Depolymerization of lignin using acidic ionic liquids

Thesis Submitted to AcSIR
For the Award of the Degree of
DOCTOR OF PHILOSOPHY
In CHEMISTRY

By
Sandip Kumar Singh
(Enrollment No. 10CC12A26037)

Under the guidance of
Dr. Paresh Laxmikant Dhepe

Catalysis & Inorganic Chemistry Division
CSIR- National Chemical Laboratory
Pune- 411008, India

May, 2017

सीएसआईआर - राष्ट्रीय रासायनिक प्रयोगशाला
(वैज्ञानिक तथा औद्योगिक अनुसंधान परिषद्)
डॉ. होमी भाभा मार्ग, पुणे - 411 008. भारत

CSIR - NATIONAL CHEMICAL LABORATORY
(Council of Scientific & Industrial Research)
Dr. Homi Bhabha Road, Pune - 411 008, India

nCL

CERTIFICATE

This is to certify that the work incorporated in this Ph. D. thesis entitled "**Depolymerization of lignin using acidic ionic liquids**" submitted by **Mr. Sandip Kumar Singh** to Academy of Scientific and Innovative Research (AcSIR) in fulfilment of the requirements for the award of the Degree of **Doctor of Philosophy in Chemistry**, embodies original research work under my supervision/guidance. I further certify that this work has not been submitted to any other University or Institution in part or full for the award of any degree or diploma. Research material obtained from other sources has been duly acknowledged in the thesis. Any text, illustration, table etc., used in the thesis from other sources, have been duly cited and acknowledged.

May, 2017

Ph. D. student
(Sandip Kumar Singh)

Supervisor
(Dr. Paresh Laxmikant Dhepe)
Senior scientist, CSIR-NCL, Pune, India-411008
Assistant Professor, AcSIR, New Delhi, India-110025

DECLARATION

I hereby declare that the thesis entitled **"Depolymerization of lignin using acidic ionic liquids"** submitted for the award of the degree of **Doctor of Philosophy in Chemistry** to the **Academy of Scientific & Innovative Research (AcSIR)**, New Delhi, has been carried out by me at Catalysis & Inorganic Chemistry Division, Council of Scientific and Industrial Research-National Chemical Laboratory, Pune, India- 411008, under the supervision of **Dr. Paresh Laxmikant Dhepe**. Research material received from other sources has been duly cited and acknowledged in the thesis. The work is original and has not been submitted as a part or full by me for any degree or diploma to this or any other university.

Date: 15th May, 2017
Place: CSIR-NCL, Pune

Sandip Kumar Singh
(AcSIR Enrollment No. 10CC12A26037)

Dedicated to………………………

My elder brother (Deepak Singh) and

younger sister (Gunjan Singh)

Acknowledgements

It is a great pleasure to express my sprinkling power words into writing. First and foremost, I would like to express my heart-felt gratitude my research supervisor and mentor Dr. Paresh Laxmikant Dhepe for providing me the admirable opportunity, to learn the first step in the scientific research carrier. I want to thank him for his excellent guidance, continuous encouragement and sincerely advice to think differently, when I was both on and off to research. His inspiration suggestion always gave a third angle to everything, I subsequently find out. His kind suggestions for being a great thinker, researcher in science as well as responsible person in the social life are absolutely inspiring. I considered very honoured for my association with him, which has given a valuable decisive turn and a significant boost in my research carrier. I would like to pay my sincere gratitude to him for all support and care, which I received from him throughout research period.

I want to express my gratitude to all my doctoral advisory committee members, Dr. V Panchagnula, Dr. D. Srinivas and Dr. A. A. Kelkar for their routine guidance and valuable suggestions throughout my research work. I thankful from the bottom of my heart to Dr. Rajamohanan, Dr. R Nandini Devi, Dr. D. Srinivas, Dr. Sayam Sen Gupta, Dr. V. Panchagnula, Dr. Jayakannan, Dr. T. Raja, Dr. C. V. V Satayanarayana, Dr. C. P. Vinod, Dr. S. B. Umbarkar, Dr. C. S. Gopinath, and Dr. E. Balaraman for their helping me in all the possible way of my research carrier.

I wish to thank to Dr. Kumar Vanka and Mr. S. Banerjee for his discussion and in collaborative theoretical work.

I would like to thank to Dr. R. K Jain for his support in the compositional analysis of the crop waste samples. I pay my gratitude to Dr. Jains group; Sandip, Priyanka, Chetna, Dhermander, Diwakar and Vipin, it was my great pleasure to analyse the sample with them.

I would like to convey my deepest thanks to Dr. D. Srinivas, Chairperson of the Catalysis and Inorganic Chemistry Division and Dr. A. P. Singh, former Chairperson of the Catalysis and Inorganic Chemistry division for providing their unconditional support to use the available facilities and also personally help whenever required. I am also thankful to Dr. (Mrs) S. Deshpande, Dr. Tejas Gaydhankar, Dr. Savita Shingoate, Ms. Samuel Violet,

……………Sandip Kumar Singh Raghuwanshi

CONTENTS

Chapter 1: Introduction and literature Review

| **Chapter 2:** | **Synthesis and characterization of ionic liquids** | **35** |
| **Section 2A:** | **Homogeneous Brønsted acidic ionic liquids** | **36** |

List of Schemes

Chapter 1

Chapter 2

Chapter 4

List of Figures

Chapter 1

Chapter 2

Chapter 3

Chapter 4

Chapter 5

List of Abbreviations

1D	One dimensional
2D	Two dimensional
AILs	Acidic ionic liquids
ATR	Attenuated total reflection
BA	Bond angle
BAILs	Brønsted acidic ionic liquids
BG	Bagasse
BL	Bond length
BLAILs	Brønsted and Lewis acidic ionic liquids
BHT	Butylated hydroxyl toluene
CHNS	Carbon, Hydrogen, Nitrogen, Sulphur
DEE	Diethyl ether
DMF	Dimethylformanide
DMSO	Dimethyl sulfoxide
DSC	Differential scanning calorimetry
DFT	Density functional theory
EtOAc	Ethyl acetate
EDX	Energy dispersive X-ray analysis
FAS	Ferrous ammonium sulphate
FID	Flame ionization detector
FT-IR	Fourier transformation-infra red
GC	Gas chromatography
GC-MS	Gas chromatography-mass spectrometry
GPC	Gel permeation chromatography
HPLC	High performance chromatography
H-BEA	Beta zeolite (H-Form)
H-USY	Ultra stable zeolite Y (H-form)
HSQC	Heteronuclear single quantum coherence
HMBC	Heteronuclear multiple bond Correlation
I-BAIL	Immobilized-Brønsted acidic ionic liquid
ICP-OES	Inductively couple plasma-optical emission spectroscopy
LC-MS	Liquid chromatography-mass spectrometry
ORGL	Organosolv lignin
Mn	Number average molecular weight
Mw	Weight average molecular weight
MMT	Million metric tons
NMR	Nuclear magnetic resonance
NOESY	Nuclear Overhauser effect spectroscopy
PDI	Polydispersity index
RH	Rice husk
SEM	Scanning electron microscopy
TCD	Thermal conductivity detector
THF	Tetrahydrofuran
TLC	Thin layer chromatography
TGA-DTA	Thermogravimetric analysis-differential thermal analysis
TPO-MS	Temperature program oxidation-mass spectrometry
UV-Vis	Ultraviolet-visible
XRD	X-ray diffraction
WC	Wood chip
WS	Wheat straw

[BMIM][Cl]	1-butyl-3-methylimidazolium chloride
[C$_3$SO$_3$HMIM][Cl]	1-methyl-3-(3-sulphopropyl)-imidazolium chloride
[C$_3$SO$_3$HMIM][HSO$_4$]	1-methyl-3-(3-sulphopropyl)-imidazolium hydrogensulphate
[C$_3$SO$_3$HMIM][H$_2$PO$_4$]	1-methyl-3-(3-sulphopropyl)-imidazolium dihydrogenphosphate
[C$_3$SO$_3$HMIM][PTS]	1-methyl-3-(3-sulphopropyl)-imidazolium p-toluenesulphonate
[C$_3$SO$_3$H(C$_6$H$_5$)$_3$P][HSO$_4$]	3-sulfopropyl-P,P,P-triphenylphosphonium hydrogensulfate
[C$_3$SO$_3$HBenzMIM][HSO$_4$]	1-methyl-3-(3-sulfopropyl)-benzimidazolium hydrogensulfate
[C$_3$SO$_3$HMIM][CuCl$_3$]	1-methyl-3-(3-sulfopropyl)-imidazolium cupric chloride
[C$_3$SO$_3$HMIM][FeCl$_4$]	1-methyl-3-(3-sulfopropyl)-imidazolium ferric chloride
[C$_3$SO$_3$HMIM][SnCl$_3$]	1-methyl-3-(3-sulfopropyl)-imidazolium stannic chloride
[C$_3$SO$_3$H(C$_2$)$_3$N][HSO$_4$]	N, N, N-triethyl-3-sulfopropanaminium hydrogensulfate
[C$_3$SO$_3$H(C$_2$)$_3$N][PTS]	N, N, N-triethyl-3-sulfopropanaminium p-toluenesulfonate
[C$_3$SO$_3$H(C$_2$)$_3$N][Cl]	N, N, N-triethyl-3-sulfopropanaminium chloride
[C$_3$SO$_3$H(C$_2$)$_3$N][H$_2$PO$_4$]	N, N, N-triethyl-3-sulfopropanaminium dihydrogenphosphate

Abstract of the Thesis

Introduction

In view of the environmental concerns caused by depletion of fossil feedstock, it is compelling to develop alternative renewable, sustainable and eco-friendly source of elements (C, H, O etc.). In view of this, the sole renewable lignocellulosic biomass, which has several benefits such as, carbon neutrality, abundant and sustainable availability, homogeneous distribution around globe etc. is of interest[1, 2] It is mainly composed of cellulose (polymer of C6 sugar), hemicellulose (copolymer of C5 and C6 sugars) and lignin (copolymer of C9 phenylpropenoid unit). Lignin is ca. 30% by *wt.* and 40% by energy of dried lignocellulosic biomass and made up of 3 major units; coumaryl (*H*), coniferyl (*G*) and sinapyl (*S*) alcohols.[2] It is a 3D amorphous copolymer and consists of several types of linkages (e.g. β-O-4, α-O-4, β-5, β-1, β–β, 4-O-5 etc.).[3] It becomes attractive to make high value low molecular weight aromatic chemicals from this rich source of phenolic copolymer. In view of this, series of catalytic processes based on mineral acids,[4] solid acids,[5] alkalis,[1] depolymerization into low molecular aromatic compounds. While, these processes are associated with several drawbacks like; employment of homogeneous catalysts, application of harsh reaction conditions (T ≥250 °C), formation of degradation products, use precious metal catalysts etc. these in turn increases the cost of the reaction etc.[6, 7] Recently, use of ionic liquids (ILs) in the biomass conversion is intensifying because ILs are regarded as green solvents or catalysts and have exploitable tunable properties.[8] Although, as a drawback in most of the studies ILs are used as solvents along with other catalysts.[9] Hence, it was proposed to use acidic ionic liquids (Brønsted acidic ionic liquids (BAILs) and immobilized-BAIL (I-BAIL)) as catalyst for lignin depolymerization under milder reaction conditions (BAILs at ≤120 °C, and I-BAIL at ≤200 °C, 1h). Further, to achieve maximum products yield and correlate the catalytic activity between the aromatic monomers, dimmer, lignin and ILs using experimental and theoretical analytical studies were undertaken as my Ph. D. work (Scheme 1).
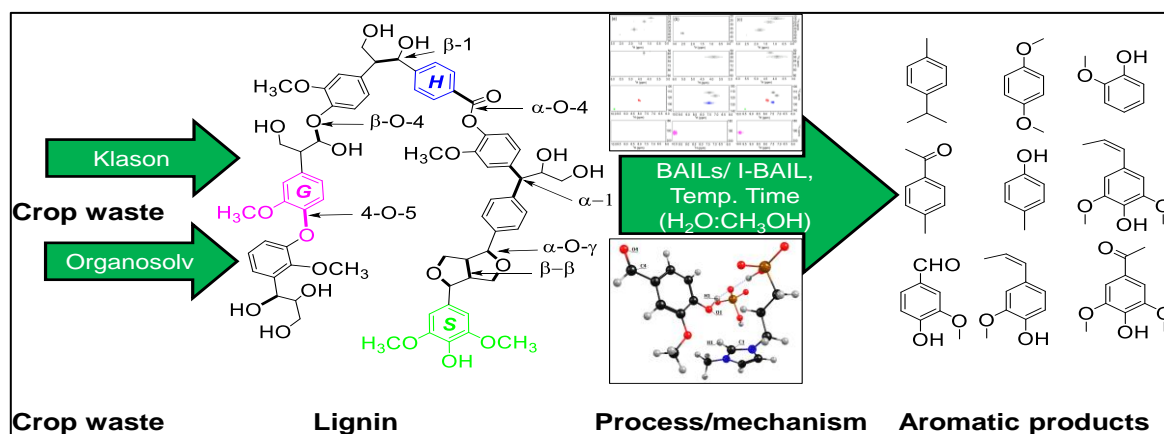
Scheme 1. Isolation and depolymerization of lignin into phenolic products using BAILs/I-BAIL.

Including 1st chapter, introduction and literature review, my thesis is divided in to six chapters. In 2nd chapter, synthesis and characterization of BAILs/I-BAIL is discussed. Characterization of commercial lignin and its depolymerization using BAILs/I-BAIL is described in 3rd chapter. In 4th chapter, isolation of Klason and organosolv lignin from various crop wastes and wood chip, their characterization and depolymerization using BAILs/I-BAIL is discussed. In 5th chapter, experimental and theoretical investigation to gain mechanistic insight on lignin depolymerization using ILs is explained. Finally, summary and conclusions are described in 6th chapter.

Statement of Problem

There are several issues associated with the above discussed known methods of lignin depolymerization processes[6, 7] and those are mentioned below,

- Use of lignin model compounds (dimmer/trimer): not actual lignin substrate.
- Use of homogeneous catalysts: very difficult to recycle the catalyst, toxicity, corrosiveness etc.
- Use of harsh reaction conditions (T≥ 250 °C): formation of char, tar, gases, degradation products etc.
- Use of ILs as solvent: costly process, viscous ILs can become a hurdle in achieving maximum yield etc.
- Poor yield of organic solvent soluble products.

To solve above mentioned issues, an efficient, green and recyclable BAILs/I-BAIL catalytic method needs to be developed for the lignin (actual substrate) depolymerization into low molecular weight phenolic products under mild reaction conditions. Additionally, the mechanistic correlation of lignin depolymerization should be developed using theoretical (DFT) and experimental (NMR (1D and 2D) and RAMAN) analysis to establish the catalytic result.

Methodology used

- BAILs were synthesized by quaternization and direct combination method using various cations (imidazolium, benzimidazolium, phosphonium and ammonium), and anions (HSO_4, H_2PO_4, Cl, PTS etc.). Along with this, synthesis of I-BAIL (immobilization of IL on silica framework) was also undertaken. Catalysts were characterized using CHNS, NMR (^{1}H, ^{13}C, and ^{29}Si), SEM, TEM, FT-IR, TGA, UV-Vis, etc. techniques.
- Isolation of Klason and organosolv lignin from various crop waste and wood chip, their (isolated and commercial lignin) characterization and depolymerization were carried out using BAILs/I-BAIL as catalysts into low molecular phenolic products (<220 g/mol). Further to observe the changes transpiring in lignin structure and existence of several functional groups in both, lignin and product on bulk and molecular level analysis were done.

- Experimental (NMR (^{1}H, ^{13}C, HSQC and NOESY), and RAMAN) and theoretical (DFT) mechanistic investigation studies were done to correlate the catalytic activity between ILs and aromatic monomers, dimmer and lignin.

Sample results

Synthesized BAILs and I-BAIL were evaluated to depolymerize commercial lignins into THF soluble products with high yields (78-91%).[10, 11] Further, the presence of various functional groups, moieties (*H*, *G* and *S*), etc. between lignin and THF soluble products were correlated using FT-IR, NMR (1D and 2D), etc. techniques, and identified the formation of different products with diversity in functional groups. Additionally, this work has extended into the studies of the isolation as well as physico-chemical characterization of isolated Klason and organosolv lignins from crop waste and wood chip samples collected from different states of India.[12] The isolated (Klason and organosolv) lignins depolymerization process was done using BAIL/I-BAIL as catalysts into low molecular weight phenolic products (50-90% yield). However, the maximum aromatic products yield was achieved with BAILs compared to other catalysts. To explore this phenomenon, experimental and theoretical calculation were checked to confirm that ILs have interaction with substrate molecules.[10, 13]

Depolymerization of commercial lignin: Recyclable BAILs with $-SO_3H$ groups in catalytic quantity under ambient pressure at 120 °C, were evaluated in batch mode Parr autoclave for the lignin depolymerization (60 kDa). The BAILs yielded THF soluble products with high efficiency (78% yield, 95±5% mass balance Figure 1). Analysis of the THF soluble products was carried out using various techniques such as FT-IR, NMR (1D (^{1}H and ^{13}C), 2D (HSQC), DSC, TGA, UV-Vis, GC, GC-MS, LC-MS, GPC, MALDI-TOF MS etc. Results show formation of low molecular weight (<220 g/mol) phenolic products. The GC-MS

Fig. 1. Depolymerisation of lignin. Reaction condition: lignin (0.5g), catalyst (0.5g), $H_2O:CH_3OH$ (30mL, 1:5*v/v*), 120 °C, 1 h, 1000 rpm.
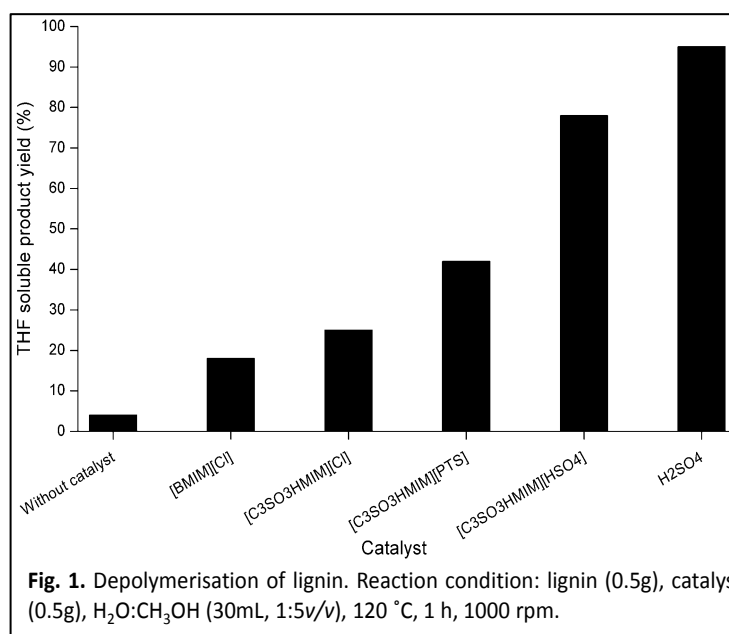
profile of the H_2SO_4 catalyzed reaction showed only a few peaks compared with $[C_3SO_3HMIM][HSO_4]$, signifying that BAIL has superior capability to yield low molecular weight aromatic products even if H_2SO_4 exhibited higher yield (98%) than BAILs (Figure 1). To check the effect of BAILs on lignin depolymerization, the correlation of the catalytic efficiency was checked by 1D (^{1}H), 2D (HSQC/NOESY) NMR and RAMAN analytical studies.

Isolation of lignin, their characterization and depolymerization using BAIL/I-BAIL The complete compositional analysis (TAPPI method) of the crop waste (rice husk, bagasse and wheat straw) and wood chip samples was done to find out the concentrations of the components present in these samples. Klason and organosolv processes were carried out to isolated lignin from the crop waste and wood chip samples, collected from different states of India. Various physico-chemical and analytical techniques were used to characterize the crop waste, wood chip, pulp and lignin, samples. The isolated lignin underwent depolymerization using BAIL (120 °C) and I-BAIL (200 °C) as catalyst and gave the low molecular weight (<220 g/mol) aromatic products yield in the range between 50-90%.

Experimental and theoretical investigation to gain mechanistic insight on lignin depolymerisation

The difference in activity between BAIL and H_2SO_4 are anticipated because of ILs ionic nature through which it can interact with lignin moieties. This would facilitate cleavage of C-O-C bonds. To check this phenomenon, ^1H NMR (Figure 2) studies were performed with cumene, vanillin (monomers), guaiacol glyceryl ether (dimmer) and lignin (copolymer) molecules. In the spectra recorded for adduct of IL and vanillin (Figure 2b), chemical shifts of proton in IL (δppm: 9.43→9.36 (NCHN, 'h'), shielding) and vanillin (δppm: 10.27→10.60 (-OH, 'o'), 6.98→7.10 and 6.94→7.06 (doublet, Ar-H, 'k'), deshielding] compared to neat spectra (IL and vanillin) were observed. This effect is best explained on the basis of transfer of electron density (through 'O' of –OH) from vanillin to electron deficient imidazolium ring (cation of IL). To eliminate the possibility of involvement of the pi electrons, NMR spectra also were recorded with

Figure 2. 1D ^1H NMR spectra. a) neat [BMIM][Cl], neat cumene and [BMIM][Cl] cumene adduct; b) neat [BMIM][Cl], neat vanillin and [BMIM][Cl] vanillin adduct. All the spectra were recorded in DMSO-d$_6$.
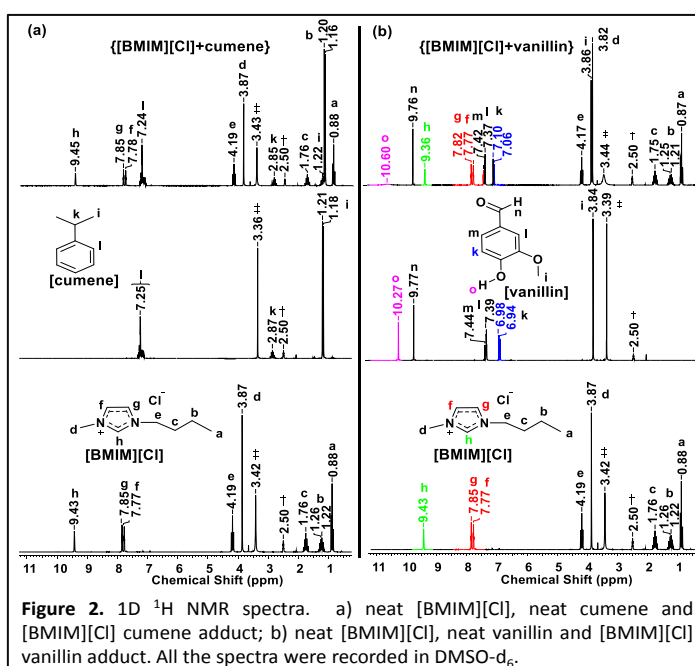
cumene (without –OH, -OCH$_3$, -CHO groups) molecule and as anticipated no shift in proton peaks were seen (Figure 2a), which reaffirmed that IL interact with substrates having –OH groups *via* 'O'. Next, interaction study was performed with guaiacol glyceryl ether and lignin molecules, and analogous trend in chemical shift was observed. To support the experimental explanations derived from 1D (^1H) NMR, interactions studies also were recorded with the help of 2D (HSQC) NMR & RAMAN analysis (between the aromatic monomers, lignin and IL) and theoretical (DFT) analysis. RAMAN spectra also explained the shift (blue and red) in IL and

vanillin adduct compared to neat samples. These results also were correlated with DFT calculations and data shows that BAIL and substrate both have strong and weak hydrogen bonding interactions. This suggests that BAIL plays a crucial role by having interactions with substrate, which, in turn is responsible in producing higher yields.

To summarize, depolymerization of lignin having C-O-C and C-C linkages into low molecular aromatic products (78% yields, with 95±5% mass balance) was achieved with recyclable BAILs as catalyst at ambient pressure at 120 °C within 1h. In order to comprehend the differences in activity between BAIL and other catalysts, experimental (NMR, RAMAN) and theoretical (DFT) studies were undertaken.

References

1. C. Li, X. Zhao, A. Wang, G. W. Huber and T. Zhang, *Chem. Rev.*, 2015, **115**, 11559-11624.
2. A. J. Ragauskas, C. K. Williams, B. H. Davison, G. Britovsek, J. Cairney, C. A. Eckert, W. J. Frederick, J. P. Hallett, D. J. Leak, C. L. Liotta, J. R. Mielenz, R. Murphy, R. Templer and T. Tschaplinski, *Science*, 2006, **311**, 484-489.
3. H. Nimz, *Angew. Chem. Int. Ed.*, 1974, **13**, 313-321.
4. M. R. Sturgeon, S. Kim, K. Lawrence, R. S. Paton, S. C. Chmely, M. Nimlos, T. D. Foust and G. T. Beckham, *ACS Sustainable Chem. Eng.*, 2014, **2**, 472-485.
5. A. K. Deepa and P. L. Dhepe, *ACS Catal.*, 2015, **5**, 365-379.
6. A. Corma, S. Iborra and A. Velty, *Chem. Rev.*, 2007, **107**, 2411-2502.
7. J. Zakzeski, P. C. A. Bruijnincx, A. L. Jongerius and B. M. Weckhuysen, *Chem. Rev.*, 2010, **110**, 3552-3599.
8. N. Sun, H. Rodriguez, M. Rahman and R. D. Rogers, *Chem. Commun.*, 2011, **47**, 1405-1421.
9. J. Zakzeski, A. L. Jongerius and B. M. Weckhuysen, *Green Chem.*, 2010, **12**, 1225-1236.
10. S. K. Singh and P. L. Dhepe, *Green Chem.*, 2016, **18**, 4098-4108.
11. S. K. Singh and P. L. Dhepe, manuscript communicated, 2016.
12. S. K. Singh and P. L. Dhepe, *Bioresour. Technol.*, 2016, **221**, 310-317.
13. S. K. Singh, S. Banerjee, K. Vanka and P. L. Dhepe, Submitted, 2016.

Chapter 1:

Introduction and literature review

1.1. Introduction

There are numerous chemicals that we use in our day to day life, which are derived from non-renewable resources such as fossil feedstocks (coal, crude-oil, natural gas, nuclear fuel, etc.). But, the major problems associated with these resources are limited stock, high consumption rate, heterogeneous distribution around the globe, rising prices etc. Another major problem is an environmental issue due to formation of oxides of carbon (CO and CO_2), sulphur (SO_2 and SO_3), and nitrogen (NO_2 and N_2O). These gases are emitted to atmosphere during the utilization of fossil feedstocks, which leads to global warming, acid rain, etc.

Generally, the demand for fuels, chemicals and energy is increasing with the increase in the population. But, the resources for their synthesis are limited and the main feedstock, fossil (crude oil) is depleting very rapidly. By considering these drawbacks, finding some alternative renewable resources for the synthesis of fuels, chemicals and energy is inevitable. However, this alternative resource should be economically sustainable, eco-friendly and renewable. There are several renewable, sustainable and eco-friendly resources of energy like lignocellulosic biomass, tidal, hydrothermal, geothermal, etc. However, sole lignocellulosic biomass is the key components for the production of renewable, sustainable and eco-friendly source of fuels, chemicals, and energy, rest resources are only energy efficient processes. The advantage of working with lignocellulosic biomass is that it can produce fuels, chemicals and energy, mainly due to its C, H and O elemental constituents. Moreover, it has wide distribution, minimal environmental impact (acid rain, CO_2 neutral, etc.) and is affordable etc.[1]

1.2. Biomass

Various kinds of bio-species are present on the Earth and those are named as plant, animal, microorganism, etc. The plant, animal and microorganism (living or dead) derived species are collectively called as biomass. Plant derived biomass is generally, agricultural crop waste, forest residue, wood chips etc. This biomass is currently used to generate heat, electricity, etc. Although, it is a good source of C, H and O, which can be valorised into fuel, chemicals and energy *via* bio-refinery concept.

1.3. Bio-refinery concept

The petro-refinery and bio-refinery are and can be used to synthesize transport fuels and chemicals but the nature of raw material taken as feedstocks are different in both the cases. However, due to the fast depletion of fossil feedstocks biomass feedstocks are fetching the importance worldwide through bio-refinery concept. The utilization of biomass (preferably lignocellulosic) into valuable chemicals, fuels and energy can be employed through bio-refinery pathway as shown in Figure 1.1. Since, the generated valuable chemicals from biomass are basically made up of carbon, hydrogen and oxygen, upon usage of these chemicals release oxides of carbon (e.g. CO and CO_2) in the atmosphere. The released carbon dioxide is consumed

by the plant *via* photosynthesis process in the presence of water and sunlight. Further, these plants (dead) are again used for bio-refinery concept to fetch fuels, chemicals and energy. Consequently, it can be said that the utilization of fuels and chemicals obtained from lignocellulosic biomass, allows a re-utilization of these in a recycle way (carbon neutral way), which generally reducing the CO_2 levels in the atmosphere. The whole bio-refinery concept is shown in the Figure 1.1. While, in use of fossil feedstocks, a million of years are essential for the natural conversion of biomass into fossil feedstocks. In the meanwhile, large amount of CO_2 will be released in the atmosphere, which is the major reason for global warming. Hence, it is vital to use biomass besides fossil feedstocks which may curtail the problems associated with fossil feedstocks.
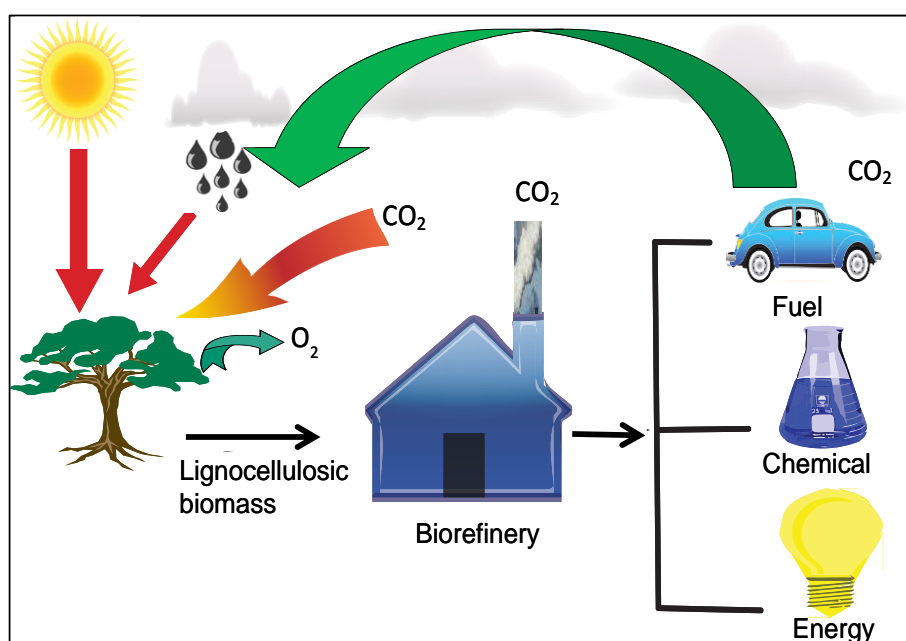
Figure 1.1. Bio-refinery concept for the conversion of lignocellulosic biomass.

1.4. Classification of biomass

The biomass is broadly categorized into two classes as animal and plant derived depending on the origin, and the details on the classification of biomass are discussed below.

1.4.1. Animal derived biomass

Chitin is one of the example of animal derived biomass and it is the second most abundant polymer and made-up of long chain N-modified polysaccharide polymer of N-acetylglucosamine $(C_8H_{13}O_5N)_n$ linked through β-(1→4) units. It is characteristic component of cell wall of fungi or the exoskeleton of arthropods, insects, etc.

1.4.2. Plant derived biomass

Plant derived biomass consists of plant residues or its derived products. It can be further sub-classified into edible (eatable for human being) and non-edible (non-eatable for human being).

1.4.2.1. Edible biomass

Starch $(C_6H_{10}O_5)_n$, oil (mustard oil, coconut oil, corn oil etc.) etc. are called as edible plant derived biomass (Figure 1.2), which are used by humans in their daily life. Starch is a polysaccharide and it is consisting of a large number of D-glucose units linked by α-(1→4) glycoside bonds. Generally, it consists of two major units, branched and linear. Starch is made up of amylose (10-20%) and amylopectin (80-90%). Edible oil consists of long chains of triglyceride fatty acids.
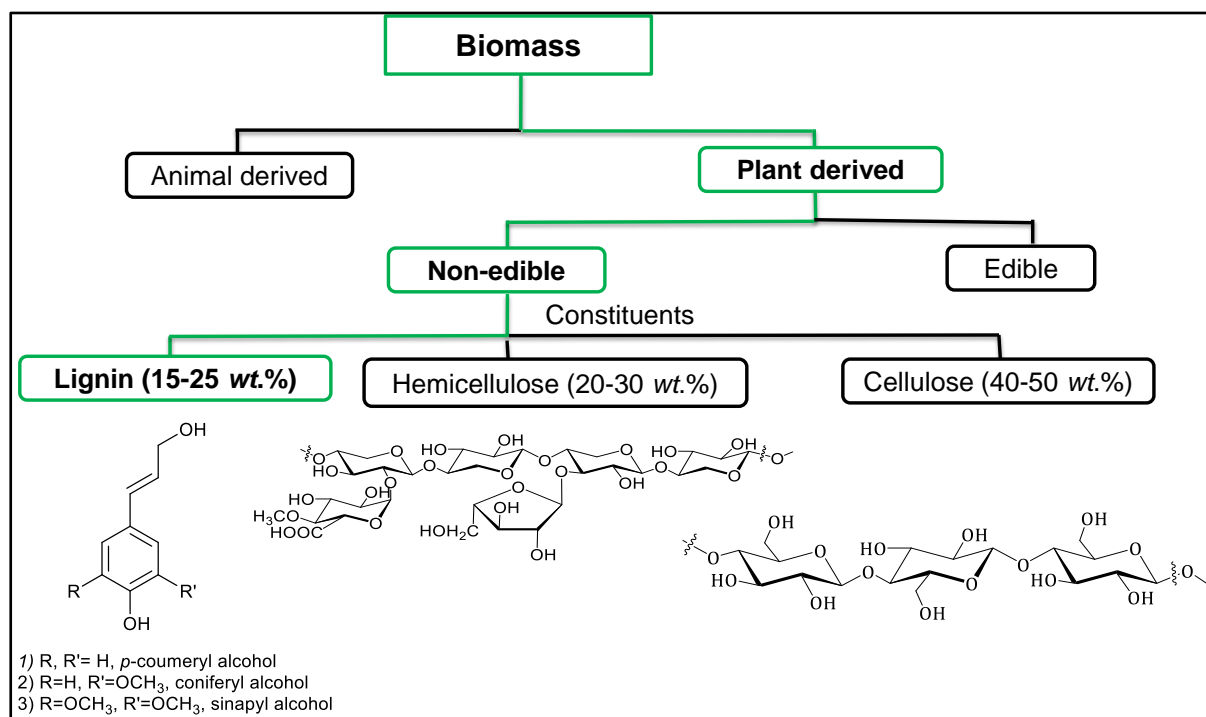
Figure 1.2. Classification of biomass.

1.4.2.2. Non-edible biomass

Lignocellulosic biomass (plant derived) is called as non-edible biomass, which is composed of cellulose (40-50 dried *wt*.%), hemicellulose (20-30 dried *wt*.%), lignin (15-25 dried *wt*.%), etc.[2-4] Cellulose and hemicellulose are collectively called as polysaccharides. These are linked by various covalent and non-covalent bonds[5] and lignin acts as glue between cellulose and hemicellulose.

1.4.2.2.1. Polysaccharides (Cellulose and hemicellulose)

Cellulose (C6 glucose polymer) is the largest abundant renewable polymer on the earth.[6] Its annual production is ca. 10×10^{10} tons[7, 8] and consists of linear chain of D-glucose units joined by β-(1→4) glycosidic linkages. It is crystalline in nature due to presence of intra, inter and inter-sheet hydrogen bonding.[9]

The second most abundant lignocellulosic biomass hemicellulose, which is composed of five carbon (e.g. xylose, arabinose, etc.) and six carbon (e.g. glucose, galactose, mannose, etc.) sugar

units, linked *via* β-(1→4) glycoside linkages in variable aspect depending on the type of plants, isolation procedure, etc.

1.4.2.2.2. Lignin

The 'Lignin' word was first coined by *de Candolle* in 1819, which was derived from the Latin word 'lignum' and the actual meaning of lignum is wood. The function of plant lignin cells is to assist the movement of water and also act as barrier to evaporate the water through its cellular struture.[10] Lignin is the third most abundant composition of lignocellulosic biomass after cellulose and hemicellulose, and its annual production is 20 billion metric tons.[11] It is estimated that ca. 125 million metric tons/year lignin produced from crop waste (Based on Technology Information, Forecasting and Assessment Council, (TIFAC)-2009) in India.[12] It is the only one renewable resource of aromatic copolymer on the Earth and is present in all the terrestrial plants like hardwood, softwood, shrubs, aquatic and marine algae, etc. Lignin also provides the mechanical strength to the plant *via* acting as glue between cellulose and hemicellulose. It is three dimensional, amorphous in nature, copolymer mainly made up of three basic units like coumaryl, coniferyl and sinapyl alcohols (Figure 1.3), and its modified units are called as *p*-hydroxyphenyl, guaiacol and syringol alcohols, respectively (Figure 1.3).[10] Lignin is considered as the outer cover of plant cell wall, for example; in the plant cell wall middle lamella is mainly composed of coumaryl alcohol.[13, 14] Coniferyl alcohol forms the secondary cell wall of the xylem element and sinapyl alcohol is considered as the contrast region of the fibre-forming cell wall.[13-15] It is bio-synthesised in the plant, through radical mechanism using three phenolic building units as shown in Figure 1.4.[15]
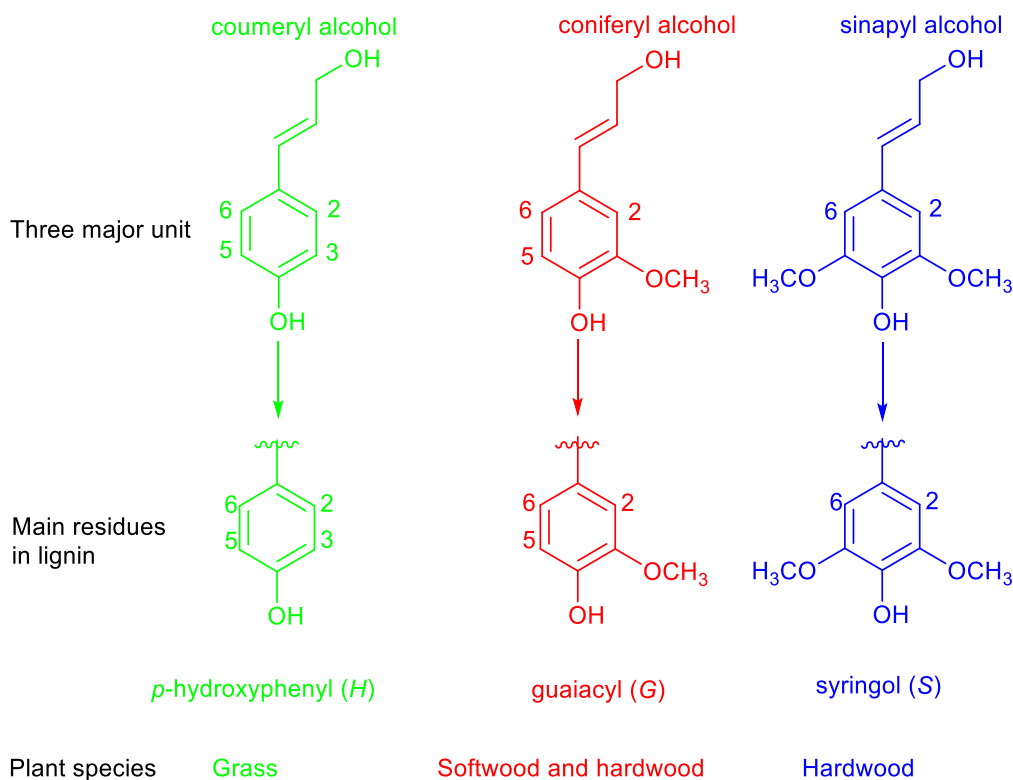
Figure 1.3. Lignin monomers building block, residues in different plants species.

1.5. Evolutionary aspects of lignin linkages

Lignin is made up of aromatic phenolic units and the actual mechanisms for the formation of various types of inter-linkages are shown in the Figure 1.4. It is synthesised by two ways namely; dimerization and lignification.[16-18] In the dimerization step, two coumaryl alcohols get ionised and is followed by formation of β-O-4 (β-ether), β-β (pinoresinol), β-5 (phenyl coumaran) linkages.[16] However, the formation of different types of linkages like β-5, 5-5, 4-O-5, β-O-4, etc. is done *via* lignification process. These inter and intra-molecular bonds formation happen through radical coupling reaction[16] in dimerization or lignification processes (Figure 1.4). These linkages vary depending upon local weather, soil condition, humidity, temperature, growth time/period, etc. along with age of plant, species, etc.[19] The β-O-4 linkage is the most dominant in all the lignins as shown in Table 1.1. As shown in Figure 1.5, it is evident that depending on the lignocellulosic source, the coumaryl, coniferyl and sinapyl alcohols units also vary. The coumaryl, coniferyl and sinapyl alcohols units are present in grass, softwood and hardwood respectively (Figure 1.3).[20] Depending upon the plant, age, climate, it contains various types of ≡C-O-C≡ and ≡C-C≡ bonds (Figure 1.5) and these bonds have different types of bond dissociation enthalpy as shown in Table 1.1.
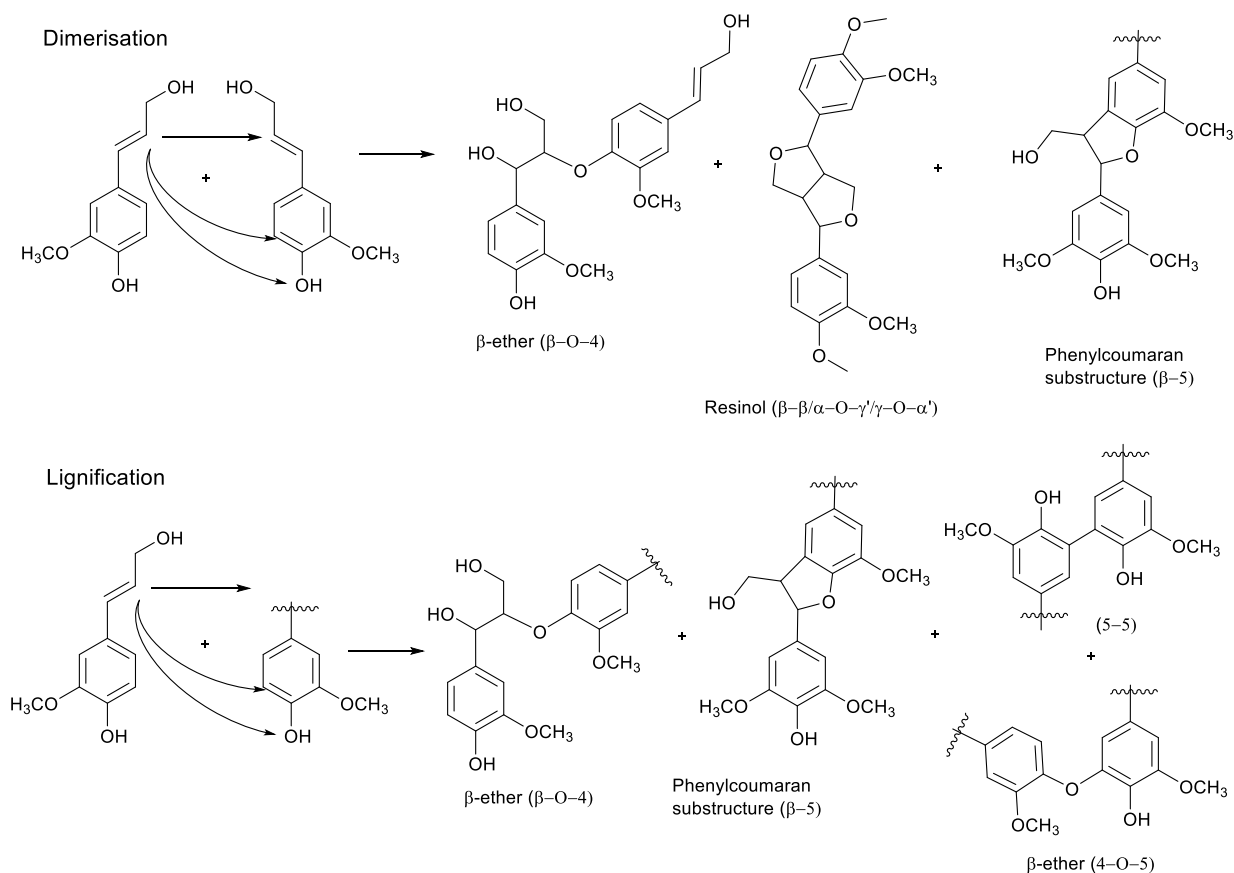
Figure 1.4. Inter-unit bond formation in the lignin structure.

Table 1.1. Nature of bonding in lignin, their abundance (hardwood and softwood) and bond dissociation enthalpy (BDE; kJ/mol).

Types of linkages	Abundance in hardwood, (%) [2, 21, 22]	Abundance in softwood, (%) [2, 21, 22]	Bond dissociation enthalpy (kJ/mol) [23-27]
β-O-4	46-65	43-50	290-335
α-O-4	4-8	6-8	215-270
4-O-5	3-7	2-5	330
α-O-γ′	-	-	270
5-5'	4-11	10-25	490
β-β	3-7	2-4	335
β-1	5-7	3-7	270-289
α-1	-	-	360-390
β-5	4-6	9-12	-
-OCH$_3$	-	-	255-275
others	5-13	-	-
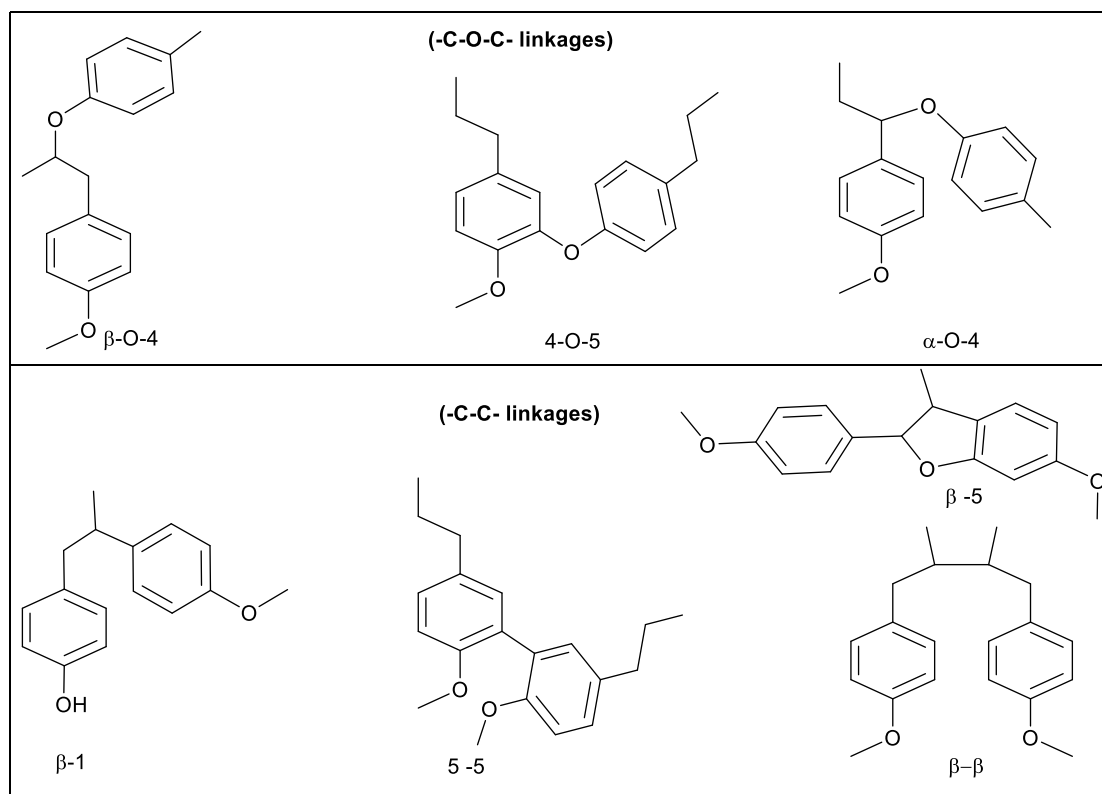
Figure 1.5. Various types of bonding in lignin.

As illustrated in the Figures 1.5 and 1.6, lignin copolymer contains various types of linkages along with several types of functional groups, like aliphatic hydroxyl, phenolic hydroxyl, benzyl hydroxyl (alky/aryl), carbonyl, ether, ester, alkoxy, aldehyde groups at the side chain. Table 1.2 represents the various functional groups are present 100 phenylpropenoids (C9) parts per unit (ppu) of hardwood and softwood lignin. These functional groups vary depending upon the isolation procedure of lignin, type of plant, age, climate etc. and hence only the approximate values of functional groups are represented here.

Table 1.2. Functional groups present in lignins derived from different sources (functional groups per 100 ppu).[28, 29]

Functional group	Hardwood	Softwood
Carboxyl	11–13	-
Carbonyl	3–17	20
Methoxy	132–146	92–96
Aliphatic hydroxyl	-	120
Benzyl hydroxyl	-	16
Phenolic hydroxyl	9–20	20–28

Based on the several observations at the bio-synthesis of the lignin, researchers have proposed the structure of the lignin. In 1977 Alder *et al.* reported the structure of lignin, which is widely accepted and referred till date (Figure 1.6).[30]
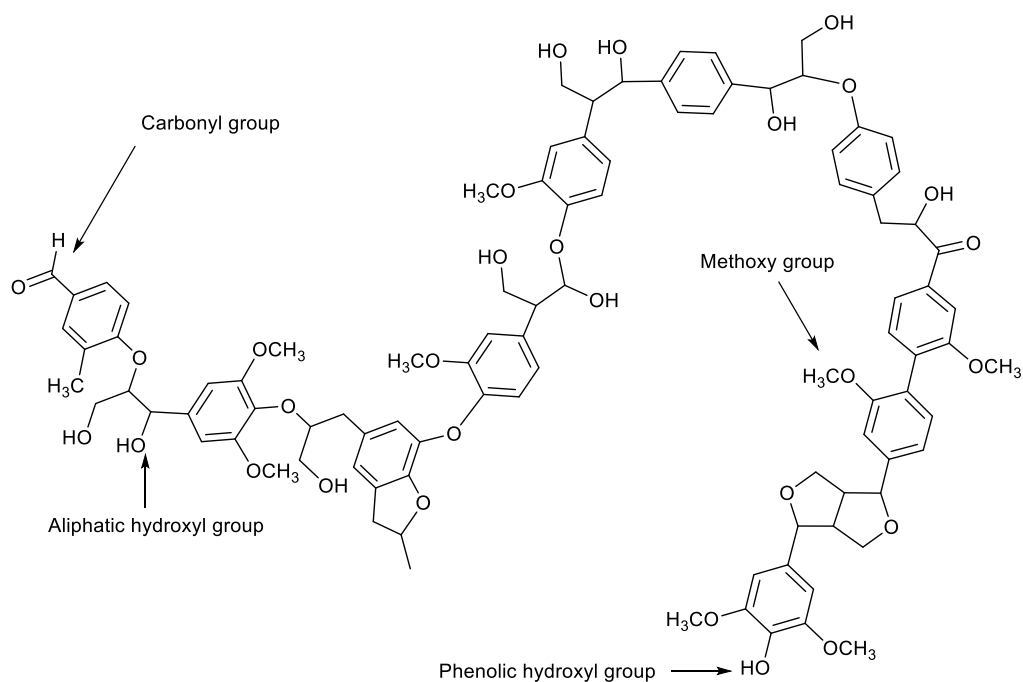
Figure 1.6. Representative structure of lignin.

1.6. Technical lignin production from lignocellulosic biomass

Pretreatment is the initial stage of bio-refinery concept to know the chemical composition of cellulose, hemicellulose, lignin, etc. in the lignocellulosic biomass. After pretreatment, lignocellulosic biomass constituents are fractioned into smaller components, than the actual molecular weight. There are several methods used for the isolation of lignin from the lignocellulosic biomass. Structure, composition, molecular weight, etc. of lignin varies depending upon the techniques used for its isolation, source of substrate (either softwood, hardwood or grass) etc.

Lignin isolation process is broadly classified into four major categories; (1) Physical isolation process (ball milling, etc.), (2) Solvent fraction (organosolv fraction along with small amount of acids like sulphuric acid, ionic liquids, etc.) (3) Chemical isolation process (acidic, alkali, alkaline, oxidative, etc.) and (4) Biological isolation process (enzymatic, fungi, etc.).[31-33] Each process has few advantages and disadvantages.

These isolation processes are further classified into sub-isolation categories. During the isolation process, the polysaccharide can be soluble and lignin may remain as solid (i.e. Klason method, etc.) and, in the second class lignin is soluble and polysaccharide will remain as insoluble (i.e. organosolv, Kraft method, etc.). Details on the isolation process used for the lignin from the lignocellulosic biomass are summarised as below.

1.6.1. Kraft lignin

Kraft process is the most dominant globally accepted industrial isolation method, which is used for the extraction of lignin from the lignocellulosic biomass. It operates at high pH and uses

substantial amount of Na_2S and NaOH (known as white liquor) at temperatures ranging between 150-180 ℃ for 2 h.[33-35]

The general monomeric molecular formula for Kraft lignin as $C_9H_{8.5}O_{2.1}S_{0.1}(OCH_3)_{0.8}(CO_2H)_{0.2}$ has been claimed.[36] MeadWestvaco, USA is the world largest Kraft lignin producing company and another company is Metso corporation, in which lignin is extracted from pulp mill.[33]

1.6.2. Lignosulfonate lignin

Lignosulfonate lignin is well known process and commonly used at paper and pulp industries.[37, 38] This process covers a wide range of pH (2-12), temperature (>120 ℃), using either calcium or magnesium with sulphite as counterion.[38] The obtained lignosulfonate lignin possesses hydrophilic and hydrophobic properties.

Lignin derived from lignosulfonate process exhibits higher number molecular weight (*Mn*) and weight average molecular weight (*Mw*), than Kraft lignin due to sulphonation on the arene bonds. The proposed monomeric molecular formula of softwood and hardwood lignosulfonate lignin are $C_9H_{8.5}O_{2.5}(OCH_3)_{0.85}(SO_3H)_{0.4}$ and $C_9H_{7.5}O_{2.5}(OCH_3)_{1.39}(SO_3H)_{0.6,}$ respectively.[36]

1.6.3. Organosolv lignin

The organosolv lignin process covers the broad temperature range from 140 to 210 ℃.[39] In this process hydrolytic cleavage of ether ($\equiv$C-O-C$\equiv$) bonds is observed and the fragmented molecules are soluble in the mixture of the organic solvent. Various organic solvents are used like methanol, ethanol, propanol, butanol, acetone, etc. The further details on the organic solvents and types of lignin are shown in Table 1.3. Depending upon the solvent used, names of the isolated organosolv lignin vary. When ethanol/water mixture is used to isolate, it is called Alcell lignin, and acetic acid/water composition is used for acetocell lignin, etc.

Table 1.3. Types of organosolv lignin.

Types of lignin	Organic solvent used in the processes[17, 40-42]
Organocell	Methanol is used, followed by methanol and NaOH and antraquinone pulping
Alcell	Ethanol/water
Alcetocell	Acetic acid/water
Acetosolv	Acitic acid/HCl pulping
Formacell	Acetic acid/formic acid/ water
Milox	Formic acid/hydrogen peroxide

The concentration of water varies 40-80% depending upon the process used for the isolation of organosolv lignin. To enhance the yield of organosolv lignin extraction, acids and alkalis are also used as catalyst. As shown in Table 1.3, Alcell and organocell processes are the major class of organosolv method.

Organosolv lignin has lower molecular weight (1000-5000 g/mol) compared to Kraft and lignosulfonate lignin. Organosolv lignin is insoluble at low pH (2-4), while it is soluble under

alkaline condition or in several polar solvents. A monomeric molecular formula for the organosolv lignin is calculated as $C_9H_{8.53}O_{2.45}(OCH_3)_{1.04}$ with calculated average molecular weight of 188 g/mol.[36] This process has several advantages, and those are shown as below.

1) Organosolv process (sulphur and metal free) is considered more eco-friendly than Kraft and lignosulfonate lignin (generally used sulphur, metal containing materials) isolation procedures. Disposal of black liqueur is major hazardous problem, which is generated in Kraft and lignosulfonate processes.

2) Recycling of organic solvent by simple rotavap and using for the next isolation procedure is possible. This is not possible with Kraft and lignosulfonate processes. Thus, organosolv is an economical process.

Extraction of oraganosolv lignin also has some disadvantages; recovery of solvents (high boiling point, e.g. 1,4- dioxane B.P.= 101.0 °C, butanol, B.P.= 117.7 °C, etc.) and handling of organic solvents.

In 1989 first organosolv lignin isolation process was established by Repap Enterprises in Canada. While, Alcell lignin was laid by Lignol Innovations Corporation of Vancouver B. C., Canada on a commercial scale.[36]

1.6.4. Klason lignin

Klason method is known for the accuracy of the lignin content in lignocellulosic biomass.[43, 44] Klason lignin content in the lignocellulosic biomass is the addition of acid soluble and insoluble lignin (acid soluble contents measured by UV-Vis spectroscopy). In this method lignocellulosic biomass is treated with 72%*wt./wt.* (12 M) sulphuric acid at 10-20 °C temperature for 2 h. Further this solution is diluted up to 3%*wt./wt.* (0.51 M) sulphuric acid and then is refluxed for 4 h.[43, 45] In this two-steps process polysaccharides are completely soluble and lignin is precipitated out. Filter the resultant mixture and wash the acid insoluble Klason lignin with hot water to remove the polysaccharides and sulphuric acid contamination. The precipitated acid insoluble Klason lignin content is filtered and washed with hot water (to remove the polysaccharides and sulphuric acid contamination) and weighed. The filtrate (liquid sample) is used for the UV-Vis analysis to calculate the acid soluble lignin, through comparing the UV-Vis absorbance to a standard at 205 or 278 nm.[44, 45]

Along with these lignin isolation methods, several other methods are also known for the isolation of lignin, like pyrolysis lignin, steam exploded lignin, cellulolytic enzymatic process, etc. details on these methods are given in the Table 1.4.

Table 1.4. Brief summary on the lignin isolation methods.

Lignin	Process	Conditions	Remarks	Refs.
Pyrolysis lignin	Pyrolysis process	High temp. (>400 ^{o}C), 2 sec.	Char, gases, low molecular weight lignin	33, 36, 46
Steam explosion lignin	Steam explosion process	Temp. 180-230 ^{o}C, high pressure 1.4-3.5 MPa, time 1-20 min.	Used for preparing cellulose pulp, alkali washing and low molecular weight lignin	36, 47
Cellulolytic enzyme lignin (CEL)	Cellulolytic enzyme process	Cellulolytic enzyme	Enzymes are used to remove carbohydrates up to 85-88%, low molecular weight lignin	32
Alkaline oxidative lignin	Alkaline oxidative process	O_2 or H_2O_2 used as oxidant	More carbonyl and carboxylic group, low molecular weight than Kraft and lignosulfonate lignin	36
Lignin	Dilute acid process	Dilute acid, HNO_3 with N_2O_5	Hydrolysis of polysaccharides, lignin as precipitated	36
Lignin	Ionic liquids (ILs) process	ILs (e.g. 1-ethyl-3-methylimidazolium acetate)	Hydrolysis of polysaccharide, lignin as precipitated	48

1.7. Availability of lignin

For the sustainability of the lignin derived product, it is desired to know the availability of the resources. Lignin is generated from the paper and pulp industries as a by-product and also from the cellulose to ethanol production process. One kilogram ethanol production from cellulosic feedstocks generates three kilogram lignin as by-product. It is estimated that natural production of lignin globally is ca. 20 billion metric tons/year. However, approximately 0.70 billion metric tons/year lignin is generated using Kraft process from paper and pulp industry. In addition to Kraft process, sulphite and soda industries also generate ca. 0.01 billion metric tons/year of lignosulfonate and ca. 10000 metric tons/year of soda lignin, respectively.[49] Lignin is mainly used to generate heat *via* burning process or ca. 2% is used as additive in the cement, binder, animal feed pallet, etc.[36]

1.8. Up-gradation of lignin

Lignin is obtained in cellulose to ethanol process as a by-product and from paper and pulp industries in huge amounts. Currently, it is burned to get heat and power, during which large quantity of CO_2 is emitted into the atmosphere. This is one of the major issues of global warming. Therefore, if lignin is valorised for the production of chemicals, materials, fuels and energy, it can significantly reduce the global warming.[36] Lignin is a significant component of total carbon in the lignocellulosic biomass, and it will be better to upgrade this fraction. It is also a requirement to achieve atom efficiency with value-addition in bio-refinery concept. Since,

lignin is the only renewable resource of aromatic products, it even becomes crucial to convert lignin into aromatic monomers, which can be used as fuels, chemicals and energy.

Lignin is generally made up of carbon, hydrogen and oxygen elements (Figure 1.6). These units are linked *via* ≡C-O-C≡ or ≡C-C≡ bonds (Figure 1.5), within the molecule. After selective cleavage of their linkages present in it, lignin produces aromatic derived monomers, which have a wide range of application in various fields like polymers, petrochemicals, materials etc. As fossil feedstocks have limitation and increasing prices of their products, lignin is the only renewable resource for the production of high amount of the aromatic monomers that can be used as materials, fuels, chemicals and energy.

Hydrocarbons such as benzene, toluene, xylene etc. are synthesised from the lignin using pyrolysis or hydro-deoxygenation processes.[50, 51] Guaiacol, phenol, catechols, cresol, etc. are aromatic monomers, which could be obtained from lignin hydrolysis process.[52, 53] These chemicals have wide range of applications,[54] while lignin alone is the base materials for the platform chemicals.[55] Vanillin is the most consumable chemicals used as flavouring agent like chocolate and ice-cream industry. It is also used in coco-cola foodstuffs and baked food which are obtained from the lignin oxidation reaction.[56] Similarly, vanillic acid, syringaldehyde, etc. are chemicals which are synthesised from the lignin oxidation reaction. Lignin oxidised products are highly bio-based potential chemicals and used as an intermediate for many industrial applications like, hydrogel, pharmaceutical, polymers, etc.[54, 57] Lignin is a macromolecule, after isolation of lignin by using various processes, they are further utilized as polymers to polyol substituted lignin, carbons fibres etc.[58] These bio-derived polymer materials have a very short term bio-durability and mechanical strength.[57] Therefore, it is significant to convert lignin efficiently and selectively into low molecular weight aromatic products.

1.9. Depolymerization of lignin

The depolymerization of technical (isolated lignin) lignin is a challenge due to its heterogeneous nature, intrinsic linkages (Figures 1.5-1.6 and Table 1.1), various functional groups, high molecular weight (>3,000 Da), etc. which makes it very complicate to selectively convert into aromatic monomers. Some of the potential routes for the lignin depolymerization into aromatic products are discussed in various papers and reviews. The main purpose is to valorise lignin copolymer into aromatic monomers, which can find applications as materials, fuels and platform chemicals. There is broad classification of lignin depolymerization into biological, chemical and thermal processes.

1.9.1. Biological depolymerization of the lignin

Lignin undergoes depolymerization into low molecular weight aromatic products, the details of the biological process is given below.

1.9.1.1. Enzymatic process

It is very difficult to selectively cleave the $\equiv$C-O-C$\equiv$/$\equiv$C-C$\equiv$ bonds having random structure of the lignin into aromatic products and prevent the repolymerization process.[59] Although, the enzymatic process is not well known for the lignin depolymerization. However, some interesting results have been obtained with the use of fungi in lignin depolymerization process. *Phanerochaete chrysosporium and Pycnoporus cinnabarinus* are used for the depolymerization of lignin into low molecular weight aromatic products.[60]

1.9.2. Thermal depolymerization of lignin

In this scenario some of the thermal process (gasification, pyrolysis, combustion and supercritical) are used to convert lignin into valuable products.

1.9.2.1. Gasification

Gasification process generates synthesis gas (syngas), which is a mixture of hydrogen and carbon monoxide with very small quantity of carbon dioxide at 700-1000 ^{o}C.[61-63] Further utilization of syngas is done by two processes, Fischer-Tropsch process[64] and methanol/dimethyl ether process.[65] Similarly, supercritical water (Tc= 374 ^{o}C, Pc= 22.09 MPa) with or without metal catalysts is used for the lignin gasification reaction.[66-68] Under gasification reaction, various products are also obtained like gasoline, jet-fuels, diesel, etc.[69] Among the various metal supported catalysts, Ru/TiO$_2$ is the good catalyst for the conversion of alkylphenol (lignin model compound) into syngas in presence of supercritical water at 400 ^{o}C.[70] Commercial Ni catalyst is also evaluated in supercritical conditions (380-480 ^{o}C) for the lignin gasification reaction into 20% yield of gas products within 1 h.[71] The Ni/MgO catalyst is also studied for the H$_2$ generation in presence of supercritical water at 400 ^{o}C.[72] Although, gasification process is well established for the coal and natural gas, still there are challenges to work with the lignin gasification reaction.[36]

1.9.2.2. Pyrolysis

Pyrolysis process refers to the thermal degradation of lignin to get low molecular weight of bio-oil in absence of O$_2$ or air. Generally, it depends on the several factors like heating rate, type of feedstocks, reaction temperature, etc.[73] It is one of the important phenomenon of the thermochemical process, which is used to generate bio-oils or low molecular products directly from the lignocellulosic biomass, which could be utilised as biofuels and aromatic chemicals.[74] Pyrolysis process occurs at 450-600 ^{o}C with or without catalyst to convert lignin into non-condensed gases, liquid (tar) and solid (char) products.[75] Depending upon the heating rate; pyrolysis process is divided into two types; (i) Slow pyrolysis, this process requires several hours to complete the reaction, which gives less yield of the products. (ii) Fast pyrolysis (100 ^{o}C/sec) process is the most dominant because, it yields high amount of bio-oils.[76, 77] The yield of bio-oil ca. 40-60*wt*.% and ca. 8-20*wt*.% gases have obtained by lignin pyrolysis process.

Derivatives of phenols, char etc. are the main components of the bio-oil. The bio-oil yield increases by using Cr_2O_3/Al_2O_3 and $NiMo/SiO_2-Al_2O_3$ as catalysts.[78] Similarly, ZSM-5 is also used to enhance the bio-oil yield.[79] Klein and Virk have proposed lignin degradation *via* free radical process.[80] Britt *et al.* reported that pyrolysis happened in multiple parallel radical and rearrangement processes.[79] The lignin pyrolysis chemistry has been discussed in detail by Ragauskas *et al.*[81] Beste and Buchanan have also predicted the density functional theory (DFT) for the conversion of the lignin or lignin model compounds by pyrolysis process.[82]

1.9.3. Chemical depolymerization of lignin

Several chemical processes are used to depolymerize lignin into aromatic products, which are (a) acid catalysed; (b) base catalysed; (c) metal catalysed; (d) supercritical fluids assisted; (e) oxidative methods and (i) ionic liquids assisted.

1.9.3.1. Acid catalysed lignin depolymerization

Earlier, acids were known for pulping/bleaching of the lignin from the lignocellulosic biomass, rather to use for the depolymerization of lignin into low molecular weight aromatic products. Acid catalysed process is further classified into several categories like mineral acid, Lewis acid and solid acid, and their utilisation for the lignin depolymerization is discussed below.

1.9.3.1.1. Mineral acid

Mineral acid catalysed lignin depolymerization into low molecular weight aromatic products is known. Hagglund and Bjorkman have used dilute hydrochloric acid solution for the lignin depolymerization into phloroglucinol, barbituric acid etc.[83] For the first time, Adler *et al.* have reported the Bjorkman lignin hydrolysis using mineral acids.[84] Johansson and Miksche have shown that the rate of acid hydrolysis of lignin model compound of α-aryl ether bond cleavage is 102 times faster than β-aryl ether bond.[85] Although, the rate of activation energy for the acid hydrolysis of β-aryl ether (148-151 kJ/mol) bond is higher than α-aryl ether (80-118 kJ/mol) bond.[86, 87] Recently, Ekerdt *et al.* have shown the use of hydrochloric acid as catalyst for the hydrolysis of phenolic β-O-4 bond of the lignin model compounds like guaiacylglycerol-β-guaiacyl ether (GG) and nonphenolic veratrylglycerol-β-guaiacyl ether (VG) molecules into aromatic monomers.[88] In the case of α-aryl ether linkage, acid catalysed hydrolysis reaction follows the S_N1-type mechanism and the first order kinetic as represented in the following equations 1.1 and 1.2;[89]

Aryl-CH$_2$-Aryl' +   H$_3$O$^+$ →   Aryl'-OH + Aryl-CH$_2$O$^+$ (1.1)

Aryl-CH$_2$O$^+$ +   ROH   →   Aryl-CH$_2$-OR   (1.2)

Rate of reaction of the lignin derived model compounds is usually faster in alcohol or phenols, than water due to solvent effects.[86, 90] It might be due to presence of phenolic –OH, which initiated nucleophile substitution reaction and forms phenolate bi-product and alcohols which have more proton donation capability during the reaction than water.[91]

1.9.3.1.2. Lewis acid

Phenolic derivative products were obtained from the lignin depolymerization reactions using Lewis acid catalysts such as $FeCl_3$, $AlCl_3$, BF_3, $ZnCl_2$, etc.[92, 93] In the presence of Lewis acid catalyst, it was observed that the reaction was thermodynamically favourable.[94] The activity of the depolymerization reaction was enhanced by the Lewis acid sites, which are converted into Brønsted acid sites in the course of the reaction.[92, 95, 96] During the above reaction Brønsted acid sites formed from Lewis acid catalyst in the presence of polar protic solvents. Hence, Lewis acid catalysts along with water or alcoholic solvent (methanol, ethanol, propanol, etc.) were reported for the lignin depolymerization reaction. Till now, the mechanism for lignin depolymerization reaction using Lewis acid catalyst is not clear.[2]

1.9.3.1.3. Organic acid

Organic acids have Brønsted acidic protons, which play an important role during the lignin hydrolysis or protonation of ether linkage ($\equiv$C-O-C$\equiv$). It is seen from Figure 1.5 and Table 1.1, that the lignin substructures have major units of β-O-4, α-O-4 linkages. Triflic acid is used to hydrolyse lignin model compound contained β-O-4 linkage into guaiacol monomeric unit.[97] Oxalic acid along with tetra-methylammonium hydroxide is used for the lignin depolymerization into phenolic products.[87] Depolymerization of oxidised lignin under milder reaction conditions in the presence of the aqueous solution of formic acid shows >60% yield of low molecular weight phenolic products.[98] Furthermore, formic acid along with Pd/C is used for the depolymerization of alkali lignin into >90% monomeric phenolic compounds in subcritical water at 265 °C, 6.5 MPa, 1-6 h.[99]

1.9.3.1.4. Solid acid

Solid acid catalysts are known for their specific properties such as, acid sites (strong and weak), Lewis and Brønsted acidity, pore size, pore volume, amorphous, crystalline structure, etc.[100-102] Zeolites were demonstrated for the lignin depolymerization into fuels range hydrocarbons.[103-106] During the lignin depolymerization, it was observed that zeolite shows dual roles.[104] Acidic sites play an important role for the depolymerization of lignin into aromatic products, while the pore size selectively passed molecules from the pore channel and the small pore size prevent the repolymerization of the formed liquid products. By optimising the pore size and acidity of the zeolites, the desired products could be achieved selectively.[104] Solid acid catalysts such as ion exchange resins (Nafion silica (SAC-13), amebrlist-15) are known for the lignin depolymerization but the problem associated with these catalysts is that they are unstable at <150 °C.[107] The lignin depolymerization activity was also monitored with different acidity, which has different pore diameters, pore volume etc. of the zeolites. It was observed that with HUSY having largest pore size, it produced 75% yield of liquid products from the alkaline lignin, while, ZSM-5 having low acidity, which produced sole 51% of liquids products.[104] In another

study, deactivation of HUSY was observed due to char and tar formation. The resultant products were adsorbed on the active site of the catalyst.[105] First time from our group lignin depolymerization into low molecular weight aromatic products was carried out using solid acid catalysts at ≥ 250 °C. Depolymerization of lignin into low molecular weight aromatic products (ca. 62%), was achieved using HUSY and metal oxide (SiO_2/Al_2O_3), catalysts in water and methanol binary solvent.[108] Although, the structure of the catalyst was disturbed and hampered the further recycle activity.[108, 109] It was also observed that the SBA-15 showed the best yield of 23% syringol products among the SBA-15, MCM-41, ZrO_2-SBA-15 and ZrO_2-MCM-41 solid acid catalysts at 300 °C for 1 h,.[106]

Several studies are also performed with precious or non-precious supported metal catalysts for the lignin depolymerization reactions. The cerium incorporated with ZSM-5 produced hydrocarbons (benzene, xylene and toluene).[110] Researcher have used Pt/Al_2O_3 (1%*wt./wt.*), catalyst for the conversion of lignin into low molecular weight aromatic products at 300 °C, for 2 h, using 2.0 MPa (H_2) pressure.[111] Another studies the cupper doped porous metal oxide catalyst was also used for the lignin depolymerization reaction at different temperature from 140 to 220 °C for 8-20 h using 4 MPa (H_2) pressure, which gives the >90% yield of aromatic products (mainly catechol derivatives).[112] The Pt supported on carbon catalyst along with H_3PO_4 was evaluated to convert lignin into dimer and monomer aromatic products (ca. 60%) in water and dioxane solvent at 200 °C, for 4 h using 0.4 MPa (H_2) pressure.[113] Further, zeolite supported Ni nanoparticle catalyst was used for organoslov lignin depolymerization reaction into hydrocarbons yield (70±5%) at 320 °C using 2.0 MPa (H_2) pressure.[114]

1.9.3.1.5. Ionic liquids (ILs) assisted

Ionic liquids (ILs) are salts having melting point (m.p.) below the boiling point (b.p.) of water. They have very characteristic physico-chemical properties based on their choice of cation and anion combinations, such as very low vapour pressure, good thermal stability, etc.[115, 116] ILs are known for the dissolution of lignocellulosic biomass and it used for extraction of lignin from lignocellulosic biomass.[117] Recently, Yinghuai *et al.* described an applications of ILs for lignin chemistry.[118] Mostly, ILs are studies as solvent for the conversion of lignin model compounds (dimers/trimers) into aromatic monomers. The cleavage of the β-O-4 bond of lignin model compound using 1-H-3-methylimidazole chloride [HMIM][Cl], acidic ionic liquid along with HCl as catalyst is known for the guaiacol formation.[88] The 1-ethyl-3-methylimidazolium tri-fluoromethanesulfonate [EMIM][CF_3SO_3], IL as solvent and ($Mn(NO_3)_2$), as catalyst could use to depolymerized lignin into aromatic products.[119] The Brønsted acidic catalysts along with ILs were used to convert lignin model compounds into 11.5% of dealkylated products.[120] The anions and Hammett acidity (H_0) effects were demonstrated for the degradation of lignin model compounds in 1-butyl-3-methylimidazolium hydrogensulphate [BMIM][HSO_4], IL for the

formation of guaiacol and Hibberts ketone types product.[121] Transition metal ($CoCl_2.6H_2O$) catalyst is also known for the oxidation of various types of lignin such as an alcell lignin, soda lignin and lignin model compounds in the presence of 1-ethyl-3-methylimidazolium di-ethylphosphate [EMIM][DEP], IL at 80 °C, within 1-4 h using 0.5 MPa (O_2) pressure, the functionalized aromatic monomer were obtained.[122] In another report, the computational studies was employed to cleave the lignin model compound *via* β-O-4 bond in IL as solvent.[123] A huge work is done by Jia *et al.* for the lignin transformations using acidic ILs but no change in molecular weight of lignin was reported in their works.[88, 124, 125] However, Zakzeski *et al.* has shown the oxidative cleavage of alcell lignin using ($CoCl_2·6H_2O$) as catalyst with NaOH as an additive within 1-ethyl-3-methyl imidazolium di-ethylphosphate [EMIM][Et_2PO_4], IL as solvent at 80 °C, for 3 h to oxidize lignin into aldehyde types product.[126] Chen *et al.* have developed the mix metal (e.g. ruthenium/vanadium/titanium) based active electrode catalyst for the Kraft lignin conversion into oxidised products like vanillin, benzaldehyde, acetovanillone, syringol, guaicol, etc., in the presence of 1-ethyl-3-methylimidazolium bis-(tri-fluoromethylsulfonyl) imide [EMIM][NTf_2] and tri-ethylammonium methanesulfonate [$(Et)_3NH$][$MeSO_3$] ILs.[127] The depolymerization of lignin extracted from bagasse into 65% conversion and 13.5% yield of phenolic monomer without any char formation was known with 1-butyl-3-methylimidazolium hydrogensulphate [C_4SO_3HMIM][HSO_4] IL at <250 °C in 15-75 minutes.[128]

1.9.3.2. Base catalysed

The depolymerization of lignin study was devoted for exploring the effect of alkaline additives such as NaOH, KOH, Na_2CO_3 or K_2CO_3, on lignin pyrolysis reaction into aromatic compounds. While, the use of carbonate additives facilitated the production of alkyl and alkoxy containing phenols were generated with the hydroxide additives. Analysis showed that all the alkaline additives promoted the reactions of decarboxylation or decarbonylation and also assisted the removal of unsaturated alkyl branch chains.[129] Shabtai *et al.* has shown the two steps process for lignin depolymerization; in the first step, base catalysed lignin depolymerization (BCD) reaction was occurred, and in the second steps, partially or totally oxygen was removed. The obtained products was a mixture of phenyl, cycloalkyl methyl ethers, alkylbenzene, branched paraffins, alkylated cycloalkanes, etc.[130] The depolymerization of lignin into derivatives of phenol products was obtained using aqueous solution of sodium hydroxide. Lavoie *et al.* has used softwood and hemp lignin with 5*wt.*% of NaOH aqueous solution and the formation of low molecular weight aromatic products were observed at 300-330 °C, 9-13 MPa (N_2) pressure.[131] The base catalysed reaction was carried out to convert organosolv lignin into syringol and hydroxyacetophenone products at 300 °C and 25.0 MPa (N_2) pressure by Roberts *et al.*[132] The olive tree pruning lignin depolymerization reaction into phenolic products have reported by in aqueous solution KOH, NaOH, $Ca(OH)_2$, LiOH and K_2CO_3 bases.[133] A computational study based

on the intermediate oxiranes into the base catalysed depolymerization of lignin is also known for getting aromatic monomers.[134] In another study organic base such as sodium phenoxide and guanidine carbonate were also evaluated for the lignin depolymerization reaction into low molecular fragments in aqueous medium along with H_2O_2.[135] In presence of Cs_2CO_3 for the cleavages of β-O-4 linkage into methoxy benzene derivatives was also reported at 180 °C within 8 h.[136]

Matthew *et al.* have reported the use of solid base catalyst for lignin depolymerization into low molecular weight aromatic monomers. The double layered hydroxides as recyclable, heterogeneous catalysts used for the lignin depolymerization into aromatic monomers.[137] Beckham *et al.* has also developed depolymerization of lignin using Ni supported on solid double layer structural catalyst.[138] While the use of 5*wt.*% Ni-HT catalysed cleaved lignins (organosolv and ball-milled lignins), which gives the alkylated aromatic products. From our group, various recyclable solid base catalysts (NaX, NaY, NaP, etc.) were used to depolymerize lignin into low molecular weight aromatic products at 250 °C within 1 h.[139]

1.9.3.3. Metal catalysed

Harris and co-workers in 1938 have used the metal oxide (Cu-Cr oxide) catalyst for the depolymerization of hardwood lignin into propylcyclohexanol.[140] The Alcell lignin depolymerization reaction was showed with Ru (C, Al_2O_3 and TiO_2), Pd (C and Al_2O_3), and Cu/ZrO_2 catalysts into the formation of benzene, toluene, xylene, and catechol at 400 °C, 4 h using 10 MPa (H_2) pressure.[141] The formation of monomeric phenols was achieved from cellulosic enzymatic lignin over zeolite supported by Raney nickel at 250 °C, within 30 min using 0.1 MPa (N_2) pressure.[142] Peppar *et al.* has studied the catalytic depolymerization of spruce wood lignin into aromatic monomers (4-propyl guaiacol and diconiferyl alcohol) using Ru/C, Pd/C, Ru/Al_2O_3 at 195 °C, 3.5 MPa (H_2) pressure.[143] The selective cleavage of ≡C-C≡ and ≡C-O-C≡ bonds present in the lignin derived model compound into phenolic monomeric products were studied with vanadium catalyst at 80 °C in 40 h.[144] Researcher has reported the aerobic oxidation of lignin derived model compound into 1,2-dihydroxy ether compounds using metal vanadium catalyst at 100 °C in 6 h or 25 °C for 3 weeks.[145] In another studies with ferrous sulphite as co-catalysts along with metal catalyst (e.g. Cu, Ag, Sn, Co, Cr, Ni, Zn or Mo) were recorded at 250-450 °C with 15.0-46.0 MPa (H_2) pressure for lignin hydrogenolysis reaction, this process is named Noguchi process.[146] Kou *et al.* have reported that lignin undergoes hydrogenation and gives 46*wt.*% phenolic products using activated carbon supported on Pt, Ru, Pd and Rh noble metal under 4.0 MPa (H_2) pressure. Metal (Ni-W_2C/C) catalytic activity was exhibited with lignin and it was found that lignin undergone catalytic hydrogenation reaction and produced guaiacol and syringol (46%) types products at 235 °C under 6.0 MPa (H_2) pressure.[147]

1.9.3.4. Supercritical fluids assisted

Supercritical conditions are typically achieved at very high temperatures and high pressures and under these conditions solvents exhibited very low viscosity and change in the density. Water, methanol, ethanol, acetone, carbon dioxide, etc. are the solvents mainly used as supercritical solvents in the various chemical reactions neat or along with catalysts. Lignin or lignin model compounds are studied under the supercritical water (Tc= 374.15 ℃ and Pc= 22.1 MPa) to yield aromatic products.[72, 148, 149] The NaOH and KOH basic catalyst were checked with supercritical methanol and ethanol (Tc> 239 ℃ and Pc> 8.0 MPa) solvents for the hydrolysis of ≡C-O-C≡ and ≡C-C≡ linkages present in lignin or lignin model compounds to form low molecular weight phenolic compounds.[86, 150] Saisu *et al.* have studied the lignin depolymerization into low molecular weight aromatic products with methanol as solvent at 400 ℃.[151] Meredith *et at.* have demonstrated the role of gases (N_2 or H_2 or CO or CO_2) for the depolymerization of organosolv lignin into aromatic products in subcritical water at 365 ℃ for 30 min.[152] Catalytic depolymerization of alkali lignin into aromatic products was noted in the presence of supercritical water along with formic acid and Pd/C catalyst at 265 ℃, within 1–6 h using 6.5 MPa (N_2) pressure.[99] Seiichi *et al.* have shown the selective production of 2-(hydroxybenzyl)-4-methylphenol from organosolv lignin depolymerization process in to a mixture of supercritical water and *p*-cresol solvent.[153]

1.9.3.5. Oxidative

Compared to the lignin derived model compounds, lignin (real molecule) oxidation reactions are limited. Oxidation process is a very crucial reaction in the lignin chemistry due to presence of various functional groups such as hydroxyl, aldehyde, carboxylic, etc. those are linked with aryl or alkyl chains. Aromatic aldehyde or acid is the main product obtained after lignin oxidation depolymerization in the presence of hydrogen peroxide along with alkali metal or mineral acid.[154] In few reports, lignin oxidation reaction is less efficient due to radical generation, which enhances repolymerization and generates many complex molecules.[22, 33, 52, 155] Bjørsvik *et al.* have achieved ca. 15% vanillin from lignin oxidation reaction.[156] Alkaline oxidation of soda lignin is also used for the production of vanillin (ca. 12%) with $PdCl_3.3H_2O/Al_2O_3$ catalyst at 100-250 ℃ using 0.2-1.0 MPa (O_2) pressure.[157, 158] Lignin underwent catalytic oxidation process to yield ca. 10% aldehyde products.[122] Acetic acid formation is achieved using wet oxidation with lignin derived aromatic monomer like guaiacol, phenol and syringol.[159]

1.10. Ionic liquids (ILs)

Ethyl ammonium nitrate [EtNH$_3$][NO$_3$] (m.p. 12 ^{o}C) is the first IL introduced in the literature in 1914.[160] In 1940 Frank Hurley and Tom Weir working at Rice Institute of Texas, invented salt that is liquid at room temperature. The warm powder of organic salt (alkylpyridinium chloride) is added in aluminium chloride and a clear colourless liquid was formed as an IL. Their discovery of the ILs remained a chemical curiosity for the several decades.

Ionic liquid is a salt that is liquid below 100 ^{o}C, or even at ambient temperature. It is a combination of organic cation (derivatives of *N*, *N'*-substituted imidazolium, *N*-substituted pyridinium, tetra-alkylated ammonium, tetra-alkylated phosphonium, etc.) and organic or inorganic anion (CF$_3$COO, HSO$_4$, Cl, etc.).[161] It is also called as room/low/ambient temperature molten salts/ionic fluid/liquid organic salts/neoteric solvent.

1.10.1. Classification of ILs

Based on cation and anion combination, ILs are classified into several categories; which are shown below.

1.10.1.1. Switchable polarity solvent ionic liquids (SPSILs)

SPSILs equilibrate in the range between higher and lower polarity combination of cation and anion, when a trigger is applied. Secondary amine is used to get SPSILs, with carbon dioxide used as a trigger agent, forming carbamate salt equation 1.3.[118]

$$NHR_2 \underset{}{\overset{+ \ CO_2}{\rightleftharpoons}} R_2NCOOH \underset{}{\overset{+ \ NHR_2}{\rightleftharpoons}} [R_2NH_2][R_2NCOO] \qquad (1.3)$$

Carbamic acid   Carbamate salt

1.10.1.2. Task specific ionic liquids (TSILs)

It is possible to incorporate some active sites into the ILs either by the combination of the anion or the cation to synthesize TSILs, and explore their specific activity for the catalytic reactions.[162, 163] The first TSIL is 3-sulphopropyl tri-phenylphosphonium *p*-toluenesulphonate (Figure 1.7).[164] The TSILs are studied for several catalytic reaction, which is esterification, dehydration, pinacol reaction, etc.[163]

3-sulfopropyl- triphenylphosphonium
p-toluenesulfonate

Figure 1.7. First task specific ionic liquid.[164]

1.10.1.3. Chiral ionic liquids (CILs)

The chiral ionic liquids (CILs) are one of the important class of TSILs. They have chiral centre either at cation or anion or at the both within the ILs. It is very difficult to synthesize them. The CILs are generally used as a chiral solvent for the asymmetric synthesis.[165] Figure 1.8 represent some examples of the CILs.

Chirality on the cation

Chirality on the anion
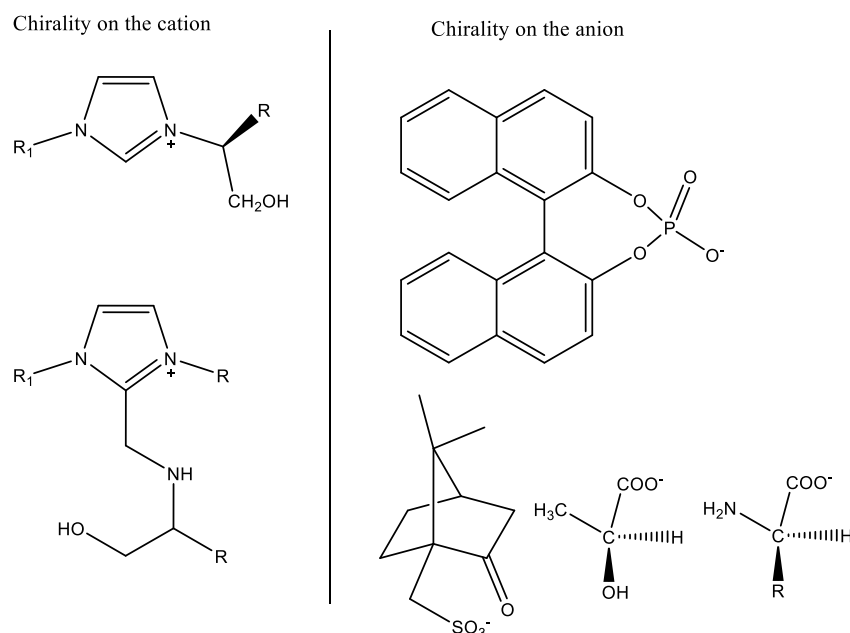
Figure 1.8. Chiral ionic liquids.

1.10.1.4. Protic ionic liquids (PILs)

The major differences between protic and other ionic liquids are the presence of exchangeable Brønsted acidic proton. So, it can be used as catalyst or solvent for the reactions such as hydrolysis, dehydration, fuel cell chemistry, etc.[166] Some of the examples of PILs are shown in Figure 1.9.
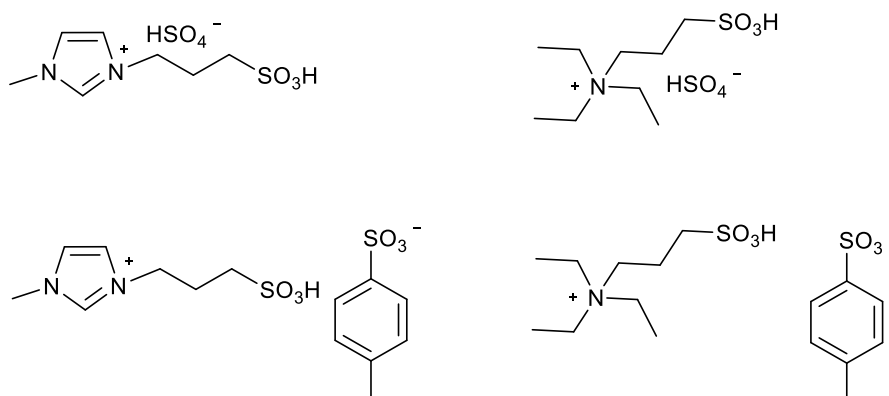
Figure 1.9. Protic ionic liquids.

1.10.1.5. Metallic ionic liquids (MSILs)

Most of the metal salt ionic liquids (MSILs) are synthesised with imidazolium or pyridium based cations. To enhance their Brønsted and Lewis acidic characteristic properties, chlorometalate salts (e.g. $[CuX_3]^-$; $[FeX_4]^-$; $[NiCl_4]^-$; $[SnCl_3]^-$; etc. are used as an anion counter part of the ILs. Compared to other ILs, metal halides ILs are more viscous.[167] Few of the metal halide based ILs are shown in Figure 1.10.
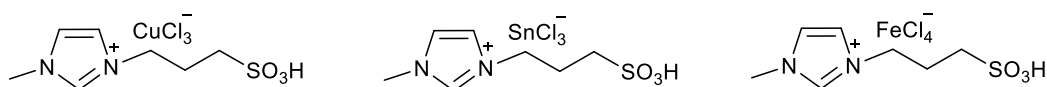
Figure 1.10. Metal halide based ionic liquids.

1.11. Application of ionic liquids

Scientists and engineers have an expectation to develop less toxic materials and more eco-friendly source for the chemical, energy, fuels, etc. generation. So, ILs are considered for a wide range of application due to its green prospects for the solvents or catalysts.[168, 169] Some of the vital applications are shown in as below;[166, 168, 170-173]

- Separation purpose (gas separation, extractive distillation, etc.)
- Analysis (MALDI-TOF matrix, protein crystallization, etc.)
- Solvent (bio-catalysis, polymerization, etc.)
- Electrostatic materials (artificial muscles, robotics, etc.)
- Catalyst (hydrolysis, dehydration, etc.)
- Electrolysis (fuel cell, sensors, batteries, coating, etc.), etc.

1.12. Synthesis of ionic liquids (ILs)

Before describing the application (for lignin depolymerization as catalysts) of ILs, their synthesis and purification methods are obligatory to discuss in details. Eventually, there are two basic methods employed for the synthesis of ILs.[174] The general procedure used to synthesis the ILs is summarized in the Figure 1.11.

Normally in most of the cases, single step is required to synthesize ILs e.g. 1-butyl-3-methylimidazolium chloride, ethylammonium nitrate, etc. Although, in many of the ILs synthesis reactions, cations are generated as zwitter ions and further react with desired anion and form the final products. In few of the ILs synthesis processes, the commercially procured cations in the form of halides are showed the anion exchange reaction.

```
┌─────────────┐
│     NR₃     │
└─────────────┘
       │
      R'H
       ↓
┌─────────────────┐
│  [NR₃R']⁺[X]⁻   │
└─────────────────┘
```

1. + Lewis acid [M]⁺[A]⁻-MX

2. + Brønsted acid [H]⁺[A]⁻-HX

3. + Ion exchange resin

+ Lewis acid MX_Y

$$[NR_3R']^+[MX_{Y+1}]^- \qquad [NR_3R']^+[A]^-$$
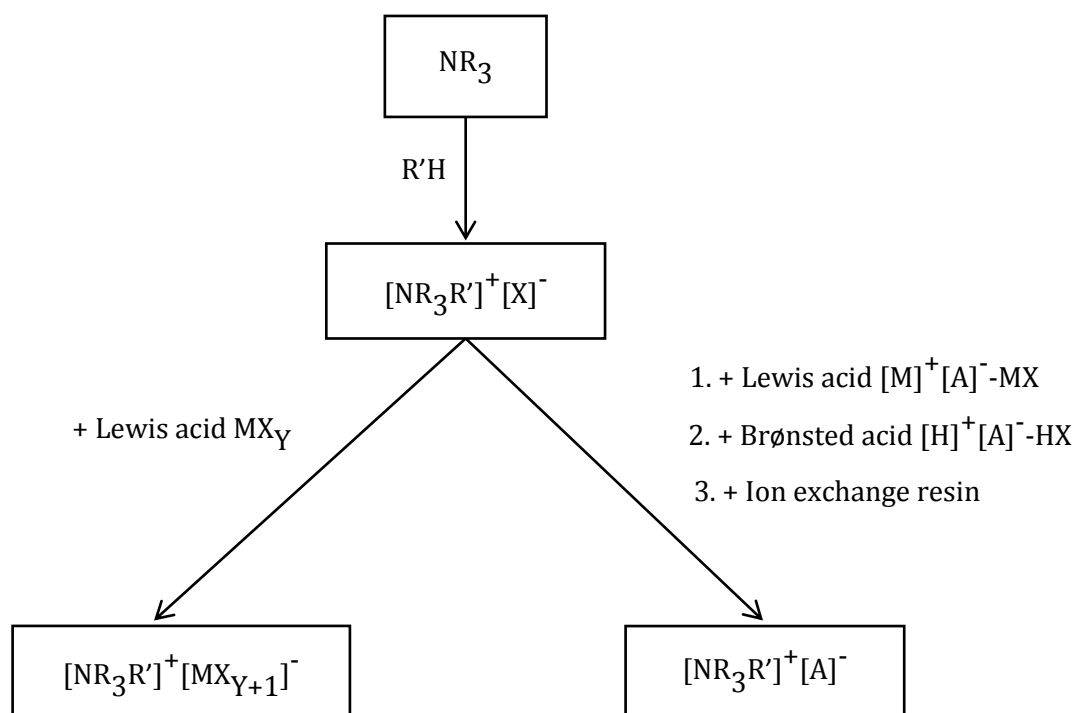
Figure 1.11. General pathway for the synthesis ILs.

As shown in the Figure 1.11, synthesis of desired ILs such as Lewis acid ILs, is done by addition reaction. Brønsted and ion exchange resin based ILs are also synthesised *via* anion exchange reaction. However, it is also necessary to know the purity, thermal stability, acidity, polarity, etc. To know this, various physico-chemical methods are used to characterise these ILs.

1.13. Characterization of ionic liquids (ILs)

Before the use of ILs in the various applications, it is essential to understand their physico-chemical properties, for their catalyst or solvent capability. Several characteristic analytical techniques are used to elaborate their physico-chemical properties such as elemental analysis, nuclear magnetic resonance [NMR, 1D (^{1}H and ^{13}C) and 2D (HSQC, HMBC etc.)], Fourier transformation-infra red (FT-IR), ultra violet-visible (UV-Vis, Hammett acidity function (H_0)), thermodynamic parameters (K_{eq}, ΔG, ΔH, ΔS, $E_a H^+$ etc.), thermal gravimetric analysis (TGA), etc. These characterization techniques help to understand their purity, thermal stability, acidity, etc. The synthesised and characterized ILs could be further used for the various chemical reactions and correlate their activity for achieving varying result.

1.14. Motivation of the work

➢ Lignin is the third major component of lignocellulosic biomass after cellulose and hemicellulose, and its annual production is approximately 20 billion metric tons.[11] It is estimated that ca. 125 million metric tons/year lignin is produced from crop waste (Based on TIFAC-2009) in India.[12] It is only one renewable resource of aromatic copolymer on the earth and is present in hardwood, softwood and grasses. Currently, it is burned to get heat and

power, during which large quantity of CO_2 is emitted into the atmosphere. Due to its heterogeneous nature, intrinsic linkages (Figures 1.5-1.6 and Table 1.1), various functional groups, high molecular weight (>3,000 Da), etc., which makes it difficult to depolymerise, only few reports are available on the conversion of lignin into value added products (Section 1.9). After selective cleavage of their linkages present in it, lignin can produce aromatic derived monomers, which have a wide range of application in various fields like polymers, petrochemicals, materials etc. (For more details please see the Section 1.8).

➢ Considering importance of products derived from lignin, biological (enzymatic, etc.), chemical (acid catalysed; base catalysed; metal catalysed; supercritical fluids assisted; oxidative methods, ionic liquids assisted etc.) and thermal (gasification, pyrolysis, combustion and supercritical) methods are developed to convert lignin into value added products. However, these known methods have few drawbacks as listed below,

- Thermal (pyrolysis and gasification): Requires >400 °C and formation of tar and char reduces the yield of desired products (low molecular weight aromatic products).

- Supercritical fluids assisted: *Tc* and *Pc* of water are, 373.6 °C and 22.1 MPa, respectively which again requires special reaction vessels and materials. Achieving high yields of desired products is detrimental due to side reactions under severe reaction conditions.

- Mineral acids (HCl, H_2SO_4): Corrosion to reaction vessels and handling hazards are major drawbacks along with non-recyclability of catalyst (thus generation of neutralization waste).

- Base catalysed (NaOH, CsOH): Operates >250 °C and has again similar problem as that with mineral acid.

- Metal catalysed: Use of high hydrogen pressures (>4 MPa) and employment of precious metals is mostly unavoidable to achieve good yields under relatively milder conditions.

- Enzymatic: Takes long times for depolymerization of lignin, which is energy consuming.

- Ionic liquids: Used as solvent along with supplementary catalyst. Use of ILs as solvent is not feasible due to high cost. Moreover, viscous nature of ILs can become hurdle in separation of the products from reaction mixture.

➢ Ionic liquid (IL) is a salt that is liquid below 100 °C, or even at ambient temperature. ILs have tuneable properties by altering the combination of cations and anions. So, ILs are considered for a wide range of application due to its green prospects for the solvents or catalysts. [169] As known from the literature, Brønsted proton (H^+) in mineral acid and solid acid catalysts, [99, 108, 109, 175, 176] help to cleave the $\equiv$C-O-C$\equiv$ linkages in lignin to yield low molecular weight aromatic compounds. Considering this researchers have employed acidic ionic liquids (ILs) as solvent along with supplementary catalyst for lignin depolymerization (For more details please see Section 1.9.3.1.5).

➤ Based on the above points such as, huge availability of lignin, lack of detailed work on lignin valorisation, importance of lignin derived aromatic products and drawbacks associated with prior methods used for conversion of lignin, it is desired to develop newer methods for depolymerization of lignin. Similarly, ILs having wide range of applications due to their tuneable properties are considered as important for their applications in biomass valorisation.

➤ Considering all above points, motivation for carrying out my Ph. D. work was to use acidic ILs in catalytic amount (homogeneous or heterogeneous) for depolymerization lignin to yield low molecular weight aromatic products under milder reaction conditions.

1.15. Objectives and scope of the thesis

Considering the importance of aromatic products, the main aim of my proposed work is to develop an efficient, green and recyclable Brønsted acidic ionic liquids (BAILs)/ Immobilized-BAIL (I-BAIL) based catalytic method which operates under milder conditions (than reported) for the depolymerization of lignin (actual substrate) into low molecular weight aromatic products.

Additionally, the mechanistic correlation study of lignin depolymerization would be established using experimental (NMR (1D and 2D) and RAMAN) and theoretical (DFT) analysis to establish the catalytic result.
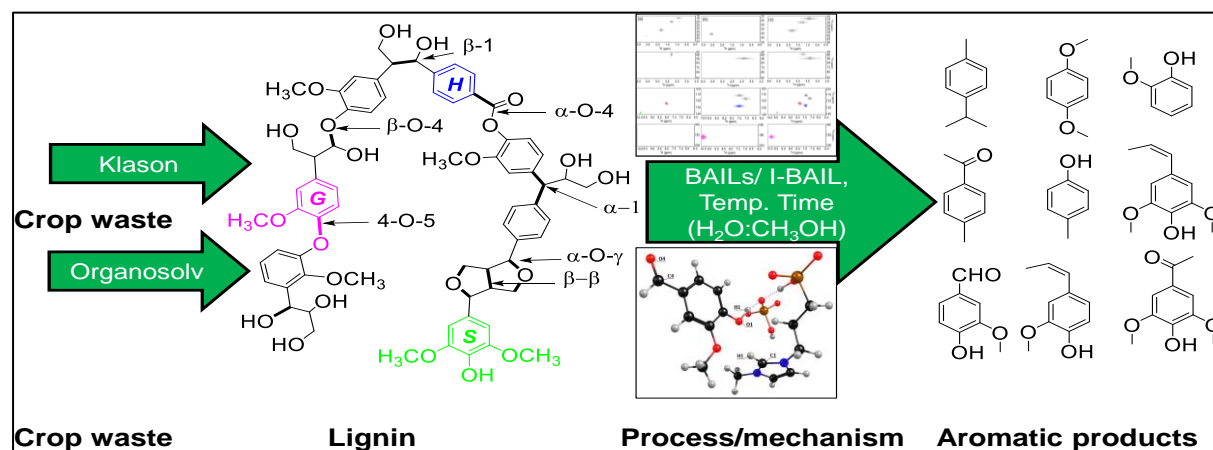
Scheme 1.1. Isolation and depolymerization of lignin into phenolic products using BAILs/I-BAIL.

By considering the above discussions, the more significant objectives are set for my Ph. D. work;

➤ **Synthesis and characterization of acidic ionic liquids**

Brønsted acidic ionic liquids (BAILs) and Immobilized-BAIL (I-BAIL) will be synthesized by applying the quaternization, direct combination and crystallization methods. Further, the synthesized BAILs/I-BAIL will be characterized using several analytical techniques [elemental analysis, NMR (^{1}H, ^{13}C and ^{29}Si), FT-IR, TGA, UV-Vis (Hammett acidity function (H_0), and

thermodynamic parameters such as ΔG, ΔH, ΔS, K_{eq} and E_aH^+), XRD, SEM, TEM, etc.], to confirm the acidity, purity, thermal stability and extent of immobilization of ILs on/in the silica framework, etc. These studies will help to draw the correlations of ILs with the catalytic activity in lignin depolymerization reactions.

> **Isolation and characterization of lignin from various substrates**

The complete compositional analysis using Technical Association of the Pulp and Paper Industries (TAPPI) method will be done to determine the exact percentage of the components present in crop waste and wood chip (collect from the different state of India) samples. Klason and organosolv methods will be employed to isolate Klason and organosolv lignins, respectively. To check the structural differences in the lignins, various bulk and molecular level advance characterization techniques would be employed. GPC and MALDI-TOF can be used to find out the molecular weight of the lignins. NMR [1D (^{1}H and ^{13}C, 2D (HSQC)], spectra of lignin samples would be helpful to understand the structural moieties (proton and carbon environment) and various linkages present in lignin. FT-IR technique would be employed to identify the presence of various functional groups in lignins. For the phase identification (crystalline or amorphous) XRD study will be done. The elemental analysis (CHNS), EDX and ICP-OES results will be useful to quantify the CHNS and nutrients present in samples. The thermal analysis such as TGA-DTA, TPO-MS and DSC will help to define their thermal stability, degradation pattern, melting point(s) and glass transition temperature(s) respectively.

> **Use of commercial and isolated lignins**

It would be a challenge to work with real lignin substrates for lignin depolymerization instead of model compounds such as dimers/trimers mostly used in the literature. This is because; real lignin substrate will have variety of linkages, high molecular weight and impurities present. Several lignin samples (commercial and isolated) will be studied for their depolymerization into low molecular weight aromatic product.

> **Development of a method for depolymerization of lignin under mild reaction conditions**

Employment of milder reaction conditions (T$\geq$ 150 ^{o}C, ambient pressure @ RT) will be preferred to enhance the lignin depolymerization products yield. Use of BAILs/I-BAIL as catalyst may help to achieve this objective due to anticipated interaction. This also would suppress the formation of degradation products such as char, tar and gases. Optimization of reaction parameters [temperature, pressure, time, reaction medium, catalyst(s), catalyst concentration, etc.], will be done to obtain higher yields of low molecular weight aromatic products.

Thermal stability of the GC/GC-MS identified aromatic products would be checked to understand the phenomenon of repolymerization and to achieve better yields.

The comparison study of BAILs with homogeneous and solid acid catalysts will be undertaken. Additionally, the I-BAIL as solid acid catalyst will be employed in lignin depolymerization reaction.

➢ **Isolation and characterization of catalysts**

After the reaction, isolate catalysts (spent catalyst) will be probed for any changes by virtue of NMR (^{1}H and ^{13}C), FT-IR, elemental analysis, TGA, XRD, SEM, TEM, etc. techniques.

➢ **Isolation of aromatic monomers from depolymerized products using column chromatography and their characterization**

Since lignin depolymerization yield mixture of products, it is desired to use column chromatography to isolate aromatic monomers from the mixture of aromatic products in pure form and their further confirmation can be carried out using GC, GC-MS, NMR, etc. analytical techniques.

➢ **Correlation studies between substrate with catalysts and substrate with products**

To find out the role of catalysts with substrate, the methodical investigations on the correlation of lignin with catalysts can be checked. The detailed characterization of substrate (lignin) and catalysts will be helpful in this regard. The experimental [1D (^{1}H and ^{13}C) and 2D (HSQC, HMBC and NOESY) NMR, and RAMAN] and theoretical (DFT) mechanistic investigation studies would be monitored to correlate the catalytic activity between ILs and aromatic monomers, dimers and lignin.

Further, the presence of various functional groups, moieties (*H*, *G* and *S*), linkages ($\equiv$C-O-O$\equiv$, and $\equiv$C-C$\equiv$) etc. between lignin and products can also be correlated using FT-IR, DSC, TGA, NMR (1D and 2D), etc. analytical techniques.

1.16. Outline of the thesis

Thesis is divided into six chapters and brief summary of each chapter is given below,

In the current chapter (Chapter 1) brief introduction on biomass, its classification and composition, pretreatment processes, availability is discussed. Also details on the lignin depolymerization methods along with their advantages and disadvantages are discussed. The uniqueness of ILs, their synthesis, characterization and their application in the various fields are deliberated. Lastly, motivation of work, scope and objectives of the Ph. D. work along with hypothesis is also mentioned.

In the second chapter, synthesis and characterization of various catalysts are discussed in detail. This Chapter is divided into two sections i.e. Section 2A and 2B. In Section 2A, synthesis procedures of ILs and followed by their characterization by several analytical techniques like NMR (^{1}H and ^{13}C), FT-IR, elemental analysis, TGA, UV-Vis [Hammett acidity function (H_0), thermodynamic parameters such as ΔG, ΔH, ΔS, K_{eq}, E_aH^+, etc.], are discussed. In the Section 2B,

the synthesis of Immobilized-BAIL and it's characterization using NMR (^{13}C and [29]Si), FT-IR, elemental analysis, TGA, UV-Vis, XRD, SEM, TEM, etc. analytical techniques is discussed.

Chapter 3 is divided into three sections i.e. Section 3A, 3B and 3C. The details on the physico-chemical analytical techniques used to characterize commercial (dealkaline, alkaline, alkali and industrial lignin) and isolated lignin (Klason and organosolv) samples are given in Section 3A. Additionally, characterization of commercial lignins is given in Section 3A. The catalytic results on the depolymerization of commercial lignin into low molecular weight aromatic product using ILs is described in Section 3B. The analysis and confirmation of formation of low molecular weight aromatic products is discussed with the help of several analytical techniques like GC, GC-MS, GPC, HPLC, LC-MS, elemental analysis, NMR, FT-IR etc. is done in Section 3B. In Section 3C details on the I-BAIL catalyzed lignin depolymerization reactions are mentioned.

Chapter 4 is divided into two sections i.e. Section 4A and 4B. The complete compositional analysis of the crop waste (rice husk, bagasse and wheat straw) samples using TAPPI method is given in Section 4A. Details on isolation of Klason lignin from different crop wastes and their characterization & depolymerization using BAILs and I-BAIL are discussed in Section 4A. The isolation of organosolv lignin, their characterization (by applying the similar analytical techniques as mentioned in Section 4A) and depolymerization is discussed in Section 4B.

In Chapter 5, experimental (1D, 2D (HSQC, NOESY and HMBC) NMR, RAMAN) and theoretical (DFT) investigations to gain mechanistic insights on lignin depolymerization using ILs are discussed.

In Chapter 6, main results and important revelations from the study along with novelty of the works are summarized.

1.17. References

1. M. Stocker, *Angew. Chem. Int. Ed.*, 2008, **47**, 9200-9211.
2. C. Li, X. Zhao, A. Wang, G. W. Huber and T. Zhang, *Chem. Rev.*, 2015, **115**, 11559-11624.
3. P. Bhaumik and P. L. Dhepe, *Catalysis Reviews*, 2016, **58**, 36-112.
4. A. J. Ragauskas, C. K. Williams, B. H. Davison, G. Britovsek, J. Cairney, C. A. Eckert, W. J. Frederick, J. P. Hallett, D. J. Leak, C. L. Liotta, J. R. Mielenz, R. Murphy, R. Templer and T. Tschaplinski, *Science*, 2006, **311**, 484-489.
5. J. Pérez, J. Muñoz-Dorado, T. de la Rubia and J. Martínez, *Int. Microbiol.*, 2002, **5**, 53-63.
6. Y. Habibi, L. A. Lucia and O. J. Rojas, *Chem. Rev.*, 2010, **110**, 3479-3500.
7. French, A. D.; Bertoniere, N. R.; Brown, R. M.; Chanzy, H.; Gray, D.; Hattori, K.; Glasser, W. In Kirk-Othmer Encyclopedia of Chemical Technology 5th ed.; Seidel, A., Ed.; John Wiley & Sons, Inc.: New York, 2004; Vol. 5.
8. V. K. Varshney and S. Naithani, in *Cellulose Fibers: Bio- and Nano-Polymer Composites: Green Chemistry and Technology*, eds. S. Kalia, S. B. Kaith and I. Kaur, Springer Berlin Heidelberg, Berlin, Heidelberg, 2011, DOI: 10.1007/978-3-642-17370-7_2, pp. 43-60.
9. C. J. Barrett and T. U. o. W.-. Madison, *Renewable Liquid Fuels from Catalytic Reforming of Biomass-derived Oxygenated Hydrocarbons*, University of Wisconsin--Madison, 2008.
10. D. Donald, in *Lignin and Lignans*, CRC Press, 2010, DOI: doi:10.1201/EBK1574444865-c1 10.1201/EBK1574444865-c1, pp. 1-10.

11. D. S. Argyropoulos and S. B. Menachem, in *Biopolymers from Renewable Resources*, ed. D. L. Kaplan, Springer Berlin Heidelberg, Berlin, Heidelberg, 1998, DOI: 10.1007/978-3-662-03680-8_12, pp. 292-322.

12. A. B. Pandey, S. ; Sukumaran, R.; Kausik, N, *Journal*, Exploitation (Ed.: R. Chidamabaram), Technology Information and Forecasting and Assessment Council (TIFAC) Report India, 2009.

13. P. Whiting and D. A. I. Goring, *Wood Sci. Technol.*, 1982, **16**, 261-267.

14. N. Terashima and K. Fukushima, *Wood Sci. Technol.*, 1988, **22**, 259-270.

15. L. B. Davin and N. G. Lewis, *Curr. Opin. Biotechnol.*, 2005, **16**, 407-415.

16. W. Boerjan, J. Ralph and M. Baucher, *Annu. Rev. Plant Biol.*, 2003, **54**, 519-546.

17. R. A. Dixon, F. Chen, D. Guo and K. Parvathi, *Phytochemistry*, 2001, **57**, 1069-1084.

18. J. M. Humphreys and C. Chapple, *Curr. Opin. Plant Biol.*, 2002, **5**, 224-229.

19. S. K. Singh and P. L. Dhepe, *Bioresour. Technol.*, 2016, **221**, 310-317.

20. R. Vanholme, B. Demedts, K. Morreel, J. Ralph and W. Boerjan, *Plant Physiol.*, 2010, **153**, 895-905.

21. H. Nimz, *Angew. Chem. Int. Ed.*, 1974, **13**, 313-321.

22. M. P. Pandey and C. S. Kim, *Chem. Eng. Technol*, 2011, **34**, 29-41.

23. X. Wang and R. Rinaldi, *ChemSusChem*, 2012, **5**, 1455-1466.

24. R. Parthasarathi, R. A. Romero, A. Redondo and S. Gnanakaran, *J. Phys. Chem. Lett.*, 2011, **2**, 2660-2666.

25. J. M. Younker, A. Beste and A. C. Buchanan, *ChemPhysChem*, 2011, **12**, 3556-3565.

26. E. Dorrestijn, L. J. J. Laarhoven, I. W. C. E. Arends and P. Mulder, *J. Anal. Appl. Pyrolysis*, 2000, **54**, 153-192.

27. R. Rinaldi, in *Catalytic hydrogenation for biomass valorization*, ed. R. Rinaldi, The Royal Society of Chemistry, UK, 2015, vol. --, ch. 4, pp. 74-98.

28. D. V. Evtuguin, C. P. Neto, A. M. S. Silva, P. M. Domingues, F. M. L. Amado, D. Robert and O. Faix, *J. Agric. Food Chem.*, 2001, **49**, 4252-4261.

29. P. C. Rodrigues Pinto, E. A. Borges da Silva and A. E. Rodrigues, *Ind. Eng. Chem. Res.*, 2011, **50**, 741-748.

30. E. Adler, *Wood Sci. Technol.*, 1977, **11**, 169-218.

31. N. Mosier, C. Wyman, B. Dale, R. Elander, Y. Y. Lee, M. Holtzapple and M. Ladisch, *Bioresour. Technol.*, 2005, **96**, 673-686.

32. H. Lange, S. Decina and C. Crestini, *Eur. Polym. J.*, 2013, **49**, 1151-1173.

33. J. Zakzeski, P. C. A. Bruijnincx, A. L. Jongerius and B. M. Weckhuysen, *Chem. Rev.*, 2010, **110**, 3552-3599.

34. A. R. Gaspar, J. A. F. Gamelas, D. V. Evtuguin and C. Pascoal Neto, *Green Chem.*, 2007, **9**, 717-730.

35. L. da Costa Sousa, S. P. S. Chundawat, V. Balan and B. E. Dale, *Curr. Opin. Biotechnol.*, 2009, **20**, 339-347.

36. J. F. W. Holladay J. E., J. J Bozell and D Johnson., *Top Value-Added Chemicals from Biomass Volume II—Results of Screening for Potential Candidates from Biorefinery Lignin, PNNL-16983, Pacific Northwest National Laboratory, Richland, WA.*, 2007.

37. J. B. Lindsey and B. Tollens, *Justus Liebigs Ann. Chem.*, 1892, **267**, 341-366.

38. F. G. Calvo-Flores and J. A. Dobado, *ChemSusChem*, 2010, **3**, 1227-1235.

39. H. H. Nimz, in *Ullmann's Encyclopedia of Industrial Chemistry*, Wiley-VCH Verlag GmbH & Co. KGaA, 2000, DOI: 10.1002/14356007.a15_305.pub2.

40. A. Lindner and G. Wegener, *J. Wood Chem. Technol.*, 1988, **8**, 323-340.

41. J. C. Parajó, J. L. Alonso, D. Vázquez and V. Santos, *Holzforschung*, 1993, **47**, 188-196.

42. Laamanen, L.A. Sundquist, J.J. Wartiovaara, I.Y.P. Kauliomaki, S.V. and Poppius, K.J., 27 Dec 1988, U.S. Pat. No. 06/936,344.

43. M. López, O. Huerta-Pujol, F. X. Martínez-Farré and M. Soliva, *Resour., Conserv. Recycl.*, 2010, **55**, 171-181.

44. W. Zhu, G. Westman and H. Theliander, *J. Wood Chem. Technol.*, 2014, **34**, 77-97.

45. M. Bunzel, A. Schüßler and G. Tchetseubu Saha, *J. Agric. Food Chem.*, 2011, **59**, 12506-12513.
46. X. Jiang, E. Naoko and Z. Zhong, *Chinese Science Bulletin*, 2011, **56**, 1417-1421.
47. J. Li, G. Gellerstedt and K. Toven, *Bioresour. Technol.*, 2009, **100**, 2556-2561.
48. A. M. Socha, R. Parthasarathi, J. Shi, S. Pattathil, D. Whyte, M. Bergeron, A. George, K. Tran, V. Stavila, S. Venkatachalam, M. G. Hahn, B. A. Simmons and S. Singh, *Proc. Natl. Acad. Sci.*, 2014, **111**, E3587-E3595.
49. E. K. Pye, in *Biorefineries-Industrial Processes and Products*, Wiley-VCH Verlag GmbH, 2008, DOI: 10.1002/9783527619849.ch22, pp. 165-200.
50. C. Xu, R. A. D. Arancon, J. Labidi and R. Luque, *Chem. Soc. Rev.*, 2014, **43**, 7485-7500.
51. M.-h. Fan, S.-m. Deng, T.-j. Wang and Q.-x. Li, *Chin. J. Chem. Phys.*, 2014, **27**, 221-226.
52. H. Wang, M. Tucker and Y. Ji, *J. Appl. Chem.*, 2013, **2013**, 1-9.
53. A. McVeigh, F. P. Bouxin, M. C. Jarvis and S. D. Jackson, *Catal. Sci. Technol.*, 2016, **6**, 4142-4150.
54. A. Llevot, E. Grau, S. Carlotti, S. Grelier and H. Cramail, *Macromol. Rapid Commun.*, 2016, **37**, 9-28.
55. D. Stewart, *Ind. Crops Prod.*, 2008, **27**, 202-207.
56. S. Rautiainen, J. Chen, M. Vehkamäki and T. Repo, *Top. Catal.*, 2016, DOI: 10.1007/s11244-016-0633-8, 1-5.
57. L. Passauer, T. Hallas, E. Bäucker, G. Ciesielski, S. Lebioda and U. Hamer, *ACS Sustainable Chem. Eng.*, 2015, **3**, 1955-1964.
58. Argyropoulos, D.S., Oct. 3 2013, U.S. Pat. No. 20130255216 A1
59. T. K. Kirk and R. L. Farrell, *Annu. Rev. Microbiol.*, 1987, **41**, 465-501.
60. C. Eggert, P. R. LaFayette, U. Temp, K. E. Eriksson and J. F. Dean, *Appl Environ Microbiol*, 1998, **64**, 1766-1772.
61. A. Yamaguchi, N. Hiyoshi, O. Sato and M. Shirai, *Top. Catal.*, 2012, **55**, 889-896.
62. R. Isha and P. T. Williams, *J. Energy Inst.*, 2011, **84**, 80-87.
63. A. Farzaneh, T. Richards, E. Sklavounos and A. van Heiningen, *A Kinetic Study of CO2 and Steam Gasification of Char from Lignin Produced in the SEW Process*, 2014.
64. G. P. Van Der Laan and A. A. C. M. Beenackers, *Catalysis Reviews*, 1999, **41**, 255-318.
65. P. J. A. Tijm, F. J. Waller and D. M. Brown, *Appl. Catal., A*, 2001, **221**, 275-282.
66. K. Kang, R. Azargohar, A. K. Dalai and H. Wang, *Energy Fuels*, 2015, **29**, 1776-1784.
67. A. Yamaguchi, N. Hiyoshi, O. Sato, M. Osada and M. Shirai, *Energy Fuels*, 2008, **22**, 1485-1492.
68. A. Yamaguchi, N. Hiyoshi, O. Sato, M. Osada and M. Shirai, *Chem. Lett.*, 2010, **39**, 1251-1253.
69. Y.-C. Lin and G. W. Huber, *Energy Environ. Sci.*, 2009, **2**, 68-80.
70. T. Sato, M. Osada, M. Watanabe, M. Shirai and K. Arai, *Ind. Eng. Chem. Res.*, 2003, **42**, 4277-4282.
71. T. Minowa, F. Zhen and T. Ogi, *J. Supercrit. Fluids*, 1998, **13**, 253-259.
72. T. Yoshida and Y. Matsumura, *Ind. Eng. Chem. Res.*, 2001, **40**, 5469-5474.
73. J. Cho, S. Chu, P. J. Dauenhauer and G. W. Huber, *Green Chem.*, 2012, **14**, 428-439.
74. D. Mohan, C. U. Pittman and P. H. Steele, *Energy Fuels*, 2006, **20**, 848-889.
75. H. B. Goyal, D. Seal and R. C. Saxena, *Renewable Sustainable Energy Rev.*, 2008, **12**, 504-517.
76. M. M. Wright, D. E. Daugaard, J. A. Satrio and R. C. Brown, *Fuel*, 2010, **89,** Supplement 1, S2-S10.
77. M. Windt, D. Meier, J. H. Marsman, H. J. Heeres and S. de Koning, *J. Anal. Appl. Pyrolysis*, 2009, **85**, 38-46.
78. D. Meier, R. Ante and O. Faix, *Bioresour. Technol.*, 1992, **40**, 171-177.
79. C. A. Mullen and A. A. Boateng, *Fuel Process. Technol.*, 2010, **91**, 1446-1458.
80. M. T. Klein and P. S. Virk, *Ind. Eng. Chem. Fundam.*, 1983, **22**, 35-45.
81. M. Kosa, H. Ben, H. Theliander and A. J. Ragauskas, *Green Chem.*, 2011, **13**, 3196-3202.

82. A. Beste, A. C. Buchanan, P. F. Britt, B. C. Hathorn and R. J. Harrison, *J. Phys. Chem. A*, 2007, **111**, 12118-12126.
83. Hagglund, E.; Bjorkman, C. B. Lignin hydrochloride. Biochem. Z. 1924, 147, 74.
84. E. Adler, J. M. Pepper and E. Eriksoo, *Ind. Eng. Chem.*, 1957, **49**, 1391-1392.
85. Johansson, B.; Miksche, G. Über die Benzyl-arylätherbindungim Lignin. II. Versuche an Modellen. Acta Chem. Scand. 1972, 26, 289−301.
86. J. E. Miller, L. Evans, A. Littlewolf and D. E. Trudell, *Fuel*, 1999, **78**, 1363-1366.
87. U. Wongsiriwan, Y. Noda, C. Song, P. Prasassarakich and Y. Yeboah, *Energy Fuels*, 2010, **24**, 3232-3238.
88. S. Jia, B. J. Cox, X. Guo, Z. C. Zhang and J. G. Ekerdt, *ChemSusChem*, 2010, **3**, 1078-1084.
89. Meshgini, M.; Sarkanen, K. V. Synthesis and Kinetics of Acid- Catalyzed Hydrolysis of Some Alpha-Aryl Ether Lignin Model Compounds. Holzforschung 1989, 43, 239−243.
90. Z. Yuan, S. Cheng, M. Leitch and C. C. Xu, *Bioresour Technol*, 2010, **101**, 9308-9313.
91. L. Lin, M. Yoshioka, Y. Yao and N. Shiraishi, *Journal*, 1997, **51**, 333.
92. M. M. Hepditch and R. W. Thring, *Can. J. Chem. Eng.*, 2000, **78**, 226-231.
93. S. Constant, C. Basset, C. Dumas, F. Di Renzo, M. Robitzer, A. Barakat and F. Quignard, *Ind. Crops Prod.*, 2015, **65**, 180-189.
94. T. R. Varga, Z. Fazekas, Y. Ikeda and H. Tomiyasu, *J. Supercrit. Fluids*, 2002, **23**, 163-167.
95. S. Jia, B. J. Cox, X. Guo, Z. C. Zhang and J. G. Ekerdt, *Ind. Eng. Chem. Res.*, 2011, **50**, 849-855.
96. Vuori, A.; Niemela, M. Liquefaction of Kraft Lignin 0.2. Reactions with a Homogeneous Lewis Acid Catalyst under Mild Reaction Conditions. Holzforschung 1988, 42, 327−334.
97. P. J. Deuss, M. Scott, F. Tran, N. J. Westwood, J. G. de Vries and K. Barta, *J. Am. Chem. Soc.*, 2015, **137**, 7456-7467.
98. A. Rahimi, A. Ulbrich, J. J. Coon and S. S. Stahl, *Nature*, 2014, **515**, 249-252.
99. J. A. Onwudili and P. T. Williams, *Green Chem.*, 2014, **16**, 4740-4748.
100. H. Hattori and Y. Ono, *Solid Acid Catalysis: From Fundamentals to Applications*, Pan Stanford, 2015.
101. M. H. Lim, C. F. Blanford and A. Stein, *Chem. Mater.*, 1998, **10**, 467-470.
102. C. J. Rhodes, *Annu. Rep. Prog. Chem., Sect. C*, 2007, **103**, 287-325.
103. X. Li, L. Su, Y. Wang, Y. Yu, C. Wang, X. Li and Z. Wang, *Front. Environ. Sci. Eng.*, 2012, **6**, 295-303.
104. Z. Ma, E. Troussard and J. A. van Bokhoven, *Appl. Catal., A*, 2012, **423–424**, 130-136.
105. Z. Ma and J. A. van Bokhoven, *ChemCatChem*, 2012, **4**, 2036-2044.
106. T. Klamrassamee, N. Laosiripojana, D. Cronin, L. Moghaddam, Z. Zhang and W. O. S. Doherty, *Bioresour. Technol.*, 2015, **180**, 222-229.
107. W. M. Alvino, *Ind. Eng. Chem. Prod. Res. Dev.*, 1980, **19**, 276-281.
108. A. K. Deepa and P. L. Dhepe, *RSC Adv.*, 2014, **4**, 12625-12629.
109. A. K. Deepa and P. L. Dhepe, *ACS Catal.*, 2015, **5**, 365-379.
110. G. T. Neumann and J. C. Hicks, *ACS Catal.*, 2012, **2**, 642-646.
111. F. P. Bouxin, A. McVeigh, F. Tran, N. J. Westwood, M. C. Jarvis and S. D. Jackson, *Green Chem.*, 2015, **17**, 1235-1242.
112. K. Barta, G. R. Warner, E. S. Beach and P. T. Anastas, *Green Chem.*, 2014, **16**, 191-196.
113. N. Yan, C. Zhao, P. J. Dyson, C. Wang, L.-t. Liu and Y. Kou, *ChemSusChem*, 2008, **1**, 626-629.
114. S. Kasakov, H. Shi, D. M. Camaioni, C. Zhao, E. Barath, A. Jentys and J. A. Lercher, *Green Chem.*, 2015, **17**, 5079-5090.
115. D. A. Fort, R. C. Remsing, R. P. Swatloski, P. Moyna, G. Moyna and R. D. Rogers, *Green Chem.*, 2007, **9**, 63-69.
116. N. Sun, H. Rodriguez, M. Rahman and R. D. Rogers, *Chem. Commun.*, 2011, **47**, 1405-1421.
117. N. Sun, R. Parthasarathi, A. M. Socha, J. Shi, S. Zhang, V. Stavila, K. L. Sale, B. A. Simmons and S. Singh, *Green Chem.*, 2014, **16**, 2546-2557.
118. Zhu Yinghuai, K. T. Yuanting and a. N. S. Hosmane, in *Ionic Liquids - New Aspects for the Future*, ed. D. J.-i. Kadokawa, InTech, 2013, DOI: 10.5772/51161., ch. 13.
119. K. Stärk, N. Taccardi, A. Bösmann and P. Wasserscheid, *ChemSusChem*, 2010, **3**, 719-723.

120. J. B. Binder, M. J. Gray, J. F. White, Z. C. Zhang and J. E. Holladay, *Biomass Bioenergy*, 2009, **33**, 1122-1130.
121. B. J. Cox, S. Jia, Z. C. Zhang and J. G. Ekerdt, *Polym. Degrad. Stab.*, 2011, **96**, 426-431.
122. J. Zakzeski, A. L. Jongerius and B. M. Weckhuysen, *Green Chem.*, 2010, **12**, 1225-1236.
123. B. G. Janesko, *Phys. Chem. Chem. Phys.*, 2014, **16**, 5423-5433.
124. B. J. Cox and J. G. Ekerdt, *Bioresour Technol*, 2012, **118**, 584-588.
125. S. Jia, J. Cox Blair, X. Guo, Z. C. Zhang and G. Ekerdt John, *Holzforschung*, 2010, **64**, 577-580.
126. J. Zakzeski, P. C. A. Bruijnincx and B. M. Weckhuysen, *Green Chem.*, 2011, **13**, 671-680.
127. A. Chen, E. I. Rogers and R. G. Compton, *Electroanalysis*, 2010, **22**, 1037-1044.
128. J. Long, W. Lou, L. Wang, B. Yin and X. Li, *Chem. Eng. Sci.*, 2015, **122**, 24-33.
129. C. Peng, G. Zhang, J. Yue and G. Xu, *Fuel Process. Technol.*, 2014, **124**, 212-221.
130. Shabtai, J.S. Zmierczak, W.W. Chornet, E. U.S. Pat. No. 5959167 A Sep. 28, 1999.
131. J.-M. Lavoie, W. Baré and M. Bilodeau, *Bioresour. Technol.*, 2011, **102**, 4917-4920.
132. V. M. Roberts, V. Stein, T. Reiner, A. Lemonidou , X. Li and J. A. Lercher, *Chem. Eur. J.*, 2011, **17**, 5939-5948.
133. A. Toledano, L. Serrano and J. Labidi, *J. Chem. Technol. Biotechnol.*, 2012, **87**, 1593-1599.
134. T. Lankau and C.-H. Yu, *Green Chem.*, 2016, **18**, 1590-1596.
135. G.-G. Xia, B. Chen, R. Zhang and Z. C. Zhang, *J. Mol. Catal. A: Chem.*, 2014, **388–389**, 35-40.
136. S. Dabral, J. Mottweiler, T. Rinesch and C. Bolm, *Green Chem.*, 2015, **17**, 4908-4912.
137. *US Pat.,* Beckham, Gregg T.Biddy, Mary J.Chmely, Stephen C., Sturgeon, Matthew R. U. S. Pat. No. 20140107381 A1 Apl. 17 2014.
138. M. R. Sturgeon, M. H. O'Brien, P. N. Ciesielski, R. Katahira, J. S. Kruger, S. C. Chmely, J. Hamlin, K. Lawrence, G. B. Hunsinger, T. D. Foust, R. M. Baldwin, M. J. Biddy and G. T. Beckham, *Green Chem.*, 2014, **16**, 824-835.
139. R. Chaudhary and P. L. Dhepe, *Green Chem.*, 2017, **19**, 778-788.
140. E. E. Harris, J. D'Ianni and H. Adkins, *J. Am. Chem. Soc.*, 1938, **60**, 1467-1470.
141. A. Kloekhorst and H. J. Heeres, *ACS Sustainable Chem. Eng.*, 2015, **3**, 1905-1914.
142. Y. Jiang, Z. Li, X. Tang, Y. Sun, X. Zeng, S. Liu and L. Lin, *Energy Fuels*, 2015, **29**, 1662-1668.
143. J. M. Pepper and Y. W. Lee, *Can. J. Chem.*, 1969, **47**, 723-727.
144. Y. Y. Jiang, L. Yan, H.-Z. Yu, Q. Zhang and Y. Fu, *ACS Catal.*, 2016, **6**, 4399-4410.
145. S. K. Hanson, R. T. Baker, J. C. Gordon, B. L. Scott and D. L. Thorn, *Inorg. Chem.*, 2010, **49**, 5611-5618.
146. D. W. Goheen, in *Lignin Structure and Reactions*, AMERICAN CHEMICAL SOCIETY, 1966, vol. 59, ch. 14, pp. 205-225.
147. C. Li, M. Zheng, A. Wang and T. Zhang, *Energy Environ. Sci.*, 2012, **5**, 6383-6390.
148. T. L. K. Yong and Y. Matsumura, *Ind. Eng. Chem. Res.*, 2012, **51**, 11975-11988.
149. K. Ehara, D. Takada and S. Saka, *J. Wood Sci.*, 2005, **51**, 256-261.
150. E. Minami, H. Kawamoto and S. Saka, *J. Wood Sci.*, 2003, **49**, 158-165.
151. M. Saisu, T. Sato, M. Watanabe, T. Adschiri and K. Arai, *Energy Fuels*, 2003, **17**, 922-928.
152. M. A. Hill Bembenic and C. E. Burgess Clifford, *Energy Fuels*, 2012, **26**, 4540-4549.
153. S. Takami, K. Okuda, X. Man, M. Umetsu, S. Ohara and T. Adschiri, *Ind. Eng. Chem. Res.*, 2012, **51**, 4804-4808.
154. A. Rahimi, A. Azarpira, H. Kim, J. Ralph and S. S. Stahl, *J. Am. Chem. Soc.*, 2013, **135**, 6415-6418.
155. T. Nakamura, H. Kawamoto and S. Saka, *J. Wood Chem. Technol.*, 2007, **27**, 121-133.
156. H.-R. Bjørsvik and L. Liguori, *Org. Process Res. Dev.*, 2002, **6**, 279-290.
157. F. G. Sales, C. A. M. Abreu and J. A. F. R. Pereira, *Braz. J. Chem. Eng.*, 2004, **21**, 211-218.
158. F. G. Sales, L. C. A. Maranhão, N. M. L. Filho and C. A. M. Abreu, *Chem. Eng. Sci.*, 2007, **62**, 5386-5391.
159. H. Suzuki, J. Cao, F. Jin, A. Kishita, H. Enomoto and T. Moriya, *J. Mater. Sci.*, 2006, **41**, 1591-1597.
160. S. Sugden and H. Wilkins, *J. Chem. Soc.*, 1929, DOI: 10.1039/JR9290001291, 1291-1298.
161. M. Moniruzzaman, N. Kamiya and M. Goto, *Org. Biomol. Chem.*, 2010, **8**, 2887-2899.
162. C. Yue, D. Fang, L. Liu and T.-F. Yi, *J. Mol. Liq.*, 2011, **163**, 99-121.

163. R. Giernoth, *Angew. Chem. Int. Ed.*, 2010, **49**, 2834-2839.
164. A. C. Cole, J. L. Jensen, I. Ntai, K. L. T. Tran, K. J. Weaver, D. C. Forbes and J. H. Davis, *J. Am. Chem. Soc.*, 2002, **124**, 5962-5963.
165. C. Baudequin, J. Baudoux, J. Levillain, D. Cahard, A.-C. Gaumont and J.-C. Plaquevent, *Tetrahedron: Asymmetry*, 2003, **14**, 3081-3093.
166. S. K. Singh and P. L. Dhepe, *Green Chem.*, 2016, **18**, 4098-4108.
167. I. J. B. Lin and C. S. Vasam, *J. Organomet. Chem.*, 2005, **690**, 3498-3512.
168. D. Zhao, M. Wu, Y. Kou and E. Min, *Catal. Today*, 2002, **74**, 157-189.
169. N. V. Plechkova and K. R. Seddon, *Chem. Soc. Rev.*, 2008, **37**, 123-150.
170. B. M. Matsagar, M. K. Munshi, A. A. Kelkar and P. L. Dhepe, *Catal. Sci. Technol.*, 2015, **5**, 5086-5090.
171. D. R. MacFarlane, N. Tachikawa, M. Forsyth, J. M. Pringle, P. C. Howlett, G. D. Elliott, J. H. Davis, M. Watanabe, P. Simon and C. A. Angell, *Energy Environ. Sci.*, 2014, **7**, 232-250.
172. L. Liang, Q. Gan and P. Nancarrow, *J. Membr. Sci.*, 2014, **450**, 407-417.
173. S. Weidmann, S. Kemmerling, S. Madler, H. Stahlberg, T. Braun and R. Zenobi, *Eur J Mass Spectrom (Chichester, Eng)*, 2012, **18**, 279-286.
174. R. Ratti, *Advances in Chemistry*, 2014, **2014**, 1-16.
175. R. K. Sharma and N. N. Bakhshi, *Bioresour. Technol.*, 1991, **35**, 57-66.
176. M. R. Sturgeon, S. Kim, K. Lawrence, R. S. Paton, S. C. Chmely, M. Nimlos, T. D. Foust and G. T. Beckham, *ACS Sustainable Chem. Eng.*, 2014, **2**, 472-485.

Chapter 2:
Synthesis and Characterization of ionic liquids

Section 2A:

Homogeneous Brønsted acidic ionic liquids

2A.1. Introduction

The conversion processes of polysaccharides (cellulose and hemicellulose) into fuels and chemicals are well known in the literature.[1-4] While, depolymerization of lignin into selective products is still a challenge, due to its non-uniformity, complex structure, high molecular weight, different linkages (Chapter 1, Figure 1.5 and Table 1.1) and the presence of alkali/alkaline metal or sulphur contaminants, etc.[5, 6] As discussed in the Chapter 1, ionic liquids (ILs) are used as a solvent along with supplementary catalysts for the depolymerization of lignin or lignin model compounds (dimers/trimers) into low molecular weight aromatic products. The use of ILs as solvent is not economically favourable, due to its high cost. After completion of reaction it becomes hurdle to isolated products from the highly viscous reaction mixture. Another problem is associated with the management of impure/by-product ionic liquids in the bulk quantities, which is also not feasible with respect to environmental aspects. ILs are considered as a green solvent or catalysts, which can have tuneable properties by altering the combination of cations and anions. Considering the importance of ILs as shown in the Chapter 1, it is vital to use ILs as catalysts along with the polar protic solvent (like dissolve like) like, methanol, ethanol, propanol, butanol, water, formic acid, etc. The various combinations of cations and anions of ILs were synthesized such as Brønsted acidic ionic liquids (BAILs) [C_3SO_3HMIM][HSO_4], [C_3SO_3HMIM][Cl], [C_3SO_3HMIM][PTS], etc., Brønsted and Lewis acidic ILs [C_3SO_3HMIM][$FeCl_4$], [C_3SO_3HMIM][$CuCl_3$], etc. and without acidity (neutral) IL [BMIM][Cl]. Further, the synthesised ILs were subjected for their physico-chemical characterization using several techniques to correlate their catalytic activity with various properties. Subsequently, synthesized ILs (catalysts) were evaluated for the depolymerization of commercial and isolated lignin into the low molecular weight aromatic products. Characterization of spent ILs is also carried out to understand the changes occurred during reactions.

Section 2A discusses synthesis procedures of ILs using quarterisation or direct combination methods, along with the details of chemicals used for the synthesis. Several analytical techniques are used for the characterization of ILs and the results of each characterization are discussed in details.

2A.2. Ionic liquids synthesis

2A.2.1. Materials

Various chemicals were used for the synthesis of ILs such as; 1,3-propanesultone (Alfa Aesar India, 99%); triethylamine (Alfa Aesar India, 99%); 1-methyl imidazole (Sigma Aldrich USA, ≥99%); 1-methyl-benzimidazole (Alfa Aesar UK, 99%); triphenylphosphine (Alfa Aesar UK, 99%); 1-chlorobutane (Alfa Aesar India, 99.5%), *p*-toluenesulfonic acid monohydrate (Sigma-Aldrich USA, 98.5%), sulphuric acid (Loba Chemie India, 98%), hydrochloric acid (Loba Chemie

India, 35%), orthophosphoric acid (Merck India, 85%), toluene (Loba Chemie India, 99.5%), 1,2-dichloroethane (Loba Chemie India, 99%), diethyl ether (Loba Chemie India, 99%) were purchased and used as such without any further treatment.

2A.2.2. Synthesis of ionic liquids (ILs)

Various imidazolium, phosphonium, benzimidazolium and ammonium based BAILs/IL (As shown in Table 2A.1) were synthesized in a two-step method.[7-14] Along with BAILs, neutral IL, 1-butyl-3-methylimidazolium chloride [BMIM][Cl] was also synthesized. The structures of the synthesized ILs are shown in the Figure 2A.1.

Table 2A.1. Full name and abbreviation of ionic liquids (ILs).

Full name of ILs	Abbreviation of the ILs
1-methyl-3-(3-sulfopropyl)-imidazolium hydrogensulfate	$[C_3SO_3HMIM][HSO_4]$
1-methyl-3-(3-sulfopropyl)-imidazolium p-toluenesulfonate	$[C_3SO_3HMIM][PTS]$
1-methyl-3-(3-sulfopropyl)-imidazolium chloride	$[C_3SO_3HMIM][Cl]$
1-methyl-3-(3-sulfopropyl)-imidazolium dihydrogenphosphate	$[C_3SO_3HMIM][H_2PO_4]$
1-methyl-3-(3-sulfopropyl)-benzimidazolium hydrogensulfate	$[C_3SO_3HBenzMIM][HSO_4]$
3-sulfopropyl-P,P,P-triphenylphosphonium hydrogensulfate	$[C_3SO_3H(C_6H_5)_3P][HSO_4]$
1-methyl-3-(3-sulfopropyl)-imidazolium cupric chloride	$[C_3SO_3HMIM][CuCl_3]$
1-methyl-3-(3-sulfopropyl)-imidazolium ferric chloride	$[C_3SO_3HMIM][FeCl_4]$
1-methyl-3-(3-sulfopropyl)-imidazolium stannic chloride	$[C_3SO_3HMIM][SnCl_3]$
1-butyl-3-methylimidazolium chloride	$[BMIM][Cl]$
N, N, N-triethyl-3-sulfopropanaminium hydrogensulfate	$[C_3SO_3H(C_2)_3N][HSO_4]$
N, N, N-triethyl-3-sulfopropanaminium p-toluenesulfonate	$[C_3SO_3H(C_2)_3N][PTS]$
N, N, N-triethyl-3-sulfopropanaminium chloride	$[C_3SO_3H(C_2)_3N][Cl]$
N, N, N-triethyl-3-sulfopropanaminium dihydrogenphosphate	$[C_3SO_3H(C_2)_3N][H_2PO_4]$

Figure 2A.1. Structural combination of cations and anions of the ILs.

2A.2.2.1. Synthesis of imidazole, benzimidazole and triphenylphosphine based ILs

In a typical procedure, under slow stirring (100 rpm), to a solution of R (R; 1-methylimidazole, triphenylphosphine or 1-methyl-benzimidazole) (36.58 mmol) dissolved in toluene (50 mL) is added drop wise into 1, 3-propanesultone, (36.58 mmol) at 0 °C (ice bath) under inert atmosphere (N_2). The solution is slowly warmed to reflux temperature and stirred (600 rpm) for 12 h. The resulting mixture is filtered to obtain the zwitterions as white solid. The white solid is washed with toluene (3×25 mL) to remove any unreacted substrates. Next, this solid is dried in vacuum oven (-0.101 MPa) at 80 °C for 4 h. In the second step; to a zwitterion, for e.g. [C_3SO_3MIM], stoichiometric amount of acid (HX; H_2SO_4, *p*-toluenesulfonic acid monohydrate, HCl or H_3PO_4) is added and the mixture is stirred at 100 °C for 12 h to obtain highly viscous colourless liquid [C_3SO_3HMIM][HSO_4], [C_3SO_3HMIM][PTS], [C_3SO_3HMIM][Cl] and [C_3SO_3HMIM][H_2PO_4] ILs. This highly viscous liquid is washed with diethyl ether (3×50 mL) to remove any impurities and it is further dried under reduced pressure to remove remains of solvent. Similarly, in the [$C_3SO_3BenzMIM$] or [$C_3SO_3(C_6H_5)_3P$] zwitterions, stoichiometric amount of H_2SO_4 is added and the mixture is stirred at 100 °C for 12 h and obtain highly viscous colourless liquid [$C_3SO_3HBenzMIM$][HSO_4] and [$C_3SO_3H(C_6H_5)_3P$][HSO_4] ILs. Finally, these highly viscous liquids are washed with diethyl ether (3×50 mL) and dried under reduced pressure to remove remains of solvent. After the characterization of these synthesised ILs, the catalytic activities are checked in lignin depolymerization reactions to yield low molecular weight aromatic products. The details of the ILs synthesis procedure are shown in Scheme 2A.1 and structures of the BAILs based on imidazole, benzimidazole and triphenylphosphine are shown in Figure 2A.1.

Quaternization method
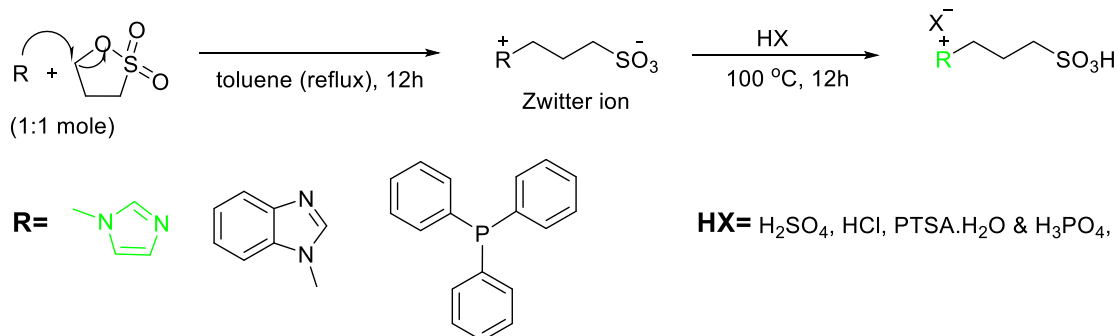
Scheme 2A.1. Schematic representation of the synthesis of imidazole, benzimidazole and triphenylphosphine based ionic liquids.

2A.2.2.2. Synthesis of imidazole based ILs with metal halide

1-methyl-3-(3-sulfopropyl)-imidazolium chloride, [C_3SO_3HMIM][Cl] was synthesised same as mentioned in Section 2A.2.2.1. In the next step for the synthesis of metallic ILs, equimolar amount (20.8 mmol) of $CuCl_2$, $FeCl_3$ or $SnCl_2$ was added to [C_3SO_3HMIM][Cl] IL at 0 °C (ice bath) under inert atmosphere (N_2) and kept for constant stirring at 100 °C for 24 h and obtain highly viscous colourless [C_3SO_3HMIM][$CuCl_3$], [C_3SO_3HMIM][$FeCl_4$] or [C_3SO_3HMIM][$SnCl_3$] ILs. These synthesised ILs were washed with diethyl ether (3×50 mL) and subjected at reduced pressure to remove remains of solvent. Synthesis procedure for the metallic ILs is shown in Scheme 2A.2 and structure of the metallic ionic liquids based on imidazole ILs is also shown in Figure 2A.1.

Direct combination

MX_Y= $FeCl_3$, $CuCl_2$ and $SnCl_2$

Scheme 2A.2. Schematic representation of the synthesis of metallic ILs.

2A.2.2.3. Synthesis of amine based ILs

In a typical procedure under slow stirring (100 rpm), the mixture of triethylamine (36.58 mmol) in 1, 2-dichloroethane (50 mL) was drop wise added into 1, 3-propanesultone (36.58 mmol) at 0 °C (ice bath) under inert atmosphere (N_2). The solution was slowly warmed to 60 °C and stirred (600 rpm) for 12 h. The resulting mixture was filtered and washed with 1, 2-dichloroethane (3×50 mL) to obtain the zwitterions as white solid. The obtained solid was dried in vacuum oven (-0.101 MPa) at 50 °C for 4 h. In the second step; in [$C_3SO_3(C_2)_3N$] zwitterions, stoichiometric amount of acid (HX; H_2SO_4, *p*-toluene sulfonic acid monohydrate, HCl or H_3PO_4) was added and the mixture was stirred at 80 ℃ for 12 h and gave highly viscous colourless [$C_3SO_3H(C_2)_3N$][HSO_4], [$C_3SO_3H(C_2)_3N$][PTS], [$C_3SO_3H(C_2)_3N$][Cl] and [$C_3SO_3H(C_2)_3N$][H_2PO_4] ILs. This liquid is washed with diethyl ether (3×50 mL) to remove any impurities and subjected to

reduced pressure to remove remains of solvent. The structure and synthesis scheme for the amine based ILs are shown in Scheme 2A.3 and Figure 2A.1.

HX= H_2SO_4, HCl, PTSA.H_2O and H_3PO_4
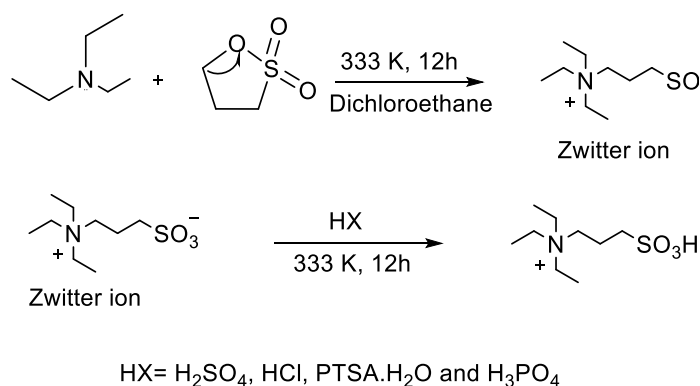
Scheme 2A.3. Schematic representation of the synthesis of amine based ILs.

The synthesized ILs as shown in Figures 2A.1, is evaluated for the lignin depolymerization into low molecular weight aromatic products.

2A.3. Rationalization behind use of various ILs

As discussed in Chapter 1 and Section 2A.1, ILs were used as solvent along with mineral acids or metal halides for the depolymerization of lignin or lignin model compounds. Considering use of ILs in bulk quantity is not an economical process, the aim of this work is to study the lignin depolymerization reaction using ILs in catalytic amount. The rationalizations behind the synthesis of various ILs are discussed as below.

2A.3.1. Rationalization between imidazole based with or without Brønsted acidic ionic liquids (BAILs)

Lignin has various types of linkages such as, ≡C-O-C≡ (ca. 70%) and ≡C-C≡ (ca. 30%) and to cleave these bonds, Brønsted acidity and Lewis acidity are required. This will help to achieve maximum yield of aromatic products. So, it was planned to synthesize with [C_3SO_3HMIM][HSO_4] or without [BMIM][Cl], BAILs (Figure 2A.2). These ILs can be used to understand the role of acidity (in term of H⁺) in the lignin depolymerization reaction.

Figure 2A.2. Structures of acidic and neutral ILs

2A.3.2. Rationalization between imidazole based Brønsted acidic and Lewis acidic ILs

To achieve the maximum yield of aromatic products from the lignin depolymerization, it was hypothesize that if the ILs having both Brønsted and Lewis acidity, better result for the lignin depolymerization could be observed. So, the combination of Lewis and Brønsted acidic ILs are synthesised (Figure 2A.3). The catalytic results of various ILs are discussed in Chapter 3.
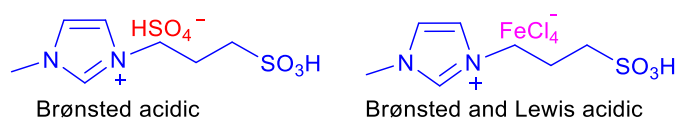
Figure 2A.3. Structures of imidazole based Brønsted and Brønsted-Lewis acidic ILs.

2A.3.3. Rationalization behind imidazole and amine based BAILs

To understand the role of imidazole (sp^2) and amine (sp^3) geometry on the lignin depolymerization activity, these catalysts were synthesized. While imidazole based ILs have planar geometry (Figure 2A.4), the amine based ILs have non planar (tetrahedral) geometry, and this may show either positive or negative effect on the activity of catalysts. To check the effect of geometry, it was planned to synthesize various kinds of ILs having different geometries.
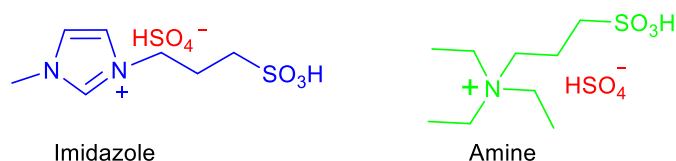
Figure 2A.4. Structures of imidazole and amine based ILs.

2A.3.4. Rationalization behind synthesis of imidazole, benzimidazole and triphenylphosphine based ILs

Since lignin is made up of derivatives of benzene rings having planar geometry, the effect of geometry or Π stacking during lignin depolymerization reaction was studied with various ILs consisting planar geometry such as imidazole, benzimidazole and triphenylphosphine having nonplanar (tetrahedral) geometry were synthesized (Figure 2A.5).
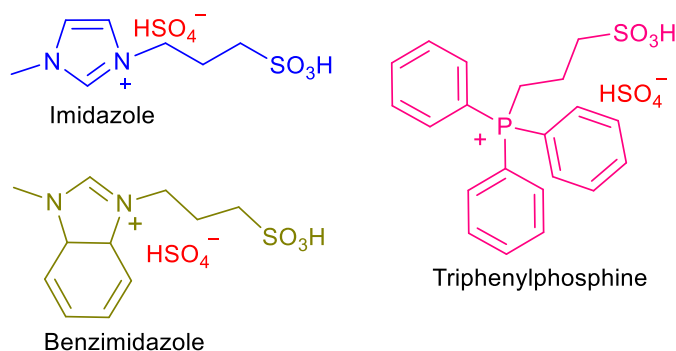
Figure 2A.5. Structures of imidazole, benzimidazole and triphenylphosphine based ILs.

2A.4. Catalysts characterization

Characterization was performed to understand the physico-chemical properties of the synthesized catalysts. All the synthesized ILs (catalysts) were characterized using various characterization techniques like elemental analysis, NMR (^{1}H and ^{13}C), Fourier transformation-infra red (FT-IR) spectroscopy, thermogravimetric analysis (TGA) and Ultra Violet- visible (UV-Vis) analytical instrument. These analytical techniques were used to define purity, thermal

stability, Hammett acidity function (H_0) and thermodynamic parameters of ILs. The details of the characterization techniques and results are studied elaborately in the current section.

2A.4.1. Solubility of ionic liquids

In the current work, various ILs are synthesized and those are made up of various combinations of cations and anions; and every cation and anion differs in polarity. Due to variable polarity, they show difference in solubilities in various solvents as shown in Table 2A.2. Further, the solubility of lignin (substrate) is also checked and the details are shown in Chapter 3, Section 3A. If both the substrate and catalyst have solubility in the same solvent, then if reaction is carried out in the same solvent, better interaction or contact between catalyst and substrate is anticipated. This in turn can give better results for the lignin depolymerization. Moreover, the catalyst recycle problem can be conquered using the solvomorphic or anti-solvent separation process.

Table 2A.2. Solubility of ILs in various solvents.†

Ionic Liquids (ILs)	Solvents, polarity index										
	H₂O, 10.2	MeOH, 5.1	EtOH, 4.3	Acetone, 5.1	Toluene, 2.4	MIBK, 4.2	DCM, 3.1	DMSO, 7.2	THF, 4.0	DEE, 2.8	EtOAc, 4.4
[C₃SO₃HMIM][HSO₄]	S	S	S	I.S.	I.S.	I.S.	I.S.	I.S.	I.S.	I.S.	I.S.
[C₃SO₃HMIM][PTS]	S	S	S	I.S.	I.S.	I.S.	I.S.	I.S.	I.S.	I.S.	I.S.
[C₃SO₃HMIM][Cl]	S	S	S	I.S.	I.S.	I.S.	I.S.	I.S.	I.S.	I.S.	I.S.
[C₃SO₃HMIM][H₂PO₄]	S	S	S	I.S.	I.S.	I.S.	I.S.	I.S.	I.S.	I.S.	I.S.
[C₃SO₃HMIM][CuCl₃]	S	S	S	I.S.	I.S.	I.S.	I.S.	I.S.	I.S.	I.S.	I.S.
[C₃SO₃HMIM][FeCl₄]	S	S	S	I.S.	I.S.	I.S.	I.S.	I.S.	I.S.	I.S.	I.S.
[C₃SO₃HMIM][SnCl₃]	S	S	S	I.S.	I.S.	I.S.	I.S.	I.S.	I.S.	I.S.	I.S.
[BMIM][Cl]	S	S	S	I.S.	I.S.	I.S.	S	S	I.S.	I.S.	I.S.
[C₃SO₃HBenzMIM][HSO₄]	S	S	S	I.S.	I.S.	I.S.	S	S	I.S.	I.S.	I.S.
[C₃SO₃H(C₆H₅)₃P][HSO₄]	S	S	S	I.S.	I.S.	I.S.	S	S	I.S.	I.S.	I.S.
[C₃SO₃H(C₂)₃N][HSO₄]	S	S	S	I.S.	I.S.	I.S.	I.S.	I.S.	I.S.	I.S.	I.S.
[C₃SO₃H(C₂)₃N][PTS]	S	S	S	I.S.	I.S.	I.S.	I.S.	S	I.S.	I.S.	I.S.
[C₃SO₃H(C₂)₃N][Cl]	S	S	S	I.S.	I.S.	I.S.	I.S.	S	I.S.	I.S.	I.S.
[C₃SO₃H(C₂)₃N][H₂PO₄]	S	S	S	I.S.	I.S.	I.S.	I.S.	S	I.S.	I.S.	I.S.

†solubility is checked by dispersing 10 mg of IL in 5 mL solvent; Note: S- solubility; I.S.- insoluble

2A.4.2. Elemental analysis of the ILs

Elemental analysis of the ILs was done using Thermo Finnigan, Italy; model EA1112 Series Flash Elemental Analyzer. The amounts of CHNS in samples were determined by rapid combustion of small amounts (10-15 mg) of the sample in pure O_2 (Dumas method or 'flash combustion'). Elemental analysis is done to quantify the carbon, hydrogen, sulphur and nitrogen present in the ILs samples. In the normal form, CHNS analysis require high temperature combustion (an oxygen rich environment) and the data is calculated based on the classical Pregl and Dumas method. Based on the CHNS results, a general monomeric molecular formula of ILs can be drawn. The experimental data of the ILs obtained matches well with the theoretical values, (Table 2A.3). Considering the data obtained from experimental and theoretical results, it is concluded that the synthesized ILs are in pure form without any impurity.

Table 2A.3. Elemental analysis of ILs.

ILs	Experimental (%)				Theoretical (%)			
	C	H	N	S	C	H	N	S
$[C_3SO_3HMIM][HSO_4]$	28.0	4.4	9.4	20.9	27.8	4.7	9.3	21.2
$[C_3SO_3HMIM][Cl]$	35.0	5.7	7.4	13.8	34.9	5.4	11.6	13.3
$[C_3SO_3HMIM][PTS]$	44.3	5.4	7.4	17.3	44.7	5.4	7.4	17.0
$[C_3SO_3HMIM][H_2PO_4]$	27.9	4.7	8.9	10.5	27.8	5.0	9.3	10.6
$[BMIM][Cl]$	54.8	8.4	15.6	-	55.0	8.7	16.0	-
$[C_3SO_3HMBenzIM][HSO_4]$	37.3	4.4	7.8	17.9	37.5	4.6	8.0	18.2
$[C_3SO_3H(C_6H_5)_3P][HSO_4]$	53.1	5.0	-	13.5	52.3	4.8	-	13.3
$[C_3SO_3H(C_2H_5)_3N][HSO_4]$	34.2	7.6	4.6	20.3	33.6	7.2	4.4	20.0
$[C_3SO_3H(C_2H_5)_3N][Cl]$	41.8	8.9	5.7	13.0	41.6	8.5	5.4	12.3
$[C_3SO_3H(C_2H_5)_3N][PTS]$	49.0	7.6	3.8	17.1	48.6	7.4	3.5	16.2
$[C_3SO_3H(C_2H_5)_3N][H_2PO_4]$	33.3	7.9	4.3	10.2	33.6	7.5	4.4	10.0
$[C_3SO_3HMIM][CuCl_3]$	21.9	4.4	8.2	7.8	22.4	3.5	7.6	8.6
$[C_3SO_3HMIM][FeCl_4]$	20.2	3.1	6.9	7.7	20.9	3.3	7.0	8.0
$[C_3SO_3HMIM][SnCl_3]$	18.9	2.8	6.4	7.3	19.5	3.0	6.5	7.5

2A.5. NMR (¹H and ¹³C) and FT-IR

2A.5.1. Nuclear magnetic resonance (NMR)

The ¹H and ¹³C liquid NMR spectra were recorded for ILs, by dissolving ca. 25 mg IL in ca. 600 μL D_2O or DMSO-d_6 solvent in a NMR tube. The solvent peak present in the spectrum is considered as reference peak (D_2O, δ= 4.80 ppm and DMSO-d_6, δ= 2.50 ppm). The ¹H and ¹³C NMR spectra of the ILs are recorded and shown in Figures 2A.6-2A.20.

2A.5.2. Fourier transform infrared spectroscopy (FT-IR)

The presence of various functional groups in IL samples were analysed using FT-IR (FT-IR-8300 Shimadzu) technique. For the analysis, pellets were made with KBr by maintaining 1*wt.*% concentration.

1-Methyl-3-(3-sulfopropyl)-imidazolium hydrogensulphate, [C₃SO₃HMIM][HSO₄]

¹H-NMR (200 MHz, D_2O, δ= ppm): 8.56 (s, 1H), 7.42 (s, 1H), 7.35 (s, 1H), 4.26 (t, 2H), 3.79 (s, 3H), 2.82 (t, 2H) and 2.21 (m, 2H).

¹³C-NMR (50.3MHz, D_2O, δ= ppm): 136.16, 123.74, 122, 47.69, 47.19, 35.66 and 25.05

FT-IR (reflectance, cm⁻¹): 3412, 3157, 3090, 2959, 2880, 1722, 1650, 1600, 1500, 1463, 1236, 1037, 847, 825, 750, 690 and 623.
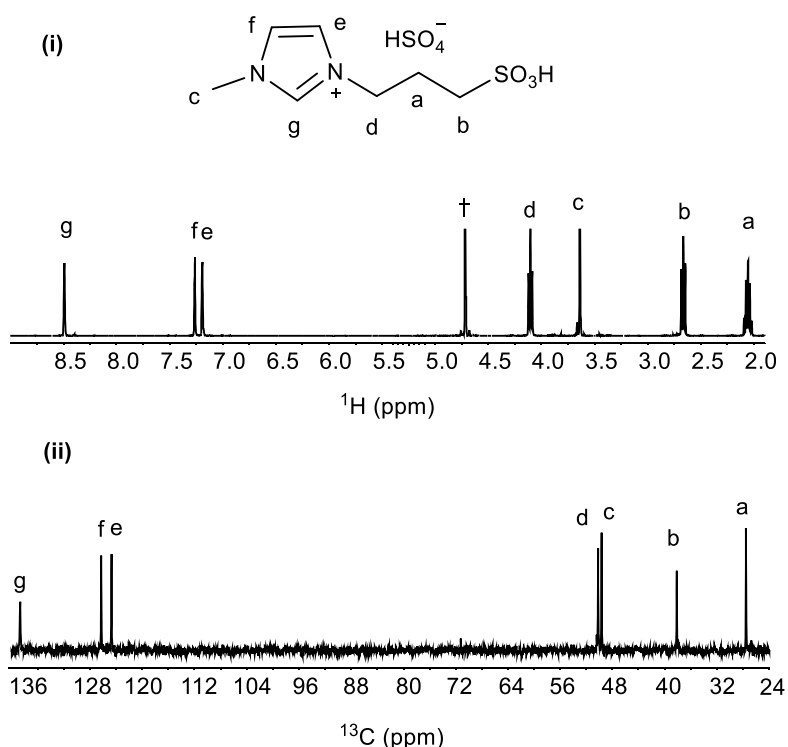
Figure 2A.6. (i) ¹H and (ii) ¹³C NMR spectra of [C₃SO₃HMIM][HSO₄] IL, († indicate the solvent peak).

1-Methyl-3-(3-sulfopropyl)-imidazolium *p*-toluenesulphonate, [C₃SO₃HMIM][PTS]

^{1}H-NMR (200 MHz, D$_2$O, δ= ppm): 8.59 (s, 2H), 7.55 (d, 2H), 7.36 (s, 1H), 7.30 (s, 1H), 7.27 (d, 2H), 4.11 (t, 2H), 3.76 (s, 3H), 2.83 (t, 2H) 2.28 (s, 3H) and 1.90 (m, 2H).

^{13}C-NMR (50.3 MHz, D$_2$O, δ= ppm): 142.42, 139.43, 136.09, 129.40, 125.31, 123.72, 122.14, 47.69, 47.17, 35.66, 25.05 and 20.44.

FT-IR (reflectance, cm^{-1}): 3412, 3157, 3090, 2959, 2930, 2880, 1722, 1600, 1559, 1501, 1463, 1236, 1175, 1129, 1037, 1012, 847, 825, 750, 690 and 623.
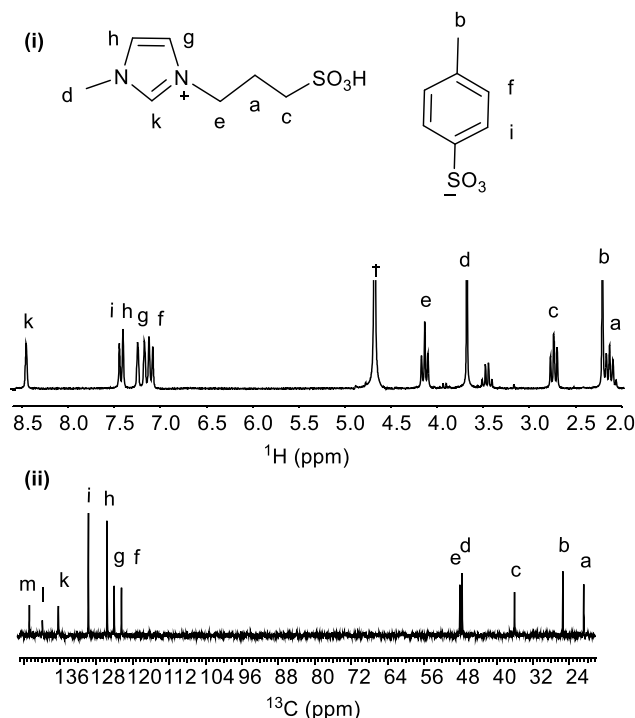
Figure 2A.7. (i) ^{1}H and (ii) ^{13}C NMR spectra of [C₃SO₃HMIM][PTS] IL, († indicate the solvent peak).

1-Methyl-3-(3-sulfopropyl)-imidazolium chloride, [C₃SO₃HMIM][Cl]

^{1}H-NMR (200 MHz, D$_2$O, δ= ppm): 8.53 (s, 1H), 7.40 (s, 1H), 7.32 (s, 1H), 4.24 (t, 2H), 3.77 (s, 3H), 2.80 (t, 2H) and 2.19 (m, 2H).

^{13}C-NMR (50.3 MHz, D$_2$O, δ= ppm): 137.19, 123.76, 122.18, 47.72, 47.18, 35.7 and 25.08.

FT-IR (reflectance, cm^{-1}): 3412, 3157, 3090, 2959, 2880, 1722, 1600, 1559, 1463, 1236, 1129, 1037, 847, 825, 750, 690 and 623.
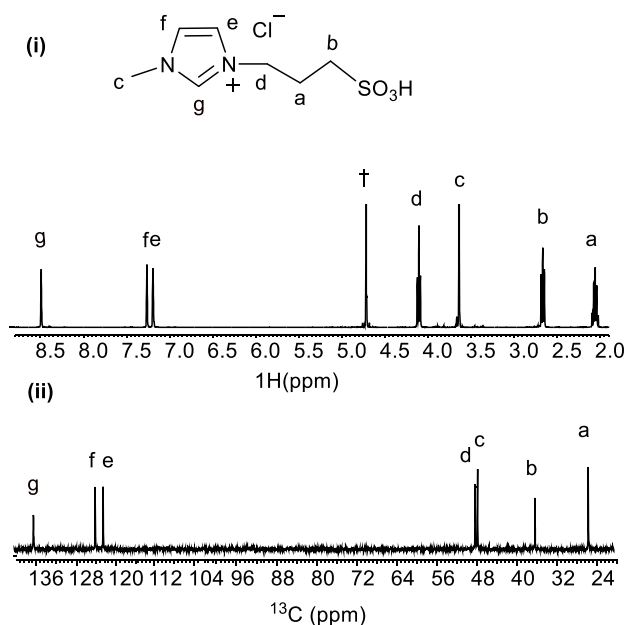
Figure 2A.8. (i) ^{1}H and (ii) ^{13}C NMR spectra of [C$_3$SO$_3$HMIM][Cl] IL, († indicate the solvent peak).

1-butyl-3-methylimidazolium chloride, [BMIM][Cl]

^{1}H-NMR (200MHz, D$_2$O, δ= ppm): 8.51 (s, 1H), 7.33 (s, 1H), 7.32 (s, 1H), 4.24 (t, 2H), 3.75 (s, 3H), 1.77 (quart, 2H), 1.35 (quint, 2H) and 0.57 (t, 3H).

^{13}C-NMR (50.3 MHz, D$_2$O, δ= ppm): 137.14, 123.76, 122.18, 49.32, 35.7, 31.2, 19.12 and 12.34.

FT-IR (reflectance, cm^{-1}): 3450, 3330, 3153, 3111, 2959, 2923, 1604, 1569, 1494, 1453, 1231, 1122 and 1031.
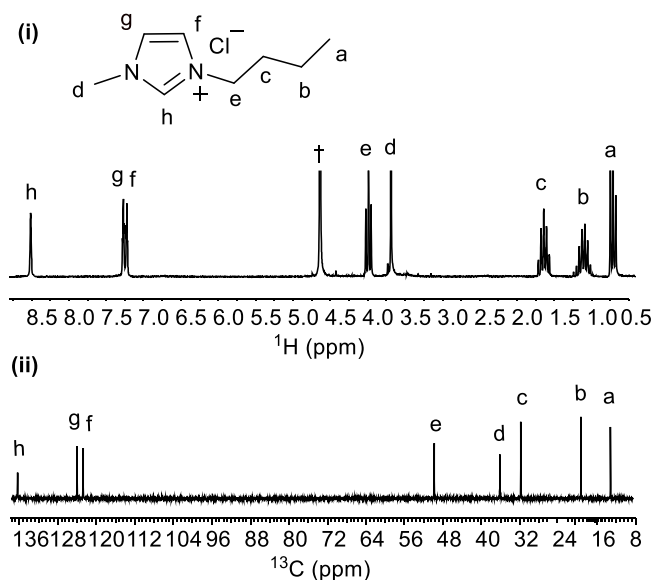
Figure 2A.9. (i) ^{1}H and (ii) ^{13}C NMR spectra of [BMIM][Cl] IL, († indicate the solvent peak).

1-Methyl-3-(3-sulfopropyl)-imidazolium dihydrogenphosphate, [C₃SO₃HMIM][H₂PO₄]

^{1}H-NMR (200 MHz, D$_2$O, δ= ppm): 8.61 (s, 1H), 7.38 (s, 1H), 7.30 (s, 1H), 4.22 (t, 2H), 3.76 (s, 3H), 2.79 (t, 2H) and 2.21 (m, 2H)

^{13}C-NMR (50.3 MHz, D$_2$O, δ= ppm): 136.09, 123.70, 122.11, 47.65, 47.15, 35.64 and 25.01.

FT-IR (reflectance, cm^{-1}): 3370, 3170, 3106, 2930, 2867, 1621, 1573, 1462, 1206, 1174, 1142, 966, 887, 839 and 743.
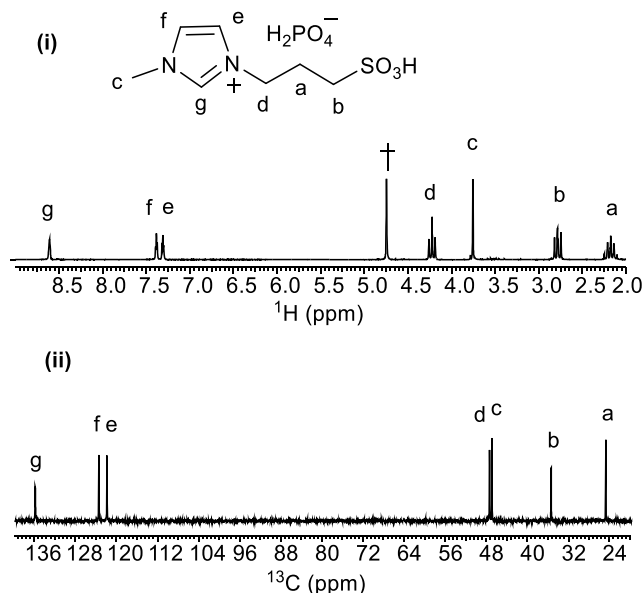
Figure 2A.10. (i) ^{1}H and (ii) ^{13}C NMR spectra of [C₃SO₃HMIM][H₂PO₄] IL, († indicate the solvent peak).

1-methyl-3-(3-sulfopropyl)-benzimidazolium hydrogensulphate, [C₃SO₃HBenzMIM][HSO₄]

^{1}H-NMR (200 MHz, D$_2$O, δ= ppm): 9.18 (s, 1H), 7.78 (s, 1H), 7.60 (s, 1H), 4.55 (t, 2H), 3.99 (s, 3H), 2.82 (t, 2H) and 2.32 (m, 2H).

^{13}C-NMR (50.3 MHz, D$_2$O, δ= ppm): 141.45, 132.15, 131.09, 126.94, 126.91, 113.05, 112.95, 47.39, 45.36, 32.94 and 24.29.

FT-IR (reflectance, cm^{-1}): 3493, 3128, 3105, 2939, 1594, 1552, 1399, 1174, 1097, 1056, 926, 861, 790, 702 and 643.
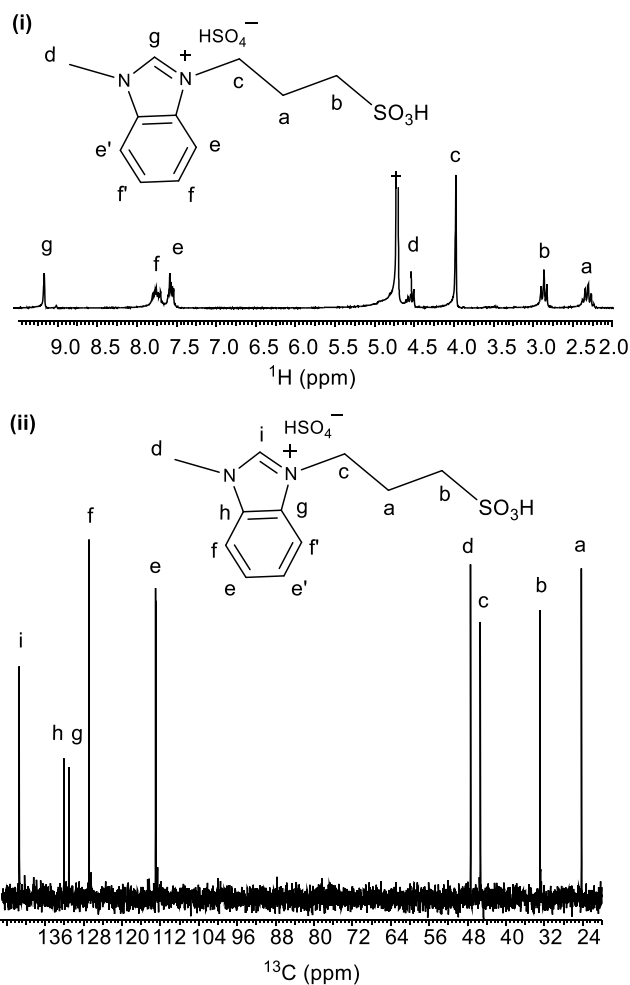
Figure 2A.11. (i) ^{1}H and (ii) ^{13}C NMR spectra of [C$_3$SO$_3$HBenzMIM][HSO$_4$] IL, († indicate the solvent peak).

Tri-phenyl-(3-sulfopropyl)-phosphonium hydrogensulphate, [C$_3$SO$_3$H(C$_6$H$_5$)$_3$P][HSO$_4$]

^{1}H-NMR (200 MHz, D$_2$O, δ= ppm): 7.52 (m, 15H), 3.26 (t, 2H), 2.76 (t, 2H) and 1.82 (m, 2H)

^{13}C-NMR (50.3 MHz, D$_2$O, δ= ppm): 134.41, 133.31, 117.2, 116.7, 49.89, 49.61 and 17.06.

FT-IR (reflectance, cm^{-1}): 3370, 3170, 1621, 1573, 1462, 1206, 1174, 1142, 966, 887, 839 and 765.
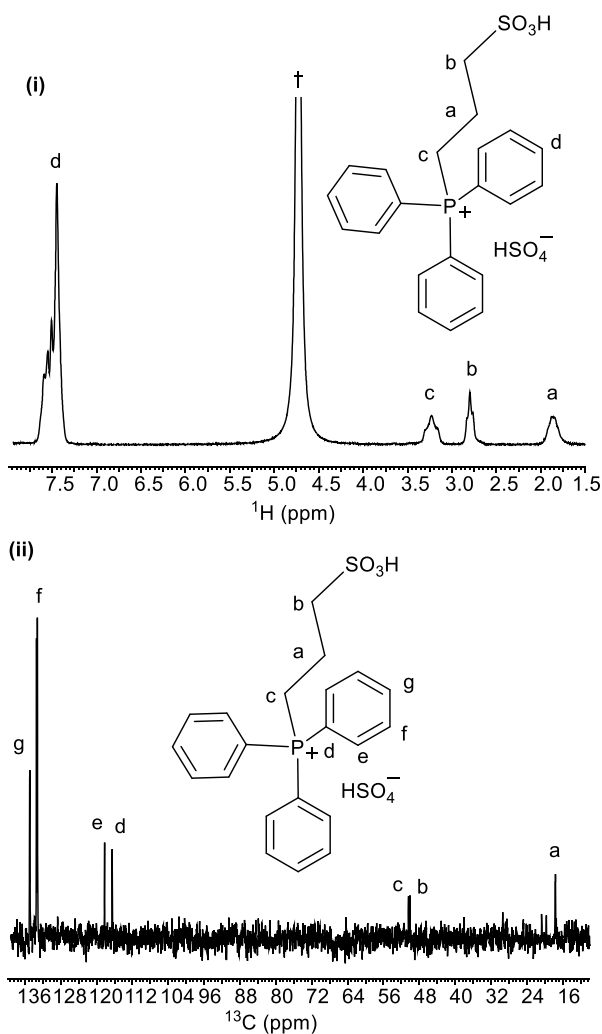
Figure 2A.12. (i) ^{1}H and (ii) ^{13}C NMR spectra of [C$_3$SO$_3$H(C$_6$H$_5$)$_3$P][HSO$_4$] IL, († indicate the solvent peak).

1-methyl-3-(3-sulfopropyl)-imidazolium cupric chloride, [C$_3$SO$_3$HMIM][CuCl$_3$]

^{1}H-NMR (200 MHz, D$_2$O, δ= ppm): 8.61 (s, 1H), 7.38 (s, 1H), 7.30 (s, 1H), 4.22 (t, 2H), 3.76 (s, 3H), 2.79 (t, 2H) and 2.21 (m, 2H).

^{13}C-NMR (50.3 MHz, D$_2$O, δ= ppm): 136.09, 123.70, 122.11, 47.65, 47.15, 35.64 and 25.01.

FT-IR (reflectance, cm^{-1}): 3403, 3077, 2956, 2894, 2826, 1619, 1570, 1463, 1373, 1212, 1149, 1038, 957, 832, 805, 751, 658, 622, 590, 528 and 451.
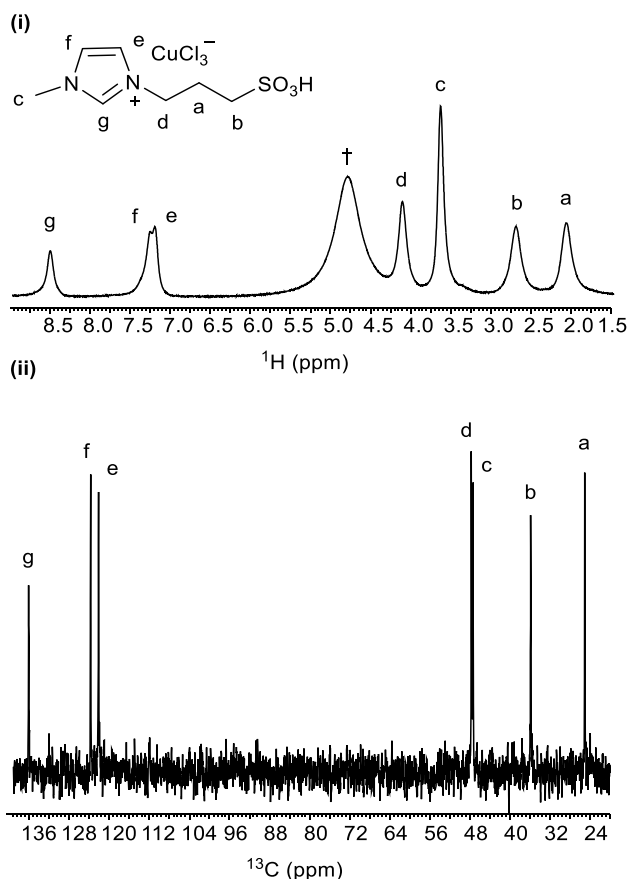
Figure 2A.13. (i) ¹H and (ii) ¹³C NMR spectra of [C₃SO₃HMIM][CuCl₃]IL, († indicate the solvent peak).

1-methyl-3-(3-sulfopropyl)-imidazolium stannic chloride, [C₃SO₃HMIM][SnCl₃]

¹H-NMR (200 MHz, D₂O, δ= ppm): 8.05 (s, 1H), 6.72 (s, 1H), 6.63 (s, 1H), 3.25 (t, 2H), 2.79 (s, 3H), 1.38 (t, 2H) and 1.02 (m, 2H).

¹³C-NMR (50.3 MHz, D₂O, δ= ppm): 136.09, 123.70, 122.11, 47.65, 47.15, 35.64 and 25.01.

FT-IR (reflectance, cm⁻¹): 3413, 3082, 2958, 2892, 2823, 1620, 1580, 1465, 1380, 1210, 1151, 1040, 960, 834, 810, 752, 659, 624, 591 and 530.
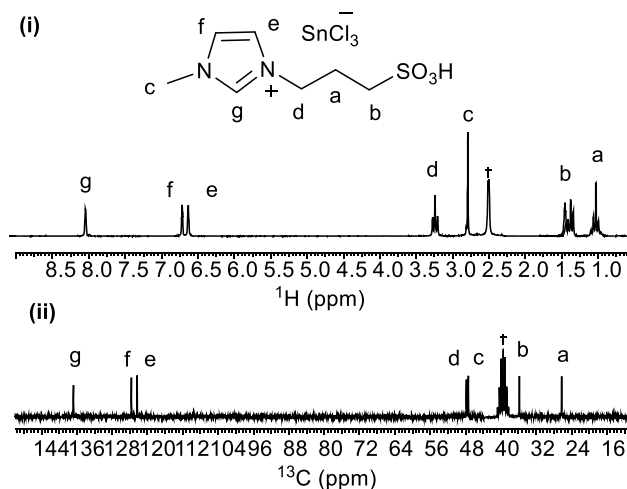
Figure 2A.14. (i) ¹H and (ii) ¹³C NMR spectra of [C₃SO₃HMIM][SnCl₃] IL, († indicate the solvent peak).

N,N,N-triethyl-3-sulfopropanaminium hydrogensulphate, [C₃SO₃H(C₂)₃N][HSO₄]

^{1}H-NMR (200 MHz, D₂O, δ= ppm): 3.21 (quart, 8H), 2.86 (t, 2H), 2.00 (quart, 2H) and 1.16 (t, 9H).

^{13}C-NMR (50.3 MHz, D₂O, δ= ppm): 57.30, 55.19, 49.75, 19.74 and 9.11.

FT-IR (reflectance, cm⁻¹): 3340, 2990, 2935, 2865, 1730, 1665, 1485, 1400, 1220, 1130, 1025, 860 and 735.
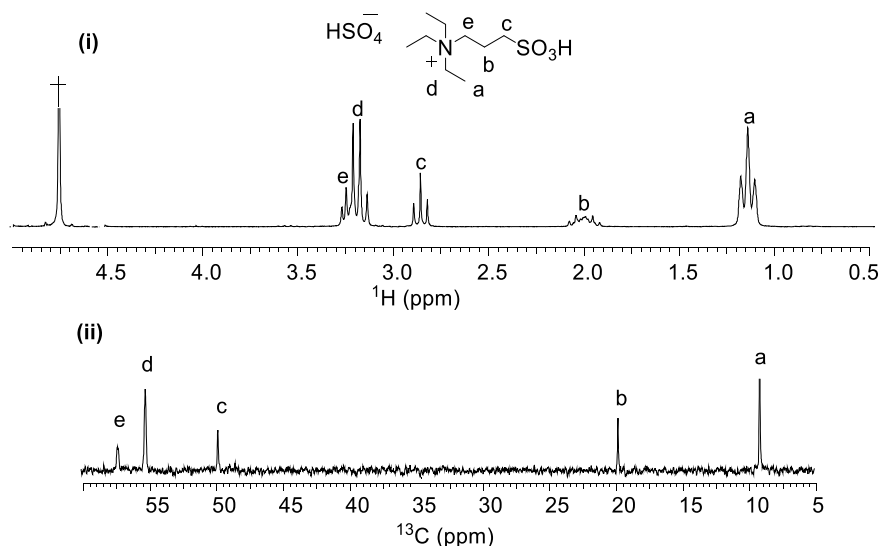
Figure 2A.15. (i) ^{1}H and (ii) ^{13}C NMR spectra of [C₃SO₃H(C₂)₃N][HSO₄] IL, († indicate the solvent peak).

N,N,N-triethyl-3-sulfopropanaminium *p*-toluenehydrogensulphate, [C₃SO₃H(C₂)₃N][PTS]

^{1}H-NMR (200MHz, D₂O, δ= ppm): 7.60(s, 1H), 7.56 (s, 1H), 7.28 (s, 1H), 7.24 (s, 1H), 3.19(quart, 6H, t, 2H), 2.86 (t, 2H), 2.28 (s, 3H), 2.00 (quart, 2H) and 1.16 (t, 9H).

^{13}C-NMR (50MHz, D₂O, δ= ppm): 142.45, 129.43, 125.34, 54.67, 52.66, 47.20, 20.45, 17.21 and 6.57.

FT-IR (reflectance, cm⁻¹): 3370, 2993, 2930, 2850, 1725, 1670, 1610, 1470, 1405, 1225, 1110, 1005, 810, 730 and 675.
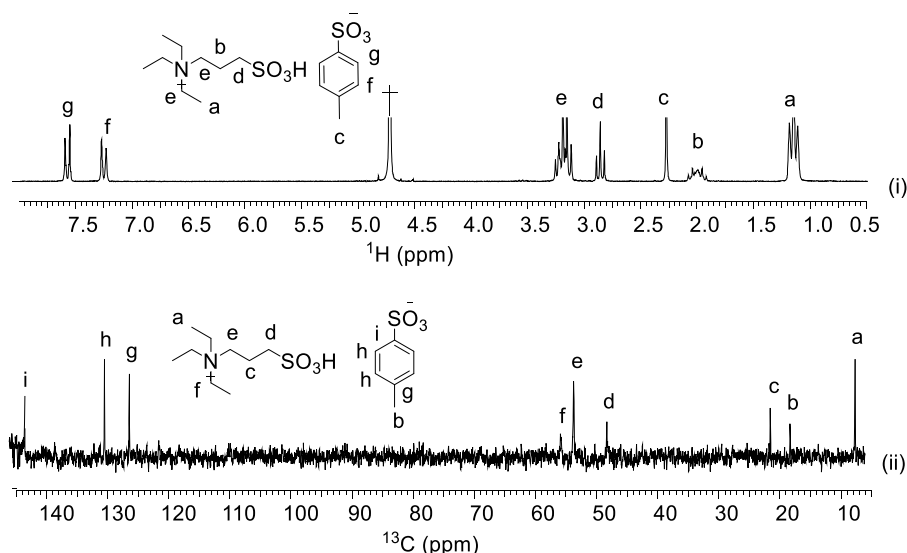
Figure 2A.16. (i) ^{1}H and (ii) ^{13}C NMR spectra of [C$_3$SO$_3$H(C$_2$)$_3$N][PTS] IL, († indicate the solvent peak).

N,N,N-triethyl-3-sulfopropanaminium chloride, [C$_3$SO$_3$H(C$_2$)$_3$N][Cl]

^{1}H-NMR (200MHz, D$_2$O, δ= ppm): 3.22 (quart, 8H), 2.87 (t, 2H), 2.01 (quart, 2H) and 1.17 (t, 9H).
^{13}C-NMR (50MHz, D$_2$O, δ= ppm): δ 54.81, 52.73, 47.27, 17.27 and 6.64.
FT-IR (reflectance, cm^{-1}): 3360, 2980, 2930, 2365, 2245, 1735, 1655, 1480, 1400, 1215, 1145, 1035, 790 and 725.
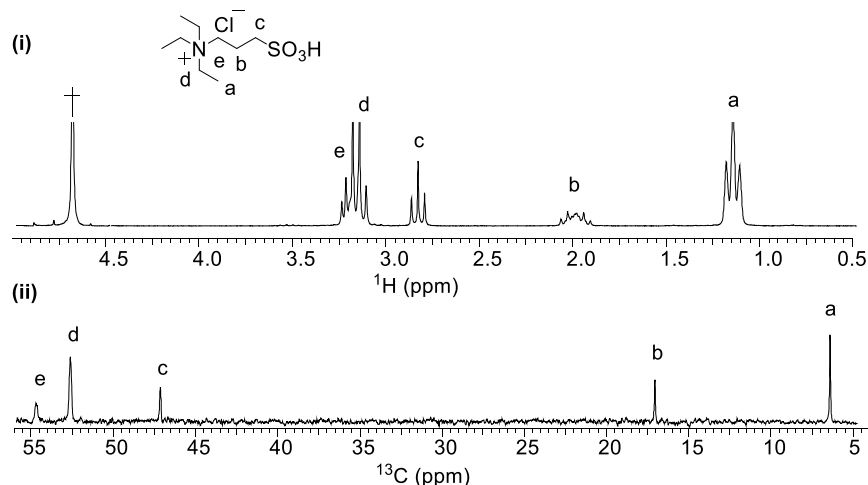
Figure 2A.17. (i) ^{1}H and (ii) ^{13}C NMR spectra of [C$_3$SO$_3$H(C$_2$)$_3$N][Cl] IL, († indicate the solvent peak).

N,N,N-triethyl-3-sulfopropanaminium dihydrogenphosphate [C$_3$SO$_3$H(C$_2$)$_3$N][H$_2$PO$_4$]

^{1}H-NMR (200MHz, D$_2$O, δ= ppm): 3.21(quart, 8H), 2.86 (t, 2H), 2.01 (quart, 2H) and 1.16 (t, 9H).
^{13}C-NMR (50.3 MHz, D$_2$O, δ= ppm): 54.59, 52.55, 47.12, 17.10 and 6.5.
FT-IR (reflectance, cm^{-1}): 3360, 2990, 2895, 2365, 2270, 1730, 1655, 1475, 1340, 1210, 1140, 1055, 830, 750 and 685.
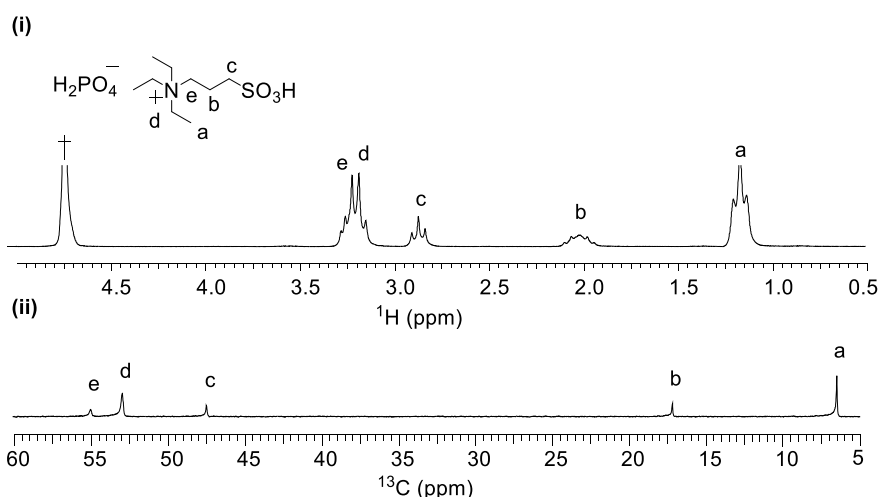
Figure 2A.18. (i) ^{1}H and (ii) ^{13}C NMR spectra of $[C_3SO_3H(C_2)_3N][H_2PO_4]$ IL, († indicate the solvent peak).

The ^{1}H and ^{13}C NMR chemical shifts were recorded using tetramethylsilane (TMS) as an internal standard and also solvent peaks were considered as reference. The multiplicity of the each peaks are abbreviated as s = singlet, d = doublet, t = triplet, quart = quartet, quint = quintet and m = multiplet. All the characteristic (^{1}H and ^{13}C) NMR peaks are present in synthesized ILs, which confirmed that ILs are synthesized in the pure form. In case of $[C_3SO_3HMIM][HSO_4]$ IL, the alkylated proton peaks are assigned as δ= 2.21 ppm (m, 2H) for 'a' protons; δ= 2.82 ppm (t, 2H), for 'b' protons, which are close to –SO$_3$H group; δ= 3.79 ppm (s, 3H) for 'c' protons, which are near to imidazolium nitrogen and δ= 4.26 ppm (t, 2H), for 'd' protons which are closed to nitrogen of imidazolium ring (linked with methyl groups). Similarly, the proton peaks for the imidazolium ring are assigned as δ= 7.35 ppm (s, 1H), for 'e' proton close to imidazolium nitrogen (further liked with propylsulphonated groups), δ= 7.42 ppm (s, 1H), for 'f' proton closed to imidazolium nitrogen (which is linked with methyl groups) and the most deshielded proton peaks at δ= 8.66 (s, 1H) for 'g' proton, this proton is located between two nitrogen atoms, Similarly, ^{1}H and ^{13}C NMR spectra for all the synthesized ILs can be described.

The functional groups present in the synthesized IL samples are confirmed with the help of FT-IR spectra. Moreover from the peaks assignment, it was observed that there were no additional peaks to be assigned for undesired functional groups in the FT-IR spectra of the ILs, which again emphasized that the synthesized ILs are free from any contamination.

2A.6. TGA analysis of ionic liquids

Thermogravimetric analysis (TGA) is the analytical technique used for the determination of thermal stability with respect to weight loss in the ILs. Generally air atmosphere is used to check the thermal stability of the ILs. During typically experiment molecules allow to decompose into gases form. Nature of decomposition and formation of gases products depends upon the strength of the bond present in the particular molecules.

The TGA experiments of the samples were conducted using METTLER TOLEDO TGA/SDTA851 series, USA; instrument. The following program was used for the analysis of the samples;

50 ^{o}C$\rightarrow$ 10 °C/min $\rightarrow$ 800 °C under (air).
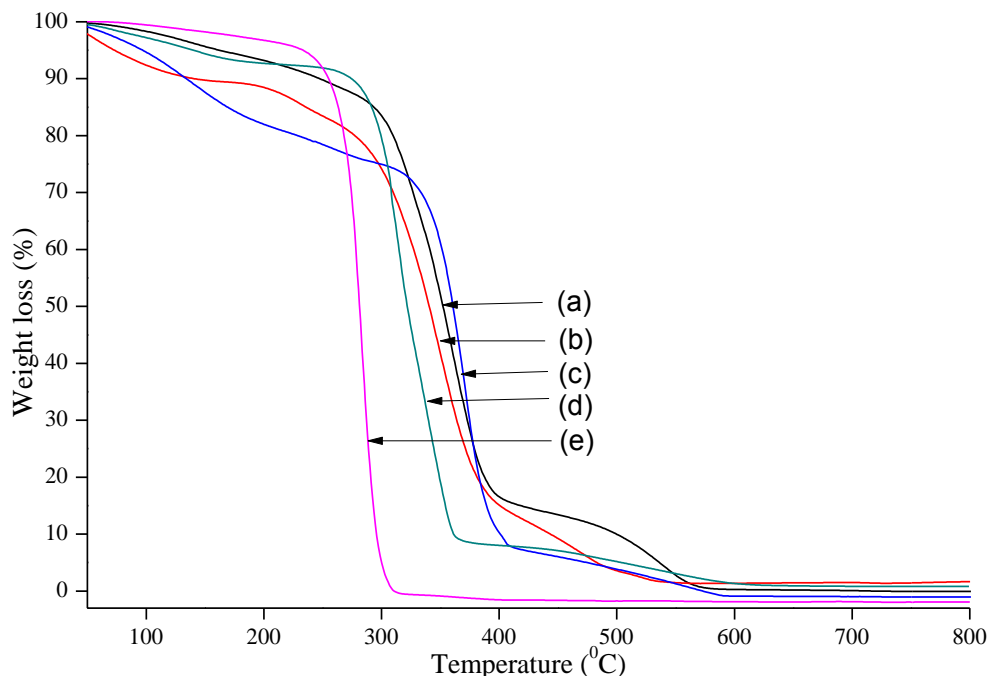
Figure 2A.19. TGA (air) analysis of (a) [C$_3$SO$_3$HMIM][HSO$_4$], (b) [C$_3$SO$_3$HMIM][PTS], (c) [C$_3$SO$_3$HMIM][Cl], (d) [C$_3$SO$_3$HMIM][H$_2$PO$_4$] and (e) [BMIM][Cl] ILs.
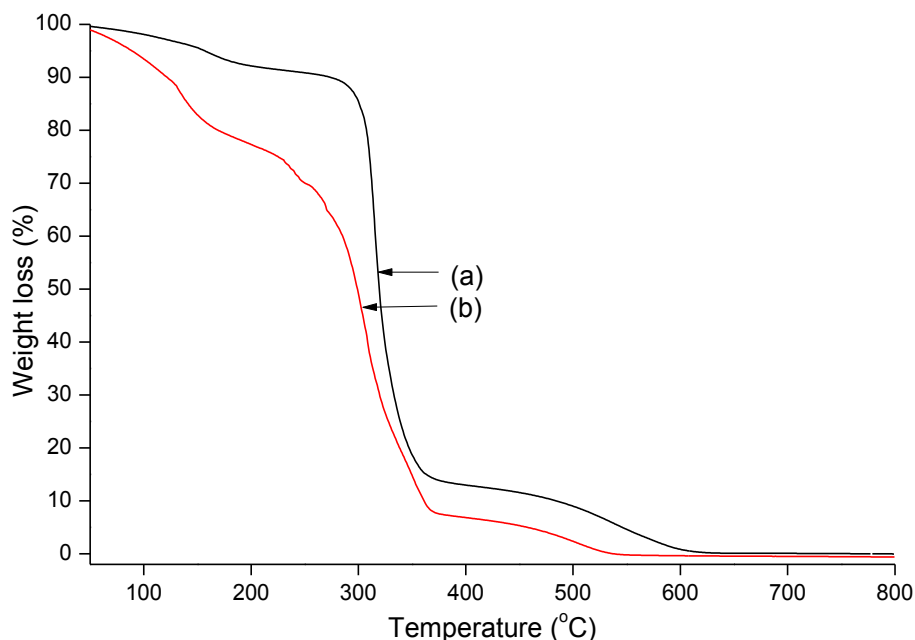
Figure 2A.20. TGA (air) analysis of (a) [C$_3$SO$_3$H(C$_2$)$_3$N][HSO$_4$], and (b) [C$_3$SO$_3$H(C$_2$)$_3$N][Cl] ILs.

The TGA study was used to analyse ILs in presence of air. From the TGA profiles, it is observed (Figures 2A.19-2A.20) that ILs are stable up to 250 ^{o}C (except [C$_3$SO$_3$H(C$_2$)$_3$N][Cl], IL). In the

beginning, weight loss was noticed due to loss of physically absorbed moisture from the ILs. Hence, as mentioned above the TGA result implies that ILs can be used for lignin depolymerization reaction at ≤250 °C.

2A.7. UV-Vis spectra for Hammett acidity function (H_0) of ILs and mineral acids (weight and mole basis)

The acid strength reflects the extent of a catalyst to liberate/donate proton. For the determination of the acid strength in ILs and homogeneous acids, Hammett acidity function (H_0) was measured using UV-Vis absorption spectroscopy (Perkin Elmer spectrophotometer (Model-Lambda 650)). The purpose of this study is to draw a correlation between catalytic activity between ILs and homogeneous acids with respect to acid strength. The determination of Hammett acidity was carried out using *p*-nitroaniline (PNA) basic indicator. It is known that with an increase in the acidic strength of the sample, the absorbance of the un-protonated form of basic indicator decreases. Whereas the protonated form of indicator could not be seen in the UV-Vis absorbance spectra because of its small molar absorptivity. With higher acid concentration, absorbance coefficient value will be low and H_0 will be more at 380.4 nm due to less resonance between amine and nitro groups present in the basic indicator that will stabilise the molecules *via* protonation. The Hammett acidity function has been calculated under the same concentration of PNA (2 mg/L, *pKa*= 0.99) with respect to weight basis (25 mg) and mole basis (H+= 50 mmol) of BAILs/IL and homogeneous acids (in Millipore water) solution. Hammett acidity function is calculated using the following equation (2A.1),

$$H_0 = pka + \log\frac{[I]}{[HI]} \qquad\qquad (2A.1)$$

Where, [I] and [HI] are the molar concentrations of unprotonated and protonated forms of indicator in solvent. The calculated H_0 value of the BAILs and homogeneous acids are summarised in Tables 2A.4-2A.5.

Table 2A.4. Hammett acidity function (H_0) of ILs and homogeneous acids (weight basis).[a]

Sr. no.	Indicator and ILs	Absorbance (a.u.)	[I]	[HI]	H_0
1	*p*-nitroaniline	0.1998	100	-	-
2	[BMIM][Cl]	0.2026	-	-	-
3	[C$_3$SO$_3$HMIM][Cl]	0.1895	95.22	4.78	2.29
4	[C$_3$SO$_3$H(C$_2$H$_5$)$_3$N][Cl]	0.1844	92.28	7.72	2.08
5	[C$_3$SO$_3$HMIM][HSO$_4$]	0.1824	91.29	8.71	2.01
6	[C$_3$SO$_3$H(C$_2$H$_5$)$_3$N][HSO$_4$]	0.1732	86.74	13.26	1.81
7	[C$_3$SO$_3$HBenzMIM][HSO$_4$]	0.1743	87.23	12.76	1.82
8	[C$_3$SO$_3$H(C$_6$H$_5$)$_3$P][HSO$_4$]	0.1860	93.09	6.91	2.12
9	[C$_3$SO$_3$HMIM][PTS]	0.1922	96.19	3.81	2.39
10	[C$_3$SO$_3$H(C$_2$H$_5$)$_3$N][PTS]	0.1853	92.75	7.25	2.10
11	[C$_3$SO$_3$HMIM][H$_2$PO$_4$]	0.1854	92.78	7.22	2.10
12	[C$_3$SO$_3$H(C$_2$H$_5$)$_3$N][H$_2$PO$_4$]	0.1797	96.90	3.10	2.48
13	[C$_3$SO$_3$HMIM][CuCl$_3$]	0.1877	93.94	6.06	2.18
14	[C$_3$SO$_3$HMIM][SnCl$_3$]	0.1767	84.46	15.54	1.72
15	H$_2$SO$_4$	0.1547	77.42	22.58	1.53
16	HCl	0.1627	81.41	18.58	1.63
17	H$_3$PO$_4$	0.1771	88.64	11.36	1.88
18	PTSA. H$_2$O	0.1873	93.77	6.23	2.16

Note: [a]H_0 values calculated with the help of UV-Vis spectroscopy using PNA indicator. Absorption recorded at 380.4 nm with ILs and homogeneous acids (25 mg in 50 mL PNA solution).

Table 2A.5. Hammett acidity function (H_0) of ILs and homogeneous acids (mole basis).[a]

Sr. no.	Indicator and ILs	Absorbance (a.u.)	[I]	[HI]	H_0
1	*p*-nitroaniline	0.1968	100	-	-
2	[BMIM][Cl]	0.2000	-	-	-
3	[C$_3$SO$_3$HMIM][Cl]	0.1549	78.70	21.29	1.56
4	[C$_3$SO$_3$H(C$_2$H$_5$)$_3$N][Cl]	0.1592	80.88	19.12	1.62
5	[C$_3$SO$_3$HMIM][HSO$_4$]	0.1369	69.56	30.44	1.35
6	[C$_3$SO$_3$H(C$_2$H$_5$)$_3$N][HSO$_4$]	0.1337	67.83	32.17	1.31
7	[C$_3$SO$_3$HBenzMIM][HSO$_4$]	0.1364	69.31	30.69	1.34
8	[C$_3$SO$_3$H(C$_6$H$_5$)$_3$P][HSO$_4$]	0.1849	93.9	6.1	2.18
9	[C$_3$SO$_3$HMIM][PTS]	0.1479	75.15	24.85	1.47
10	[C$_3$SO$_3$H (C$_2$H$_5$)$_3$N][PTS]	0.1422	72.28	27.72	1.41
11	[C$_3$SO$_3$HMIM][H$_2$PO$_4$]	0.1739	88.38	11.62	1.87
12	[C$_3$SO$_3$H(C$_2$H$_5$)$_3$N][H$_2$PO$_4$]	0.1742	95.22	4.78	2.29
13	[C$_3$SO$_3$HMIM][CuCl$_3$]	0.1849	94.00	6.00	2.18
14	[C$_3$SO$_3$HMIM][SnCl$_3$]	0.1740	88.43	11.56	1.87
15	H$_2$SO$_4$	0.1230	62.5	37.5	1.21
16	HCl	0.1318	66.99	33.01	1.30
17	H$_3$PO$_4$	0.1624	82.52	17.48	1.66
18	PTSA. H$_2$O	0.1873	72.28	27.72	1.41

Note:[a] H_0 values calculated with the help of UV-Vis spectroscopy using PNA indicator. Absorption recorded at 380.4 nm with ILs and homogeneous acids (H$^+$= 50 mmol in 50 mL PNA solution).

The following trend of Hammett acidity function (weight basis) for all the BAILs is observed, [C$_3$SO$_3$HMIM][SnCl$_3$]> [C$_3$SO$_3$H(C$_2$H$_5$)$_3$N][HSO$_4$]> [C$_3$SO$_3$HBenzMIM][HSO$_4$]> [C$_3$SO$_3$HMIM][HSO$_4$]> [C$_3$SO$_3$H(C$_2$H$_5$)$_3$N][Cl]> [C$_3$SO$_3$HMIM][H$_2$PO$_4$]~ [C$_3$SO$_3$H(C$_2$H$_5$)$_3$N][PTS]> [C$_3$SO$_3$H(C$_6$H$_5$)$_3$P][HSO$_4$]~ [C$_3$SO$_3$HMIM][CuCl$_3$]> [C$_3$SO$_3$HMIM][Cl]> [C$_3$SO$_3$HMIM][PTS]> [C$_3$SO$_3$H(C$_2$H$_5$)$_3$N][H$_2$PO$_4$]. The Hammett acidity function (H_0) of the BAIL samples is observed in the range between 1.74-2.48. From the obtained results, it can be concluded that [C$_3$SO$_3$HMIM][SnCl$_3$] has maximum Hammett acidity function (H_0) than other BAILs. Similarly, the Hammett acidity function (mole basis) of all the BAILs is also calculated and obtained trend of the acid strength is as follows; [C$_3$SO$_3$H(C$_2$H$_5$)$_3$N][HSO$_4$]> [C$_3$SO$_3$HBenzMIM][HSO$_4$]> [C$_3$SO$_3$HMIM][HSO$_4$]> [C$_3$SO$_3$H(C$_2$H$_5$)$_3$N][PTS]> [C$_3$SO$_3$HMIM][PTS]> [C$_3$SO$_3$HMIM][Cl]> [C$_3$SO$_3$H(C$_2$H$_5$)$_3$N][Cl]> [C$_3$SO$_3$HMIM][H$_2$PO$_4$]> [C$_3$SO$_3$HMIM][SnCl$_3$]> [C$_3$SO$_3$H(C$_6$H$_5$)$_3$P][HSO$_4$]~ [C$_3$SO$_3$HMIM][CuCl$_3$]> [C$_3$SO$_3$H(C$_2$H$_5$)$_3$N][H$_2$PO$_4$]. Among all (mole basis) H_0 values,

$[C_3SO_3H(C_2H_5)_3N][HSO_4]$ BAIL showed maximum acid strength. The data obtained on H_0 may help to explain the activity of catalysts in the depolymerization reactions.

2A.8. UV-Vis spectra for the calculation of the thermodynamic parameters

2A.8.1. Calculation of thermodynamic parameters (K_{eq}, ΔG, ΔH, ΔS and ΔE$_a$,H$^+$) of the BAILs and mineral acid (25 mg sample in 10 mL PNA solution)

Thermodynamic parameter reflects the extent of a catalyst that can act as spontaneous or nonspontaneous reaction. For the spontaneous reaction, ΔG (change in Gibb's free energy) should be negative or <0, it means that reaction is kinetically or thermodynamically favourable. If the ΔG value is positive or >0 the reaction/process will be nonspontaneous. The thermo dynamic parameters (K_{eq}, ΔG, ΔH, ΔS and ΔE$_a$,H$^+$) of BAILs and mineral acid are calculated using UV-Vis spectroscopy. The purpose of this study is to draw a correlation between catalytic activity of the BAILs and mineral acid, with their thermodynamic parameters. The determinations of thermodynamic parameters are carried out using basic *p*-nitroaniline (PNA) indicator. The thermodynamic parameters have calculated under the same concentration of PNA (2mg/L, *pKa*= 0.99) solution with respect to weight basis (25 mg) of BAILs and mineral acid (in Millipore water) solution. With increase in proton donation ability or acid strength in sample, the absorbance of the unprotonated form of basic indicator decreases. Whereas the protonated form of indicator could not be observed because of its small molar absorptivity coefficient. The UV-Vis absorption of BAILs and mineral acid are recorded between a range of 25-65 °C with respect to different concentration (weight and moles basis). The indicator (protonated and unprotonated) absorption ratios ([HI$^+$]/[I]) are calculated by the absorbance recorded in UV-Vis spectroscopy.

The protonation equilibrium between the indicator and BAILs or minerals acid (HA) are shown in equation 2A.2,

$$I + HA \leftrightarrow HI^+ + A^- \qquad (2A.\ 2)$$
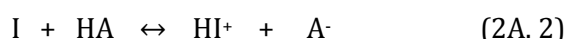
The equilibrium constant (K_{eq}) for the dissociation of BAILs and mineral acid are shown in equation 2A.3,

$$Keq = \frac{[HI+][A-]}{[I][HA]} \qquad (2A.\ 3)$$

The ([HI$^+$]/[I]) ratio is obtained from the difference in the absorbance of PNA solution and BAILs or mineral acid in adduct form. The ([X$^-$]/[HA]) value is obtained from the pH data of the adduct of PNA solution with BAILs or mineral acid.

Similarly, the temperature variable and concentration dependent K_{eq} values are calculated for the BAILs and mineral acid. Furthermore, with the help of K_{eq} the other thermodynamic parameters such as ΔG, ΔH and ΔS can be calculated.

The linear dependence of K_{eq} on the temperature is given by the van't Hoff equation:

$$\Delta G = -RT \ln K_{eq} \qquad\qquad (2A.4)$$

or

$$\ln K_{eq} = -\Delta G/RT \qquad\qquad (2A.4)$$

At particular temperature, ΔG depends on ΔH and ΔS as it is shown in the following equation,

$$\Delta G = \Delta H - T\Delta S \qquad\qquad (2A.5)$$

From equations 2A.4 and 2A.5, the linear form of van't Hoff equation can be written as;

$$\ln Keq = -\frac{\Delta H}{RT} + \frac{\Delta S}{R} \qquad\qquad (2A.6)$$

A linear plot of $\ln K_{eq}$ verses 1/T gives a straight line with slope= -ΔH and intercept= ΔS/R.

A typical graph of $\ln K_{eq}$ verses 1/T for BAILs and mineral acid are shown in Figure 2A.21.

2A.8.1.1. Activation energy (E_a,H^+)

The activation energy of proton transfer (E_a,H^+) is a measure of the hindrance provided by the medium in the protonated indicator. The E_a,H^+ is obtained from the temperature dependent H_0 measurement. When the temperature dependent H_0 fitted in the Arrhenius equation, linear relationship between $\ln H_0$ and 1/T is observed.

E_a,H^+ is calculated from the slope of linear fit;

$$\ln H_0 = \ln(H_0)_0 - E_a,H^+/RT \qquad\qquad (2A.7)$$

Whereas, $(H_0)_0$ is the Hammett acidity at room temperature, E_a,H^+ is the activation energy of proton transfer, and R is the universal gas constant.

The thermodynamic parameters (K_{eq}, ΔG, ΔH, ΔS and $\Delta E_a,H^+$) of BAILs and mineral acid are calculated using 2A.3-2A.7 equations and the obtained result is summarized in the Tables 2A.6-2A.21.

2A.8.1.2. pH measurement

The pH of equimolar mixture of PNA and adduct at variable temperature are measured by using the calibrated pH meter (DPH 504).

Table 2A.6. pH of BAILs and mineral acid (25 mg in 10 mL PNA solution) at different temperatures.

ILs and mineral acid	T, (K)				
	298.15	308.15	318.15	328.15	338.15
PNA	7.95	7.92	7.89	7.81	7.86
H_2SO_4	1.70	1.65	1.62	1.60	1.55
$[C_3SO_3HMIM][HSO_4]$	2.05	2.03	1.99	1.94	2.01
$[C_3SO_3HMIM][PTS]$	2.47	2.46	2.39	2.34	2.40
$[C_3SO_3HMIM][Cl]$	2.39	2.36	2.31	2.34	2.38
$[C_3SO_3HMIM][H_2PO_4]$	2.42	2.40	2.38	2.39	2.41

Table 2A.7. Absorbance (A max. 380.4 nm) of PNA with BAILs and mineral acid adduct at different temperatures.

T, (K)	PNA	H_2SO_4	$[C_3SO_3HMIM]$ $[HSO_4]$	$[C_3SO_3HMIM]$ $[PTS]$	$[C_3SO_3HMIM]$ $[Cl]$	$[C_3SO_3HMIM]$ $[H_2PO_4]$
298.15	0.2316	0.1570	0.1860	0.2038	0.2151	0.2105
308.15	0.2314	0.1634	0.1891	0.2081	0.2193	0.2134
318.15	0.2308	0.1700	0.1918	0.2099	0.2208	0.2134
328.15	0.2291	0.1762	0.1928	0.2100	0.2205	2143
338.15	0.2268	0.1777	0.1934	0.2100	0.2198	0.2136

Table 2A.8. Hammett acidity function (H_0) of PNA with BAILs and mineral acid adduct at different temperatures.

T, (K)	(H_0)				
	H_2SO_4	$[C_3SO_3HMIM]$ $[HSO_4]$	$[C_3SO_3HMIM]$ $[PTS]$	$[C_3SO_3HMIM]$ $[Cl]$	$[C_3SO_3HMIM]$ $[H_2PO_4]$
298.15	1.31	1.60	1.59	2.11	1.99
308.15	1.37	1.64	1.94	2.31	2.1
318.15	1.44	1.68	1.99	2.33	2.12
328.15	1.51	1.72	2.03	2.40	2.15
338.15	1.55	1.75	2.09	2.49	2.20

Table 2A.9. Chemical equilibrium (Keq) of PNA with BAILs and mineral acid adduct at different temperatures.

T, (K)	Keq				
	H_2SO_4	[C_3SO_3HMIM] [HSO_4]	[C_3SO_3HMIM] [PTS]	[C_3SO_3HMIM] [Cl]	[C_3SO_3HMIM] [H_2PO_4]
298.15	0.80	0.5	0.62	0.18	0.24
308.15	0.69	0.45	0.28	0.11	0.19
318.15	0.57	0.40	0.24	0.10	0.18
328.15	0.48	0.37	0.21	0.09	0.17
338.15	0.43	0.35	0.19	0.07	0.15

Table 2A.10. Gibbs free energy (ΔG) of PNA with BAILs and mineral acid adduct at different temperatures.

T, (K)	ΔG, (J/K mol)				
	H_2SO_4	[C_3SO_3HMIM] [HSO_4]	[C_3SO_3HMIM] [PTS]	[C_3SO_3HMIM] [Cl]	[C_3SO_3HMIM] [H_2PO_4]
298.15	553.1	1718.4	1185.7	4250.9	3535.5
308.15	962.8	2022.9	3303.7	5580.6	4297.4
318.15	1476.9	2393.0	3796.1	5973.5	4577.3
328.15	2002.7	2749.0	4258.5	6540.1	4916.4
338.15	2384.5	2974.8	4640.1	7253.4	5354.3

Table 2A.11. lnKeq verses 1/T, (K) of PNA with BAILs and mineral acid adduct at different temperatures.

1/T, (K)	lnKeq				
	H_2SO_4	[C_3SO_3HMIM] [HSO_4]	[C_3SO_3HMIM] [PTS]	[C_3SO_3HMIM] [Cl]	[C_3SO_3HMIM] [H_2PO_4]
0.00335	-0.2232	-0.6932	-0.4781	-1.7150	-1.4274
0.00325	-0.3711	-0.7987	-1.2732	-2.2077	-1.6610
0.00314	-0.5622	-0.9165	-1.4274	-2.303	-1.7150
0.00305	-0.7341	-0.9944	-1.5609	-2.3973	-1.8021
0.00296	-0.8441	-1.0500	-1.6610	-2.3973	-1.9042

Table 2A.12. lnH_0 verses 1/T, (K) of PNA with BAILs and mineral acid adducts at different temperatures.

1/T, (K)	lnH_0				
	H_2SO_4	[C$_3$SO$_3$HMIM] [HSO$_4$]	[C$_3$SO$_3$HMIM] [PTS]	[C$_3$SO$_3$HMIM] [Cl]	[C$_3$SO$_3$HMIM] [H$_2$PO$_4$]
0.00335	0.27	0.47	0.46	0.75	0.69
0.00325	0.31	0.49	0.66	0.84	0.74
0.00314	0.36	0.52	0.69	0.85	0.75
0.00305	0.41	0.54	0.71	0.88	0.77
0.00296	0.44	0.56	0.74	0.91	0.7
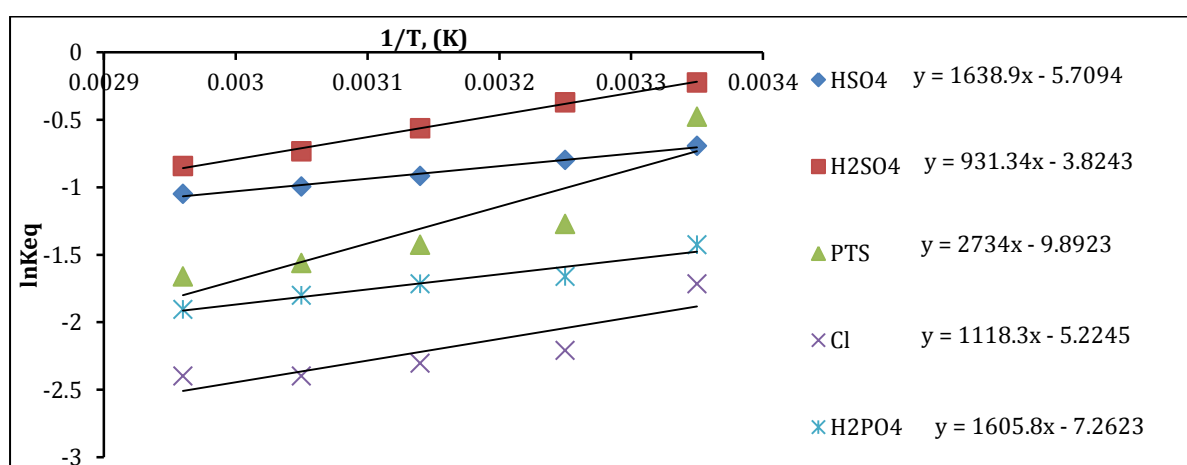
Figure 2A.21. Plot of lnKeq against 1/T, (K) for BAILs and mineral acid (25 mg sample in 10 mL PNA solution). The abbreviations assigned as in Figure 2A.21 are HSO4= [C$_3$SO$_3$HMIM][HSO$_4$], PTS= [C$_3$SO$_3$HMIM][PTS], Cl= [C$_3$SO$_3$HMIM][Cl] and H2PO4= [C$_3$SO$_3$HMIM][H$_2$PO$_4$] BAILs.
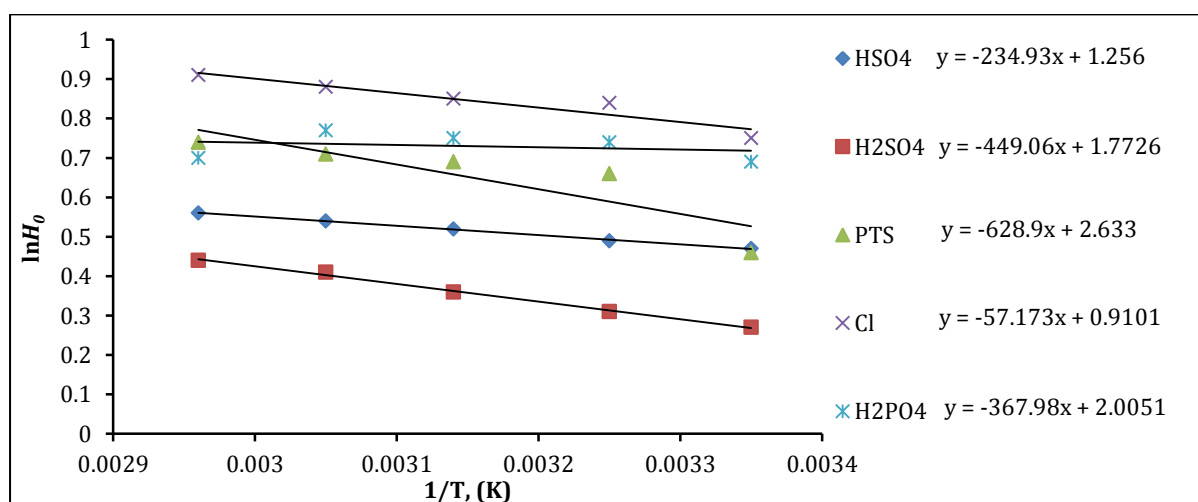
Figure 2A.22. Plot of lnH_0 verses against 1/T, (K) for BAILs and mineral acid (25 mg sample in 10 mL PNA solution). The abbreviations assigned as in Figure 2A.22 are HSO4= [C$_3$SO$_3$HMIM][HSO$_4$], PTS= [C$_3$SO$_3$HMIM][PTS], Cl= [C$_3$SO$_3$HMIM][Cl] and H2PO4= [C$_3$SO$_3$HMIM][H$_2$PO$_4$] BAILs.

Table 2A.13. Thermodynamic parameter (ΔH, ΔS and ΔE_aH^+) of PNA with BAILs and mineral acid adduct at different temperatures.

BAILs and mineral acid	Linear equation	ΔH (KJ/mol)	ΔS (J/K mol)	Linear equation	ΔE_aH^+ (KJ /mol)
H_2SO_4	y= 931.34x - 3.8243	-7.7	-31.8	y= -449.06x + 1.7726	3.7
$[C_3SO_3HMIM][HSO_4]$	y = 1638.9x - 5.7094	-13.6	-47.4	y= -234.93x + 1.256	1.9
$[C_3SO_3HMIM][PTS]$	y= 2734x - 9.8923	-22.7	-82.3	y= -628.9x + 2.633	5.2
$[C_3SO_3HMIM][Cl]$	y= 1118.3x - 5.2245	-9.3	-43.4	y= -57.173x + 0.9101	0.5
$[C_3SO_3HMIM][H_2PO_4]$	y= 1605.8x - 7.2623	-13.3	-60.4	y= -367.98x + 2.0051	3.1

2A.8.2. Calculation of thermodynamic parameters of BAILs and mineral acid on mole basis (H^+= 2.78 mmol)

With the help of UV-Vis spectroscopy, thermodynamic parameters (K_{eq}, ΔG, ΔH, ΔS and E_aH^+) are calculated for the BAILs and mineral acid (H^+= 2.78 mmol) in PNA solution (2 mg in 1000 mL Millipore water). Details of the methods used for the calculation of thermodynamic parameters are given in Section 2A.8. However, the data generated by using equations 2A.2 to 2A.7 are tabulated below.

Table 2A.14. pH of BAILs and mineral acid (H^+= 2.78 mmol in 10 mL PNA solution) at different temperatures.

ILs and mineral acid	T, (K)				
	298.15	308.15	318.15	328.15	338.15
PNA	7.95	7.92	7.89	7.81	7.86
H_2SO_4	2.94	2.90	2.86	2.79	2.86
$[C_3SO_3HMIM][HSO_4]$	2.85	2.84	2.80	2.76	2.73
$[C_3SO_3HMIM][PTS]$	2.78	2.69	2.57	2.68	2.72
$[C_3SO_3HMIM][Cl]$	2.97	2.96	2.94	2.79	2.88
$[C_3SO_3HMIM][H_2PO_4]$	3.21	3.11	3.09	2.98	3.23

Table 2A.15. Absorbance (A max. 380.4 nm) of PNA with BAILs and mineral acid adduct at different temperatures.

T, (K)	PNA	H_2SO_4	$[C_3SO_3HMIM]$ $[HSO_4]$	$[C_3SO_3HMIM]$ $[PTS]$	$[C_3SO_3HMIM]$ $[Cl]$	$[C_3SO_3HMIM]$ $[H_2PO_4]$
298.15	0.2316	0.2103	0.2054	0.2109	0.2136	0.2150
308.15	0.2314	0.2104	0.2060	0.2157	0.2171	0.2175
318.15	0.2308	0.2099	0.2060	0.2169	0.2183	0.2198
328.15	0.2291	0.2081	0.2054	0.2157	0.2165	0.2239
338.15	0.2268	0.2052	0.2056	0.2147	0.2147	0.2246

Table 2A.16. Hammett acidity function (H_0) of PNA with BAILs and mineral acid adduct at different temperatures.

T, (K)	(H_0)				
	H_2SO_4	$[C_3SO_3HMIM]$ $[HSO_4]$	$[C_3SO_3HMIM]$ $[PTS]$	$[C_3SO_3HMIM]$ $[Cl]$	$[C_3SO_3HMIM]$ $[H_2PO_4]$
298.15	1.98	1.88	1.99	2.06	2.06
308.15	1.99	1.89	2.13	2.17	2.18
318.15	1.99	1.91	2.18	2.23	2.29
328.15	1.99	1.93	2.19	2.22	2.62
338.15	1.97	1.98	2.22	2.24	2.99

Table 2A.17. Chemical equilibrium (Keq) of PNA with BAILs and mineral acid adduct at different temperatures.

T, (K)	Keq				
	H_2SO_4	$[C_3SO_3HMIM]$ $[HSO_4]$	$[C_3SO_3HMIM]$ $[PTS]$	$[C_3SO_3HMIM]$ $[Cl]$	$[C_3SO_3HMIM]$ $[H_2PO_4]$
298.15	0.30	0.36	0.27	0.25	0.25
308.15	0.24	0.35	0.20	0.20	0.20
318.15	0.28	0.34	0.16	0.17	0.15
328.15	0.28	0.32	0.17	0.16	0.07
338.15	0.30	0.28	0.16	0.16	0.03

Table 2A.18. Gibbs free energy (ΔG) of PNA with BAILs and mineral acid adduct at different temperatures.

T, (K)	ΔG, (J/K mol)				
	H_2SO_4	[C$_3$SO$_3$HMIM] [HSO$_4$]	[C$_3$SO$_3$HMIM] [PTS]	[C$_3$SO$_3$HMIM] [Cl]	[C$_3$SO$_3$HMIM] [H$_2$PO$_4$]
298.15	2999.0	2503.3	3219.2	7963.4	7962.6
308.15	3660.1	2612.5	4180.2	4189.0	4138.4
318.15	3407.4	2874.4	4772.6	4711.4	4935.9
328.15	3457.2	3147.2	4891.1	4960.1	7286.4
338.15	3376.5	3563.7	5150.5	5109.9	9680.9

Table 2A.19. lnKeq verses 1/T, (K) of PNA with BAILs and mineral acid adduct at different temperatures.

1/T, (K)	lnKeq				
	H_2SO_4	[C$_3$SO$_3$HMIM] [HSO$_4$]	[C$_3$SO$_3$HMIM] [PTS]	[C$_3$SO$_3$HMIM] [Cl]	[C$_3$SO$_3$HMIM] [H$_2$PO$_4$]
0.00335	-1.21	-1.01	-1.298	-1.395	-1.395
0.00325	-1.43	-1.05	-1.632	-1.635	-1.615
0.00314	-1.29	-1.09	-1.804	-1.78	-1.87
0.00305	-1.27	-1.15	-1.79	-1.82	-2.67
0.00296	-1.2	-1.27	-1.832	-1.818	-3.44
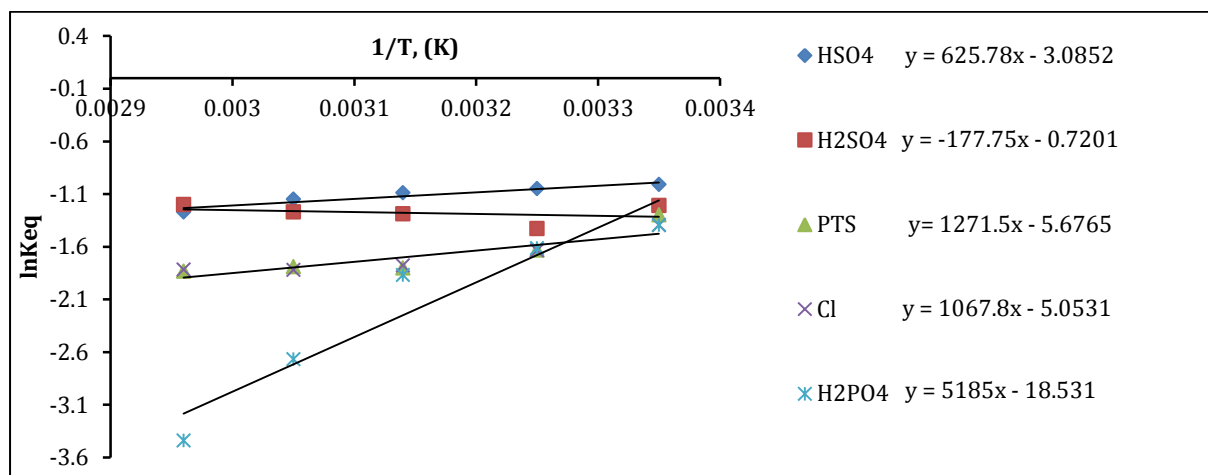
Figure 2A.23. Plot of lnKeq against 1/T, (K) for BAILs and mineral acid (H$^+$= 2.78 mmol sample in 10 mL PNA solution). The abbreviations assigned as in the Figure 2A.23 are HSO4= [C$_3$SO$_3$HMIM][HSO$_4$], PTS= [C$_3$SO$_3$HMIM][PTS], Cl= [C$_3$SO$_3$HMIM][Cl] and H2PO4= [C$_3$SO$_3$HMIM][H$_2$PO$_4$] BAILs.

Table 2A.20. $\ln H_0$ verses $1/T$, (K) of PNA with BAILs and mineral acid adducts at different temperatures.

1/T, (K)	$\ln H_0$				
	H_2SO_4	$[C_3SO_3HMIM]$ $[HSO_4]$	$[C_3SO_3HMIM]$ $[PTS]$	$[C_3SO_3HMIM]$ $[Cl]$	$[C_3SO_3HMIM]$ $[H_2PO_4]$
0.00335	0.683	0.631	0.69	0.72	0.72
0.00325	0.69	0.64	0.76	0.77	0.78
0.00314	0.69	0.65	0.78	0.8	0.83
0.00305	0.69	0.66	0.78	0.8	0.96
0.00296	0.68	0.68	0.8	0.81	1.1
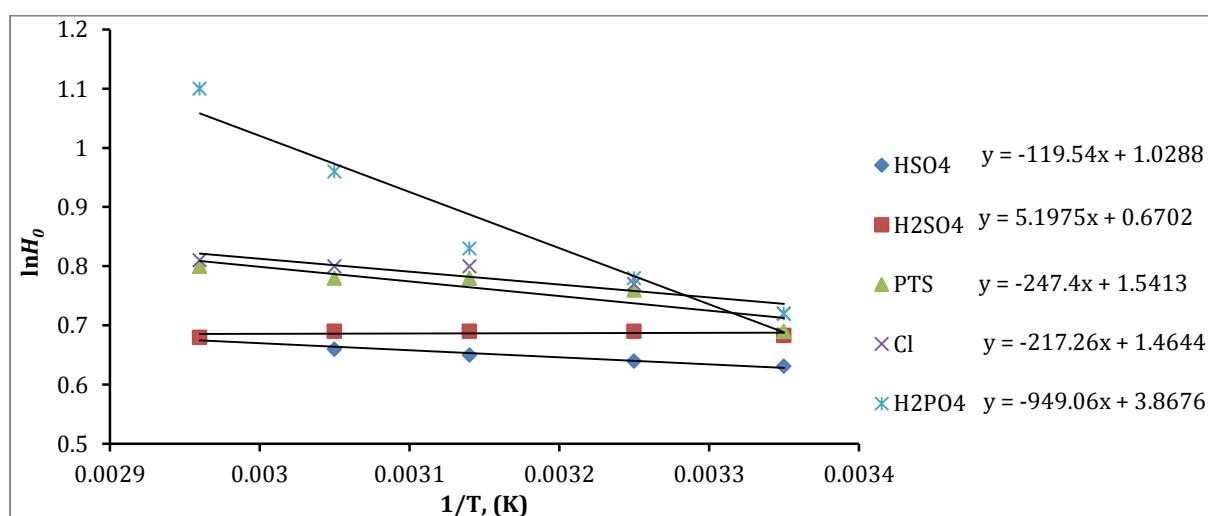
Figure 2A.24. Plot of $\ln H_0$ against $1/T$, (K) for BAILs and mineral acid (H^+= 2.78 mmol sample in 10 mL PNA solution). The abbreviations assigned as in the Figure 2A.24 are HSO4= $[C_3SO_3HMIM][HSO_4]$, PTS= $[C_3SO_3HMIM][PTS]$, Cl= $[C_3SO_3HMIM][Cl]$ and H2PO4= $[C_3SO_3HMIM][H_2PO_4]$ BAILs.

Table 2A.21. Thermodynamic parameter (ΔH, ΔS and ΔE_{aH^+}) of adducts at different temperatures.

BAILs and mineral acid	Linear equation	ΔH (KJ/mol)	ΔS (J/K mol)	Linear equation	$\Delta E_a H^+$ (KJ/mol)
H_2SO_4	y= -177.75x - 0.7201	1.5	-6.0	y= 5.1975x + 0.6702	-0.04
$[C_3SO_3HMIM]$ $[HSO_4]$	y = 625.78x - 3.0852	-5.2	-25.6	y= -119.54x + 1.0288	1.0
$[C_3SO_3HMIM]$ $[PTS]$	y= 1271.5x - 5.6765	-10.6	-47.2	y= -247.4x + 1.5413	2.1
$[C_3SO_3HMIM]$ $[Cl]$	y = 1067.8x - 5.0531	-8.9	-42.0	y= -217.26x + 1.4644	1.8
$[C_3SO_3HMIM]$ $[H_2PO_4]$	y = 5185x - 18.531	-42.9	-154.1	y= -949.06x + 3.8676	7.9

The thermodynamic parameters (ΔG, Keq, ΔH, ΔS and $\Delta E_a H^+$) are calculated for the BAILs and mineral acid, and the data is given in Tables 2A.6-2A.21. It is observed from tables that ΔG is positive, which conclude that reactions will not proceed spontaneous. By definition, there are evidently, two factors which contribute to the value of ΔG. These are the energy factor ΔH and the entropy ΔS. Both are having the similar contribution for the spontaneous reaction. For negative ΔG values, the ΔH values should be negative and TΔS positive. While at high temperature entropy factor are predominant (i.e. endothermic reaction). Although at low temperature energy factor (i.e. exothermic reaction) ΔH always negative and decrease in the entropy. To sum up of the above statement, it is clear that for the spontaneous reaction, ΔG should be negative.

Another factor for the reaction to achieve better yield is the activation energy ($\Delta E_a H^+$). Lower the activation barrier means lower the activation energy, which favours the faster reaction towards the forward direction.

More details on thermodynamic parameter and their correlation with lignin depolymerization studied are discussed in Chapter 3.

2A.9. Conclusions

A number of ILs are synthesized to evaluate their activities in lignin depolymerzaition studies to yield low molecular weight aromatic products. To check the effect of anions, cations and acidity in lignin depolymerization reaction various types of ILs with Brønsted acidity, Lewis acidity, without acidity and combination of Brønsted and Lewis acidity are synthesised (using quarterisation and direct combination methods), and characterised in details using several techniques (NMR, FT-IR, elemental analysis, TGA and UV-Vis). These characterizations revealed that synthesized ILs are pure and stable up to 250 °C. Thermodynamic parameters of the BAILs

and mineral acid have also been calculated using UV-Vis absorption studies by comparing the difference in absorbance of neat PNA solution and adduct forms of PNA solution with BAILs and mineral acid.

From the Hammett acidity (H_0) function and thermodynamic parameters results, it is understandable that the chemical properties (acidity, enthalpy, entropy, activation energy, etc.) of the BAILs and mineral acid vary by virtue of cations, anions and their combinations. Effects of the various physical and chemical properties of the BAILs and mineral acid on the depolymerization of lignin into low molecular weight aromatic products have been studied in details and the discussions are made in Chapter 3. Next section i.e. 2B contains the details on the synthesis and characterization of Immobilized-Brønsted acidic ionic liquid.

2A.10. References

1.	G. W. Huber, S. Iborra and A. Corma, *Chem. Rev.*, 2006, **106**, 4044-4098.
2.	P. Bhaumik and P. L. Dhepe, *Catalysis Reviews*, 2016, **58**, 36-112.
3.	G. W. Huber and A. Corma, *Angew. Chem. Int. Ed.*, 2007, **46**, 7184-7201.
4.	C.-H. Zhou, X. Xia, C.-X. Lin, D.-S. Tong and J. Beltramini, *Chem. Soc. Rev.*, 2011, **40**, 5588-5617.
5.	A. Corma, S. Iborra and A. Velty, *Chem. Rev.*, 2007, **107**, 2411-2502.
6.	J. Zakzeski, P. C. A. Bruijnincx, A. L. Jongerius and B. M. Weckhuysen, *Chem. Rev.*, 2010, **110**, 3552-3599.
7.	B. M. Matsagar and P. L. Dhepe, *Catal. Sci. Technol.*, 2015, **5**, 531-539.
8.	G. A. Kraus and T. Guney, *Green Chem.*, 2012, **14**, 1593-1596.
9.	R. Kore, T. J. D. Kumar and R. Srivastava, *J. Mol. Catal. A: Chem.*, 2012, **360**, 61-70.
10.	R. Kore and R. Srivastava, *Tetrahedron Lett.*, 2012, **53**, 3245-3249.
11.	L. Zhang, M. Xian, Y. He, L. Li, J. Yang, S. Yu and X. Xu, *Bioresour. Technol.*, 2009, **100**, 4368-4373.
12.	E. Delahaye, R. Gobel, R. Lobbicke, R. Guillot, C. Sieber and A. Taubert, *J. Mater. Chem.*, 2012, **22**, 17140-17146.
13.	D. Fang, K. Gong, Q. Shi and Z. Liu, *Catal. Commun.*, 2007, **8**, 1463-1466.
14.	S. K. Singh and P. L. Dhepe, *Green Chem.*, 2016, **18**, 4098-4108.

Section 2B:

Immobilized-Brønsted acidic ionic liquid

(I-BAIL)

2B.1. Introduction

The molten salts having melting point <100 ^oC are called ionic liquids (ILs). Due to their important properties, such as low vapour pressure, high thermal stability, excellent solubility, tuneable acidity or basicity by changing the combination of cations or anions, etc. those find much uses in several chemical transformations.[1-8] ILs have also been used as solvent or catalyst in the conversion of lignocellulosic biomass.[9] The use of ILs as solvent is a costly process and it is economically unfavourable and because of their highly viscous nature, it becomes hurdle to achieve maximum yield of the products. At the large scale, disposal of the recovered impure IL samples is another major problem. A lot of research has been devoted towards immobilization of ILs to overcome the problem of easy seperation.[10-14]

Maryam Nouri *et at.* has shown the preparation of N-(3-silicapropyl) imidazolium hydrogen sulphate supported ILs as solid acid catalysts.[12] Authors have refluxed the silica propyl chloride with excess quantity of imidazole mixture in anhydrous toluene. The resultant mixture of silica chemically bonded with imidazole was dried and further used for N-(3-silicapropyl) imidazolium hydrogen sulphate preparation. Into the dried solid, concentrated H_2SO_4 was added and the resulting mixture was kept for stirring under reflux condition for 48 h. Finally the silica based ILs as solid catalyst was obtained after washing and drying the resultant mixture. From the elemental and TGA analysis, they have concluded that only 4 *wt.*% organic moieties are present in the N-(3-silicapropyl) imidazolium hydrogen sulphate catalyst.[12] The details about the synthesis procedure are given in Scheme 2B.1.

([Sipim]H₂SO₄)

(a) (MeO)₃Si-(CH₂)₃-Cl, toluene(dry), Et₃N, reflux, 48 h;   (b) Imidazole, toluene (dry), 24 h, reflux;
(c) Dry under vaccum (50 °C), 4 h;   (d) CH₂Cl₂ (dry, H₂SO₄ (97%), 48 h, reflux
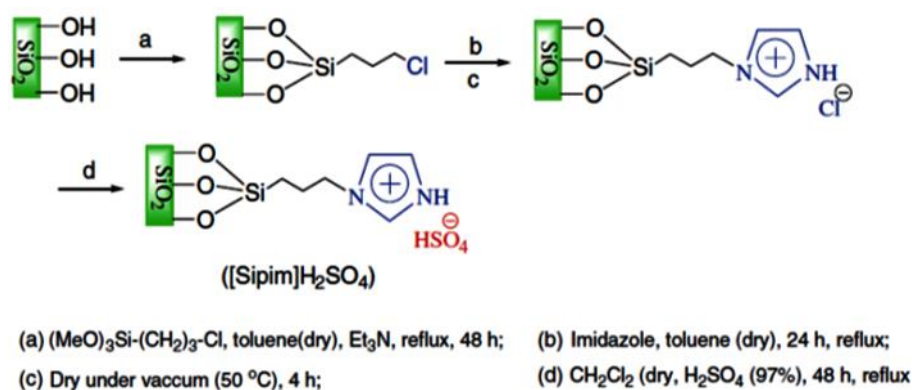
Scheme 2B.1. Synthesis of silica supported IL.[12]

In other report Qiang Zhang *et al.* has shown another way to synthesis silica gel supported IL. Authors have shown the covalent attachment of ILs to the silica surface. The TGA and elemental analysis of synthesized supported ILs catalyst showed that 24 *wt.*% grafting of ILs on/in silica surface is possible.[11] The details of the synthesis procedure of silica gel supported acidic ILs are given in Scheme 2B.2.
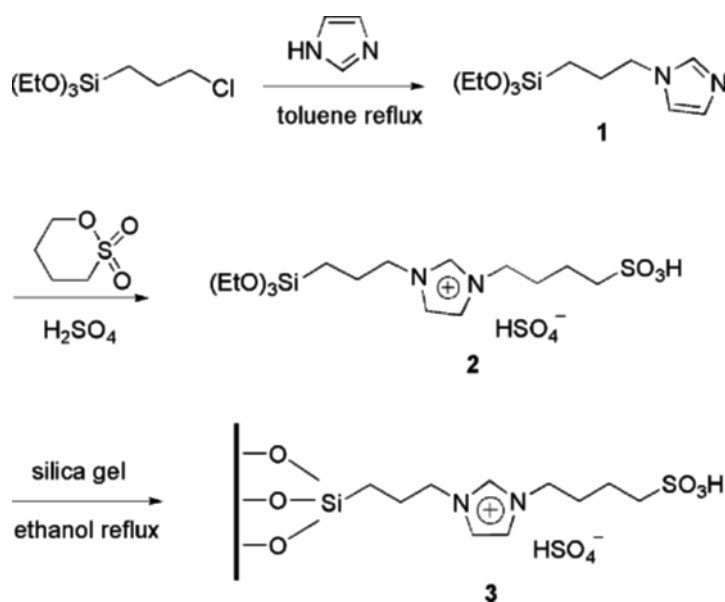
Scheme 2B.2. Synthesis of solid acid catalyst by the silica gel supported IL.[11]

Similarly, Abhishek K. G. *et al.* has used sol-gel method to synthesis supported ILs. In this method, researchers have used the different steps for the synthesis of low density ionogel samples. Particular molar ratio of tetraethylorthosilane, formic acid and the ILs are mixed and allowed to gellify at 30 ℃ for 5-6 days.[15] For more details about the synthesis procedure of the supported ILs please refer Scheme 2B.3.
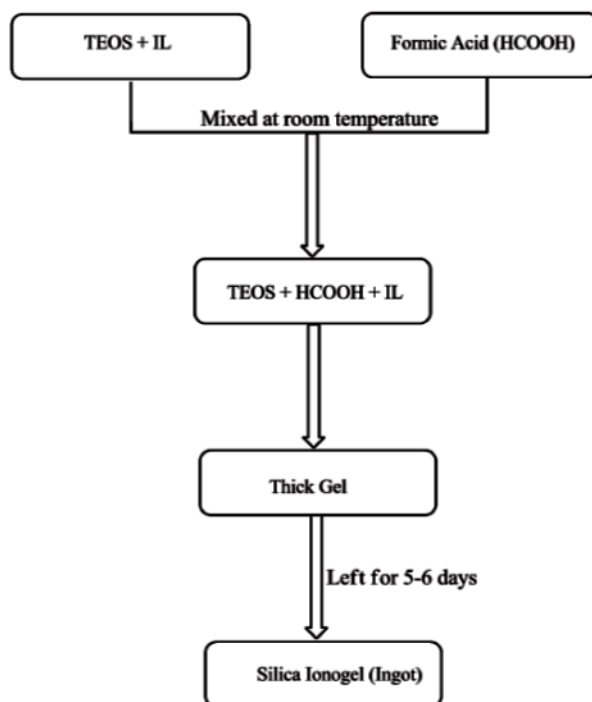
Scheme 2B.3. Steps used in the synthesis of ionogels *via* the sol-gel path.[15]

The supported IL as solid acid catalysts was synthesized with covalent anchoring method, which was prepared by the addition of *N*-3-(3-triethoxysilylpropyl)-4,5-dihydroimidazol and 1-chlorobutane to form 1-butyl-3-(3-triethoxysilylpropyl)-4,5-dihydroimidazolium chloride.

However, maximum 25 *wt.*% loading of ILs on/in silica support materials was analysed.[14] For more details about the synthesis procedure of the supported ILs please see Scheme 2B.4.
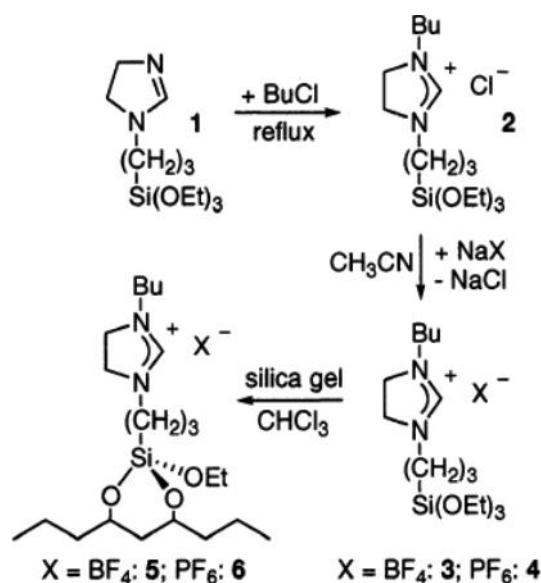
Scheme 2B.4. Synthesis of surface anchored IL.[14]

The intense research activity has been focussed on/in modifying the surface morphology of silica materials with functionalising ILs to get supported ILs as solid acid catalysts. However, due to low degree of immobilization of ILs (in the range between 4-28%) on/in the silica framework, use of excess amount reagents, leaching of ILs during the reaction from the supports and lower thermal stability are major problems with reported methods. Considering this improvements in immobilization processes are required. Another importance of the immobilization requirement is that ILs are homogeneous in nature and thus it is difficult to separate those from reaction mixture.[11-15] By virtue of immobilizing those, easy separation is possible. However, still the efficient immobilization processes is largely unaddressed.

Objective of the current study is to provide a new process for the synthesis of Immobilized-Brønsted acidic ionic liquid (I-BAIL) as solid acid catalyst by virtue of developing efficient method. The I-BAIL has potential to be used as solid acid catalysts in the lignin depolymerization reaction. Details on the synthesis of I-BAIL are as below.

2B.2. Experimental

2B.2.1. Materials

Imidazole (Alfa Aesar UK, 99%), 1,3-propanesultone (Alfa Aesar India, 99%), sulphuric acid (Loba Chemie India, 98%), 3-chloropropyl trimethoxysilane (Sigma Aldrich USA, 97%), tetraethoxysilane (Sigma Aldrich USA, 98%), and ethanol (Changshu Yangyuan Chemical China, 99.9%), used as received.

2B.2.2. Synthesis of Immobilized-Brønsted acidic ionic liquid (I-BAIL)

I-BAIL materials were synthesized as shown in Figure 2B.1 and as mentioned below,

Solution 'a':

Molar composition= 1.0 imidazole: 1.0 1,3-propanesultone: 1.0 sulphuric acid

3.0 g imidazole was taken in a beaker and the beaker was kept in water bath maintained at room temperature (27 ^{o}C). To imidazole, 5.4 g 1,3-propanesultone was added dropwise within 5 minute. Subsequently, 10 mL distilled water was added and the mixture was stirred (over magnetic stirrer) at room temperature for 2 h. To this solution, 4.4 g H_2SO_4 was added drop wise under slow stirring. This solution was stirred vigorously at room temperature for 2 h. This solution is named as 'a'.

Solution 'b':

Molar composition= 4.0 3-chloropropyl trimethoxysilane: 3.0 tetraethoxysilane

In a beaker, 9.0 g 3-chloropropyl trimethoxysilane was taken and to it 6.9 g tetraethoxysilane dissolved in 20 mL ethanol was added. The resulting solution was stirred at room temperature for 4 h. This solution is named as 'b'.

Afterwards, solution 'a' was added dropwise into solution 'b' at room temperature (27 ^{o}C) under slow stirring over magnetic stirrer. After immediate addition of solution 'a' into 'b', solution becomes turbid but slowly it changes to transparent solution. Further, this solution is stirred for 5 h at room temperature. Then the resulting solution was transferred into three Teflon lined steel autoclaves and subjected to aging (crystallization) for time period [168 h (7 days)] at 100 ^{o}C under atmospheric pressure at static condition. After cooling down the autoclave, solid materials were filtered, washed with 600 mL distilled water to remove unreacted reagents and H_2SO_4 and dried in an oven maintained at 55 ^{o}C for 2 h. Later, solid material was dried in vacuum (-0.101 MPa) oven at 100 ^{o}C for 4 h. Material with crystallization time of 168 h (7 days) named as I-BAIL. Similar process was used for the synthesis of silica.
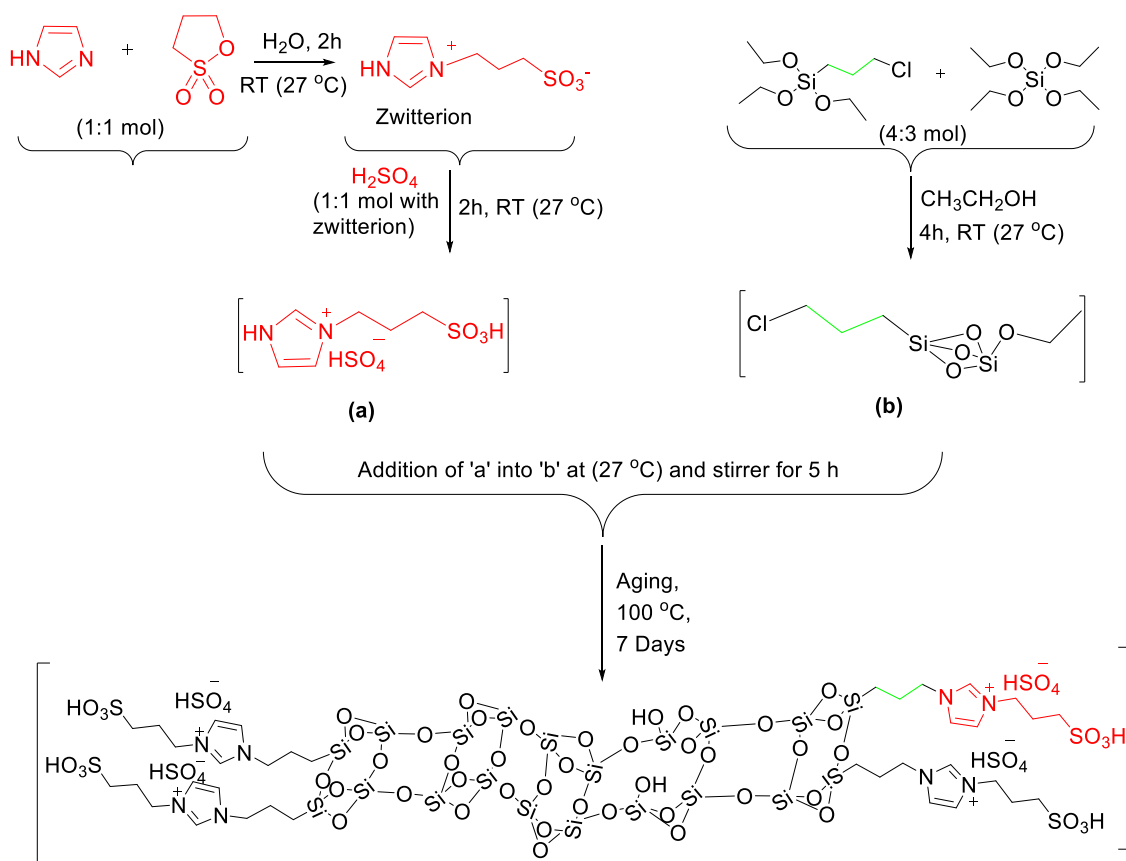
Figure 2B.1. Synthesis of Immobilized-Brønsted acidic ionic liquid (I-BAIL) and proposed structure of I-BAIL.

2B.3. Characterization of Immobilized-Brønsted acidic ionic liquid (I-BAIL)

I-BAIL was characterized with the help of elemental analysis, thermogravimetric analysis-differential thermal analysis (TGA-DTA), X-ray diffraction (XRD), solid state ^{13}C and ^{29}Si magic-angle spectroscopy (MAS) nuclear magnetic resonance (NMR), Fourier transformation–infra red (FT-IR), ultra violet-visible (UV-Vis) spectroscopy, scanning electron microscopy along with energy dispersive X-ray diffraction (SEM-EDX) and transmission electron microscopy (TEM).

2B.3.1. Elemental analysis of I-BAIL

Elemental analysis was done in Thermo Finnigan, Italy; model EA1112 Series Flash Elemental Analyzer. The amount of C, H, N and S in sample is determined by rapid combustion of small amount (ca. 10 mg) of the sample in pure O_2 (Dumas method or "flash combustion").

The CHNS elemental analysis of I-BAIL is (%); C, 17.60, H, 3.01, N, 4.39 and S, 10.51). This result is similar to decomposition mass loss of I-BAIL through TGA (ca. 45 *wt.* %).

2B.3.2. Thermogravimetric analysis-differential thermal analysis (TGA-DTA) of silica and I-BAIL

The TGA-DTA (air) of I-BAIL and silica samples were studied using METTLER TOLEDO TGA / SDTA851 series, USA; instrument. The following program is used for the analysis;

50 °C→ 10 °C/min → 800 °C (air).

TGA-DTA study was performed under air environment. TGA-DTA graph of silica and I-BAIL are shown in Figure 2B.2. As seen, I-BAIL is stable until 250 °C and then weight loss of ca. 45% is seen until 700 °C. After this temperature, no weight loss is observed up to 800 °C due to presence of silica in the I-BAIL catalyst. The weight loss observed until 700 °C is mainly due to loss of organic moieties such as IL immobilized on/in silica.[11]
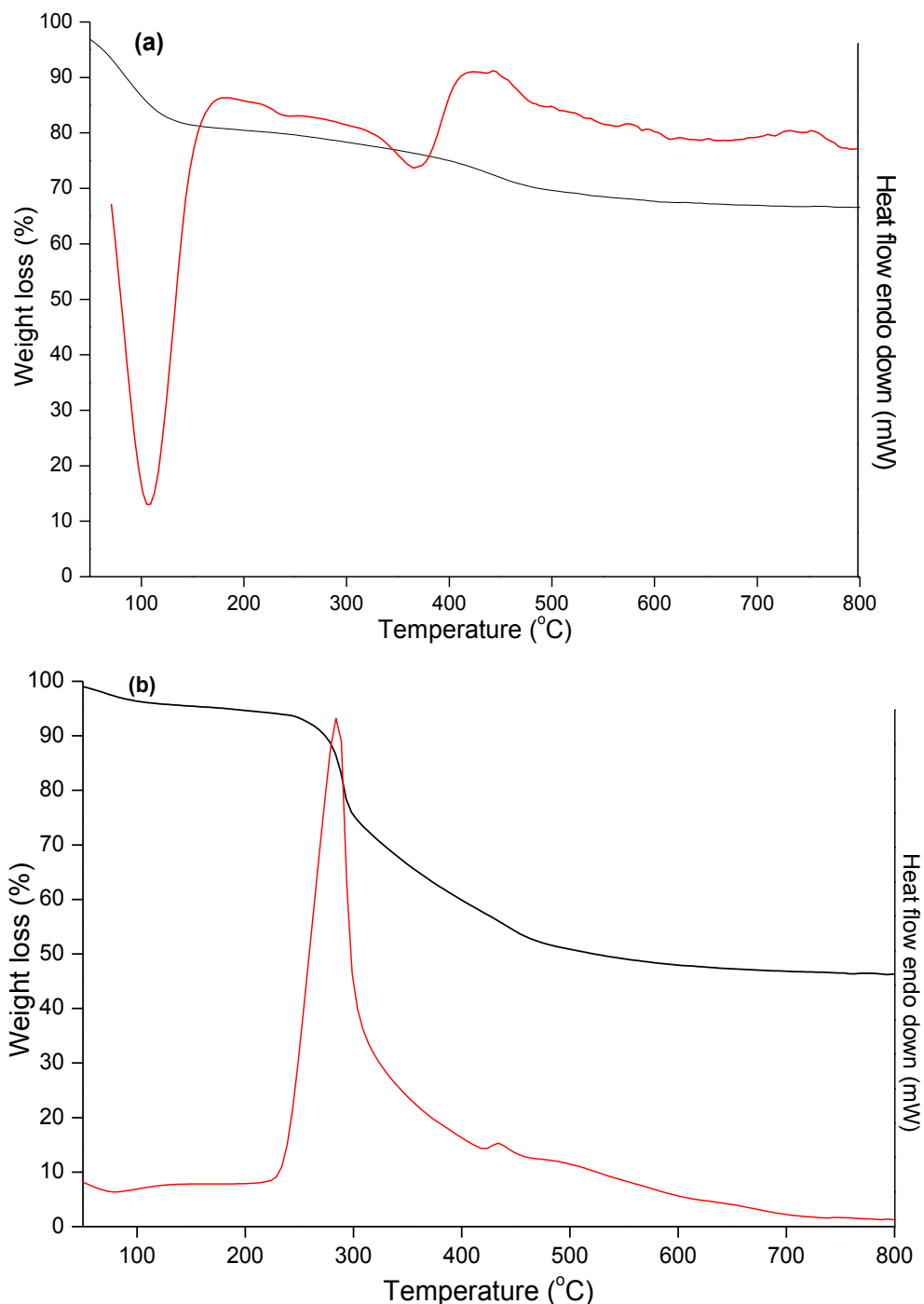
Figure 2B.2. Thermogravimetric analysis-differential thermal analysis (TGA-DTA, Air) of (a) silica and (b) I-BAIL.

To compare the results, silica (SiO_2) prepared in the laboratory using TEOS is subjected to TGA-DTA analysis and it is observed that it losses ca. 11% weight until 150 °C mainly due to loss

of physically adsorbed water. Silica has more hydrophilic nature than I-BAIL, due to presence of maximum surface (inner or outer) hydroxyl groups, which is confirmed from FT-IR spectrum of silica. Similarly, I-BAIL has maximum organic moieties (confirmed by CHNS and TGA-DTA analysis), because of same, it will show the hydrophobicity or less moisture to the I-BAIL sample, which is confirmed from the TGA-DTA analysis of I-BAIL sample.

From the weight loss of BAIL in I-BAIL, it was calculated that 45% of IL is immobilized in/on silica surface. This value matches well with elemental analysis (%); C-17.60, H-3.01, N-4.39 and S-10.51. According to the mole basis addition, the weight loss of BAIL in I-BAIL should be ca. 70%. However, the difference of 25% (70-45) is due to the fact that not all BAIL is immobilized on the silica surface. These values conclude that the above proposed structure is similar to the CHNS value.

2B.3.3. X-ray diffraction (XRD) of silica and I-BAIL

The Rigaku Miniflex 600, with duel goniometer diffractor instrument was used for the analysis. The source of X-ray was used Cu Kα (1.5418 Å radiation) with Ni filter. The samples were scanned from a 2θ value of 2 to 40 ° at the rate of 1°/min. The XRD pattern of the silica and I-BAIL are presented in Figure 2B.3. These XRD patterns indicate that while only silica shows broad peak at 2θ= 23.23o for amorphous nature, I-BAIL show one additional peak at 2θ = 7.16o. This peak may be assigned to T^3 type species of silica that is assigned as silica propyl (Si-$CH_2CH_2CH_2$-N) chain attached to the imidazole ring.[16]
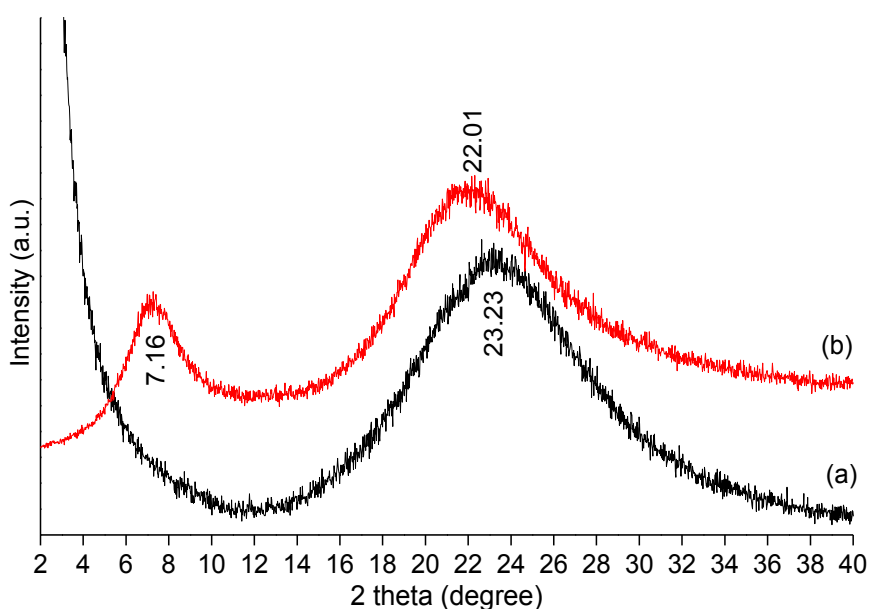
Figure 2B.3. XRD patterns of (a) silica and (b) I-BAIL catalyst.

2B.3.4. ^{13}C and ^{29}Si MAS NMR of I-BAIL

The ^{29}Si magic-angle spinning nuclear magnetic resonance (MAS NMR) and ^{13}C cross polarisation/MAS NMR spectra were recorded at 79.49 and 100.61 MHz, on a Bruker Avence-300 MHz spectrometer respectively. The adamantine and tetramethylsilane molecules were used as an internal standard for ^{13}C CP-MAS and ^{29}Si MAS NMR respectively.

The ^{29}Si MAS NMR spectrum of the I-BAIL is shown in Figure 2B.4. Silicon sites are labelled according to usual NMR notation: Q^n represents Si atoms quaternary oxygen linked, i.e. bound to (4-n) OH groups. Hence, Q^4 represents the internal siloxane type Si atoms in $Si(OSi)_4$, while Q^2 and Q^3 correspond to surface Si atoms bound to hydroxyl groups $Si(OSi)_2(OH)_2$ and $Si(OSi)_3OH$, respectively.[17] The peaks at -93.03, -102.16 and -110.57 ppm are assigned respectively to Q^2, Q^3 and Q^4 Si sites, similar to literature.[17] Besides the Q^n resonances, the spectra display a peak at -66.70 ppm in the typical range of organosiloxane Si atoms (T^3) $RSi(OSi)_3$ (R= $-(CH_2)_3-N$ (imidazole)), thus providing evidence for the chemical bonding of with SiI-IL silica-immobilized ionic liquid (SiI-IL) to the siliceous network. The intensity of this resonance increased markedly with increasing SiI-IL relative amount. The shoulder at -58.30 ppm is assigned to T^2 environments ($RSi(OSi)_2(OCH_2CH_3)$).[17]

The ^{13}C CP/MAS NMR spectrum of the I-BAIL sample is shown in Figure 2B.5. The three peaks at 10.46 (C_1), 26.92 (C_2) and 47.78 (C_3) ppm are characteristic of the Si-bonded propyl chains.[18, 19] While the N atom (imidazole) bonded propyl chains carbon is shown 47.78 (C_1), 26.92 (C_2) and 47.78 (C_3) and 115.81, 116.59 and 132.70 ppm peaks belong to imidazole ring carbon atom.[11]
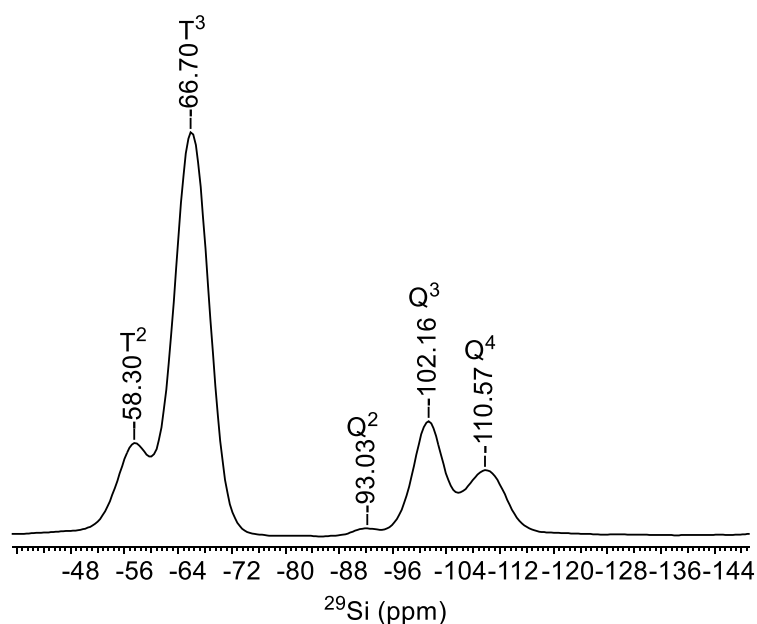
Figure 2B.4. ^{29}Si NMR of I-BAIL.
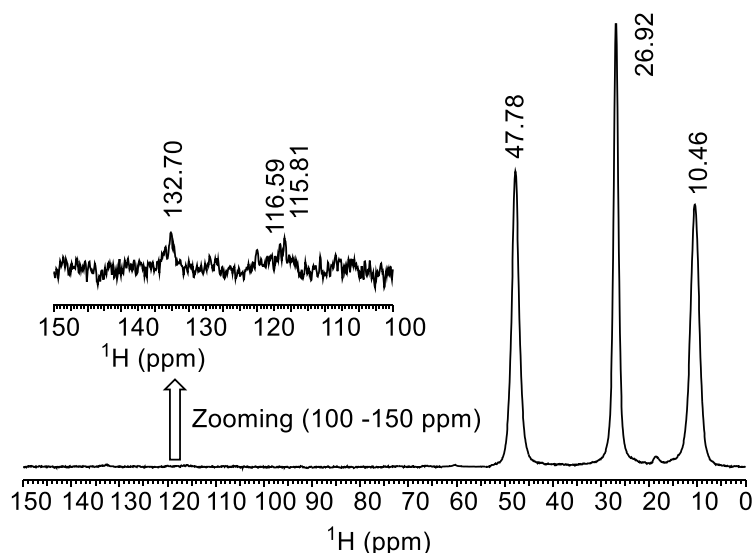
Figure 2B.5. ^{13}C NMR of I-BAIL.

2B.3.5. UV-Visible spectra of silica and I-BAIL

The electronic transition in I-BAIL and silica were identified with the help of UV-Vis absorption measurement of the sample using UV-2700 spectrophotometer Shimadzu, Japan. Solid samples were analysed from a range of λ = 200-800 nm.

UV-Vis spectra of silica and I-BAIL are shown in Figure 2B.6. In I-BAIL spectrum, peaks at 212, 242 and 280 nm belong to π-π electronic transition of aromatic/imidazole ring. While 280 and 212 nm peaks are absent in the silica. It is confirmed that I-BAIL contained imidazole ring attached with silica molecule.
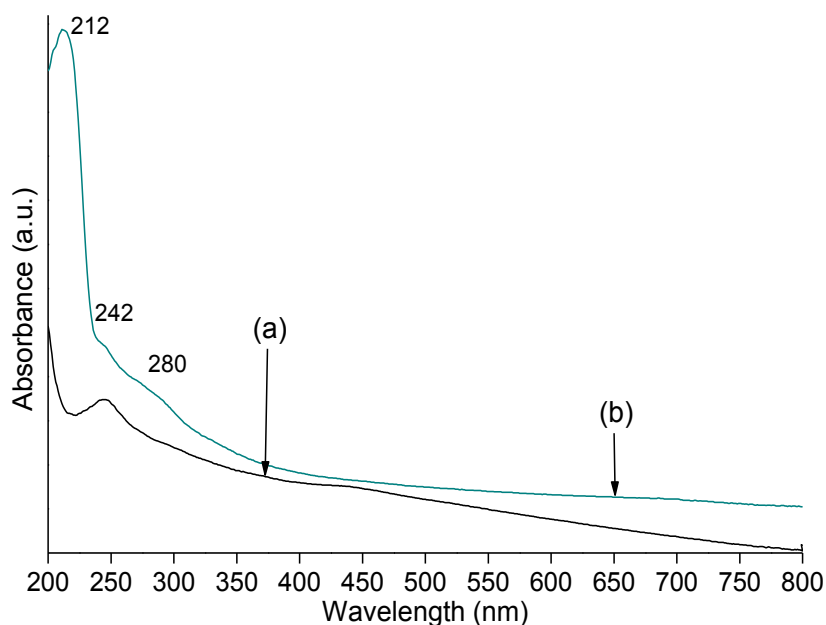
Figure 2B.6. UV-Vis spectra of (a) silica and (b) I-BAIL.

2B.3.6. FT-IR spectra of silica and I-BAIL

Presence of the functional groups on I-BAIL and silica were analysed using FT-IR (FT-IR-8300 Shimadzu) technique. For the analysis, pellets were made with KBr by maintaining 1*wt.*% concentration. The normalization of intensities was discussed based on the exact concentration used for making pellets.

FT-IR spectra of SiO_2 and I-BAIL are shown in Figure 2B.7. The amorphous SiO_2 shows the typical absorption band at 1087 cm^{-1} due to asymmetric Si–O–Si stretching mode, whereas band at 797 cm^{-1} are attributed to the symmetric Si–O–Si stretching vibration.[20] The absorption band at 465 cm^{-1} is assigned to O–Si–O deformation vibrations and stretching vibrations of Si–OH surface groups, respectively.[21] In all the samples a broad band at 3436 cm^{-1} due to moisture (H–OH) chemisorbed in the samples is visible.[22] Other peaks at 3630 cm^{-1} and 3436 cm^{-1} are assigned to the asymmetric and symmetric stretching in -OH group attached to the silica atom. While the other peaks at 2990, 2962 and 2900 cm^{-1} belonging to the symmetric and asymmetric CH_2 and CH_3 group in alkyl chain present in I-BAIL. The absorption band at 1454 cm^{-1} belong to symmetric stretching of >S=O bond of sulphur dioxide group.[23] The peaks at 1134 and 1046 cm^{-1} confirms the >S=O stretching vibration attached to R-SO_3H and HSO_4^- groups.[11] Another band at 1628 cm^{-1} is assigned to C=C stretching modes of imidazole ring and 1134 cm^{-1} also is assigned to N-C-H bending modes.[23] In imidazole ring amine, C-N stretching bands is observed in the range 1380-1250 cm^{-1}.[24] The bands at 797, 756, 647 cm^{-1} were due to in plane of imidazole ring.[23] The presence of these peaks confirmed the various groups (e.g. –C-H, N-CH_3, N-CH_2-) are linked to Immobilized-Brønsted acidic ionic liquid (I-BAIL).
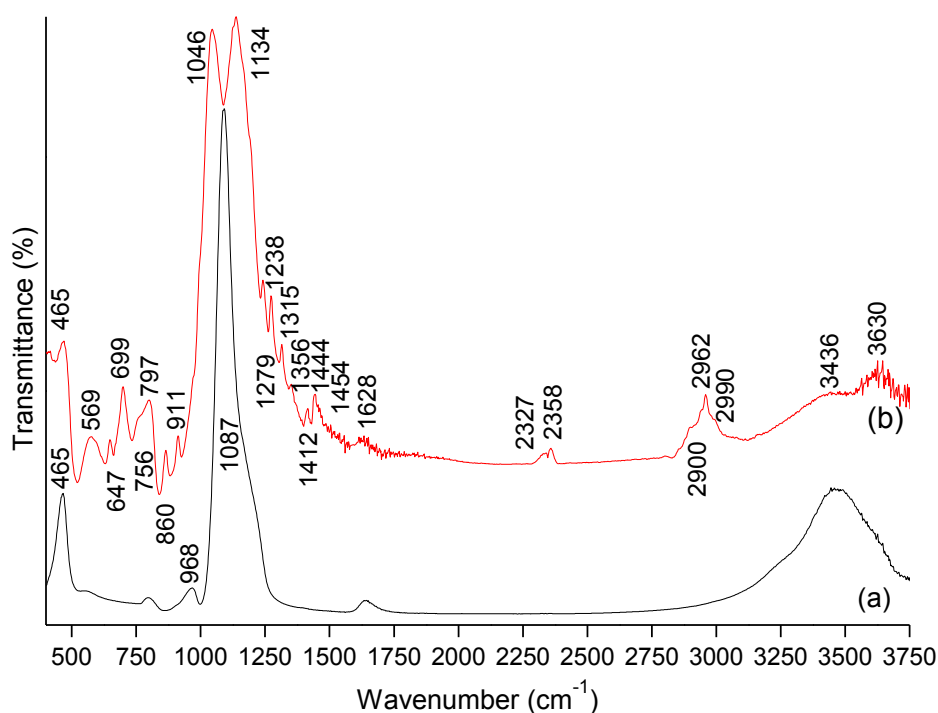
Figure 2B.7. FT-IR spectra of (a) silica and (b) I-BAIL.

2B.3.7. SEM images of silica and I-BAIL

The details on shape and morphology of the silica and I-BAIL samples were obtained in a Leo Leica Cambridge UK Model Stereo scan 440 scanning electron microscope, with an electron beam of 5-50 eV. Non-uniform morphology of silica and I-BAIL with particle size ranging from <1 μm to 10 μm in the SEM images are seen from Figure 2B.8. The rough surface of silica is shown in the Figure 2B.8a, which affirms the absence of IL on the silica surface. After immobilization of IL on/in the silica framework the smooth morphology of I-BAIL was formed, as shown in the Figure 2B.8b. The change in the morphological appearance of I-BAIL (obtained from silica) emphasized that immobilization of IL on the silica framework is successful.
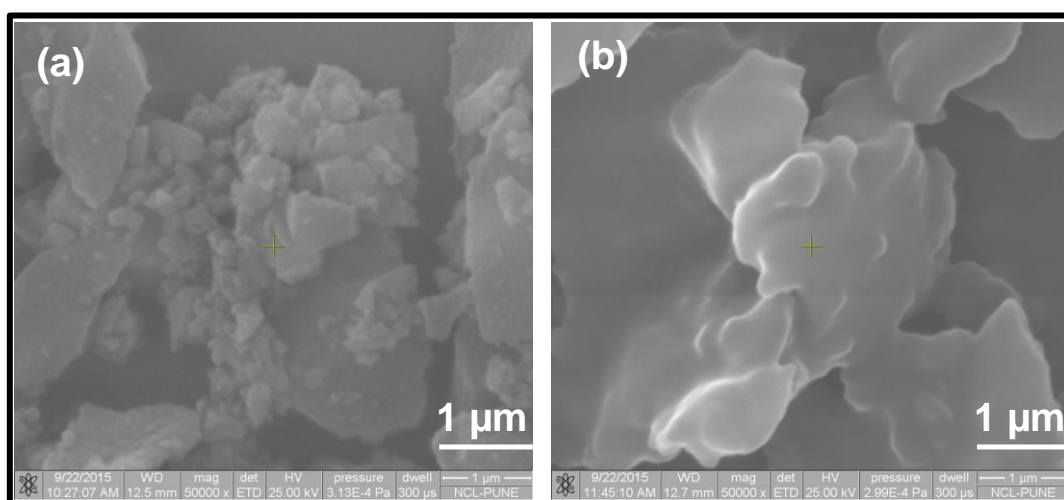
Figure 2B.8. SEM images of (a) silica and (b) I-BAIL.

2B.3.8. TEM images of silica and I-BAIL

TEM images of silica and I-BAIL samples (Figure 2B.9) were taken with FEI TECNAI T20 Model instrument operated at an accelerating voltage of 200 kV. Samples were prepared by mixing of sample in isopropanol solvent for homogeneous dispersion, and then transferred the samples on a polymeric carbon coated copper grid. The TEM image of silica (Figure 2B.9a) is differed in appearance to I-BAIL image (Figure 2B.9b). The appearance of the embedded 'void' is seen in the TEM image of I-BAIL, which confirmed that immobilization of IL on/in silica framework.
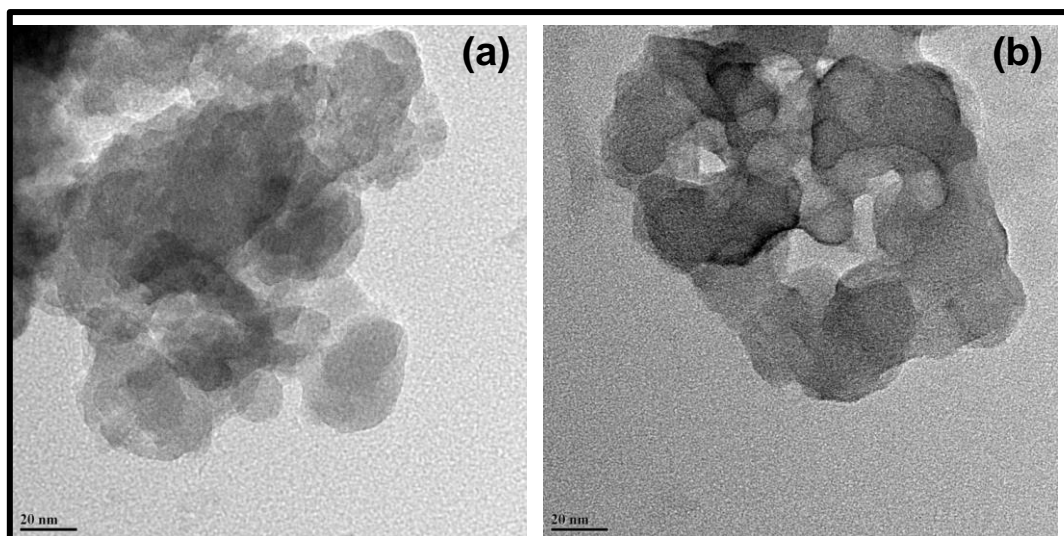
Figure 2B.9. TEM images of (a) silica and (b) I-BAIL.

2B.4. Conclusions

In the summary, I-BAIL is synthesised using quarterisation, combination and crystallization methods for the depolymerzaition of commercial and isolated (Klason and Organosolv) lignins into low molecular weight aromatic products. To check the effect of immobilization of BAIL, an aging for 7 days was applied to synthesize I-BAIL. The synthesised I-BAIL was subjected for characterization using several techniques like NMR (^{13}C and ^{29}Si), FT-IR, elemental analysis, TGA-DTA, XRD, UV-Vis, TEM, and SEM. These characterizations techniques revealed that the synthesised I-BAIL is stable up to 250 °C and 42 *wt.*% immobilisation of BAIL on/in the silica framework is possible. In the next Chapter, the characterization of commercial lignin and its depolymerization using ILs and I-BAIL as catalyst into low molecular weight aromatic products is discussed.

2B.5. References

1.   B. J. Cox and J. G. Ekerdt, *Bioresour Technol*, 2012, **118**, 584 - 588.
2.   A. George, K. Tran, T. J. Morgan, P. I. Benke, C. Berrueco, E. Lorente, B. C. Wu, J. D. Keasling, B. A. Simmons and B. M. Holmes, *Green Chem.*, 2011, **13**, 3375 - 3385.
3.   Z. C. Zhang, *Wiley Interdiscip. Rev.: Energy Environ.*, 2013, **2**, 655-672.
4.   Y. Yang, H. Fan, J. Song, Q. Meng, H. Zhou, L. Wu, G. Yang and B. Han, *Chem. Commun.*, 2015, **51**, 4028-4031.
5.   G. Chatel and R. D. Rogers, *ACS Sustainable Chem. Eng.*, 2014, **2**, 322-339.
6.   E. Reichert, R. Wintringer, D. A. Volmer and R. Hempelmann, *Phys Chem Chem Phys*, 2012, **14**, 5214 - 5221.
7.   H. Wang, M. Tucker and Y. Ji, *J. Appl. Chem.*, 2013, **2013**, 1-9.
8.   J. Long, W. Lou, L. Wang, B. Yin and X. Li, *Chem. Eng. Sci.*, 2015, **122**, 24-33.
9.   N. Sun, H. Rodriguez, M. Rahman and R. D. Rogers, *Chem. Commun.*, 2011, **47**, 1405-1421.
10.   B. Xin and J. Hao, *Chem. Soc. Rev.*, 2014, **43**, 7171-7187.
11.   Q. Zhang, J. Luo and Y. Wei, *Green Chem.*, 2010, **12**, 2246-2254.
12.   M. Nouri Sefat, D. Saberi and K. Niknam, *Catal Lett*, 2011, **141**, 1713-1720.

13. A. Chrobok, S. Baj, W. Pudło and A. Jarzębski, *Appl. Catal., A*, 2009, **366**, 22-28.
14. C. P. Mehnert, R. A. Cook, N. C. Dispenziere and M. Afeworki, *J. Am. Chem. Soc.*, 2002, **124**, 12932-12933.
15. A. K. Gupta, M. P. Singh, R. K. Singh and S. Chandra, *Dalton Transactions*, 2012, **41**, 6263-6271.
16. D. R. d. Carmo, M. d. S. Magossi, U. d. O. Bicalho and D. R. Silvestrini, *Int. J. Chem.*, 2014, **6**, 22-33.
17. G. B. B. Varadwaj, S. Rana, K. Parida and B. B. Nayak, *J. Mater. Chem. A*, 2014, **2**, 7526-7534.
18. S. L. C. Pinho, H. Faneca, C. F. G. C. Geraldes, M. H. Delville, L. D. Carlos and J. Rocha, *Biomaterials*, 2012, **33**, 925-935.
19. X. Zhang and Y. Fan, *J. Non-Cryst. Solids*, 2012, **358**, 337-341.
20. M. A. Mondragon, V. M. Castano, M. J. Garcia and S. C.A. Tellez, *Vib. Spectrosc.*, 1995, **9**, 293-304.
21. J. Lin, H. Chen, Y. Ji and Y. Zhang, *Colloids Surf., A*, 2012, **411**, 111-121.
22. I. A. Rahman, M. Jafarzadeh and C. S. Sipaut, *Ceram. Int.*, 2009, **35**, 1883-1888.
23. P. Gupta, M. Kour, S. Paul and J. H. Clark, *RSC Adv.*, 2014, **4**, 7461-7470.
24. H. U. Gremlich, in *Handbook of Analytical Techniques*, Wiley-VCH Verlag GmbH, 2008, DOI: 10.1002/9783527618323.ch17, pp. 465-507.

Chapter 3:

Characterization of commercial lignin and its depolymerization using acidic ionic liquids

Section 3A:

Characterization of lignin

3A.1. Lignin and catalyst characterization techniques

The structures of lignin molecules are dependent on several factors such as age/type of plant species, weather, soil nutrients, isolations procedures, etc.[1-4] In most of the lignin depolymerization studied, researchers have used lignin model compounds as initial substrate and converted those in to monomer units.[5, 6] Characterization of lignin model compounds are comparatively easier owing to their low molecular weight and less intrinsic structure than lignin (real) molecules.[7, 8] However, in the current work, lignin (real lignin) depolymerization reactions were carried out using homogeneous or immobilized-Brønsted acidic ionic liquids into low molecular weight aromatic products. Before lignin depolymerization reaction, it was essential to characterize lignins on bulk and molecular levels to understand their various physico-chemical properties.[9-11] The details on the analytical instruments, sample preparation and analysis methods used for the lignin characterization are described below.

3A.1.1. Gel permeation chromatography (GPC)

GPC analysis is similar to size exclusive chromatography or molecular sieve chromatography. These instruments are used to determine the molecular weight of the compounds based on their size or hydrodynamic volume and also it is an useful technique for determining the molecular weight of the polymers. The dissolved macromolecule lignin sample in THF, DMF or water solvents is passed through the column, which is filled with stationary materials like gel or porous beads (styragel or PL gel). Mainly THF, DMF or water solvents are used as mobile phase and sample should be absolutely soluble into these solvents at room temperature. In a typical GPC analysis molecules of smaller size penetrate into porous gel which delays their elution and in contrast larger molecules which cannot enter porous gel elutes fast. UV-Vis, refractive index (RI) and light scattering detectors are mainly used in GPC analysis. For the number average molecular weight (Mn) and weight average molecular weight (Mw) sample analysis, polystyrene is mainly used as a calibration standard. The ratio of the weight average molecular weight and number average molecular weight gives the polydispersity index (P.D.I=Mw/Mn). GPC of the lignin and depolymerized product samples were performed using Viscotek VE 1122 pump, Viscotek VE 3580 RI detector and Viscotek VE 3210 UV–Vis detector in tetrahydrofuran (THF) or dimethyl formamide (DMF) solvent using polystyrene as a calibration standard. The detector and column temperature were kept at 35 ºC with a constant flow rate of mobile phase (1 mL/min) used for the GPC analysis.

The weight and number average molecular weight of the samples were calculated with the help of following equation 3A.1.

$$Mw = \frac{\sum NiMi2}{\sum Ni} \; and \; Mn = \frac{\sum NiMi}{\sum Ni} \qquad (3A.\,1)$$

The Polydispersity index (PDI) was calculated using equation 3A.2.

$$PDI = \frac{Mw}{Mn} \qquad \qquad (3A.2)$$

The GPC (DMF) VISKOTEK TDA 305-040 Triple Detector Array refractive index (RI), viscometer (VISC), low angle light scattering (LALS), right angle light scattering (RALS) GPC/SEC MODULE was used. The separations were achieved by using different columns (T6000M, GENERAL MIXED ORG, 300 X 7.8 mm; TGAURD, ORG GUARD COL, 10 x 4.6 mm) and dimethylformamide (DMF) was used as mobile phase at 60 °C under a constant flow rate of 1 mL/min. GPC samples were prepared at concentrations of 10 mg/mL.

3A.1.2. Matrix assisted laser desorption ionisation- time of flight mass spectrometry (MALDI-TOF MS)

MALDI-TOF MS is a soft ionisation technique used for the analysis of the molecular weight of the bio-molecules like DNA, proteins, peptides, sugars, lignin, etc. It tends to fragment the molecules, when it is ionised by more suitable convenient matrix assisted laser desorption ionisation methods. MALDI-TOF MS analysis is three steps process wherein the first step is the sample preparation with suitable matrix materials and further applied on the golden MALDI-TOF MS target plate and in second step a pulse laser irradiation on the sample is done. Finally, the sample gets ionised in protonated (m/z+ 1), and deprotonated (m/z -1) form and shows the molecular mass of the materials.

MALDI-TOF MS for lignin samples were recorded using Voyager DE-STR instrument. It was equipped with a N_2 laser (337 nm, 3 ns pulse, 20 Hz maximum firing rate) and the matrix compound used was 2, 5-dihydroxy benzoic acid (DHB). Lignin was dissolved in acetonitrile with a concentration of 1 mg/mL and lignin samples (1 µL) were overlaid on the matrix (1 µL) placed on the golden MALDI-TOF MS target plate, the plate was kept for drying until the solvent was evaporated and then subjected for the analysis. The lignin had a high molecular weight in the range of 10-100 kDa which is in good correlation with GPC data.

3A.1.3. Temperature program oxidation- mass spectrometry (TPO-MS)

To understand the thermal response of the sample, temperature program oxidation-mass spectrometry (TPO-MS) was used in which a qualitative analysis for the formation of various oxidative or hydrocarbons products having different m/z was measured in presence of air or inert (Helium) condition. The mass analyser was calibrated using H_2, CH_4, CO, CO_2, C_6H_6, etc. standards before performing the sample analysis.

TPO-MS (Micromeritics autochem II chemisorption analyzer-Pfieffer instrument) attached with thermal conductivity detector (TCD) and mass-spectrometer was used for the study. The experiments were performed under 5% O_2+ 95% He (*v/v*) or 100% He, to understand the effect

of environment on the product formation after lignin decomposition. The following TPO program was used;

a) Pre-treatment for removal of moisture:

RT $\rightarrow$ 5 ^{o}C/min $\rightarrow$ 120 ^{o}C (hold time: 2 h) $\rightarrow$ Cooling (50 ^{o}C in presence of He, Flow rate 30 mL/min)

b) Analysis:

50 ^{o}C$\rightarrow$ 5 ^{o}C/min $\rightarrow$ 800 ^{o}C (hold time: 10 min) $\rightarrow$ Cooling (RT, in presence of He, flow rate 30 mL/min)

(Oxidation/decomposition in the presence of 5% O_2 + 95% He (*v/v*) *or* 100% He)

Heats of decomposition for each sample were measured during continuous heating at a prescribed heating rate. The decomposition generally started in lignin sample in case of 100% He, at 200 ^{o}C and it was seen until 770 ^{o}C. While in case of 5% O_2 + 95% He, decomposition started at ca. 300 ^{o}C and was completed at 550 ^{o}C in a series of endothermic and exothermic reactions.

3A.1.4. Differential scanning calorimetry (DSC) analysis

DSC is a thermoanalytical technique, which tells the amount of heat essential due to change in physico-chemical properties of samples as a function of temperature. The sample and reference temperature were maintained throughout the analysis. The melting and crystalline temperatures of lignins and THF soluble products were recorded on DSC Q-10 (TA instruments, USA) under N_2 atmosphere with a heating rate of 10 ^{o}C/min from 50 to 300 ^{o}C.

3A.1.5. Inductively coupled plasma-optical emission spectroscopy (ICP-OES) and Scanning electron microscopy-energy-dispersive X-ray (SEM-EDX)

ICP-OES is an important analytical technique, which is used to determine the parts per million (PPM) levels of the elements present in the samples. It is a type of emission spectroscopy that is based on the inductively coupled plasma, which excites the atoms and ions to emit the electromagnetic radiation at a particular wavelength for a specific element. The qualitative and quantitative elemental analysis of the samples is possible by calibrating the instrument with standard solutions of precisely known concentration.

Samples were analysed in SPECTRO ARCOS Germany, FHS 12 ICP-OES instrument. The sample was prepared as follows; the crop waste, wood chip, pulp and lignin samples were first calcined at 620 ^{o}C for 6 h under air and after burning the entire C, H and O are eliminated as gases products which leaves back inorganic ash as the residue. The elemental analysis of this ash revealed that it does not contain any organic matter (C, H, N). Later, 0.05 g ash was weighed in the polypropylene bottle and to this ca. 400 μL of HF was added. The mixture was heated at 60 °C to remove the excess HF. The resulting dried mixture was dissolved in 5 mL freshly

prepared aquaregia (HCl:HNO$_3$; 1:3 *v/v*), which was diluted to 50 mL. The resulting solution was filtered using 0.22 micron filter and the filtered solution was analysed by ICP-OES.

The elemental composition of the sample was confirmed using the EDX, attached with the SEM instrument which clearly indicated that carbon, oxygen, sodium and sulphur are present in the lignin sample. In this technique, X-rays source is used to eject an electron present in the inner shell and create vacancy in samples. Through this phenomenon energy is liberated and it is known as x-rays energy and this generated x-rays are measured which are characteristic for the specific elements. The SEM-EDX of the samples was obtained on a Leo Leica Cambridge UK Model Stereoscan 440 scanning electron microscope, with an electron beam of 5-50 eV.

3A.1.6. Attenuated total reflection- Infra-red (ATR-IR) spectroscopy

Attenuated total reflection (ATR) or Fourier transform infrared (FT-IR) spectroscopy was used to analyse the various functional groups present in the molecules. This is non-destructive and simple analytical tool for the qualitative and quantitative analysis of chemical composition present in the molecules. It deals with the stretching and bending modes of the vibration of the chemical bonds present in a molecule, which are observed at various frequencies depending upon the functional groups and nature of chemical bonds. After absorbing infrared electromagnetic radiation, the frequencies of the chemical bonds increases due to leading of the transitions between ground state to various excited states. The FT-IR or ATR spectra are recorded for the samples to the mid-infrared region (600-4000 cm^{-1}) of the electromagnetic spectrum. The presence of various functional groups in ionic liquids, crop waste, lignin, THF soluble products, etc. were analysed using FT-IR (FT-IR-8300 Shimadzu) and an alpha-T Bruker [(ATR), eco ZnSe] spectrophotometer technique. For FT-IR analysis of samples, pellets were made with KBr by maintaining 1*wt.*% concentration. The normalization of intensities was discussed based on the exact concentration used for making pellets.

3A.1.7. Nuclear magnetic resonance (NMR) analysis

Nuclear magnetic resonance (NMR) spectroscopy is a widespread analytical technique, which exploits the magnetic behaviour of the assured atomic nuclei. The change in the spin states of a nuclear magnetic moment is observed, while the nucleus absorbs the electromagnetic radiation in presence of applied strong magnetic field. The atomic nuclei having odd number of protons and/or neutrons and retaining a nuclear spin I≠0 (^{1}H, ^{13}C, ^{29}Si, etc.), are NMR active, and if the nuclear spin of molecules, I=0 (^{12}C, ^{16}O, ^{32}S, etc.), will be NMR inactive. The skeleton structural properties of the molecules can be illustrated by the NMR spectroscopy, in which they existed. NMR analysis gives the detailed information pertaining to structure, dynamics and chemical environment of the atoms present in molecules.

3A.1.7.1. ¹H NMR

The 500.13, 399.78 and 200.13 MHz frequency, Bruker Avance and JEOL-500, 400 and 200 NMR instrument were used for ¹H NMR spectra at 25.9±2 ᵒC DMSO-d_6 solvents. The ¹H NMR spectra for the lignins and products samples were recorded with 20-70 mg of samples in 600±100 μL DMSO-d_6 solvents.

3A.1.7.2. ¹³C NMR

The 125.76 and 50.32 MHz frequency Bruker Avance-500 and 200 NMR instrument were used for ¹³C spectra at 25.9±2 ᵒC in DMSO-d_6 solvents. The ¹³C NMR spectra for the lignins and products samples were recorded with 20-70 mg of samples in 600±100 μL DMSO-d_6 solvents.

3A.1.7.3. 2D (¹H/¹³C HSQC) NMR

Two dimensional heteronuclear single quantum coherence (HSQC) NMR was recorded at 25±2 ᵒC using Bruker Avance-500 MHz (operating at a frequency of 500.13 MHz) spectrometer and 20-70 mg sample dissolved in 600±100 μL DMSO-d_6 solvent.

3A.2. Results and Discussions

In this Chapter details of the characterization techniques and physico-chemical properties of various types of lignins are discussed. Dealkaline lignin (CAS Number : 9005-53-2   Product Number : L0045, TCI Chemical Japan); alkaline lignin (CAS Number : 8068-05-1   Product Number : L0082, TCI Chemical, Japan); alkali lignin (CAS Number : 8068-05-1   Product Number : 370959, Aldrich, USA) were purchased and used without any further pre-treatment. Along with commercial lignin samples, lignin was also collected from local industries like industrial lignin. Subsequently it identified that it is made up of *H*, *G* and *S* units along with various linkage, which are dependent on the type/age of plant, isolations procedures, etc. So, it is essential to probe the substructure units and various types of linkages. Therefore, lignin was systematically characterized by several physico-chemical analytical techniques. The analytical techniques used are elemental analysis, XRD, ICP-OES, TGA, NMR (¹H, ¹³C and HSQC), FT-IR, SEM-EDX, GPC, MALDI-TOF MS, etc. These techniques confirmed the monomers molecular formula, solubility of lignin, higher heat potentials, double bond equivalence, thermal stability/phase changes, protons, carbons skeletons, functional groups, morphology, molecular weight etc. of the lignin molecules. However, detailed characterization of ionic liquids and isolated (Klason and organosolv lignin) lignin samples are discussed in the Chapters 2 and 4, respectively. In this chapter, the detailed characterizations of the commercial lignins are discussed.

3A.2.1. Solubility of lignin

Solubility of commercial lignin samples were checked with various solvents and binary mixtures of solvents. The details on lignins solubility, Hansen solubility parameter and polarity index of various solvents are given in Table 3A.1.

The solubility of lignins was determined in several solvents and the obtained results are given in Table 3A.1. The main purpose of the solubility are; (i) to find a suitable solvent for the lignin depolymerization reaction, (ii) separation of products from the lignin depolymerized reaction mixture and (iii) correlation of lignin solubility data with catalyst solubility data for easy recycle of catalysts after the reaction using suitable solvent in which both are insoluble.

Lignin has several functional groups (-OH, -OCH$_3$, -COO-, -CO, -COOH, etc.), aromatic moieties and several types of linkages ($\equiv$C-O-C$\equiv$ and $\equiv$C-C$\equiv$), which defined the polar nature of lignin molecules. Lignin is a copolymer unit of sinapyl, coumaryl and coniferyl alcohols moieties, these separate monomer moieties have wide range of solubility than the actual lignin molecules. As shown in the Table 3A.1, dealkaline lignin is 44% soluble in water and 74% soluble in methanol, while dealkaline lignin is 100% soluble in the binary solvent mixture water:methanol (1:5, *v/v*). The data obtained from solubility result of dealkaline lignin in the water:methanol, (1:5 *v/v*) solvent mixture would be the significant solvent for transforming the lignin depolymerization reaction. Hansen solubility parameter (HSP) of lignin is 28.6 MPa$^{1/2}$ while the monomeric solvents which have HSP values higher or close to lignin HSP values in which lignin is partially soluble, e.g. HSP value of water (solubility, 44%) is 48.0MPa$^{1/2}$ and methanol (solubility, 74%) is 29.7 MPa$^{1/2}$ respectively. Lignin is insoluble in several solvents such as THF, EtOAc, DEE, etc. The HSP values of these solvents are low(er) than lignin and also HSP values are closer to aromatic compounds and low molecular weight aromatic compounds are soluble into these solvents. Hence, these solvents are used to extract products from the lignin depolymerization reaction mixture. As observed from the Table 3A.1, lignin is more soluble in polar solvent than in non-polar solvents (Polarity index, 0-9.0). Considering the obtained result from the solubility of lignin, water:methanol, 1:5 (*v/v*) solvent ratios was chosen to carry out all the lignin depolymerization reactions.

Table 3A.1. Solubility, Hansen solubility parameter and polarity index of various solvents, used for dealkaline lignin solubility and extraction of depolymerized products.

Solvent/mixture/ aromatic monomers	Hansen solubility parameter (δ; MPa$^{1/2}$)[12-15]	Polarity index	Lignin solubility[*] and [≠](%)
Water	48.0	9.0	44
Methanol	29.7	5.1	74
Ethanol	26.2	5.2	IS
Propanol	23.5	5.1	IS
Butanol	23.3	1.0	IS
Acetone	19.7	5.1	IS
Ethyl acetate (EtOAc)	18.1	4.4	IS
Chloroform	18.9	4.1	IS
Tetrahydrofuran (THF)	19.4	4.0	IS
Dichloromethane (DCM)	20.8	3.1	IS
Diethyl ether (DEE)	15.8	2.8	IS
Glycerol	34.1	-	42
Ethylene glycol	33.7	-	66
1,2-propylene glycol	29.5	-	48
Toluene	14.3	2.4	IS
Methyl isobutyl ketone (MIBK)	15.5	4.0	IS
Binary mixtures			
Water:Methanol (1:5 *v/v*)	-	-	100
Water:Methanol (1:1 *v/v*)	32.4	-	68
Water:ethanol (1:1 *v/v*)	27.9	-	52
Water:n-propanol (1:1 *v/v*)	25.1	-	30
Water:i-propanol (1:1 *v/v*)	25.3	-	IS
Water:acetone(1:1 *v/v*)	21.5	-	82
Water:tetrahydrofuran (1:1 *v/v*)	20.2	-	IS
Water:1,4-dioxane(1:1 *v/v*)	21.8	-	IS
Toluene:water (1:1 *v/v*)	-	-	6
Toluene:water:methanol (1:1:1 *v/v/v*)	-	-	34
MIBK: water (1:1 *v/v*)	-	-	10
MIBK:water:methanol (1:1:1 *v/v/v*)	-	-	58

Water:methanol (1:5*v/v*)	-	-	Alkali lignin= 90
Water:methanol (1:5 *v/v*)	-	-	Alkaline lignin=60
Water:methanol (1:5 *v/v*)	-	-	Industrial lignin=30
Aromatic compounds			
p-cresol	22.7	-	
Phenol	24.1	-	
Vanillin	25.2	-	
Eugenol	22.8	-	
Resorcinol	29.0	-	
Benzene	18.7	-	
Toluene	18.3	-	
Xylene	18.2	-	
Styrene	19.0	-	
Acetophenone	19.6	-	
Benzaldehyde	22.5	-	
Benzylalcohol	25.2	-	
Lignin	28.6	-	
[*]lignin 250 mg, solubilized in solvent 5mL, at RT (25±3 ^{0}C). IS: Insoluble.[≠] unless it is revealed all the solubility data are mentioned for dealkaline lignin			

3A.2.2. X-ray diffraction of dealkaline, alkaline, alkali and industrial lignin

The XRD analysis was done for various lignin (dealkaline, alkaline, alkali and industrial) samples (Figure 3A.1). Due to the amorphous nature of lignin broad peaks were observed in XRD. However, lignin is isolated with the lignocellulosic biomass which may be contaminated with crystalline or amorphous cellulose impurity. The peak corresponding to crystalline cellulose appears at 22.5^o and the amorphous peak of lignin at 17.7 and 18.5^o. In order to check the cellulose impurity in various lignin samples, XRD pattern was recorded (Figure 3A.1) in which a broad peak in a range between 8-32° appeared which confirms that the lignin is amorphous in nature. Along with this broad peak, few extra sharp peaks were also observed at 2θ value of 18.8, 28, 29, 32, 34 and 49° due to the presence some impurities in the dealkaline and industrial lignins. These peaks matched well with XRD pattern of Na_2SO_4 (JCPDS file No. 36-0397). The presence of Na and S in dealkaline and industrial lignins was also confirmed from elemental, SEM-EDX and ICP-OES analysis. This is likely due to the extraction of dealkaline and industrial lignin by same isolation procedure.
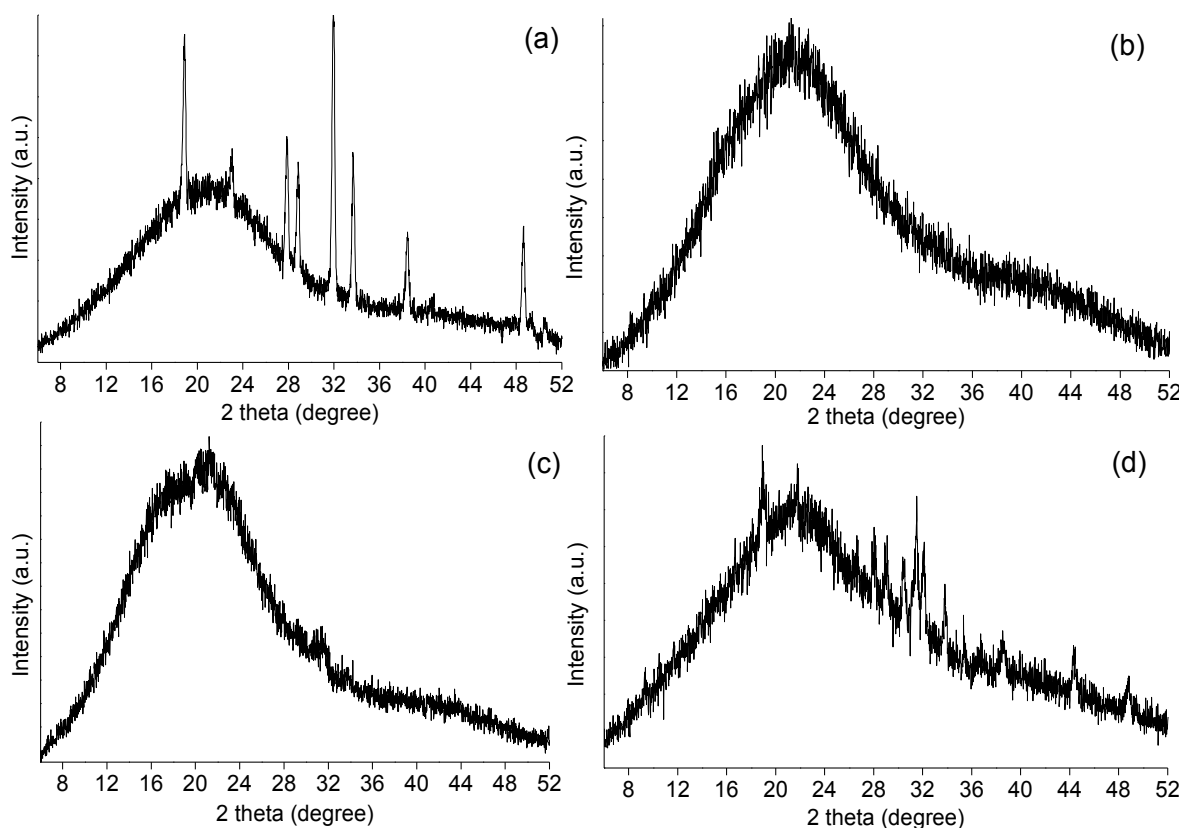
Figure 3A.1. XRD diffraction patterns of (a) dealkaline, (b) alkaline, (c) alkali and (d) industrial lignin samples.

3A.2.3. SEM images and EDX of lignin samples

The scanning electron microscopy (SEM) was used to examine the micro and morphological structure of the commercial lignin (dealkaline, alkaline, alkali and industrial lignin) samples. The non-uniform/unstructured morphology of the lignin samples with particle size ranging from <1 μm to 30 μm were observed (Figure 3A.2). The elemental composition of the sample was determined using the EDX (Figure 3A.2), attached with the SEM instrument. The data clearly indicates that carbon, oxygen, sodium and sulphur are present in the lignin samples. The ICP-OES and EDX analysis revealed the presence of Na and S in dealkaline, alkali and industrial lignin samples. These samples might have been separated using Kraft process, in which NaOH and Na_2S reagents were taken. However, Na and S both are present in the alkaline sample, which was confirmed by the ICP-OES analysis but these elements were not observed in EDX analysis (Figure 3A.2f). This is because EDX is provides only surface composition whereas ICP-OES can provide the precise data of the digestive samples at the ppm level.
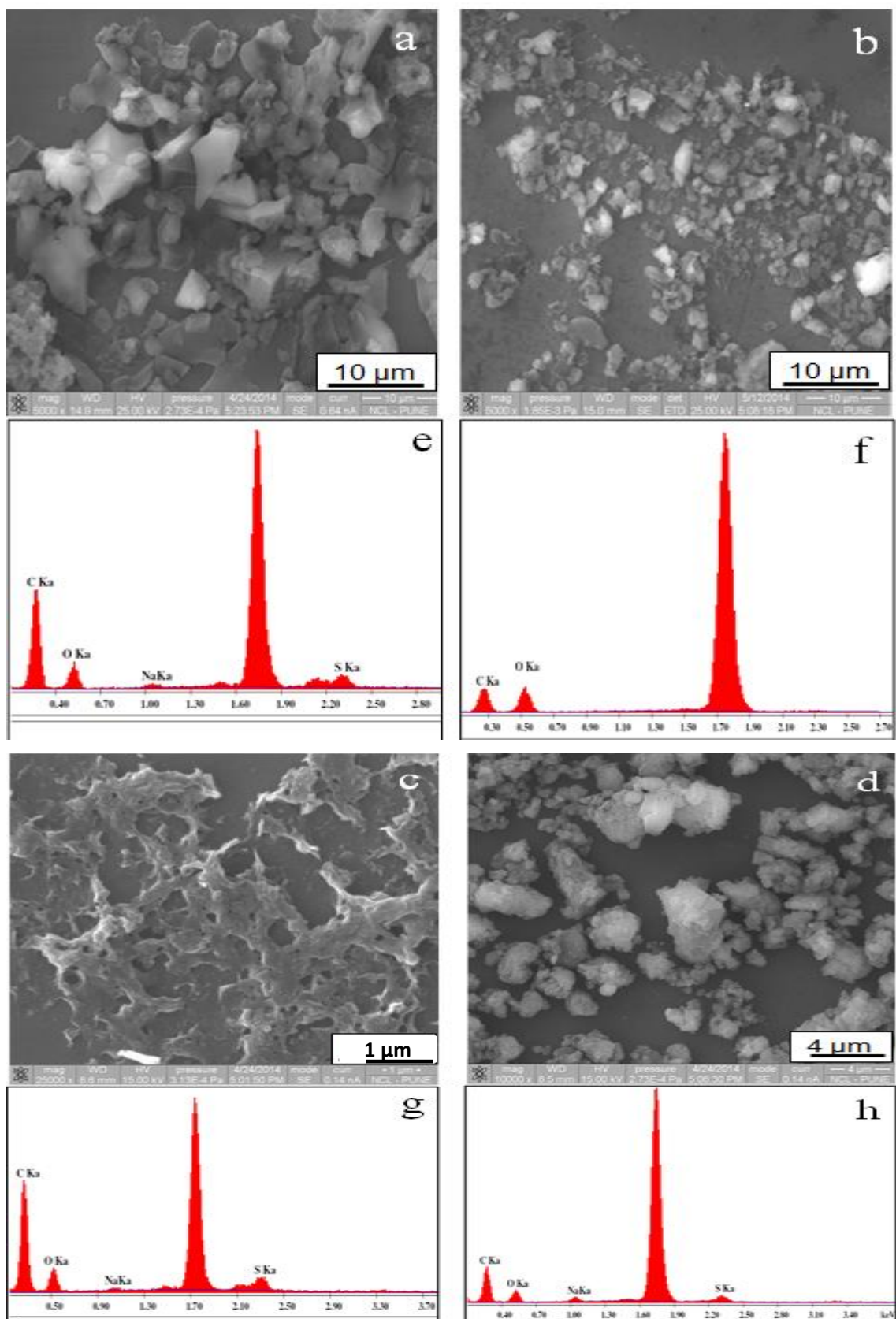
Figure 3A.2. SEM images: (a) dealkaline, (b) alkaline, (c) alkali, (d) industrial and EDX analysis of (e) dealkaline, (f) alkaline, (g) alkali and (h) industrial lignin samples.

3A.2.4. Gel permeation chromatography

Molecular weight of the lignin samples is a vital physical property to be analysed in order to understand the lignin activity during the catalytic reaction. GPC analysis was used to determine the molecular weight of dealkaline lignin in which dimethylformamide (DMF) was used as solvent. In GPC chromatogram (Figure 3A.3) dealkaline lignin showed peaks corresponding to 60 kDa molecular weight. Literature reports supports that alkaline lignin have weight average molecular weight, (Mw) 60 kDa with 10 kDa number average molecular weight (Mn) and polydispersity index (PDI)= 6.[16] Similarly, the molecular weight of alkali lignin was found; Mn= 5 kDa, Mw= 28 kDa and PDI= 5.6, from the Aldrich supplier. These results represented the nature of lignin is heterogeneous fractions and also have high molecular weights. In most of the work, depolymerization studies were carried out with lignin model compounds (dimers/trimers) but in the current work real lignin substrate have used.
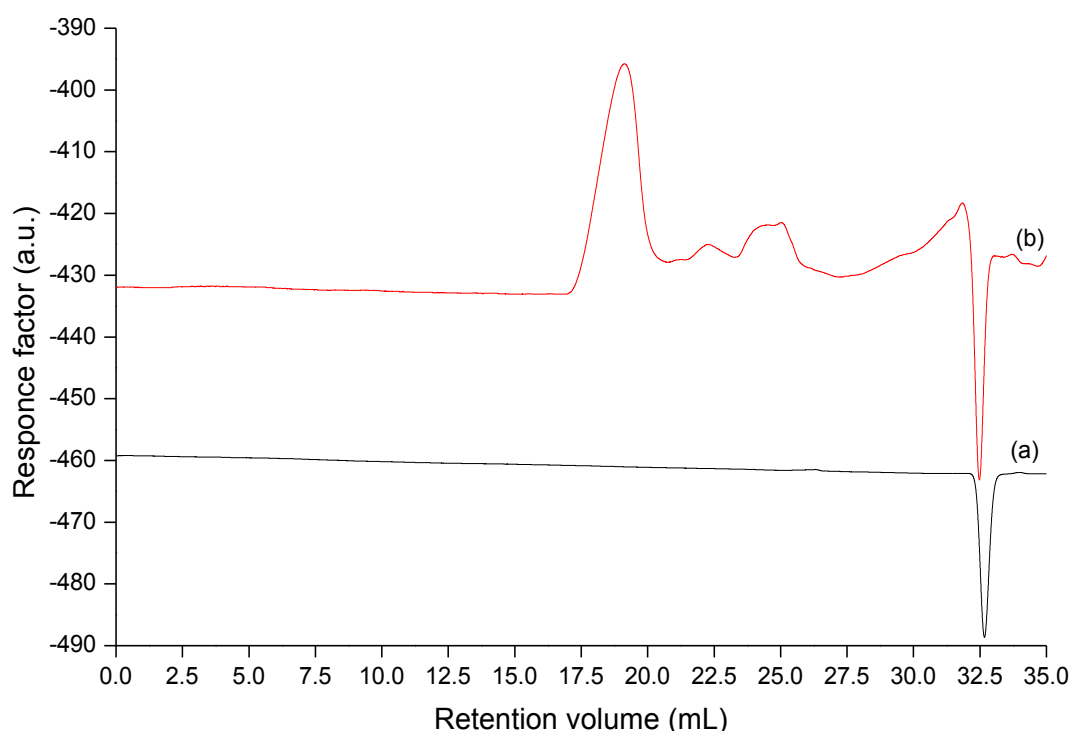
Figure 3A.3. GPC (DMF) chromatogram for (a) DMF solvent and (b) dealkaline lignin.

3A.2.5. MALDI-TOF MS

The MALDI-TOF analysis of the lignin sample was analysed to find out the molecular weight of dealkaline lignin in the range between 10-100 kDa (Figure 3A.4). A broad peak was observed with a peak maximum at ca. 60 kDa, which is close to the significant result obtained with GPC data of dealkaline lignin. Broadening of peak was observed due to its poor ionization and poor ability to carry out the charge for the mass spectrometric analyser which is also reported in earlier literature.[17] In this work, alkaline, alkali and industrial lignin samples were also checked

for the MALDI-TOF MS analysis in which due to poor ionisation of these samples, it was very difficult to get the MALDI-TOF MS analyser peaks for these samples.
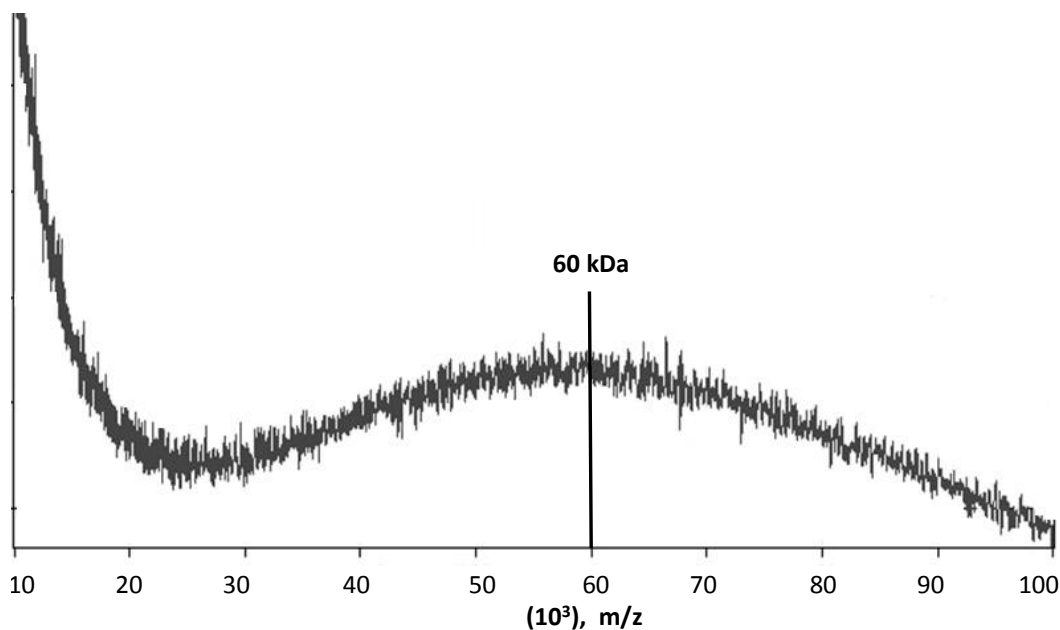
Figure 3A.4. MALDI-TOF MS analysis profile of dealkaline lignin.

3A.2.6. Thermogravimetric analysis (TGA) of dealkaline, alkaline, alkali and industrial lignin (Air and N$_2$)

The TGA thermogram obtained for lignin samples in presence of air and inert (N$_2$) are presented in Figures 3A.5A and 5B. The TGA analysis (Air) for commercial lignin samples are shown in Figure 4A.5A. Around 200 ^{o}C the weight loss of about 2-12% was observed which may be due to removal of physically absorbed moisture and complete degradation of the organic moieties was observed around 800 ^{o}C. TGA curve reveal the mass loss or phase changes (solid to liquid and further liquid to gases) as function of temperature. The weight losses of the lignin samples were seen in the two steps in which at first step the weight loss in the range between 30-40% was observed from 210 ^{o}C to 400 ^{o}C is due to the decomposition of cross linked alkyl units which might be due to side chain alkyl units, linked such as $\equiv$C-C$\equiv$/ $\equiv$C-O-C$\equiv$ bond attached to the aromatic ring, and further it might be contributed by aromatic ring present in the lignin samples.[18, 19] Similarly, in the second step, weight loss of around 50-60% were observed in the range between 450 ^{o}C to 800 ^{o}C, which is the degradation region for the aromatic and ethylene groups.[19] As seen in (Figure 3A.5), lignin samples are stable until 250 ^{o}C and even after heating lignin up to 800 ^{o}C, some amount of lignin remains unburnt which is due to presence of inorganic residue (ash) in lignin samples. These inorganic residues are mostly Na$_2$SO$_4$ which was evident from CHNS and ICP-OES analysis that Na and S are present in dealkaline and industrial lignin samples (Table 3A.2).

The thermal degradation analysis of dealkaline and alkaline lignin samples was also carried out up to 800 ^{o}C in N$_2$ atmosphere in which 30-40% unburnt materials were observed

(Table 3A.3). However, ca. 75% of carbon was burnt because a lignin molecule has carbon hydrogen and oxygen, which helped to form CO, CO_2, CH_4, H_2O etc. Based on the results obtained in TGA and understanding from the general monomeric formula of lignin ($C_{10}H_{12-13}O_3S_{0.01-0.09}$), it is anticipated that lignin may decompose as CO, CO_2, CH_4, H_2, etc. To understand this, TPO-MS experiments were performed for the dealkaline lignin and it was observed that besides these gases some other gases are also formed, which are shown in Table 3A.3 and Figure 3A.6.

The TGA values obtained in air and N_2 environments showed that, the thermal decomposition of the lignin samples showed significant differences in both conditions. It may be possible that this variation is related to the susceptibility of lignin with air during its decomposition. There are several methods which have been used to calculate the activation energy as a function of extent of thermal degradation. Under the nitrogen environment, the thermal degradation energy of polymers has high activation energies than the thermal degradation in presence of oxygen[20] due to which difference is observed in the thermograms of lignin in air and N_2 environment.

In the next Sections 3B and 3C, lignin depolymerization reactions were carried out at 120 ºC and 200 ºC which emphasizes lignin self-degradation will not occur under the reaction conditions.
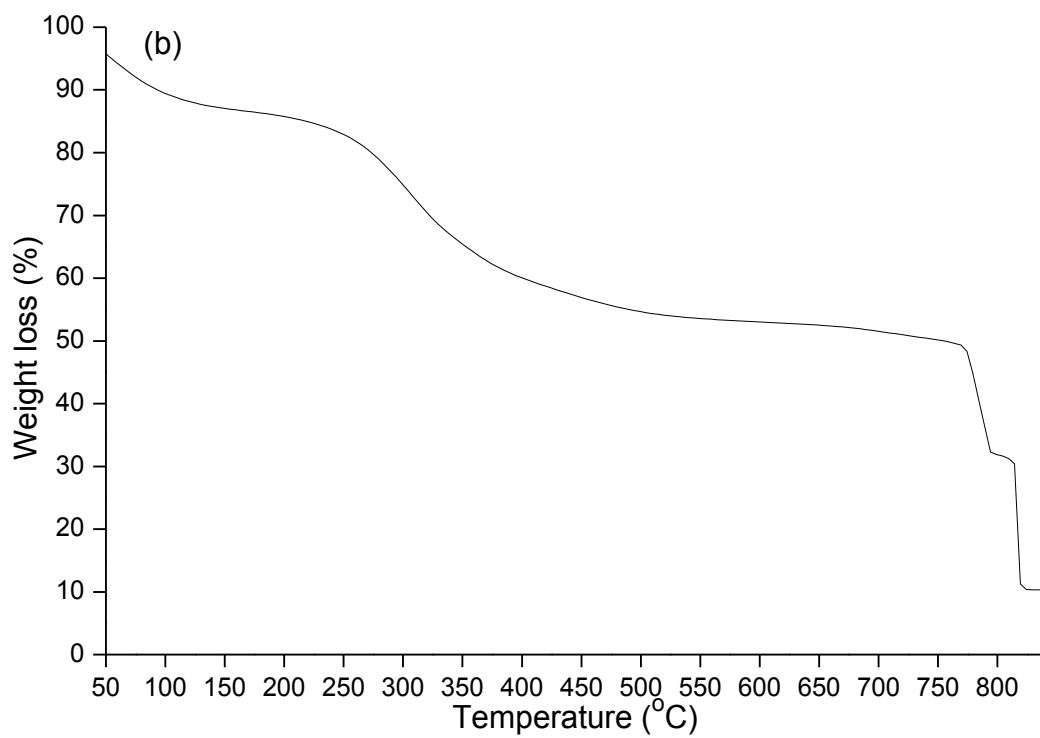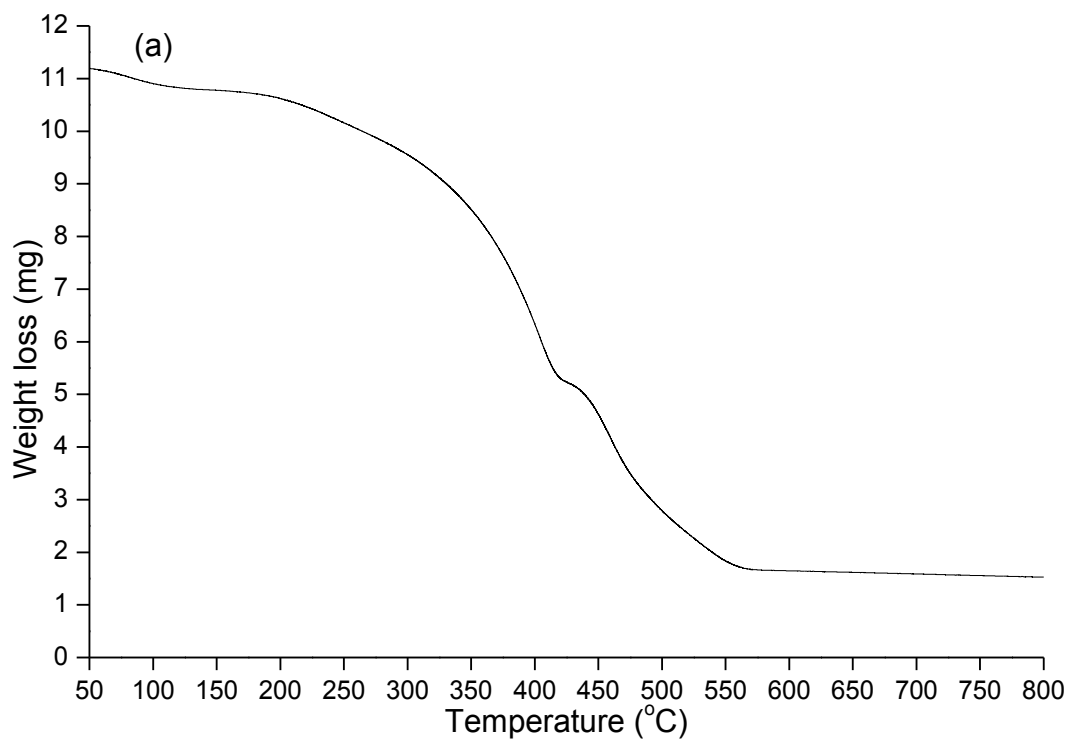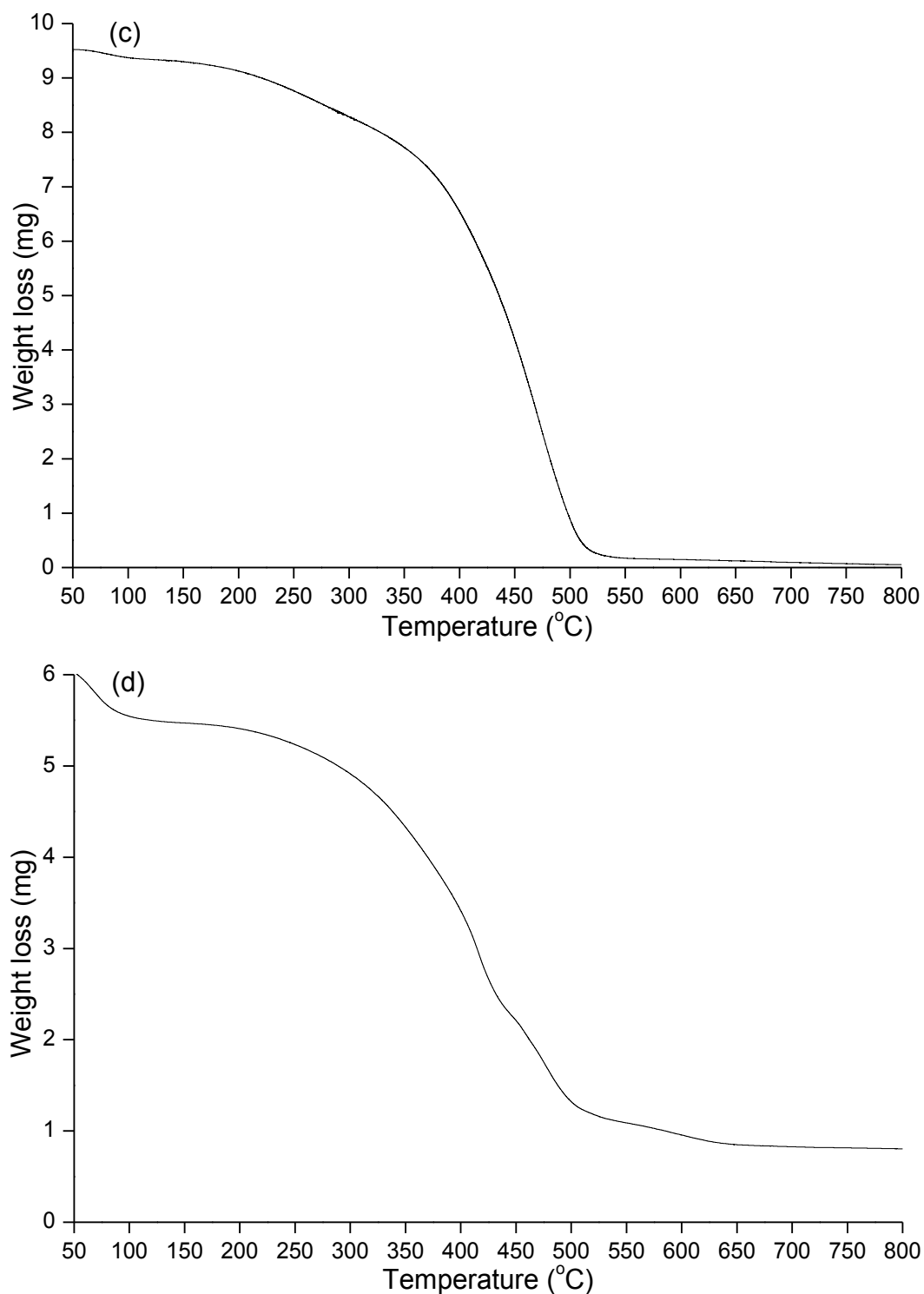
Figure 3A.5A. Thermogravimetric analysis (air), of (a) dealkaline, (b) alkaline, (c) alkali and (d) industrial lignin samples.
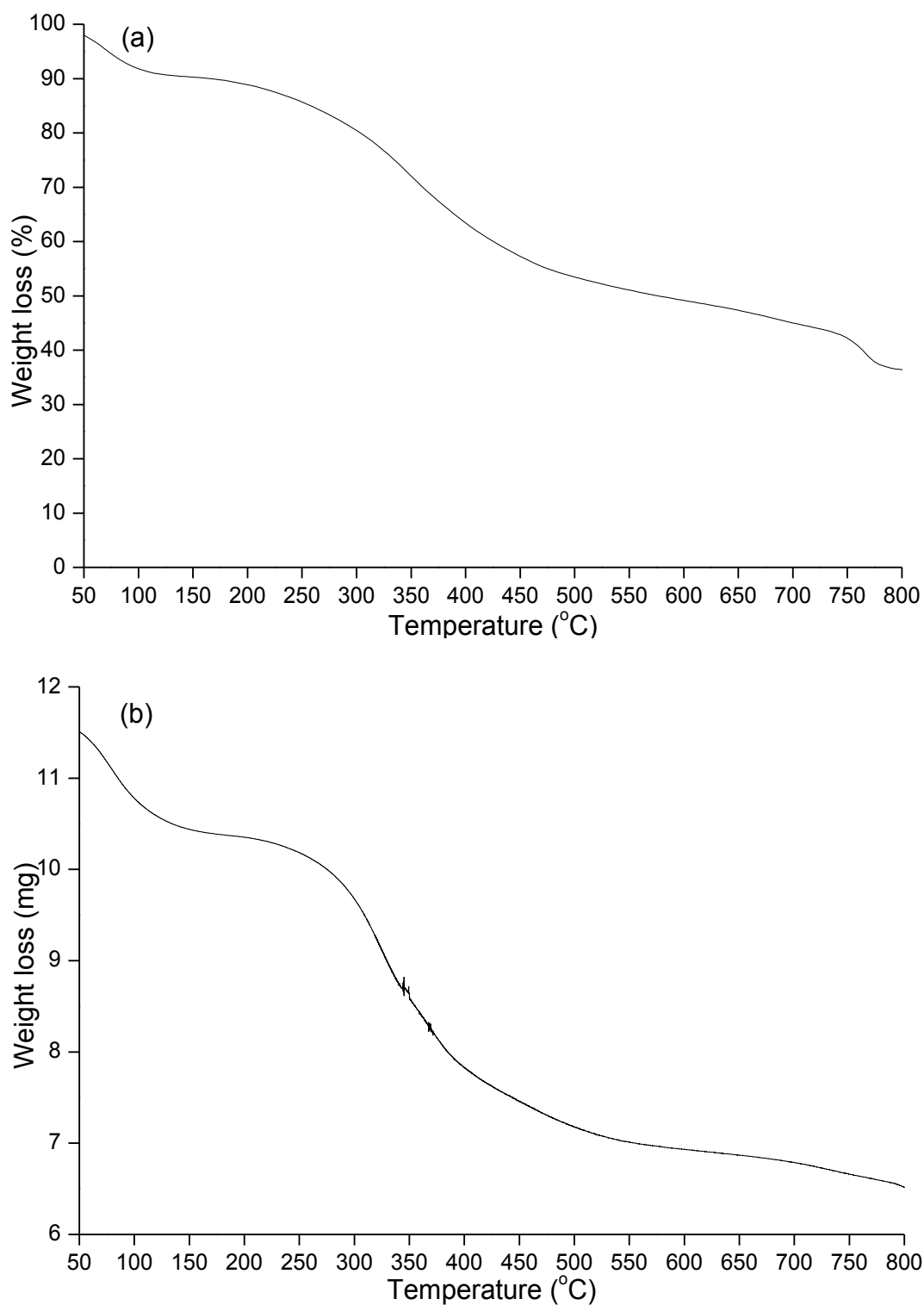
Figure 3A.5B. Thermogravimetric analysis (N_2), of (a) dealkaline and (b) alkaline lignin samples.

3A.2.7. Temperature programme oxidation-mass spectrometry (TPO-MS)

The lignin samples were subjected to TPO-MS studies in order to understand their thermal conversion behaviour. The decompositions for each sample were measured during continuous heating at a prescribed heating rate. For the pre-treated lignin sample in 100 % He atmosphere the onset of decomposition was at 200 °C and at 770 °C a complete decomposition was observed. In case of 5% O_2 + 95% He decomposition started at ca. 300 °C and completed at 550 °C in a series of endo and exothermic reactions. To understand the effect of conditions (in inert or in presence of O_2), on the products formation, sulphur dioxide, carbon monoxide, carbon dioxide, methane, hydrogen, oxygen etc. were used to calibrate the TPO-MS instrument.

As observed from the TCD chromatograph of the pre-treated dealkaline lignin sample in presence of the 100% He, the thermal decomposition of lignin is observed in two ranges. It is obviously due to the two types of moieties present within lignin structure; (i) cross side chains and (ii) aromatic moieties. However, four TCD signals were detected in the presence of 5% O_2 with 95% He, the first signal starting from 50-150 °C, which is due to moisture present in the 5%O_2 and second minor signal from 150-300 °C, for the surface hydroxyl groups in the lignin. These minors signals are not detected in the 100% He TCD chromatogram due to the absence of moisture in the 100% He. Similarly, two major signals were detected in the TCD chromatogram in 100% He or 5% O_2 with 95% He, these signals have arisen due to the cross side chains and aromatic moieties. While in the presence of 100% He, these signals are too apart from each other due to the dimerization of the ionised aromatic monomers leading to dimers formation (e.g. phenanthroline, etc.) in inert environment at high temperature.[21] These moieties have high heat of decomposition due to which these decompose at higher temperature. While in presence of 5% O_2 with 95% He, the complete decomposition of organic moieties is observed at 550 °C. This is because under the oxygen environment, the thermal degradation energy of polymers has low(er) activation energies than the thermal degradation in presence of helium (inert gas).[20]

As shown in Figure 3A.6, lignin showed decomposition over a broad range of temperatures due to the presence of various types of linkages (Tables 3A.4 and 3A.5), functional groups and bond dissociation enthalpies of lignin [Chapter 1, Table 1.1 and Figure 1.5]. As given in Chapter 1, Table 1.1, depending on the temperature, cleavage of aryl-aryl/alkyl ($\equiv$C-C$\equiv$) or aryl-ether ($\equiv$C-O-C$\equiv$) linkages is possible.[22, 23] It is worth noting here that when experiment was done with 5% O_2, highly intense peaks for gaseous products (CO, CO_2, CH_4, H_2 etc. Table 3A.2, equations 3A.3-3A.18) are observed and these are less under inert atmosphere (100% He). Importantly, observance of ozone under both the conditions is possible due to a radical mechanism under thermal conditions. However, for the explanations of ozone formation,[24] typically a radical mechanism is discussed.
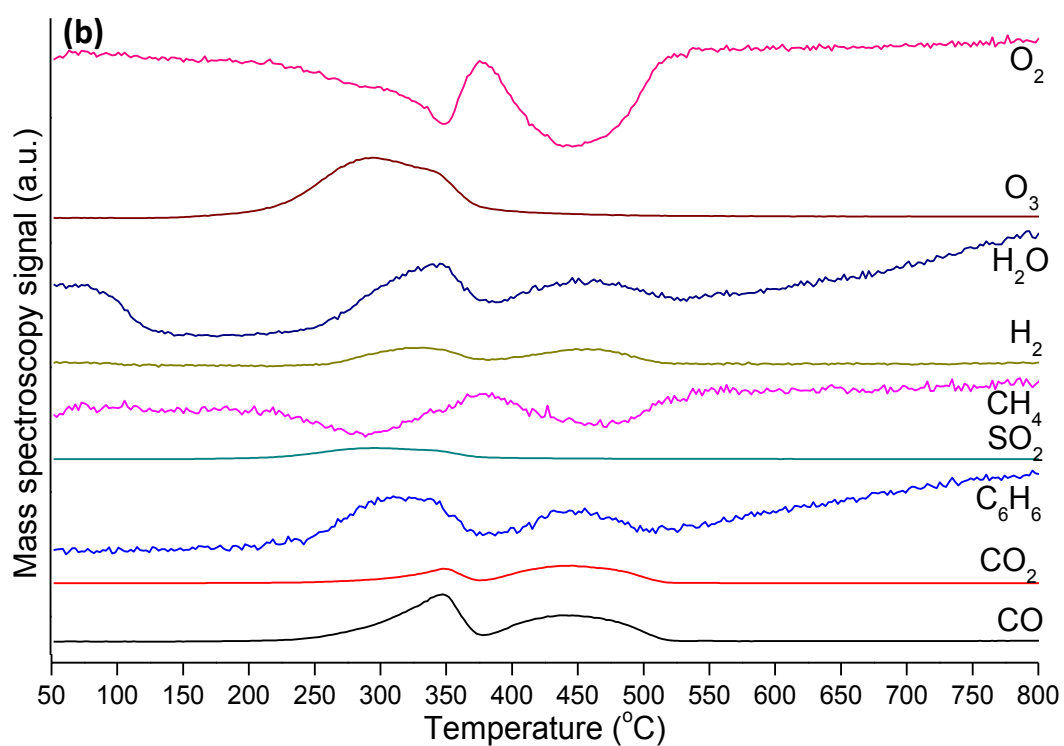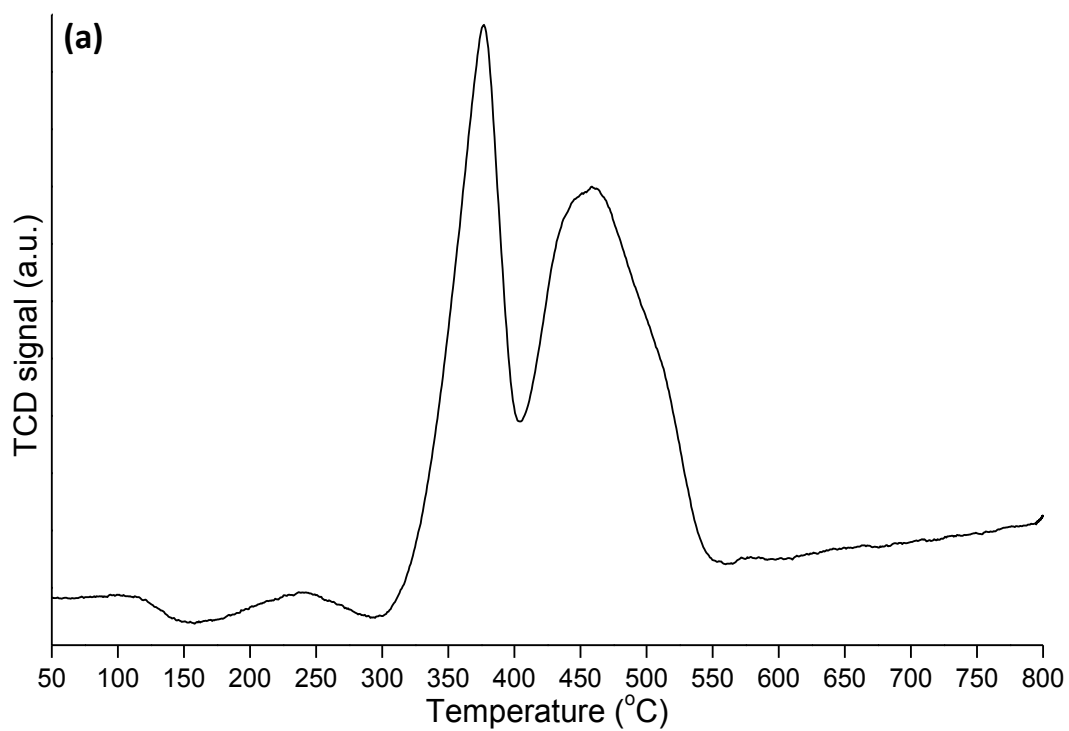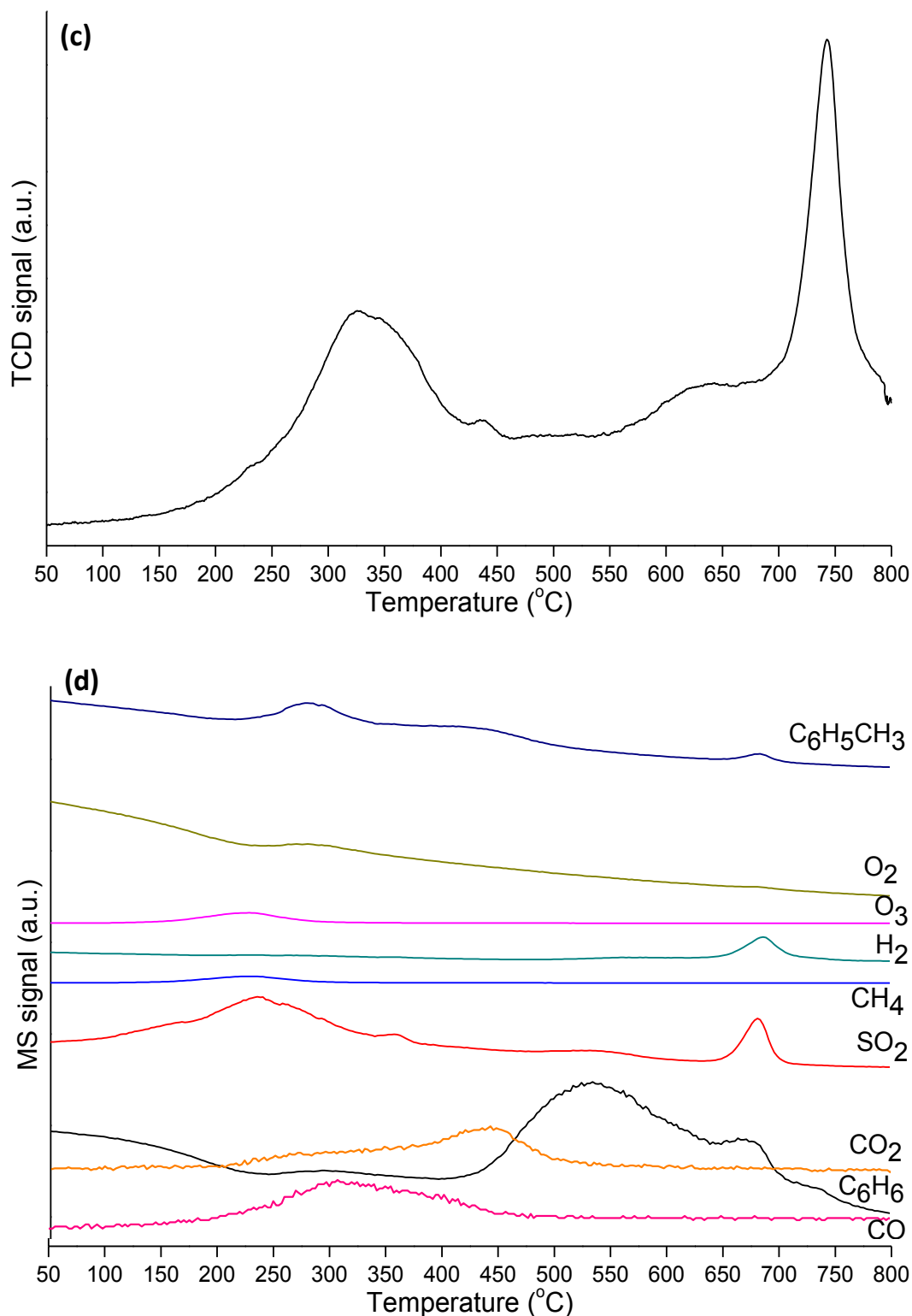
Figure 3A.6. Temperature programme oxidation-mass spectrometry (TPO-MS) of lignin. (a) TCD-(5% O_2 +95% He *v/v*), (b) MS profile-(5% O_2 +95% He *v/v*), (c) TCD-100% He and (d) MS profile-100% He.

Based on these observations following equations are proposed;

$$RH \longrightarrow R^{\bullet} + H^{\bullet} \qquad \text{3A.3}$$

$$R^{\bullet} + O_2 \longrightarrow R\text{-}OO^{\bullet} \qquad \text{3A.4}$$

$$R\text{-}OO^{\bullet} + RH \longrightarrow R\text{-}OOH + R^{\bullet} \qquad \text{3A.5}$$

$$2H^{\bullet} \longrightarrow H_2 \qquad \text{3A.6}$$

$$ROOH \longrightarrow RO^{\bullet} + {}^{\bullet}OH \qquad \text{3A.7}$$

$$2ROOH \longrightarrow RO^{\bullet} + ROO^{\bullet} \qquad \text{3A.8}$$

$$RO^{\bullet} \longrightarrow CO + R^{\bullet} \qquad \text{3A.9}$$

$$ROO^{\bullet} \longrightarrow CO_2 + R^{\bullet} \qquad \text{3A.10}$$

$$Na_2SO_4 \longrightarrow Na^{\bullet} + SO_4^{\bullet} \qquad \text{3A.11}$$

$$SO_4^{\bullet} \longrightarrow SO_2 + OO^{\bullet} \qquad \text{3A.12}$$

$$O_2 + OO^{\bullet} \longrightarrow O_3 + O^{\bullet} \qquad \text{3A.13}$$

$$RCH_3 \longrightarrow R^{\bullet} + CH_3^{\bullet} \qquad \text{3A.14}$$

$$CH_3^{\bullet} + H^{\bullet} \longrightarrow CH_4 \qquad \text{3A.15}$$

$$R\text{-}O\text{-}CH_3 \longrightarrow RO^{\bullet} + CH_3^{\bullet} \qquad \text{3A.16}$$

$$ROO^{\bullet} + O^{\bullet} \longrightarrow O_2 + R\text{-}O^{\bullet} \qquad \text{3A.17}$$

$$R^{\bullet} + CH_3^{\bullet} \longrightarrow RCH_3 \qquad \text{3A.18}$$
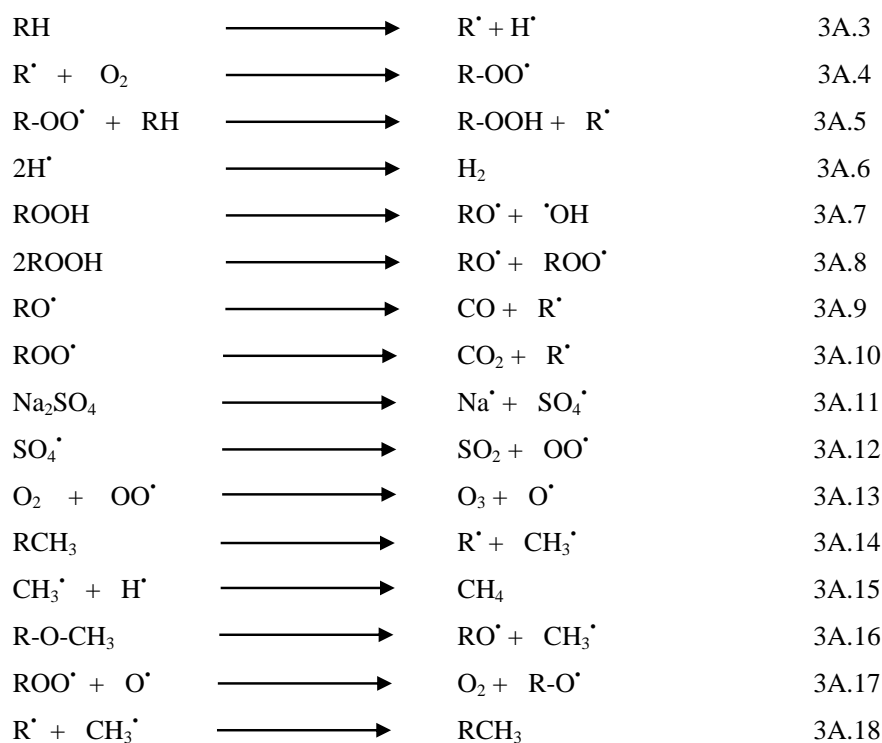
Table 3A.2. Decomposition of lignin into various products in TPO-MS experiment.

Molecules (m/z, g/mol)	Temperature (±2.0 °C) 100% He	Temperature (±2.0 °C) 5% O_2 + 95% He
Carbon monoxide (28)	310	350, 450
Carbon dioxide (44)	445	350, 450
Benzene (78)	540, 675	325, 405
Sulphur dioxide (64)	240, 355, 690	310
Methane (16)	225	(-290, -460)*, 375
Hydrogen (2)	690	335, 455
Ozone (48)	225	310, 340
Oxygen (32)	(-235)*, 275	(-340, -445)*, 375
Toluene (92)	(-225)*, 280, 440, 680	-
Water (18)	-	(-210, -380)*, 340, 450
Notes: *energy consumed during decomposition, - value indicates consuming process		

3A.2.8. Differential scanning calorimetry

DSC analysis was used to analyse the melting and glass transition temperature of dealkaline lignin samples and this process was carried out in the presence of inert (N_2) atmosphere. The sample (ca. 10 mg) was taken in aluminium pan and transferred for the DSC analysis in the range between 50-350 °C. The analysis showed two peaks i.e. energy absorbed and released peaks which are known as endothermic or melting point (heat absorption) and exothermic or

glass transition temperature (heat released). In the thermogram obtained from DSC analysis of dealkaline lignin (Figure 3A.7), peaks are recorded at 230 and 245 °C, due to melting (endothermic) and crystallization/char (exothermic), respectively. This analysis measured that dealkaline lignin sample has high boiler as observed from the Figure 3A.7.
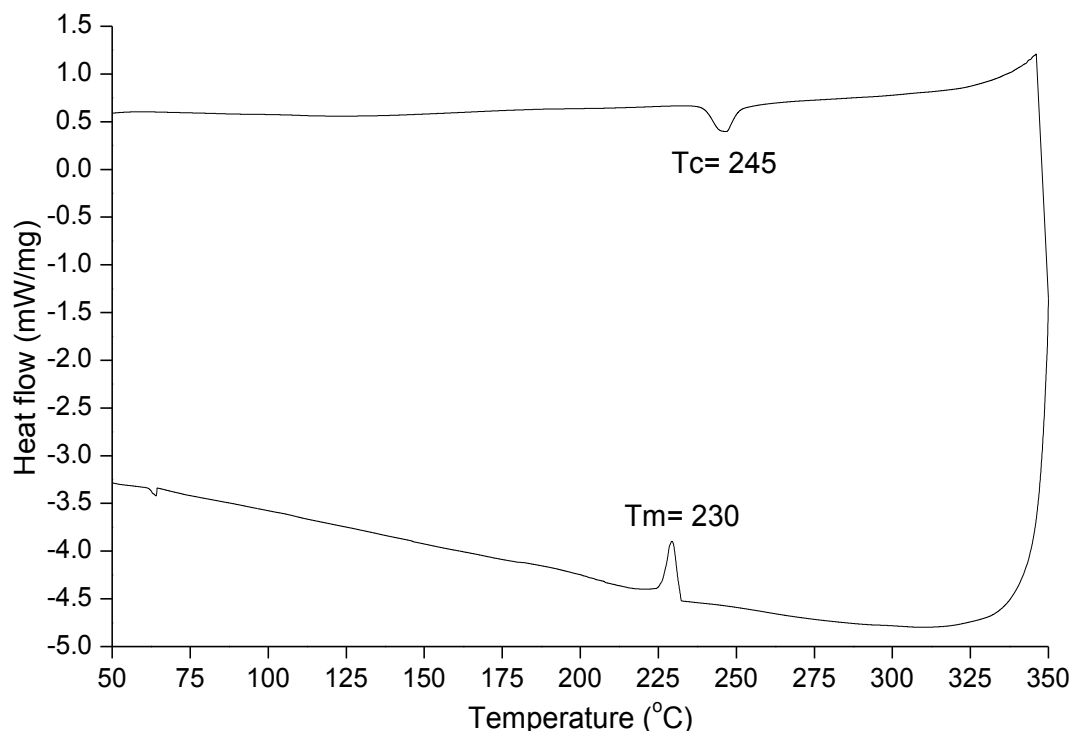
Figure 3A.7. DSC analysis of dealkaline lignin sample.

3A.2.9. Elemental analysis of lignin

During the calculation of monomer molecular formula, HHV and DBE, the ash correction was given for the lignin samples. Based on the CHNS analysis, monomeric molecular formula for lignin samples was calculated as, $C_{10}H_{12-13}O_3S_{0.01-0.09}$ which matches well with the literature.[25, 26] The higher heat values (HHV) of lignin samples were also calculated by using equation 3A.19. It is observed that the HHV (range 26.10-27.90) is almost similar in all lignin samples. The double bond equivalence (DBE) number (also known as degree of unsaturation) calculated for lignin samples based on equation 3A.20 and considering MMF, reveals it to be between 4.5 and 5.0. Usually, benzene and phenol has DBE number of 4 each (considering one for ring and one each for one double bond). In lignin samples, DBE number of 4.5-5.0 suggests aromatic ring with one double bond substitution (alkene substituent). This is obvious since coumaryl alcohol, coniferyl alcohol and sinapyl alcohol, which are the three main building units of lignins have DBE number of 5. The DBE number of 4.5-5.0 also implies that few of the aromatic rings might be devoid of alkene substitution. Moreover, the GPC results, the MALDI-TOF MS analysis of dealkaline lignin were carried out and the results obtained with GPC (~60 kDa) and MALDI-TOF MS (~60 kDa)

are similar to tentative 333 phenyl propenoid units, which is calculated based on dealkaline lignin monomeric formula $C_{10}H_{13}O_3S_{0.09}$ (molecular weight- ca. 180 g/mol).

Table 3A.3. Physical properties of lignin samples.[27]

Properties	Dealkaline lignin	Alkaline lignin	Alkali lignin	Industrial lignin
Moisture, (%)	11.20	13	7	12
ICP-OES[a] Na (mg/g)	28.8	52.0	70.1	63.0
TGA residue %, (N_2)	35.72	42.2	-	-
TGA residue % ,(Air)	16.97	17.35	3.15	13.5
pH[b]	4.16	9.10	6.23	4.15
colour	dark brown	black	brown	brown
Elemental composition (%)				
C	65.92	65.48	66.14	66.92
H	7.02	6.97	7.07	6.70
O[c]	25.87	27.21	25.92	26.19
S	0.98	0.106	0.72	-
O/C, ratio	0.30	0.30	0.30	0.30
MMF[d]	$C_{10}H_{13}O_3S_{0.09}$	$C_{10}H_{12}O_3S_{0.01}$	$C_{10}H_{13}O_3S_{0.04}$	$C_{10}H_{12}O_3$
Higher heat value,[28] (HHV, MJ/kg)[e]	36.82	28.27	34.56	27.58
DBE[f]	4.5	5.0	4.5	5.0
Molecular weight (kDa)[g]	~60	~60	~28	-
Where, [a]Inductively coupled plasma-optical emission spectroscopy (ICP-OES) results for 1.0 g of lignin, [b]100 mg sample was suspended in 6 mL millipore water and shaking was done for 5 min. Later lignin which is insoluble in water was allowed to settle down and then pH was measured (pH of millipore water was 6.92 at 25.6 °C)6.31, [c]- calculation based on elemental analysis by using ('O' *wt.*%, after ash correction) = 100-('C' *wt.*% + 'H' *wt.*%), [d]-MMF-monomer molecular formula, [e]-HHV-higher heat value in MJ/kg, calculated using Dulong formula, [f]DBE: double bond equivalence and, [g]dealkaline molecular weight calculated using MALDI-TOF and GPC, alkaline and alkali lignins molecular weight obtained from the literature and Sigma-Aldrich supplier respectively.				

The HHV have been calculated using "Dulong formula applying equation 3A.19;

$$HHV = 0.3383 \times C + 1.442 \times \left(H - \frac{O}{8}\right) + 9.248 \times S \qquad 3A.19$$

Where C= weight basis % of the carbon, H= weight basis % of the hydrogen, O= weight basis % of the oxygen and S= weight basis % of the sulphur.

DBE can be calculated using the following equation 3A.20;

$$DBE = C - \left(\frac{H}{2}\right) + \left(\frac{N}{2}\right) + 1 \qquad\qquad 3A.\,20$$

Where C, H and N = number of carbon, hydrogen and nitrogen atoms obtained from the monomer molecular formula.

3A.2.10. Ultraviolet-visible spectra of dealkaline, alkaline, alkali and industrial lignin

The UV-Visible spectra of 1 mg commercial lignin samples dissolved in 10 mL methanol solvent are shown in Figure 3A.8. In UV-Vis spectra (Figure 3A.8) various characteristic bands of lignin samples were observed. Normally, absorption bands observed in the range of 200-220 nm are due to Π-Π* transition of the aromatic ring (-CH=CH-). Similar double bond observation is confirmed by the DBE (4.5-5.0) of the lignin samples, which means that one benzene ring and one additional double bond (Section 3A.2.9). Observance of shoulder band at 230 nm can be assigned to the mono- or di-substituted aromatic rings (e.g. –OCH$_3$, -CHO, -OAr, etc.). The absorption bands for syringyl (*S*), guaiacyl (*G*) and *p*-hydroxyphenyl (*H*) units at 280±2, 277±2 and 313±2 nm, are observed respectively.[29-31] In case of alkali derived, λmax seen at 281 nm suggests that lignin contains majority of *S* units. However, in case of industrial lignin sample, band observed at decreased wavelength (278 nm) suggests that lignin has major contribution from *G* units. Additionally, it has been established that absorption bands in the range of 270-290 nm are due to nonconjugated phenolic compounds.[31] The absorption band between 300-320 nm indicates the presence of aromatic conjugated structures (Cα, C=C and C=O) or guaiacyl moieties, which can reinforce one DBE.[32]
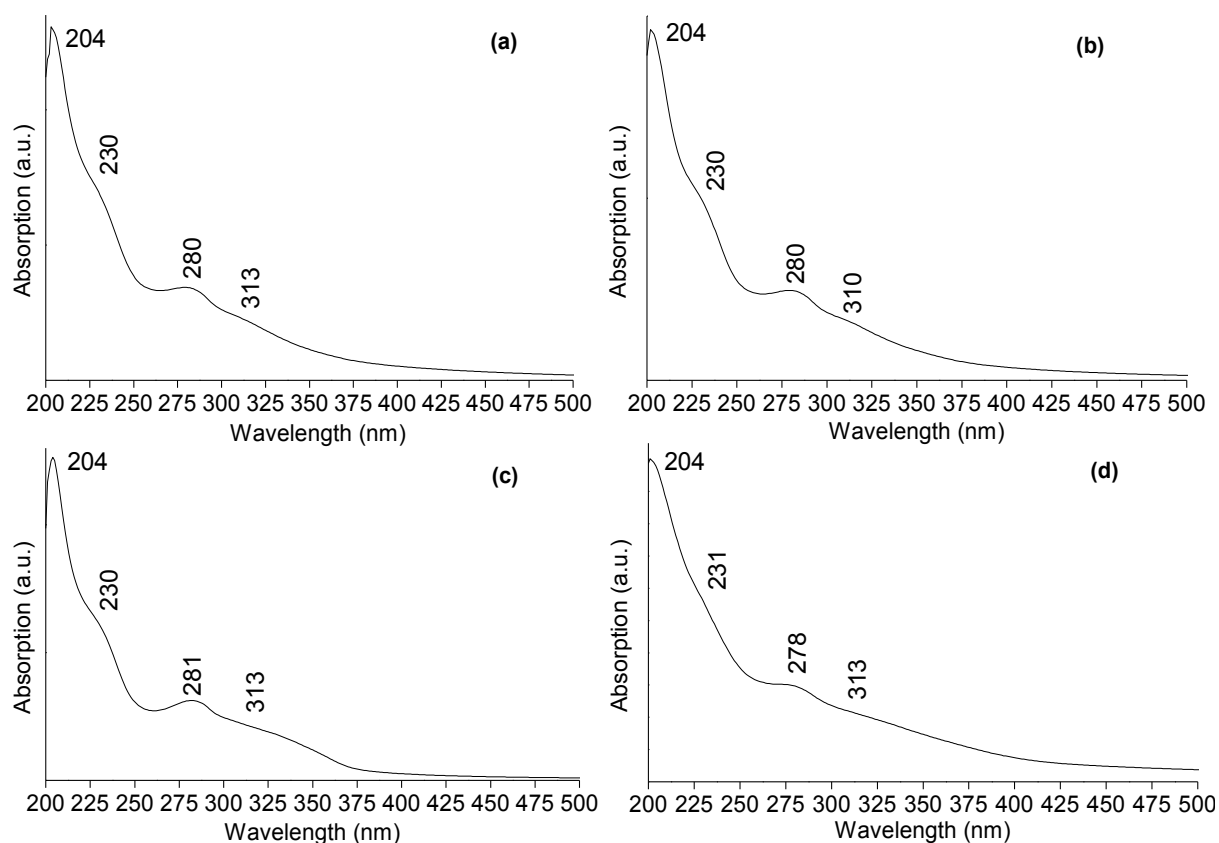
Figure 3A.8. UV-Vis spectra: (a) dealkaline, (b) alkaline, (c) alkali and (d) industrial lignin samples; 1 mg sample is dissolved in 10 mL methanol solvent.

3A.2.11. Attenuated total reflection (ATR) spectra of dealkaline, alkaline, alkali and industrial lignin

In ATR spectra typical bands for the lignin samples were recorded (Figure 3A.9), and the presence of various functional groups were correlated with the literature.[33-35] A broad band at 3410-3380 cm^{-1} is attributed to the hydroxyl groups attached with phenolic and aliphatic units, while peaks in the range between 2970-2880 cm^{-1} and 2860-2830 cm^{-1} are due to by C–H stretching vibrations in methoxy, methyl, methylene and aldehyde groups. The bands at 1610-1580 cm^{-1}, 1515-1505 cm^{-1}, 1440-1420 cm^{-1} and 1440-1420 cm^{-1} are assigned to skeletal vibrations of aromatic moieties (C=C) and C=O stretching group in the syringyl and guaiacyl aromatic rings present in lignin samples. The relatively higher intensity of the band at 1610-1580 cm^{-1}, in comparison with that of the band at 1515-1505 cm^{-1}, is due to presence of a considerable amount of *p*-hydoxyphenyl fragments, as well as of some condensed aromatic structures, favouring an increase in the intensity of this absorption band. The interesting band in the 1740-1770 cm^{-1}, 1740-1680 cm^{-1} and 1681-1640 cm^{-1} range may be assigned to the presence of unconjugated and conjugated carbonyl and aromatic carboxyl groups attached with lignin molecules. As shown in the Table 3A.3, lignin samples have DBE = 4.5-5, which suggests that lignin contained one phenolic units and one double bond that may be conjugated or unconjugated carbonyl, alkene or carboxylic groups attached with lignin. Similar results were

observed with ATR spectra of lignin samples. A shoulder at 1370-1350 cm^{-1} appears due to the presence of phenolic hydroxyl groups and aliphatic C–H in methyl groups, linked to side alkylated chains or aromatic rings. The higher intensity of the band at 1230-1200 cm^{-1}, in comparison to the band at 1275-1250 cm^{-1}, may be determined by the presence of both *p*-hydroxyphenyl derivatives and guaiacyl containing fragments. A very strong band at 1120-1115 cm^{-1} may be due to the C–H deformation in syringyl units and secondary alcohols, or by C=O stretching vibrations. The strong band at 1035-1025 cm^{-1} is complex and may be governed both by the deformation vibrations of C–H in the aromatic structures with predominating guaiacyl units, and by the deformation vibrations of C–O in the primary and stretching vibrations of unconjugated C=O group.The summary of the various mode of ATR bands present in the lignin are consolidated in the Table 3A.4.
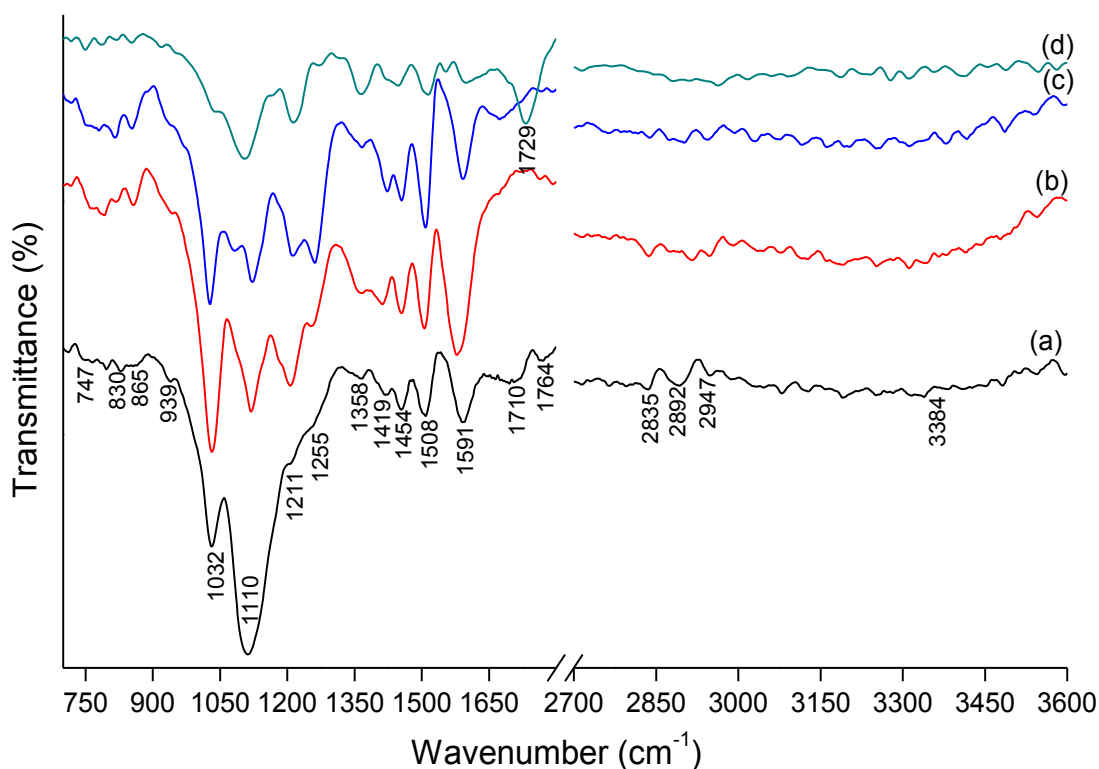
Figure 3A.9. ATR spectra: (a) dealkaline, (b) alkaline, (c) alkali and (d) industrial lignin.

Table 3A.4. ATR peaks assignments of commercial lignin samples.

Lignin peaks position (cm⁻¹)				Peaks (cm⁻¹)	Assignments
Dealkaline	Alkaline	Alkali	Industrial		
3384 (b)	3403 (b)	3403 (b)	3400 (b)	3410-3380	O-H stretching
2947 (w), 2892 (w)	2948 (w), 2918 (w)	2945 (w), 2898 (w)	2963 (w), 2882 (w)	2970-2880	C-H asymmetric stretching in methyl and methylene group
2835 (m)	2838 (m)	2838 (m)	2835 (m)	2860-2830	C-H symmetric stretching in methyl and methylene group
1764 (m)	1761 (w)	1761 (w)	-	1740-1770	C=O stretching in unconjugated ketone, carbonyl and ester groups
1710 (w)	1730 (w)	1729 (s)	1726 (w)	1740-1680	C=O stretching in unconjugated ketone, carbonyl and ester groups
-	1670 (w)	1675 (w)	-	1680-1640	C=O stretching in conjugated *p*-substituted aryl ketones
1591 (s)	1580 (s)	1592 (s)	1592 (m)	1610-1580	Aromatic skeleton vibration plus C=O stretching
1508 (s)	1505 (s)	1509 (s)	1512 (m)	1515-1505	Aromatic skeleton vibrations
1454 (s)	1454 (s)	1454 (w)	1445 (m)	1470-1450	C-H deformation (asymmetric in -CH₃ and –CH₂-)
1419 (m)	1413 (w)	1422 (w)	1416 (m)	1440-1420	Aromatic skeleton vibrations combined with C-H in plane deformations
1358 (w)	1365 (w)	1365 (w)	1365 (w)	1370-1350	Aliphatic C-H stretching in CH₃ (not –OCH₃) and phenolic -O-H
1255 (w)	1253 (m)	1262 (m)	1273 (m)	1275-1250	stretching C-H of *G* units
1211 (w)	1202 (s)	1208 (s)	1211 (s)	1230-1200	C-C plus C-O plus C=O stretching (*G* condensed >*G* etherified, typical of *G* units)
1110 (s)	1119 (s)	1116 (s)	1119 (s)	1120-1115	Aromatic C-H in plane deformation
1029 (s)	1019 (s)	1019 (s)	1003 (s)	1035-1025	Aromatic C-H in plane deformation (*G*>*S*) plus C-O deformation in primary alcohols plus C=O stretching (unconjugated)
939 (w)	942 (w)	933 (w)	920 (w)	945-920	-
865 (w)	856 (m)	853 (m)	853 (w)	865-	-

				850	
836 (m)	830 (s)	833 (s)	848 (w)	850-830	*p*- substituted phenolic unit
Note: (b) broad, (w) weak, (m) medium & (s) strong band intensities.					

3A.2.12. Nuclear magnetic resonance (NMR) spectroscopy

3A.2.12.1. ^{1}H and ^{13}C NMR of dealkaline lignin

To probe more about the skeleton (proton and carbon) of the dealkaline lignin, ^{1}H and ^{13}C NMR spectra were recorded (500 MHz). ^{1}H NMR spectrum for the dealkaline lignin is shown in Figure 3A.10. As observed from the spectrum, the peaks for $-CH_3$, $-CH_2-$, and $-CH-$ alkyl groups are observed around 0.5–1.80 ppm in ^{1}H NMR spectrum of lignin sample. The appearance of peaks from 2.00-2.80 ppm can be assigned to the proton α to the carbonyl group ($R-CO-CH_3$; R-alkyl or aryl) or benzylic proton ($Ar-CH_3$) or ester ($R-CH_2-COOR$; R= alkyl or aryl) groups. Another peak in the range between 3.7-3.9 ppm is due to the presence of methoxy (CH_3-O-) or $Ar-OCH_3$ or an ester group ($R-COOCH_2R$; R=alkyl or aryl), etc. Aromatic proton peaks are assigned between 6.0 and 8.5 ppm region for the *S*, *G* and *H* phenolic moieties present in the lignin samples and the peak at 9.9 ppm is assigned for the aldehyde proton R-C(O)H peaks. Similarly, the presence of aldehyde group is in lignin samples are also confirmed by the ATR spectra for carbonyl groups in the range between 1710-1740 cm^{-1}.

To understand the skeleton of the lignin samples, ^{13}C NMR spectra were recorded (Figure 3A.10). The peaks in the range of 20–50 ppm are typically for CH_3CO- species or R_3CH (R-alkyl) species. The peaks at 55-90 ppm are assigned to the carbon next to heteroatom (oxygen) ($R-CH_2-O-$; $R_2-CH-O-$; R_3-C-O-; R=alkyl or aryl group), etc. The peaks for aromatic regions are observed between 110–150 ppm and for alkenes between 110–140 ppm. Further, the peaks in the range of 170-180 ppm are assigned to carbon in ester/aldehyde groups ($R-CO-R$, R-alkyl or aryl), etc. The appearance of carbonyl groups (in the range between 1680-1770 cm^{-1}) in the lignin samples are confirmed by the ATR spectra (Figure 3A.9).
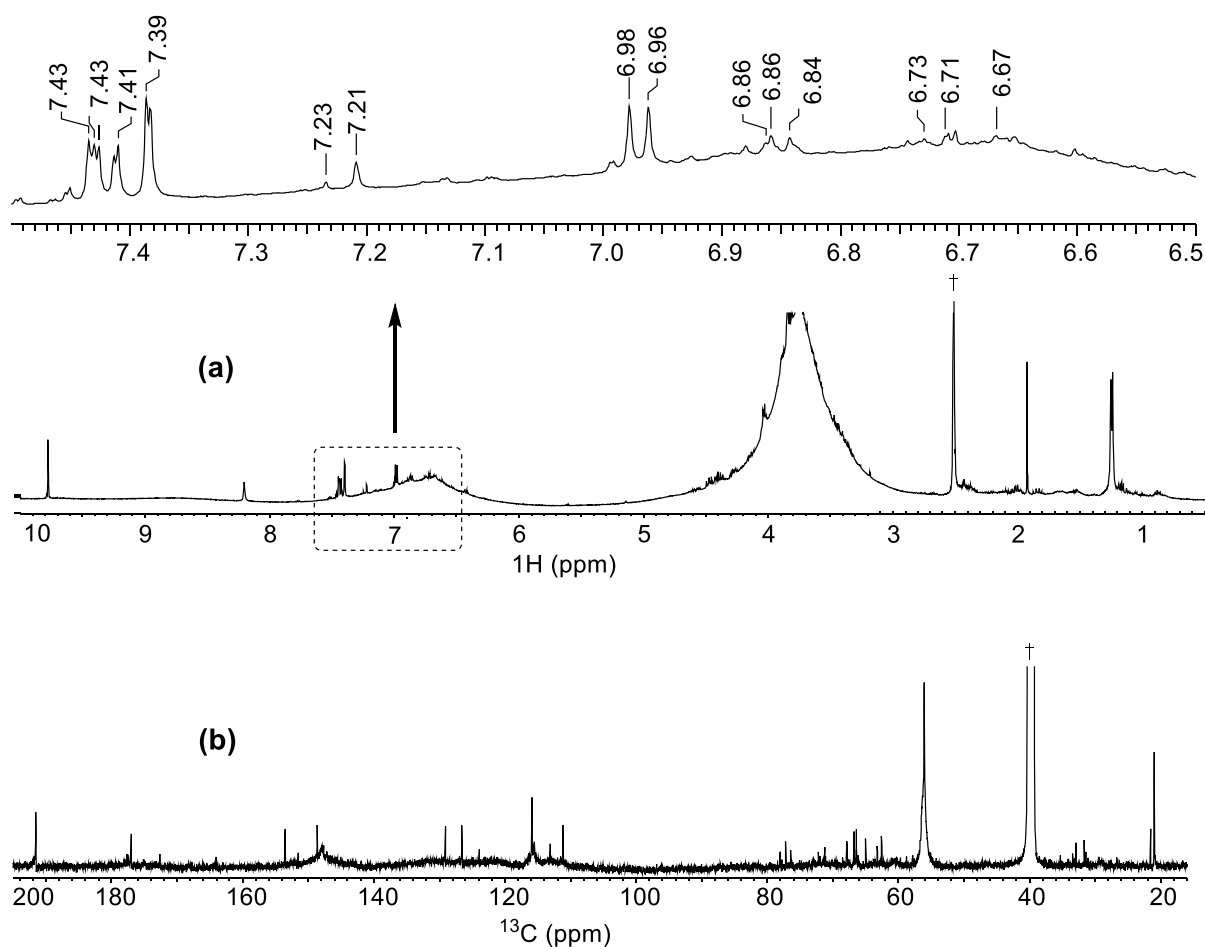
Figure 3A.10. (a) ^{1}H and (b) ^{13}C NMR spectra of dealkaline lignin. NMR spectra were recorded in DMSO-d_6 solvent. † peak assigned for the solvent peak.

3A.2.12.2. Heteronuclear single quantum coherence (HSQC) NMR of dealkaline lignin

To find out more information on the structure of lignin, two dimensional heteronuclear single quantum coherence (2D, HSQC), NMR spectroscopy was carried out to characterize dealkaline lignin in deuterated DMSO solvent. The peaks at δ= 2.5 ppm (^{1}H NMR) and δ= 39.5 ppm (^{13}C NMR) were considered as reference peaks to assign the 2D (HSQC) NMR signals for the lignin. To understand the various types of substructure unit, linkages and the presence of chemical moieties (*S*, *G* and *H*) in the lignin molecule, the assigned 2D (HSQC) NMR results are correlated with available reports.[3, 35-38] However, the variable chemical composition of the linkages present in the lignin sample [i.e., β-O-4′ ether linkage (A); phenylcoumaran (β-5′; α-O-4′ linkage) (B); phenyl propenoid units : *p*-hydroxyphenyl alcohol (*H*), guaiacyl alcohol (*G*), syringyl alcohol (*S*) and *p*-hydroxybenzoate (PB)], were observed and confirmed with the help of 2D (HSQC) NMR spectrum (Figure 3A.11).

The 2D (HSQC) NMR spectrum of the lignin sample is divided into three subsequent regions; 1) alkylated side chain region or saturated hydrocarbons (δ$_H$/δ$_C$= 0.5-2.5/10.0-50.0 ppm); 2)

oxygenated aliphatic/aromatic regions (δ_H/δ_C= 2.5-6.0/50.0–90.0 ppm) and 3) olefinic/aromatic regions (δ_H/δ_C= 6.0-8.5/100.0-140.0 ppm), present in the lignin.

Alkylated side chain region

The signals for alkylated side chain regions are observed in the range of δ_H/δ_C= 0.5-2.5/10.0-50.0 ppm. For the terminal or bridge aliphatic hydrocarbons, close to the carbonyl or olefinic or aromatic moieties are observed in the range of 0.5-2.5/10.0-50.0 ppm. However, the signals present for the side chain of the alkylated groups clearly support the fact that inter linkage units are present in the lignin molecules. Accordingly, based on the 2D (HSQC) NMR spectra of alkylated region δ_H/δ_C= 0.5-2.5/10.0–50.0 ppm, it is difficult to differentiate the lignin sub-structural moieties.

Linkages region

The side chain region of the 2D (HSQC) NMR spectrum provides the useful data pertaining to various inter-unit linkages present in the lignin molecule. The linkage units (alkylated group attached with hetero atom or next to olefins/aromatic rings) present in the lignin sample are visible in the range between δ_H/δ_C= 2.5-6.0/50.0–90.0 ppm in the 2D (HSQC) NMR spectrum (Figure 3A.11). The 2D (HSQC) NMR showed prominent signal at δ_H/δ_C=3.73/56.05 ppm which correspond to –OCH$_3$ group present in the lignin which may be attached with the alkylated chain or at the aromatic rings (*S* and *G* moieties) as shown in Figure 3A.11d. The 2D (HSQC) signal at δ_H/δ_C= 3.39/60.88 ppm is assigned to the presence of Hγ-Cγ within Aγ lignin substructure for β-O-4' linkage. The presence of phenyl coumaran substructure linkage Hγ-Cγ correlation in β-5' unit is obtained at δ_H/δ_C= 3.59/63.14 ppm in the 2D (HSQC) NMR spectrum of the lignin. The signal at δ_H/δ_C= 3.35/62.32 ppm are assigned for the Cγ-Hγ at β-5' phenyl coumaran (Bγ) structural unit. However, in 2D (HSQC), few of the linkage signals could not be assigned based on the literature and these signals are alkylated side chain attached with the heteroatoms or olefinic bonds.
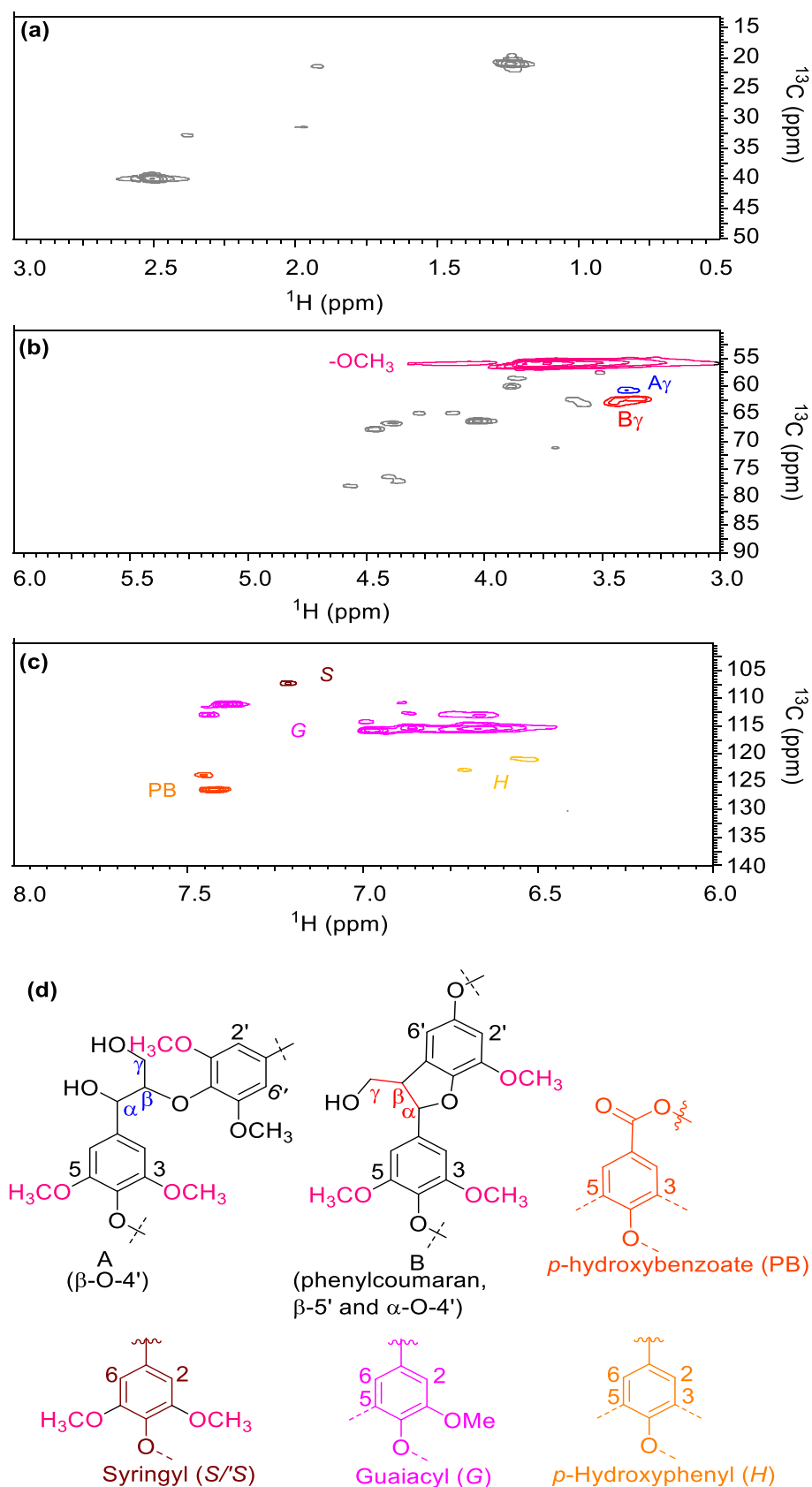
Figure 3A.11. 2D (HSQC) NMR spectrum of dealkaline lignin (a) Alkylated side chain region, (b) linkage region, (c) olefinic/aromatic region and (d) substructure units. The NMR spectrum was recorded in the DMSO-d_6 solvent.

Olefinic/aromatic region

The lignin structural units are made up of alkylated, arylated (*S*, *G* and *H* units), olefinic and various types of linkages as shown in Figure 3A.11. The details of the 2D (HSQC) NMR signals for olefinic/aromatic (*p*-hydroxyphenyl alcohol (*H*), guaiacyl alcohol (*G*), syringyl alcohol (*S*) and to *p*-hydroxybenzoates moieties assigned, which are correlated from the literature. The 2D (HSQC) NMR signals at δ_H/δ_C= 6.88/110.88 ppm correspond to G_2 and signals at δ_H/δ_C= 6.75-6.67/115.59 ppm are matched with G_5 signals present in lignin sample. The oxidised $S_{2,6}$ structural units present in the lignin sample are detected at δ_H/δ_C= 7.21/107.41 ppm. Interestingly, in the 2D (HSQC) NMR spectrum, it is possible to see the two signals at δ_H/δ_C= 6.99/114.30 ppm and δ_H/δ_C= 7.42/126.52 ppm corresponding to the $H_{3,5}$ unit and $H_{2,6}$ moieties. Signals due to *p*-hydroxybenzoate ($PB_{3,5}$) are also seen at δ_H/δ_C= 7.44/127.9 ppm in the lignin samples.

3A.3. Conclusions

In the summary, as properties of lignins differ based on the type/age of plant and isolations procedures, it becomes important to understand those before depolymerization and hence commercially procured lignin samples were systematically characterized by assorted thermal/spectroscopic techniques. The solubility studies of lignin were checked in various solvents and water:methanol (1:5 *v/v*) ratio was selected as the best solvent ratio for completely solubilising dealkaline lignin. Based on HSP values, it was easy to select solvent for extraction of low molecular weight aromatic products from the lignin depolymerized reaction mixture. The X-ray diffraction (XRD) measurements were carried out for understanding the morphologies of commercial lignin samples, which showed amorphous nature of lignin with Na_2SO_4 contamination in dealkaline and industrial lignin samples. It may be possible due to Kraft isolation process which is used to extract lignin, where white liquor (NaOH and Na_2S) solution are used. Scanning electron microscopy helped to suggest the unstructured morphology of commercial lignin and energy dispersive X-ray spectroscopy (EDX) attached with SEM also confirmed the C, O, Na, S present in lignin. ICP-OES analysis also confirmed the Na and S impurities present in the lignin. Though, conclusive estimation of the molecular weight of lignin samples is not possible due to lack of standards for the same, gel permeation chromatography (GPC) analysis was carried out to get an idea about molecular weight distribution and it observed 60 kDa molecular weight of dealkaline lignin. The matrix assisted laser desorption ionisation - time of flight mass spectrometry (MALDI-TOF MS), also affirms the molecular weight observed in GPC analysis. The GPC and MALDI-TOF MS analysis of dealkaline lignin were carried out and obtained results (~60 kDa) are similar to tentative 333 phenylpropenoid monomeric units, which is calculated based on dealkaline lignin monomeric formula $C_{10}H_{13}O_3S_{0.09}$ (molecular weight- ca. 180 g/mol). To understand the thermal response of

lignin TPO-MS studies were undertaken and it was observed that lignin decomposes in a wide range of temperature, probably because it contains various linkages, functional groups and bond dissociation enthalpies etc. It is worth noting that when experiment was performed with 5% oxygen (*v/v*), intense peaks for gases products ($CO/CO_2/CH_4/H_2$ etc.) were observed at lower temperatures (<550 °C), but formation of these products was less under helium atmosphere even until 800 °C as oxygen helps degradation. The melting (*Tm*= 230 °C) and crystalline (*Tc*= 245 °C) temperature of the dealkaline sample was monitored with the help of DSC thermal analysis. Elemental analysis was used to quantify the carbon, hydrogen and oxygen present in lignin, which defined the monomer molecular formula in the range between $C_{10}H_{12-13}O_3S_{0.01-0.09}$, with 4.5-5 double bond equivalence numbers, which showed one aromatic ring (DBE= 4) along with one double (DBE= 1) bond present in phenylpropenoid unit. The presence of electronic transitions in the lignin samples were monitored with UV-Visible spectroscopy. The functional groups present in commercial lignin samples were checked with attenuated total reflection (ATR) spectroscopy. The lignin skeleton (proton and carbon) environment was examined using 1D (^1H and ^{13}C) and 2D (HSQC) nuclear magnetic resonance spectroscopy technique. Similarly, the aromatic moieties are also confirmed by the ATR and NMR analytical techniques. In the next sections 3B and 3C, lignin depolymerization studies are discussed using $-SO_3H$ functionalized homogeneous and immobilized ionic liquids, respectively.

3A.4. References

1. W. Boerjan, J. Ralph and M. Baucher, *Annu. Rev. Plant Biol.*, 2003, **54**, 519-546.
2. M. Frei, *Sci. World J.*, 2013, **2013**, 25.
3. S. K. Singh and P. L. Dhepe, *Bioresour. Technol.*, 2016, **221**, 310-317.
4. J. J. Stewart, T. Akiyama, C. Chapple, J. Ralph and S. D. Mansfield, *Plant Physiol.*, 2009, **150**, 621-635.
5. S. Jia, B. J. Cox, X. Guo, Z. C. Zhang and J. G. Ekerdt, *ChemSusChem*, 2010, **3**, 1078-1084.
6. B. J. Cox, S. Jia, Z. C. Zhang and J. G. Ekerdt, *Polym. Degrad. Stab.*, 2011, **96**, 426-431.
7. A. Rahimi, A. Azarpira, H. Kim, J. Ralph and S. S. Stahl, *J. Am. Chem. Soc.*, 2013, **135**, 6415-6418.
8. F. Cheng and C. E. Brewer, *Renewable Sustainable Energy Rev.*, 2017, **72**, 673-722.
9. J. S. Lupoi, S. Singh, R. Parthasarathi, B. A. Simmons and R. J. Henry, *Renewable Sustainable Energy Rev.*, 2015, **49**, 871-906.
10. S. H. Ghaffar and M. Fan, *Biomass Bioenergy*, 2013, **57**, 264-279.
11. J.-X. Sun, X.-F. Sun, R.-C. Sun, P. Fowler and M. S. Baird, *J. Agric. Food Chem.*, 2003, **51**, 6719-6725.
12. M. Belmares, M. Blanco, W. A. Goddard, R. B. Ross, G. Caldwell, S. H. Chou, J. Pham, P. M. Olofson and C. Thomas, *J. Comput. Chem.*, 2004, **25**, 1814-1826.
13. C. M. Hansen, *Hansen Solubility Parameters: A User's Handbook, Second Edition*, CRC Press, 2007.
14. in *Journal of Chromatography Library*, ed. J. S. Peter, Elsevier, 1986, vol. Volume 35, pp. 20-36.
15. G. C. Vebber, P. Pranke and C. N. Pereira, *J. Appl. Polym. Sci.*, 2014, **131**, n/a-n/a.

16.   Z. Yuan, S. Cheng, M. Leitch and C. Xu, *Bioresour. Technol.*, 2010, **101**, 9308-9313.

17.   M. L. Mattinen, S. Tapani, R. Gosselink, D. S. Argyropoulos, D. Evtuguin, A. Suurnäkki, E. de Jong and T. Tamminen, *BioResources*, 2008, **3**, 549.

18.   R. A. Fenner and J. O. Lephardt, *J. Agric. Food Chem.*, 1981, **29**, 846-849.

19.   R. Sun, J. Tomkinson and G. Lloyd Jones, *Polym. Degrad. Stab.*, 2000, **68**, 111-119.

20.   J. D. Peterson, S. Vyazovkin and C. A. Wight, *Macromol. Chem. Phys.*, 2001, **202**, 775-784.

21.   P. S. B. dos Santos, P. H. G. de Cademartori, R. Prado, D. A. Gatto and J. Labidi, *Wood Sci. Technol.*, 2014, **48**, 873-885.

22.   S. Zhao, Y. Luo, Y. Su, Y. Zhang and Y. Long, *Energy Fuels*, 2014, **28**, 5049-5056.

23.   A. I. Afifi, J. P. Hindermann, E. Chornet and R. P. Overend, *Fuel*, 1989, **68**, 498-504.

24.   *US Pat.,* U.S. Pat. No. 3,726,850, 1973.

25.   J. Zakzeski, P. C. A. Bruijnincx, A. L. Jongerius and B. M. Weckhuysen, *Chem. Rev.*, 2010, **110**, 3552-3599.

26.   E. O. S. Saliba, N. M. Rodriguez, D. Piló-Veloso and S. A. L. Morais, *Arq. Bras. Med. Vet. Zootec.*, 2002, **54**, 42-51.

27.   X. Zhang, Q. Zhang, J. Long, Y. Xu, T. Wang, L. Ma and Y. Li, *BioResources*, 2014, **9**, 3347-3360.

28.   J. Long, X. Li, B. Guo, F. Wang, Y. Yu and L. Wang, *Green Chem.*, 2012, **14**, 1935-1941.

29.   H. Yang, Y. Xie, X. Zheng, Y. Pu, F. Huang, X. Meng, W. Wu, A. Ragauskas and L. Yao, *Bioresour. Technol.*, 2016, **207**, 361-369.

30.   K. Mononen, A.-S. Jaaskelainen, L. Alvila, T. Pakkanen Tuula and T. Vuorinen, *Holzforschung*, 2005, **59**, 381-388.

31.   X. Zhao, L. Dai and D. Liu, *J. Appl. Polym. Sci.*, 2009, **114**, 1295-1302.

32.   U. Westermark, *Wood Sci. Technol.*, 1985, **19**, 223-232.

33.   G. Gellerstedt, J. Li, I. Eide, M. Kleinert and T. Barth, *Energy Fuels*, 2008, **22**, 4240-4244.

34.   G. Zhou, G. Taylor and A. Polle, *Plant Methods*, 2011, **7**, 1-10.

35.   S. K. Singh and P. L. Dhepe, *Green Chem.*, 2016, **18**, 4098-4108.

36.   N. D. Bonawitz, J. I. Kim, Y. Tobimatsu, P. N. Ciesielski, N. A. Anderson, E. Ximenes, J. Maeda, J. Ralph, B. S. Donohoe, M. Ladisch and C. Chapple, *Nature*, 2014, **509**, 376-380.

37.   M. Foston, R. Samuel, J. He and A. J. Ragauskas, *Green Chem.*, 2016, **18**, 608-621.

38.   J. Rencoret, J. Ralph, G. Marques, A. Gutiérrez, Á. T. Martínez and J. C. del Río, *J. Agric. Food Chem.*, 2013, **61**, 2434-2445.

Section 3B:

Depolymerization of lignin using Brønsted acidic ionic liquids

3B.1. Introduction

Lignin is ca. 30% by *wt.* and 40% by energy constituent of dried lignocellulosic biomass.[1-3] It is 3 dimensional, amorphous copolymer and mainly composed of 3 major phenyl propenoid units, which are coumaryl (*H*), coniferyl (*G*) and sinapyl (*S*) alcohols, linked *via* ≡C-O-C≡ and ≡C-C≡ bonds.[4-6] The composition of *H, G* and *S* units vary with age of plant, type of plant, environment, soil conditions, isolation procedures, etc.[7] Currently, it is burned to get heat and power, during which large quantity of CO_2 is produced into the atmosphere. Depolymerization of lignin can produce aromatic derived products, which have a wide range of application in various fields like polymers, petrochemicals, materials etc. Therefore, development of an efficient catalytic process for lignin depolymerization in to higher yield of low molecular weight aromatic monomers is very important.

Several methods have been employed for the depolymerization of lignin (Please see the Chapter 1, Section 1.9). To the best of my knowledge there are no reports available on Brønsted acidic ionic liquids (BAILs) as catalysts for lignin depolymerization into low molecular weight aromatic products under the milder reaction conditions (T ≤120 °C). Hence, it was anticipated that lignin can be depolymerized into low molecular weight aromatic products first time using only BAILs as catalysts under milder reaction conditions. Details on reaction conditions are discussed in the Section 3B.

In this Section, 4 different types of actual lignin have been used to depolymerize into low molecular weight aromatic products. Additionally, to avoid the formation of side products such as char, tar and gases, the thermal stability of products was done under the similar reaction conditions, as employed for lignin depolymerization. Subsequently in this work, reasonable deliberations on structures and various functional groups correlation in lignin and in products are discussed by meticulous characterization techniques.

3B.2. Experimental

3B.2.1. Materials

Dealkaline lignin (CAS Number : 9005-53-2   Product Number : L0045, TCI Chemical, Japan); alkaline lignin (CAS Number : 8068-05-1   Product Number : L0082, TCI Chemical, Japan); alkali lignin (CAS Number : 8068-05-1   Product Number : 370959, Aldrich, USA) were purchased and used without any further pre-treatment. Along with commercial lignin samples, lignin was also collected from local industries like industrial lignin. The vanillin (99%), eugenol (99%), 1,3-dimethoxybenzene (99%) were purchased from Aldrich USA. Methyl vanillate (99%) and *m*-cresol from Acros organic India, guaiacol (99%), sulphuric acid (98%), hydrochloric acid (35%), tetrahydrofuran (THF, 99.5%, AR), methanol (99.8%, AR), toluene (99.5%, AR), iso-propyl alcohol (99.5%, AR), diethyl ether (DEE, 99%, AR) and ethyl acetate (EtOAc, 99.8%) were

purchased from Loba Chemia, India and ethanol absolute (99.9%) Changshu Yangyuan chemical China was purchased. These chemicals were used as such without any further treatment.

3B.2.2. Synthesis and characterization of catalysts

The phosphonium, ammonium, benzimidazolium and imidazolium cation based BAILs/IL with various anions were synthesised in two steps (except [BMIM][Cl]). In a first step, zwitterion formation or quarterisation was done and in the second (final) step synthesis of ILs *via* direct combination method was carried out. The details of the synthesis procedures and structures of the ILs are given in Chapter 2, Sections 2A.2.2 and Table 3B.1. The various physico-chemical analytical techniques (CHNS, NMR (1D- ^{1}H and ^{13}C), FT-IR, TGA and UV-Vis) (Chapter 2, Section 2A.5), revealed that ILs are obtained in pure form and are stable until 250 ^{o}C and those possess different Hammett acid functions (H_0) (Chapter 2, Sections 2A.6-2A.7).

Table 3B.1. Full name and abbreviation of ionic liquids (ILs).

Full name of ILs	Abbreviationof the ILs
1-methyl-3-(3-sulfopropyl)-imidazolium hydrogensulfate	$[C_3SO_3HMIM][HSO_4]$
1-methyl-3-(3-sulfopropyl)-imidazolium *p*-toluenesulfonate	$[C_3SO_3HMIM][PTS]$
1-methyl-3-(3-sulfopropyl)-imidazolium chloride	$[C_3SO_3HMIM][Cl]$
1-methyl-3-(3-sulfopropyl)-imidazolium dihydrogenphosphate	$[C_3SO_3HMIM][H_2PO_4]$
1-methyl-3-(3-sulfopropyl)-benzimidazolium hydrogensulfate	$[C_3SO_3HBenzMIM][HSO_4]$
3-sulfopropyl-P,P,P-triphenylphosphonium hydrogensulfate	$[C_3SO_3H(C_6H_5)_3P][HSO_4]$
1-methyl-3-(3-sulfopropyl)-imidazolium cupric chloride	$[C_3SO_3HMIM][CuCl_3]$
1-methyl-3-(3-sulfopropyl)-imidazolium ferric chloride	$[C_3SO_3HMIM][FeCl_4]$
1-methyl-3-(3-sulfopropyl)-imidazolium stannic chloride	$[C_3SO_3HMIM][SnCl_3]$
1-butyl-3-methylimidazolium chloride	[BMIM][Cl]
N, N, N-triethyl-3-sulfopropanaminium hydrogensulfate	$[C_3SO_3H(C_2)_3N][HSO_4]$
N, N, N-triethyl-3-sulfopropanaminium *p*-toluenesulfonate	$[C_3SO_3H(C_2)_3N][PTS]$
N, N, N-triethyl-3-sulfopropanaminium chloride	$[C_3SO_3H(C_2)_3N][Cl]$
N, N, N-triethyl-3-sulfopropanaminium dihydrogenphosphate	$[C_3SO_3H(C_2)_3N][H_2PO_4]$

3B.2.3. Characterization of lignin

In my work, depolymerization of real lignin (instead of model compounds such as dimers/trimers) is done and since it is recognized that the properties of lignins are dependent on the type/age of plant and isolations procedures, it was decided to characterize lignins using several thermal and spectroscopic techniques. The details on lignin characterizations are already discussed in Chapter 3, Section 3A. In this section of the Chapter 3, discussions on the results obtained in catalytic depolymerization of lignin carried out with homogeneous ionic

liquids is done. Furthermore, deliberations on the correlations studies between lignin and depolymerized products are done based on several thermal, spectroscopic and chromatographic techniques.

3B.2.4. Lignin depolymerization

Depolymerization reactions of lignin were conducted at desired temperatures for required time in a batch mode reactor of 150 mL capacity (Parr Autoclave, USA). Unless specified, in all the reactions, lignin (2 *wt.*% solution H_2O:CH_3OH, 1:5 *v/v*= 30 mL) and catalyst (0.5 g) were charged and the reactor was heated to desired temperature under slow stirring (100 rpm). Unless mentioned all the reactions were carried out with dealkaline lignin. After attaining the desired temperature, stirring was increased to 1000 rpm and this time was considered as starting time of a reaction. At this temperature the pressure generated in the autoclave was 0.35 MPa due to water and methanol. After completion of reaction, reactor was allowed to cool to room temperature under the flow of air and slow stirring (100 rpm).

3B.2.5. Work-up procedure

After completion of reaction, reactor was allowed to cool to room temperature under the flow of air and slow stirring (100 rpm). Reaction mixture was collected and solvent (water and methanol) was evaporated using rotary vacuum evaporator (Figure 3B.1). Care was taken to trap all the low volatile products by arranging 3 ice traps in series before vacuum pump. The analysis of any collected solvent in these traps revealed no loss of products. The reaction mass (ILs + products + unreacted lignin) obtained after removing solvent was dried at 55 ℃ for 16 h and further under vacuum at 80 ℃ for 4 h. The weight of the dried viscous mass ('a' in Figure 3B.1) was taken to check the mass balance and to the dried mass, 30 mL of tetrahydrofuran (THF) was added to dissolve the products ('b' in Figure 3B.1). THF was chosen to extract the products as it does not dissolve lignin (Chapter 3, Section 3A.2.1, Table 3A.1). Similarly, it was also observed that ILs are not soluble in THF (Chapter 2, Section 2A. Table 2A.2) and hence it was anticipated that the solvent will only extract aromatic products. Similar to THF extraction, products were also extracted using 30 mL diethyl ether (DEE, 'c' in Figure 3B.1) and ethyl acetate (EtOAc, 'd' in Figure 3B.1).
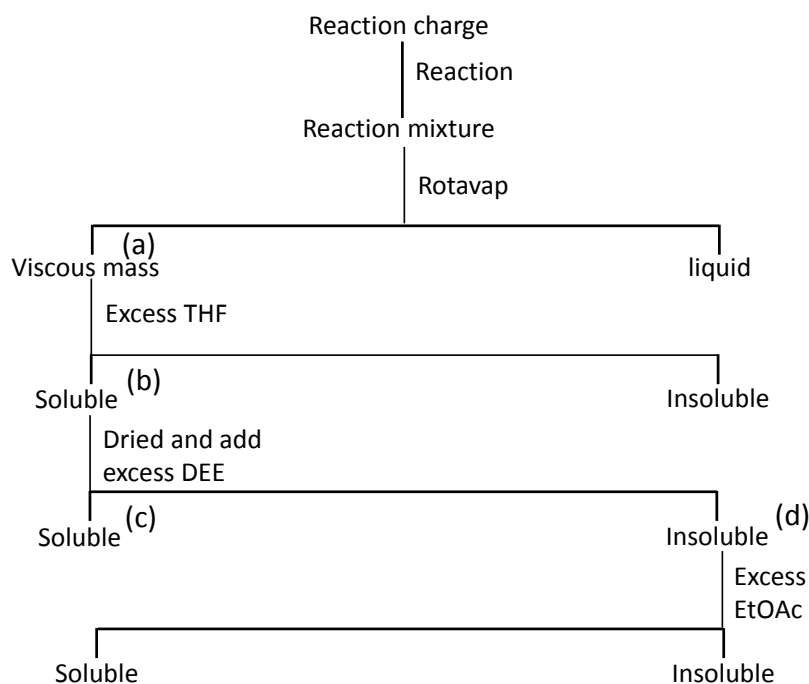
[a]depolymerized, repolymerized, unconverted lignin BAILs and IL

[b]THF soluble low molecular weight aromatic products (analysed by GC, HPLC, LC-MS, GPC, FT-IR, ^{1}H and^{13}C NMR, TGA (Air) etc.

[c]DEE soluble products, lower molecular weight aromatic products and

[d]ILs, repolymerized and unconverted lignin

Figure 3B.1. Extraction of organic solvent soluble products from reaction mixture.

3B.2.6. Analysis of THF, EtOAc and DEE soluble liquid products

The lignin depolymerization into THF, EtOAc and DEE soluble low molecular weight aromatic products was confirmed using several analytical techniques such as, GC, GC-MS, HPLC, LC-MS, GPC, NMR (1D-^{1}H and ^{13}C, and 2D-HSQC), FT-IR, DSC, TGA, CHNS and UV-Vis.

3B.2.6.1. Gas chromatography (GC)

THF soluble low molecular weight aromatic products were analysed using GC (Varian CP 3800, Netherland) attached with flame ionization detector (FID) and CPSIL 8CB capillary column (5% phenyl 95% dimethyl polysiloxane) (30 m x 0.25 mm x 0.32 μm). N$_2$ (inert gas) was used as a carrier gas (flow rate 0.6 mL/min). The column oven program; 100 ^{o}C (hold time: 4 min) $\rightarrow$ 10 ^{o}C/min $\rightarrow$ 280 ^{o}C (hold time: 20 min) was used along with injector temperature of 275 °C and detector temperature of 280 °C. The split ratio used was 40:1 for sample delivery.

3B.2.6.2. Gas chromatography-mass spectrometry (GC-MS)

The Varian 3800 GC-MS, (Saturn 2000MS) equipped with the VF-5 capillary column (5% phenyl 95% dimethyl polysiloxane) (30 m x 0.25 mm x 0.25 μm) was used and helium (0.6 mL/min) was used as a carrier gas. The similar column oven program used for GC analysis was also used in this analysis. The formation of various compounds was confirmed by matching the

fragmentation pattern(s) from NIST library and by injecting commercially procured standard samples.

3B.2.6.3. High pressure liquid chromatography (HPLC)

THF soluble aromatic products were analysed using Agilent make HPLC system equipped with auto sampler, C18 column (250 mm x 4.6 mm, 30 °C) and refractive index (RI) detector (40 °C). $CH_3OH:H_2O:CH_3COOH$ (39:59:2 *v/v/v*) was used as mobile phase with a flow rate of 0.5 mL/min. The identification of the compounds in the THF soluble mixture was done by injecting commercially procured standard samples.

3B.2.6.4. Liquid chromatography-mass spectrometry (LC-MS)

The LC-MS (Thermo Finnigan Electro Spray Ionisation, Positive mode 40 volt) analysis of THF soluble products was carried out using Surveyor MSQ liquids chromatography.

3B.2.6.5. Gas chromatography-thermal conductivity detector (GC-TCD)

The gas products were analysed in Chemito 8610 model GC attached with TCD detector and is equipped with Porapack Q column (2.74 m × 2 mm). The column oven program was 100 ºC (hold time: 4 min) → 10 ºC/min → 180 ºC (hold time: 4 min) along with injector temperature of 50 °C and detector temperature of 150 °C.

3B.2.6.6. Gel permeation chromatography (GPC)

GPC analysis was carried out to check the molecular weight of the obtained products in the THF soluble low molecular weight aromatic products (Chapter 3, Section 3A.1.1).

3B.2.7. Solubility of IL in THF

Lignin depolymerization reactions were done using homogeneous ILs as catalysts. After the reaction, reaction mixture was collected, filtered and solvent was evaporated at reduced pressure to obtain viscous reaction mixture. THF was used to extract the low molecular weight aromatic products from the reaction mixture. To confirm the absence of ILs in the THF soluble low molecular weight aromatic products, solubility of ILs was checked in the THF solvent. In a typical procedure, 0.5 g IL was mixed with 30 mL THF and this mixture was stirred for 1 h at room temperature (25 ºC). It was observed that IL (lower layer) and THF (upper layer) form separate layers. The upper layer of THF was separated through separating funnel and was taken in RB. Later THF was evaporated using rotary evaporator and to the RB, water was added and this water solution was injected in HPLC. No peak for IL was observed which confirmed that IL is insoluble in THF. Moreover, weight of empty RB and after evaporation of THF was observed to be same, which again confirmed that the IL is not dissolved in THF. This observation and earlier observation of non-solubility of lignin in THF, suggests that the mass obtained in THF after the reaction does not have any contribution from IL and lignin.

3B.2.8. Yield calculation

The yield (%) for THF soluble products was calculated based on the viscous mass recovered from the THF solvent.

THF soluble products yield (%)

$$= \frac{\text{Weight of THF soluble viscous mass}}{\text{Weight (moisture and ash corrected) of lignin charged}} \times 100 \qquad (3B.1)$$

Most of the reactions were performed three times to check the reproducibility of results and the data presented in the current work is average of these three reactions.

Typically, ±3% error in the yields in repeated reactions was observed.

3B.2.9. Mass balance calculation

Mass balance of the reaction was calculated based on several weights taken during the reaction. To illustrate this further an example is shown below,

Reaction conditions: Lignin 0.5 g (2 *wt.*% solution H_2O:CH_3OH, 1:5 *v/v*= 30 mL), catalyst (ILs/acids) 0.5 g, 120 ºC, 1 h.

Total charge of the reaction is 0.945 g (lignin 0.445 g (0.5 g - 0.055 g (moisture) + catalyst 0.5 g). After following above mentioned work-up procedure, the weight of dried viscous mass (solid 'a' in Fig. 3B.1) at room temperature was 0.920 g.

Mass balance (%)

$$= \frac{\text{Weight of dried viscous mass}}{\text{Weight of actual charge}} \times 100 \qquad (3B.2)$$

$$\text{Mass balance (\%)} = \frac{0.920 \text{ g}}{0.945 \text{ g}} \times 100$$

$$= 97\%$$

3B.3. Result and discussion

3B.3.1. Depolymerization of lignin using catalyst (weight basis)

3B.3.1.1. Effect of anions

Typically, ionic liquids (ILs) based on imidazolium cation with [Cl], [PTS], [H_2PO_4] and [HSO_4] several anions were used as catalysts. These ILs with different acidity (for more details please see the Chapter 2, Section 2A.7) were chosen for the lignin depolymerization reactions. The catalytic reactions were carried out using batch mode Parr reactor with varying reaction parameters. The workup procedure, analysis of products by GC, GC-MS, HPLC, LC-MS, GPC etc. analytical techniques and calculation of products yield were done as discussed in the sections above.

Initially, the catalytic activity of imidazolium based cation with [Cl], [PTS], [H_2PO_4] and [HSO_4] several anions was evaluated for dealkaline lignin depolymerization reaction at 120 °C for 1 h, which has the molecular weight (60 kDa). The dealkaline lignin depolymerization reactions were carried out and the obtained results are shown in Figure 3B.2a. Under the desired reaction conditions without catalyst only 4% yield of low molecular weight aromatic products was obtained. But when the IL with imidazolium cation and [HSO_4] anion was used the yield for low molecular weight aromatic products increased to 78% THF soluble products. Among all the ILs, catalysts with imidazolium cation and with [Cl], [PTS], [H_2PO_4] and [HSO_4] anions having different Hammett acidity function (Chapter 2, Section 2A.7), and dissimilar dissociation constant, showed the variable activity for low molecular weight aromatic products formation (24-78% yield). Interestingly, neutral IL, [BMIM][Cl] as expected showed inferior yield (18%) compared to BAILs because of absence of –SO_3H group, yet it offered improved yield than non-catalytic reaction (4%).

As seen from Figure 3B.2a, imidazolium cation with [HSO_4] catalyst having 6.64 mmol of H^+ shows better activity (78% yield) than [H_2PO_4] anion having 9.96 mmol H^+ catalyst (38% yield). This must be due to the difference in their dissociation constants (Ka) of the H_2SO_4 and H_3PO_4 and as per the literature[8-10] survey the dissociation constant of acids are shown as below.

H_2SO_4 → HSO_4^- + H^+ (Ka1= 1.0× 10^3) (3B.3)

HSO_4^- → SO_4^{2-}+ H^+ (Ka2= 1.2 × 10^{-2}) (3B.4)

and,

H_3PO_4 → $H_2PO_4^-$ + H^+ (Ka1= 7.5 x 10^{-3}) (3B.5)

$H_2PO_4^-$ → HPO_4^{2-} + H^+ (Ka2= 6.2 x 10^{-8}) (3B.6)

HPO_4^{2-} → PO_4^{3-} + H^+ (Ka3= 4.8 x 10^{-13}) (3B.7)

As observed from the equations 3B.3-3B.7, the first dissociation constant of H_2SO_4 is strongest than the H_3PO_4 this is because of HSO_4^- have more stable confirmation due to maximum resonance of negative (-) charge at the double bond oxygen atoms compared to $H_2PO_4^-$. Similarly, second dissociation constant of H_2SO_4 is also strong to the first dissociation constant of H_3PO_4 which shows that H_2SO_4 is stronger acid than H_3PO_4. This may have effect on the activity of catalyst wherein anions are [HSO_4] and [H_2PO_4]. Considering this, even if the molar based H^+ concentration of [C_3SO_3HMIM][H_2PO_4] IL (H^+= 9.96 mmol) catalyst is higher than [C_3SO_3HMIM][HSO_4] IL (H^+=6.64 mmol), it showed inferior activity (38 verses 78%).

3B.3.1.2. Effect of cations

Considering the importance of [HSO_4] anion with imidazolium cation as discussed in Section 3B.3.1.1, [C_3SO_3HMIM][HSO_4] BAIL catalyst gave 78% yield of low molecular weight aromatic products. To understand the role of [HSO_4] anion with various cations (BAILs) (e.g. imidazolium, benzimidazolium, ammonium and phosphonium) were synthesised to depolymerise dealkaline

lignin. The lignin depolymerization reactions were carried out at optimized reaction conditions (120 °C, 1 h) in water:methanol (1:5, *v/v*= 30 mL). The results are shown in Figure 3B.2b. The BAILs with imidazolium based cation with [HSO$_4$] anion gives the maximum 78% yield of THF soluble low molecular weight aromatic products than BAILs with benzimidazolium (42%), triphenylphosphonium (19%), and triethylammonium (10%) based cations.

   The maximum yield of THF soluble products yield obtained with imidazolium cation can be explained on the basis of structural geometry of the cations. The structure of all the cations used for lignin depolymerization studies are represented in the Figure 3B.3. BAILs with imidazolium cation showed the interaction with lignin, and more discussion on the lignin with ionic liquids interaction studies are explained in Chapter 5. Moreover, the structural geometry of imidazolium based cation is planar, which can facilitate the more interaction with substrate. In case of benzimidazolium based cation it also has planar geometry but the additional benzene ring create hindrance during the interaction due to which low yield (42%) of THF soluble products were obtained than imidazolium (78%). Similarly, in case of triethylammonium based cation it does not possess planar geometry and as a consequence there is insufficient interaction between IL and lignin which gave poor yield (10%) of low molecular weight aromatic products. Similarly with triphenylphosphonium based cation with three bulky phenyl groups which also does not possess planar geometry gave the only 18% yield of low molecular weight aromatic products.

   To comprehend the structural dissimilarity of BAILs with different cations, all the structure of cations were sketched using ChemBioDraw 14.0 software. All the drawn structures were set for the lower energy job to get the most stable geometry, the obtained most stable structure are plotted in Figure 3B.3. Ionic liquids (ILs) are salts (combination of cations and anions) having melting point below the boiling point of water. They have very characteristic physico-chemical properties based on their choice of cation and anion combinations.[11, 12] One of the vital physical properties is structural geometry of cations and it is shown in Figure 3B.3. To understand the difference between the structural geometry in cations of ILs were sketched using ChemBioDraw Ultra 14.0 software and the structural colour coding is as follows: C (grey), O (red), N (blue), P (pink), S (yellow). As observed from the Figure 3B.3, imidazolium and benzimidazolium cations have planar geometry, however the benzimidazolium cation has extended planar geometry with benzene ring. On the other hand, ammonium and phosphonium based cations possess non-planar (tetrahedral) geometry. Three bulky groups like try-ethyl and tri-phenyl are attached with ammonium and phosphonium cations respectively. This study may give a hint that ILs with imidazolium and benzimidazolium cations has better interaction with the lignin because of their planar geometry and gave the better activity for lignin depolymerization reaction.

3B.3.1.3. Effect of Brønsted and Lewis acidity

From the literature, it was observed that catalysts with both Brønsted and Lewis acidity were used to depolymerize lignin into aromatic products, (Chapter 1, Section 1.9.3.1). In the current section ILs having both Brønsted and Lewis acidity was used to investigate the lignin depolymerization (Chapter 2, Figure 2A.3). Lignin depolymerization reactions were performed at optimized reaction conditioned (120 °C, 1 h) in water:methanol solvent (1:5= 30 mL). The obtained results are shown in the Figure 3B.3c, which shows the $[C_3SO_3HMIM][HSO_4]$ IL with Brønsted acidity gave the higher yield (78%) of THF soluble low molecular weight aromatic products than ILs with $[C_3SO_3HMIM][FeCl_4]$ (9% yield), $[C_3SO_3HMIM][CuCl_3]$ (4% yield) and $[C_3SO_3HMIM][SnCl_3]$ (15%) combination of both Brønsted and Lewis acidity. While the catalytic activity was checked with neutral [BMIM][Cl] IL, it showed superior activity (18% yield) than the combination of Brønsted and Lewis acidity ILs.

   The char formation was observed in the reactor, when the lignin depolymerization reactions were carried out with the combination of Brønsted and Lewis acidic ILs. It is also known from the literature that in the presence of Lewis acidic catalysts, the formed aromatic products itself undergoes repolymerization and transformed into char products.[13] Hence, low(er) yield of THF soluble low molecular weight aromatic products ware obtained (Figure 3B.2c)

3B.3.1.4. Effect of solid and homogeneous acids

The catalytic activity of $[C_3SO_3HMIM][HSO_4]$ BAIL for dealkaline lignin depolymerization reactions was compared with homogeneous and heterogeneous acids under similar reaction conditions (water:methanol, 1:5 *v/v*= 30 mL, 120 °C, 1 h). The dealkaline lignin depolymerization reactions are carried out with HCl, PTSA.H_2O (*p*-toluene sulfonic acid monohydrate), H_2SO_4 and H_3PO_4 as homogeneous acid catalysts as these acids were used for the synthesis of BAILs. In lignin depolymerization reactions at 120 °C within 1 h, 21%, 46%, 95% and 98% yield of THF soluble products were obtained with HCl, PTSA. H_2O, H_2SO_4 and H_3PO_4 as catalysts respectively (Figure 3B.2d). Compared to $[C_3SO_3HMIM][HSO_4]$ BAIL (78% of THF soluble products), homogeneous acid showed of lower yield of low molecular weight aromatic products, which is confirmed by the GC-MS chromatogram of the products (Figure 3A.4). So it can be concluded that HCl, PTSA.H_2O, H_2SO_4 and H_3PO_4 as homogeneous acid catalysts gave mainly dimer and oligomer products beside to form aromatic monomers.

   Similarly, the result obtained with $[C_3SO_3HMIM][HSO_4]$ BAIL catalyst was compared with solid acids catalyst such as HUSY (Si/Al=15), H-BEA (Si/Al= 19) and amberlyst-15 under the similar reaction conditions (120 °C, 1 h) and the obtained results are shown in the Figure 3B.2d. The results indicate that at 120 °C with 1 h, 2%, 3% and 60% yield of THF soluble products were achieved with HUSY, H-BEA and amberlyst-15 catalysts respectively. The difference in the catalytic results between BAIL and solid acids is due to difference in their catalytic reaction

systems. The BAIL is soluble in the water:methanol (1:5 *v/v*= 30 mL) solvent mixture, while solid acids is insoluble and formed a heterogeneous phase during the reaction. These results suggest that there was a poor interaction of substrate (lignin) with catalysts. Also, with solid acids catalysts, there are problem of diffusion limitation during the reactions, which can suppress the rate of catalytic activity and another reason might be the pore size of the solid acid catalysts. Dealkaline lignin molecules have larger size between <1 to 30 μm so the lignin molecules cannot pass through the small pore size (6-7.5 Å) of solid acid catalysts. These findings (diffusion limitation and small pore size) of solid acid catalysts confirmed the under these reaction conditions (120 ᵒC, 1 h) lignin depolymerization into higher yield of low molecular weight aromatic product could not be possible.
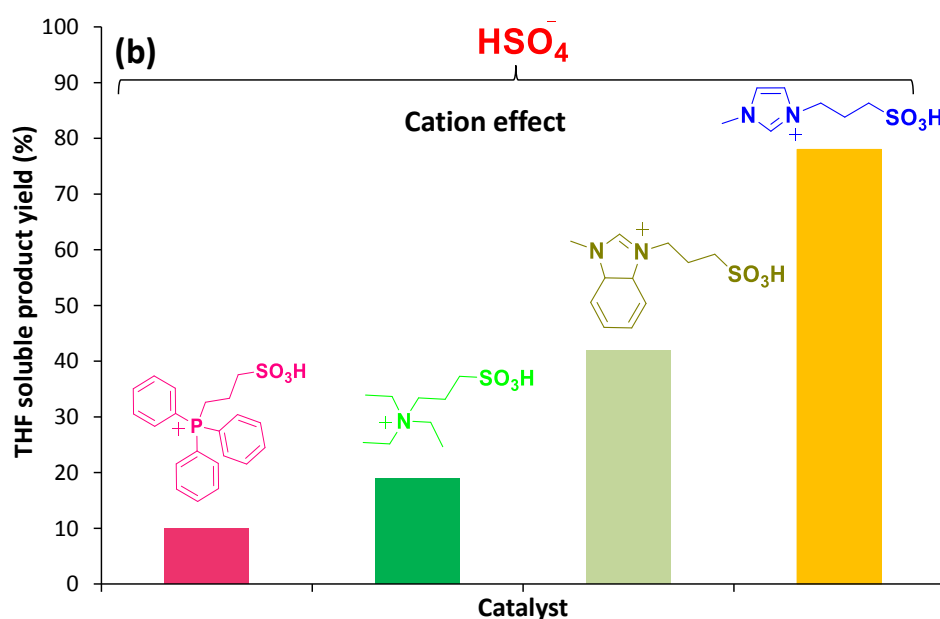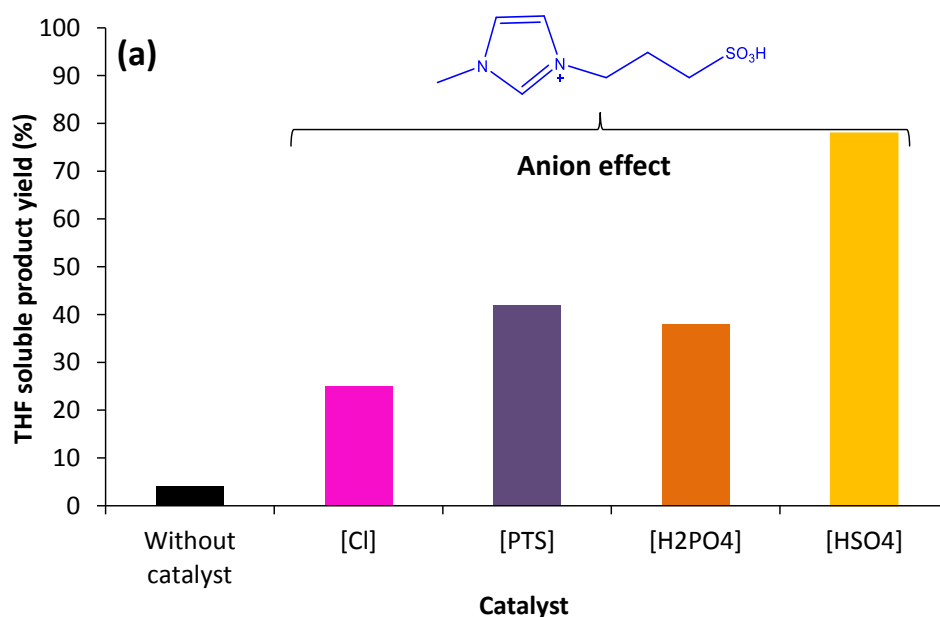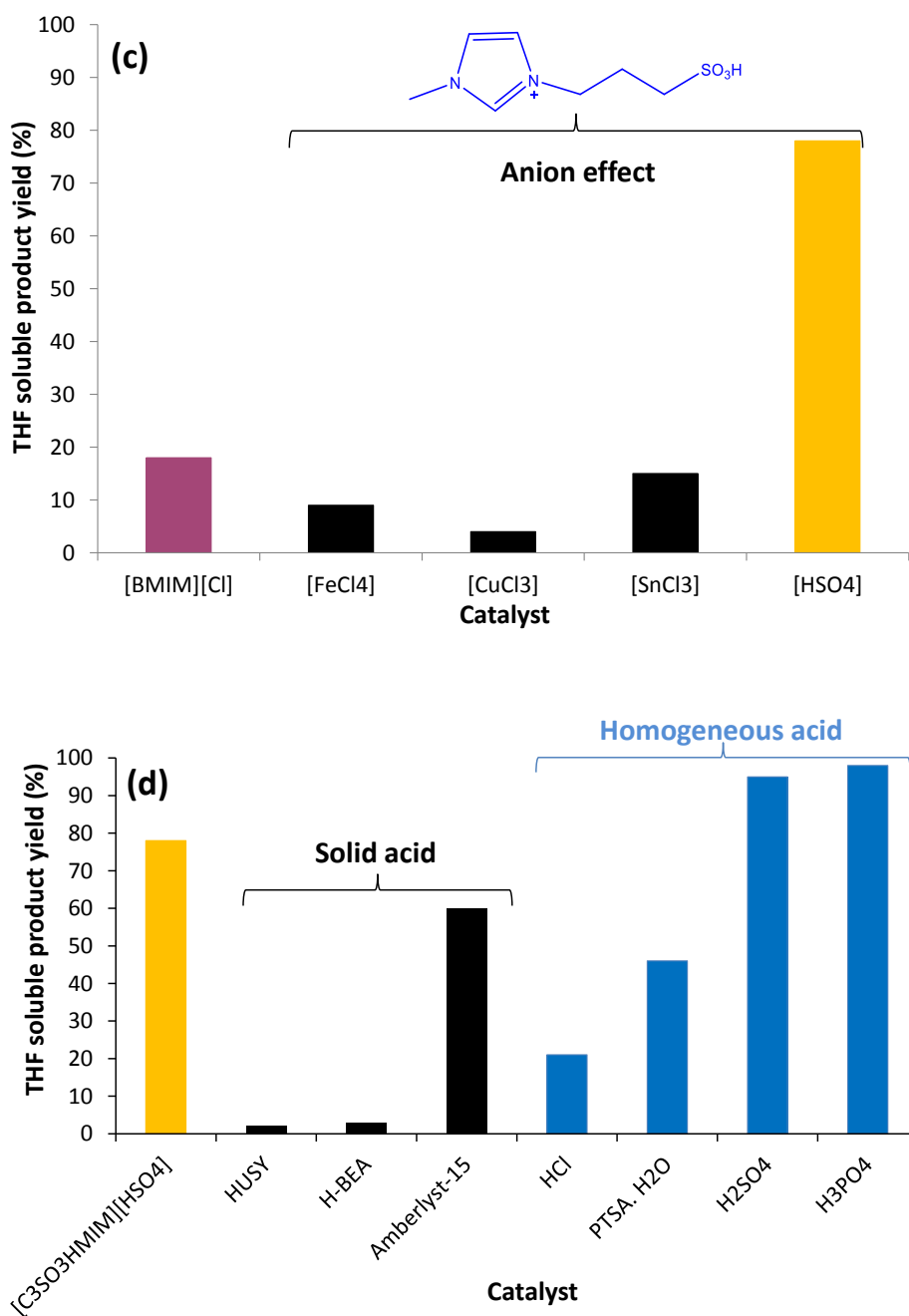
Figure 3B.2. Summary on the yield of THF soluble products in catalyst evaluation study for depolymerization of dealkaline lignin. (a) effect of anions with constant cation (C_3SO_3HMIM) (b) effect of cations with constant anion (HSO_4), (c) effect of Brønsted and Lewis acidity of ILs and (d) effect of homogeneous and heterogeneous acid catalysts. Reaction condition: dealkaline lignin (2 *wt*.% solution H_2O:CH_3OH, 1:5 *v/v*= 30 mL), catalyst (0.5 g) 120 °C, 1 h, 1000 rpm. Values are average of three reactions with ±3% error observed.
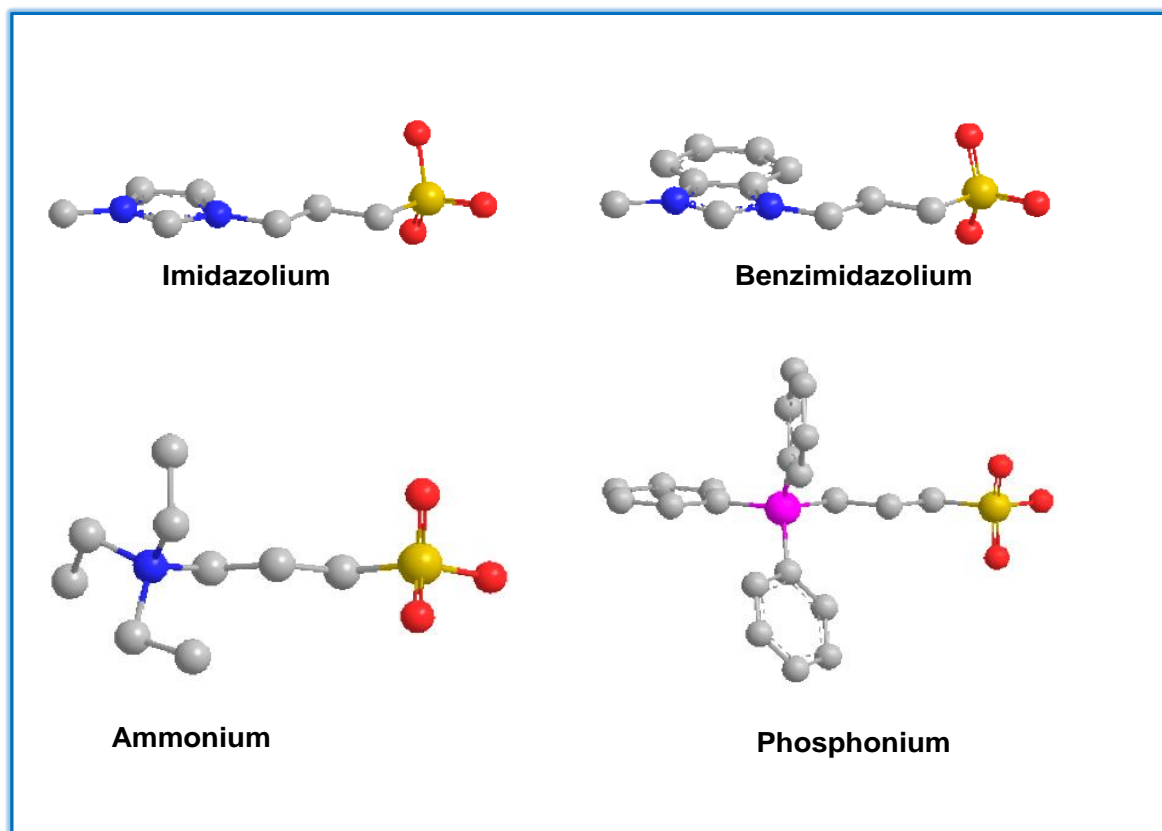
Figure 3B.3. 3-dimensional geometry of the cations. Colour coding for atoms is as follows: C (grey), O (red), N (blue), P (pink) and S (yellow).

3B.3.1.5. Confirmation of aromatic monomers formation

The lignin depolymerization into THF, EtOAc and DEE soluble low molecular weight aromatic products is confirmed using several analytical techniques. Those analytical techniques are GC, GC-MS, HPLC, LC-MS, GPC, etc.

The obtained results using several analytic techniques imply that majority of the formed products under the optimized reaction conditions are low molecular weight aromatic products, which are confirmed by GC-MS and GC chromatograms (Figures 3B.4-3B.6). Further, THF soluble obtained products were analysed by the LC-MS (Figure 3B.7) and HPLC (Figure 3B.8) analytical techniques. The obtained products in the HPLC analysis are similar to the products identified by the GC and GC-MS techniques and few product peaks were overlapping in the HPLC chromatogram. Also LC-MS analysis confirmed the formation of THF soluble low molecular weight aromatic products after the dealkaline lignin depolymerization reaction using [C$_3$SO$_3$HMIM][HSO$_4$] as catalyst.
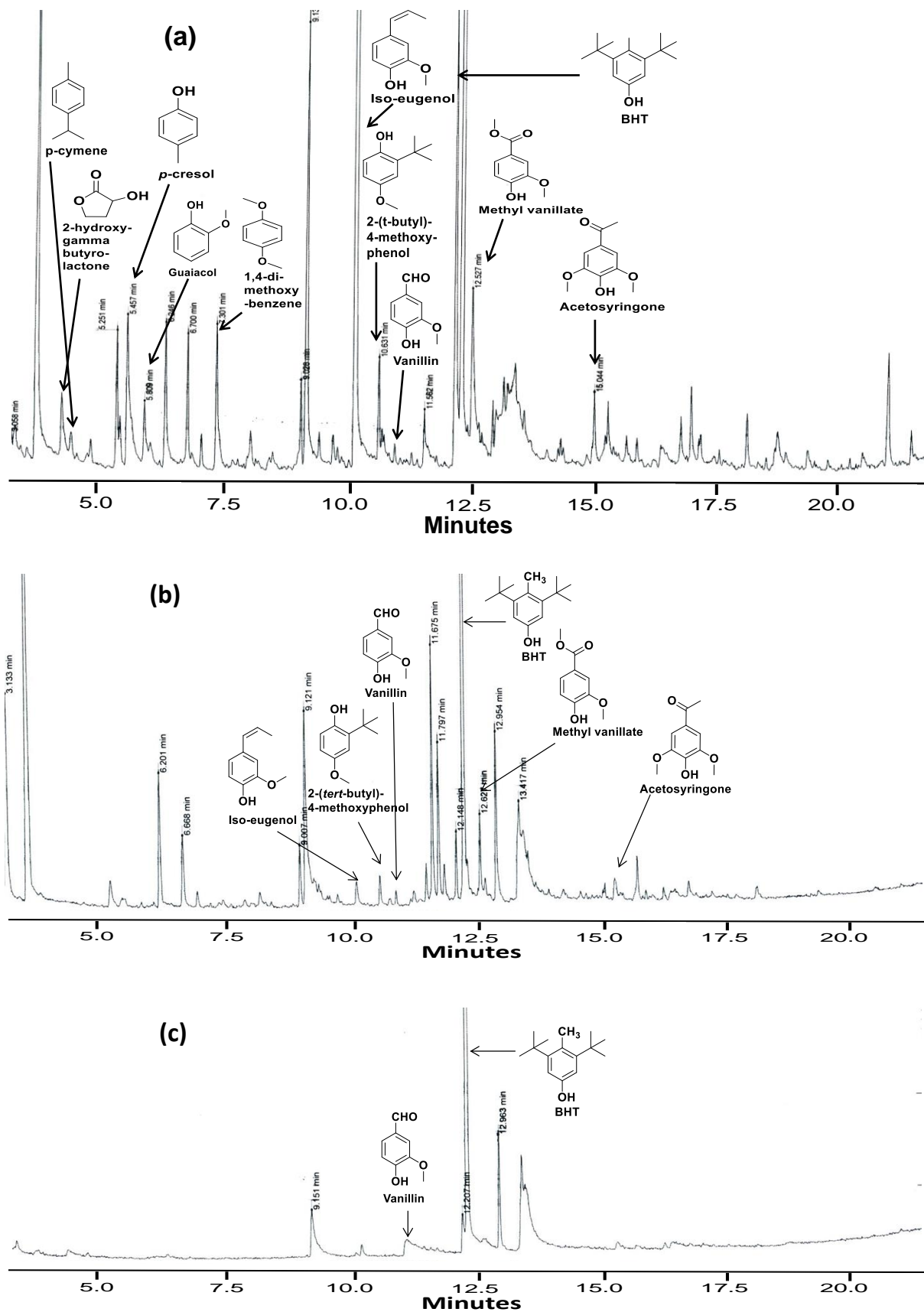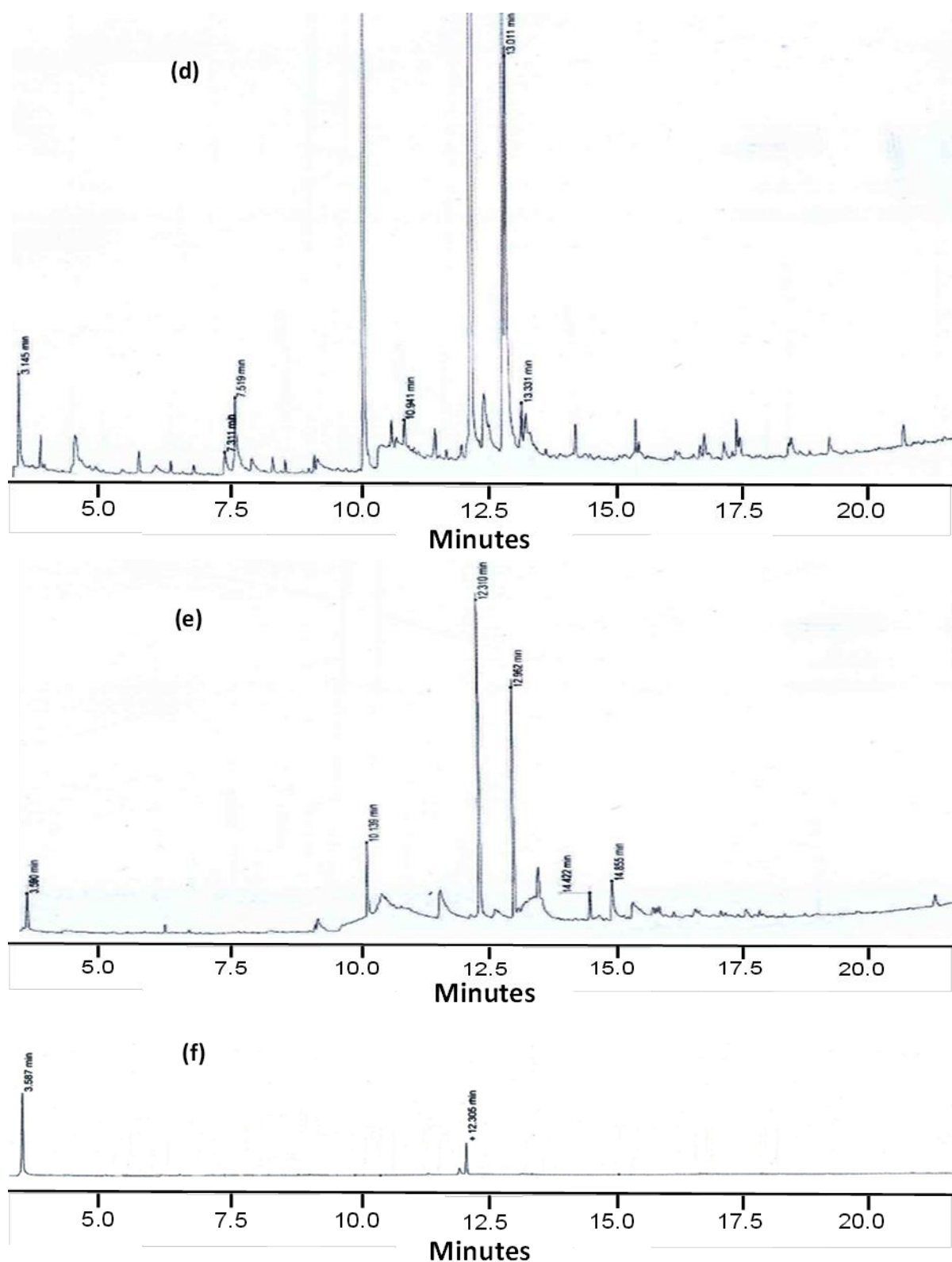
Figure 3B.4. GC-MS of THF soluble products obtained using (a) [C$_3$SO$_3$HMIM][HSO$_4$], (b) [C$_3$SO$_3$HMIM][PTS], (c) [C$_3$SO$_3$HMIM][Cl] catalysts. GC-MS of (d) ethyl acetate (EtOAc), (e) diethyl ether (DEE) soluble products obtained using [C$_3$SO$_3$HMIM][HSO$_4$] catalyst and (f) THF soluble products with H$_2$SO$_4$ catalyst. Reaction conditions: dealkaline lignin (2 *wt.*% solution H$_2$O:CH$_3$OH, 1:5 *v/v* = 30 mL), catalyst (0.5 g), 120 ºC, 1 h, 1000 rpm.
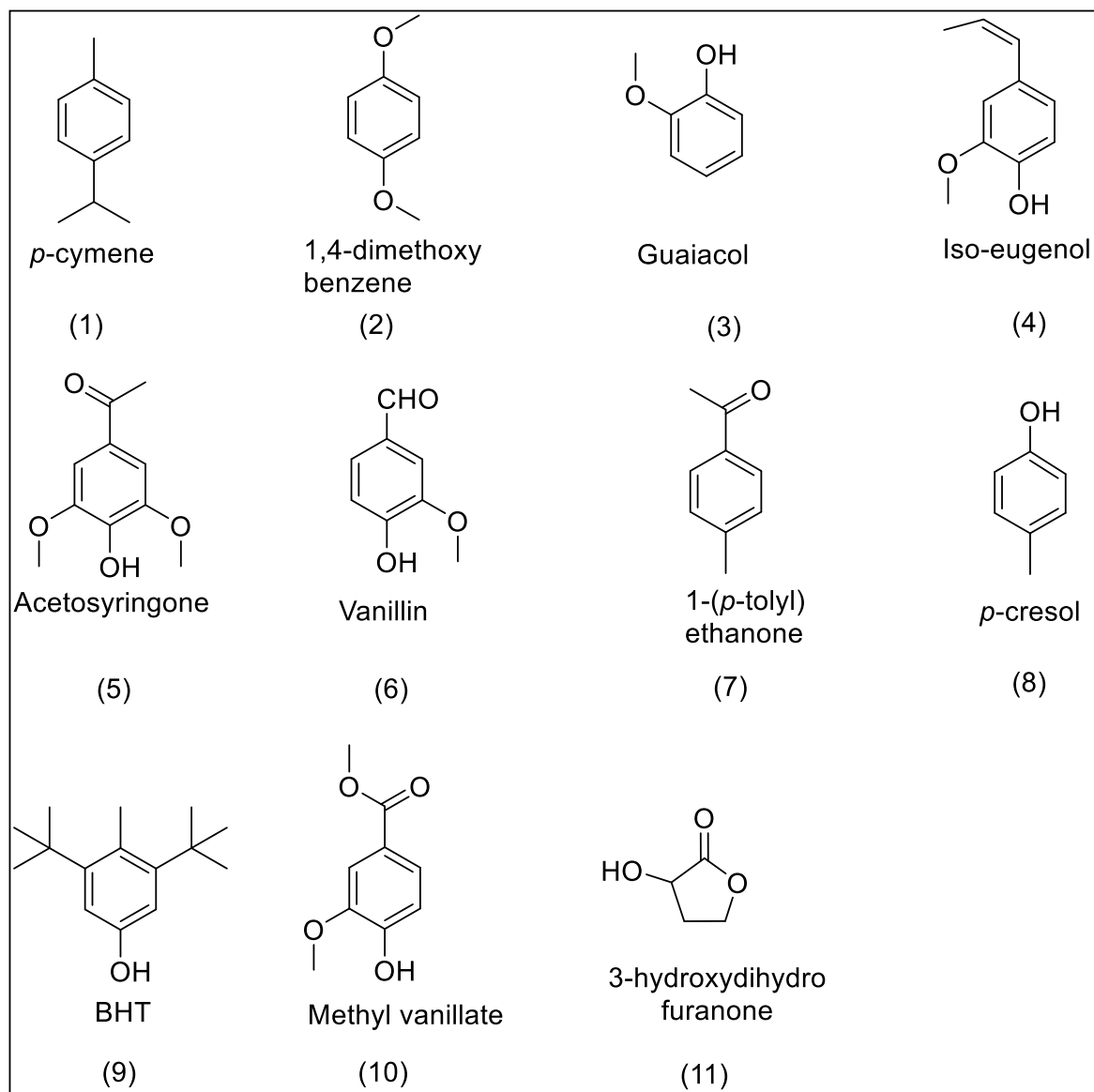
Figure 3B.5. GC-MS identified low molecular weight aromatic products in the THF soluble products. Reaction conditions: dealkaline lignin (2 *wt.*% solution $H_2O:CH_3OH$, 1:5 *v/v*= 30 mL), [C_3SO_3HMIM][HSO_4] (0.5 g), 120 ^{o}C, 1 h, 1000 rpm.
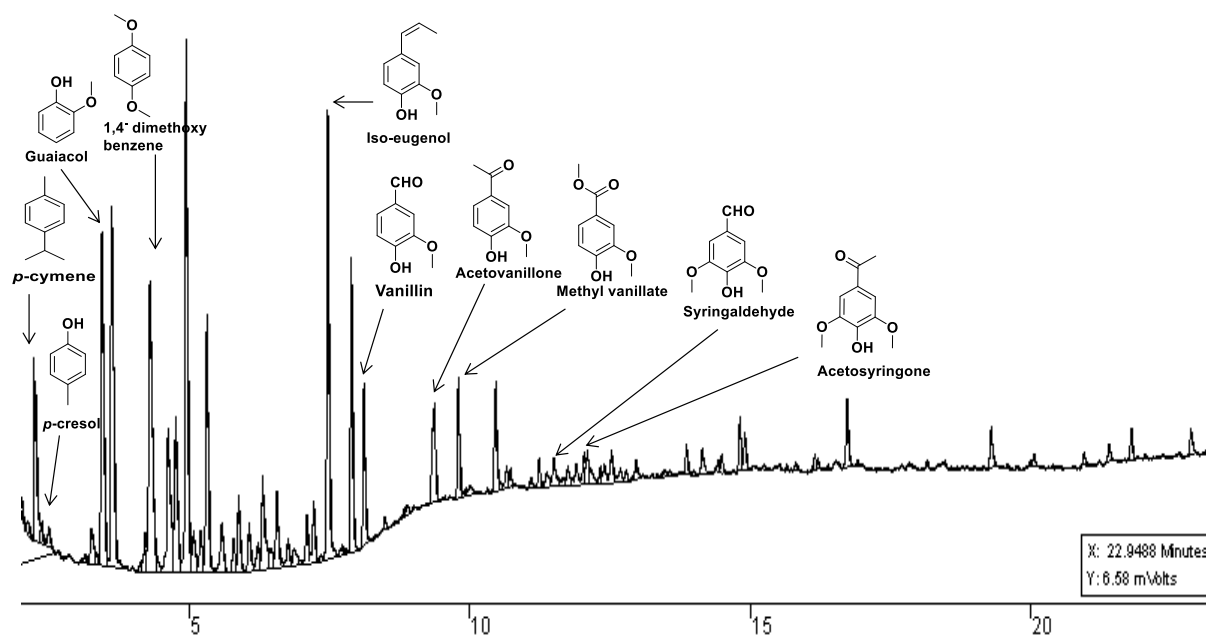
Figure 3B.6. GC-FID of THF soluble products obtained using [C₃SO₃HMIM][HSO₄] catalyst. Reaction conditions: dealkaline lignin (2 *wt.*% solution $H_2O:CH_3OH$, 1:5 *v/v*= 30 mL), [C₃SO₃HMIM][HSO₄] (0.5 g), 120 ᵒC, 1 h, 1000 rpm.
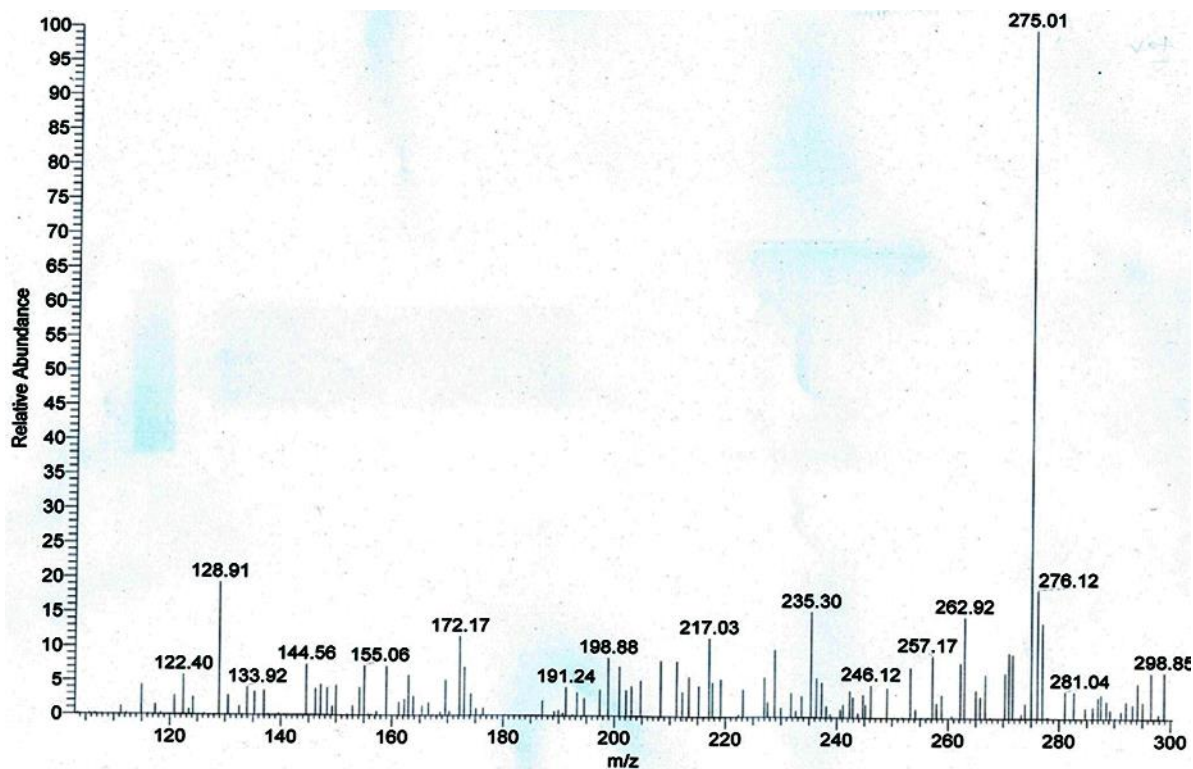
Figure 3B.7. LC-MS of THF soluble products in methanol obtained using [C₃SO₃HMIM][HSO₄] catalyst. Reaction conditions: dealkaline lignin (2 *wt.*% solution $H_2O:CH_3OH$, 1:5 *v/v*= 30 mL), [C₃SO₃HMIM][HSO₄] (0.5 g), 120 ᵒC, 1 h, 1000 rpm.
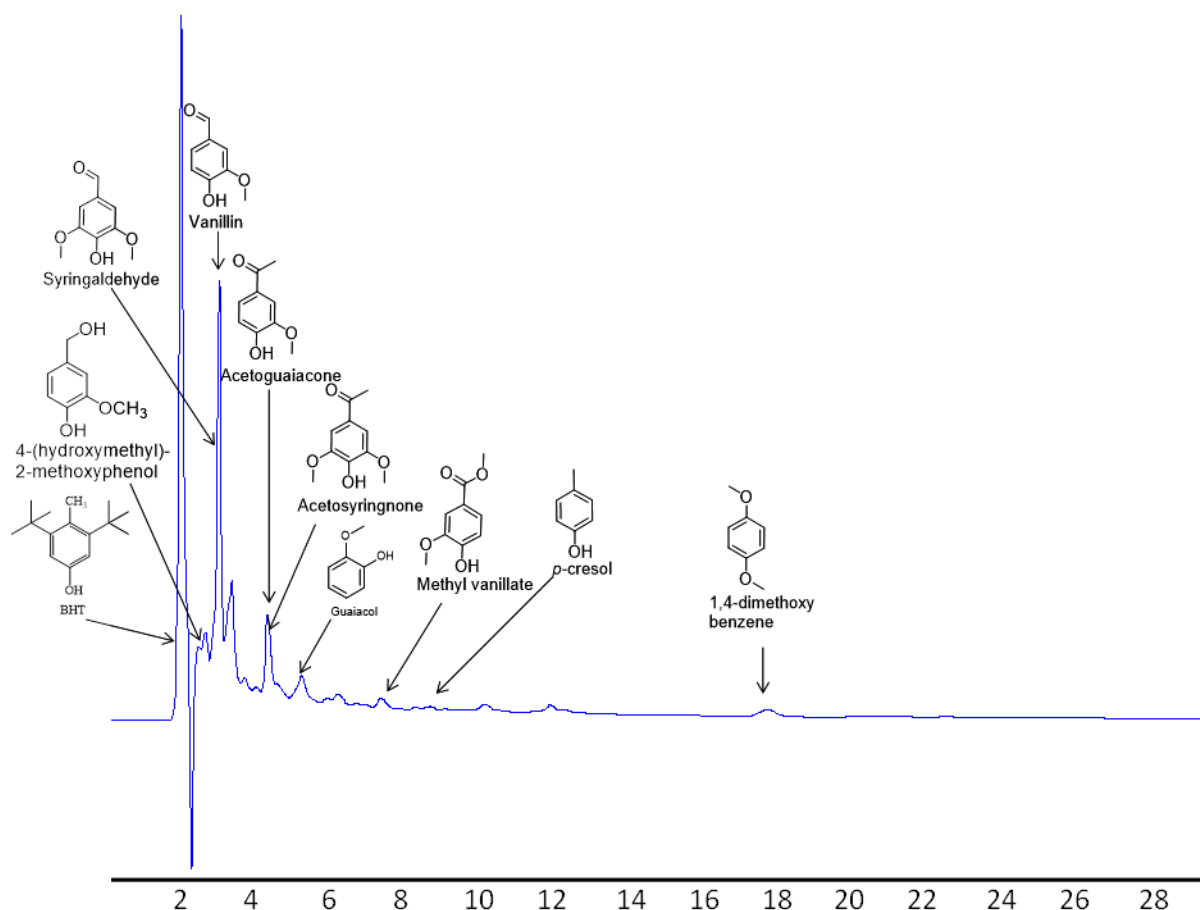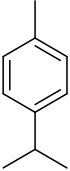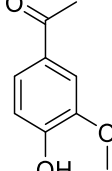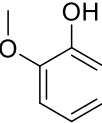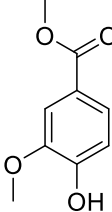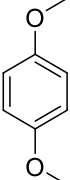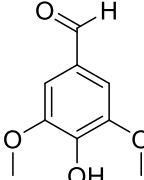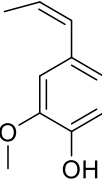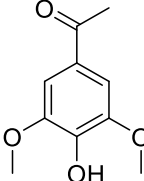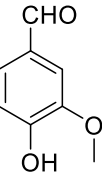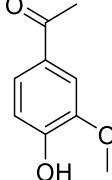
Figure 3B.8. HPLC of THF soluble products obtained using [C$_3$SO$_3$HMIM][HSO$_4$] catalyst. Reaction condition: dealkaline lignin (2 *wt.*% solution H$_2$O:CH$_3$OH, 1:5, *v/v*= 30 mL), [C$_3$SO$_3$HMIM][HSO$_4$] (0.5 g), 120 °C, 1 h, 1000 rpm.

3B.3.1.6. Quantification of aromatic monomers

Using various chromatographic (GC, GC-MS, HPLC, LC-MS; Figures 3B.4-3B.8) analytical techniques the depolymerization of dealkaline lignin into low molecular aromatic products confirmed and identified (monomers Table 3B.2). To quantify the formation of low molecular weight aromatic products, GC-MS identified products were commercially procured and injected in GC and GC-MS to confirm the compounds with retention time and mass fragmentations and in addition calibration curve was derived. The aromatic monomers distribution obtained from GC analysis were low molecular weight aromatic products (124–196 g/mol) which are given in Table 3A.2. However, few of the GC-MS identified products are still not quantified because those are not commercially available and therefore their calibration could not be carried out. Based on the results from GC analysis, it was estimated that ca. 45% yield of the products extracted in THF soluble products had a molecular weight in the range 124–196 g/mol.

Table 3B.2. Summary on the GC and GC-MS identified low molecular weight aromatic products in the THF soluble product and their yields.*

Aromatic monomers	Structure	Aromatic monomer distribution (*wt. %*)	Aromatic monomers	Structure	Aromatic monomer distribution (*wt. %*)
p-cymene		4.8	1-(-hydroxy-3-methoxy phenyl) ethanone		8.0
2-methoxy phenol		22.3	methyl 4-hydroxy-3-methoxybenzoate		5.7
1,4-dimethoxy benzene		24.8	4-hydroxy-3,5-dimethoxy benzaldehyde		2.2
2-methoxy-4-(propenyl) phenol		23.0	1-(4-hydroxy-3,5-dimethoxy phenyl) ethanone		1.2
4-hydroxy-3-methoxy benzaldehyde		8.1	1-(-hydroxy-3-methoxy phenyl) ethanone		8.0

*Reaction condition: dealkaline lignin (2 *wt.*% solution H_2O:CH_3OH, 1:5 *v/v*= 30 mL), [C_3SO_3HMIM][HSO_4] (0.5 g), 120 ºC, 1 h, 1000 rpm.

3B.3.2. Depolymerization of lignin using catalyst (mol basis)

3B.3.2.1. Substrate mole calculation

Based on elemental analysis of dealkaline lignin, the monomer molecular formula (MMF) was calculated as $C_{10}H_{13}O_3S_{0.09}$ (Chapter 3, Section 3A.2.9, Table 3A.3). The molecular weight of the monomer formula derived from dealkaline lignin is ca. 180 g/mol. Considering this, if 0.5 g of dealkaline lignin is taken for the reaction, it calculates to 2.78 mmol (0.5 g/180 g/mol = 0.002777 mol). Similar to substrate mole, ILs catalysts (H^+, 2.78 mmol) was taken for the dealkaline lignin depolymerization.

3B.3.2.2. Effect of various ILs

Although, in all the reaction, similar quantity of catalyst (0.5 g) was taken, it was expected that due to dissimilarity in H^+ concentration at 0.5 g loading of catalyst (H^+= H_3PO_4, 15.3 mmol; H_2SO_4, 10.2 mmol; HCl, 13.7 mmol; [C_3SO_3HMIM][HSO_4], 3.32 mmol; [C_3SO_3HMIM][PTS], 1.33 mmol; [C_3SO_3HMIM][Cl], 2.07 mmol) variation in activity was observed (21-98% yield). To nullify this effect, reactions were performed using comparable (substrate/catalyst ratio= 1) H^+ concentration (2.78 mmol) in the reaction mixture by altering the catalyst quantities (Figure 3B.9).

3B.3.2.3. Effect of anions

Lignin depolymerization (2 *wt.*% solution H_2O:CH_3OH, 1:5 *v/v*= 30 mL), 120 °C, 1 h, 1000 rpm) studies were performed using H^+= 2.78 mmol of ILs as catalyst and the results are plotted in Figure 3B.9a. Since, in all the experiments same quantity of catalyst (0.5 g) was used, it was expected that due to disparity in H^+ concentration at 0.5 g loading of catalyst (H_2SO_4, 10.2 mmol; [C_3SO_3HMIM][HSO_4], 3.32 mmol; [C_3SO_3HMIM][PTS], 1.33 mmol) variation in activity was observed (95, 78 and 42% yield of low molecular weight of aromatic products). To nullify this effect, reactions were performed using comparable (substrate/catalyst, 2.78/2.78= 1) H^+ concentration (2.78 mmol) in the reaction mixture by altering the catalyst quantities and the following order of activity was seen,

[H_2SO_4] (96%) > [C_3SO_3HMIM][HSO_4] (52%) > [C_3SO_3HMIM][PTS] (49%).

This shows that if H^+ concentration is kept constant, analogous activity (52, 49%, yield of low molecular weight of aromatic products) can be observed with all ILs with varying anions. This implies that the anion does not provide any contribution to the activity (Figure 3B.9a).

3B.3.2.4. Effect of cations

The ammonium, phosphonium, benzimidazolium and imidazolium cations with [HSO_4] anion as catalysts were checked for lignin depolymerization using (2 *wt.*% solution H_2O:CH_3OH, 1:5 *v/v*= 30 mL), catalyst (H^+= 2.78 mmol) at 120 °C for 1 h (Figure 3B.9.b). Again, it was observed that imidazolium cation gives maximum 52% yield of THF soluble low molecular weight aromatic product. It might be due to the better interaction of imidazole ring (N-CH-N), with -C-O-R (R-H, alkyl) ether group of aromatic ring in lignin molecules. It means that both cations and anions have effective role for lignin depolymerization into low molecular weight aromatic products but the anions have lesser effect than cations (For more details please see the Chapter 5, Section 5.3.2.
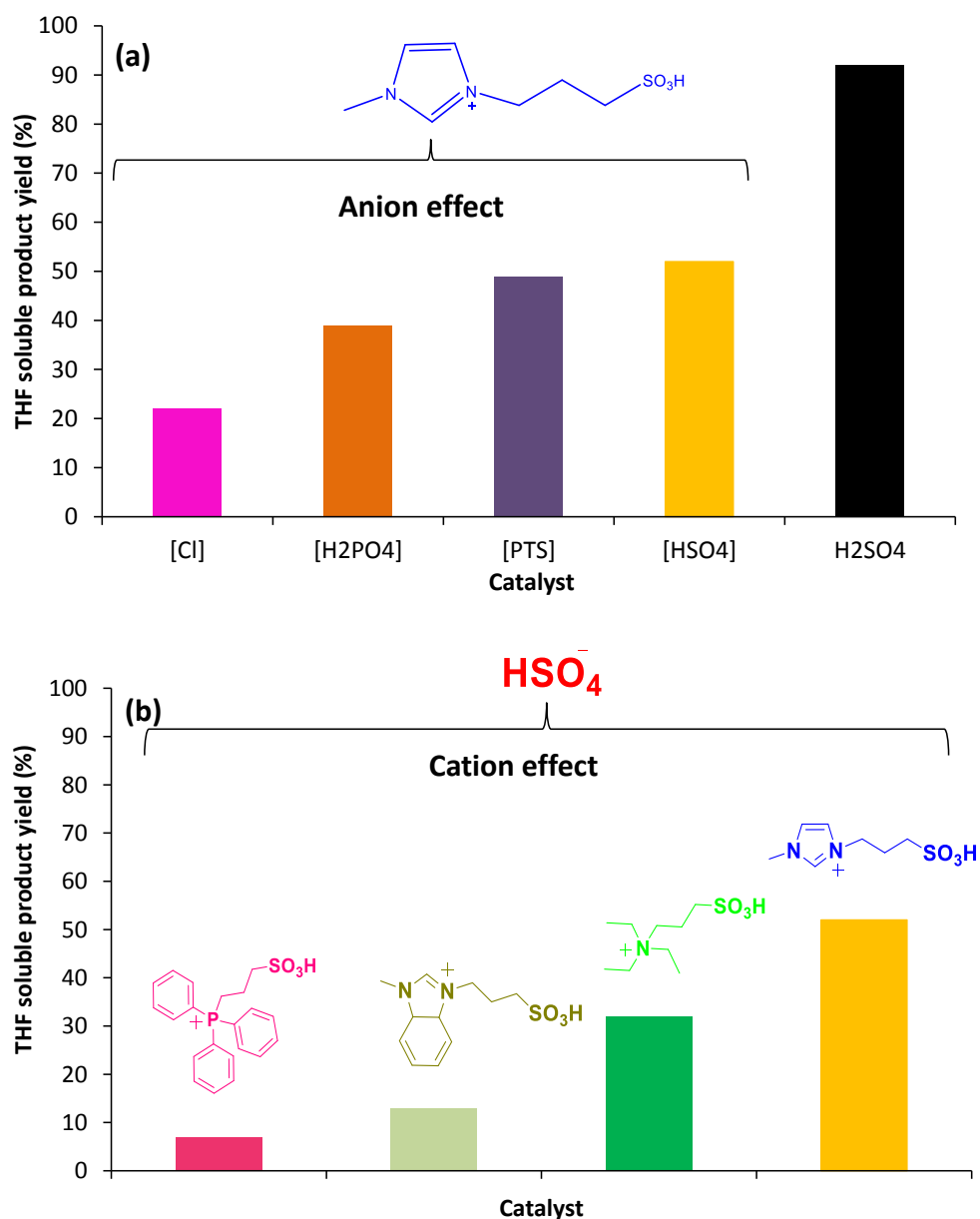
Figure 3B.9. Summary on the yield of THF soluble products in catalyst evaluation study for depolymerization of dealkaline lignin. (a) effect of anions with constant cation (C_3SO_3HMIM) (b) effect of cations with constant anion (HSO_4). Reaction conditions: Dealkaline lignin (2 *wt.*% solution $H_2O:CH_3OH$, 1:5 *v/v*= 30 mL), catalyst (2.78 mmol), 120 ºC, 1 h, 1000 rpm. Values are average of three reactions with ±3% error observed.

As shown above depolymerization of dealkaline lignin was successfully done by charging the same quantity of (weight, 0.5 g) various ILs, solid acids, mineral and organic acids. Similarly, reactions were also done by maintaining constant H^+ concentration (2.78 mmol) of ILs and H_2SO_4. From both the studies it is learnt that best result (78% yield) could be obtained with [C_3SO_3HMIM][HSO_4] catalyst when reactions are done with same quantity of catalyst (0.5 g). Based on the results obtained with various catalysts on weight and mole basis, it was decided to carry out further reactions using similar weight basis (0.5 g).

3B.3.3. Repolymerization study

Literature reports suggest that at higher temperatures and under acidic conditions aromatic products (obtained in depolymerization reaction) undergo repolymerization.[2, 4, 14-16] To overcome this, researchers have used capping agents such as boric acid, phenol etc. in which the interaction of these with –OH groups decrease the repolymerization.[15, 17, 18] In this work, it was observed that the IL interacts with –OH groups (For more details please see Chapter 5, Section 5.3.2) and this might suppress the repolymerization and improve the activity in case of BAIL catalysed reaction in comparison to H_2SO_4 catalysed reaction. To check the possibility of repolymerization in this work specifically to explain whether this gives rise to difference in activity between BAIL and H_2SO_4, commercially procured chemicals (identified by GC/GC-MS in depolymerization study) were taken as substrates (*p*-cresol= 60 mg, guaiacol= 60 mg, 1,4-dimethoxybenzene= 60 mg, eugenol= 80 mg vanillin= 80 mg, methyl vanillate= 20 mg) and charged with H_2SO_4 or [C_3SO_3HMIM][HSO_4] catalyst (0.5 g) in water:methanol (1:5 *v/v*= 30 mL). This mixture was stirred for 1 h at 120 °C and 170 °C and the GC chromatographs for the initial and after reaction are summarized in Figures 3B.10A and 3A.10B. The results indicate that irrespective of whether BAIL is used or H_2SO_4 is used in the reaction, slight decrease in peak intensities were seen at elevated temperatures compared with initial samples. However, a careful look shows that the most decrease in the intensity was for eugenol compound in case of BAIL catalysed reaction and along with that peak intensities for other compounds were also decreased when BAIL is used in the reaction. Interestingly, only a slight decrease in peak intensities was observed when H_2SO_4 was used as a catalyst in comparison to BAIL catalyst. Nonetheless, contrary to results obtained with H_2SO_4, BAIL will act as capping agent it was still active. Nevertheless, based on this data, it can be suggested that the BAIL is capable of depolymerising lignin in more efficient way than H_2SO_4.
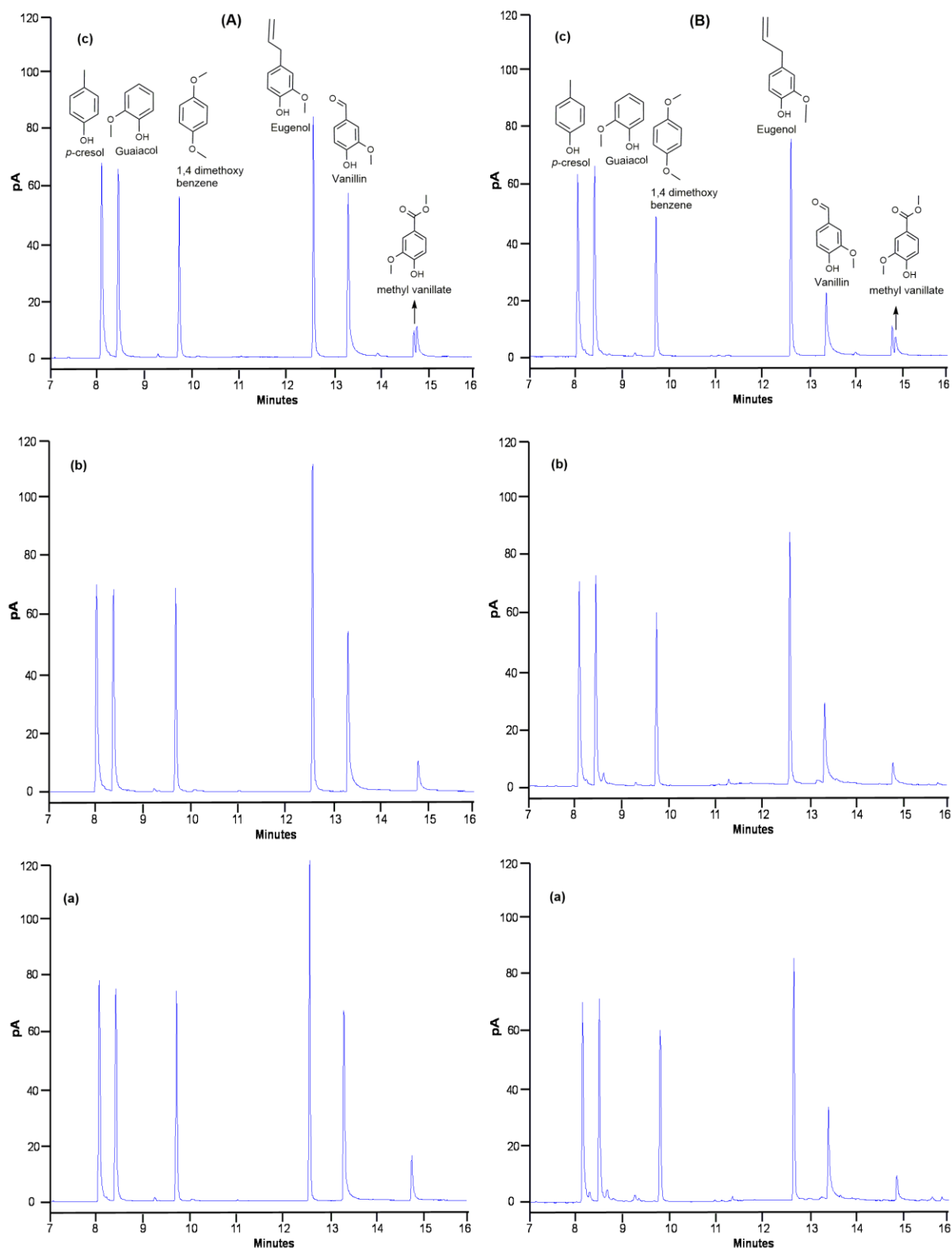
Figure 3B.10. Repolymerization study with *p*-cresol, guaiacol, 1,4-dimethoxybenzene, eugenol, vanillin and methyl vanillate in presence of (A) [C₃SO₃HMIM][HSO₄] and (B) H₂SO₄ as catalysts at (a) room temperature (25 °C)-initial sample, (b) 120 °C, 1 h and (c) 170 °C, 1 h.

3B.3.4. Effect of temperature

Depolymerization of lignin at various temperature (70-170 °C) was investigated and the optimized reaction temperature was 120 °C wherein dealkaline lignin depolymerization gave 78% yield of low molecular weight aromatic products (Figure 3B.11). Increasing the temperature (range, 70-120 °C) would promote the depolymerization of the lignin and degradation/repolymerization (range, after 120-170 °C) of the THF soluble product at higher temperatures, as it was observed in repolymerization studies (Figure 3B.10) which is similar to the results reported.[19] It is shown that the depolymerization favours at lower temperature (<120 °C) while the degradation/repolymerization reaction become predominant at higher temperature. Further, reactions were performed for shorter time 30 min at higher temperature 130 and 140 °C for lignin depolymerization into THF soluble products 53% and 65% yield respectively and this shows that there is no improvement in the products yield.
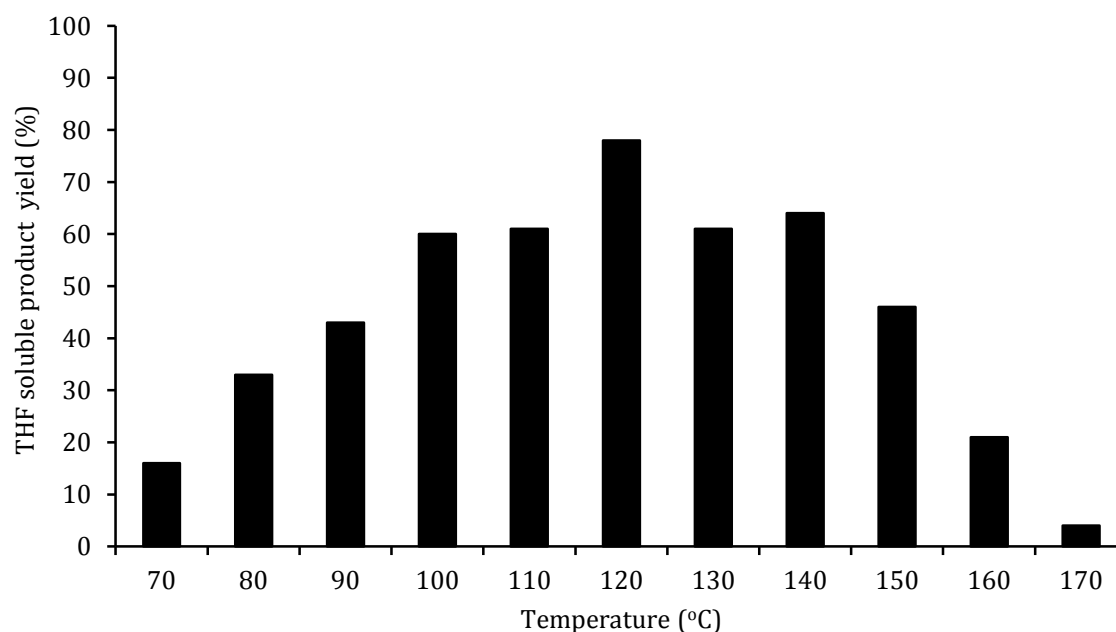
Figure 3B.11. Effect of temperature on lignin depolymerization. Reaction condition: dealkaline lignin (2 *wt.*% solution $H_2O:CH_3OH$, 1:5 *v/v*= 30 mL), $[C_3SO_3HMIM][HSO_4]$ (0.5 g), 70-170 °C, 1 h, 1000 rpm.

Values are average of three reactions with ±3% error observed.

3B.3.5. Effect of time

The Effect of time on THF soluble low molecular weight aromatic products was studied at a range between 15-360 min at 120 °C using $[C_3SO_3HMIM][HSO_4]$ IL (0.5 g), in water:methanol (1:5, *v/v*= 30 mL) solvent. As shown in Figure 3B.12 within 15 min, 20%; 30 min, 38% and after 60 min, 78% yields are obtained. However as the reaction time lengthened from 60 to 360 min the yield of THF soluble products is almost similar (70-80%). It may be due to lignin contained ≡C-O-C≡ (ca. 70%) linkage, under the reaction conditions, ≡C-O-C≡ bond hydrolysis is

happening so the yield could not be observed more than 75±10%. Therefore, 60 min would be a best reaction time for lignin depolymerization into THF soluble low molecular weight aromatic products at 120 °C.
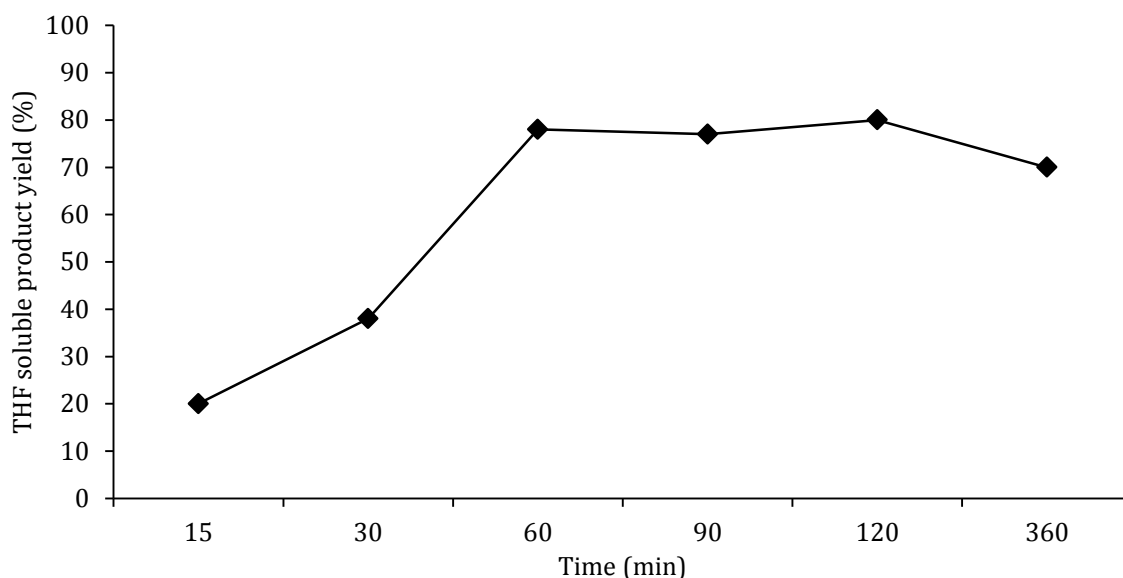
Figure 3B.12. Effect of time on lignin depolymerization. Reaction condition: dealkaline lignin (2 *wt.*% solution H_2O:CH_3OH, 1:5 *v/v*= 30 mL), [C_3SO_3HMIM][HSO_4] (0.5 g), 120 °C, 15-360 min, 1000 rpm.

Values are average of three reactions with ±3% error observed.

3B.3.6. Effect of pressure

To examine the effect of pressure (Inert N_2) on the THF soluble low molecular weight aromatic products yield, reactions were done with lignin (0.5 g) and [C_3SO_3HMIM][HSO_4] (0.5 g), at 120 °C for 1 h under N_2 pressure ranging from 0.5-3.0 MPa (Figure 3A.13). As pressure increased the yield of THF soluble products decreased which was due to formation of char. These results suggest that maximum THF soluble low molecular weight aromatic products yield could be achieved in the absence of N_2 pressure.
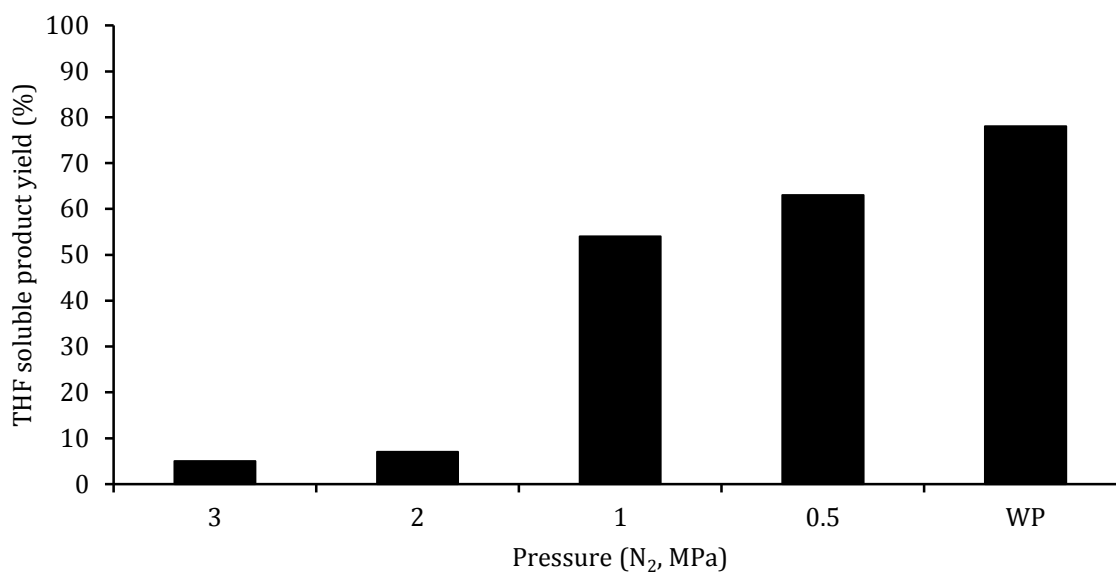
Figure 3B.13. Effect of N_2 pressure on lignin depolymerization. Reaction condition: dealkaline lignin (2 *wt.*% solution H_2O:CH_3OH, 1:5 *v/v*= 30 mL), [C_3SO_3HMIM][HSO_4] (0.5 g), atmospheric pressure to 3.0 MPa N_2 @ RT, 120 ºC, 1 h, 1000 rpm.

Where, WP-without pressure.

Values are average of three reactions with ±3% error observed.

3B.3.7. Effect of reaction medium

During the lignin depolymerization into THF soluble low molecular weight aromatic products, the effect of solvents was evaluated (Figure 3B.14) in presence of [C_3SO_3HMIM][HSO_4] IL as a catalyst and at 120 ºC for 1 h. As observed, 78% THF soluble products yield was obtained with water:methanol ratio of 1:5, *v/v*. In this solvent ratio, dealkaline lignin is observed to be completely soluble (100%). If the concentration of water in water:methanol ratio (1:1 *v/v*) was increased, the THF soluble products yield was declined (51%). It was observed that with only water as a solvent very low yield (16% yield) is possible to achieve. This phenomenon of decrease in yield with an increase in water concentration might be due to only 44% solubility of lignin in water in comparison to complete solubility in water:methanol (1:5, *v/v*) system. THF soluble low molecular weight aromatic products yield increased from 16 to 78%, with decrease in water concentration in water:methanol solvent system. It might be due to the suppression of the formation of repolymerized products at water:methanol, (1:5 *v/v)* ratio. The methanol helped to dissolve dealkaline lignin (Please see Chapter 3, Section 3A.2.1, Table 3A.1) and suppressed the yield of repolymerized products.[20-22] It may be due to the hydrogen-donor capability of methanol which leads to stabilization of the free radicals generated from lignin depolymerization reaction, which in turn suppressed the formation of repolymerized products.[23] Water with ethanol or iso-propanol solvent systems with 1:5 (*v/v*) ratios are used for dealkaline lignin depolymerization into THF soluble products (Figure 3B.14). As seen in Figure 3B.14, water with methanol ratio produces better result as compared to ethanol and

iso-propanol. It might be due to better solubility[24] (Please see Chapter 3, Section 3A.2.1, Table 3A.1) of dealkaline lignin. Another, reason may be auto-generated pressure (0.35 MPa) during the reaction in case water:methanol mixture, similarly the auto-generated pressure with water:ethanol (1:5 *v/v*) and with water:iso-proponal (1:5 *v/v*) solvents during the reaction was 0.31 and 0.28 MPa respectively. Similarly, the reactions were carried out using toluene with or without water and methanol solvents. The obtained results are shown in Figure 3B.14. While using toluene as reaction medium low yield was obtained (5-13%), which might be due to low(er) solubility of dealkaline lignin in particular solvent ratios, for more details please see Chapter 3, Section 3A.2.1, Table 3A.1.
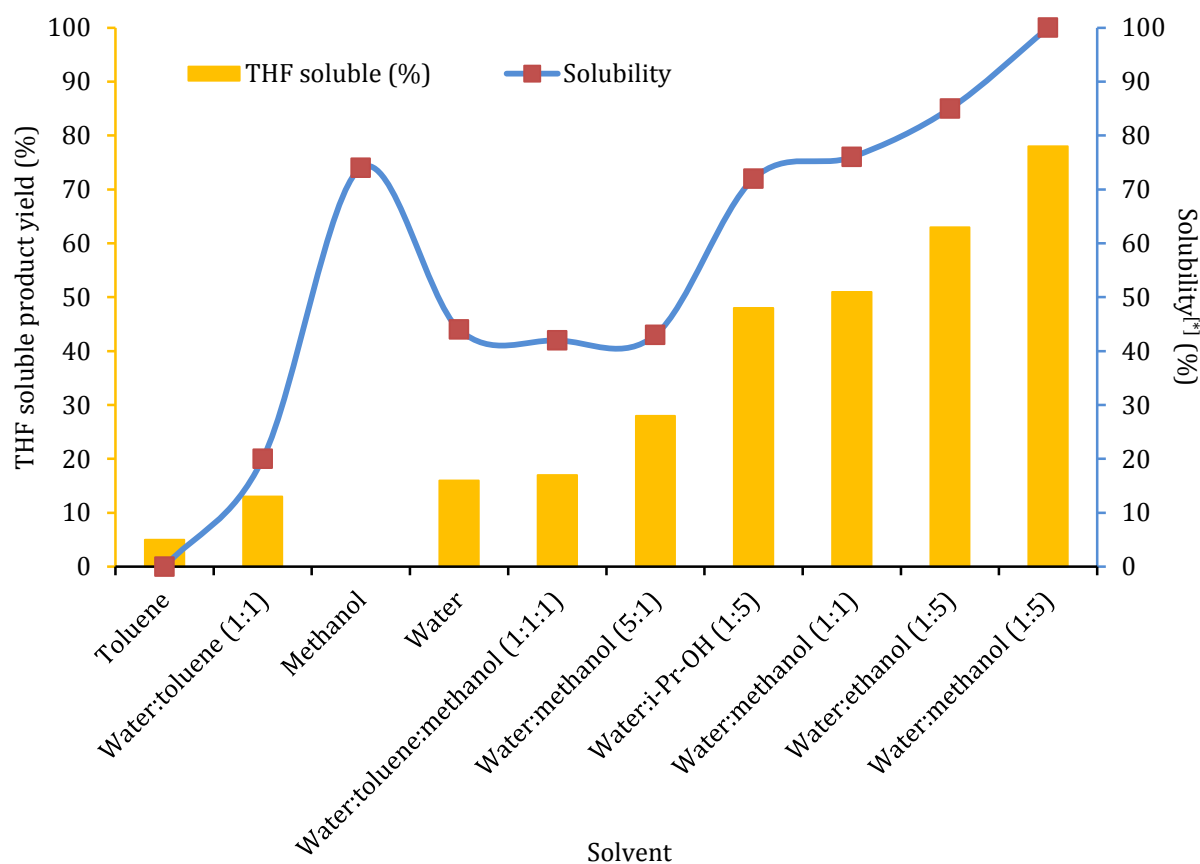
Figure 3B.14. Effect of solvent on lignin depolymerization. Reaction condition: dealkaline lignin (2 *wt.*% solution various solvent *v/v*= 30 mL), [C$_3$SO$_3$HMIM][HSO$_4$] (0.5 g), 120 ^{o}C, 1 h, 1000 rpm.

[*]lignin 250 mg, solubilized in solvent 5 mL, at RT (25±3 ^{o}C).

Values are average of three reactions with ±3% error observed.

Higher the solubility, maximum yield of THF soluble low molecular weight aromatic product yield is observed (Figure 3B.14). It might be suggest that for lignin depolymerization, lignin should be soluble in the respective solvents.

3B.3.8. Effect of various substrates

The depolymerization of various (industrial, alkali, alkaline and dealkaline lignin) lignin samples were carried out using $[C_3SO_3HMIM][HSO_4]$ IL as catalyst in water:methanol (1:5, *v/v*= 30 mL) ratio at 120 ℃ for 1 h (Figure 3B.15). Among all substrate, alkali lignin gave better yield of THF soluble low molecular weight aromatic product (96%) but aromatic monomers detected by GC, GC-MS and HPLC were less as compared to dealkaline lignin. Lignin depolymerization to THF soluble low molecular weight aromatic product yield was 78% with dealkaline, 48% with industrial and 55% with alkaline lignin. It is because dealkaline lignin is completely soluble in solvent (water:methanol, 1:5, *v/v*), while the industrial, alkaline and alkali lignin were 30%, 60% and 90% soluble (Table 3B.3) respectively. It was analysed that alkali lignin have high solubility in particular ratio and also it has low molecular weight (typically, *Mw*= 28 kDa) than dealkaline (*Mw*= 60 kDa) and alkaline (*Mw*= 60 kDa) lignin. Similarly, it might be due structural dissimilarity as represented in the scanning electron microscopy (Chapter 3, Section 3A,2.3, Figure 3A.2) and various types of moieties and linkages shown in FT-TR spectra (For more details please see Chapter 3, Sections 3A.2.11-3A.2.12, Figures 3A.9-3A.11 and Table 3A.4).
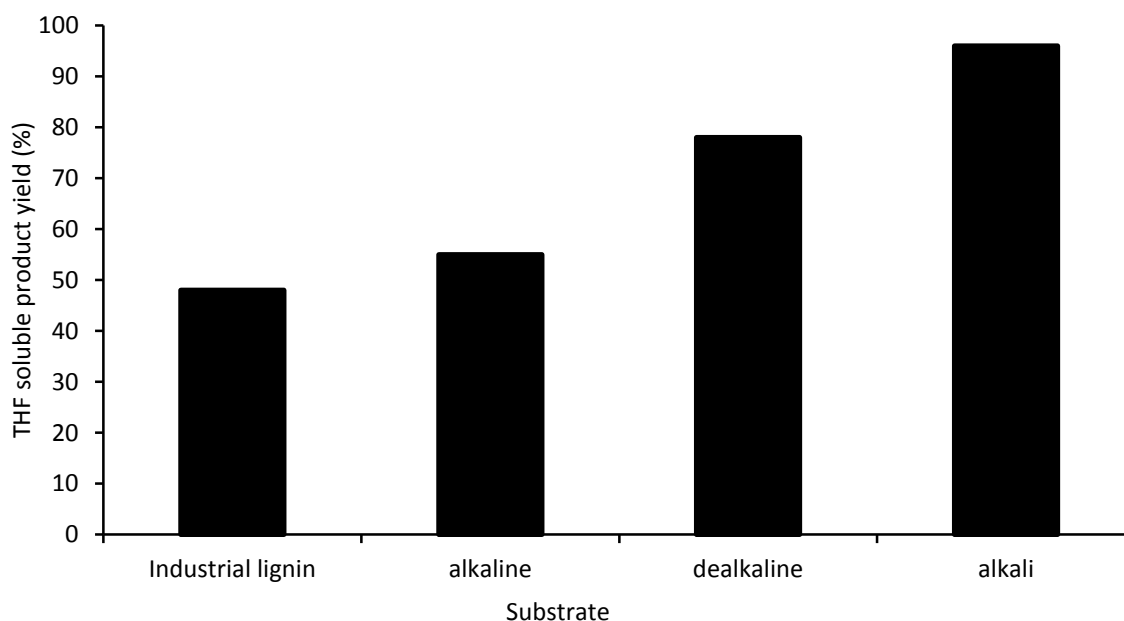
Figure 3B.15. Effect of various substrates on lignin depolymerization. Lignin (2 *wt.*% solution $H_2O:CH_3OH$, 1:5, *v/v*= 30 mL), $[C_3SO_3HMIM][HSO_4]$ (0.5 g), 120 ℃, 1 h, 1000 rpm.

Values are average of three reactions with ±3% error observed.

Table 3B.3. Properties of lignins.

Properties of lignin	Industrial	Alkaline	Deakaline	Alkali
Mol. *wt.* (Da)	-	60,000	60,000	28,000
Solubility (%)	32	62	100	100
Na (mg/g)	63	52	29	70

3B.3.9. Recycle study of the catalyst

The reuse of the BAILs, after extracting the products in THF soluble low molecular weight aromatic product (in which IL is not soluble; Section 3B.2.7), water was added to THF insoluble mass to separate unreacted lignin and water insoluble products from BAIL. The water soluble BAIL was again subjected to rotary evaporator and after evaporation, viscous mass was dried at 55 ^oC for 6 h and later dried in vacuum oven at 120 ^oC for 4 h. 0.5 g recovered BAIL contained 603 ppm Na as determined by ICP-OES technique. To remove the contamination of Na from recovered BAIL, HCl (2.94 mmol) was added to BAIL solution (1.0 g recovered BAIL in 20 mL water) stirrer at room temperature for 4 h to form NaCl salt. Again after evaporation of water, ethanol was added to the viscous mass and some white coloured solid (mostly NaCl) to separate BAIL from NaCl. This is possible since NaCl is insoluble in ethanol but BAIL is soluble. After separation of ethanol solution from solid (NaCl), ethanol was evaporated and the recovered BAIL was again subjected to ICP-OES technique in which Na was not observed. The analysis confirmed absence of Na and thus this BAIL was further used in next runs and recycled catalyst gave similar activity for 6 cycles (Figure 3B.16). Moreover, to check the presence of Cl$^-$ in BAIL, silver chloride (mirror) test was done and the results illustrate that BAIL was not contaminated with any Cl$^-$.
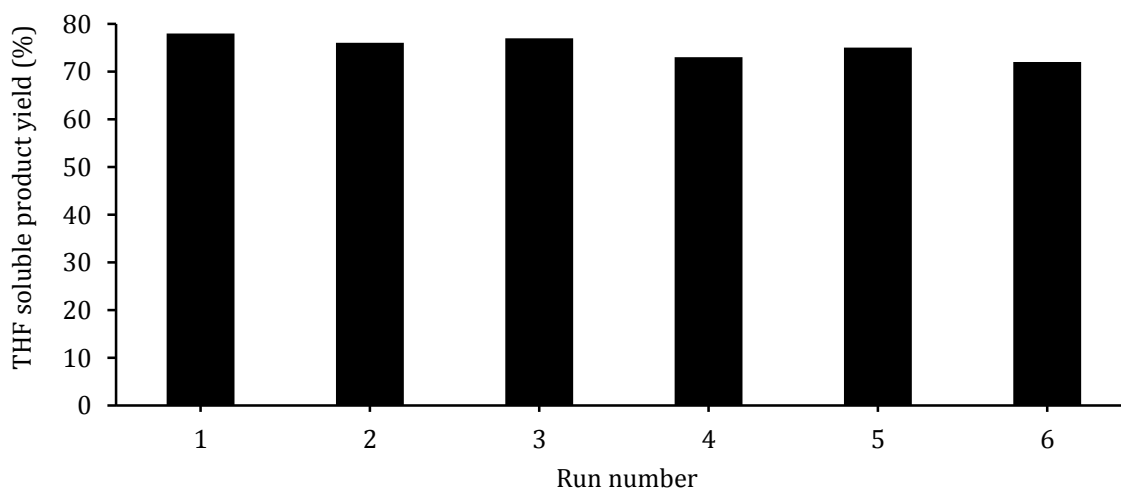
Figure 3B.16. Reuse study of [C$_3$SO$_3$HMIM][HSO$_4$] BAIL. Dealkaline lignin (2 *wt.*% solution H$_2$O:CH$_3$OH, 1:5, *v/v*= 30 mL), [C$_3$SO$_3$HMIM][HSO$_4$] (0.5 g), 120 ^oC, 1 h, 1000 rpm.

Values are average of three reactions with ±3% error observed.

Recovered IL was characterised by NMR, (^{1}H and ^{13}C), FT-IR, CHNS, ICP-OES and TGA. Characterization result is similar with fresh IL as shown below.

3B.3.10. Characterization of spent [C₃SO₃HMIM][HSO₄] BAIL

The spent [C₃SO₃HMIM][HSO₄] BAIL as catalyst was characterized by various physico-chemical analytical techniques to check their purity and thermal stability.

¹H and ¹³C-NMR spectra of fresh and spent [C₃SO₃HMIM][HSO₄] BAIL

Fresh [C₃SO₃HMIM][HSO₄] BAIL

¹H-NMR (200 MHz, D₂O): δ, 8.56 (s, 1H), 7.42 (s, 1H), 7.35 (s, 1H), 4.26 (t, 2H), 3.79 (s, 3H), 2.82 (t, 2H) and 2.21 (m, 2H).

¹³C-NMR (50.3MHz, D₂O): δ, 136.16, 123.74, 122.0, 47.69, 47.19, 35.66 and 25.05.

Spent [C₃SO₃HMIM][HSO₄] BAIL

¹H-NMR (200 MHz, D₂O): δ, 8.57 (s, 1H), 7.46 (s, 1H), 7.36 (s, 1H), 4.24 (t, 2H), 3.80 (s, 3H), 2.83 (t, 2H) and 2.23 (m, 2H).

¹³C-NMR (50.3MHz, D₂O): δ, 136.18, 123.76, 122.10, 47.71, 47.19, 35.68 and 25.09.
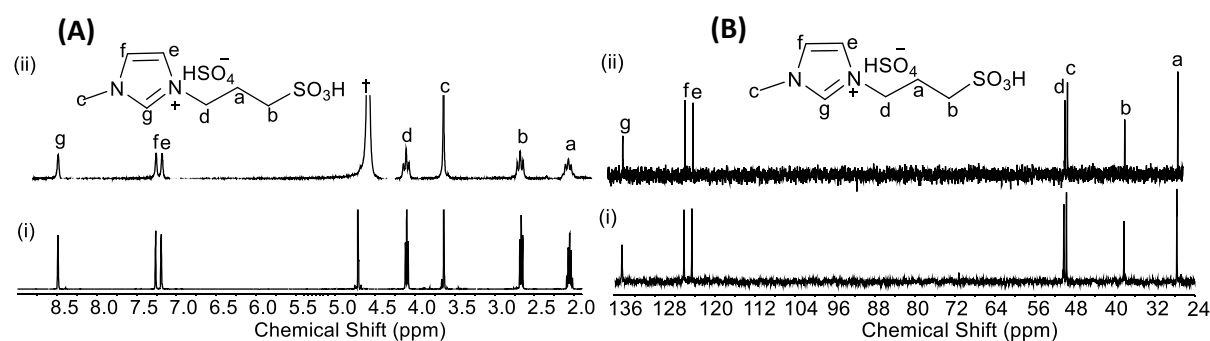
Figure 3B.17. (A) ¹H and (B) ¹³C NMR spectra of fresh (i) and spent (ii) up to 5ᵗʰ run of [C₃SO₃HMIM][HSO₄] BAIL, († indicate the solvent peak).

FT-IR spectra of fresh and spent [C₃SO₃H MIM][HSO₄] BAIL†

Fresh [C₃SO₃HMIM][HSO₄] BAIL
FT-IR (reflectance, cm⁻¹): 3412, 3157, 3090, 2959, 2880, 1722, 1650, 1600, 1500, 1463, 1236, 1037, 847, 825, 750, 690, 623.
Spent [C₃SO₃HMIM][HSO₄] BAIL
FT-IR (reflectance, cm⁻¹): 3415, 3162, 3095, 2963, 2892, 1719, 1658, 1601, 1503, 1467, 1240, 1041, 850, 830, 755, 692, 627.

Table 3B.4. Elemental analysis of fresh and spent [C₃SO₃HMIM][HSO₄] BAIL.

BAIL	Fresh (%)				Spent (%)			
	C	H	N	S	C	H	N	S
[C₃SO₃HMIM][HSO₄]	28.01	4.35	9.39	20.90	27.78	4.20	8.96	21.01

The isolated spent [C₃SO₃HMIM][HSO₄] BAIL catalyst was characterised by several analytical techniques such as elemental analysis, NMR, FT-IR and TGA analysis. The elemental analysis of spent [C₃SO₃HMIM][HSO₄] BAIL matched well with the fresh catalyst (Table 3B.4). The NMR (¹H and¹³C) (Figure 3B.17) and FT-IR characterizations reveal that the spent ILs is obtained in the

pure form. The TGA analysis (air) of spent [C$_3$SO$_3$HMIM][HSO$_4$] BAIL catalyst showed weight loss similar to fresh [C$_3$SO$_3$HMIM][HSO$_4$] BAIL catalyst. This analysis confirmed [C$_3$SO$_3$HMIM][HSO$_4$] BAIL catalyst is stable under reaction conditions.

3B.4. Isolation of aromatic monomers using column chromatography

Once the reaction was done with dealkaline lignin (2 *wt.*% solution H$_2$O:CH$_3$OH, 1:5, *v/v*= 30 mL), [C$_3$SO$_3$HMIM][HSO$_4$] (0.5 g) catalyst, at 120 °C for 1 h, the obtained THF soluble low molecular weight aromatic products were first analysed with GC, GC-MS, HPLC, LC-MS. Later, isolation of aromatic monomers soluble in THF was done using column chromatography. It was very difficult to isolate the aromatic monomers from the THF soluble products due to close polarity of the identified aromatic monomers. However, the three aromatic monomers were separated out from the reaction mixture using column chromatography, further those are quantified and characterised by ^{1}H NMR, GC and GC-MS; namely vanillin (m/z-152), methyl vanillate (m/z-182) and acetoguaiacone (m/z-166). It is much interesting that first time vanillin ca. 7 mg (ca. 2.5%) is isolated in pure form, 281 mg of THF soluble low molecular aromatic products using column chromatography (Figure 3B.18).

Column chromatography was carried out to isolate aromatic monomers in the pure form from THF soluble low molecular weight aromatic products using silica gel (230-400 mesh) as stationary phase. Pet ether and different concentration of EtOAc were taken as mobile phase. Initially, the slurry of THF soluble products was prepared in the DCM (5 mL) and with silica gel (ca. 1.0 g, 230-400 mesh). The obtained slurry was transferred at reduced pressure to get dried slurry (mixture of silica gel and THF soluble products). The dried slurry was loaded in pre-prepared 30 cm length column (filled with silica gel and with 100% pet ether). It was very difficult within a single step to separate aromatic monomers, so in beginning three aromatic monomers (in mixture) were separated out, which was further subjected for second steps to isolate individually three aromatic monomers in pure form. Initially, mixtures of three aromatic monomers were obtained at 80:20% *v/v* pet ether:EtOAc solvent ratios, which was confirmed by the GC-MS and GC. The mixtures of three aromatic monomers were again loaded for column chromatography. The mixtures of aromatic monomers were separated individually, which was confirmed by the GC, GC-MS and ^{1}H NMR (Figures 3B.19-3B.20) analysis. These compounds were also confirmed in the mixture of THF soluble low molecular weight aromatic products (Table 3B.2).
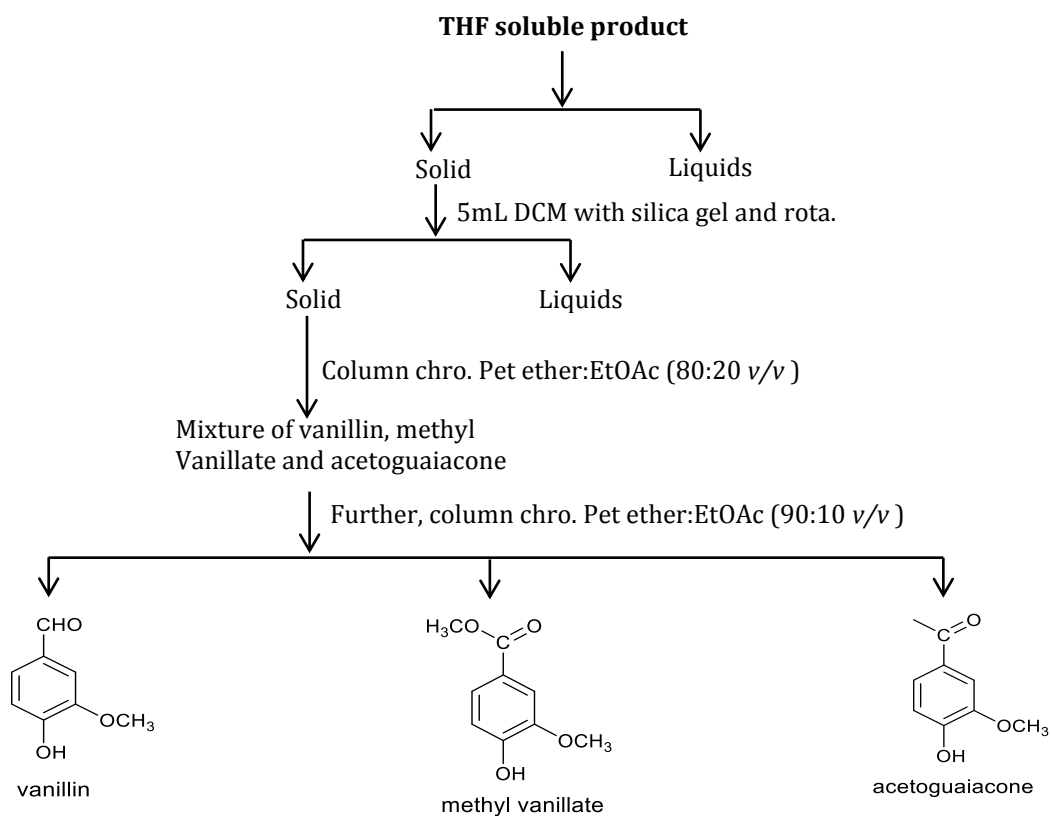
Figure 3B.18. Scheme for the isolation of aromatic monomers using column chromatography from THF soluble products.
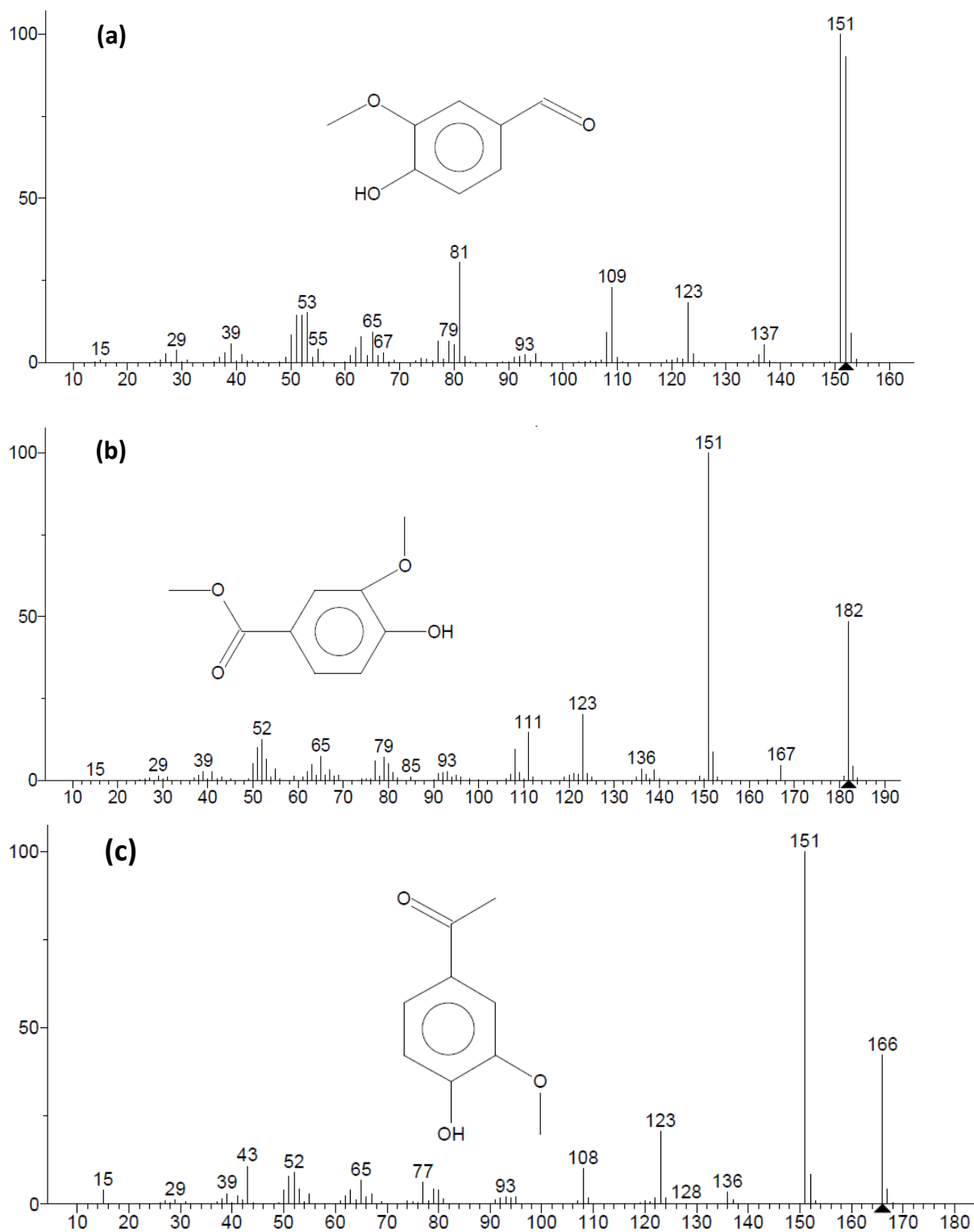
Figure 3B.19. GC-MS of column chromatography identified aromatic monomers. Reaction conditions. Dealkaline lignin (2 *wt.*% solution $H_2O:CH_3OH$, 1:5, *v/v*= 30 mL), [C_3SO_3HMIM][HSO_4] (0.5 g), 120 °C, 1 h, 1000 rpm.
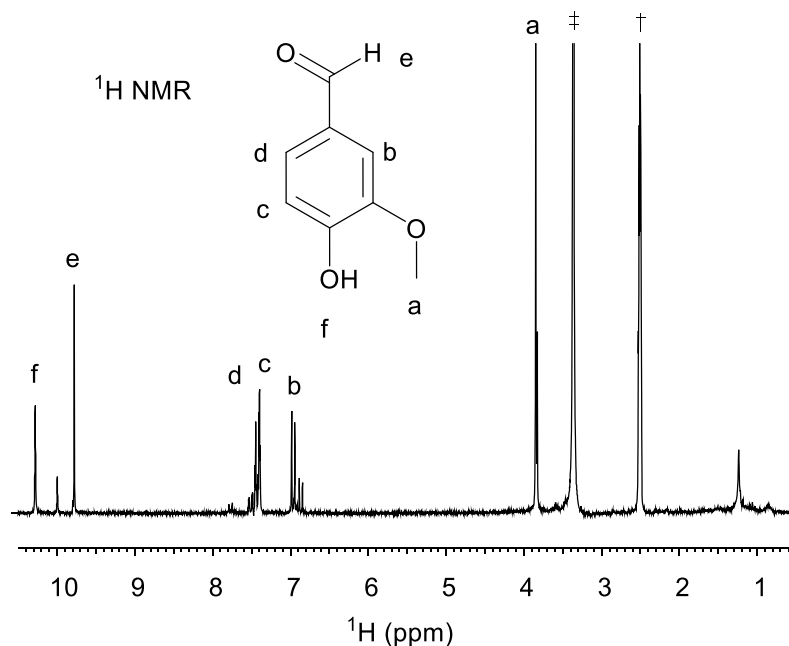
Figure 3B.20. ^{1}H NMR of isolated vanillin recorded in DMSO-d_6 solvent († peak for the DMSO solvent and ‡ for the water present in the DMSO solvent).

3B.5. E-factor

One of the most important green chemistry aspects is E-Factor, which gives more impetus for growing cleaner and more sustainable processes. Green chemistry is: (i) reduce the waste generation and (ii) avoid usage of toxic/hazardous materials. The E-factor is calculated based on the equation 3B.8. Higher the E-factor value means more waste generated in the process.[25]

$$\text{E} - \text{Factor} = \frac{\text{Amount of waste}}{\text{Amount of product}} \quad\quad (3B.8)$$

In a typical reaction done with lignin (2 *wt.*% solution H_2O:CH_3OH, 1:5 *v/v*= 30 mL), catalyst (0.5 g) at 120 ºC for 1 h, THF soluble products yield of 78% was achieved with high efficiency (95±5% mass balance). Considering this, an E-factor of 0.28 is calculated. This value is close to ideal (E-factor= 0) value of E-factor and similar to E-factor of industrial bulk chemicals.[25]

3B.6. Correlation between lignin and THF soluble products

As discussed above, substantiation for formation of low molecular weight aromatic products was done by chromatographic techniques as discussed in the sections 3B.3.1.5. Nonetheless, to perceive the changes transpiring in lignin structure and existence of several functional groups in both dealkaline lignin and in THF soluble low molecular weight aromatic products on bulk and molecular levels were done using several chromatographic, spectroscopic and thermal analytical techniques (TGA, GPC, DSC, UV-Vis, FT-IR, 1D and 2D (HSQC) NMR, etc.).

3B.6.1. Thermogravimetric analysis (TGA)

The TGA graphs obtained for dealkaline lignin and THF soluble products are presented in Figure 3B.21. As seen in (Figure 3B.21), lignin is stable up to 250 °C, while THF soluble low molecular weight aromatic products are stable up to 150 °C, which shows that lignin undergoes depolymerization into low molecular weight aromatic products, which have low degradation points than lignin. Even after heating lignin up to 700 °C, some amount of lignin remains unburnt (ignition residues). This is due to presence of inorganic residue (ash) in lignin. Based on the results obtained in TGA and understanding the structure of lignin ($C_{10}H_{13}O_3S_{0.09}$) and THF soluble products, it is predicted that lignin and THF soluble low molecular weight aromatic products may decompose as CO, CO_2, CH_4 and H_2, which was discussed in Section 3A.2.7.
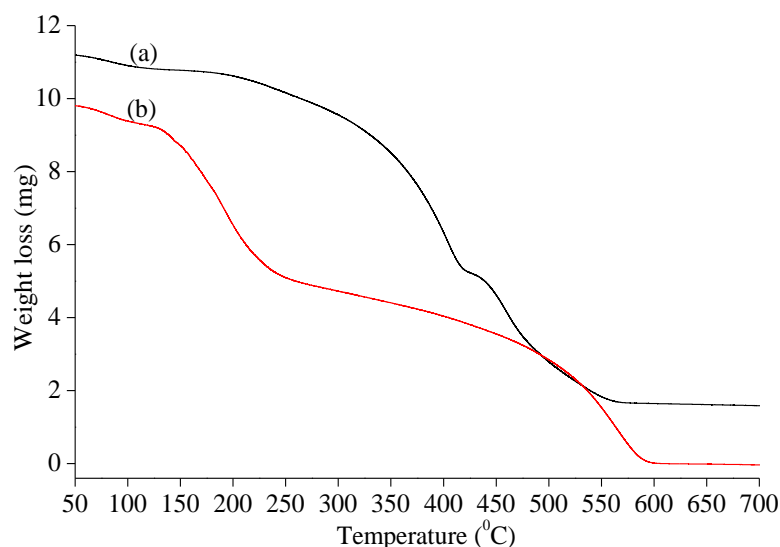
Figure 3B.21. Thermogravimetric analysis profiles (air) of (a) dealkaline lignin and (b) THF soluble products. Reaction conditions: dealkaline lignin (2 *wt.*% solution H_2O:CH_3OH, 1:5 *v/v*= 30 mL),[C_3SO_3HMIM][HSO_4] (0.5 g), 120 °C, 1 h, 1000 rpm.

3B.6.2. Gel permeation chromatography (GPC)

The formation of low molecular weight aromatic products and to confirm the changes occurred in dealkaline lignin GPC analysis was done. Similarly, in previous reports researchers have employed the GPC analysis to correlate the lignin and aromatic products obtained after depolymerization.[13, 26] For the GPC analysis, samples were prepared with 10 mg/mL concentrations in DMF solvent and the instrument was calibrated using polystyrene standards. Though, this technique estimation of molecular weight of dealkaline lignin and THF soluble low molecular weight aromatic products from GPC analysis is not feasible owing to complex structure of lignin and non-availability of standards for calibration. As seen from Figure 3B.22, [C_3SO_3HMIM][HSO_4] catalysed lignin depolymerized products has peak at high retention volume that conclude the formation of low molecular weight aromatic products. It is noticed from the GPC chromatogram (Figure 3B.22), that lignin undergoes depolymerization as emergence of

new peak along with solvent which is detected in products and also disappearance of major peak in the THF soluble products, which is present in GPC chromatograph of lignin at 19.0 retention volume. Since from the GPC chromatogram of THF soluble products peaks are eluted along with solvent indicates that THF soluble products obtained have low molecular weight ≤1000 g/mol. This results is good correlated with the unidentified peaks were noted in the GC-MS and LC-MS analysis, with having high molecular weight as dimers, trimers (300-550 g/mol). Accordingly, the result obtained with GPC analysis is good correlation with the GC, GC-MS, HPLC and LC-MS analysis.
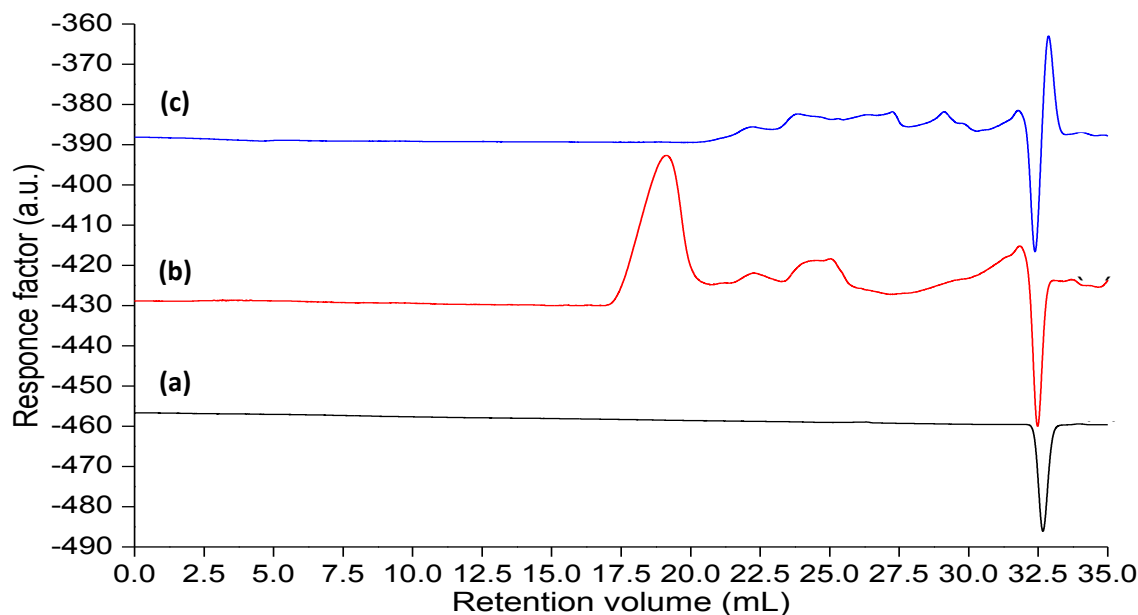
Figure 3B.22. GPC (DMF) analysis profiles of (a) DMF solvent, (b) dealkaline lignin and (c) THF soluble low molecular weight aromatic products. Reaction conditions: dealkaline lignin (2 *wt.*% solution H_2O:CH_3OH, 1:5 *v/v*= 30 mL), [C_3SO_3HMIM][HSO_4] (0.5 g), 120 °C, 1 h, 1000 rpm.

3B.6.3. Differential scanning calorimetric analysis (DSC)

In the thermogram obtained from DSC analysis of lignin (Figure 3B.23a), peaks were recorded at 228 and 244 °C, due to melting (endothermic) and crystallization/char (exothermic), respectively. Nonetheless, absence of these peaks in the THF soluble low molecular weight aromatic products and observance of multiple new peaks (Figure 3B.23b) denote that lignin was depolymerised into low molecular weight aromatic products, which have diverse transition temperatures. Additionally, it is advocated that the products are low boilers (<300 °C) as no peak for crystallization was spotted and subsequent to analysis, sample pan was empty. This finding is in line with the products ascertained from chromatography analysis.
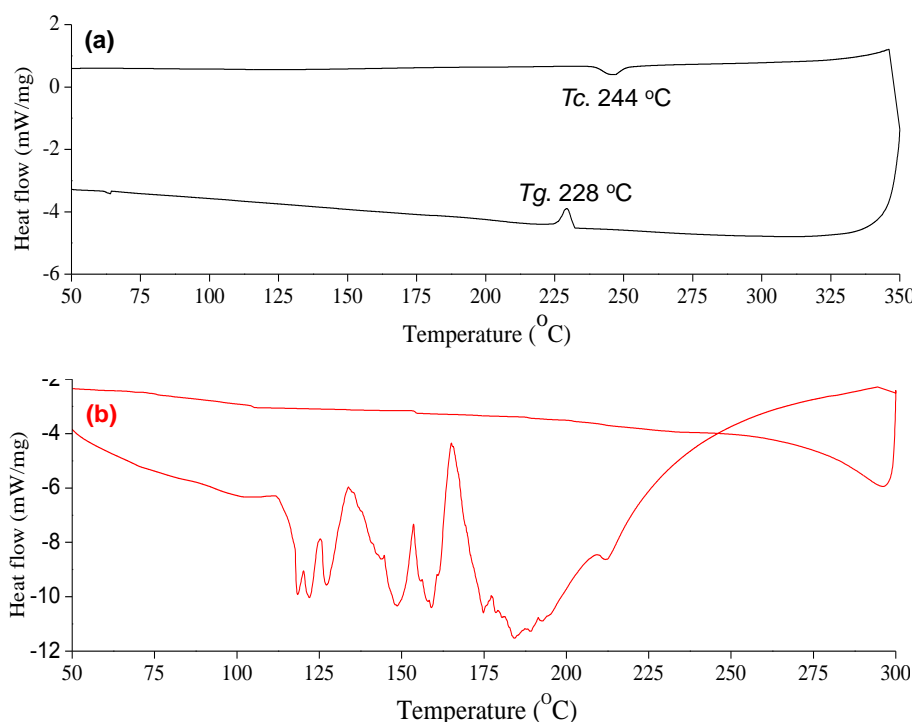
Figure 3B.23. DSC analysis of (a) dealkaline lignin and (b) THF soluble products.

Reaction conditions: dealkaline lignin (2 *wt.*% solution H_2O:CH_3OH, 1:5 *v/v*= 30 mL), [C_3SO_3HMIM][HSO_4] (0.5 g), 120 ℃, 1 h, 1000 rpm.

3B.6.4. UV-Visible (UV-Vis) spectra

The UV-Vis absorption spectroscopy is primarily employed to define the multiple bond (single, double and triple) or aromatic conjugation within lignin and THF soluble products. As seen from Figure 3B.24, in UV-Vis spectra for various characteristic bands for lignin and THF soluble products samples are observed. Normally, absorption bands observed in the range of 200-220 nm are due to Π-Π* electronic transition of the aromatic ring (-CH=CH-). Observance of shoulder band at 230 nm can be assigned to the mono- or di-substituted aromatic rings (e.g. –OCH_3, -CHO, -OAr etc.), in both lignin and products spectra. The absorption bands for guaiacyl (*G*), syringyl (*S*) and *p*-hydroxyphenyl (*H*) units at 280±4 and 313±2 nm are observed in dealkaline lignin and in products samples.[27-29] Additionally, it has been established that absorption bands in the range of 270-290 nm are due to non-conjugated phenolic compounds.[29] The absorption band between 300-320 nm indicates the presence of aromatic conjugated structures (Cα C=C and C=O) or guaiacyl moieties.[30] Efforts were undertaken to identify functionalities (conjugation, function groups) by UV-Vis (Figure 3B.24) absorption measurement study and as seen, in both the samples, existence of four peaks (313, 280, 230, 204 nm) due to occurrence of various types of chromophores/substituent in aromatic compounds proved that almost all the functionalities are preserved in products, as such present in dealkaline lignin.
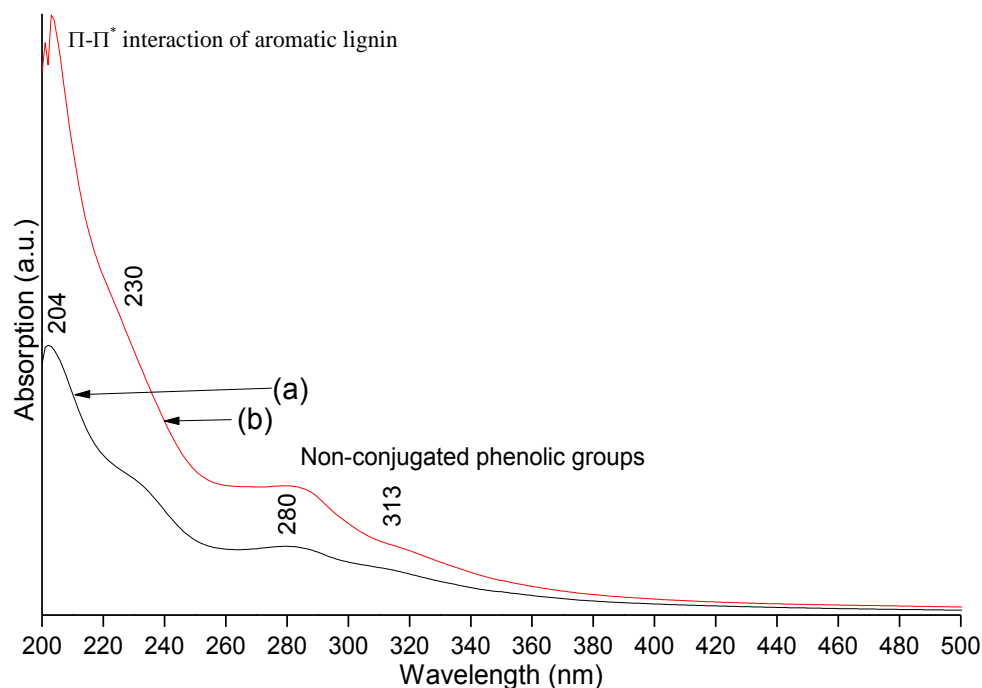
Figure 3B.24. UV-Vis spectra of (a) dealkaline lignin and (b) THF soluble products in methanol. Reaction conditions: dealkaline lignin (2 *wt.*% solution $H_2O:CH_3OH$, 1:5 *v/v*= 30 mL), [C_3SO_3HMIM][HSO_4] (0.5 g), 120 ℃, 1 h, 1000 rpm.

3B.6.5. Fourier transform infrared (FT-IR) spectra

The presence of various functional groups in dealkaline lignin and THF soluble products were analysed using FT-IR (FT-IR-8300 Shimadzu) technique and occurrence of numerous functional groups in both are established with the literature.[31-33] For the analysis, pellets were made with KBr by maintaining 1*wt.*% concentration. The normalization of intensities was performed based on the exact concentration used for making pellets.

The FT-IR spectrum (Figure 3B.25a) of lignin illustrates presence of various functional groups such as hydroxyl (~3400 cm^{-1}), methoxy C-H (~2935 cm^{-1}), and carbonyl (~1730, 1770 cm^{-1}). Multiple peaks for aromatic C=C (in ring) (1400-1600 cm^{-1}), ether bonds (~1125, 1200-1270 cm^{-1}), and primary alcohols (1040-1060 cm^{-1}) etc. were also observed in the spectrum. The FT-IR study of THF soluble low molecular weight aromatic products (Figure 3B.25b) demonstrate that besides peaks observed in parent lignin sample with similar or different intensities, emergence of few new peaks was seen. A new peak appeared at 1180 cm^{-1} (s) is assigned to C–O (stretch) in phenol or to C-O (stretch) in lactone and acyl group. Another major peak visible at 1068 cm^{-1} is assigned to (sp^3) alkoxy C-O group. Peaks at 850 and 885 cm^{-1} are assigned for (sp^2) C-H bending in substituted benzene and $R_2C=CH_2$ (germinal disubstituted alkene). Twin peaks visible at 1730, 1770 cm^{-1} are due to C=O stretch in acids/esters/aldehydes/ketones. The increase in peak intensity (2875 cm^{-1}) in products implies that this contribution is primarily from aldehyde group (C-H stretch). Appearance of peak at

2945 cm^{-1} because of C-H stretching in (sp[3]) alkanes is in line with multiple peaks observed for alkanes (1380-1460 cm^{-1}) in products. An enhancement in intensity of broad peak in products at 3200-3500 cm^{-1} is due to RO-H (alcohol) implies that lignin undergoes depolymerization. A decline in intensity for peaks at 1040 (aromatic) and 1125 cm^{-1} (aliphatic) is due to ether linkages in products compared with lignin again corroborate that lignin undergoes depolymerization. This study reveals that most of the functionalities present in lignin are conserved in products and also some new functionality are introduced because of cleavage of several bonds in lignin. Similar results are seen with the other lignin (alkali, alkaline and industrials lignin). Table 3B.2, consolidated for the products obtained in dealkaline lignin depolymerization reaction (from GC, GC-MS, HPLC and LC-MS) with having several functional groups, which are good matches with the significant result obtained with FT-IR data.
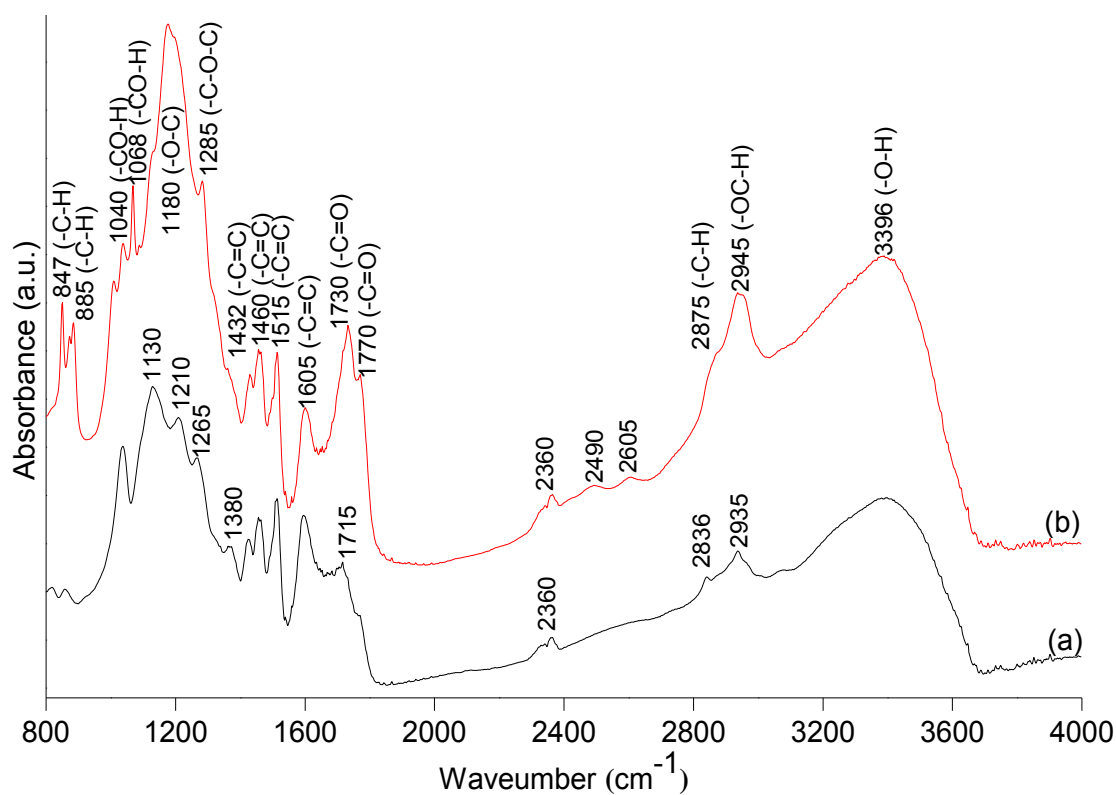
Figure 3B.25. FT-IR spectra of (a) dealkaline lignin and (b) THF soluble products.

Reaction condition: lignin (2 *wt.*% solution H_2O:CH_3OH, 1:5 *v/v*= 30 mL), [C_3SO_3HMIM][HSO_4] (0.5 g), 120 °C, 1 h, 1000 rpm.

3B.6.6. Nuclear magnetic resonance (NMR) spectra

3B.6.6.1. ^{1}H and ^{13}C NMR spectra of dealkaline lignin and THF soluble products

The changes transpiring in lignin structure and THF soluble products were characterized using 1D (^{1}H and ^{13}C) and 2D (HSQC) NMR spectra. The DMSO-d_6 solvent was used an internal standard δ_C= 39.5 ppm for ^{13}C and δ_H= 2.5 ppm for ^{1}H NMR.

To study more about the skeleton (proton and carbon) of the dealkaline lignin and THF soluble low molecular weight aromatic products obtained after lignin depolymerization, [1]H

NMR spectra were recorded (500 MHz) in DMSO-d_6 (Figures 3B.26a-3B.26b). As observed from the spectra, most of the peaks present in dealkaline lignin are retained in the THF soluble products, however there is a difference in the intensities. Typically, peaks for $-CH_3$, $-CH_2-$, and $-CH-$ alkyl groups are observed around 0.5–1.8 ppm in lignin and these peaks are more intense in THF soluble products. The appearance of peaks from 2.0-2.8 ppm can be assigned to the proton attached with α to the carbonyl group ($R-CO-CH_3$; R-alkyl or aryl) or benzylic proton ($Ar-CH_3$) or ester ($R-CH_2-C(O)OR$; R= alkyl or aryl) groups. The appearance of a peak at 3.7-3.9 ppm is due to the presence of methoxy (CH_3-O-) or $Ar-OCH_3$ or an ester group ($R-C(O)OCH_2R$; R=alkyl or aryl). Aromatic protons are assigned between 6.0-8.5 ppm regions for the *H*, *G* and *S* moieties. The ^{1}H NMR data thus bring us to the conclusion that an increase in 0.5-2.7 ppm region is in the THF soluble products data and ultimately supports our efforts to statement that lignin undergoes depolymerization.

To expanse more related to skeleton of the dealkaline lignin and THF soluble products, ^{13}C NMR are represented in the Figure 3B.26c-3B.26d. All the peaks observed in the dealkaline lignin are assigned in THF soluble products with more intense of alkyl, hetero atom near to alkyl, aryl or aromatic regions. Increase in the intensity in the range between 10-40 ppm (alkylated region) derived from ^{13}C NMR spectrum of THF soluble products, which is in line with the ^{1}H NMR data. It is clearly emphasized that after lignin depolymerization similar types of functional group is retained in THF soluble products. Peaks assigned in the range of between 20–50 ppm are typically for CH_3CO- or R_3CH (R-alkyl) species. The peaks at 55–90 ppm is assigned to the carbon next to heteroatom (oxygen) ($R-CH_2-O-$; $R_2-CH-O-$; R_3-C-O-; R=alkyl or aryl group). The ^{13}C NMR peaks for the aromatics (*H*, *G* and *S* moieties) carbons are seen in the range between 110–150 ppm and alkenes (110–140 ppm), which are clearly observed in lignin and in THF soluble products, however the more intense peaks for the aromatic carbons are observed in the THF soluble product. It is obvious lignin is copolymer, which possess high molecular weight (60 kDa) and after depolymerization they convert into low molecular weight aromatic products so these are more intense in products. The peaks in range 170-180 ppm are assigned to carbon associated with an carbonyl group ($R-C(O)-R'$, $R-C(O)O-R'$, R= alkyl or aryl). As seen peak for carbonyl group in the THF soluble products is observed in ^{13}C NMR spectrum, is in line with the result obtained from FT-IR spectrum (1730 and 1730 cm^{-1}, Figure 3B.25) of the products (GC and GC-MS identified aromatic monomers, Table 3B.2). It was also observed that the products attained the similar functional groups as confirmed with the help of several chromatography and mass analyser as GC, GC-MS, HPLC and LC-MS, (Figures 3B.4-3B.8) and analysis (Table 3B.2).
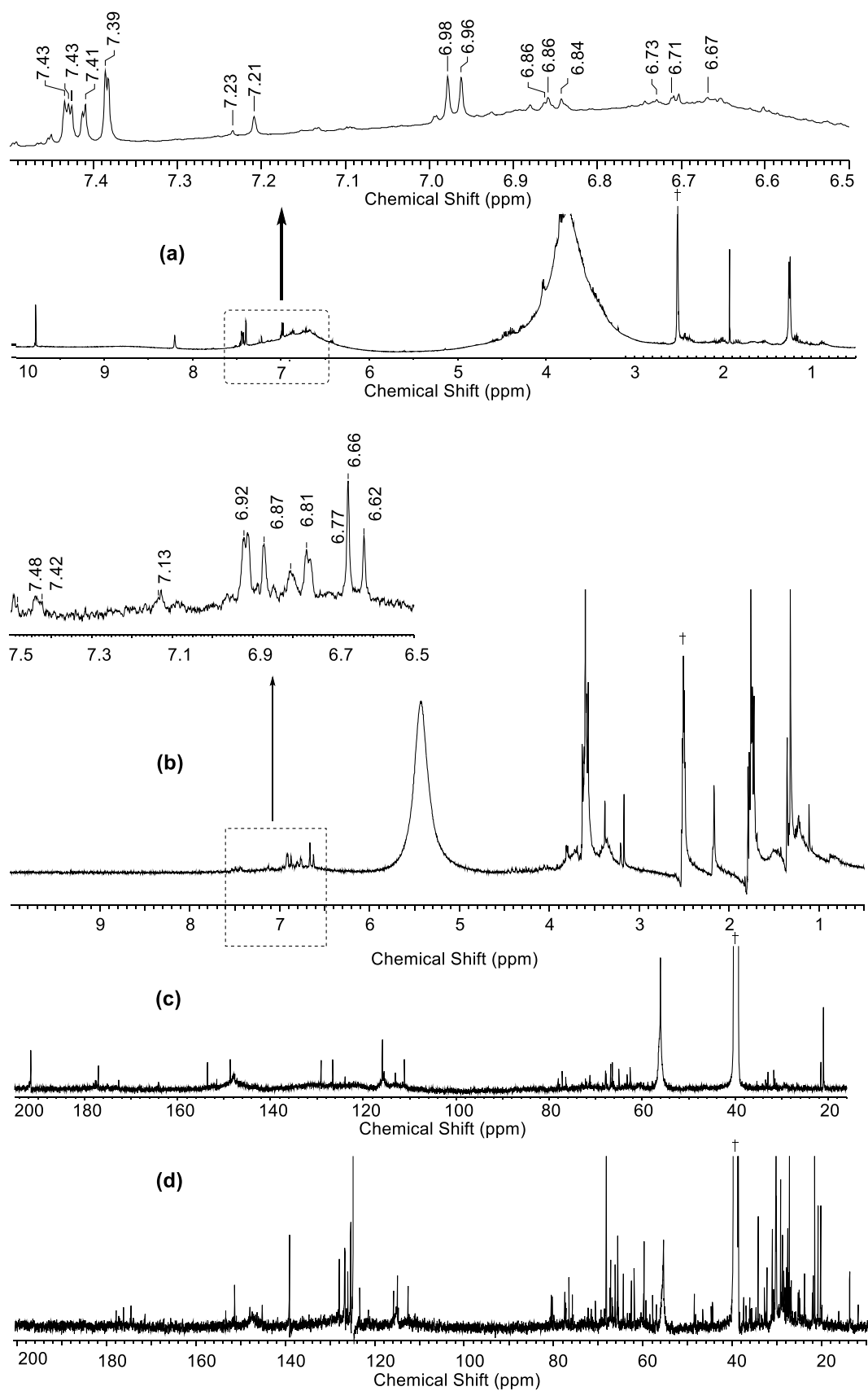
Figure 3B.26. ^{1}H and ^{13}C NMR spectra of (a, c) dealkaline lignin and (b, d) THF soluble products. Reaction conditions: dealkaline lignin (2 *wt.*% solution H_2O:CH_3OH, 1:5 *v/v*= 30 mL), [C_3SO_3HMIM][HSO_4] (0.5 g), 120 °C, 1 h, 1000 rpm. All the spectra were recorded in DMSO-d$_6$.

3B.6.6.2. 2D heteronuclear single quantum coherence (HSQC) NMR spectra of dealkaline lignin and THF soluble products

To ascertain the linkages and functional groups present in lignin and products, advance analytical tool, 2D (HSQC) NMR was carried out (Figure 3B.27). The 2D (HSQC) spectrum shows signals for oxygenated aliphatic and aromatic of lignin in the range between δ_C/δ_H= 50-90/2-6 and 100-140/6-8 ppm, respectively.[6, 34-38] In lignin sample, strong signal for –OR groups (etherified) was observed at δ_C/δ_H= 56/3.2-4.0 ppm (Figure 3B.26a). Nonetheless, in products, the intensity of this signal was decreased (Figure 3B.26d) manifesting that during depolymerization, most of the ether linkages were cleaved. Similar observation is made by the FT-IR spectra (Figure 3B.25), the disappearance peaks at 1130 and 1210 cm^{-1} in THF soluble products, which correspond to ≡C-O-C≡ group linkage and present in dealkaline lignin. However, presence of few –OR groups in products is in line with the products identified (Figure 3B.27) with –OCH$_3$ groups. Likewise, in products (Figure 3B.27d), low intensity signals (δ_C/δ_H= 62-64/3.2-3.65 ppm) for C$_\gamma$-H$_\gamma$ was observed compared with lignin sample (Figure 3B.26a) implying decrease in concentration of these species. On the contrary increase in intensity for signal (δ_C/δ_H= 60-62/3.2-3.5 ppm) assigned to C$_\gamma$-H$_\gamma$ specifies emergence of new moieties in products. The nonappearance of signals for A$_\beta$ (δ_C/δ_H= 84.2/4.3 ppm) for guaiacyl moiety (*G*) and Bα (δ_C/δ_H= 85.5/4.6 ppm) in products (Figure 3B.27e) again emphasized that lignin (Figure 3B.27b) undergoes depolymerization. Generally, the cross-signals observed at δ_C/δ_H= 100-140/6-8 ppm corresponds to aromatic moieties such as, *p*-hydroxyphenyl (*H*), guaiacyl (*G*) and syringyl (*S*) alcohols (Figure 3B.27). While in lignin sample (Figure 3B.27c), prominent signals for '*G*' units are observed (δ_C/δ_H= 111/7.4, 115.4-115.7/6.7-7.0 ppm for C$_2$-H$_2$, C$_5$-H$_5$ and C$_6$-H$_6$ in '*G*' units), those were decreased in products (Figure 3B.27f) due to cleavage of –OR bonds. The observance of new signals for '*H*' units (δ_C/δ_H= 125.4-127.1/6.0-7.1 ppm) in products (Figure 3B.27f) again emphasized that lignin is depolymerised. The same observation is made for A$_\beta$ (δ_C/δ_H= 84.2/4.3 ppm) as reviewed above. Since similar 2D (HSQC) NMR results were also observed when other BAILs were used in these reactions, which is also found from GC-MS analysis (Figure 3B.4).
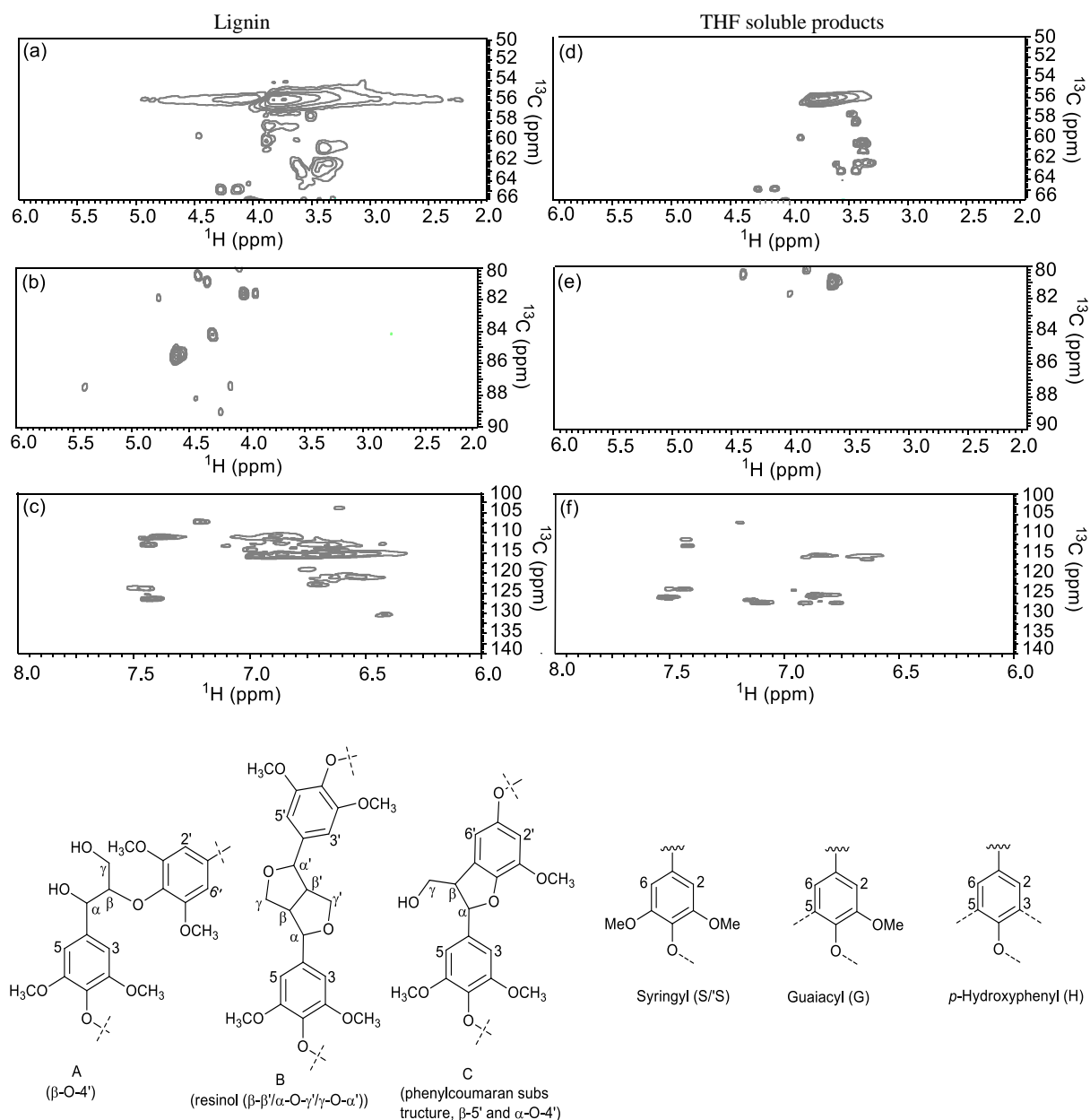
Figure 3B.27. 2D (HSQC) NMR spectra of (a, b, c) dealkaline lignin and (d, e, f) THF soluble products. All the spectra were measured after dissolving samples in DMSO-d_6.

A few low intense peaks present in NMR spectra may be from countless derivative on aromatic rings (lignin and THF soluble low molecular aromatic products), but due to the complex structure of lignin copolymer and high molecular weight (60 kDa), it would be very challenging to define all peaks. The analytical tools revealed the fact that the few functional groups and aromaticity were seen in lignin, which are retained in products and identification of products could be achieved with the help of NMR spectroscopic along with GC, GC-MS, HPLC, and LC-MS chromatograms attached with mass analyser techniques.

3B.7. Conclusions

In summary, depolymerization of various lignins (alkali, alkaline, dealkaline and industrial lignins) into low molecular weight aromatic products was studied over several BAILs/IL catalysts. Various types of phosphonium, ammonium, benzimidazolium and imidazolium cations with the combination of [HSO$_4$], [Cl], [PTS], [H$_2$PO$_4$] anions based ILs as catalysts were evaluated for dealkaline lignin depolymerization to yield low molecular weight aromatic products. Among several BAILs/IL catalysts evaluated, [C$_3$SO$_3$HMIM][HSO$_4$] was found to be the best catalyst for the lignin depolymerization reaction which yielded 78% of THF soluble low molecular weight aromatic products. Optimization of reaction conditions was carried out to improve the yield of low molecular weight aromatic products. Reaction conditions such as temperature, time, pressure, concentration of catalysts (weight and mole basis), reaction medium etc. were studied in detail to achieve higher yield THF soluble products. After thorough study, following reaction condition is considered as optimum condition to yield highest amount of THF soluble products (78%),

Lignin (2 *wt.*% solution H$_2$O:CH$_3$OH, 1:5 *v/v* = 30 mL), [C$_3$SO$_3$HMIM][HSO$_4$] (0.5 g), 120 °C, 1 h.

From 78% THF soluble products, three aromatic monomers were successfully isolated in pure form *via* applying column chromatography. These products were characterized for their purity using NMR, GC and GC-MS analytical techniques. Correlation between the effect of acidity (Brønsted, Lewis and both) in BAILs, their comparison with solid acids (HUSY, H-BEA and amberlyst-15), homogeneous mineral and organic acids (HCl, H$_2$SO$_4$, H$_3$PO$_4$ and PTSA.H$_2$O) etc. was done and it was found that imidazolium cation with [HSO$_4$] anion gave highest yield of THF soluble low molecular weight aromatic products. It was also observed that with the combination of Brønsted and Lewis acidity, ILs catalyse degradation reactions (char, coke and gas) which decreased the yield of desired products. Recyclability of [C$_3$SO$_3$HMIM][HSO$_4$] catalyst shown that the catalyst is recyclable and the spent catalyst was characterized using CHNS, TGA, FT-IR and NMR techniques for any changes. These characterization studies revealed that it is obtained in pure form and is stable under the reaction conditions. The reaction path for lignin depolymerization proceeded *via* ester (-C(O)O-) and ether (≡C-O-C≡) bonds cleavage in a hydrolysis reaction. The cleavage of ≡C-O-C≡ bond was proven by (¹H, ¹³C and HSQC) NMR (disappearance of linkage region in the 2D (HSQC) NMR) and FT-IR analytical techniques (missing of ≡C-O-C≡ peaks at 1130 and 1210 cm⁻¹ in the products). The aromatic monomers formations were confirmed by various chromatograms attached with mass analyser techniques such as GC, GC-MS, HPLC, LC-MS and GPC. The quantification of these aromatic monomers was carried out by injecting the calibration standards, which were commercially available and it was found that 45% of aromatic monomers are present in 78% yield of THF soluble low molecular weight aromatic products. Correlation studied between the substrate (lignin) and THF soluble

low molecular weight aromatic products were done by various meticulous analytical techniques such as FT-IR, NMR, DSC, GPC, TGA, UV-Vis, etc. These analyses again emphasised that lignin molecule depolymerised into low molecular weight aromatic products.

3B.8. References

1. A. Rahimi, A. Azarpira, H. Kim, J. Ralph and S. S. Stahl, *J. Am. Chem. Soc.*, 2013, **135**, 6415-6418.

2. J. Zakzeski, P. C. A. Bruijnincx, A. L. Jongerius and B. M. Weckhuysen, *Chem. Rev.*, 2010, **110**, 3552-3599.

3. P. C. A. Bruijnincx and B. M. Weckhuysen, *Nat Chem*, 2014, **6**, 1035-1036.

4. S. Nanayakkara, A. F. Patti and K. Saito, *Green Chem.*, 2014, **16**, 1897-1903.

5. H. Nimz, *Angew. Chem. Int. Ed.*, 1974, **13**, 313-321.

6. N. D. Bonawitz, J. I. Kim, Y. Tobimatsu, P. N. Ciesielski, N. A. Anderson, E. Ximenes, J. Maeda, J. Ralph, B. S. Donohoe, M. Ladisch and C. Chapple, *Nature*, 2014, **509**, 376-380.

7. K. Stärk, N. Taccardi, A. Bösmann and P. Wasserscheid, *ChemSusChem*, 2010, **3**, 719-723.

8. D. D. Perrin, *Ionization constants of inorganic acids and bases in aqueous solution, second edition*, Pergamon, Oxford, UK, 1982.

9. J. House, *Inorganic Chemistry* Academic Press, 2nd edn., 2012.

10. B. R. Puri, L. R. Sharma and M. S. Pathania, *Principles of physical chemistry*, Vishal Publishing CO., India, 44 edn., 2011.

11. S. Tsuzuki, H. Tokuda and M. Mikami, *Phys. Chem. Chem. Phys.*, 2007, **9**, 4780-4784.

12. R. P. Matthews, I. J. Villar-Garcia, C. C. Weber, J. Griffith, F. Cameron, J. P. Hallett, P. A. Hunt and T. Welton, *Phys. Chem. Chem. Phys.*, 2016, **18**, 8608-8624.

13. A. Toledano, L. Serrano and J. Labidi, *Fuel*, 2014, **116**, 617-624.

14. C. Xu, R. A. D. Arancon, J. Labidi and R. Luque, *Chem. Soc. Rev.*, 2014, **43**, 7485-7500.

15. A. Toledano, L. Serrano and J. Labidi, *Fuel*, 2014, **116**, 617-624.

16. J. Li, G. Henriksson and G. r. Gellerstedt, *Bioresour. Technol.*, 2007, **98**, 3061-3068.

17. V. M. Roberts, V. Stein, T. Reiner, A. Lemonidou, X. Li and J. A. Lercher, *Chem. Eur. J.*, 2011, **17**, 5939-5948.

18. T. Belkheiri, C. Mattsson, S.-I. Andersson, L. Olausson, L.-E. Åmand, H. Theliander and L. Vamling, *Energy Fuels*, 2016, **30**, 4916-4924.

19. W. J. Connors, L. N. Johanson, K. V. Sarkanen and P. Winslow, *Journal*, 1980, **34**, 29-37.

20. Z. Yuan, S. Cheng, M. Leitch and C. Xu, *Bioresour. Technol.*, 2010, **101**, 9308-9313.

21. A. K. Deepa and P. L. Dhepe, *RSC Adv.*, 2014, **4**, 12625-12629.

22. W. Xu, S. J. Miller, P. K. Agrawal and C. W. Jones, *ChemSusChem*, 2012, **5**, 667-675.

23.   X. Z. Yuan, H. Li, G. M. Zeng, J. Y. Tong and W. Xie, *Energy*, 2007, **32**, 2081-2088.

24.   J. Zakzeski, A. L. Jongerius, P. C. A. Bruijnincx and B. M. Weckhuysen, *ChemSusChem*, 2012, **5**, 1602-1609.

25.   R. A. Sheldon, *Chem. Commun.*, 2008, 3352-3365.

26.   Y. Ye, Y. Zhang, J. Fan and J. Chang, *Ind. Eng. Chem. Res.*, 2011, **51**, 103-110.

27.   H. Yang, Y. Xie, X. Zheng, Y. Pu, F. Huang, X. Meng, W. Wu, A. Ragauskas and L. Yao, *Bioresour. Technol.*, 2016, **207**, 361-369.

28.   K. Mononen, A.-S. Jaaskelainen, L. Alvila, T. Pakkanen Tuula and T. Vuorinen, *Holzforschung*, 2005, **59**, 381-388.

29.   X. Zhao, L. Dai and D. Liu, *J. Appl. Polym. Sci.*, 2009, **114**, 1295-1302.

30.   U. Westermark, *Wood Sci. Technol.*, 1985, **19**, 223-232.

31.   G. Gellerstedt, J. Li, I. Eide, M. Kleinert and T. Barth, *Energy Fuels*, 2008, **22**, 4240-4244.

32.   G. Zhou, G. Taylor and A. Polle, *Plant Methods*, 2011, **7**, 1-10.

33.   S. K. Singh and P. L. Dhepe, *Green Chem.*, 2016, **18**, 4098-4108.

34.   F. Tran, C. S. Lancefield, P. C. J. Kamer, T. Lebl and N. J. Westwood, *Green Chem.*, 2015, **17**, 244-249.

35.   P. Ferrini and R. Rinaldi, *Angew. Chem. Int. Ed.*, 2014, **53**, 8634-8639.

36.   J. M. W. Chan, S. Bauer, H. Sorek, S. Sreekumar, K. Wang and F. D. Toste, *ACS Catal.*, 2013, **3**, 1369-1377.

37.   S. Van den Bosch, W. Schutyser, R. Vanholme, T. Driessen, S. F. Koelewijn, T. Renders, B. De Meester, W. J. J. Huijgen, W. Dehaen, C. M. Courtin, B. Lagrain, W. Boerjan and B. F. Sels, *Energy Environ. Sci.*, 2015, **8**, 1748-1763.

38.   M. Foston, R. Samuel, J. He and A. J. Ragauskas, *Green Chem.*, 2016, **18**, 608-621.

Section 3C:

Depolymerization of lignin using

Immobilized-Brønsted acidic ionic liquid

3C.1. Introduction

Now-a-days, use of ionic liquids (ILs) as solvent or catalysts in the conversions of lignocellulosic biomass is growing. This is due to their important properties (low vapour pressure, high thermal stability, excellent solubility in wide range of solvents etc.), which help in achieving desired results. ILs are also considered as eco-friendly solvent and their numerous tuneable properties (e.g. acidic, basic, solubility, etc.) again drive the reactions towards obtaining desired products.[1, 2] Literature suggests that the use of ILs as a solvent along with supplementary catalyst(s) in the lignin depolymerization helps to achieve better results.[3-5] But, recycling of ILs is the major problem associated with these reactions. Considering this, the immobilization of ILs over silica framework is proposed.[6-10] However, due to low quantity of immobilization of ILs (28%)[7] and lower thermal stability of immobilized ILs; improvements in immobilization processes are still required. As shown in Chapter 3B, BAILs can depolymerise lignin into low molecular weight aromatic products. In view of this, the Immobilized-Brønsted acidic ionic liquid (I-BAIL) has a potential to be used as solid acid catalysts in lignin depolymerization reactions to yield low molecular weight aromatic products. To the best of my knowledge, lignin depolymerization using I-BAIL catalyst is not known. The lignin depolymerization reactions using I-BAIL as solid acid catalyst are discussed in details in this section.

3C.2. Experimental

3C.2.1. Materials

Detailed descriptions of the materials characterization were already discussed in Chapter 2, Section 2B.3.

3C.2.2. Characterization of substrate

Detailed descriptions on lignin characterizations were already discussed in Chapter 3, Section 3A.2.

3C.2.3. Synthesis and characterization of Immobilized-Brønsted acidic ionic liquid (I-BAIL)

I-BAIL was synthesised in two steps, wherein the first step-gel formation and in second step-crystallization process completed. The details descriptions of the catalyst synthesis procedures and proposed structures of the I-BAIL are given in Chapter 2, Sections 2B.2.2. The various physico-chemical analytical techniques (CHNS, NMR, FT-IR, TGA, XRD, TEM, SEM and UV-Vis; discussed in Chapter 2, Section 2B.3), showed that 42$wt.$% immobilization of ILs on/in silica framework is possible and it is stable till 250 ^{o}C.

3C.2.4. Lignin depolymerization

Lignin depolymerization reaction was carried out at desired temperature for required time in a batch mode reactor (Parr Autoclave= 150 mL capacity). Unless specified, in all the reactions, dealkaline lignin (2 $wt.$% solution H_2O:CH_3OH, 1:5 v/v= 30 mL) and catalyst (I-BAIL, 0.5 g) were

taken in reactor (150 mL) and the reactor was sealed and heated to desired temperature (200 ^oC) under slow stirring (100 rpm). After attaining the desired temperature, stirring was increased to 1000 rpm and this time was noted as initial reaction time (Auto generated pressure= 3.2 MPa). After completion of reaction, reactor was allowed to cool to room temperature (25 ^oC) under constant flow of air and under slow stirring (100 rpm).

3C.2.5. Work-up procedure

After completion of reaction, the reactor was allowed to cool to room temperature under the flow of air and slow stirring (100 rpm). Reaction mixture was collected, centrifuged, filtered and washed with water:methanol (1:5 *v/v*) solvent ratio. Solvent (water and methanol) was evaporated by using rotary vacuum evaporator (Figure 3C.1). Care was taken to trap all the low volatile products by arranging three ice traps in series before vacuum pump. The analysis of collected solvent in these traps revealed no loss of products. The reaction mass (products + unreacted lignin) obtained after removing solvent was dried at 55 ^oC for 16 h and further under vacuum at 80 ^oC for 4 h. To the dried mass, 30 mL of tetrahydrofuran (THF) was added to dissolve the products. THF was chosen to extract the products because it does not dissolve lignin (for more details descriptions please see lignin characterization Chapter 3, Section 3A.2.1, Table 3A.1) and hence would only extract aromatic products.
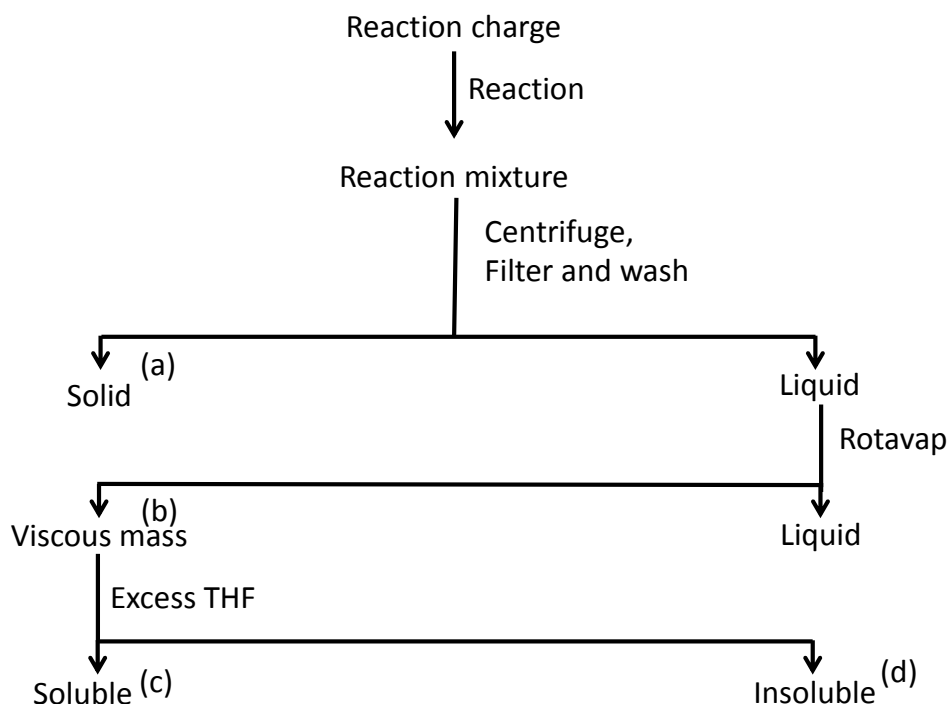
(a)recovered I-BAIL catalyst

(b)depolymerised, repolymerised, and unconverted lignin

(c)THF soluble products (analysed by GC, GC-MS, FT-IR, NMR, etc. and

(d)repolymerised and unconverted lignin

Figure 3C.1. Extraction of organic solvent soluble products from reaction mixture.

3C.2.6. Analysis of THF soluble products

The lignin depolymerization into THF soluble low molecular weight aromatic products was confirmed by using several analytical techniques, such as GC, GC-MS, NMR, FT-IR, CHNS, etc.

3C.2.7. Yield calculation

The yield (%) for THF soluble products was calculated based on the viscous products recovered from the THF solvent.

THF soluble products yield (%)

$$= \frac{\text{Weight of THF soluble dried viscous mass}}{\text{Weight (moisture and ash corrected) of lignin charged}} \times 100 \qquad (3C.1)$$

Most of the reactions were performed three times to check the reproducibility of results and the data presented in the current work is average of three reactions.

Typically, ±2% error in yield was observed on repeating the reactions.

3C.2.8. Mass balance calculation

Reaction conditions: dealkaline lignin (0.5 g), (H_2O:CH_3OH, 1:5 v/v= 30 mL), I-BAIL (0.5 g), 120 ᵒC, 1 h. Total reaction charge was 0.945 g (lignin 0.445 g (0.5-0.055 g (moisture)) + catalyst 0.5 g. After work-up procedure, the weight of dried viscous mass (products, unconverted and repolymerized lignin) and I-BAIL at room temperature was 0.91 g.

Mass balance =

$$\frac{\text{Weight of dried viscous mass } + \text{ Weight of I} - \text{BAIL}}{\text{Weight of actual charge}} \times 100 \qquad (3C.2)$$

$$\text{Mass balance} = \frac{0.91 \text{ g}}{0.945 \text{ g}} \times 100$$

= 96%

3C.3. Results and discussion

3C.3.1. Catalyst evaluation

As discussed in previous Chapter 3, Section 3B, lignin depolymerization reactions were carried out using dealkaline lignin (2 $wt.$% solution H_2O:CH_3OH, 1:5 v/v= 30 mL), [C_3SO_3HMIM][HSO_4] BAIL (0.5 g), which gave yield of 78% THF soluble products at 120 ᵒC within 1 h. For easy recycling of catalyst, dealkaline lignin depolymerization studies were continued using I-BAIL as solid acid catalyst using lignin (2 $wt.$% solution H_2O:CH_3OH, 1:5 v/v= 30 mL), I-BAIL (0.5 g) at 200 ᵒC for 1 h. The auto-generated pressure was 3.2 MPa under these reaction conditions. The result obtained using I-BAIL catalyst for dealkaline lignin is shown in Figure 3C.2. I-BAIL catalyst gave 90% yield of THF soluble low molecular weight aromatic products with >96±5%

mass balance (Section 3C.2.8). Similarly, the catalytic result obtained with silica (Synthesized using similar processes as used for I-BAIL), showed only 3% THF soluble products, this result revealed that Brønsted acidity is required for $\equiv$C-O-C$\equiv$ bond cleavage. However, this result is similar to the result obtained without using catalyst (yield 4% of THF soluble products).
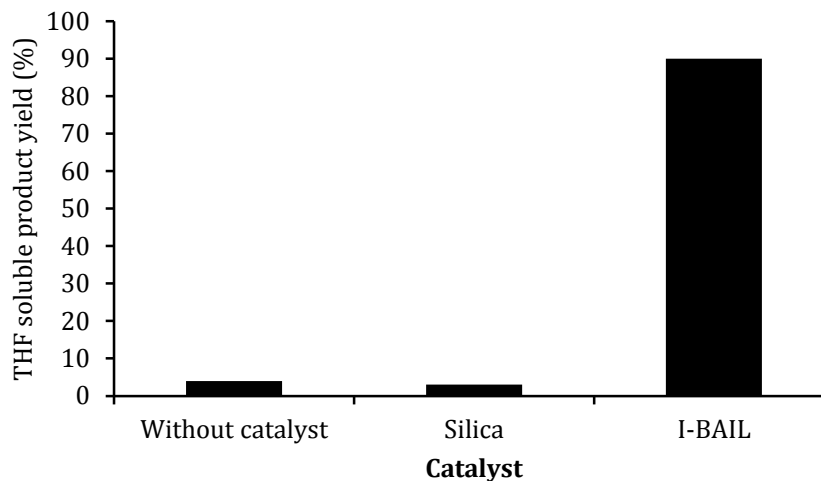
Figure 3C.2. Depolymerization of dealkaline lignin. Reaction conditions: lignin (2 *wt.*% solution, H_2O:CH_3OH, 1:5 *v/v*= 30 mL), catalyst (0.5 g), 200 ℃, 1 h, 1000 rpm.

Values are average of three reactions with ±2% error observed.

3C.3.2. Effect of temperature

As shown in the Chapter 3, Section 3B.3.4, [C_3SO_3HMIM][HSO_4] IL as catalyst was capable of depolymerising dealkaline lignin to yield 78% THF soluble low molecular weight aromatic products at 120 ℃ in 1 h. To improve the yield of THF soluble products, reactions were performed with I-BAIL at altered reaction temperature in the range between 120-250 ℃ (Figure 3C.3). Since in earlier reports lignin depolymerization reactions were carried out using solid acid catalyst at higher (≥250 ℃) temperature, it was decided to perform reactions at temperature ≥120 ℃, because in the previous Chapter 3, Section 3B.3.4, significant result (78% yield) was obtained at 120 ℃. It was found that as reaction temperature elevated from 120 ℃ to 200 ℃, the yield of THF soluble low molecular weight aromatic products enhanced from 5% to 90% Figure 3C.3. In the previous Chapter 3, Section 3B.3.4, lignin depolymerization studies were optimized at 120 ℃. It is because ILs form homogeneous phase with the reaction mixture, leading to better interaction of substrate with catalyst. In the current scenario, I-BAIL as solid acid catalyst formed different phase from the reaction mixture, which required higher energy for better interaction, so that I-BAIL as catalyst in lignin depolymerization reaction may be used at high temperature. According to Sabatier principle, if the reaction rate is high(er), then substrate and solid acid catalyst have maximum interaction energy, which is known as Sabatier's maximum.[11] The optimized temperature for the lignin depolymerization using I-BAIL as a catalyst is 200 ℃ to give 90% yield of THF soluble products. This catalytic result revealed

that I-BAIL as solid acid catalyst is highly active with increase in temperature may help to degrade maximum lignin contents into products. Further decrease in yield (due to char formation) was observed at higher temperature as 250 °C. However, I-BAIL is also unstable at temperature ≥250 °C, it undergoes degradation at higher temperature as shown in Chapter 2, Section 2B.3.2, Figure 2B.2. It was clearly emphasised that the formed product at higher temperature undergoes self-condensation or repolymerization reactions, which are known from the literature.[12]
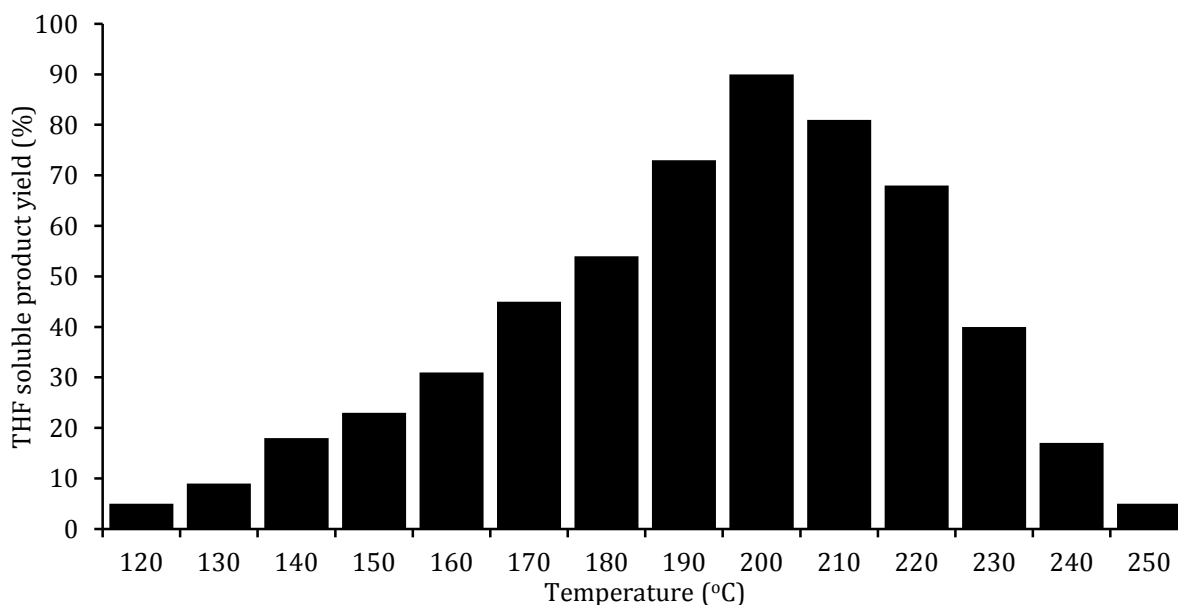
Figure 3C.3. Effect of temperature on depolymerization of dealkaline lignin. Reaction conditions: lignin (2 *wt.*% solution, $H_2O:CH_3OH$, 1:5 *v/v*= 30 mL), I-BAIL (0.5 g), 120-250 °C, 1 h, 1000 rpm.

Values are average of three reactions with ±2% error observed.

3C.3.3. Effect of time

After narrowing down the reaction parameters for lignin depolymerization with I-BAIL catalyst to gain maximum yield of THF soluble low molecular weight aromatic products at 200 °C using lignin (2 *wt.*% solution, $H_2O:CH_3OH$, 1:5 *v/v* =30 mL), all the further reactions were performed using the similar reaction conditions. To improve the products yield, typically reactions were done in the range between 15 to 120 min. It was observed from the Figure 3C.4 that, as the reaction time increased from 15 min to 60 min, THF soluble products yield also increased from 48% to 90% respectively. Further increase in reaction time (120 min) did not enhance in yield (91%) of THF soluble low molecular weight aromatic products, but the formation of char in reactor was seen in minor quantity.
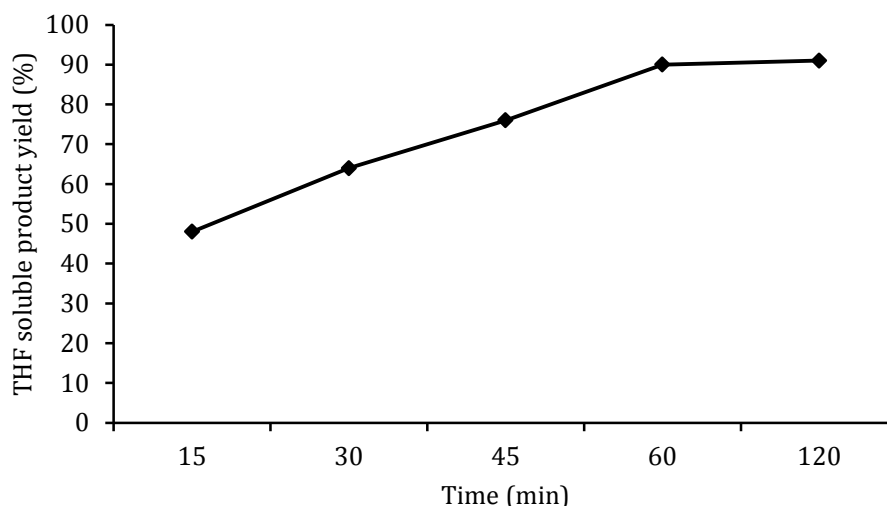
Figure 3C.4. Effect of time on depolymerization of dealkaline lignin. Reaction conditions: lignin (2 *wt*.% solution, H_2O:CH_3OH, 1:5 *v/v*= 30 mL), I-BAIL (0.5 g), 200 ^oC, 15-120 min, 1000 rpm. Values are average of three reactions with ±2% error observed.

3C.3.4. Effect of various substrates

As details description discussed in the Chapter 3, Section 3A.2, physico-chemical properties of various lignin samples varied due to presence of various functional groups, moieties (*S*, *G* and *H*), linkages, etc. in lignin. The depolymerization of lignin like industrial, alkali, alkaline and dealkaline lignin was carried out using I-BAIL as catalyst in water:methanol (1:5, *v/v*= 30 mL) solvent ratio at 200 ^oC in 1 h, auto-generated pressure (3.2 MPa) (Figure 3C.5). Depolymerization of dealkaline, industrial, alkaline and alkali lignin gave THF soluble low molecular weight aromatic products with 90%, 78%, 36% and 12% yields respectively. Among all the substrates, dealkaline lignin gave maximum yield (90%) of THF soluble products, while very low yield (12%) of THF soluble products was observed with alkali lignin. It may be possible due to that the depolymerized products converted into the char products, which were observed in major quantity after completion of the reaction in autoclave. THF soluble low molecular weight aromatic products were analysed by GC, GC-MS and HPLC, while depolymerization of dealkaline lignin generated the maximum aromatic monomers, it might be due to structural dissimilarity as observed in the physico-chemical properties of lignin (for more details descriptions please see the Chapter 3, Section 3A.2).
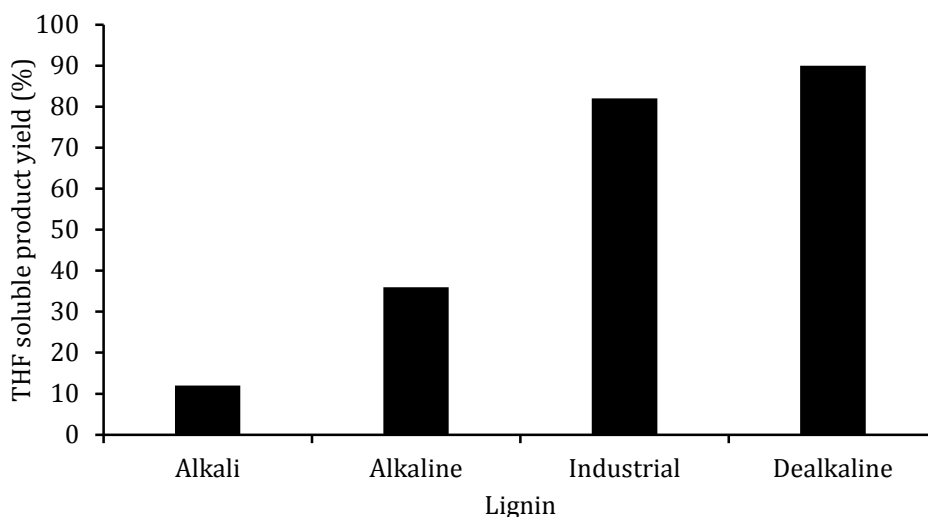
Figure 3C.5. Depolymerization of various substrates. Reaction conditions: lignin (2 *wt.*% solution, $H_2O:CH_3OH$, 1:5 *v/v* = 30 mL), I-BAIL (0.5 g), 200 °C, 1 h, 1000 rpm.

Values are average of three reactions with ±2% error observed.

Table 3C.1. Properties of various lignin samples.

Properties of lignin	Alkali	Alkaline	Industrial	Deakaline
Mol. *wt.* (Da) [*]	28,000	~60,000	-	~60,000
Solubility[‡] (%)	100	62	32	100
Na (mg/g)[#]	70	52	63	29
[*]for more details please see the section 3A.2.4, [‡]lignin (250 mg), suspended in solvent (water:methanol 1:5 *v/v* = 5 mL), at RT (27±2 °C), [#]calculated using ICP-OES methods.				

3C.3.5. Catalyst recycle

For reuse study of I-BAIL, after completion of the reaction, the catalyst was recovered from the reaction mixture by centrifugation (5000 rpm for 10 min) and then was filtered and washed with water:methanol (1:5 *v/v*) solvent. The recovered I-BAIL catalyst was dried in oven at 55 °C for 2 h and then transferred to vacuum oven at 90 °C for 2 h. The recycled catalyst was used for the further dealkaline lignin depolymerization reaction (Figure 3C.6). The yield declined after each run, it might be due to the sodium contamination (29 mg/g) present in dealkaline lignin (Chapter 3, Section 3A.3.2. and Tables 3A.3) which killed the active sites (H^+) of catalyst, leading to conversion of $-SO_3H$ into $–SO_3Na$ functional groups. The presence of Na on the recovered catalyst was proven by the ICP-OES analysis. Fresh I-BAIL catalyst does not have sodium element, while after first run catalyst contained 25.3 mg/g sodium and after 5th run sodium quantity was analysed to be 68 mg/g through ICP-OES analysis. After 5th run, 0.05 mmol H^+ acidic sites were available on the catalyst, which is insufficient to depolymerise lignin into low molecular weight aromatic products (Figure 3C.6). As observed from the ICP-OES analysis of the spent catalyst, after first run 0.55 mmol of H^+ ($-SO_3H$) acid site was poisoned by Na ($-SO_3Na$).

Nearly all the H$^+$ (-SO$_3$H) acid sites available within catalyst were converted into Na (-SO$_3$Na) group till 5th run (Table 3C.2), thus the lower catalytic activity was observed.
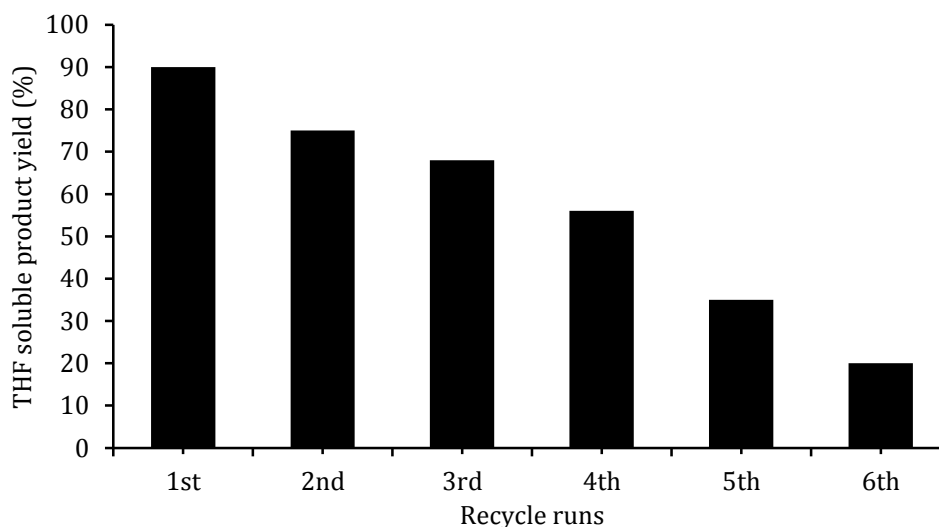
Figure 3C.6. Reuse study for depolymerization of dealkaline lignin. Reaction conditions: lignin (2 *wt*.% solution H$_2$O:CH$_3$OH, 1:5 *v/v*= 30 mL), I-BAIL (0.5 g), 200 °C, 1 h, 1000 rpm. Values are average of three reactions with ±2% error observed.

Table 3C.2. ICP-OES analysis for Na content (dealkaline lignin and spent catalyst) and H$^+$ (mmol) concentration on fresh and spent catalysts (based on theoretical calculation).

	Recycle run					
	Fresh	1st	2nd	3rd	4th	5th
Na content (mg/ 0.5 g) on catalyst	0	12.65	-	-	-	34
Na content (mmol) on lignin (0.5 g)	0.63	-	-	-	-	-
H$^+$ concentration (mmol) on catalyst (0.5 g)	1.39	0.84	-	-	-	0.05
H$^+$ concentration poisoned due to Na on catalyst (mmol)	0	0.55	-	-	-	1.34

3C.4. Correlation between lignin and products

As discussed, lignin (Chapter 3, Section 3A) and products (Chapter 3, Section 3B) characterization studies were done by various thermal/spectroscopic analytical techniques. Nonetheless, to perceive the changes transpiring in lignin structure and existence of several functional groups in both, lignin and product, on bulk and molecular level analysis were done using several analytical techniques like UV-Vis, FT-IR, 1D and 2D (HSQC) NMR, etc., which are in line as detailed discussed in the Chapter 3, Section 3B.6. However, the GC-MS chromatogram of THF soluble low molecular weight aromatic products obtained with dealkaline lignin depolymerization using [C$_3$SO$_3$HMIM][HSO$_4$] and I-BAIL catalysts are discussed as below Section 3C.4.1.

3C.4.1. Correlation between homogeneous [C$_3$SO$_3$HMIM][HSO$_4$] and heterogeneous (I-BAIL) catalytic activity

The activity of homogeneous [C$_3$SO$_3$HMIM][HSO$_4$] BAIL catalyst was compared with heterogeneous (I-BAIL) catalyst under similar reaction conditions, dealkaline lignin (2 *wt*.% solution H$_2$O:CH$_3$OH, 1:5 *v/v*= 30 mL), catalyst (0.5 g), except temperature 120 ₒC for [C$_3$SO$_3$HMIM][HSO$_4$] and 200 oC for (I-BAIL), 1 h, 1000 rpm. Yield of 78% and 90% THF soluble products were obtained with [C$_3$SO$_3$HMIM][HSO$_4$] and (I-BAIL) catalysts respectively. But the THF soluble products obtained with [C$_3$SO$_3$HMIM][HSO$_4$] catalysed reaction showed mostly low molecular weight aromatic products, which were confirmed by the GC-MS chromatograms (Figure 3C.7). Few products like *p*-cymene, *p*-cresol, guaiacol, vanillin, methyl vanillate, etc. corresponding to aromatic monomers peaks were observed in the THF soluble products obtain, when [C$_3$SO$_3$HMIM][HSO$_4$] catalyst was employed for dealkaline lignin depolymerization, while corresponding peaks of these aromatic monomers were absent in THF soluble products obtained with I-BAIL catalysed dealkaline lignin depolymerization reaction. So, it can be concluded that homogeneous [C$_3$SO$_3$HMIM][HSO$_4$] catalysed dealkaline lignin depolymerization gave aromatic monomers, while I-BAIL catalysed reaction gave mainly dimers and oligomers products, instead of forming aromatic monomers under the above reaction conditions. The homogeneous [C$_3$SO$_3$HMIM][HSO$_4$] catalyst gave more aromatic products than heterogeneous I-BAIL catalyst. It may be possible that, during the reaction better interaction (for more details descriptions please see the Chapter 5) of lignin with [C$_3$SO$_3$HMIM][HSO$_4$] catalyst is able to transform lignin into low molecular weight aromatic products. While I-BAIL catalyst formed the heterogeneous phase during the reaction so may be better interaction is not possible compared to [C$_3$SO$_3$HMIM][HSO$_4$] catalysed reaction, which gave dimers and oligomers in THF soluble products. Similarly, diffusion limitation can also be conquered by the homogeneous [C$_3$SO$_3$HMIM][HSO$_4$] BAIL catalyst with lignin depolymerization reaction, while it is very difficult with lignin and I-BAIL catalytic reaction, and so poor yield of aromatic monomers was obtained with I-BAIL catalyst.
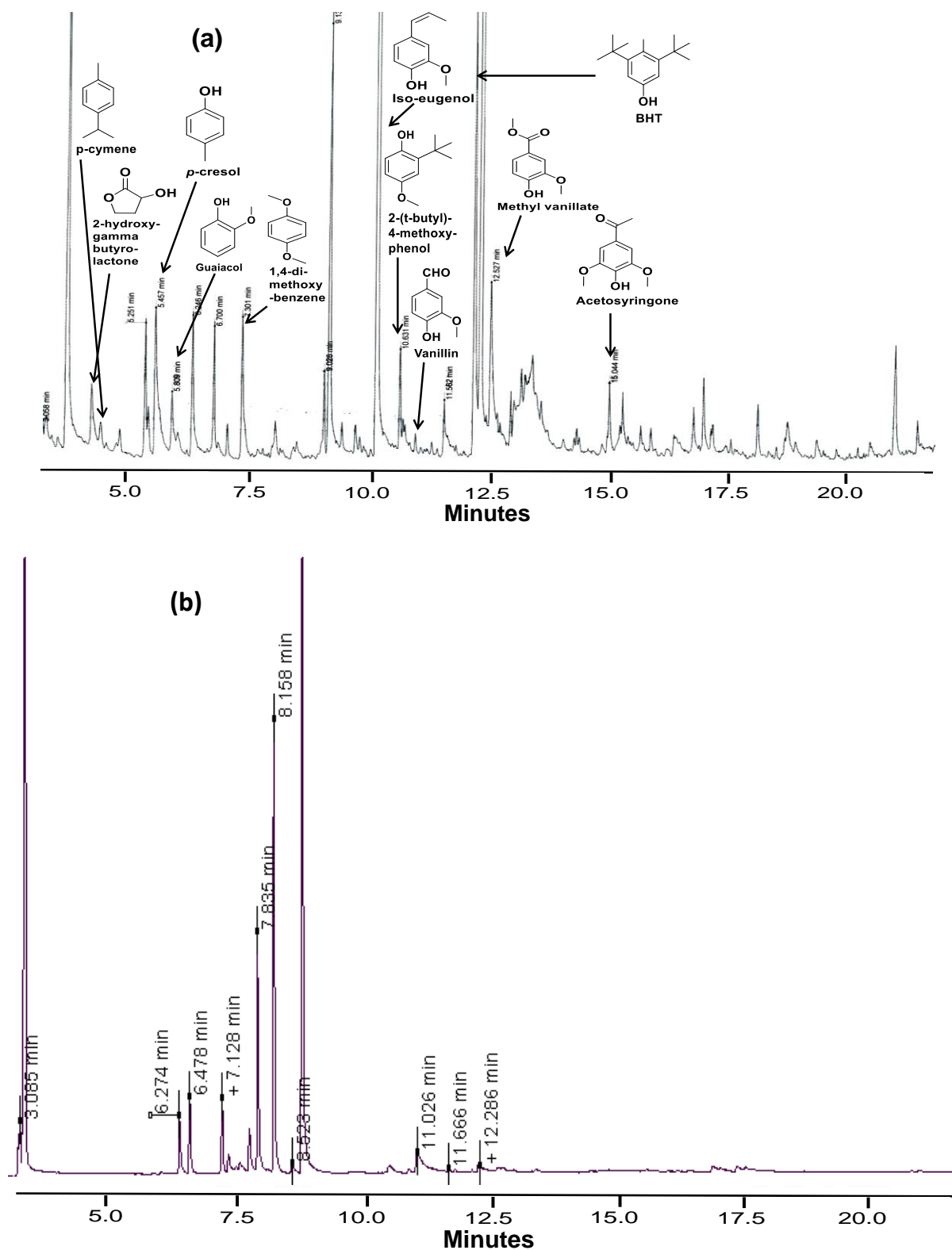
Figure 3C.7. GC-MS chromatograms of THF soluble products using (a) [C₃SO₃HMIM][HSO₄] and (b) I-BAIL catalysts. Reaction conditions: dealkaline lignin (2 *wt.*% solution $H_2O:CH_3OH$, 1:5 *v/v*= 30 mL), catalyst (0.5 g), 120 °C for [C₃SO₃HMIM][HSO₄] and 200 °C for (I-BAIL), 1 h, 1000 rpm.

3C.5. Conclusions

In summary, depolymerization of dealkaline lignin with I-BAIL catalyst was studied. The I-BAIL catalyst added the importance of ILs as solid acid catalyst which allowed the use of ILs in significant amounts and easy recyclability of catalyst. Various reaction parameters were applied to depolymerize lignin. It was observed that dealkaline lignin depolymerization was successfully achieved into THF soluble low molecular weight aromatic products yield (90%, with 96±5% mass balance) at 200 °C in 1 h. A significant comparison study was made between $[C_3SO_3HMIM][HSO_4]$ and I-BAIL catalysed lignin depolymerization reactions. The $[C_3SO_3HMIM][HSO_4]$ catalyst produced maximum aromatic products compared to I-BAIL catalyst, which was confirmed by the GC-MS chromatographs of THF soluble products. The recycled I-BAIL catalyst was contaminated by sodium, which was confirmed by the ICP-OES analysis. The sodium content was increased in each run till the presence of active Brønsted protons in I-BAIL.

3C.6. References

1.   N. Sun, R. Parthasarathi, A. M. Socha, J. Shi, S. Zhang, V. Stavila, K. L. Sale, B. A. Simmons and S. Singh, *Green Chem.*, 2014, **16**, 2546-2557.
2.   N. Sun, H. Rodriguez, M. Rahman and R. D. Rogers, *Chem. Commun.*, 2011, **47**, 1405-1421.
3.   J. Zakzeski, A. L. Jongerius and B. M. Weckhuysen, *Green Chem.*, 2010, **12**, 1225-1236.
4.   K. Stärk, N. Taccardi, A. Bösmann and P. Wasserscheid, *ChemSusChem*, 2010, **3**, 719-723.
5.   M. E. Zakrzewska, E. Bogel-Lukasik and R. Bogel-Lukasik, *Energy & Fuels*, 2010, **24**, 737-745.
6.   M. Nouri Sefat, D. Saberi and K. Niknam, *Catal Lett*, 2011, **141**, 1713-1720.
7.   Q. Zhang, J. Luo and Y. Wei, *Green Chem.*, 2010, **12**, 2246-2254.
8.   A. Chrobok, S. Baj, W. Pudło and A. Jarzębski, *Appl. Catal., A*, 2009, **366**, 22-28.
9.   A. K. Gupta, M. P. Singh, R. K. Singh and S. Chandra, *Dalton Transactions*, 2012, **41**, 6263-6271.
10.   C. P. Mehnert, R. A. Cook, N. C. Dispenziere and M. Afeworki, *J. Am. Chem. Soc.*, 2002, **124**, 12932-12933.
11.   R. A. van Santen and M. Neurock, in *Molecular Heterogeneous Catalysis*, Wiley-VCH Verlag GmbH & Co. KGaA, 2007, DOI: 10.1002/9783527610846.ch10, pp. 409-422.
12.   W. J. Connors, L. N. Johanson, K. V. Sarkanen and P. Winslow, *Journal*, 1980, **34**, 29-37.

Chapter 4:

Isolation of lignins from crop waste, their characterization and depolymerization using acidic ionic liquids

Section 4A:

Klason lignin

4A.1. Introduction

Until now, characterization and lignin depolymerization reactions (Details descriptions in Chapter 3, Sections 3A-3C) are discussed with the commercially procured lignin samples. These lignin samples are contaminated with sodium metal, which is confirmed by the ICP-OES and XRD studies. As mentioned in the Chapter 1, lignocellulosic biomass is mainly composed of polysaccharides and lignin units. The polysaccharide (cellulose and hemicellulose) contents present in the lignocellulosic biomass are collectively known as holocellulose.[1] It is further classified into α-, β- and γ-cellulose (for more details descriptions see the T-203 cm-99 process).[2] Pre-treatment is a preliminary step in the bio-refinery concept, wherein separation of cellulose, hemicellulose and lignin units is carried out. However, during the isolation process their structural units are altered. Though, in case of cellulose and hemicelluloses major changes in their structures occurred in terms of alteration in their degree of polymerization but in lignin, concentrations of *p*-coumaryl alcohols (*H)*, coniferyl alcohols (*G)* and sinapyl alcohols (*S)*, elemental composition (C, H and O), linkages and molecular weights are varied. Considering this, lignin isolation processes (Kraft, soda, lignosulphate, hydrolysis, enzymatic, ionic liquids processes, etc.)[3-8] and their effects on the composition of lignin are briefly described in the Chapter 1, Section 1.6. With most of these processes, metals (Na, Mg, Ca, etc.) impurity, use of high cost of solvents (ionic liquids economically not favourable), longer time (enzyme took several weeks to complete the process), use of high temperature etc. are few drawback associated. However, it is a need to develop, metal free, highly efficient, cheap, safe and environmentally benign process to isolate lignin from crop waste. Looking at the above concerns, Klason method (using acidic hydrolysis) was chosen because it is one of the methods which allows isolation of lignin from crop waste samples in pure form.

The approximate quantity of the crop waste production per annum in India and in world is consolidated in the Table 4A.1.

Table 4A.1. India and world scenario of crop waste production.[9]

Source	Region/ country	2010 (MMT)	2011 (MMT)	2012 (MMT)	2013 (MMT)	2014 (MMT)
Rice husk (RH)	India	1.4×10^8	1.6×10^8	1.6×10^8	1.6×10^8	1.6×10^8
	World	7.0×10^8	7.2×10^8	7.4×10^8	7.4×10^8	7.4×10^8
India/World ratio (%)		20	22.2	21.6	21.6	21.6
Bagasse (BG)	India	8.0×10^7	8.7×10^7	9.4×10^7	9.3×10^7	9.4×10^7
	World	6.5×10^8	7.0×10^8	6.9×10^8	7.2×10^8	7.3×10^8
India/World ratio (%)		12.3	12.4	13.6	12.9	12.9
Wheat straw (WS)	India	2.9×10^8	3.4×10^8	3.5×10^8	3.4×10^8	3.5×10^8
	World	1.7×10^9	1.8×10^9	1.9×10^9	1.9×10^9	1.9×10^9
India/World ratio (%)		17.1	18.9	18.4	17.9	18.4

Considering this abundant availability of crop wastes (RHs, BGs and WS) that India generates per annum, which typically consists of cellulose, hemicellulose and lignin constituents, it can be used to synthesize chemicals and mainly production of aromatic monomers from the isolated Klason lignin.

In the current Chapter, work is reported on the isolation of Klason lignin (acid soluble and insoluble lignin) and the complete quantification of α-, β- and γ-cellulose, inorganic nutrients, etc. in these crop wastes. To quantify each component within crop waste samples, Technical Association of the Pulp and Paper Industry (TAPPI) method is followed. Further, the details on the physico-chemical analysis of isolated Klason lignin from the various crop waste samples have been discussed. The depolymerization of isolated lignin into low molecular weight aromatic products is also discussed in Section 4A.

4A.2. Experimental

4A.2.1. Materials

The various crop waste samples were collected from different states of India; rice husk (RH I) from Karnataka; bagasse (BG I) from Maharashtra; RH II, bagasse (BG II) and wheat straw (WS) from Uttar Pradesh and RH III were collected from Odisha. Before use, the crop waste sample was sieved to get ca. 45 μm size. Sulphuric acid (Loba Chemie, India, 98%), methanol (Loba Chemie, India, 99.80%), isopropyl alcohol (Loba Chemie India, >99.50%), hydrofluoric acid (Loba Chemie India, 40.0%), hydrochloric acid (Loba Chemie India, 35.50%), nitric acid (Loba Chemie India, 69.0-72.0%), sodium chlorite (Thomas Baker India, 80.0%), glacial acetic acid (Thomas Baker India, 99.8%), NaOH (Loba Chemie India, 98.0%), potassium dichromate (Loba Chemie India, 99.50%), ferroin solution (Loba Chemie India, AR 0.025 M), ferrous ammonium sulphate hydrate (FAS, Loba Chemie India, 98.50%,) were purchased and used without any further purification.

4A.2.2. Characterization of samples

Since it has been recognized that the properties of lignins are dependent on the type/age of plant and isolations procedures, it was obligatory to investigate those and therefore, isolated Klason lignin samples were systematically characterized by thermal/spectroscopic techniques (XRD, SEM-EDX, TGA, elemental analysis, UV-Vis, ATR, ^{13}C CP-MAS NMR etc. For details description on instruments and methods of sample preparation, please see Chapter 3, Section 3A.

4A.3. Compositional analysis of crop waste

4A.3.1. Analysis of moisture content

Crop waste sample was weighed (ca. 1.0 g) and was allowed to dry at 100 ^{o}C for 4 h in oven. The moisture content in the crop waste sample was calculated by difference in weight of the sample before and after drying using the following equation 4A.1.

$$\Delta W = Wx - Wy \qquad \qquad (4A.1)$$

Where,

ΔW= Difference in weight

W_x= Weight of sample before drying and

W_y= Weight of sample after drying

4A.3.2. Quantification of ash content

Oven dried crop waste samples were exposed to calcination in the presence of air from room temperature (27±2 ^{o}C) to 620 ^{o}C using 10 ^{o}C/min ramping rate (4 h holding time) to determine the amount of ash (Table 4A.2). It was clear from the Table 4A.2, that rice husk (RH) samples contained the maximum inorganic residue compared to bagasse (BG) and wheat straw (WS). At the higher temperature, >620 ^{o}C polysaccharides (cellulose, hemicellulose) and lignin are degraded as CO, CO_2, CH_4 etc. which confirmed from TPO-MS studies (Details descriptions, Chapter 3, Section 3A.2.7). The remaining part is ash which consists of silica and other inorganic nutrients. The obtained solid was weighed to calculate the exact amount of ash present in known quantity of sample by the difference in the weight of the sample before and after calcination using following equation 4A.2,

$$\Delta W = Wx - Wy \qquad \qquad (4A.2)$$

Where,

ΔW= Difference in the weight (inorganic residue) of sample,

W_x= Weight of sample before calcination and

W_y= Weight of sample after calcination

Muffle furnace programme for ash analysis (air)

Room temperature → (10 °C/min) → 620 °C (4 h, hold time) → cooling to room temperature.

4A.3.3. Isolation of Klason lignin from crop waste samples

Isolation of Klason (acid soluble and acid insoluble) lignins from crop waste such as rice husk (RH I, II and III), bagasse (BG I and II) and wheat straw (WS) samples was carried out using reported method with minor modifications.[10-12] To achieve complete saccharification of the crop waste sample, 72% *wt./wt.* H_2SO_4 (12±0.02 M) was chosen because in a reported process when it is carried out with <72% *wt./wt.* H_2SO_4 solution, complete polysaccharides extraction is not possible. The use of >72% *wt./wt.* H_2SO_4 solution poses a problem of transformation of C6 and C5 polysaccharides into insoluble products.

4A.3.3.1. Analysis of insoluble Klason lignin

In a typical procedure, 1.0 g oven dried crop waste sample was taken in a 100 mL beaker and to it added 15 mL 72 % *wt./wt.* (12±0.02 M) H_2SO_4 solution, while stirring for 2 h. The addition was done under maintained temperature of 20 to 25 °C by adding ice into the water bath (concentrated H_2SO_4 reacts with crop waste sample exothermically). The colour of the mixture changes (brown colour samples changed into dark golden), and the crop waste sample swells. The polysaccharides hydrolysis is achieved at desired concentration of (12±0.02 M) H_2SO_4. Further, the digested samples with H_2SO_4 (72.0% *wt./wt.* sulphuric acid) were washed thoroughly with 600 mL hot water (80±5 °C) and washed solution was transferred into 1000 mL RB (current sulphuric acid= 3% *wt./wt.*).The washed solution was placed in preheated oil bath for 4 h, at this reaction condition the remaining (unhydrolyzed) polysaccharides were completely hydrolysed. Consequently, the RB with resultant solution was kept at 50 °C for 12 h for settling down the precipitated Klason lignin. Filtered the resultant mixture using G2 crucible and washed the residue with 200 mL hot water (80±5 °C, known quantity) to remove the polysaccharides and sulphuric acid contamination from acid insoluble Klason lignin. The filtrate solutions were kept for quantification of acid soluble lignin (UV-Vis spectroscopy). Dried the filtrate sample with G2 crucible, firstly at room temperature (30±2 °C) for 6 h, later in the oven at 60±2 °C for 6 h, then transferred the oven dried sample in vacuum oven (-0.101 MPa) at 100±2 °C for 2 h. The 22.6±3 *wt.*% acid insoluble and soluble (Table 4A.3) Klason lignins were isolated from crop waste samples with 95±3% mass balance. The obtained solid mass (Klason lignin) was known as uncorrected lignin. Subsequently, the accurately weighed uncorrected lignin was subjected for calcination at 620 °C for 4 h in presence of air, for ash correction (as defined in Section 4A.3.2). For more details on compositional (holocellulose, pentosan, silica content, nutrients) analysis of the crop waste samples are discussed in the following sections and the percentage of the chemical constituents are consolidated in the Table 4B.2. All the extraction processes were accomplished three times to duplicate the results.

Table 4A.2. Summary on the composition of crop wastes (rice husk, bagasse and wheat straw).*

Component (%)	RH I	RH II	RH III	BG I	BG II	WS
Lignin (acid soluble + acid insoluble)	23.9	22.3	21.5	20.0	20.6	18.1
Pentosan	15.4	12. 4	11.7	20.1	20.1	16.9
Holocellulose (α-+β-+γ- cellulose)	61.0	52.9	52.2	70.1	68.0	62.9
α-cellulose	37.3	34.7	28.2	40.7	38.8	36.2
β-cellulose	9.5	6.1	11.3	14.3	15.3	16.8
γ-cellulose	13.2	11.8	17.3	13.9	12.9	8.8
Ignition residues (SiO_2 + nutrients)	15.8	16.5	17.3	3.1	3.0	16.6
SiO_2	10.0	14.1	9.8	1.7	1.6	9.2

*Determined by Technical Association of the Pulp and Paper Industry (TAPPI) method

4A.3.3.2. Analysis of acid soluble Klason lignin

The amount of acid soluble lignin was quantified with the help of UV-Vis absorption spectroscopy at 278 nm by using the following equation (4A.3) (Figure 4A.1);[13]

$$\text{Acid soluble lignin (\%)} = \frac{DV\,(As - Ab)}{a \times w} \times 100 \qquad (4A.3)$$

Where,

D-dilution ratio; V- filtrate volume (in litre); As- absorbance of sample; Ab- absorbance of solvent (blank solution), a- molar absorptivity of the soluble lignin, w- oven dried weight of crop waste sample (g).

The molar absorptivity of the soluble lignin was used 23.3 at 278 nm (for softwood lignin).[13]

Table 4A.3. Quantification of Klason lignin (acid insoluble and soluble lignin).

Sr. no.	Crop waste	Acid insoluble lignin (%)	Acid soluble lignin (%), at 278 nm	Total (Acid soluble and insoluble lignin) (%)
1	RH I	22.6	1.3	23.9
2	RH II	21.7	0.8	22.5
3	RH III	20.2	1.1	21.3
4	BG I	20.1	0.9	20.0
5	BG II	19.3	1.3	20.6
6	WS	16.5	1.6	18.1
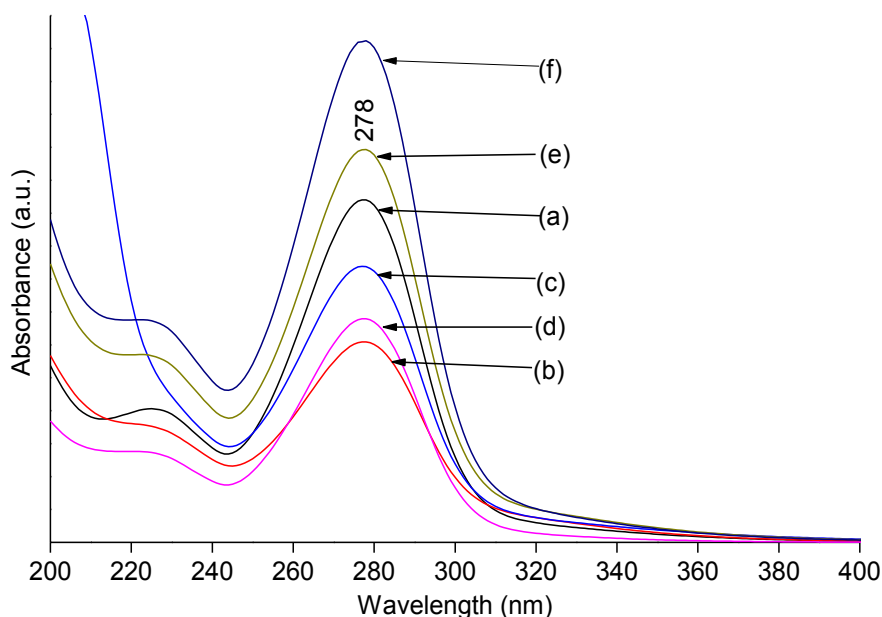
Figure 4A.1. UV-Vis spectra of acid soluble Klason lignins derived from (a) RH I, (b) RH II, (c) RH III, (d) BG I, (e) BG II and (f) WS crop waste samples.

Overall procedure for the Klason lignin determination can be depicted as Scheme 4A.1.
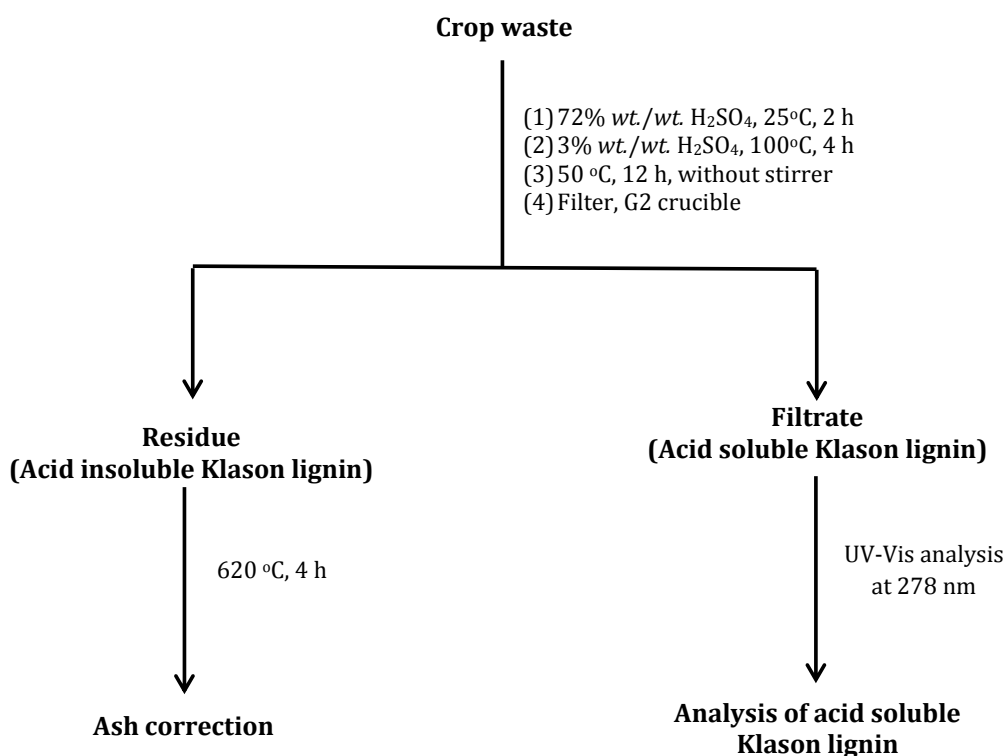
Scheme 4A.1. Flowchart for the Klason lignin analysis of crop waste.

The total lignin contents present in the crop waste samples can be estimated by the TAPPI methods, which is the main objective of Klason lignin (Acid soluble and insoluble lignin) analysis. This analysis provides the importance of acid soluble lignin for the analysis of accurate lignin present in the samples. As shown in the Table 4A.3, that acid insoluble lignin contents is

much higher than the acid soluble, which is in line with the available report for acid soluble Klason lignin.[14]

4A.3.4. Quantification of polysaccharides (holocellulose; mixture of cellulose and hemicellulose)

Generally, holocellulose is called as mixture of cellulose and hemicellulose (polysaccharides) in the lignocellulosic biomass. The lignin removal process of the crop waste samples was carried out to get holocellulose (as white powder). Basically, holocellulose is the building block of three types of polymers such as α-, β- and γ- cellulose. After removal of lignin, the α-, β- and γ-cellulose compositional analysis of the crop waste samples was done by using T-203 cm-99 method.[2] So the crop waste samples were processed to remove lignin before being subjected to the analysis of holocellulose.

4A.3.4.1. Analysis of holocellulose

Distilled water 160 mL was taken in 250 mL conical flask and to this 1.5 g crop waste sample was suspended. The mouth of the conical flask was capped with glass lid. The conical flask containing reaction mixture was warmed up to 70±2 °C for 1 h in a preheated oil bath. While heating, 1.5 g sodium chlorite ($NaClO_2$) and 1.0 mL glacial acetic acid were added 3 to 4 times (with the gap of 15 min) under constant stirring (600 rpm), during the addition of the $NaClO_2$ and acetic acid, stirring was kept at 100 rpm. During this procedure, colour of the resultant mixture was changed from brown to light golden. After completion of reaction, the resultant mixture was allowed to cool at room temperature and then filtration was done using G2-sintered glass crucible (pore size 15-40 μm). In this process, lignin was obtained in soluble form and lignin free solid pulp was gained, which is called as holocellulose (white colour). Further the filtrate was washed with 100 mL preheated hot water 70±2 °C, followed by washing with 150 mL acetone (to remove lignin contaminant from holocellulose). Then filtrate was first dried at room temperature (27±2 °C, for 6 h), after that dried in oven at (50±2 °C for 2 h), then transferred into vacuum (-0.101 MPa) oven 105±2 °C for 2 h for removing solvent contamination. Presence of lignin content was considered after subtracting the weight of dried holocellulose from the weight of dried crop waste sample. The obtained holocellulose consisted of inorganic ash, consequently considering the weight of actual holocellulose, the weight of ash correction had to be subtracted (ash modification).

4A.3.4.2. Quantification of α-, β- and γ-cellulose

The determination of α-, β- and γ- cellulose contents from the crop waste samples was done using the well-known Technical Association of Pulp and Paper Industry (TAPPI) T-203 cm-99 method.[2] The quantity of α- cellulose was measured by subtracting the quantity of β- and γ-cellulose and inorganic ash from the holocellulose. The β- and γ- cellulose in the holocellulose sample derived from crop waste were measured by treating with 17.50 *wt.*% diluted solution of

NaOH at 25±2 °C. The β- and γ- cellulose contents are soluble in NaOH solution, though α-cellulose comes out as precipitate form. The quantification of β- and γ- cellulose were achieved through the oxidation *via* potassium dichromate ($K_2Cr_2O_7$) after that volumetric titration using freshly prepared ferrous ammonium sulphate (FAS) solution in the presence of ferroin indicator. The α- cellulose contains high molecular weight of cellulose (mainly insoluble in diluted NaOH solution), whereas β- and γ- cellulose contains low molecular weight of cellulose. The β-cellulose was completely soluble in the diluted NaOH solution and can be precipitated out by acidification. The γ- cellulose is soluble in both diluted NaOH and acidified mixture.

To calculate the percentage of α-, β- and γ- cellulose, lignin free pulp (holocellulose) of crop waste sample were allowed to be dried first in oven at 60±2 °C for 12 h. Precisely weighed dry pulp (holocellulose) was taken (3.0 g) in 500 mL conical flask and 200 mL of dilute NaOH (17.50 *wt.*%) solution was added to this and obtained suspension was stirred (600 rpm) to achieve finely dispersed reaction mixture. Formerly after 30 min (after addition of 17.50 *wt.*% NaOH solution), 200 mL distilled water was mixed and further suspension was stirred at 600 rpm for extra 30 min (the total stirring time was completed for 1 h after mixing of 17.50 *wt.*% NaOH solution). While addition and stirring, temperature was maintained at 25±2 ℃. The reaction mixture was filtered through G2-sintered glass crucible and filtrate was collected for further analysis [first 20 mL filtrate was thrown (avoid contamination) and remaining solution was used for further quantification of β- and γ- cellulose]. The filtrate (F1) solution contains β- and γ- cellulose although suspension solid residue consists of α- cellulose and inorganic ash, hence accurate weight of α- cellulose was considered by difference in weight of inorganic ash from solid residue (Contained α- cellulose and inorganic ash).

4A.3.4.3. Quantification of α- cellulose

The filtrate solution 25 mL (F1) was taken in conical flask (250 mL), to this 25 mL aqueous solution of $K_2Cr_2O_7$ (0.5 N) was mixed slowly and carefully. Then 50 mL concentrated H_2SO_4 was added with caution and the resultant solution was kept as such in open hood for 15 min. Afterwards, 50 mL distilled water at 27±2 °C was mixed and the resultant solution was shaken slowly and was allowed to cool by keeping the conical flask under running tap water for 10-15 min till the resultant solution attained (27±2 °C), further ferroin as a basic indicator (5-6 drops) was added into this solution. Then, the cold solution was titrated with freshly prepared 0.1 N ferrous ammonium sulphate (FAS) solution. The β- and γ- cellulose were oxidized by $K_2Cr_2O_7$ and further quantified by the volumetric titration with FAS (the purple colour was appeared at the end point). The volume of FAS used in the titration was noted (V_1). The blank titration was also completed subsequently by the same process but without the pulp filtrate solution (F1), 12.50 mL NaOH (17.50 *wt.*%), 12.50 mL distilled water + 25 mL $K_2Cr_2O_7$ (0.5 N) and 75.0 mL of concentrated H_2SO_4 was taken and the resulting mixture was allowed to cool at 27.0± 2 °C under

running tap water and further into this added 75.0 mL distilled water then 5-6 drops of ferroin indicator was added and the final volume was titrated with 0.1 N ferrous ammonium sulphate (FAS) solution. The consumed volume for blank titration was also noted as (V_2). The quantification of the β- + γ- cellulose can be obtained by following equation 4B.4;

$$[\beta - \text{cellulose (\%)} + \gamma - \text{cellulose (\%)}] = \left[\frac{6.85(V2 - V1) \times N \times 20}{A \times W}\right] \quad (4A.4)$$

Where:

V_1 and V_2= Consumed volume of FAS for the sample titration (mL) and blank titration (mL)

N= Normality of freshly prepared FAS solution

A= Volume of pulp filtrate (F1) was taken (mL)

W= Weight of (ash corrected) sample was taken (g)

Percentage of α- cellulose was found out by the difference of β- + γ- cellulose (%) from 100 using equations 4A.5-4A.6.

$$\alpha - \text{cellulose (\%)} = 100 - \left[\frac{6.85 \ (V2 - V1) \times N \times 20}{A \times W}\right] \quad (4A.5)$$

or

$$\alpha - \text{cellulose (\%)} = [100 - [\beta - \text{cellulose (\%)} + \gamma - \text{cellulose (\%)}] \quad (4A.6)$$

4A.3.4.4. Quantification of γ- cellulose

The obtained 50 mL pulp filtrate solution (F1) was filled into measuring flask with stopper and into this diluted 50 mL H_2SO_4 (3.0 N) was mixed carefully. The final 100 mL resulting solution was mixed appropriately *via* thorough inverting and shaking the measuring flask. The solution was warmed up to 80-90 ℃ for 15-20 min by simply keeping the measuring flask in to the preheated water bath (this allows to form suspension of β-cellulose). The obtained white colour suspension was allowed to keep without disturbance at 27±2 ℃ for 16 h. The formed suspension was allowed to filter using G2-sintered glass crucible and filtrate (F2) was obtained (mainly consisting β- cellulose). It was tested with $K_2Cr_2O_7$ and titrated with FAS (0.1 N) solution. For the same titration, 50 mL of filtrate solution (F2) obtained after β- cellulose extraction was taken into 250 mL conical flask and concentrated H_2SO_4 (90 mL) was mixed gently with caution. The resulting solution was kept for 15 min and further allowed to cool at 27±2 ℃ under the running tap water. 5-6 drops of ferroin indicator was added to this (room temperature, 27±2 ℃) solution and then the solution was titrated against freshly prepared FAS (0.1 N) solution. The end point was noted at the appearance of purple colour (the consumed volume of FAS solution was noted as V_3). The blank titration was done by replacing filtrate (F2) with 12.50 mL NaOH (17.50 *wt.*%), 12.50 mL distilled water and 25 mL H_2SO_4 (3 N). In this solution, concentrated H_2SO_4 (90 mL) was added gently caution. The resulting solution was kept for 15 min without disturbance and then further allowed to cool at room temperature 27±2 ℃

under the running tap water. To this, 5-6 mL ferroin indicator was added and then titrated against freshly prepared FAS solution (0.1 N). The end point was recorded by the appearance of purple colour (V_4) of the solution. The γ-cellulose (%) was measured using equation 4A.5.

4A.3.4.5. Quantification of β- cellulose

Overall the quantification of β- cellulose was done by the subtraction of α- and γ- cellulose quantity from 100 (equation 4A.7). Similarly, the percentage of holocellulose (containing α-, β- and γ- cellulose) were quantified for all crop waste like rice husk (RH I, II and III), bagasse (BG I and II) and wheat straw (WS) samples. The percentage of the compositions in the crop waste samples is consolidated in Table 4A.2.

$$β − cellulose\ (\%) = 100 − (α − cellulose\ (\%) +\ γ − cellulose) \tag{4A.7}$$

4A.3.5. Quantification of pentosan (C5 polysaccharide)

The quantity of pentosan tells the approximate amount of hemicellulose (copolymer of C5 and C6 polysaccharides) present in the rice husks, bagasse and wheat straw crop waste samples. For pentosan quantification, 5.0 g oven dried crop waste samples and 300 mL of HCl (13.50 M) were taken into 500 mL RB flask combined with distillation assembly as shown in Figure 4A.2.

Initially, the above resulting mixture was heated at 100 ℃, and the distillate sample was collected in the attached conical flask (ca. 250 mL distillate sample was collected) with distillate assembly. Through distillation, pentosan was projected to collect along with solvent in distillate form. Through the distillation process the volume of the above made mixture was maintained up to 300 mL (primarily volume) by adding HCl (13.50 M) solution dropwise. Distillate solution (contained mainly pentosan) was diluted with known quantity of water and further used for UV-Vis spectroscopy (absorption λmax at 280 nm) to calculate the percentage of pentosan present in the crop waste samples. The pentosan percentages present in the crop waste samples were calculated using following equation 4A.8;

$$Pentosan\ (\%) = \frac{absorbance\ (280\ nm)\ \times 1.563}{151 \times dried\ weight\ of\ crop\ waste} \times 100 \tag{4A.8}$$

The accurate weight of crop waste samples were deliberated after removing the percentages of the moisture and inorganic/ash impurity.

According to the earlier reports, rice husk, bagasse and wheat straw samples comprises 13.17±3% of pentosan.[15] In the line, composition of the particular crop waste samples may vary from various factors as it is discussed in the Chapter 3, Section 3A.
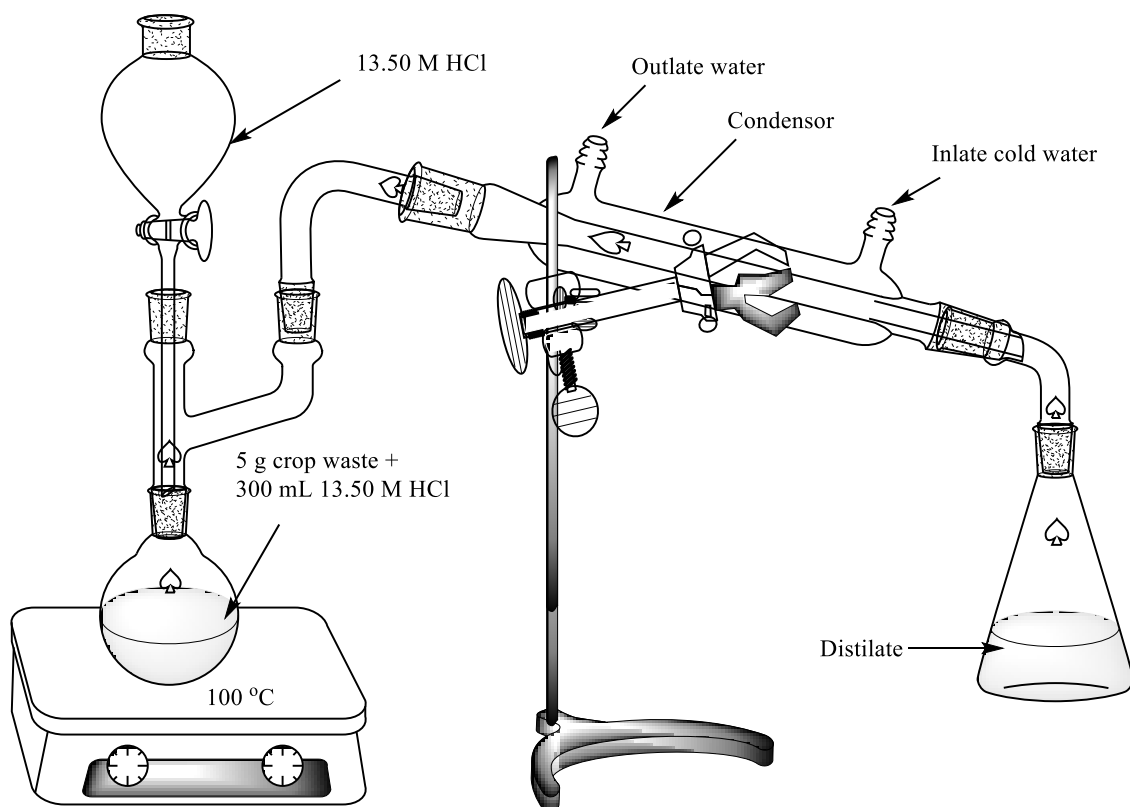
Figure 4A.2. Experimental set-up for the quantification of pentosan in the crop waste samples.

4A.3.6. Quantification of silica content in the crop waste samples

Oven dried 0.05 g ash sample was subjected into 50 mL polypropylene bottle, into this, addition of HF tilled soaked (ca. 400 ± 100 μL), and the resulting mixture was heated at 80 °C (using hot plate) to remove the excess HF (repeat 2 times to remove the complete silica content from the ash sample), to remove the silica content because the silica reacts with HF to form hexafluorosilicic acid (H_2SiF_6). The HF treatment was done in the hood with proper precaution. The HF reaction with silica can be signified as in equation 4A.8. The silica quantity was calculated by the difference in weight loss of silica before and after HF treatment by using following equation 4A.9,

$$SiO_2 + 6HF \rightarrow H_2SiF_6 (\uparrow) + 2H_2O \tag{4A.8}$$

$$\Delta W = Wx - Wy \tag{4A.9}$$

Where,

ΔW= Difference in weight of silica content present the inorganic residues,

W_x= Weight of dried ash sample before addition of HF and

W_y= Weight of dried ash sample after addition of HF

4A.3.7. Quantification of nutrients contents in crop waste samples

To quantify the different nutrients contents, sample ca. 2.0 g weighed (±0.001 g), dried (in oven for overnight at 60 °C and further vacuum (-0.101 MPa) oven drying for 6 h at 80 °C) and were

exposed to calcination for 2 h at 620 °C in presence of air. Inorganic residue ca. 0.2 g was treated with HF, to remove the silica content because silica reacts with HF to form hexafluorosilicic acid (H_2SiF_6), the HF reaction with silica can be signified as equation 4A.8.

This process was repeated till complete silica removal, remaining part of inorganic residue (ash) was dissolved in freshly prepared aqua regia (HNO_3:HCl, 1:3 *v/v*) and into this solution deionized water was added. The resulting solution was filtered through 0.22 μm, nylon syringe filter. Finally, the resulting solution was analysed using ICP-OES to obtain the nutrients content in the crop waste. From ICP-OES result, it was analysed that samples contained variable amount of many nutrients as consolidated in Table 4A.4. It was effective to determine the nutrients contents present within the crop waste samples because these metals may affect activity of the acidic/basic catalysts during the reactions and can alter the catalytic activity or active sites of catalysts. To confirm the reproducibility, all the experiments were repeated 3 times and the error in the results is ca. 2% (based on the actual value) and the obtained result is well matched with the literature result.[15]

Table 4A.4. Various nutrients contents present in crop waste.

Crop wastes	Macronutrients (mmol/g)[†]			Micronutrients (mmol/g)[†]		
	Mg	K	Ca	Na	Mn	Fe
Blank solution[≠]	-	-	-	-	-	-
RH I	0.99	0.56	0.09	0.02	0.02	0.03
RH II	0.15	1.02	0.05	0.04	0.02	0.02
RH III	0.86	0.38	0.21	0.11	0.01	0.01
BG I	0.43	1.20	0.28	0.32	0.01	0.06
BG II	0.55	0.37	0.16	0.90	0.01	0.25
WS	0.23	0.12	0.08	0.80	0.01	0.02
[†]Determined by ICP-OES (mmol of element in 1.0 g of crop waste), [≠]10 mL (3 mL aqua regia and 7 mL millipore water).						

Overall procedure for the complete compositional analysis of crop waste determination can be depicted as below in Scheme 4A.2.
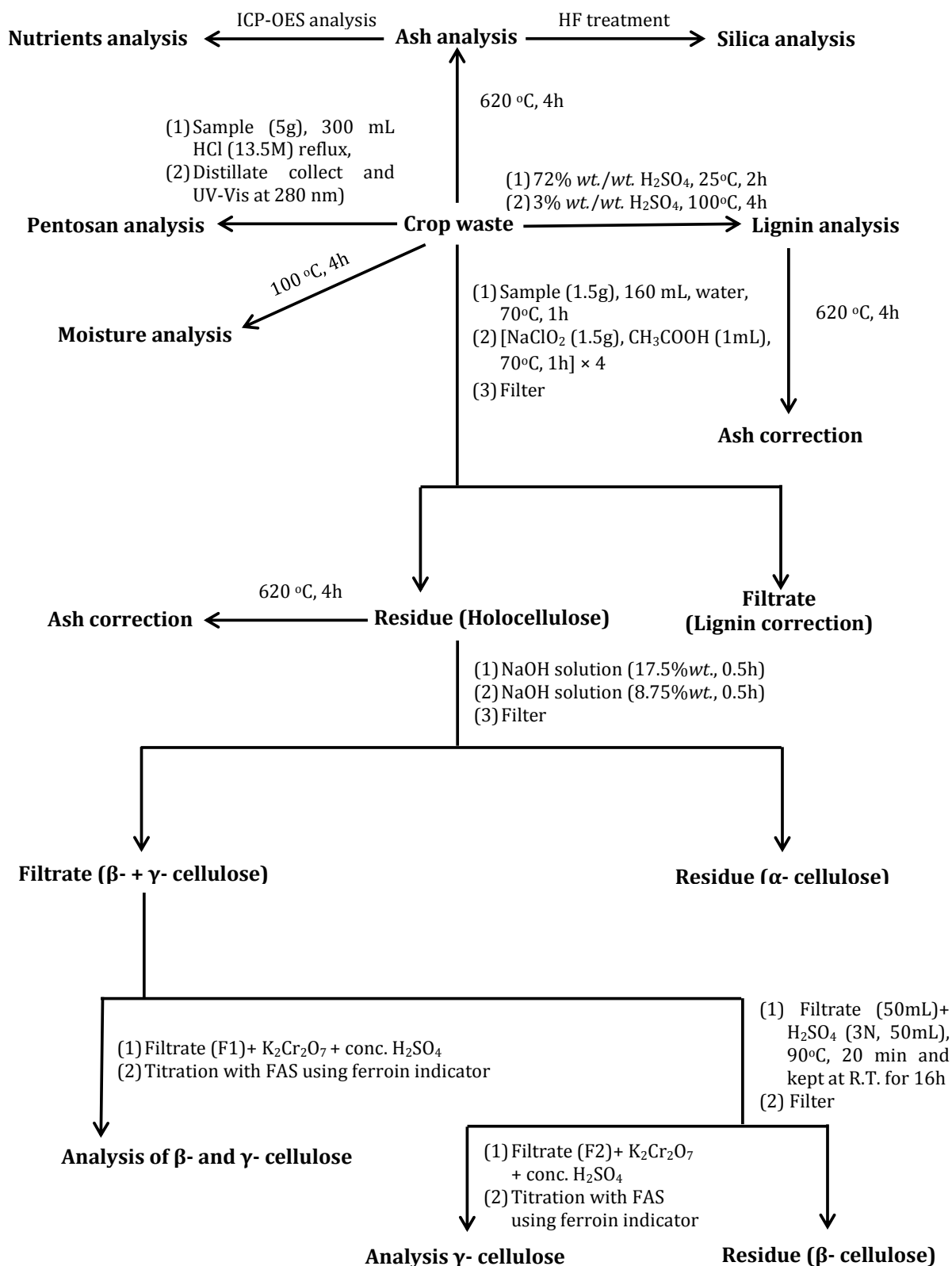
Scheme 4A.2. Flowchart for the complete compositional analysis of crop waste.

4A.4. Results and discussion

4A.4.1. Klason lignin characterization

4A.4.1.1. X-ray diffraction pattern

To understand the phase identification of the crop waste and isolated Klason lignin samples, the XRD analysis are carried out and shown in Figure 4A.3. The XRD pattern are recorded in 2θ range varying from 5 to 40° (scan rate 4°/min) for Klason lignin and crop waste samples. In the crop waste samples, the crystalline cellulose peak is observed at 22.19^o. Additionally, another two peaks at 15.26 and 17.08^o are also observed in the crop waste samples for the amorphous cellulose.
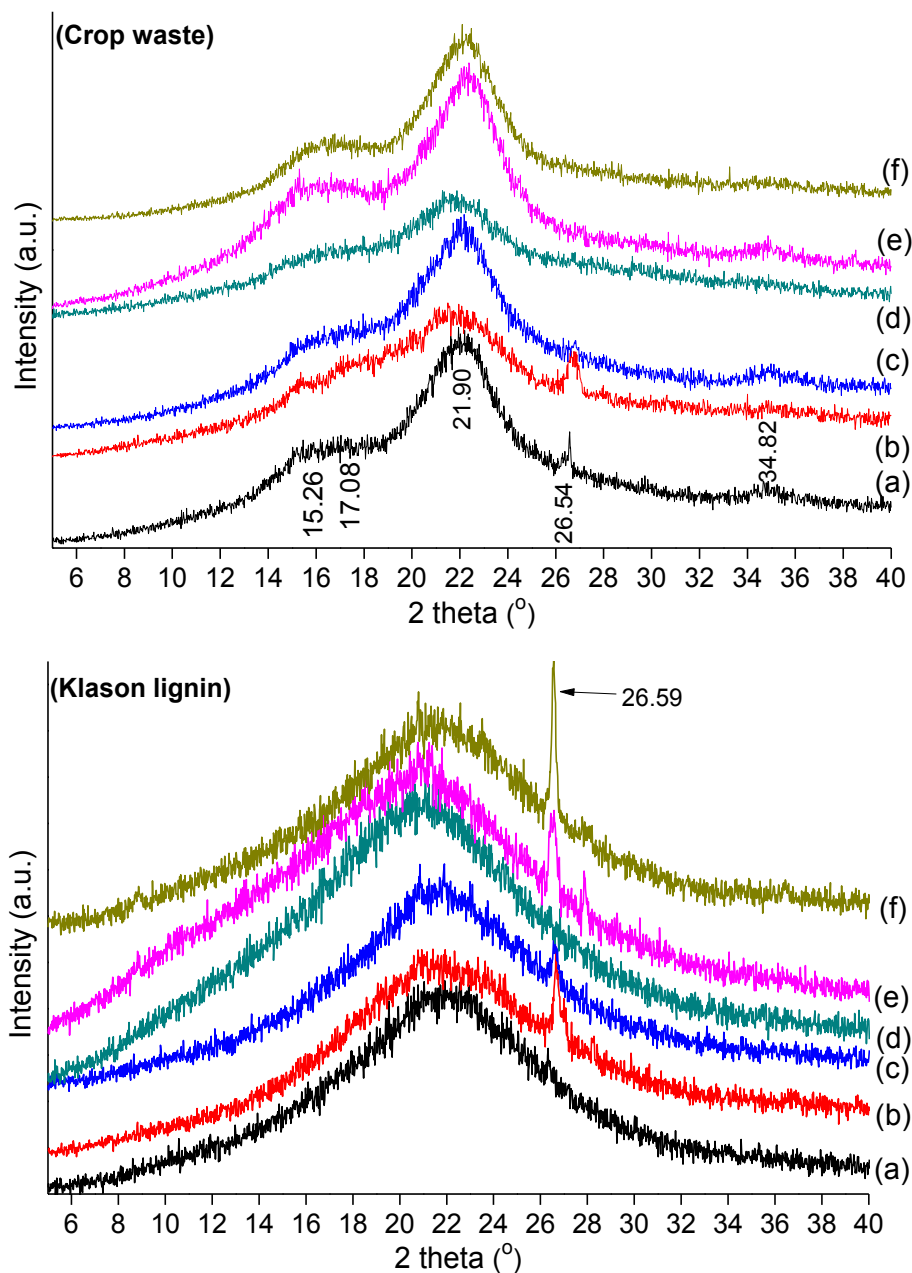
Figure 4A.3. XRD patterns of crop waste and isolated Klason lignin (a) RH I, (b) RH II (c) RH III, (d) BG I, (e) BG II and (f) WS, samples.

After removal of Klason lignin samples, as predicted no peaks are observed for the crystalline and amorphous cellulose peaks pattern. A broad XRD peak pattern is observed in lignin samples, which showed the amorphous nature of the lignin. However, an additional peak at 26.54° is observed in the isolated lignin samples for the presence of SiO_2 within the rice husk and wheat straw samples and also in the respective isolated lignins, which is similar with XRD pattern of silica (JCPDS file No. 33-1161) contents. The crop waste samples contain silica as shown in the Table 4A.2. Isolated Klason lignins are also associated with silica contents, which are affirmed by the XRD pattern.

4A.4.1.2. Scanning electron microscopy (SEM) along with energy-dispersive X-ray spectroscopy (EDX)

The SEM images of crop waste samples showed unstructured morphology of all the samples. However, after separation of lignin from these crop wastes the morphology of crop waste changes as seen from Figure 4A.4. It is interesting to note that although the morphologies of all the crop wastes were different[16] but Klason lignins separated from these crop wastes shows similar type of coagulated unstructured morphology. Typically, lignin particles with submicron size can be formed when lignin is heated above its glass transition temperature. These lignin particles have in recent times gained lot of importance due to their non-toxic nature and thus can be used in various applications e.g. animal feed pellets and molasses additive, oil well drilling, etc. In this work, the non-spherical particles agglomerated (lack of particle integrity) Klason lignins derived from RHs and WS crop waste samples were observed. However, to get bigger lignin (Figures 4A.4a, 4b, 4c and 4f) particles obtained from crop wastes showed agglomeration (lack of particle integrity) which is one of the drawbacks of acid hydrothermal treatment as known from literature.[17] Due to agglomeration of lignin particles (Figures 4A.4a, 4b, 4c and 4f), the obtained morphologies of the lignin samples are quite bigger, while the lignin particles obtained from BG crop waste showed the spherical (droplets) morphology.

Additionally, the elemental composition of the samples was also determined using the EDX (Figure 4B.4), linked to the SEM instruments. It clearly indicates that carbon, oxygen, sulphur, silicon etc. elements are present in the lignin sample. Klason isolation process is used to isolate Klason lignin, where H_2SO_4 was used as reagent.
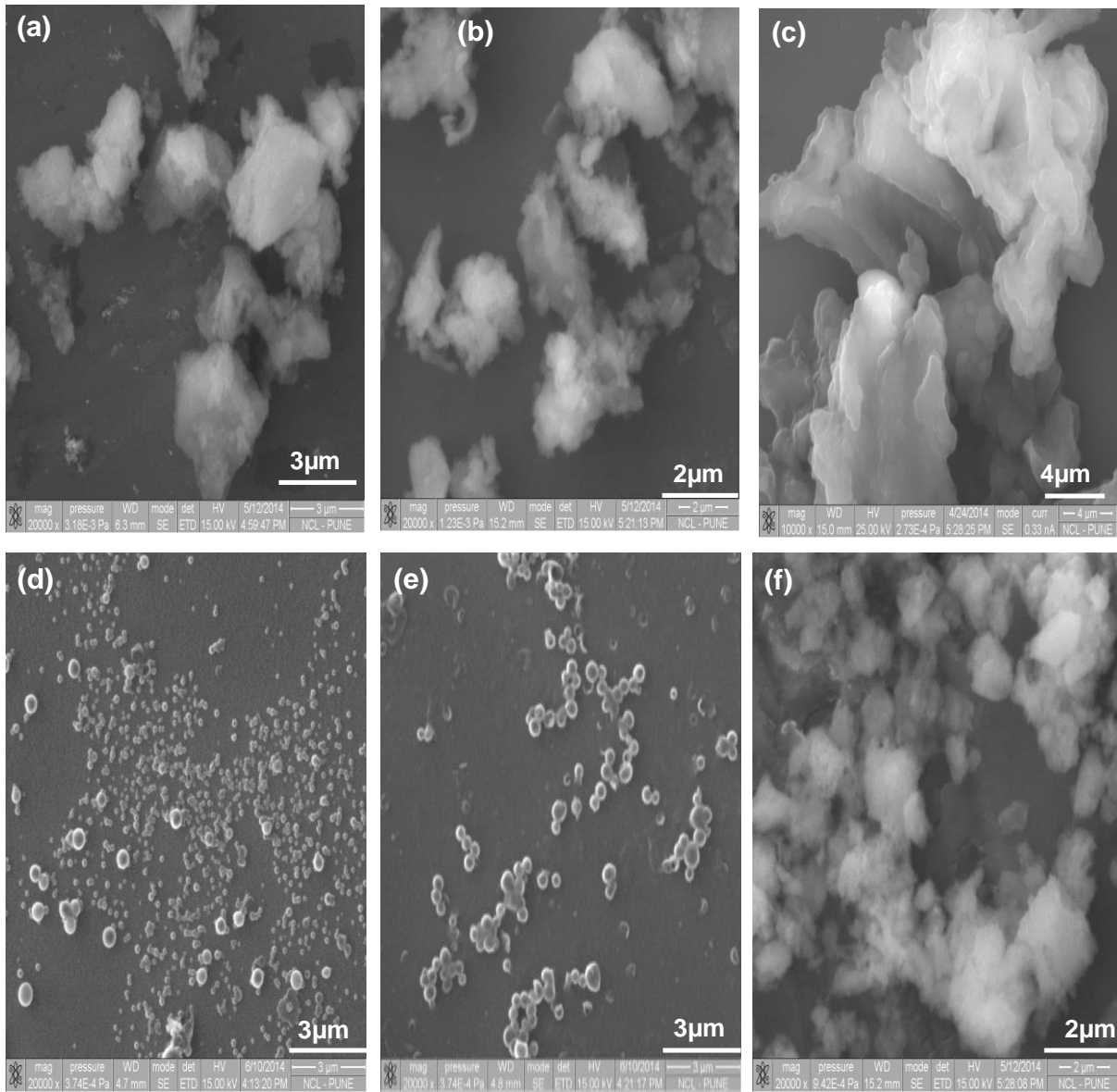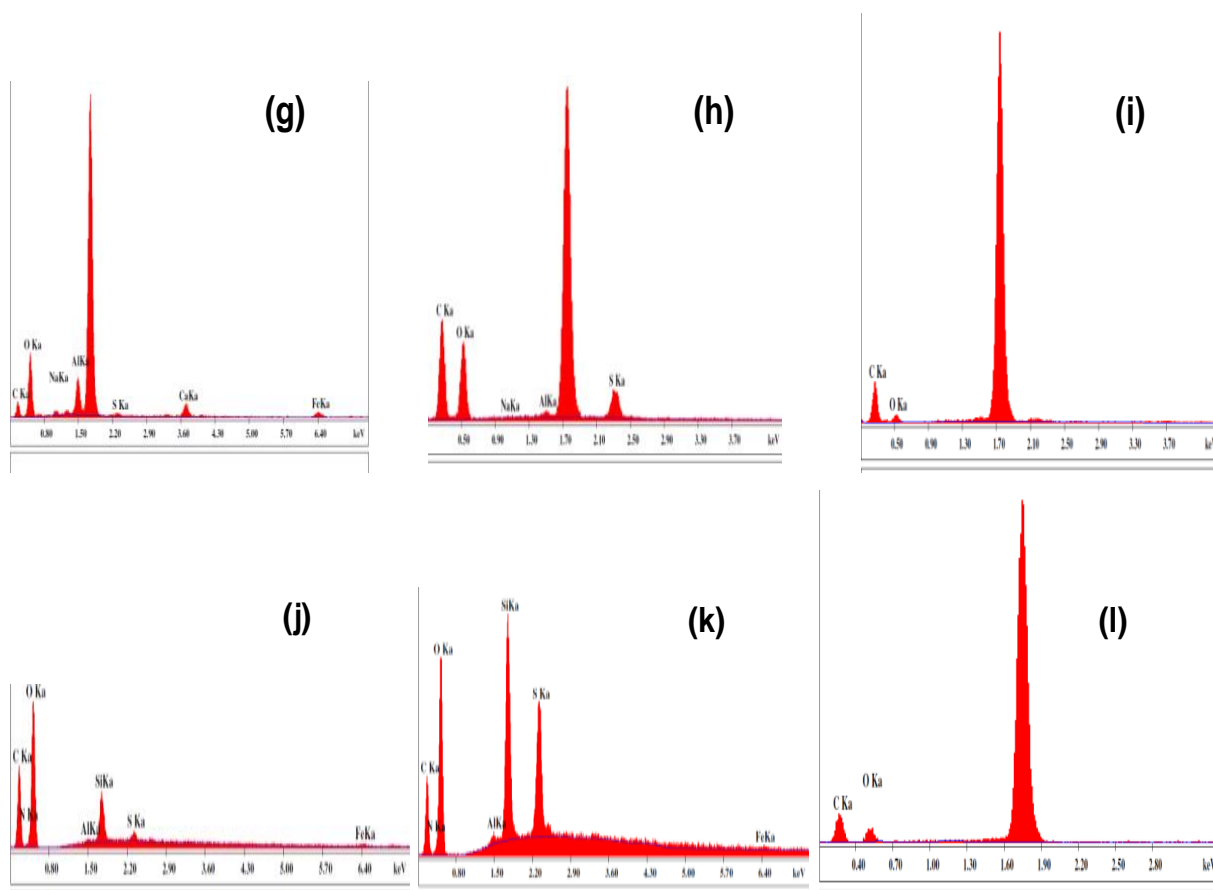
Figure 4A.4. SEM images and EDX of (a, g) RH I; (b, h) RH II; (c, i) RH III; (d, j) BG I; (e, k) BG II and (f, l) WS isolated Klason lignin.

4A.4.1.3. Thermogravimetric analysis

The TGA analysis (Air) for Klason lignins are shown in Figure 4A.5. Klason lignins are observed the weight loss ca. 15% till 200 °C, it may be removal of physically adsorbed moisture, and complete degradation of the organic moieties is observed at ~570 °C. The TGA curve reveals mass loss or phase changes (solid to liquid and further liquid to gases) as a function to temperature. Thermal degradation of Klason lignins started from 200 °C and continued till 550 °C (ca. 65% mass loss). It might be due to side chain alkyl units, linked such as ≡C-C≡/ ≡C-O-C≡ bonds attached to the aromatic ring, and further it might be contributed by aromatic ring present in the Klason lignin.[18, 19] Since, the RH I, II and III, as observed from the analysis Figure 4A.5, ca. 30-40% mass of Klason lignin remained as such in the ignition residue. During the Klason process, lignin is obtained as solid and polysaccharides as liquid, along with solid lignin, the ignition residue was also obtained in insoluble solid form. TGA analysis of lignin derived from BG II species showed very low contents of ignition residues (ca. 3%), which is in line with the data obtained for ash content present in the lignin sample (Table 4A.5). Similarly, the same trends of ash contents after burning (RH I, 35%, RH II, 36% and RH III, 28%), and solid residue obtained from TGA analysis (Solid residues; RH I, 35%, RH II, 34% and RH III, 27%) are also

determined for Klason lignins, which produced almost similar results. The presence of inorganic contents such as silica and nutrient contents in the isolated Klason lignins are confirmed by XRD pattern, EDX and ICP-OES analysis, as shown in the Figures 4A.3-4A.4 and Tables 4A.2 and 4A.4.
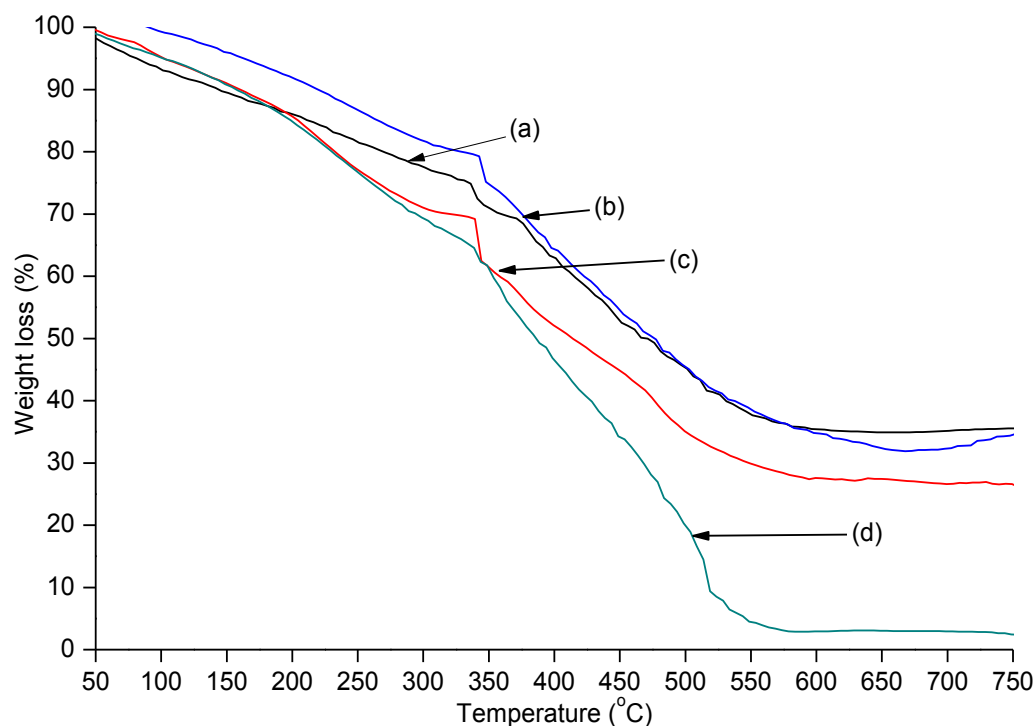
Figure 4A.5. Thermogravimetric analysis (air) of Klason lignin samples derived from (a) RH I, (b) RH II, (c) RH III and (d) BG II.

4A.4.1.4. Elemental analysis of crop waste and Klason lignin samples

Elemental analysis of the crop waste and isolated Klason lignin samples were done in detail to know the percentage of C, H and O chemical contents, as shown in Table 4A.5. Typically, the crop waste samples contains higher O/C_{eff} ratio compared to the isolated Klason lignin samples and after removal of polysaccharides contents from the crop waste samples, the oxygen percentage drop down in the Klason lignin samples. It is obvious because in cellulose C6 sugar general monomer molecular formula $C_6H_{12}O_6$ and in hemicellulose mainly C5 sugar unit $C_5H_{10}O_5$ are made up off O/C_{eff} ratio= 1. This is approximately similar to the general monomer molecular formula of the crop waste samples which is $C_{6.2-7.6}H_{10.6-11.5}O_6$. After polysaccharide removal, Klason lignin samples have monomer molecular formula in range between $C_{8.3-9.6}H_{9.9-11.3}O_3S_{0.1}$, which is well matches with the theoretical calculation. However, the higher heat values (HHV) or higher calorific values (calculated using Dulongs equation , for details descriptions please see the Chapter 3, Section 3A.2.9, equation 3A.19) of the crop waste samples are also lower than isolated Klason lignin samples because of higher oxygen content and presence of polysaccharide (which have O/C_{eff} ratio= 1) in the crop waste samples. However, considering the HHV values and lower O/C ratios of the isolated Klason lignin showed that it is good source of fuels and energy than crop waste sample. Additionally, the degree of unsaturation or double bond

equivalence of the isolated Klason lignin samples are calculated, for more details please see Chapter 3, Section 3A, equation 3A.20, and the resultant data are in the range between 4.4-5.0, Table 4A.5, it is in line with the general monomer molecular formula of the major building units of the lignin (coumaryl, coniferyl and sinapyl alcohols). For one benzene ring, it is considered four and one for exo double (-C=C-) such as propenoid units or one saturated ring which is the common for monomeric molecular formula of three building units of lignin samples as shown in the Chapter 1, Figure 1.3. Further to check the acidic, basic or neutral nature of the Klason lignin sample, the pH was measured (Table 4A.5) and it was confirmed that the isolated Klason lignin samples are acidic (pH= 2.40-2.90). It may be because of H_2SO_4 was used for the solubilisation of polysaccharide during the Klason lignin extractions. The sulphur unit (in the $-SO_3H$ form) may remain with lignin unit in the form of sulphate group, which is confirmed by ATR (S=O stretching frequency at 1040-1060 cm^{-1}), and sulphur presence in the lignin sample is also confirmed by EDX analysis and elemental analysis (Table 4A.5).

Table 4A.5. Elemental analysis of crop waste and Klason lignin samples (oven dry basis).

	Samples	Elemental analysis (*wt.*%)				MMF[b]	Ash, (*wt.*%)	HHV[c] (MJ/kg)	O/C ratio	DBE [d]	pH [e]
		C	H	S	O[a]						
Crop waste	RH I	36.9	5.6	-	47.7	$C_{6.2}H_{11.3}O_6$	14	13.1	0.97	-	-
	RH II	37.7	5.4	-	47.1	$C_{6.4}H_{11.0}O_6$	17	13.2	0.94	-	-
	RH III	37.7	5.7	-	47.4	$C_{6.3}H_{11.5}O_6$	17	14.4	0.95	-	-
	BG I	45.2	5.5	-	48.1	$C_{7.6}H_{11.4}O_6$	2	14.7	0.79	-	-
	BG II	44.7	5.5	-	49.8	$C_{7.2}H_{10.6}O_6$	3	16.6	0.83	-	-
	WS	40.9	5.5	-	46.6	$C_{7.0}H_{11.3}O_6$	13	12.6	0.86	-	-
Klason lignin	RH I	56.3	5.4	1.0	24.5	$C_{9.2}H_{10.6}O_3S_{0.1}$	35	17.9	0.33	4.9	2.4
	RH II	53.3	5.3	1.0	25.7	$C_{8.3}H_{9.9}O_3S_{0.1}$	36	16.5	0.36	4.4	2.9
	RH III	56.1	5.5	1.1	23.5	$C_{9.6}H_{11.3}O_3S_{0.1}$	28	19.0	0.31	5.0	2.5
	BG I	61.8	6.4	0.9	27.9	$C_{8.9}H_{11.0}O_3S_{0.1}$	10	18.3	0.34	4.4	2.3
	BG II	62.3	6.5	1.1	28.1	$C_{8.9}H_{11.1}O_3S_{0.1}$	6	18.5	0.34	4.4	2.7
	WS	59.9	5.8	1.1	26.2	$C_{9.2}H_{10.6}O_3S_{0.1}$	25	17.9	0.33	4.9	2.5

Where, [a]-calculation based on elemental analysis after removing ash, [b]-MMF-monomer molecular formula, [c]-HHV-higher heat value in MJ/kg, [d]-DBE= double bond equivalence and [e]-100 mg sample was suspended in 6 mL millipore water and shaking was done for 5 min. Later lignin which is insoluble in water was allowed to settle down and then pH was measured (pH of millipore water was 6.92 at 25.0 °C) 6.31

4A.4.1.5. UV-Visible spectra

The UV-Vis spectra were recorded to find out the electronic transitions present in the isolated Klason lignin (Figure 4A.6). The Klason lignin (ca. 2 mg) was suspended in 10 mL methanol and filtrate solution was analysed from a range between λ = 200-400 nm (Figure 4A.6). The normal absorption band in the range of 200-220 nm is observed due to Π- Π* transition of the aromatic ring or alkenes units. The observance of new peaks at 230 nm is shown for the presence of mono/di-substituted aromatic phenolic rings (e.g. –OH, -OCH₃, -OAr groups, etc.). The presence of 283±5, and 315±3 nm peaks for the syringyl alcohol (*S*), guaiacyl alcohol (*G*) and *p*-hydroxyphenyl alcohol (*H*) units are observed.[20] The peaks in the range between 270-290 nm are observed for the unconjugated phenolic molecules, and additional peaks at a range of 300 and 320 nm indicates for the presence of unsaturated conjugated phenolic molecules such as Cα C=C and C=O or guaiacyl moieties.[21]
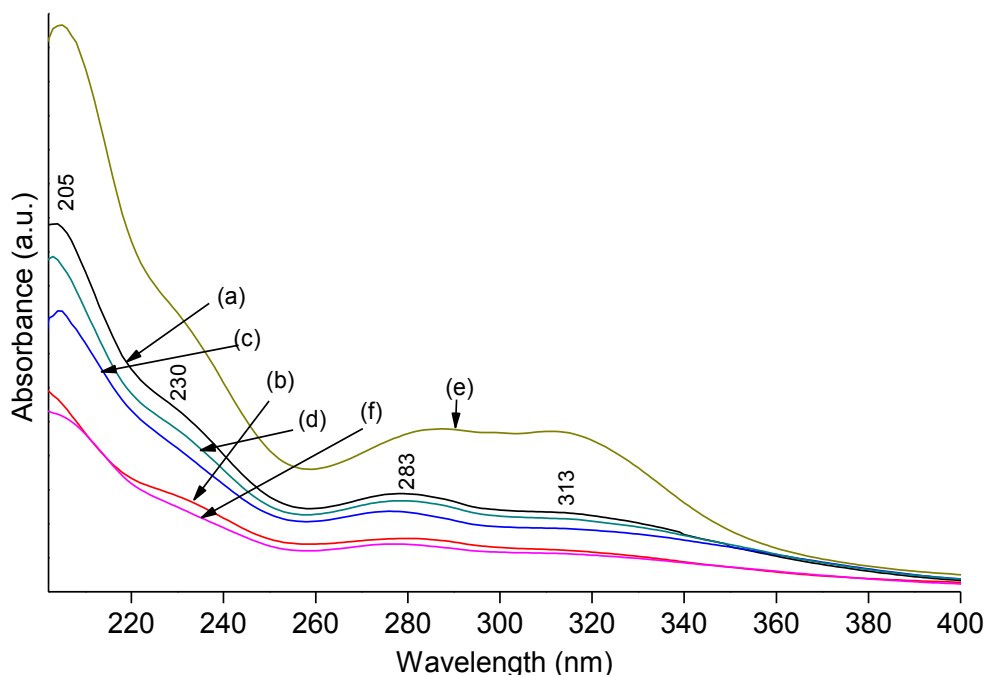
Figure 4A.6. UV-Vis spectra of Klason lignin derived from (a) RH I, (b) RH II, (c) RH III, (d) BG I, (e) BG II and (f) WS crop waste samples. Klason lignin (ca. 2 mg) sample was suspended in 10 mL methanol.

4A.4.1.6. ATR spectra

The presence of various functional groups in isolated Klason lignin samples were analysed using ATR analytical technique (Figure 4A.7) and details descriptions of the peaks are consolidated in the Table 4A.6.[16] A band in a range of 3400 to 3300 cm^{-1} was attributed to the hydroxyl groups attached with the phenolic or aliphatic substructures of the isolated lignins, while those peaks at 2924 and 2841 cm^{-1} were initiated by C–H stretching vibrations present such as methoxy, methyl and methylene groups. The peaks are belonging to the aldehyde groups in the range between 2800-2860 and 2700-2760 cm^{-1}, while for the confirmation of the aldehyde proton both peaks must be present. Interestingly, very low intensity peaks at 2841 and 2924 cm^{-1} are observed for the stretching mode –CH of group in all the isolated lignin samples. The significant functional groups present in the Klason lignin are defined in the range between 1550-1800 cm^{-1}, while the peaks present at 1730±5 and 1715±5 cm^{-1} for the stretch –C=O of unconjugated ester, ketone or aldehyde functional groups present in the Klason lignin samples, the observance of dual C-H stretching peaks at 2820-2850 and 2720-2750 cm^{-1} are missing for the characteristic peaks of the aldehyde group. Potentially aldehyde group, these peaks are absent in the Klason lignin samples. Similarly, multiple peaks in the range between 1400-1600 cm^{-1} in all the samples represent the benzene ring present in the isolated Klason lignin samples.
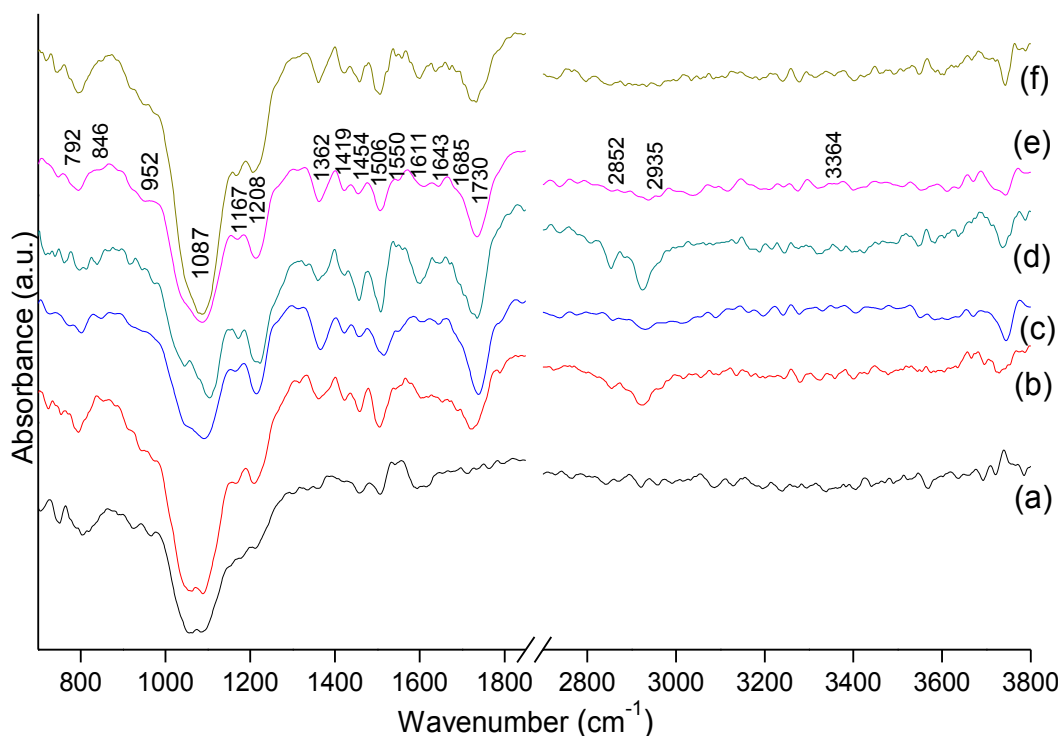
Figure 4A.7. ATR spectra of isolated Klason lignin derived from (a) RH I, (b) RH II, (c) RH III, (d) BG I, (e) BG II and (f) WS.

Beside these peaks, below 1550 cm^{-1} peaks belonging to the characteristic aromatic peaks and other functional groups, which are consolidated in the Table 4A.6 and these peaks are almost similar in all the Klason lignin samples. It is important to note that peaks observed between 1030-1270 cm^{-1} are assigned to *G*, *H* and *S* units present in lignin. Another major peak visible at 1087 cm^{-1} is assigned to alkoxy C-O group. Peaks at 845±5 and 800±5 cm^{-1} are assigned to C-H bending in substituted benzene and $R_2C=CH_2$ (geminal disubstituted alkene) groups.

Table 4A.6. ATR band of ORGL derived from RH I, RH II, RH III, BG I, BG II and WS, samples.

Bands (cm^{-1})	Assignments	Wavenumbers (cm^{-1})					
		RH I	RH II	RH III	BG I	BG II	WS
3400-3300	O-H stretching	3335 (w)	3340 (w)	3340 (w)	3365 (w)	3364 (w)	3370 (w)
2960-2920	C-H asymmetric stretching in methyl and methylene group	2921 (w)	2924 (w)	2924 (s)	2923 (s)	2935 (w)	2935 (w)
2860-2830	C-H symmetric stretching in methyl and methylene group	2841 (w)	2856 (w)	2856 (w)	2852 (m)	2852 (w)	2850 (w)
1750-	C=O stretching	-	1795	1785	-	-	-

1800	anhydride, ester, aldehyde groups		(w)	(w)			
1740-1680	C=O stretching in unconjugated ketone, carbonyl and ester groups		1736 (s)	1719 (s)	1737 (s), 1689 (w)	1730 (s), 1685 (m)	1734 (s)
1670-1620	C=O stretching in conjugated *p*-substituted aryl ketones	1621 (w)	1644 (w)	-	1643 (m)	1643 (w)	1637 (w)
1610-1590	Aromatic skeleton vibration plus C=O stretching	1591 (w)	1608 (w)	1605 (w)	1598 (s)	1611 (w)	1598 (m)
1515-1505	Aromatic skeleton vibrations	1508 (m)	1513 (m)	1506 (s)		1506 (s)	1505 (m)
1470-1450	C-H deformation (asymmetric in -CH₃ and –CH₂-)	1460 (w)	1457 (w)	1457 (w)	1457 (m)	1454 (w)	1457 (w), 1421 (w)
1370-1350	Aliphatic C-H stretching in CH₃ (not –OCH₃) and phenolic -O-H	-	1365 (s)	1362 (m)	1357 (m)	1362 (s)	1360 (s)
1230-1200	C-C plus, C-O plus, C=O stretching (*G* condensed >*G* etherified, typical of *G* units)	1211 (w)	1211 (s)	1207 (m)	1221 (s)	1206 (s)	1205 (s)
1180-1160	Typical for *H*, *G*, *S* units of lignin	1168 (w)	1168 (w)	1178 (s)	1170 (m)	1167 (w)	1170 (w)
1080-1100	-	1086 (s)	1092 (s)	1089 (s)	1102 (s)	1087 (s)	1087 (s)
1040-1060	S=O stretching	1059 (s)	1053 (s)	1059 (s)	1047 (m)	1048 (w)	1051 (w)
960-980	-	964 (w)	-	971 (w)	973 (w)	952 (w)	951 (w)
920-945	-	922 (w)	935 (w)	941 (w)	944 (m)	937 (w)	918 (w)
810-790	-	803 (s)	800 (m)	794 (s)	809 (w)	792 (s)	796 (s)
770-745	-	748 (m)	770 (w)	754 (w)	761 (w)	741 (w)	745 (w)

Notes: w: weak, m: medium and s: strong band intensities.

4A.4.1.7. ^{13}C CP-MAS NMR characterization

Klason lignin derived from crop waste samples were subjected to the solid-state cross-polarization magic angle spinning 13-carbon nuclear magnetic resonance (^{13}C CP-MAS NMR, at 79.49 on a Bruker Avence-300 MHz) analytical under similar acquisition parameter. The adamantine molecule was used as an internal standard for ^{13}C CP-MAS NMR. A comparison study of the ^{13}C CP-MAS NMR of Klason lignin samples has been done with available literature.[22,] [23] The ^{13}C CP-MAS NMR spectra recorded for Klason lignins derived from crop waste samples are shown in Figure 4A.8 and it showed the considerable difference in the peaks distribution and intensities in their chemical shift. The ^{13}C CP-MAS NMR for the alkyl side chain peaks are observed in the range of chemical shift (δ= 10–50 ppm), which were typically assigned to -CH$_3$, -CH$_2$-, -CH-, -C-, CH$_3$CO- species etc. It is documented from the spectra (Figure 4A.8) that BG II has low intensities in the alkyl region compared to the other samples, for more details please see the consolidated result for the alkyl group regions in the Table 4A.7.

Interesting results for the difference of various linkages or heteroatom ('O') next to aliphatic or aromatic carbon ('C') peaks are documented in the range between δ= 50-90 ppm. The appearance of methoxy (-OCH$_3$) group in all the lignin samples are of almost similar intensity except RH III and BG II lignin samples with minor change in the chemical shift (δ= 55.86-56.08 ppm). However, peaks for the β-O-4' substructures (Aα and Aγ; Aγ units linked with αC=O group) appeared in all the isolated Klason lignin samples with variable intensities in the range of between δ= 60.90-60.97 ppm, 68.21-68.57 ppm and 72.75-72.93 ppm. The peaks are also observed for the Cβ in dibenzodioxocin substructures (Cβ) units at δ= 83.25-83.96 ppm.

The aromatic regions of ^{13}C CP-MAS NMR spectra for Klason lignin samples were recorded in the range between δ=90-140 ppm. The peaks for the tricin molecules observed in the range between δ= 93.21-94.03 ppm (T$_8$) and 105.45-106.02 ppm (T'$_{2,6}$) in all the Klason lignin samples originated from the crop waste with variable intensities, while, the peaks for the *p*-hydroxyphenyl unit is observed at δ= 115.60-116.02 ppm and 129.22-130.17 ppm for C$_{3,5}$ and C$_{2,6}$ units present in Klason lignin samples with variable intensities. Although, peaks for the etherified guaiacyl C$_{3,4}$ units are detected at chemical shift δ= 147.59-147.74 ppm with variable concentration (Figure 4A.8). The peaks at δ= 152.35-153.13 ppm belong to the Cα in β-O-4' substructures (Aγ) linked with αC=O units with almost similar intensity in all the samples. Peak appear at δ= 182.21-182.71 ppm for C=O in spirodienone unit, but it is missing in BG II sample. Moreover, the results of the ^{13}C CP-MAS NMR of Klason lignin derived from BG II are almost different with other lignin samples, more details of the peaks assignment present in the Klason

lignin are consolidated in the Table 4A.7, few of the peaks present in the lignin samples are not assigned based on the available reports.
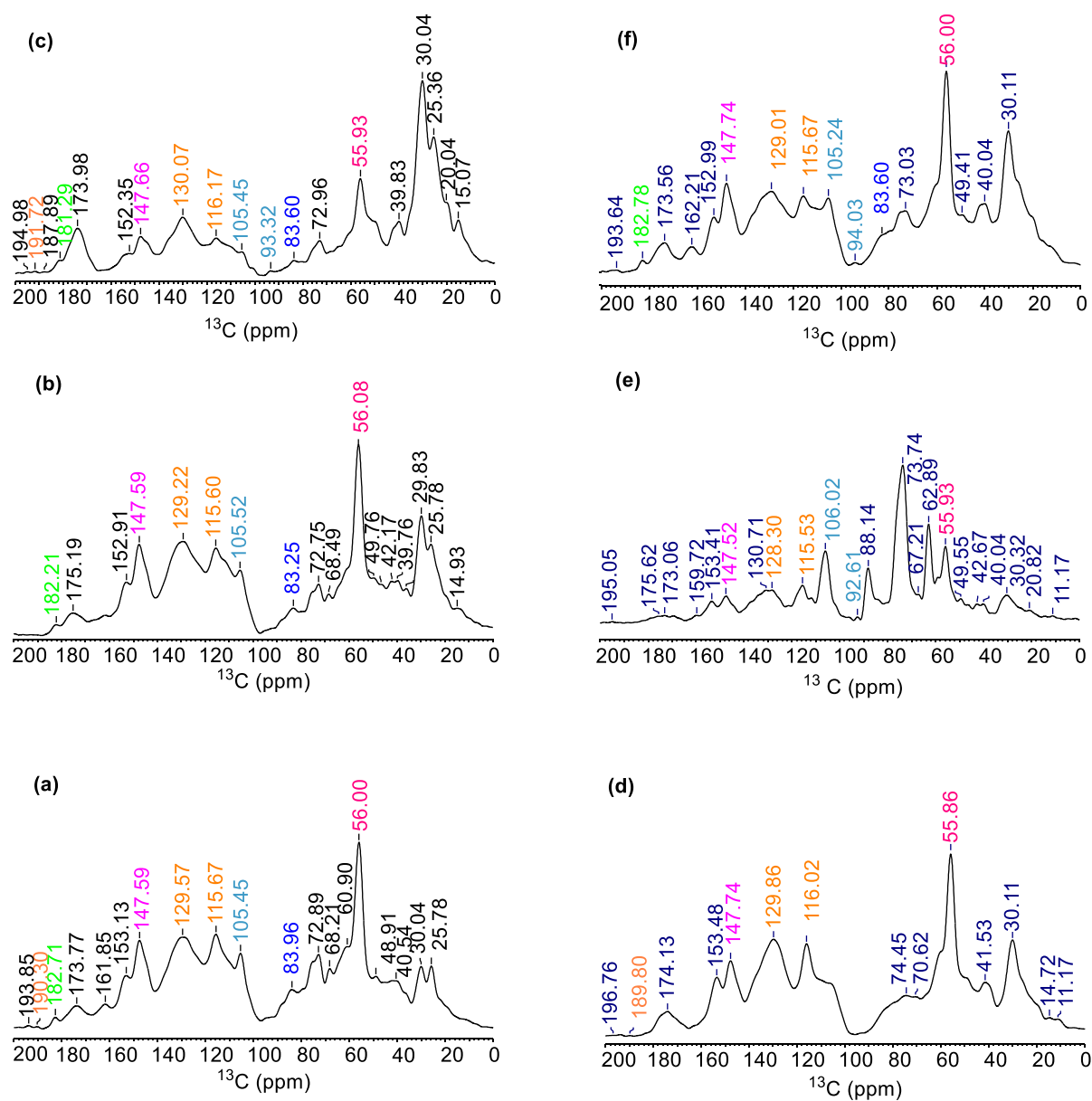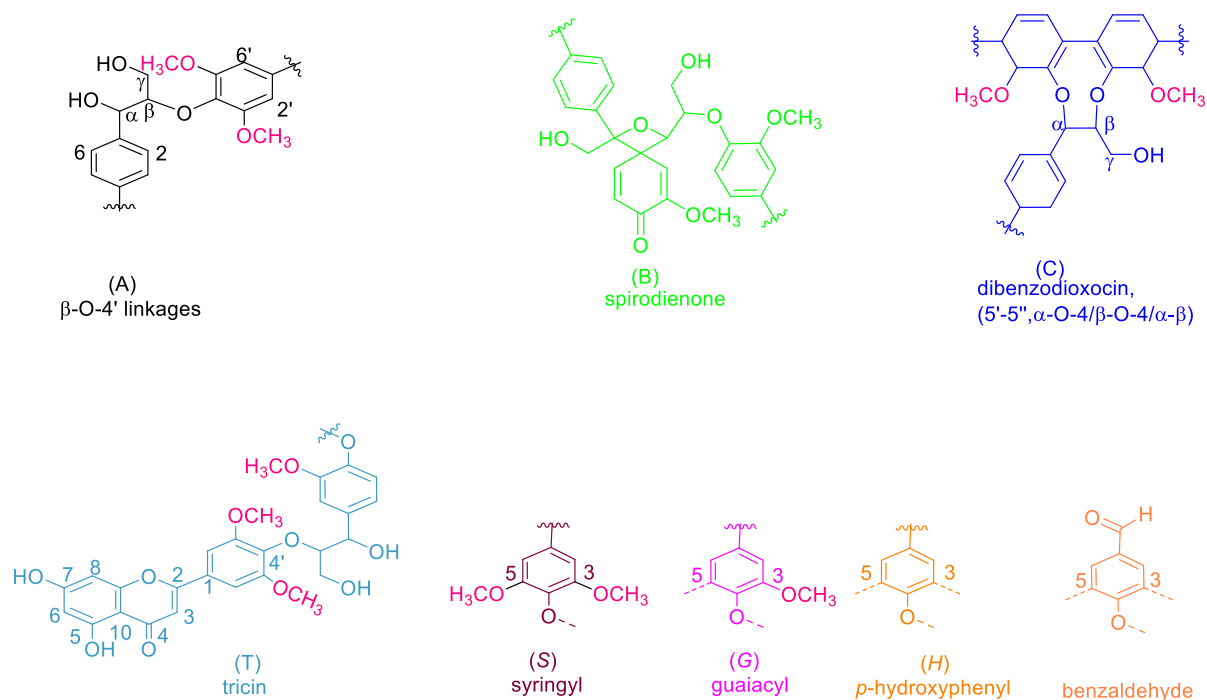
Figure 4A.8. Solid state ^{13}C CP-MAS NMR spectra of Klason lignins derived from (a) RH I, (b) RH II, (c) RH III, (d) BG I, (e) BG II and (f) WS of with lignin sub-structure units.

Table 4A.7. Assignments of ^{13}C CP-MAS NMR of Klason lignin derived from RH I, RH II, RH III, BG I, BG II and WS crop waste samples.

Assignment	Klason lignins, δ_C (ppm)					
	RH I	**RH II**	**RH III**	**BG I**	**BG II**	**WS**
-	-	-	-	11.17	11.17	-
Terminal –CH$_3$ group	-	14.93	15.07	14.72	-	-
-	-	-	20.04	-	20.82	-
-	25.78	25.78	25.36	-	-	-
-CH$_2$- alkyl group	30.04	29.83	30.04	30.11	30.32	30.11
α-carbon in phenylpropanol group	-	36.14	-	-	-	-
-	40.54	39.14	-	41.53	40.04	40.04
α-carbon CH$_2$ with aliphatic substituted group	-	42.17	-	-	42.62	-
-	-	46.64	46.73	-	-	-
-	-	49.76	-		49.55	49.41
C-H in methoxyls group	56.00	56.08	55.93	55.86	55.93	56.00
C$_\gamma$ in β-O-4' substructures (A$_\gamma$)	60.90	60.93	60.97		62.89	
C$_\gamma$ in β-O-4' substructures	68.21	68.49	68.56	70.62	-	-

(A_γ) linked units with $\alpha C=O$						
C_α in β-O-4' substructures (A_α)	72.89	72.75	72.93	74.45	73.74	73.03
C_β in dibenzodioxocin substructures (X_β)	83.96	83.25	83.60	-	-	83.60
-	-	-	-	-	88.14	-
C_8 in tricin (T_8)	93.41	93.21	93.32		92.61	94.03
$C'_{2,6}$ in tricin ($T'_{2,\,6}$)	105.45	105.52	105.45		106.02	105.24
$C_{3,5}$ in (H)	115.67	115.60	116.17	116.02	115.53	115.67
$C_{2,6}$ in (H)	129.57	129.22	130.07	129.86	128.30	129.01
	-	-	-	-	130.71	-
C_3 and C_4 in etherified guaiacyl (G)	147.59	147.59	147.66	147.74	147.52	147.74
C_α in β-O-4' substructures (A_γ) linked units with $\alpha C=O$	153.13	152.91	152.35	153.48	153.41	152.99
C_4 in (H)	161.81	161.85	-	-	159.72	162.21
-	173.77	-	-	174.13	173.06	173.56
-	-	175.19	-	-	175.62	-
C=O in spirodienone units	182.71	182.21	181.29	-	-	182.78
-	-	-	187.89	189.80	-	-
C=O in benzaldehyde units	190.30	-	191.98		-	-
$\alpha C=O$ in β-O-4' substructures (A_γ) linked units with	193.85	-	194.98	196.76	195.05	193.64
Note: (-) not assigned.						

4A.5. Depolymerization of Klason lignins

In Chapter 3, Sectiona 3B.3.1 and 3B.3.2, detailed descriptions of the lignin depolymerization into low molecular weight aromatic products have been discussed using various ILs, among all catalyst [C_3SO_3HMIM][HSO_4] IL has given the highest yield (78%) of low molecular weight aromatic products. Thus, optimized reaction parameters are applied with the isolated Klason lignin samples. Depolymerization reactions of isolated Klason lignins were carried out at desired temperature (120 ℃ for [C_3SO_3HMIM][HSO_4] and 200 ℃ for I-BAIL) for required time (1 h) in a batch mode Parr autoclave reactor of 150 mL capacity. For all the reactions, lignin (2$wt.$% solution, H_2O:CH_3OH, 1:5 v/v= 30 mL) and [C_3SO_3HMIM][HSO_4] or I-BAIL (0.5 g) catalyst were taken and the reactor was warmed up to desired temperature under slow stirring (100

rpm). After attaining the desired temperature, stirring speed was increased to 1000 rpm and this time was noted as starting time of lignin depolymerization reaction. At this temperature the auto-generated pressure was 0.35 MPa ([C_3SO_3HMIM][HSO_4]) and 3.2 MPa (I-BAIL) due to water and methanol binary solvent. After completion of reactions, reactor was allowed to cool to room temperature (27 °C) under the flow of air and slow stirring (100 rpm).

4A.5.1. Depolymerization of Klason lignins using [C_3SO_3HMIM][HSO_4]

Depolymerization studies of isolated Klason lignin shows the variable range of organic solvent soluble products 58-99% yield (Figure 4A.9), while the ash corrections (for each sample) are given during the calculation of yield. As it is observed that lignin isolated form RH I, II and III samples are showing comparable result of organic solvent soluble product. It is because of those are having the similar types of lignin sub-structural units as it is confirmed from the lignin characterization studies as mentioned in the above sections in CHNS, UV-Vis, ATR, NMR, elemental analysis. However, the organic solvent soluble product obtained from lignin isolated from wheat straw is higher than all other lignins. The lignin obtained from WS showed variable particle size as confirmed from SEM analysis and have maximum amorphous nature as visible from XRD pattern. It might be due to well dispersed particle size and amorphous nature of Klason lignin isolated from WS, it gave better result compared to other isolated lignins. Similarly, from the ATR spectrum of Klason lignin derived from WS have more intense peaks at 1087 cm^{-1}, which belongs to ether ($\equiv$C-O-C$\equiv$) linkage. During the lignin depolymerization, maximum amount of organic solvent soluble products yield are obtained through ether bond cleavage. Additionally, lignin obtained from the BG I and II samples showing the almost similar catalytic results for the organic solvents soluble products.
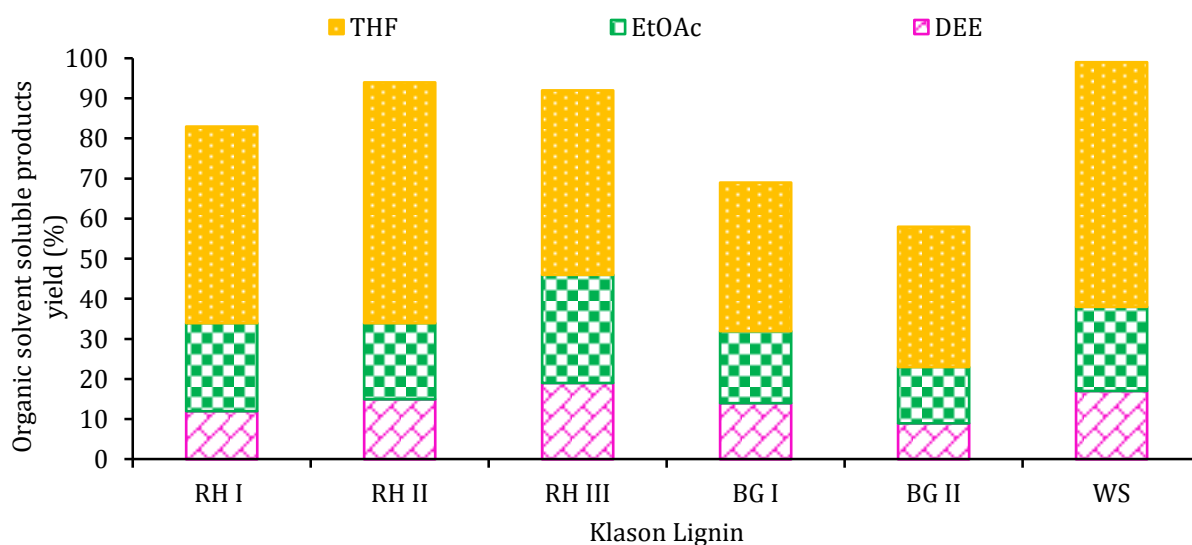
Figure 4A.9. Depolymerization of Klason lignin using [C_3SO_3HMIM][HSO_4] catalyst. Reaction condition: lignin (2 *wt*.% solution H_2O:CH_3OH, 1:5 *v/v*= 30 mL), [C_3SO_3HMIM][HSO_4] (0.5 g), 120 °C, 1 h, 1000 rpm.

Values are average of three reactions with ±4% error observed.

4A.5.2. Depolymerization of Klason lignin using I-BAIL

Optimization of reaction parameters for Klason lignin depolymerization using I-BAIL catalyst has been taken from Chapter 3, Section 3C. Lignin depolymerization using I-BAIL catalyst, the auto generated pressure was 3.2 MPa at 200 °C, it might be due to water and methanol solvent. Different organic solvent (Figure 4A.10) has been used to extract the low molecular weight organic soluble product. In the broad range of organic solvent soluble products yield (45-90%) are obtained, it is obvious due to its structural variation, which are confirmed by various analytical techniques as discussed in the Section 4A.5.1. The I-BAIL result are different with the $[C_3SO_3HMIM][HSO_4]$ catalytic result, due to applied high temperature and difference in H^+ concentration in I-BAIL as solid acid catalyst. However, Klason lignin obtained from WS is showing the good yield of organic solvent soluble products compared to other isolated lignin. For more details descriptions about the obtained result, please see the above Section 4A.5.1. Depolymerization of isolated lignins from RHs is showing almost comparable results, it may be due to structural similarities between them, as discussed in Section 4A.4.
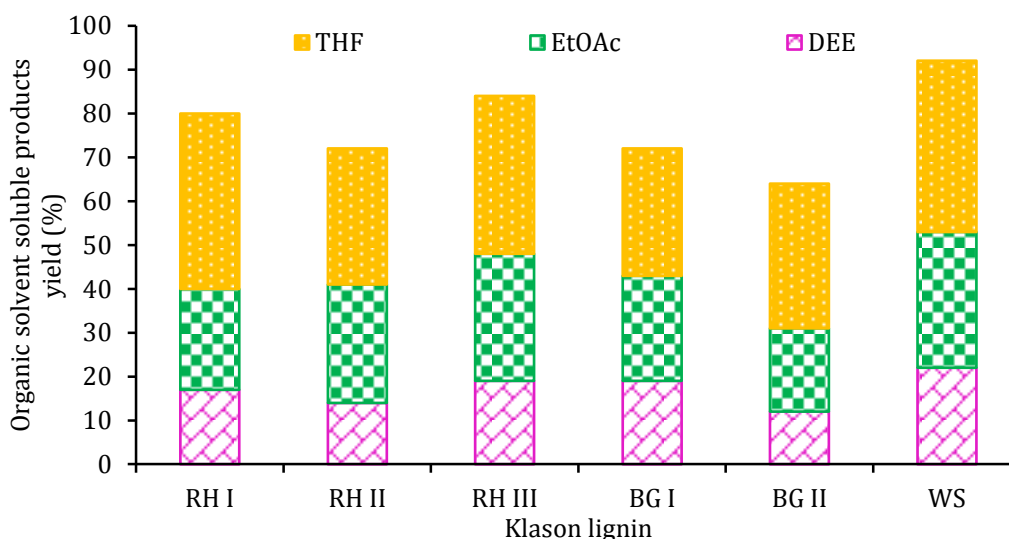
Figure 4A.10. Depolymerization of Klason lignin using I-BAIL catalyst. Reaction condition: lignin (2 *wt*.% solution $H_2O:CH_3OH$, 1:5 *v/v*= 30 mL), I-BAIL (0.5 g), 200 °C, 1 h, 1000 rpm. Values are average of three reactions with ±4% error observed.

4A.6. Correlation between lignin and products

As detailed descriptions discussed above, lignin characterization studies (Section 4A.4) and substantiation for formation of organic solvent soluble products yield were done by various spectroscopic analytical techniques (A detailed description of the lignin and products correlation were already discussed in Chapter 3, Section 3B.6). Nonetheless, to perceive the changes transpiring in lignin structure and existence of several functional groups in both, lignin

and product on bulk and molecular level were done using several analytical techniques UV-Vis, FT-IR, 1D and 2D (HSQC) NMR, etc. which are similar as discussed in the Chapter 3, Section 3B.6.

4A.7. Conclusions

In summary, the ability to isolate, characterise and quantify unknown components in the form of phenyl propenoid copolymer, will assist the efforts to convert crop waste into lignin. The results revealed the 72*wt.*% of sulphuric acid quantity produced a relatively higher yield (21±3%) of Klason lignins (acid soluble and insoluble). Further, complete composition analysis such as Klason lignin, holocellulose (α-, β- and γ- cellulose), silica, moisture, pentosan, nutrients contents, etc. predict that crop waste samples are having variable chemical contents. Additionally, complete characterization of crop waste samples along with isolated Klason lignin samples again confirmed that crop waste and Klason lignins have variable contents of different functional groups, moieties, etc. NMR spectra of isolated Klason lignin samples confirmed that the samples were not showing any polysaccharides peaks in the ^{13}C CP-MAS NMR spectra. It is further proven by XRD and elemental analysis (compared with the known literature of Klason lignins). It was observed that the Klason lignins were composed of *G* and *H* and tricin (T) units; and among all *G* units were present in the major quantity. From the elemental analysis the general monomeric formula as $C_{8.3-9.6}H_{9.9-11.3}O_3S_{0.1}$, is suggested which is similar to the guaiacyl alcohol units. Additionally, complete quantification of six crop waste species (3 rice husk, 2 bagasse and wheat straw samples) showed variable concentration of the contents. This effect may arise due to soil nutrients, age/type of plant species, weather, etc. as these samples were collected from different states of India, and treated with same Klason process. Klason lignin thus obtained had variable concentration of functional groups and aromatic moieties. It is anticipated from the literature that lignin has different linkages and moieties and on its depolymerization, variable products yield can be obtained. Considering this, depolymerization of Klason lignin samples were carried out and the varying organic solvent soluble products yield (45-99%) with $[C_3SO_3HMIM][HSO_4]$ and I-BAIL catalysts were obtained.

4A.8. References

1. A. J. Ragauskas, C. K. Williams, B. H. Davison, G. Britovsek, J. Cairney, C. A. Eckert, W. J. Frederick, J. P. Hallett, D. J. Leak, C. L. Liotta, J. R. Mielenz, R. Murphy, R. Templer and T. Tschaplinski, *Science*, 2006, **311**, 484-489.

2. Alpha-, beta- and gamma-cellulose in pulp, Test Method T 203 cm-09.

3. F. S. Chakar and A. J. Ragauskas, *Ind. Crops Prod.*, 2004, **20**, 131-141.

4. N. E. E. Mansouri and J. Salvado, *Ind. Crops Prod.*, 2006, **24**, 8-16.

5. J. Zhang, H. Deng, L. Lin, Y. Sun, C. Pan and S. Liu, *Bioresour. Technol.*, 2010, **101**, 2311-2316.

6. J. A. Perez-Pimienta, M. G. Lopez-Ortega, P. Varanasi, V. Stavila, G. Cheng, S. Singh and B. A. Simmons, *Bioresour. Technol.*, 2013, **127**, 18-24.

7. J. Long, X. Li, B. Guo, F. Wang, Y. Yu and L. Wang, *Green Chem.*, 2012, **14**, 1935-1941.

8. R. Bharadwaj, A. Wong, B. Knierim, S. Singh, B. M. Holmes, M. Auer, B. A. Simmons, P. D. Adams and A. K. Singh, *Bioresour. Technol.*, 2011, **102**, 1329-1337.

9. Food and Agriculture Organization of the United Nations, http://faostat3.fao.org/faostat.

10. R. Samuel, Y. Pu, B. Raman and A. J. Ragauskas, *Appl Biochem Biotechnol*, 2010, **162**, 62-74.

11. J. B. Sluiter, R. O. Ruiz, C. J. Scarlata, A. D. Sluiter and D. W. Templeton, *J. Agric. Food Chem.*, 2010, **58**, 9043-9053.

12. , Acid-insoluble lignin in wood and pulp, Test Method T 222 om-02.

13. E. Maekawa, T. Ichizawa and T. Koshijima, *J. Wood Chem. Technol.*, 1989, **9**, 549-567.

14. S. Yasuda, K. Fukushima and A. Kakehi, *J. Wood Sci.*, 2001, **47**, 69.

15. H. Kobayashi and A. Fukuoka, *Green Chem.*, 2013, **15**, 1740-1763.

16. S. K. Singh and P. L. Dhepe, *Bioresour. Technol.*, 2016, **221**, 310-317.

17. Y. Pu, F. Hu, F. Huang, B. H. Davison and A. J. Ragauskas, *Biotechnol. Biofuels*, 2013, **6**, 15-27.

18. R. A. Fenner and J. O. Lephardt, *J. Agric. Food Chem.*, 1981, **29**, 846-849.

19. R. Sun, J. Tomkinson and G. Lloyd Jones, *Polym. Degrad. Stab.*, 2000, **68**, 111-119.

20. H. Yang, Y. Xie, X. Zheng, Y. Pu, F. Huang, X. Meng, W. Wu, A. Ragauskas and L. Yao, *Bioresour. Technol.*, 2016, **207**, 361-369.

21. U. Westermark, *Wood Sci. Technol.*, 1985, **19**, 223-232.

22. K. M. Holtman, H. m. Chang, H. Jameel and J. F. Kadla, *J. Wood Chem. Technol.*, 2006, **26**, 21-34.

23. G. Almendros, A. T. Martinez, A. E. Gonzalez, F. J. Gonzalez-Vila, R. Fruend and H. D. Luedemann, *J. Agric. Food Chem.*, 1992, **40**, 1297-1302.

Section 4B:

Organosolv lignin

4B.1. Introduction

Amongst various procedures known for isolation of lignin, use of organosolv (ORG) process for delignification of lignocellulosic materials allows safe and clean pretreatment isolation processes. Since the lignin (ORGL) obtained from this procedure is of high-quality due to absence of sulphur, free of alkali/alkaline metals, soluble in organic solvents etc. it has attracted much interest from researchers.[1-3]

In a step further, in this study, focus is given on analysing the properties of different lignins (ORGLs) derived from same type of crop waste and wood chip samples such as, rice husk (RH), bagasse (BG), wheat straw (WS) and wood chip (WC) by isolating the same using organosolv technique. Further, the isolated ORGL samples were subjected to characterization and their depolymerization reactions using [C$_3$SO$_3$HMIM][HSO$_4$] and I-BAIL as catalysts under optimized reaction conditions.

4B.2. Experimental

4B.2.1. Materials

Crop waste samples were collected from different states of India; rice husk (RH) from Karnataka, (RH I), West Bengal (RH II), Uttar Pradesh (RH III), Odisha (RH IV), bagasse (BG) and wood chip from Maharashtra and wheat straw (WS) from Uttar Pradesh. Before use, all the samples were sieved to obtain RH I-IV, BG, WS and WC with ca. 45 micron size. These samples were named as, RH I (Karnataka state, India), RH II and WS (Uttar Pradesh state, India), RH III (West Bengal state, India), RH IV (Odisha, India), BG and WC (Maharashtra state, India). Absolute ethanol (Changshu Yangyuan Chemical China, 99.9%), sulphuric acid (Loba Chemie India, 98%), methanol (Loba Chemie India, 99.8%), 2, 5-dihydroxy benzoic acid (Sigma-Aldrich USA, >99.5%), acetonitrile (Sigma-Aldrich USA, HPLC grade 99.93%), isopropyl alcohol (Loba Chemie India, >99.5%) and tetrahydrofuran (Merck India, HPLC grade> 99.9%) were used as received.

4B.2.2. Characterization

The ORGLs derived from various crop wastes and wood chip were characterized by a range of physico-chemical characterization techniques. Detail information about the sample preparation and analytical techniques used for ORGLs characterization is given in the Chapter 3, Section 3A.1.

4B.2.3. Isolation of organosolv lignin from crop waste and wood chip samples

For the isolation of ORGLs from rice husks (RHs), bagasse (BG), wheat straw (WS) and wood chip (WC) in a typical procedure (Figure 4B.1), 8.0 g samples were dispersed in 1.024 mmol H$_2$SO$_4$ solution [distilled water-ethanol mixture (1:1 *v/v*= 60 mL)] in an autoclave coated with Teflon. The mixture was stirred (900 rpm) at 180 °C for 1 h and later autoclave was cooled to room temperature (27±2 °C) under flow of air. The mixture was filtered through whatmann

filter paper (No. 110) to separate solid (pulp; solid containing cellulose, hemicellulose, ash etc. obtained after extraction of lignin) and liquid (containing lignin and soluble sugar). Subsequently, the separated solid (pulp) was dried for 16 h in an oven maintained at 55±2 ᵒC. Later, solid was dried under vacuum (-0.101 MPa) at 90±2 ᵒC for 4 h. To the liquid fraction three volumes of distilled water (180 mL) was added in order to precipitate the hydrophobic lignin termed as organosolv lignin (ORGL). The precipitation of lignin was possible from water-ethanol mixture since lignin is insoluble in water and addition of extra water acted as an antisolvent. The precipitated ORGL was then filtered through whatmann filter paper (No. 110), washed with 100 mL of water and then dried in an oven maintained at 55±2 ᵒC for 16 h. Later it was dried under vacuum (-0.101 MPa) at 90±2 ᵒC for 4 h. The calculated mass balance of 93±5% (Section 4B.2.4) was achieved after all the isolation processes. All the isolation experiments were performed three times to check the reproducibility of isolation processes. The data presented in all the Figures and Tables given in this work are average of three experiments.

Sample

(a) 8g sample, water + ethanol, 1:1 *v/v*= 60 mL,
1.024 mmol H_2SO_4, 180 ᵒC,1 h.

Reaction mixture

(b) filter

Solid≠

Liquid

(c) 3 volume distilled water

Precipitate

(d) filter

Solid† (Organosolv lignin)
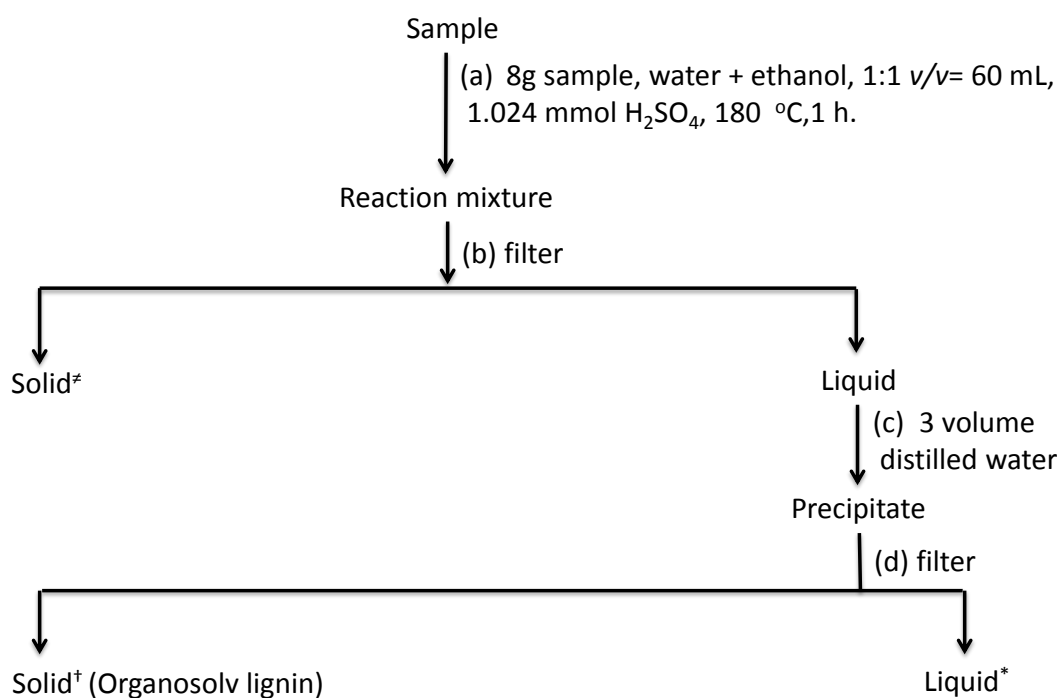
Liquid*

≠-solid sample analysed by CHNS, XRD, etc.

†-solid sample are analysed by CHNS, ATR, (NMR) (^{1}H, ^{13}C and HSQC), GPC, UV-Vis, XRD, TGA, SEM-EDX, MALDI, DSC, etc.

 *- liquid sample analysed by HPLC

Figure 4B.1. Flow chart for the extraction of ORGL from the crop waste and wood chip samples.

4B.2.4. Mass balance

The calculation of mass balance of the crop waste and wood chip samples was done as follows,

Samples contains ca. 4±2% moisture,

Reaction conditions: crop waste and wood chip samples (8.0 g), H_2SO_4, (0.1 g), solvent (water:ethanol, 1:1 *v/v*= 60 mL), 180 °C for 1 h.

So the total charge = 8.10 g [sample 7.68 g (after moisture correction) + H_2SO_4 0.1 g].

After the completion of reaction, the reaction mixture was allowed to cool to room temperature and workup was done as illustrated in Figure 4B.1. The obtained various mass (ORGL, pulp and soluble sugars and mineral acid in diluted reaction mixture) were dried first at room temperature, after that in the oven at 55±2 °C for 16 h and then transferred in vacuum (-0.101 MPa) oven at 90 ±2 °C for 4 h. The weight of solid (recovered pulp= 5.20 g, soluble sugars= 1.04 g and ORGL= 0.96 g) at room temperature was 7.20 g.

$$\text{Mass balance (\%)} = \frac{\text{(Weight of dried mass obtained after reaction)}}{\text{(Weight of total charge before isolation procedure)}} \times 100$$

$$\text{Mass balance (\%)} = \frac{7.20 \text{ g}}{7.78 \text{ g}} \times 100$$

$$= 92.5\%$$

All the isolation processes were performed 3 times to reproduce the results.

4B.3. Results and discussion

4B.3.1. Characterization of samples

4B.3.1.1. X-ray diffraction

The X-ray diffractions recorded for crop waste and wood chip (RH I, II, III, IV, BG, WS and WC), pulps (containing cellulose, hemicellulose, ash etc.) and isolated ORGLs are shown in Figure 4B.2. As seen, in each of the samples, an intense peak observed at 2θ of 22.1° is characteristically assigned to the crystalline part of cellulose. Similarly, two broad shoulder peaks at 2θ of 15.7° and 16.1° were seen in samples, which are typically ascribed to amorphous nature of cellulose. As expected, no sharp, intense peaks for hemicelluloses and lignin are observed in lignocellulosic materials due to their amorphous nature. The XRD patterns for isolated lignin (ORGL) samples showed only one very broad peak. This elucidates that ORGL samples are amorphous in nature.[4]

The BG and its derived ORGL and pulp samples showed the low intense XRD peaks patterns than the RHs, WS and WC and their derived ORGL and pulp samples respectively. This is because hemicellulose (pantosan) content in the BG sample is in higher quantity (25±2%)[5] than RH (16±2%), WS (19±2) and WC (21±2) samples.[5-7] Since, hemicellulose is amorphous in nature, the less intense peaks in XRD pattern are observed in BG sample. Moreover, absence of any intense peak at 22.1° in all the ORGL samples also established that in these samples cellulose is not present[8] and thus it suggests that during the isolation procedures, lignin is selectively isolated from crop wastes and wood chip.[9] On the contrary, presence of peaks at 2θ

of 16.6° and 22.1° in all the pulp samples again proves that cellulose is not extracted along with lignin.
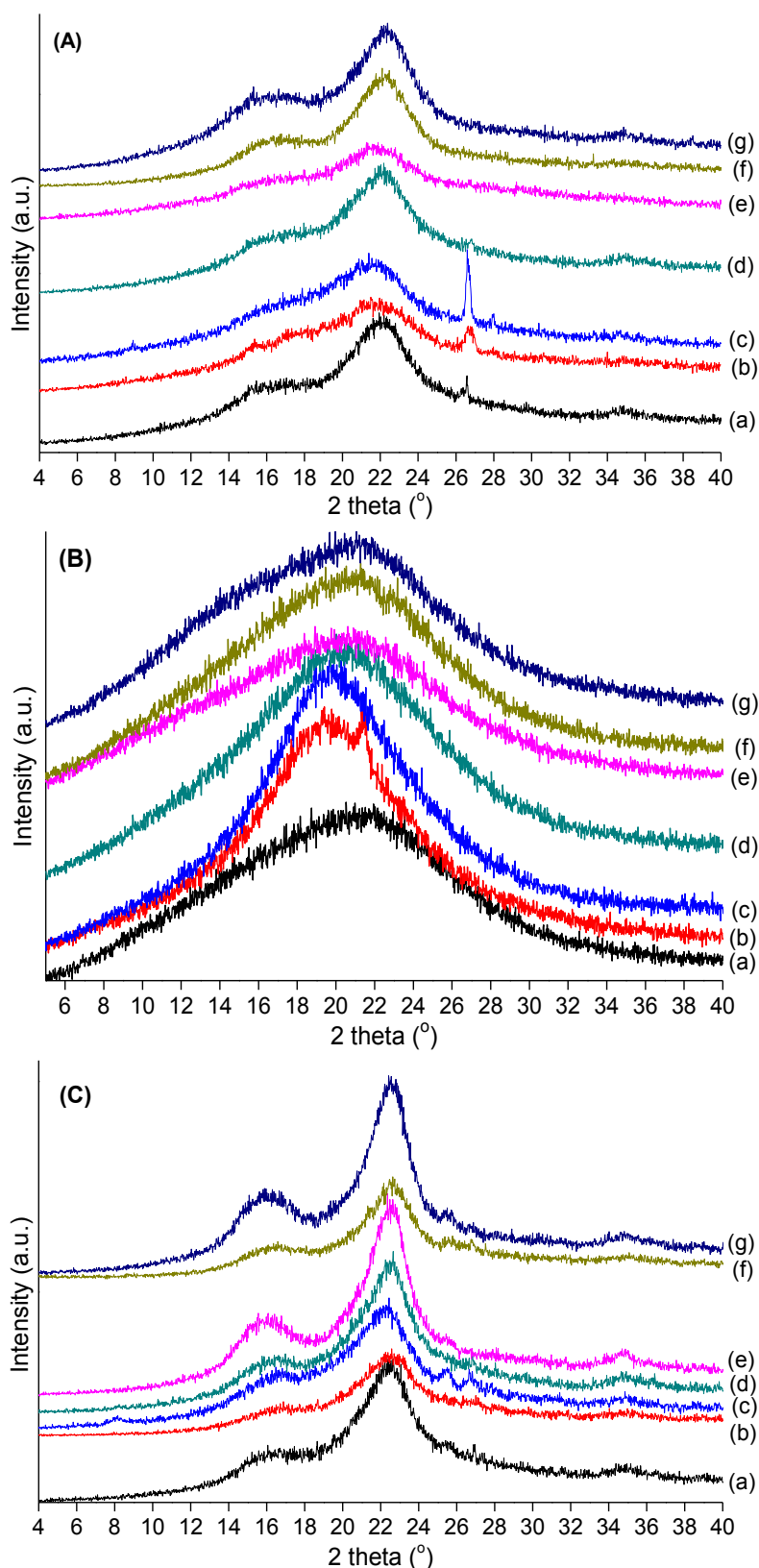
Figure 4B.2. XRD patterns of (A) crop waste and wood chip, (B) isolated ORGL and (C) Pulp of (a) RH I, (b) RH II (c) RH III, (d) RH IV, (e) BG, (f) WS and (g) WC samples.

The most intense peak observed at 2θ of 26.6° belongs to silica present in the rice husks and pulps and it is matched well with XRD of SiO_2 (JCPDS file No. 33-1161). The presence of silica was also confirmed from ash derived from rice husks samples.

4B.3.1.2. Scanning electron microscopy (SEM) along with energy-dispersive X-ray spectroscopy (EDX)

From the available literature, the SEM images of crop waste and wood chip samples (sample images were not taken) have unstructured morphology.[10] However, after separation of lignin from these crop wastes, the morphology of crop waste changes as seen from Figure 4B.3. It is interesting to note that although the morphologies of all the crop wastes were different but lignins (ORGLs) separated from these crop wastes show similar type of spherical morphology. Typically, lignin particles with nano and submicron size can be formed when lignin is heated above its glass transition temperature (170-240 °C)[11, 12] and also when oil in water type systems are used. These lignin particles have in recent times gained lot of importance due to their non-toxic nature and thus can be used in various applications. In this work, it was possible to yield perfectly spherical particles (droplets) of lignin with <200 – 600 nm size from RHs, BG, WS and WC crop wastes. However, lignin particles obtained from WS crop wastes showed agglomeration (lack of particle integrity) as known from literature as one of the drawbacks of acid hydrothermal treatment.[13] Additionally, the elemental composition of the samples were also determined using the EDX (Figure 4B.3), linked to the SEM instrument. It clearly indicates that carbon, oxygen, sulphur, etc. elements are present in the lignin sample.
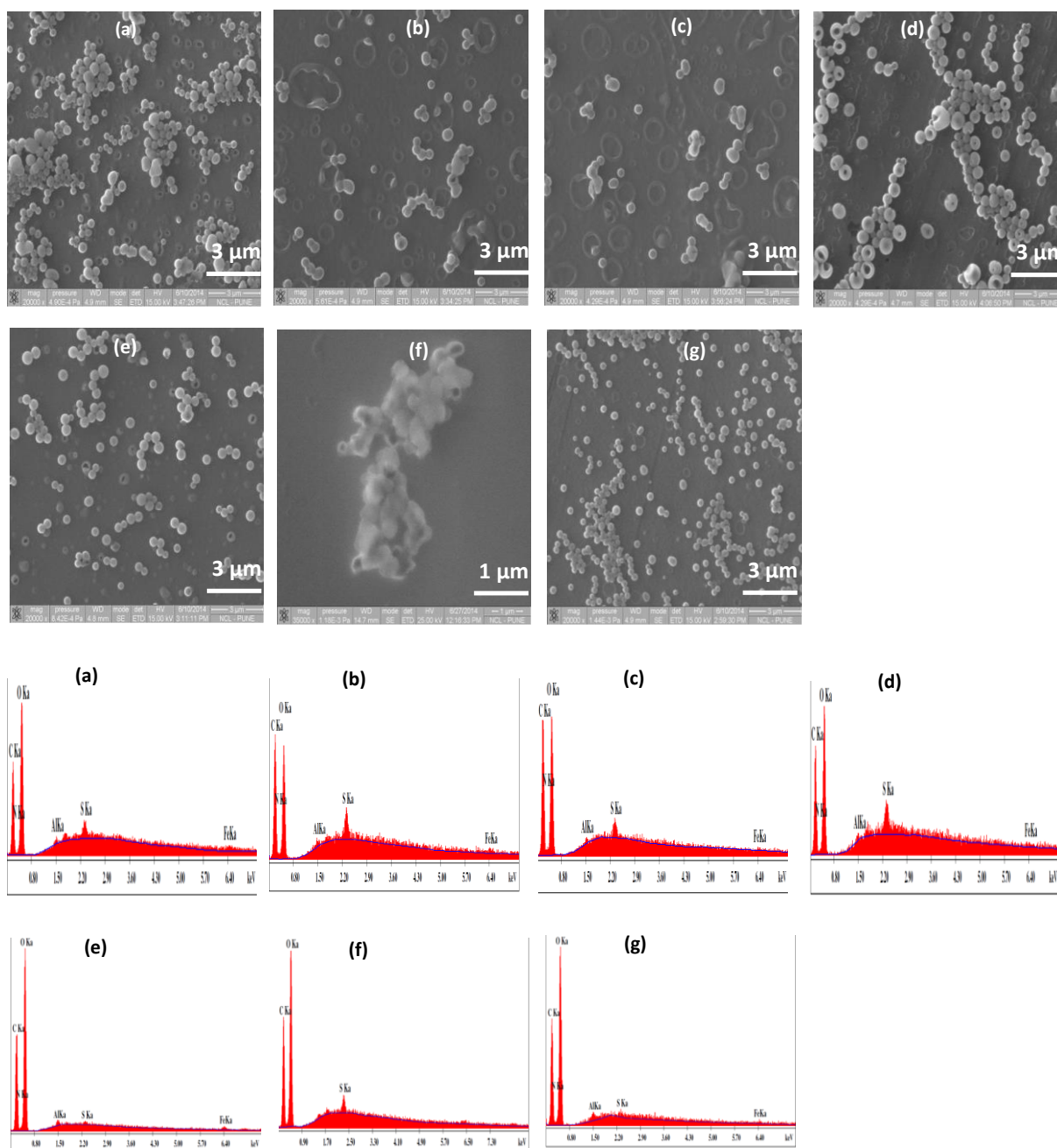
Figure 4B.3. SEM images and EDX of isolated ORGL samples of (a, h) RH I, (b, i) RH II, (c, j) RH III, (d, k) RH IV, (e, l) BG, (f, m) WS and (g, n) WC.

4B.3.1.3. Gel-permeation chromatography (GPC)

The GPC analysis is used to check the molecular weight distribution of the ORGL samples using THF as eluent solvent and polystyrene as standard for calibration. Molecular weight distribution is one of the important features of the isolated ORGL samples to understand its physico-chemical properties. For more details descriptions on the equations used for the calculation of molecular weight please see Chapter 3, Section 3A,1.1 and equations 3A.1-3A.2.

From the GPC analysis (Figure 4B.4), it is clearly seen that ORGL derived from RH, BG, WS and WC samples have variable number and weight average molecular weight distribution. The

polydispersity index (PDI, *Mw/Mn*) of the ORGL sample derived from WC is showing the high number average molecular weight. However, WS is showing high PDI (2.5) compared to other samples. The obtained results (*Mw*, *Mn* and PDI) from the GPC analysis of ORGL samples derived from RH, BG, WS and WC are summarized in the Table 4B.1. The obtained data of the ORGL samples are comparable with the reported literature.[3] Moreover, the GPC results, the MALDI-TOF MS analysis was carried out and the results obtained with GPC and MALDI-TOF MS are similar to 7 to 8 phenylpropenoid units.[3, 14, 15]

Table 4B.1. Summary on the GPC analysis result of ORGL samples (*Mw*, *Mn* and PDI (*Mw/Mn*)).

ORGL samples	*Mw* (g/mol)	*Mn* (g/mol)	PDI (*Mw/Mn*)
RH I	1082	636	1.7
RH II	1093	607	1.8
RH III	1366	784	1.7
RH IV	948	578	1.6
BG	1140	691	1.6
WS	1290	517	2.5
WC	1436	1104	1.3

Note: Gel permeation chromatography (GPC) sample was prepared with a concentration of ca. 5 mg/mL in THF solvent (HPLC grade).
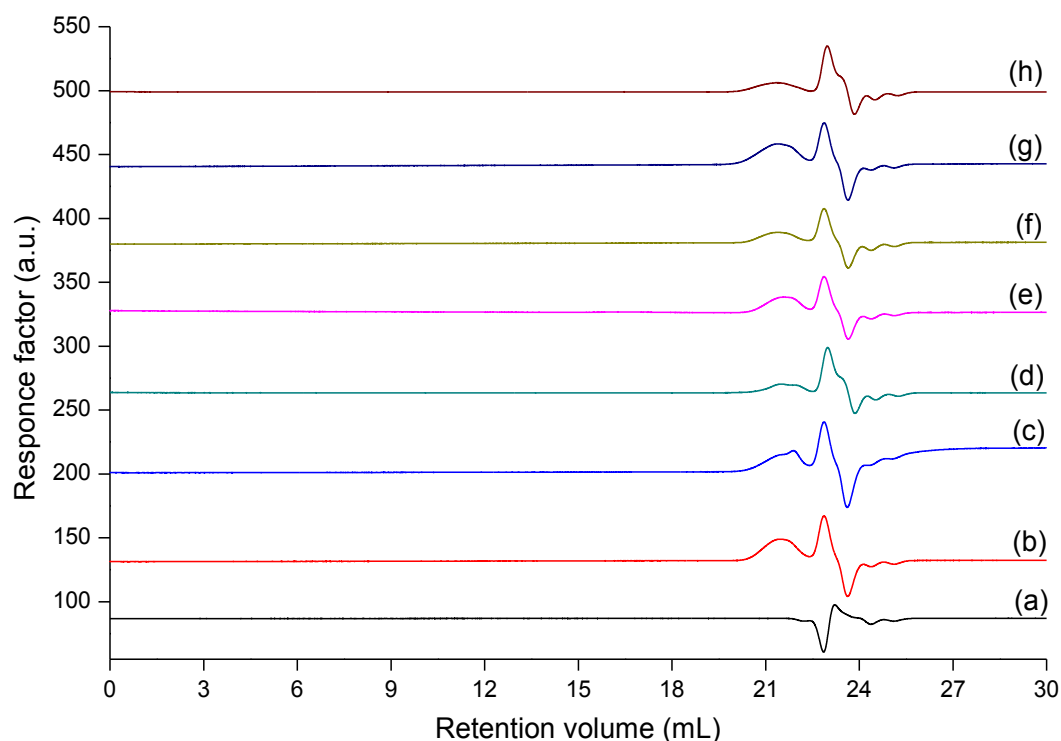
Figure 3B.4. GPC chromatograms of, (a) THF solvent, (b) RH I, (c) RH II, (d) RH III, (e) RH IV, (f) BG, (g) WS and (h) WC derived ORGL samples.

4B.3.1.4. Matrix-assisted laser desorption/ionization-time of flight mass spectrometry (MALDI-TOF MS)

The matrix assisted compound used was 2, 5-dihydroxy benzoic acid (DHB) for MALDI-TOF MS analysis. Lignin was dissolved in acetonitrile with a concentration of 1 mg/mL. The ORGL samples (1.5 µL) were overlaid on the golden MALDI-TOF MS target plate, waited for sample drying and placed matrix (1.5 µL) on the dried sample. The plate was kept for drying until the solvent was evaporated and then subjected to the analysis. The MALDI-TOF MS spectra are also in the line of average molecular weight of the ORGLs was ca. 1180 Da. The MALDI-TOF MS results were similar to the GPC results (1301, 1387, 1402 1000, 1187, 1310 and 1510 verses 1082, 1093, 1366, 948, 1140, 1290 and 1436 Da) for RH I, II, III, IV, BG, WS and WC ORGL samples, respectively, whereas the molecular weight was somewhat under estimated due to the change of GPC standard calibration sample. As the standard calibration was used unbranched/linear polystyrene and the ORGL samples were (RHs, BG, WS and WC) irregularly/branched.

4B.3.1.5. Thermogravimetric analysis (TGA)

The thermogravimetric analysis was done to check the thermal decomposition of lignin under wide range (50 to 800 °C) of temperature. As observed from Figure 4B.5, ORGLs derived from RHs, BG, WS and WC samples were stable until ∼200 °C and after that degradation or phase changes or mass loss of lignin was started. The weight losses of the ORGL samples were seen in the two steps. Wherein the first step, the weight loss (ca. 40%) was observed from 210 °C to 400 °C, it is due to the decomposition of cross link alkyl units.[15, 16] From the elemental analysis (for lignin samples), the average general monomer molecular formula of lignin was derived as $C_9H_{10}O_3$ (Table 4B.2).

From the elemental analysis (for lignin samples), the average general monomer molecular formula of lignin was derived as $C_9H_{10}O_3$ (Table 4B.2), which included the side chain and aromatic group. If the side chain is subtracted from this then the obtained formula will be C_8H_6, it mean that one aromatic ring and one ethylene group. The molecular formula weight of this (C_8H_6) is 102 g/mol, while the total molecular formula weight ($C_9H_{10}O_3$) is 166 g/mol from the average general monomer molecular formula of lignin. The general formula weight of aromatic and side ethylene groups covered the 61.44% of the total 100% of the average general monomer molecular formula of lignin, which is calculated as follows;

$$\text{The formula weight (\%)} = \frac{\text{molecular weight of aromatic and side ethelene groups}}{\text{molecular weight of the general monomer formula of lignin}} \times 100$$

$$= \frac{102}{166} \times 100$$

$$= 61.44\%$$

The total % of the general monomer molecular formula of lignin = [molecular weight of aromatic and side ethylene groups + side alkyl chain]

100%= [61.44 + side alkyl chain]%

Side alkyl chain= 38.56%

As observed from the Figure 4B.5 that lignin decomposition is seen in the two steps. Wherein, the first step decomposed ca. 40% weight loss, which belongs to side alkyl chains. Similarly, in the second steps remaining ca. 60% for the aromatic and ethylene groups were burned in the range between 450 ℃ to 620 ℃. this lignin degradation region is confirmed for the aromatic and ethylene groups.[16] Mass loss ca. <5% was remained and it devoted for mostly any inorganic compounds in the ash in all the ORGL samples.
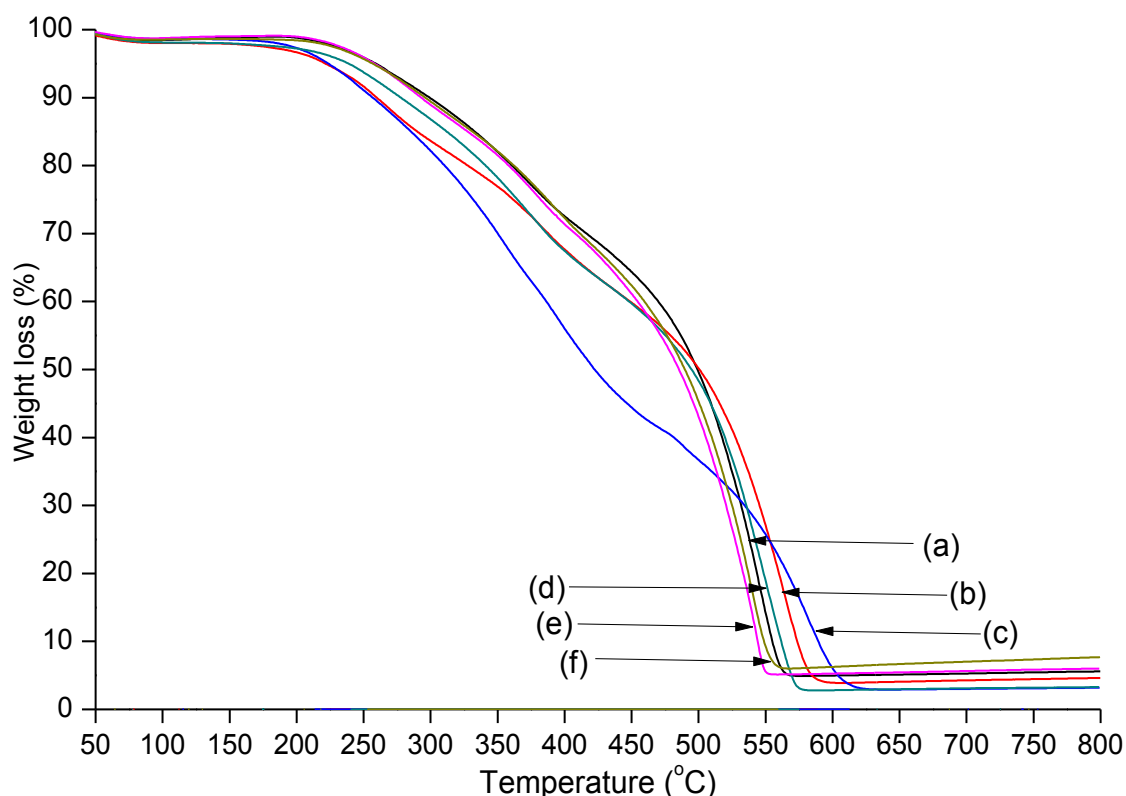
Figure 3B.5. Thermogravimetric analysis (Air) of ORGL derived from (a) RH I, (b) RH II, (c) RH III, (d) BG, (e) WS and (f) WC samples.

4B.3.1.6. Elemental analysis of crop waste, wood chip, pulp and isolated ORGL samples

The micro or elemental analysis is a crucial phenomenon for providing the exact ratios of the carbon, hydrogen, sulphur, nitrogen etc. present in the lignocellulosic materials. The C, H and O elemental composition of the crop waste and wood chip, isolated solid pulp and ORGL samples were carried out and the obtained results are consolidated in Table 4B.2.

Literature suggests that the O/C ratio in lignocellulosic materials ranges between 0.75-1.30 and in this work for RHs, BG, WS and WC samples, the observed O/C ratio ranges between 0.67-0.91. These values are very close to the literature values. After the extraction of ORGL from the

crop waste and wood chip samples, the generated pulp has higher O/C ratio (in a range between 0.9-1.4). This is because pulp has higher concentration of the polysaccharide (mixture of cellulose and hemicellulose), those have higher O/C ratio (in a range between 0.9-1.4). However, it is noticed from the Table 4B.2, the O/C ratio of the isolated lignin samples has decreased almost by two times compared to crop waste and wood chip. Due to the same observation, the higher heat values (HHV or also known as high heat potential as gross calorific value or gross energy) were obtained for these samples when calculated using Dulong's formula (Chapter 3, Section 3A.3.9. equation 3A.19).[15, 17] The HHV range between 2.0-2.5 times greater than RHs, BG, WS and WC crop waste and wood chip samples. As known the crop waste samples are consists of cellulose (mainly glucose C6 units $C_6H_{12}O_6$), hemicellulose (mainly xylose C5 units $C_5H_{10}O_5$), phenyl propenoids lignin units and inorganic constituents or ash. After extraction of ORGL from the crop waste and wood chip samples, the remaining solid pulp samples mainly have polysaccharides and ash. During the calculation of monomer molecular formula and HHV, the ash correction was given for the pulp samples. The monomer molecular formula of the pulp sample is $C_{6.0}H_{9.4}\text{-}_{9.7}O_{6.9}\text{-}_{8.3,}$ which is well matched with the theoretical values. Moreover, the double bond equivalence (DBE) or degree of unsaturation of the isolated ORGL samples was calculated (for details descriptions please see Chapter 3, Section 3A.3.9, equation 3A.20) and it is in the range of 4.3-5.3 of the ORGL samples and values are similar to the main building block units such as sinapyl, coniferyl and coumaryl alcohols (Chapter 1, Figure 1.3) present in the lignin substructure units (DBE= 5). For one benzene ring, DBE is equal to the 4.0 number and one for a double bond in conjugation (side alkene/carbonyl etc.). So the DBE ranges between 4.3- 5.3 suggests that in ORGL samples, one benzene ring along with one side chain of the double bond units is present. Further to check the acidic, basic or neutral nature of the ORGLs sample, the pH was measured (Table 4B.2) and it was confirmed that the isolated ORGL samples are neutral molecules or free from any acidic or basic contamination.

Table 4B.2. Elemental analysis of crop waste and wood chip, pulps and ORGL (oven dry basis) samples.

	Samples	Elemental analysis (wt.%)			MMF[b]	Ash, (wt.%)	HHV[c] (MJ/kg)	O/C ratio	DBE[d]	pH[e]
		C	H	O[a]						
Crop wastes and wood chip	RH I	36.9	5.6	47.7	$C_{6.2}H_{11.3}O_6$	14	11.9	1.0	-	-
	RH II	37.7	5.4	47.1	$C_{6.4}H_{11.0}O_6$	17	13.7	0.9	-	-
	RH III	37.2	5.7	47.4	$C_{6.3}H_{11.5}O_6$	12	12.3	1.0		
	RH IV	37.7	5.7	47.4	$C_{6.3}H_{11.5}O_6$	17	14.4	1.0	-	-
	BG	45.2	5.5	48.1	$C_{7.6}H_{11.4}O_6$	2	14.7	0.8	-	-
	WS	40.9	5.5	46.6	$C_{7.0}H_{11.3}O_6$	13	12.6	0.9	-	-
	WC	49.3	5.7	44.4	$C_{8.9}H_{12.3}O_6$	2	16.9	0.7		
Pulp	RH I	34.2	4.5	51.6	$C_{5.3}H_{8.2}O_{6.0}$	21	7.0	1.1		
	RH II	33.2	4.4	50.5	$C_{5.0}H_{8.0}O_{5.7}$	23	6.0	0.9		
	RH III	32.6	4.3	51.1	$C_{5.0}H_{7.9}O_{6.0}$	19	5.9	1.2		
	RH IV	33.6	4.4	51.5	$C_{6.0}H_{9.4}O_{6.9}$	22	6.5	1.2		
	BG	33.7	4.5	60.6	$C_{6.0}H_{9.6}O_{8.1}$	3	6.8	1.4		
	WS	34.1	4.5	53.4	$C_{6.0}H_{9.5}O_{7.1}$	17	7.0	1.2		
	WC	33.4	4.5	61.3	$C_{6.0}H_{9.7}O_{8.3}$	4	6.6	1.4		
ORGL	RH I	66.9	7.9	25.2	$C_{10.1}H_{12.8}O_3$	2	29.5	0.3	4.7	6.3
	RH II	68.3	8.1	23.7	$C_{11.5}H_{16.2}O_3$	2	30.5	0.3	4.4	6.5
	RH III	66.7	7.8	25.5	$C_{10.1}H_{12.8}O_3$	3	29.2	0.3	4.7	6.5
	RH IV	65.9	6.6	27.5	$C_{9.8}H_{11.6}O_3$	2	26.9	0.3	4.8	6.9
	BG	63.4	5.5	31.1	$C_{8.5}H_{8.4}O_3$	1	23.8	0.4	5.3	6.3
	WS	63.6	6.5	29.9	$C_{8.5}H_{10.4}O_3$	4	25.5	0.4	4.3	6.9
	WC	62.9	6.1	31.0	$C_{8.5}H_{9.7}O_3$	3	24.5	0.4	4.7	6.7

Where, [a]-calculation based on elemental analysis by using ('O' wt.%, after ash correction) = 100-('C' wt.% + 'H' wt.%), [b]-MMF-monomer molecular formula [c]-HHV-higher heat value in MJ/kg, [d]DBE-double bond equivalence and [e]-100 mg sample was suspended in 6 mL millipore water and shaking was done for 5 min. Later lignin which is insoluble in water was allowed to settle down and then pH was measured (pH of millipore water was 6.92 at 25.6 °C) 6.31.

4B.3.1.7. UV-Visible spectra

As it is well known from the literature, lignin contains various types of UV-Vis active functional groups such as -C=C-, -OCH$_3$, -CHO, -COOH, -OH, etc. Because of these groups biomass appears brown in colour. The characteristic UV-Vis absorption peaks for above mentioned groups were observed in ORGL samples (Figure 4B.6). Generally, benzene ring (-CH=CH-) present in the lignin structure shows absorption peak in a range between 200-220 nm for Π-Π* electronic transition. In the ORGL samples derived from the RHs, BG, WS and WC crop waste and wood chip, the UV-Vis absorption peak in this range (200-220 nm) was visible. Another absorption peak at 230 nm for the mono/di-substituted chromophoric groups such as –OCH$_3$, -CHO, -OAr, etc. with the benzene ring is observed. In the UV-Vis spectra, peaks at 280±4 nm was observed for sinapyl alcohol (*S*), 273±4 nm for guaiacyl alcohol (*G*) and 315±4 nm for *p*-hydroxyphenyl alcohol (*H*) units.[17, 18] The phenolic conjugated structural units (alkene or carbonyl units) peak patterns are also observed in the UV-Vis spectra at 300-320 nm.[19] Additionally, in the ORGL samples the UV-Vis absorption peaks observed in a range between 270-290 nm for the unconjugated phenolic group.[17] Although, the lower intensity at 278±2 nm in all the ORGL samples (except BG) are showing the low concentration of *S* units. It might be during the milder acid isolation process *S* units are converted into *G* units.
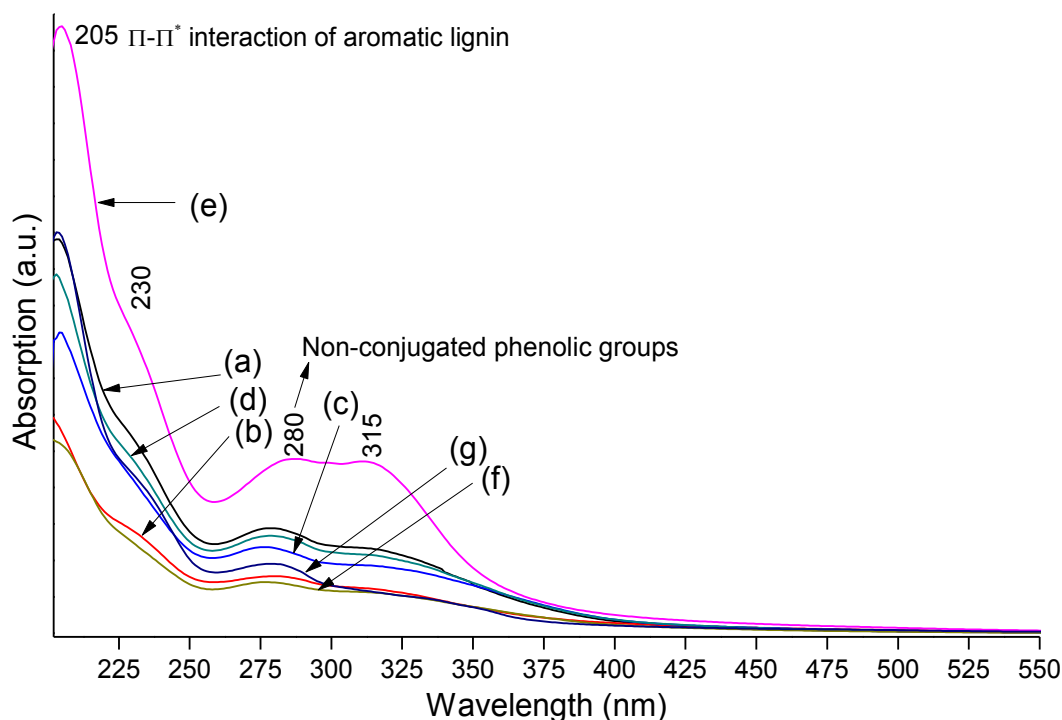
Figure 4B.6. UV-Visible spectra for ORGLs of (a) RH I, (b) RH II, (c) RH III, (d) RH IV, (e) BG, (f) WS and (g) WC, 1 mg sample was dissolved in 10 mL methanol solvent.

4B.3.1.8. ATR spectra

An advanced attenuated total reflection (ATR) technique was used to evaluate the chemical composition and functional groups present in the lignin structures. The ATR spectra for ORGL samples derived from RHs, BG, WS and WC crop waste and wood chip were recorded in the range between 700-3600 cm^{-1} and presented in Figure 4B.7. The details of the absorption peaks for the ORGL samples are also summarised in Table 4B.3.[15, 20, 21] Generally, the ATR stretching bands can be classified into three regions, 1) single bond region (-OH, -NH, -CH, etc.) from 3600 to 2750 cm^{-1}; 2) double and triple bond region (C=O, C=C, C≡C, N≡N, C≡N, etc.) from 2200 to 1500 cm^{-1} and 3) substituted or finger print or ring substituted region (ortho, meta and para, etc.) from 1500 to 700 cm^{-1}. In all the ORGL samples a weak-broad peak was observed for –OH groups in the range between 3330-3400 cm^{-1}. These –OH groups are mostly attached to aromatic skeleton and show weak intensity which implies that not many free –OH groups are available on lignin. This in turn may reflect the fact that in the *G*, *H* and *S* moieties of lignin on which free –OH groups are available are involved in formation of ether or ester linkages. It is anticipated that upon hydrolysis/depolymerization of these lignins, free –OH groups will be available on aromatic monomers. The observance of peak for –OH groups can also suggest that those are attached to aliphatic side chain structure since peaks for alkanes (-CH$_2$-OH) at ~3400 cm^{-1} and C-O stretch in alcohols (H$_2$C-OH) at ~1220 cm^{-1} were also observed. The peaks observed at 2920 and 2853 cm^{-1} are assigned to the -C-H stretching in the methyl (sp^3; -CH$_3$), methylene (sp^2; =CH$_2$ /-CH$_2$-) or methoxy (sp^3; -OCH$_3$) groups present in the isolated ORGLs structures. The two characteristic peaks for the aldehyde (-C-H) were seen in 2700-2760 and 2800-2860 cm^{-1} regions. However, a careful look at spectra reveals that in RHs (II and III) derived ORGL sample, highest peak intensity for these peaks was seen. On the other hand, BG derived ORGL sample showed lowest intensity for these peaks. This clearly indicates that RHs (II and III) containing ORGL sample has higher concentration of –CHO groups than any other samples. Thus it was possible to map the concentration of functionalities in different ORGL samples. This in turn would give understanding that upon hydrolysis it can be expected that RH derived ORGL may yield products with higher aldehyde functionality such as vanillin, cinnamaldehyde etc. In the double bond region, peaks with weak intensity observed at 1690-1735 cm^{-1} are attributed for the carbonyl stretching mode of ester (saturated) or anhydride groups or ketones in ORGL samples. A strong peak at 1705, 1740 and 1697 cm^{-1} observed in RHs (II and III) and BG derived ORGL samples reflects the fact that it can be assigned to aldehyde for RHs and ketone groups in BG since peaks for aldehyde were very intense and weak in RHs and BG samples at 2820-2720 cm^{-1}, respectively. The possibility of peak observed at 1697 cm^{-1} in BG derived ORGL sample due to ester group was less because typically they appear at higher wavenumber (>1720 cm^{-1}). The characteristic peaks at ~1600 and ~1510 cm^{-1} for aromatic

skeleton were observed in all the ORGL samples.[17, 22] Below 1500 cm^{-1} absorption peaks are typically called as finger print region or substituted functional groups at the aromatic ring (ortho, meta, para), these peaks are present in ORGL samples with having variable intensities and concise in the Table 4B.3. These bands are very difficult to assign, although most of the peaks are very complex, and also having with the contribution of the numerous vibrational mode. Yet, peaks under this region are particular to define the monolignols units like guaiacol alcohol (*G*), syringyl alcohol (*S*) and *p*-hydroxyphenol alcohol (*H*) present in the lignin substructure units. The bands of the ORGL samples represent the vibration characteristic peaks for the guaiacol alcohol unit at 1260±5 cm^{-1} and subsequent band at 1030 cm^{-1} for the C-O vibration modes of the aryl alkyl ether (Ar-O-CH$_3$) group and along with the same peaks another band at 1218 cm^{-1} are observed for the C-C, C-O or C=O stretching bands for the *G* unit. The peaks at 850 cm^{-1} is showing the C-H out of plane vibration for guaiacyl units at 2, 5 and 6 positions.[23] The spectra of the ORGL samples at 1320±5 cm^{-1}, which is the characteristic band for the aryl alkyl ether group of the syringyl alcohol (*S*) unit and 835±5 cm^{-1} peak arises for the C-H vibration out of plane in 2 and 6 positions of *S* unit.[23] A weak band in the range 1350-1370 cm^{-1} is originating for the phenolic -OH and aliphatic C-H groups, which is common for the isolated ORGL derived from RHs, BG, WS and WC samples. The stretching band with a strong vibration peak at 1210-1230 cm^{-1} can be represent for the C-C, C-O and C=O groups in ORGL samples.[23]
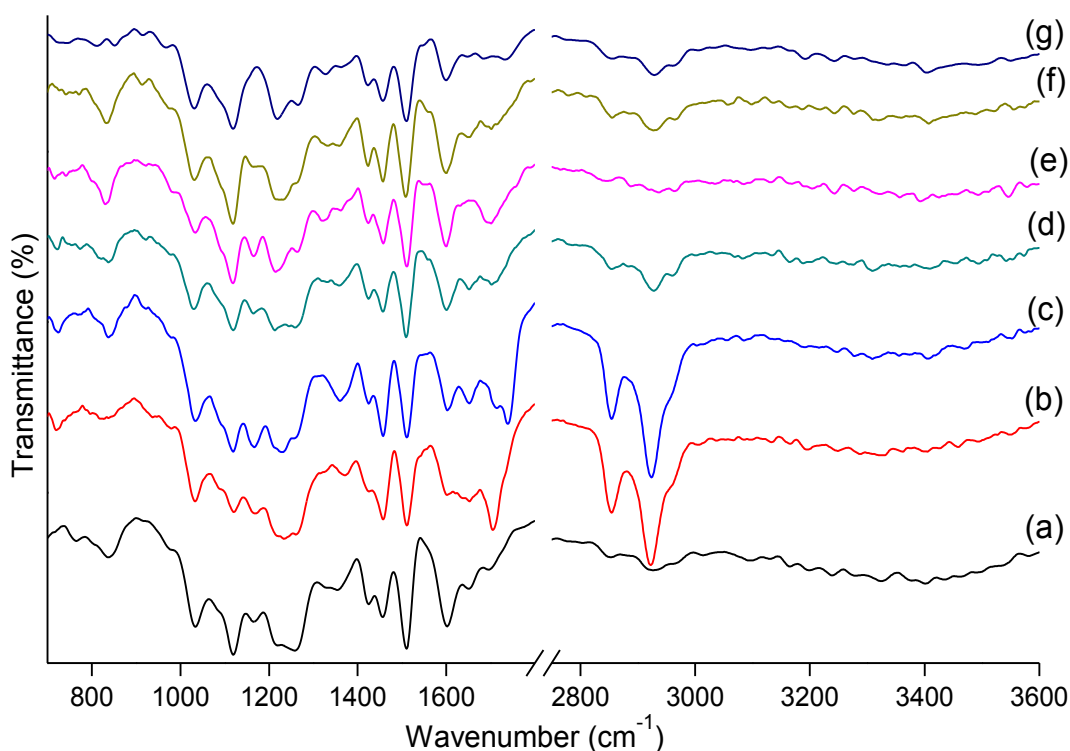
Figure 4B.7. ATR spectra of ORGL derived from (a) RH I, (b) RH II, (c) RH III, (d) RH IV, (e) BG, (f) WS and (g) WC crop waste and wood chip samples.

Table 4B.3. Summary on the ATR band of ORGL derived from RH I, RH II, RH III, RH IV, BG, WS and WC samples.

Bands (cm^{-1})	Assignments	Wavenumbers (cm^{-1})						
		RH I	RH II	RH III	RH IV	BG	WS	WC
3400-3300	O-H stretching	3395 (w)	3320 (w)	3350 (w)	3403 (b)	3403 (b)	3403 (b)	3400 (b)
2960-2920	C-H asymmetric stretching in methyl and methylene group	2960 (w), 2925 (w)	2960 (w), 2923 (s)	2960 (w), 2923 (m)	2965 (w), 2928 (m)	2967 (w), 2934 (w)	2967 (w), 2930 (m)	2967 (w), 2925 (m)
2850-2830	C-H symmetric stretching in methyl and methylene group	2850 (w)	2850 (s)	2850 (s)	2852 (m)	2846 (m)	2855 (m)	2855 (m)
1740-1680	C=O stretching in unconjugated ketone, carbonyl and ester groups	1700 (w)	1705 (s)	1740 (s), 1710 (w)	1706 (w)	1697 (m)	1700 (w)	1735 (w), 1690 (w)
1670-1640	C=O stretching in conjugated *p*-substituted aryl ketones	1650 (s)	1650 (w)	1650 (s)	1650 (w)	-	1650 (w)	1650 (w)
1610-1590	Aromatic skeleton vibration plus C=O stretching	1600 (s)	1600 (w)	1605 (m)	1600 (s)	1601 (s)	1600 (s)	1605 (s)
1515-1505	Aromatic skeleton vibrations	1510 (s)	1510 (s)	1510 (s)	1507 (s)	1510 (s)	1507 (s)	1507 (s)
1470-1450	C-H deformation (asymmetric in -CH$_3$ and –CH$_2$-)	1455 (w)	1455 (m)	1455 (s)	1456 (s)	1456 (s)	1459 (s)	1455 (s)
1440-1420	Aromatic skeleton vibrations combined with C-H in plane deformations	1420 (s)	1425 (w)	1425(m)	1423 (m)	1423 (w)	1423 (w)	1423 (m)
1370-1350	Aliphatic C-H stretching in CH$_3$ (not –OCH$_3$) and phenolic -O-H	1355 (w)	1370 (m)	1360 (s)	1354 (w)	1360 (w)	1360 (w)	1363 (w)

1270-1260	stretching C-H of *G* units	1260 (s)	1265 (w)	1265 (m)	1260 (m)	1260 (m)	1263 (m)	1266 (m)
1230-1210	C-C plus C-O plus C=O stretching (*G* condensed >*G* etherified, typical of *G* units)	1215 (s)	1230 (w)	1230 (m)	1215 (s)	1212 (s)	1231 (s)	1218 (s)
1170-1160	Typical for *H, G, S* units of lignin	1165 (m)	1170 (w)	1165 (s)	1165 (m)	1164 (m)	1164 (w)	-
1120-1115	Aromatic C-H in plane deformation	1120 (s)	1120 (m)	1120 (m)	1119 (s)	1119 (s)	1116 (s)	1119 (s)
1035-1030	Aromatic C-H in plane deformation (*G>S*) plus C-O deformation in primary alcohols plus C=O stretching (unconjugated)	1035 (s)	1035 (s)	1030 (s)	1029 (s)	1031 (s)	1031 (s)	1031 (s)
845-830	*p*- substituted phenolic	835 (s)	830 (w)	835 (m)	836 (m)	830 (s)	833 (s)	848 (w)

Notes: w: weak, m: medium and s: strong band intensities.

4B.3.1.9. 1D (^{1}H, ^{13}C) and 2D (HSQC) NMR characterization

The one dimensional (^{1}H and ^{13}C) and two dimensional (^{13}C/^{1}H) heteronuclear single quantum correlation (HSQC) NMR spectra were examined after dissolving ca. 60 mg ORGL sample in 700 μL deuterated DMSO solvent.[15, 21, 24]

4B.3.1.9.1. ^{1}H and ^{13}C NMR spectra

The ORGL derived from RHs, BG, WS and WC crop waste and wood chip samples were used for the proton NMR (Figures 4B.8a-4B.8g). The DMSO-d_6 solvent is consider as an internal reference (δ= 2.50 ppm for ^{1}H and δ= 39.50 ppm for ^{13}C). ^{1}H NMR is a reliable method to explain the proton skeleton of the ORGL samples. The proton NMR spectra in the range between δ= 0.8–1.7 ppm are elucidated the sp3 (primary), sp2 (secondary) and sp (tertiary) alkyl groups present in the ORGL samples. However, the signal for carbonyl group present in the ORGL samples linked by several functional groups (ketone/ester, Ar–CO–CH$_3$/ Ar/R–CH$_2$–COOR/Ar) or benzyl protons (Ar–CH$_3$) are assigned between the ranges of δ= 2.0-3.0 ppm. The most intense peak at δ= 3.4-3.5 ppm is assigned for the water present in the deuterated DMSO solvent. Methoxy (–OCH$_3$) and ester (Ar/R–COOCH$_2$R/Ar) proton peaks are observed at δ= 3.7-3.9 ppm in isolated ORGL samples with variable intensities.

Figure 4B.8. 1D (^{1}H and ^{13}C) NMR spectra of ORGL derived from (a, n) RH I; (b, i) RH II; (c, j) RH III; (d, k) RH IV; (e, l) BG; (f, m) WS and (g, n) WC crop waste and wood chip samples. All the NMR spectra were recorded in the DMSO-d_6 solvent. Peaks assigned by † (^{1}H) and ‡ (^{13}C) indicate for deuterated DMSO-d_6 solvent.

Another significant peak at δ= 5.3 ppm in the ORGL derived from the crop waste and wood chip samples resulted due to the presence of alkene type moieties (-CH=CH-). However, the main building block penylpropenoids units such as *S, G, H* and tricin (*T*) moieties present in the ORGL samples are observed at δ= 6.0-8.5 ppm range for the aromatic (–CH) protons with analogous peak intensities.

To correlate the peaks present in the proton NMR, ^{13}C spectra were examined for ORGL derived from RHs, BG, WS and WC samples and those are represented in Figures 4B.8h-4B.8n. Typically, ^{13}C NMR peaks for the alkyl side chains were assigned for -CH$_3$, -CH$_2$-, -CH-, -C-, CH$_3$CO- species, etc. in the range between δ= 10.0−50.0 ppm, it is documented from ^{13}C NMR spectra of ORGL samples having variable peaks intensities. Interesting results for various inter linkages units, the observance of peaks at 60−90 ppm are attributed to the carbon appearing next to allyl/oxygen/aromatic ring (-CH=CH$_2$; Ar/R−CH$_2$−O−; Ar$_2$/R$_2$−CH−O−; Ar$_3$/R$_3$−C−O−). However, peaks for the alkene (-C=C-) or aromatic (*H, G, S* and *T* moieties) carbon were also observed in the range between δ= 100-140 ppm for the isolated ORGL derived from RHs, BG, WS and WC samples.

4B.3.1.9.2. 2D (HSQC) NMR spectra

The 2D heteronuclear single quantum correlation (HSQC) NMR analysis were carried out to characterize ORGL (Figure 4B.9) derived from RHs, BG, WS and WC samples in the deuterated DMSO solvent. Signals at δ= 2.5 ppm (^{1}H NMR) and δ= 39.5 ppm (^{13}C) were considered as reference signals to assign the 2D (HSQC) NMR signals. To understand the various types of sub-structural units, different linkages and variable chemical moieties present in the isolated ORGL samples, the obtained 2D (HSQC) NMR results are correlated with available reports.[15, 21, 25-27] However, the variable chemical composition of the major inter-structural linkages units present in the ORGL samples [i.e., β-O-4′ ether linkage (A); phenylcoumaran (β-5′; α-O-4′ linkage) (B); cinnamyl alcohol (I); tricin (T); phenylpropenoid type substructure units; *p*-hydroxyphenyl alcohol (*H*), guaiacyl alcohol (*G*), syringyl alcohol (*S*) and *p*-hydroxybenzoate (PB)], were observed in the isolated ORGL samples derived from RHs, BG, WS and WC samples and confirmed with the help of 2D (HSQC) NMR spectra (Figure 4B.9).

The 2D (HSQC) NMR spectra of the isolated ORGL lignin samples are divided into three subsequent regions; wherein 1) alkylated side chain region or saturated hydrocarbons (δ$_C$/δ$_H$= 10.0-50.0/0.5-2.5 ppm); 2) oxygenated aliphatic/aromatic regions (δ$_C$/δ$_H$= 50.0−90.0/2.5-6.0 ppm) and 3) the most affective olefinic/aromatic regions (δ$_C$/δ$_H$= 100.0-140.0/6.0-8.5 ppm) present in the isolated ORGL derived from the crop waste and wood chips samples.

The alkylated signals were detected in range of δ$_C$/δ$_H$= 10.0-50.0/0.5-2.5 ppm for the terminal or bridge aliphatic hydrocarbons, it might be close to the carbonyl group or attached with the olefinic/aromatic rings, for more detailed at the obtained results for ORGL samples are

given in Table 4B.4. However, presence of the numbers of side chain of alkylated groups clearly supports that inter linkage units are present in the ORGL samples. Consequently, based on the 2D (HSQC) NMR spectra of alkylated region δ_C/δ_H= 10.0–50.0/0.5-2.5 ppm, it is not possible to differentiate the lignin sub-structural moieties.

Linkages region of the 2D (HSQC) NMR spectra

The inter linkage units (alkylated group attached with hetero atom or next to olefins/aromatic rings) present in the ORGL samples are noticed in the range between δ_C/δ_H= 50.0–90.0/2.5-6.0 ppm in the 2D (HSQC) NMR spectra Figures 4B.9a-9g.

The 2D (HSQC) NMR signals at δ_C/δ_H= 55.68-55.38/3.74-3.59 ppm are assigned to presence of –OCH$_3$ group in ORGL samples with variable intensities. However, the most intense signal for –OCH$_3$ group is observed in the ORGL derived from WS crop waste samples, which are having two methoxy (in '*S*' type moieties) groups at aromatic ring, and the 2D (HSQC) NMR signal for the '*S*' moieties is more in concentration in WS sample than ORGLs derived from RHs, BG and WS samples. The Hγ-Cγ within cinnamyl alcohol unit (Iγ) is seen at the range between δ_C/δ_H= 59.65-59.64/4.04-4.03 ppm in ORGL samples derived from the crop waste and wood chip except ORGL derived from WC sample. The 2D (HSQC) signal at δ_C/δ_H= 59.64-60.32/3.40-3.60 ppm are noticed due to presence of Hγ-Cγ within Aγ lignin substructure for β-O-4 linkage unit in all the ORGL samples with variable intensities. However, 2D (HSQC) signal ORGL derived from WS sample is having more concentration for the Aγ than the other ORGL samples. Similarly, the most intense signal for the tricin aromatic moieties is also well match to confirm the Aγ concentration in ORGL derived from WS sample. The phenylcoumaran sub-structure linkage Hγ-Cγ within β-5 unit is also seen at δ_C/δ_H= 62.59-62.18/3.73-3.36 ppm in the 2D (HSQC) NMR spectra of the ORGL samples. However, 2D (HSQC) signals at δ_C/δ_H= 63.90-63.80/3.33-3.31 ppm could not be identified based on the lignin assign NMR signal from the literature. These signals are considered for the alkylated side chain attached with the hetero atoms or olefinic bonds. It is affirmed that these signals may belong to sub-structural (A) or (B) units. As seen from Table 4B.4 for 2D (HSQC) NMR spectra peaks, ORGL derived from the WS is showing the maximum similarities with other ORGL samples, which confirmed that it contained more sub-structural units than others. The signal at δ_C/δ_H= 86.95/5.43 ppm are assigned for the Cα-Hα at β-5' phenylcoumaran (Bα) structural unit present in the ORGL derived from RHs (I and IV) and WC samples.
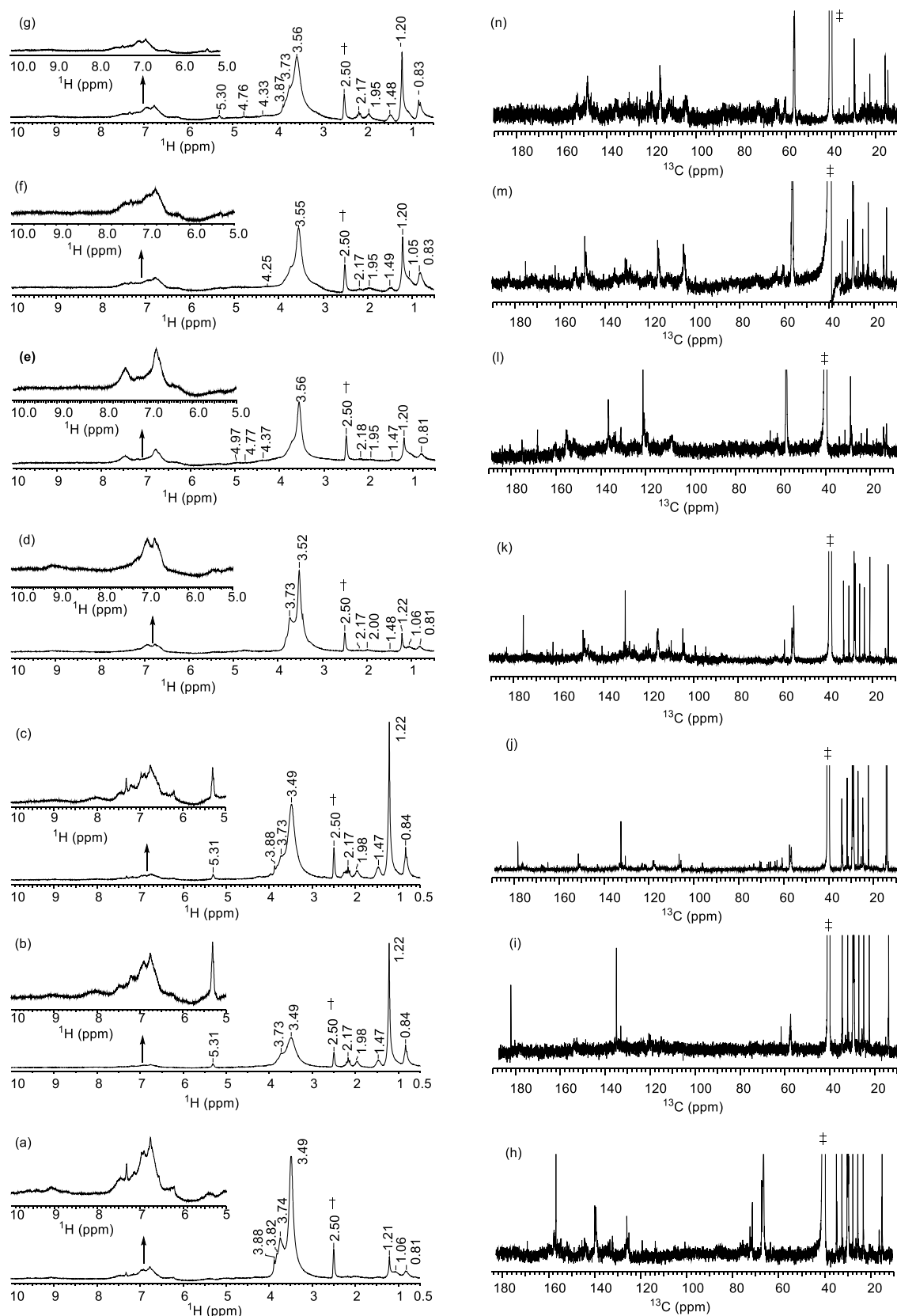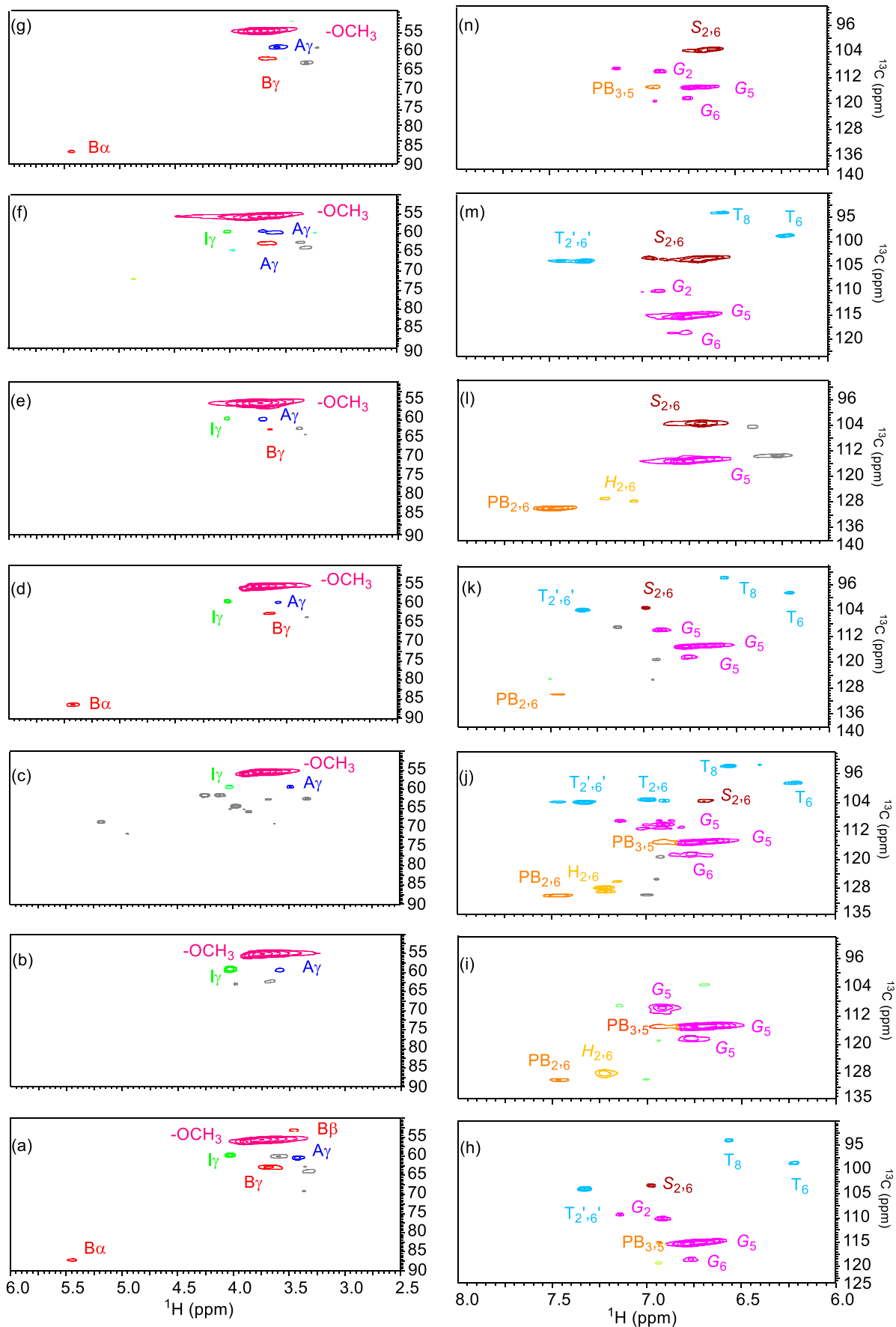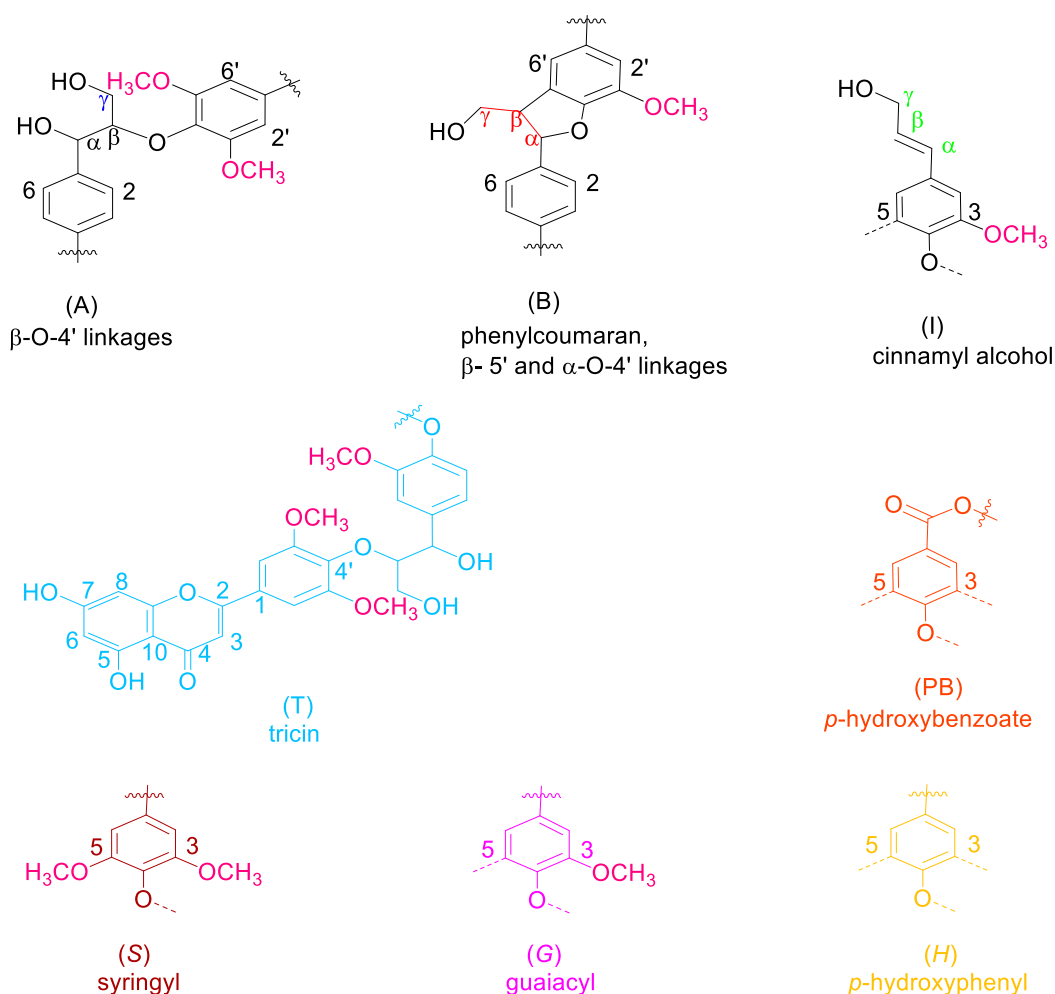
Figure 4B.9. 2D (HSQC) NMR spectra of ORGLs derived from (a, n) RH I; (b, i) RH II; (c, j) RH III; (d, k) RH IV; (e, l) BG; (f, m) WS and (g, n) WC crop waste and wood chip samples and main substructure units present in lignin. All the NMR spectra were recorded in the DMSO-d$_6$ solvent.

Olefinic/aromatic region of the 2D (HSQC) NMR spectra

The lignin sub-structural units are made up of alkylated, arylated (*S*, *G* and *H* units), olefinic and various types of inter structural linkage units as shown in Figures- 4B.9h-4B.9n. The detail of the 2D (HSQC) NMR signals for olefinic/aromatic [*p*-hydroxyphenyl alcohol (*H*), guaiacyl alcohol (*G*) and syringyl alcohol (*S*) moieties] regions are summarized in Table 4B.4. The C$_8$-H$_8$ (T$_8$, δ_C/δ_H= 93.68-94.15/6.56-6.57 ppm), C$_6$-H$_6$ (T$_6$, δ_C/δ_H= 98.37-98.73/6.21-6.23 ppm) and C'$_{2,6}$-H'$_{2,6}$ (T'$_{2,6}$, δ_C/δ_H= 103.19-103.95/6.68-6.98 ppm) within tricin (T) molecule, these signals are assigned in the ORGL originated from the RHs (I, III and IV) and WS samples. Remarkably, C$_8$-H$_8$ (T$_8$) and C$_6$-H$_6$ (T$_6$) substructure moieties were missing in ORGL samples derived from RH II, BG and WC samples (Figures- 4B.9i, 4B.9l and 4B.9n). The peaks at δ_C/δ_H= 110.05-110.17/6.91 ppm for *G*$_2$, δ_C/δ_H= 115.0-115.43/6.75-6.78 ppm for *G*$_5$ and δ_C/δ_H= 119.31/6.93 ppm for the *G*$_6$ signals are observed in the ORGL derived from crop waste and wood chip samples. The *S*$_{2,6}$ structural units present in the ORGL samples are detected at δ_C/δ_H= 103.19-103.95/6.68-6.99

ppm. The peaks at δ_C/δ_H= 114.87/6.94 ppm for the $PB_{3,5}$ unit present in the ORGL derived from RHs (I-III) and WC samples. It is fascinating result observed that the peaks because of *H* substructure is not visualised in ORGL derived from RHs (I and IV), WS and WC samples. Similarly, the $PB_{2,6}$ signals were seen in ORGL derived from RHs (II-IV) and BG samples. Beside, these peaks few phenylpropenoid peaks are also detected but those are not identified based on the available report for lignin molecules as consolidated in Table 4B.4.

Table 4B.4. Assignments of 2D (^{13}C/^{1}H, HSQC) NMR of ORGLs derived from RHs, BG, WS and WC samples.

δ_C/δ_H (ppm) ORGL samples							Labels	Assignments
RH I	RH II	RH III	RH IV	BG	WS	WC		
56.03/ 3.75	55.95/ 3.74	56.04/ 3.76	55.48/ 3.74	55.38/ 3.73	55.68/ 3.73	55.48/ 3.74	-OCH$_3$	C-H in methoxyls
60.32/ 3.42	59.97/ 3.58	59.88/ 3.49	59.64/ 3.57	59.64/ 3.71	59.84/ 3.61	59.64/ 3.59	A$_\gamma$	H$_\gamma$- C$_\gamma$ in β-O-4' substructures (A)
60.07/ 4.03	59.88/ 4.03	60.07/ 4.04	59.65/ 4.04	59.64/ 4.04	59.64/ 4.03	-	I$_\gamma$	H$_\gamma$-C$_\gamma$ in cinnamyl alcohol end group (I)
63.04/ 3.68	-	-	62.59/ 3.65	62.18/ 3.39	62.38/ 3.36	62.58/ 3.73	B$_\gamma$	H$_\gamma$-C$_\gamma$ in β-5' phenylcoumaran substructures (B)
-	-	-	-	62.48/ 3.65	62.69/ 3.67	-	-	-
63.86/ 3.33	-	63.14/ 3.34	63.86/ 3.33	63.90/ 3.31	63.80/ 3.31	63.80/ 3.32	-	-
87.60/ 5.46	-	-	86.95/ 5.43	-	-	86.95/ 5.43	B$_\alpha$	H$_\alpha$-C$_\alpha$ in β-5' phenylcoumaran substructure (B)
94.57/ 6.57	-	94.79/ 6.57	93.68/ 6.57	-	94.15/ 6.57	-	T$_8$	H$_8$-C$_8$ in tricin (T)
99.29/ 6.22	-	99.32/ 6.22	98.37/6. 21	-	98.73/ 6.23	-	T$_6$	H$_6$-C$_6$ in tricin (T)
103.95 /6.99	-	103.93/ 7.0	103.19/ 6.99	103.57/ 6.69	103.48 /6.68	103.95 /6.68	$S_{2,6}$	H$_{2,6}$-C$_{2,6}$ in (*S*)
104.68 /7.34	-	103.93/ 7.36	103.95/ 7.33	-	103.82 /7.31	-	T'$_{2,6}$	H'$_{2,6}$-C'$_{2,6}$ in tricin (T)
-	-	-	-	-	103.39	-	-	-

					/6.96			
-	-	104.60/ 7.48	-	-	103.90 /7.43	-	-	-
-	-	-	-	104.59/ 6.41	-	-	-	-
-	-	-	109.16/ 7.14	-	-	109.16 /7.14	-	-
110.71 /6.93	110.36 /6.91	110.86/ 6.92	110.05/ 6.91	-	110.09 /6.91	110.17 /6.91	G_2	H_2-C_2 in (H)
			-	113.47/ 6.27	-	-	-	-
115.7/ 6.90	115.6/ 6.92	115.76/ 6.93	-	-	-	114.87 /6.94	$H_{3,5}$	$H_{3,5}$-$C_{3,5}$ in (H)
115.85 /6.77	115.6/ 6.76	115.76/ 6.78	115.12/ 6.75	115.25/ 6.78	115.43 /6.78	115.0/ 6.75	G_5	H_5-C_5 in (G)
-	115.7/ 6.62	115.60/ 6.53	-	-	-	115.6/ 6.75	$PB_{3,5}$	$H_{3,5}$-$C_{3,5}$ in p-hydroxy benzoate (PB)
119.11 /6.78	118.92 /6.76	119.29/ 6.78	119.31/ 6.93, 118.42/ 6.76	-	-	119.32 /6.93, 118.42 /6.75	G_6	H_6-C_6 in (G)
-	128.2/ 7.22	128.4/ 7.23	-	127.05/ 7.2	127.82 /7.21	-	$H_{2,6}$	$H_{2,6}$-$C_{2,6}$ in (H)
			-	127.81/ 7.05	-	-	-	-
-	130.90 /7.49	130.5/ 7.47	130.10/ 7.46	129.97/ 7.47	130.1/ 7.44	-	$PB_{2,6}$	$H_{2,6}$-$C_{2,6}$ in p-hydroxy benzoate (PB)
Note: (-) not assigned.								

4B.4. Depolymerization of ORGLs

Among all the homogeneous acidic ionic liquids were evaluated as catalysts (Chapter 3, Sections 3B.3.1 and 3B.3.2) in dealkaline lignin depolymerization reaction, [C_3SO_3HMIM][HSO_4] and I-BAIL gave the highest THF soluble products yield 78% and 90 respectively. Considering this, further the isolated ORGLs depolymerization studies were carried out with this catalyst. After the optimization of reaction parameters for the deakaline lignin depolymerization various isolated ORGLs derived from RHs, BG, WS and WC crop waste and wood chip samples were evaluated under similar reaction parameters. For all the reactions, ORGL (2 *wt.*% solution H_2O:CH_3OH, 1:5 *v/v*= 30 mL) and [C_3SO_3HMIM][HSO_4] or I-BAIL (0.5g) catalyst were taken and the reactor was warmed up to desired temperature under slow stirring (100 rpm). After attaining the desired temperature, stirring speed was increased to 1000 rpm and this time was noted as starting time of lignin depolymerization reaction. At this 120 ºC, ([C_3SO_3HMIM][HSO_4]) or 200 ºC (I-BAIL), the pressure generated in the autoclave was 0.35 MPa or 3.2 MPa respectively due to water and methanol. After completion of reaction, reactor was allowed to cool to room temperature under the flow of air and slow stirring (100 rpm).

4B.4.1. Depolymerization of ORGLs using [C_3SO_3HMIM][HSO_4] BAIL

Depolymerization of isolated lignins was done using [C_3SO_3HMIM][HSO_4] BAIL catalyst (Figure 4B.10), and obtained product have shown variable range of organic solvent soluble (Ethyl acetate and diethyl ether) products (11-36% yield). In this wok, THF is not used to extract the products since ORGLs are soluble in THF. It is important to mention here that the obtained result confirmed that under this reaction condition, catalyst is able to convert ORGLs into low molecular weight aromatic products with diverse physico-chemical properties. Also it is vital to state that in various lignins different subunits, linkages and functional groups are present. The ORGLs are insoluble into the EtOAc and DEE so these organic solvents are selected for the extraction of obtained low molecular weight aromatic products after lignin depolymerization.
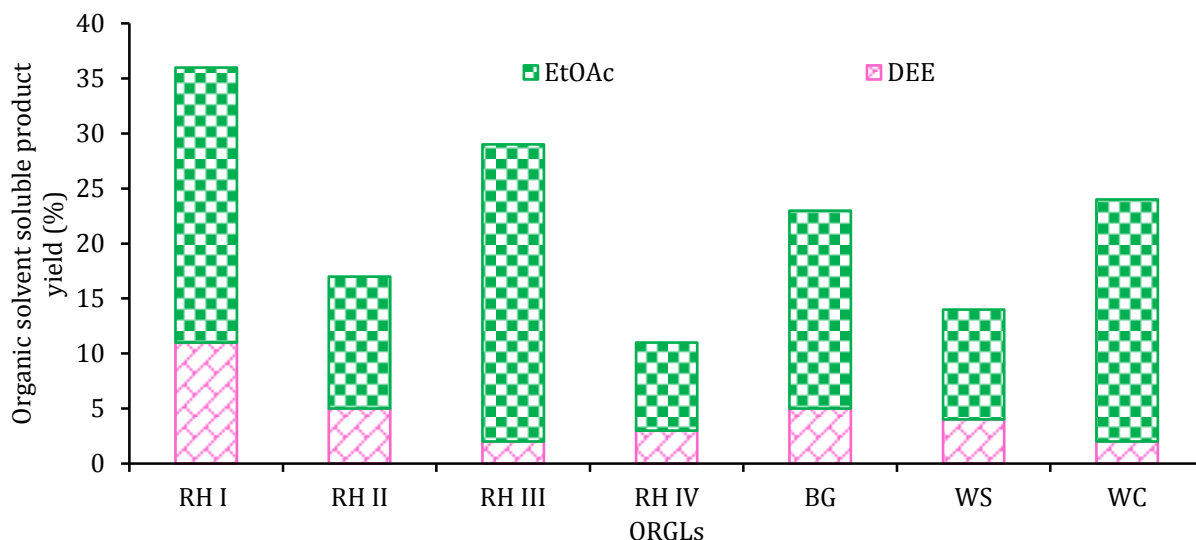
Figure 4B.10. Depolymerization of ORGLs using [C$_3$SO$_3$HMIM][HSO$_4$] catalyst. Reaction condition: lignin (2 *wt*.% solution H$_2$O:CH$_3$OH, 1:5 *v/v*= 30 mL), [C$_3$SO$_3$HMIM][HSO$_4$] (0.5 g), 120 $^{\circ}$C, 1 h, 1000 rpm.

Values are average of three reactions with ±2% error observed.

4B.4.2. Depolymerization of ORGLs using I-BAIL

As discussed in the Chapter 3, Section 3C.2.4, the I-BAIL as solid acid catalysts evaluated for dealkaline depolymerization reaction since I-BAIL gave the highest THF soluble products (90%), further the depolymerization of isolated ORGL derived from various crop waste and wood chip samples were evaluated with I-BAIL catalyst. After the dealkaline lignin depolymerization reaction with I-BAIL, the similar reaction parameters were applied with Isolated ORGL samples. For all the ORGL depolymerization reactions, lignin (2 *wt*.% solution H$_2$O:CH$_3$OH, 1:5 *v/v*= 30 mL) and I-BAIL (0.5 g) catalyst were applied at 200 $^{\circ}$C in 1 h and the reactor was warmed up to desired temperature under slow stirring (100 rpm). After reaching the desired temperature the stirrer speed was increased up to 1000 rpm and this time was considered the reaction beginning time. Under these reaction conditions, the auto-generated pressure was 3.2 MPa. After completion of reaction, reactor was allowed to cool at room temperature and further continue for the work up of reaction mixture.

After lignin depolymerization, low molecular weight aromatic products were extracted using different (EtOAc and DEE) organic solvents. The organic solvents soluble products yield were obtained in the range between 46-56%. The variation in the yield is obvious due to its structural dissimilarities, which is proven by the several characterization techniques in the current Section. The I-BAIL results are different with the [C$_3$SO$_3$HMIM][HSO$_4$] catalytic result, due to application of high temperature, auto-generated pressure (3.2 MPa) and difference in acid amount (H$^+$ concentration) in/on I-BAIL catalyst. The lignin obtained from WS is showing the good yield of organic solvent soluble products than the other ORGLs. However the isolated

ORGLs from crop waste and wood chip samples are showing almost comparable (50± 5%) results for the organic solvent soluble products.
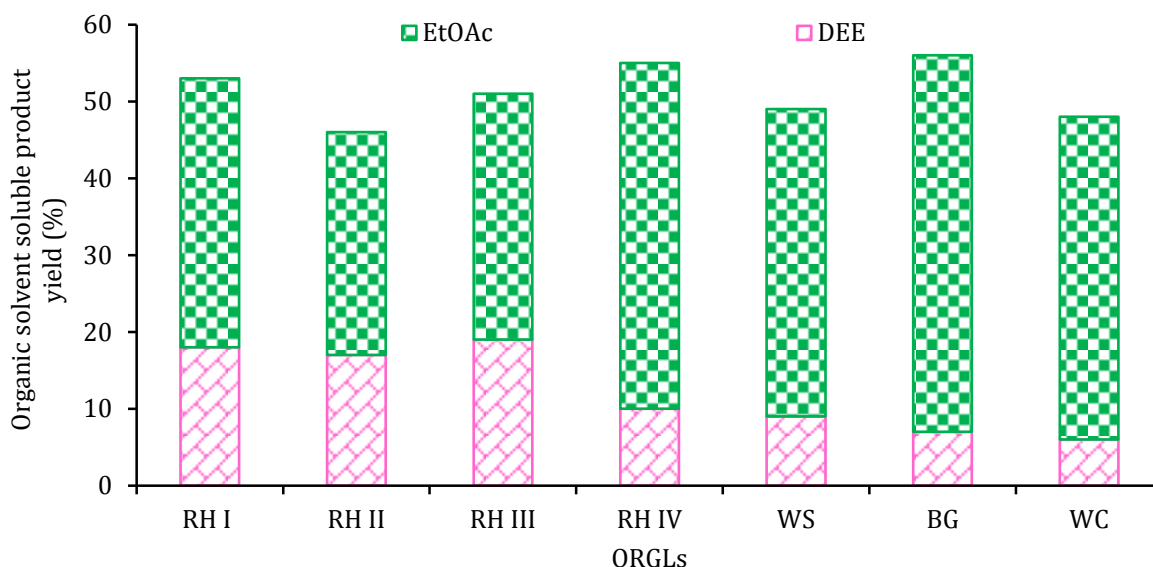
Figure 4B.11. Depolymerization of ORGLs using I-BAIL catalyst. Reaction condition: lignin (2 *wt*.% solution H_2O:CH_3OH, 1:5 *v/v*= 30 mL), I-BAIL (0.5 g), 200 °C, 1 h, 1000 rpm. Values are average of three reactions with ±2% error observed.

The result of dealkaline lignin and ORGL samples depolymerization reactions into low molecular weight aromatic products yield are different under the similar reaction condition. This dissimilarity in results is occurred due to the difference in their physico-chemical properties. As observed from the 1D (^{1}H and ^{13}C) and 2D (HSQC) NMR spectra of the dealkaline lignin and ORGL samples, the 1D spectra of dealkaline lignin is showing minimum signals (Figure 3A.10) for the alkylated regions, while in the ORGL samples, these signals are more intense. It means that ORGL samples contained maximum ≡C-C≡ units than dealkaline lignin. It is also reported in the literature that ORGL sample have maximum ≡C-C≡ linkage than the other types of lignin. Moreover to 1D result, 2D (HSQC) NMR spectra are recorded for dealkaline and ORGL samples, the dealkaline lignin has higher concentration of linkage signals (δ= 50-90/3.0-6.0 ppm), which confirmed that after lignin depolymerization under acidic condition, these bonds will get hydrolysed and gave maximum yield of low molecular weight aromatic products. Additionally, the ATR spectra of dealkaline lignin and ORGL samples are also recorded and these results are in line with the NMR result. The strong C-O bond is observed at 1029 cm^{-1} in the dealkaline lignin, while it is weak and observed at 1025-1035 cm^{-1} in the ORGL samples. The NMR and ATR molecular levels analysis suggest that dealkaline lignin have maximum linkages, so these bonds get depolymerized during the acid hydrolysis reaction and gave maximum yield of low molecular weight aromatic products.

4B.5. Conclusions

In summary, it is noted that though similar isolation method, organosolv is used to extract lignin from different crop waste and wood chip samples, their physico-chemical properties vary. ATR spectra of ORGL derived from RHs, BG, WS and WC samples demonstrated that the isolated lignins are pure without any polysaccharides contamination. Additionally, due to absence of any signals in NMR due to polysaccharides, it was further proven that the lignin extracted from crop waste and wood chip materials is pure. Inter structural units of lignin were also extensively characterized by UV-Vis, ATR and 2D (HSQC) NMR techniques (Figures 4B.7-4B.9). It was observed that the ORGLs were composed of *S*, *G* and *H* units and among them *G* units were present in the major quantity (Figures 4B.7 and 4B.9). The similar observation was also made from UV-Vis analysis. However, RHs (I and III) WS and WC derived ORGL samples, signals due to T substructure is seen. This shows that if depolymerization of these lignins is carried out products distribution would be slightly different but majority of the products formed would be similar. Furthermore, according to the MALDI-TOF MS spectra as discussed in Section 4B.3.1.4, the average molecular weight of the crop waste and wood chip extracted ORGLs was ca. 1200 Da. Consequently, it is concluded that ORGL derived from crop waste and wood chip samples are comprised of ca. 8 consistent phenyl propenoid of *H*, *G, S* and T units. GPC analysis showed the 1082, 1093, 1366,948, 1140, 1290 and 1436 Da, with a PDI of 1.7, 1.8, 1.7, 1.6, 1.6, 2.5 and 1.3 for RH I, II, III, IV, BG, WS and WC ORGL samples, respectively, MALDI-TOF MS results were in line with the observations made in GPC results (1301, 1387, 1402 1000, 1187, 1310 and 1510 verses 1082, 1093, 1366,948, 1140, 1290 and 1436 Da) for RH I, II, III, IV, BG, WS and WC ORGL samples, respectively). As it was predicted from the literature that substrate having different linkages and moieties, after depolymerization gave the different products yield. Considering this, the depolymerization of all ORGL samples were carried out and the varying organic solvent aromatic products yield (11-56%) with $[C_3SO_3HMIM][HSO_4]$ and I-BAIL catalysts were obtained even if ORGLs isolation processed under similar reaction conditions.

4B.6. References

1.   R. Behling, S. Valange and G. Chatel, *Green Chem.*, 2016, **18**, 1839-1854.

2.   M. H. Hussin, A. A. Rahim, M. N. Mohamad Ibrahim, D. Perrin, M. Yemloul and N. Brosse, *Polym. Degrad. Stab.*, 2014, **109**, 33-39.

3.   K. Barta, G. R. Warner, E. S. Beach and P. T. Anastas, *Green Chem.*, 2014, **16**, 191-196.

4.   K. V. Sarkanen, *In The Chemistry of Wood*, Browning, B. L., Ed.; Interscience, New York, 1963.

5.   A. A. Guilherme, P. V. F. Dantas, E. S. Santos, F. A. N. Fernandes and G. R. Macedo, *Braz. J. Chem. Eng.*, 2015, **32**, 23-33.

6.   P. Bhaumik and P. L. Dhepe, *RSC Adv.*, 2014, **4**, 26215-26221.

7. Congcong Chi, Z. Zhang, W. Ge and H. Jammmel, *BioResources*, 2009, **4**, 537-543.

8. S. Tang, G. A. Baker, S. Ravula, J. E. Jones and H. Zhao, *Green Chem.*, 2012, **14**, 2922-2932.

9. Y. Wu, Z. Fu, D. Yin, Q. Xu, F. Liu, C. Lu and L. Mao, *Green Chem.*, 2010, **12**, 696-700.

10. K. Chakraborty, J. Saha, U. Raychaudhuri and R. Chakraborty, *Food and Nutrition Sciences*, 2015, **Vol.06No.10**, 9.

11. S. Youssefian and N. Rahbar, *Scientific Reports*, 2015, **5**, 11116.

12. G. M. Irvine, *Wood Sci. Technol.*, 1985, **19**, 139-149.

13. Y. Pu, F. Hu, F. Huang, B. H. Davison and A. J. Ragauskas, *Biotechnol. Biofuels*, 2013, **6**, 15-27.

14. S. Kasakov, H. Shi, D. M. Camaioni, C. Zhao, E. Barath, A. Jentys and J. A. Lercher, *Green Chem.*, 2015, **17**, 5079-5090.

15. S. K. Singh and P. L. Dhepe, *Bioresour. Technol.*, 2016, **221**, 310-317.

16. R. Sun, J. Tomkinson and G. Lloyd Jones, *Polym. Degrad. Stab.*, 2000, **68**, 111-119.

17. X. Zhao, L. Dai and D. Liu, *J. Appl. Polym. Sci.*, 2009, **114**, 1295-1302.

18. H. Yang, Y. Xie, X. Zheng, Y. Pu, F. Huang, X. Meng, W. Wu, A. Ragauskas and L. Yao, *Bioresour. Technol.*, 2016, **207**, 361-369.

19. U. Westermark, *Wood Sci. Technol.*, 1985, **19**, 223-232.

20. W. Li, N. Sun, B. Stoner, X. Jiang, X. Lu and R. D. Rogers, *Green Chem.*, 2011, **13**, 2038-2047.

21. S. K. Singh and P. L. Dhepe, *Green Chem.*, 2016, **18**, 4098-4108.

22. A. Tejado, C. Pena, J. Labidi, J. M. Echeverria and I. Mondragon, *Bioresour. Technol.*, 2007, **98**, 1655-1663.

23. C. G. Boeriu, D. Bravo, R. J. A. Gosselink and J. E. G. van Dam, *Ind Crop Prod*, 2004, **20**, 205 - 218.

24. K. Barta, T. D. Matson, M. L. Fettig, S. L. Scott, A. V. Iretskii and P. C. Ford, *Green Chem.*, 2010, **12**, 1640-1647.

25. N. D. Bonawitz, J. I. Kim, Y. Tobimatsu, P. N. Ciesielski, N. A. Anderson, E. Ximenes, J. Maeda, J. Ralph, B. S. Donohoe, M. Ladisch and C. Chapple, *Nature*, 2014, **509**, 376-380.

26. M. Foston, R. Samuel, J. He and A. J. Ragauskas, *Green Chem.*, 2016, **18**, 608-621.

27. J. Rencoret, J. Ralph, G. Marques, A. Gutiérrez, Á. T. Martínez and J. C. del Río, *J. Agric. Food Chem.*, 2013, **61**, 2434-2445.

Chapter 5:

Experimental and theoretical investigations to gain mechanistic insight on lignin depolymerization

5.1. Introduction

Lignin, a 3D amorphous copolymer, is made up of substituted phenols or phenolic subunits (*p*-hydroxyphenyl (*H*), guaiacyl (*G*), syringyl (*S*) alcohols)[1] linked together *via* ≡C-C≡ (30-40% w.r.t. total linkages) or ≡C-O-C≡ (60-70% w.r.t. total linkages) linkages, and this makes it a sole source of aromatics in nature. As a result, it becomes sensible to make high value low molecular weight aromatic chemicals from this rich source of aromatic polymer, which would eventually facilitate the bio-refinery concept becoming attractive.[2] Since ionic liquids (ILs) are considered to be green due to their unique properties that also can be tuned as per the requirement, they are suitable for employment in the transformations of biomass.[3] Moreover, functionalizing ILs with acidic groups (-SO$_3$H, etc.) were used in depolymerising copolymer such as lignin under acidic conditions.[4]

Typically, the bonding and non-bonding interactions between the cations of ILs and substrates may suggest a variety of interactions (π/π, -OH/π, -NH/π, -CH/π etc.), which makes it complicated to recognize which of these interactions are actually significant and are playing a decisive role in deciding the activity of a catalyst.[5-11] An interaction between the aromatic cation and π systems is also very well known, which further complicates the scenario.[12, 13] It is also reported that the NCHN (C2-H2) in imidazolium plays a crucial role during its interaction with the anion, which influences the physico-chemical properties of ILs. Additionally, the size and electronegativity of the anions are important factors that need to be remembered while discussing the properties of ILs.[14, 15] Nevertheless, the understanding of the type of interaction(s) present between IL and lignin is not yet completely established because, unlike in cellulose which has only –OH groups present on the carbon framework, in lignin several functional groups (aromaticity, -OH, -OCH$_3$, -CHO, olefinic etc.) are present on the carbon framework that can interact differently with IL and thus can make the discussions on the type of interactions complicated. However, once this interaction is understood, it would be of great help to design ILs to depolymerize lignin or any other resembling biomass molecule in an efficient way.

Since for a substrate to undergo any transformations its contact with catalyst plays an important role, it was decided to study this aspect in detail in order to understand the difference in activity of Brønsted acidic ionic liquid (BAIL) and H$_2$SO$_4$. Consequently, to comprehend this phenomenon, with the help of experimental and theoretical studies, interactions of lignin with ILs were done. Accordingly, to establish the interactions between lignin and ILs such as [BMIM][Cl] and [C$_3$SO$_3$HMIM]HSO$_4$] experimental and theoretical studies have been leveraged. Even if lignin is an intricate molecule, which makes the interpretation of the results complicated, interaction studies on the microscopic level of lignin with IL were done with the

help of 1D (^{1}H) 2D [^{13}C/^{1}H heteronuclear single quantum correlation (HSQC); ^{15}N/^{1}H heteronuclear multiple bond correlation (HMBC); ^{1}H/^{1}H nuclear Overhauser effect spectroscopy (NOESY)] NMR and RAMAN spectroscopy. Additionally, a theoretical (DFT) study was done to ascertain the type of interactions observed from experimental studies.

5.2. Experimental

5.2.1. Experimental Details

5.2.1.1. NMR analysis

Bruker Avance NMR instruments were used to record the NMR spectra in DMSO-d$_6$ solvent. The ^{1}H NMR proton peak at 2.5 ppm and ^{13}C NMR carbon peak at 39.5 ppm are considered as reference peaks. Various monomers/dimers/lignin samples neat or adduct were characterised using 1D/2D NMR spectroscopy. The details of each sample, instruments and measurements of samples are summarized in the Tables 5.1-5.2.

Table 5.1. Detail of Bruker Avance NMR instruments operate on frequencies and temperatures.

NMR	200 MHz	400 MHz	500 MHz	Temperature (^{o}C)
^{1}H	200.13	-	500.13	25.9 ^{o}C
^{13}C	50.23	-	125.76	26.1 ^{o}C
HSQC (^{13}C/^{1}H)	-	-	125.77/500.13	25.0 ^{o}C
HMBC (^{15}N/^{1}H)	-	-	50.69/500.13	25.0 ^{o}C
NOESY (^{1}H/^{1}H)	-	400.13/400.13	-	21.0 ^{o}C

Table 5.2. Summary on the concentrations, data points and number of scans used for HSQC, HMBC and NOESY NMR studies.*

Compounds	Quantity (±0.02 mg)	Data points	Number of scans
HSQC (^{13}C/^{1}H)			
Cumene	15.8	1024	128
Vanillin	20.0		
Guaiacol glyceryl ether	26.06		
Benzyl phenyl ether	58.4		
Lignin	70.0	1024	88
[BMIM][Cl]	22.97 mg, monomers and guaiacol glyceryl ether	1024	160
[BMIM][Cl]	55.30 mg, benzyl phenyl ether		
[BMIM][Cl]	48.50 mg for lignin		
Adducts			
Cumene	15.8	1024	128
[BMIM][Cl]	22.97		
Vanillin	20	1024	128

[BMIM][Cl]	22.97		
Guaiacol glyceryl ether	26.06	1024	128
[BMIM][Cl]	22.97		
Benzyl phenyl ether	50.0	1024	128
[BMIM][Cl]	55.30		
Lignin	70.0	1024	128
[BMIM][Cl]	48.5		
HMBC ($^{15}N/^{1}H$)			
Neat [BMIM][Cl]	100	1024	128
Adducts			
Vanillin	87	1024	128
[BMIM][Cl]	100		
Lignin	103	1024	128
[BMIM][Cl]	100		
NOESY ($^{1}H/^{1}H$)			
Vanillin	20	1024	16
[BMIM][Cl]	22.97		
* All the samples were prepared in 700 μL DMSO-d_6.			

5.2.1.2. RAMAN analysis

The Lab RAM HR Evolution instrument (HORIBA Scientific) using monochromatic radiation emitted by an Ar$^+$ laser (514.5 nm) source operating at 0.5% of 100 mW was used to analyse the RAMAN shift in the neat vanillin, neat [BMIM][Cl] and vanillin-[BMIM][Cl] adduct samples.

5.2.2. Computational Details

Further, to analyse this interaction phenomenon, theoretical calculations have been carried out with Turbomole 7.0[16, 17] using the TZVP basis set.[18] Geometry optimizations have been performed using the Perdew, Burke, and Ernzerhof functional (PBE).[19] Dispersion corrections[20] have been included in all the calculations. The resolution of identity (RI)[21] along with the multipole accelerated RI (marij)[22] approximations have been used for an accurate and efficient treatment of the electronic Coulomb term in the density functional theory (DFT) calculations. Solvent corrections have also been included in all the calculations using the cosmo model,[23] with epsilon (ϵ)= 46.7, to model the DMSO solvent, to study the NMR result obtained from the experimental observations.

5.3. Results and Discussions

5.3.1. Depolymerization of lignin

Catalytic amounts (0.5 g) of Brønsted acidic ionic liquids (BAILs)[4] (For more details description please see Chapter 3, Sections 3B.3.1 and 3B.3.2) and H_2SO_4 were employed for the depolymerization of lignin (2 *wt.*% solution water:methanol, 1:5 *v/v*= 30 mL) at 120 °C to yield low molecular weight aromatic products and the catalytic results are summarized in Figure 5.1. While the maximum yield of THF soluble products (95%) was obtained when depolymerization was carried out with H_2SO_4 as a catalyst compared to BAIL, [C_3SO_3HMIM][HSO_4], catalyst (78% yield) (Figure 5.1), but the comparison of GC and GC-MS profiles of products (Chapter 3, Section 3B.3.1.5, Figures 3B.4-3B.7) shows that with BAIL as a catalyst, better yields of low molecular weight aromatic products are possible to achieve in comparison to H_2SO_4. Moreover, it is also seen that neutral IL, [BMIM][Cl] shows poor activity due to the absence of the –SO_3H group originated acidity.
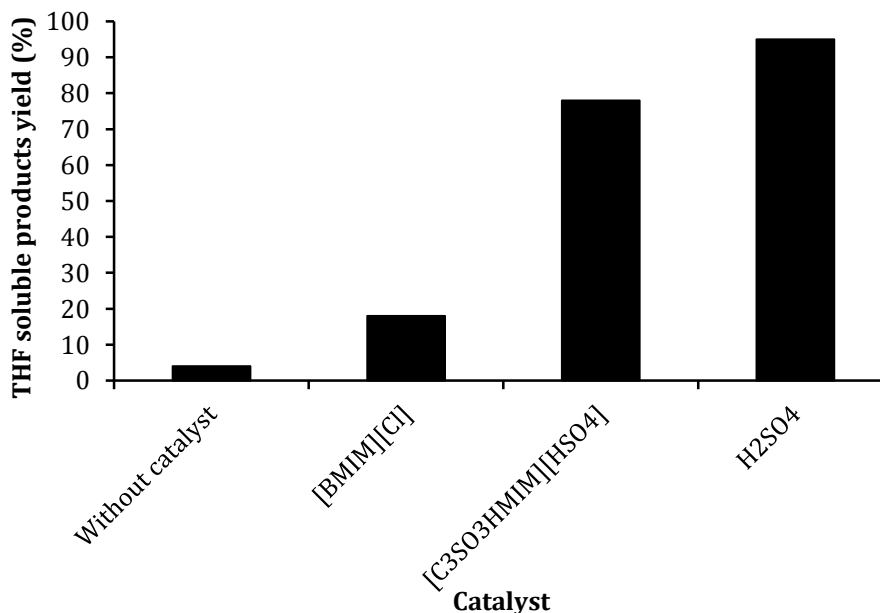
Figure 5.1. Lignin depolymerization. Reaction condition: dealkaline lignin (2 *wt.*% solution in water:methanol, 1:5 *v/v*= 30 mL), catalyst (0.5 g), 120 °C, 1 h, 1000 rpm.
Values are mean of 3 reactions with ±3% error noticed.

Dealkaline lignin having a general molecular formula, $C_{10}H_{13}O_3S_{0.09}$ (Chapter 3, Section 3A.2.9, Table 3A.3) was also thoroughly characterized using UV-Vis and FT-IR techniques (Chapter 3, Sections 3A.2.11-3A.2.12, Figures 3A.8-3A.9) to understand its physico-chemical properties and based on these studies, a correlation between the depolymerized products (obtained in BAIL catalyzed reactions) and substrate could be established. As seen from the FT-IR spectra of THF soluble products and lignin (Chapter 3, Section 3B.6.5, Figure 3B.25), after the depolymerization of lignin, peak intensity for –OH groups has increased and that of ether linkages has decreased

(in products). Moreover, peaks for other functional groups remain the same in products as observed in lignin. These results suggest that during depolymerization, lignin undergoes the acid catalysed hydrolysis reaction to yield low molecular weight aromatic products.

Even if it was relatively easy to ascertain the fact that lignin underwent the acid catalyzed hydrolysis reaction, it was rather surprising to find out that the BAIL (with -SO$_3$H) performed better than the mineral acid (H$_2$SO$_4$). To understand this difference in activity, acid strength was measured through Hammett acidity scale (for more details please see the Chapter 2, Section 2A.7 and Tables 2A.4-2A.5), (all the reactions were done using similar 0.5 g catalyst loading) and it was found that H$_2$SO$_4$ has higher acid strength (H_0= 1.53) compared to [C$_3$SO$_3$HMIM][HSO$_4$] BAIL (H_0= 2.01) when similar quantity of catalyst (0.5 g) is charged in the reaction. Further, it was observed that when depolymerization was catalyzed by H$_2$SO$_4$, higher concentration of H$^+$ (10.2 mmol) was available compared with [C$_3$SO$_3$HMIM][HSO$_4$] BAIL (3.3 mmol). Subsequently, it was believed that this higher acid concentration in H$_2$SO$_4$ catalyzed reaction might be harmful in the reaction, as it may initiate side reactions (like degradation and repolymerization). Therefore, depolymerization reactions were carried out with BAIL and H$_2$SO$_4$ by maintaining similar H$^+$ (2.78 mmol) concentration (Chapter 3, Section 3B.3.2). As seen from the data (for more details descriptions please see the Chapter 3, Section 3B.3.2), under this condition as well, H$_2$SO$_4$ gave the better yield (92%) of THF soluble products than [C$_3$SO$_3$HMIM][HSO$_4$] (52%) catalyst but from GC and GC-MS profiles it was again observed that BAIL showed higher amount of low molecular weight aromatic products formation than H$_2$SO$_4$ (for more details descriptions please see the Chapter 3, Section 3B.3.1.5, and Figures 3B.4 and 3B.7). Since for a substrate to undergo any transformations, its contact with catalyst plays an important role, it was decided to study this aspect in detail in order to understand the difference in activity between BAIL and H$_2$SO$_4$. Consequently, to comprehend this phenomenon, interactions of lignin/monomers/dimers with ILs were monitored with the help of experimental and theoretical studies.

5.3.2. Understanding the interactions between ILs and lignin

5.3.2.1. Experimental understanding- interaction studies

5.3.2.1.1. 1D (^{1}H) NMR

The [C$_3$SO$_3$HMIM][HSO$_4$] BAIL displayed better performance than H$_2$SO$_4$ catalyst (Figure 5.1), and it was anticipated that because of their ionic nature BAIL can interact with lignin moieties, which would facilitate cleavage of ≡C-O-C≡ (ether)/-C(O)O-C≡ (ester) bonds. Moreover, catalytic results point out that lignin may interact more with cation than anion (Chapter 3, Section 3B.3). Lignin contained various types of functional groups (aromaticity, -OH, -OCH$_3$, -CHO, olefinic etc.), aromatic moieties (*S*, *G* and *H*) and linkages (≡C-O-C≡ and ≡C-C≡) which are present on the carbon framework, as confirmed by the ATR and NMR studies (Chapter 3,

Sections 3A.2.11-3A.2.12). Various linkages and functional groups present in lignin can interact with ILs (cations or anions). It was hypothesised that owing to interactions, changes in electron density/bond polarization can be occurred in adducts. To unravel this phenomenon, ^{1}H NMR study was monitored between IL and substrates [monomers (cumene and vanillin), dimers (guaiacol glyceryl ether and benzyl phenyl ether) and real lignin]. As under acidic conditions it is impractical to scrutinize the change in chemicals shifts in –OH (due to fast exchange of protons),[24] it was decided to carry out the interaction studies with neutral IL, [BMIM][Cl] instead of [C_3SO_3HMIM][HSO_4] BAIL. The 1D (^{1}H) NMR studies were initially done with cumene (without any oxygen containing groups), vanillin (with –OH, -OCH_3, -CHO groups) and lignin (with several oxygen containing groups including ether linkages) (Figure 5.2). To check the possibility of participation of π electrons *via* π/π, -OH/π, -NH/π, -CH/π etc. type interactions, the NMR spectrum was also recorded with the cumene substrate but no change in the chemical shift was detected in cumene-[BMIM][Cl] adduct (Figure 5.2A). However, as seen in the adduct samples, a change in the chemical shifts of protons in IL (δ ppm= 9.43$\rightarrow$9.36 (H_2, –$N_1C_2H_2N_3$-), upfield) and vanillin (δ ppm= 10.27$\rightarrow$10.60 (H_1), 6.98$\rightarrow$7.10 and 6.94$\rightarrow$7.06 (doublet, H_5), downfield] related to neat samples of [BMIM][Cl] and vanillin were detected (Figure 5.2B). Furthermore, a sharp –OH peak present in neat sample is converted into a broad peak in the adduct, which suggests the change in chemical environment around the proton. Similar observations were also made for the NMR spectra for lignin, [BMIM][Cl] and lignin-[BMIM][Cl] adduct (Figure 5.2C). Change in chemical shift of protons in IL (δ ppm= 9.74$\rightarrow$9.46 (H_2, –$N_1C_2H_2N_3$-), upfield) and lignin (δ ppm= 8.19-6.75$\rightarrow$8.23-6.75 (aromatic protons), downfield] were observed, which highlighted that the IL interacts (imidazole ring, –$N_1C_2H_2N_3$-) with lignin (Figure 5.2C). However, an apparent shift in the H_2 proton (δ ppm= 9.74$\rightarrow$9.46 (H_2, –$N_1C_2H_2N_3$-), upfield) peak was visible in lignin-[BMIM][Cl] adduct related to neat [BMIM][Cl] IL. This is because lignin comprised higher concentration of –OH (For more details descriptions please see Section 3A.2.11, Figure 3A.9) and other functional groups (than other molecules studied here). Further the interaction of IL with dimer compound, guaiacol glyceryl ether having two –OH group along with ether linkage was checked. As seen from Figure 5.2D, in this case also change in chemical shift of protons in IL (δ ppm= 9.42$\rightarrow$9.35 (H_2, –$N_1C_2H_2N_3$-), upfield) and guaiacol glyceryl ether of two –OH groups (δ ppm=4.94$\rightarrow$5.06 (H_1) and 4.65$\rightarrow$4.80 (doublet, H_2), downfield] was observed, which again emphasized the fact that the IL interacts through oxygen atom (substrate) and C_2-H_2 (–$N_1C_2H_2N_3$-, imidazolium ring). Although, interaction between substrate and IL is proven by above mentioned studies (through oxygen on substrate), yet it was not clear whether oxygen atom in ether linkages also participate in any interaction with IL. To probe this phenomenon, an interaction study was performed with benzyl phenyl ether (with only oxygen involved in ether linkage and no other oxygen containing functional group is

present) and IL. Interestingly, as monitored through NMR spectra for neat samples (benzyl phenyl ether and [BMIM][Cl]) and benzyl phenyl ether-[BMIM][Cl] adduct (Figure 5.2E), no change in chemical shifts in H_2 in IL (δ ppm= 9.54$\rightarrow$9.50 (H_2, $-N_1C_2H_2N_3-$), no change) and H_{12} protons in benzyl phenyl ether (δ ppm= 5.10$\rightarrow$5.09 (benzyl proton), no change] were observed. This result indicates that may be due to steric hindrance created by two phenyl rings, it is not possible to have any interaction between oxygen of ether linkage and IL. In summary, the NMR findings illustrates that substrate and IL preferentially interact through 'O' and $-N_1C_2H_2N_3-$. As it observed that since oxygen of ether linkage is not involved in the interaction, it is free for protonation *via* which hydrolysis reaction proceeds.
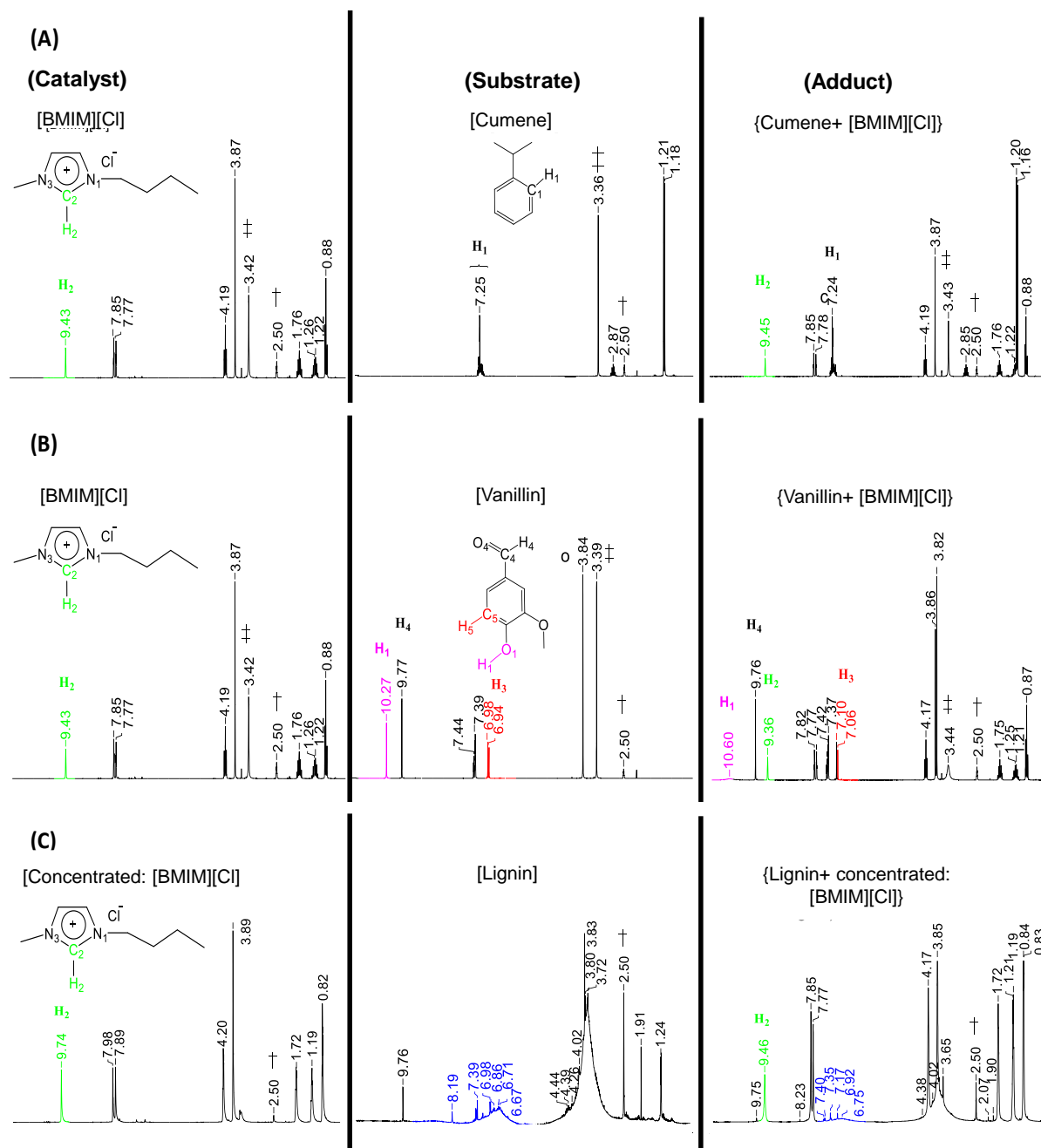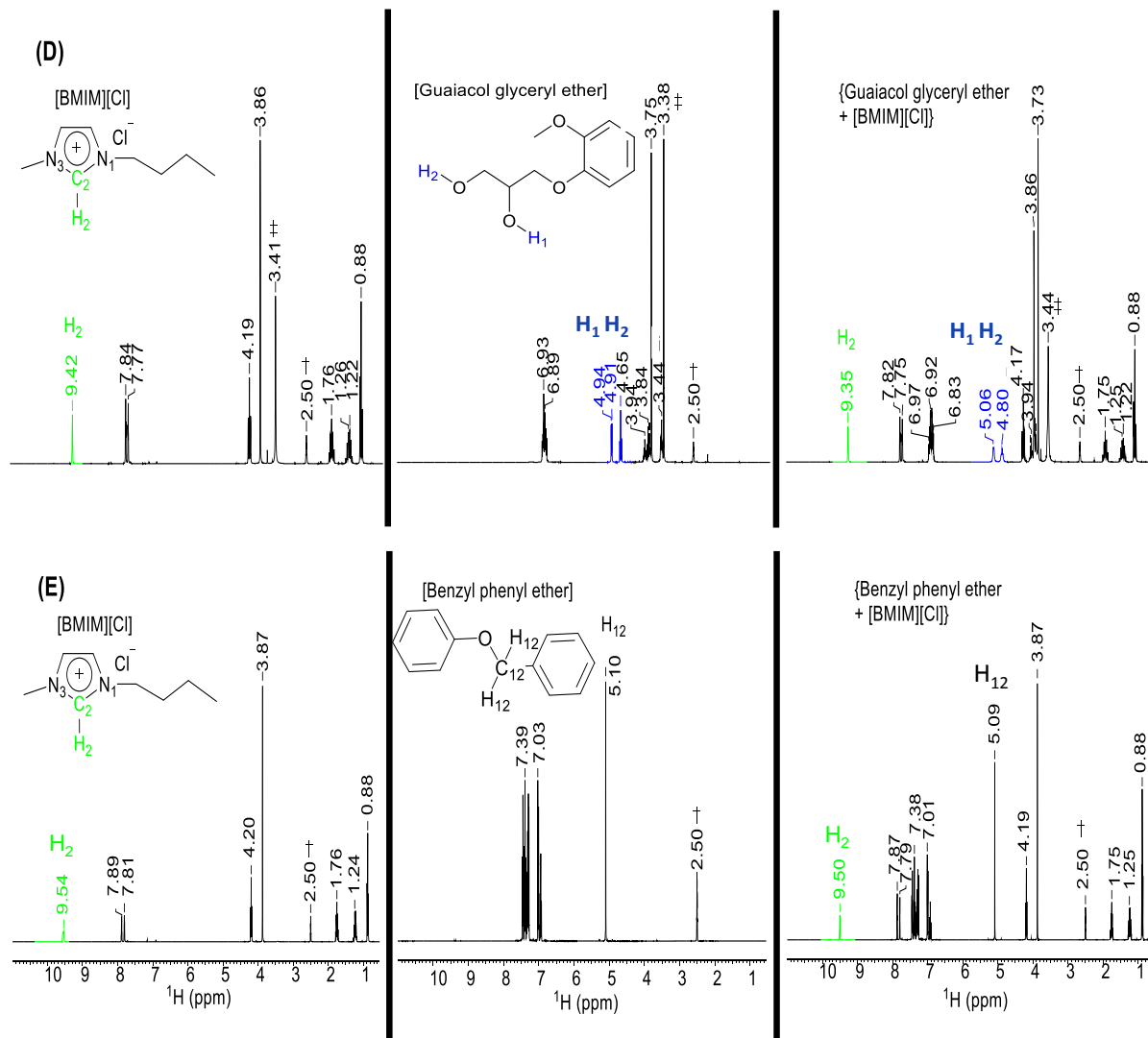
Figure 5.2. ^{1}H NMR spectra for (A) neat [BMIM][Cl], neat cumene and cumene-[BMIM][Cl] adduct; (B) neat [BMIM][Cl], neat vanillin and vanillin-[BMIM][Cl] adduct; (C) neat [BMIM][Cl], neat lignin and lignin-[BMIM][Cl] adduct; (D) neat [BMIM][Cl], neat guaiacol glyceryl ether and guaiacol glyceryl ether-[BMIM][Cl] adduct and (E) neat [BMIM][Cl], neat benzyl phenyl ether and benzyl phenyl ether-[BMIM][Cl] adduct. The spectra were recorded in DMSO-d_6 solvent and the δ=2.50 ppm is considered as reference peak. [†]Peak for the deuterated DMSO solvent and [‡]peak for the water present in DMSO-d_6 solvent.

5.3.2.1.2. 2D (^{13}C/^{1}H, HSQC) NMR

To underpin the explanations derived from 1D (^{1}H) NMR, interactions were studied with the help of 2D heteronuclear single quantum correlation (HSQC) NMR. In order to monitor interactions between IL and substrates, an advanced analytical 2D (HSQC) NMR study for [BMIM][Cl], vanillin, lignin, vanillin-[BMIM][Cl] and lignin-[BMIM][Cl] adduct samples was done in DMSO-d$_6$ solvent. As seen from Figure 5.3A, the signal for -N$_1$C$_2$H$_2$N$_3$- in [BMIM][Cl] IL was shifted to upfield (δ_C/δ_H= 136.55/9.75→136.74/9.37 ppm) in vanillin-[BMIM][Cl] adduct. Similarly, signals for -N$_1$C$_5$H$_5$C$_4$H$_4$N$_3$- (imidazolium ring) group were seen (Figure 5.3A), at lower chemical shifts (δ_C/δ_H= 122.6/7.99→122.759/7.85 and 123.95/7.89→124.56/7.79 ppm, upfield, for C$_5$-H$_5$ and C$_4$-H$_4$) in vanillin-[BMIM][Cl] adduct. The signal for Ar-H (C$_5$-H$_5$) in vanillin (Figure 5.3A) was observed at downfield in vanillin-[BMIM][Cl] adduct (δ_C/δ_H= 115.4/6.97→115.63/7.11 ppm for C$_5$-H$_5$) than Ar-H (C$_5$-H$_5$) signal for neat vanillin sample. The difference in chemical shift in vanillin-[BMIM][Cl] adduct to neat vanillin and IL, affirmed that IL (–N$_1$C$_2$H$_2$N$_3$-/-N$_1$C$_5$H$_5$C$_4$H$_4$N$_3$- groups) interact with vanillin through 'O' of –OH group. The 2D (HSQC) NMR study was also performed for neat lignin, neat [BMIM][Cl] and lignin-[BMIM][Cl] adduct, demonstrates similar observations which observed in vanillin-[BMIM][Cl] adduct. For e.g. signal for -N$_1$C$_2$H$_2$N$_3$- in IL was shifted to upfield (δ_C/δ_H= 136.55/9.72→136.57/9.47 ppm) after addition of lignin (Figure 5.3B), and signals for -N$_1$C$_5$H$_5$C$_4$H$_4$N$_3$- groups were also seen at lower chemical shifts (δ_C/δ_H= 122.6/7.99→122.49/7.85 ppm for C$_4$-H$_4$ and 123.95/7.89→123.69/7.78 ppm, for C$_5$-H$_5$, upfield) in lignin-[BMIM][Cl] adduct (Figure 5.3B) Thus, it can be affirmatively inferred from NMR studies that lignin interacts with cation (–N$_1$C$_2$H$_2$N$_3$-, imidazolium ring) of IL *via* 'O' of –OH group. It had limitations to interact with [BMIM][Cl] IL and thus chemical shifts were averaged out towards neat [BMIM][Cl] sample. But as these interactions are rapid, IL was competent of interacting with numerous vanillin molecules and thus displayed uninterrupted increase in chemical shift (Figure 5.3B) than vanillin-[BMIM][Cl] adduct.
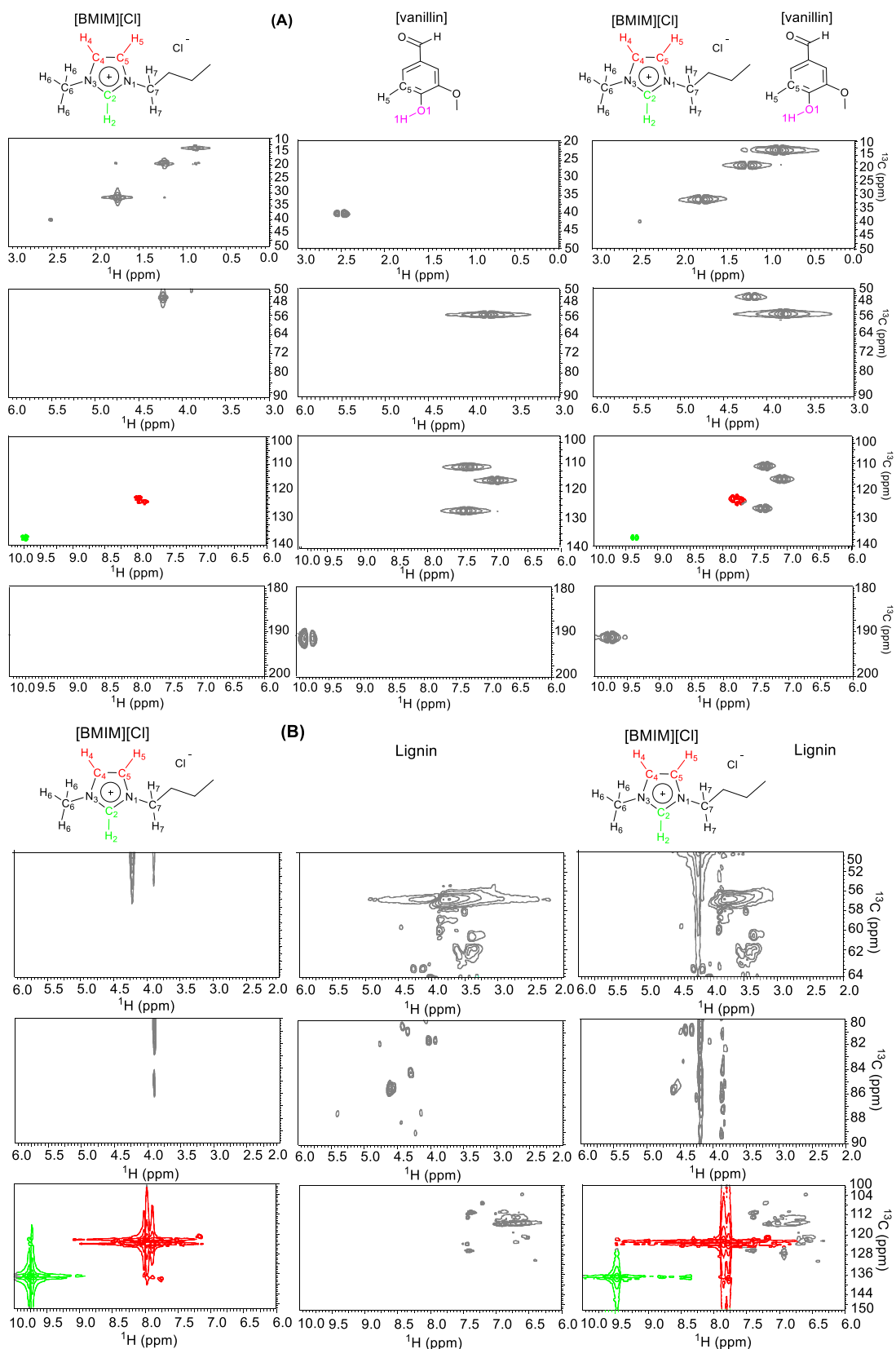
Figure 5.3. 2D (HSQC) NMR spectra of (A) neat [BMIM][Cl], neat vanillin and vanillin-[BMIM][Cl] adduct and (B) neat [BMIM][Cl], neat lignin and lignin-[BMIM][Cl] adduct. All the spectra were recorded in DMSO-d_6 solvent.

5.3.2.1.3. 2D (^{1}H/^{1}H, NOESY) NMR

Two dimensional nuclear Overhauser effect spectroscopy (NOESY) NMR was recorded at 25±2 ^{o}C using Bruker Avance-500 MHz (operating at a frequency of 500.13 MHz) spectrometer and sample (vanillin= 20 mg and [BMIM][Cl]= 22.97 mg) was dissolved in 700 μL DMSO-d$_6$ solvent. NOESY effect can be analysed between two nucleuses, which are less than 5 Å apart. Albeit from 1D (^{1}H) and 2D (HSQC) NMR results (Figures 5.2 and 5.3), the 2D (NOESY) NMR study was apprehended that substrate (–OH group) interact with IL (imidazolium ring). However to find out the mode of interaction (inter or intra) either parallel or perpendicular (Figure 5.4), 2D (NOESY) NMR study was leveraged for vanillin-[BMIM][Cl] adduct, as this technique allows to gather information for an interaction between ^{1}H-^{1}H (inter or intra molecular), if they are in close vicinity (<5 Å) with each other. 2D (^{1}H-^{1}H, NOESY) NMR spectrum of vanillin-[BMIM][Cl] adduct for H$_2$ proton in IL (–N$_1$C$_2$H$_2$N$_3$-, imidazole ring) is interacted with wide range of protons (H$_6$-H$_{10}$) present in [BMIM][Cl] molecule. Similarly, H$_4$ and H$_5$ protons in IL (-N$_1$C$_5$H$_5$C$_4$H$_4$N$_3$-, imidazole ring) showed intra molecular interaction with H$_6$, H$_7$, H$_8$ and H$_9$ protons (Figure 5.4). Additionally, 2D (^{1}H-^{1}H, NOESY) NMR spectrum of vanillin-[BMIM][Cl] adduct showed that vanillin molecule formed intra molecular interaction (Figure 5.4), such as Ho and Hl protons interacted with Hk and Hi protons respectively. From the obtained results, it concluded (Figure 5.4), that only intra-molecular H-H interaction and consequently it is believed that predominantly –OH (vanillin) and imidazolium (cation, [BMIM][Cl]) groups interact with each other in a perpendicular mode (Figure 5.5). This is evident since steric hindrance between alkyl chains, methoxy group etc. would destabilize parallel arrangement. Moreover, aromatic rings would repel each other and this will lead to almost perpendicular interaction. These results also match well with the results obtained with 1D (^{1}H) NMR of cumene spectrum where no shift in δ values was noticed because of absence of –OH groups and that there is a least prospects of Π-Π' interaction between aromatic rings in cumene and immidazolium owing to perpendicular interaction.
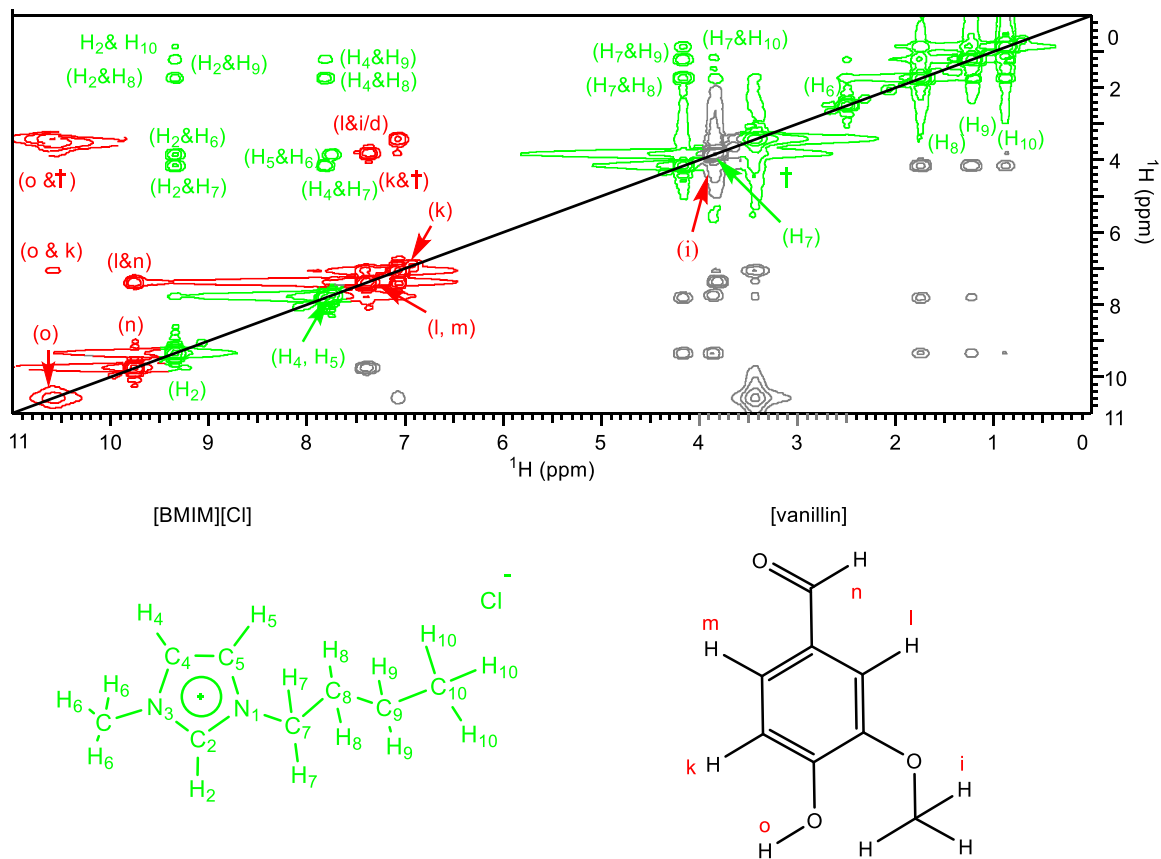
Figure 5.4. 2D (NOESY) NMR spectrum of vanillin-[BMIM][Cl] adduct. The NMR spectrum was recorded in DMSO-d_6 solvent.
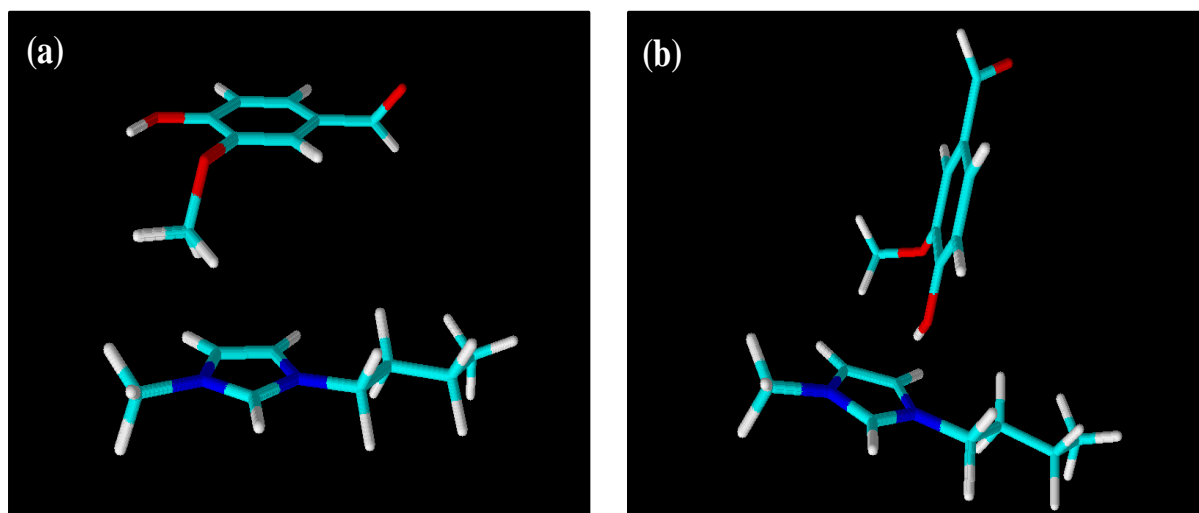
Figure 5.5. Proposed structure for the interaction of vanillin with [BMIM] cation of IL, (a) parallel and (b) perpendicular.

5.3.2.1.4. ^{1}H NMR (Molar concentration study on chemical shift)

An apparent from 1D (^{1}H) and 2D (HSQC) NMR spectra of lignin-[BMIM][Cl] and vanillin-[BMIM][Cl] adducts (Figures 5.2-5.3) that maximum difference in chemical shift in lignin-[BMIM][Cl] adduct ($\Delta\delta$= 0.28 ppm) of proton peak in IL (-$N_1C_2H_2N_3$-, cation) was observed than vanillin-[BMIM][Cl] adduct ($\Delta\delta$= 0.07 ppm) of -$N_1C_2H_2N_3$- proton peak. This is because lignin has higher concentration of –OH and other functional groups (for more details descriptions please see, Chapter 3, Section 3A.2.11) than vanillin molecule, which can interact with cation (-$N_1C_2H_2N_3$-) of IL. This effect is best explained on the basis of transfer of electron density (through 'O' of –OH) of substrates to electron deficient imidazolium ring in IL (-$N_1C_2H_2N_3$- cation), which are affirmed by 1D (^{1}H) and 2D (HSQC) NMR spectra. It was affirmatively inferred from 1D and 2D NMR studies that lignin interacts with -$N_1C_2H_2N_3$- cation of IL *via* 'O' of –OH groups. However, it (–OH groups) had limitations to interact with IL and thus chemical shifts were averaged out towards neat [BMIM][Cl] IL sample than lignin-[BMIM][Cl] adduct. But these interactions are rapid, IL was proficient of interacting with numerous vanillin molecules and thus displayed uninterrupted increase in chemical shift in lignin-[BMIM][Cl] adduct. The various concentrations of vanillin in vanillin-[BMIM][Cl] adduct were used to measure the difference in chemical shift (Table 5.3). To find out the rational number(s) of –OH groups is interacting with imidazolium ring of IL, vanillin (-OH groups) with different concentrations (0.5 to 5.0 molar) were studied, while 1.0 molar concentration of [BMIM][Cl] IL was taken for this study. The maximum (^{1}H) difference in chemical shift was observed at 0.5 and 1 molar ratio (vanillin/IL) for vanillin (Figure 5.6A) and at higher molar ratios (1.5, 3 and 5), the change in chemical shift declined. Nevertheless, at the same time continuous increase in chemical shift of -$N_1C_2H_2N_3$- proton in [BMIM][Cl] IL was seen (Figure 5.6B) up to 3 molar concentration, after that minor increment in the chemical shift ($\Delta\delta$= 0.02 ppm) was perceived, which affirmed that for 3 moles of vanillin molecule can formed the significant change in chemical shift with 1 mole of [BMIM][Cl] IL, which were seen with -$N_1C_2H_2N_3$- proton in IL and –OH proton in vanillin respectively. These contrasting results were exhibited due to change of concentration of both vanillin and IL in DMSO-d_6. Until reaching stoichiometric amount of vanillin:[BMIM][Cl] IL ratio, increase in chemical shift was observed but when surplus (above stoichiometric >1 molar ratio) vanillin concentration, the chemical shift was declined (Figure 5.6A).

Table 5.3. Summary on the concentrations study of vanillin in vanillin-[BMIM][Cl] adduct used for 1D (^{1}H) NMR studies.*

Sr. No.	Compounds	Quantity (±0.2 mg)
1	For 0.5 molar ratio	
	Vanillin	10
	[BMIM][Cl]	22.97
2	For 1 molar ratio	
	Vanillin	20
	[BMIM][Cl]	22.97
3	For 1.5 molar ratio	
	Vanillin	30
	[BMIM][Cl]	22.97
4	For 3.0 molar ratio	
	Vanillin	60
	[BMIM][Cl]	22.97
5	For 5.0 molar ratio	
	Vanillin	100
	[BMIM][Cl]	22.97

* All the samples were prepared in 700 μL DMSO-d_6.
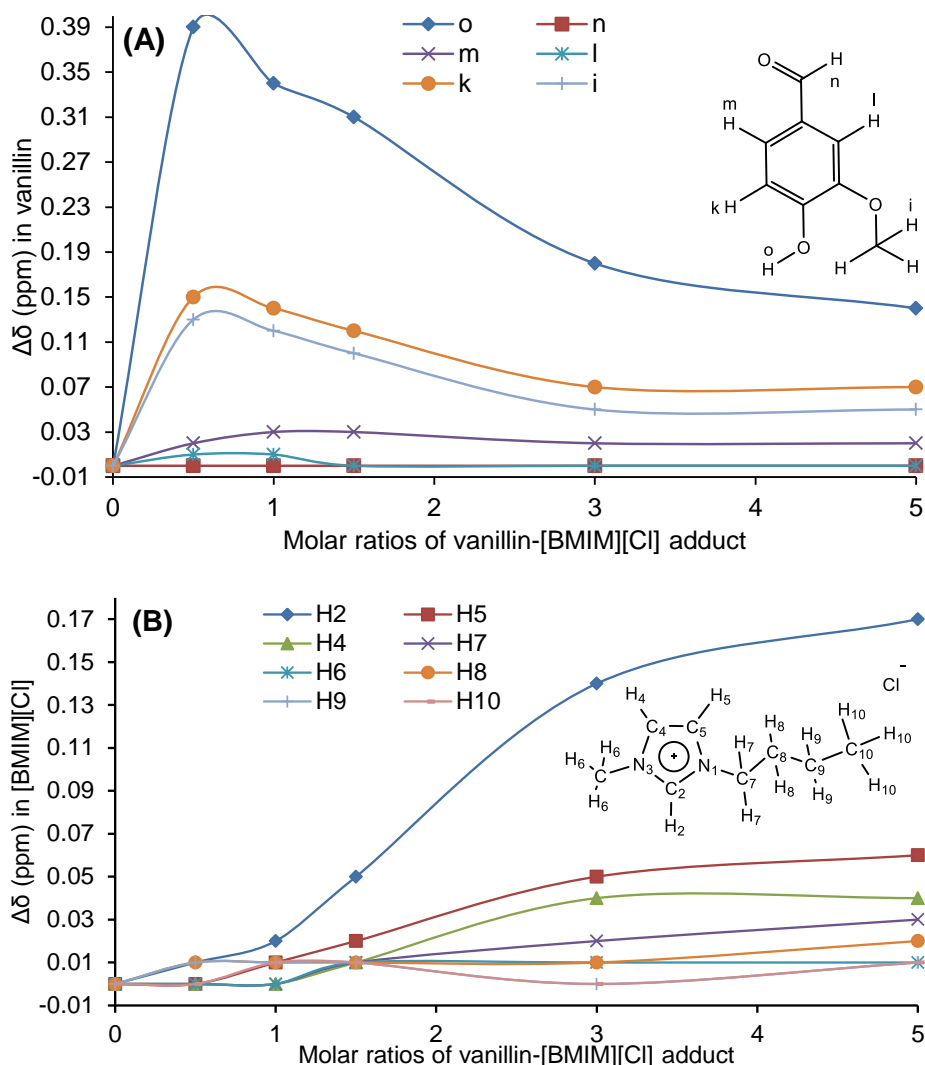
Figure 5.6. (A) Effect of molar concentration on chemical shift of vanillin for vanillin-[BMIM][Cl] adduct and (B) Effect of molar concentration on chemical shift of [BMIM][Cl] for vanillin-[BMIM][Cl] adduct. All the spectra were recorded in DMSO-d_6.

5.3.2.1.5. 2D (^{15}N/^{1}H, HMBC) NMR

The 2D heteronuclear multiple bond correlation (HMBC) NMR was recorded at 25 °C using Bruker Avance-500 MHz (operating at a frequency of 500.13 MHz) spectrometer. Ca. 87-103 g samples were dissolved in DMSO-d_6 solvent (700 μL) and 2D (HMBC) NMR spectra were recorded. To comprehend the actual mode of interaction observed through 1D (^{1}H) NMR study, an advanced 2D (^{15}N/^{1}H, HMBC) NMR characterization technique was used. Through this technique, the correlation between the hydrogen present on carbon flanked between two nitrogen atoms (-$N_1C_2H_2N_3$-) and nitrogen atoms could be observed. Moreover, it was also doable to establish the correlation between neighbouring hydrogen atoms with nitrogens. The 2D (^{15}N/^{1}H, HMBC) NMR spectra for neat [BMIM][Cl] IL, vanillin-[BMIM][Cl] adduct and lignin-[BMIM][Cl] adduct samples were recorded in deuterated DMSO solvent (Figure 5.7). As

observed from Figure 5.7, and the chemical shifts summarized in Table 5.4, in the 2D (^{15}N/^{1}H, HMBC) NMR spectrum of the neat [BMIM][Cl] sample, the signal for methylated nitrogen (N_3) of imidazole ring is observed at 171.07 ppm along with signal for methyl (C_6) protons at 3.88 ppm (N_3-H_6, Table 5.4). In case of nitrogen linked with butyl group (N_1) signal is observed at 182.85 ppm along with methylene (C_7) proton at 4.22 ppm (N_1-H_7). To confirm that the signal for N_3 and N_1 appears at 171.07 and 182.85 ppm, respectively, 1D (^{1}H) NMR spectra of 1-methylimidazole and 1-butylimidazole were recorded. As seen from Figure 5.8, in the NMR spectrum of 1-methylimidazole, a singlet was observed at 3.64 ppm for methyl (C_6) proton (H_6). Additionally, a triplet for methylene (C_7) protons (H_7) was observed at 3.94 ppm in the NMR spectrum recorded for 1-butylimidazole. The appearance of protons (H_7) in methylene (C_7) compared with methyl (C_6) proton (H_6) at higher chemical shift is because of difference in their electronegativity. Since in 2D (^{15}N/^{1}H, HMBC) NMR spectrum of neat [BMIM][Cl], two distinct signals for protons were observed at 3.88 and 4.22 ppm, it was possible to assign the signals for N_3 and N_1 related to methyl (H_6) and methylene (H_7) groups attached to nitrogen atoms. The appearance of signal for N_1 in deshielded region (182.85 ppm) relative to N_3 (171.07 ppm) in imidazolium cation is possibly due to its more electropositive character compared to N_3. The 2D (^{15}N/^{1}H, HMBC) NMR signals for $-N_1C_2H_2N_3-$ and $-N_1C_5H_5C_4H_4N_3-$ groups present in neat [BMIM][Cl] were observed at δ_N/δ_H= 171.07/9.63 (N_3-H_2) and 182.87/9.63 ppm (N_1-H_2) and (δ_N/δ_H= 171.09/7.91ppm (N_3-H_4) and 182.84/7.87 ppm (N_1-H_5)), respectively (Figure 5.7A, Table 5.4). When 2D (^{15}N/^{1}H, HMBC) NMR spectrum was recorded for vanillin-[BMIM][Cl] adduct, shielding effect was observed in case of N_1-H_2 and N_3-H_2 signals (Figure 5.7B). Although, shielding effect on proton (H_2) and N_1 signals was observed as expected but, it was rather surprising that N_3 didn't show the similar trend. Similar to vanillin-[BMIM][Cl] adduct, in case of lignin-[BMIM][Cl] adduct also shielding effect on δ_N/δ_H (N_1-H_2 and N_3-H_2) was observed. The extent of shielding effect was more evident in case of lignin than vanillin because of higher concentration of $-OH$/$-OCH_3$ groups present on lignin (ATR study, Chapter 3, Figure 3A.9), those would interact with ionic liquids. However, a careful look at 2D (^{15}N/^{1}H, HMBC) NMR spectral data (Figure 5.7, Table 5.4) reveals that compared to N_3-H_2 (0.54 ppm), the shielding effect on N_1-H_2 (3.78 ppm) is more prominent. This is because N_1 is more electropositive than N_3. Thus, from 2D (^{15}N/^{1}H, HMBC) NMR studies, the results obtained with 1D (^{1}H) NMR were corroborated and it is suggested that between lignin and cation of IL, a strong interaction is present. Further, to study the effect of the $-SO_3H$ group attached to cation *via* propyl group on the chemical shifts of nitrogen and protons was done *via* 1D (^{1}H) NMR characterization.
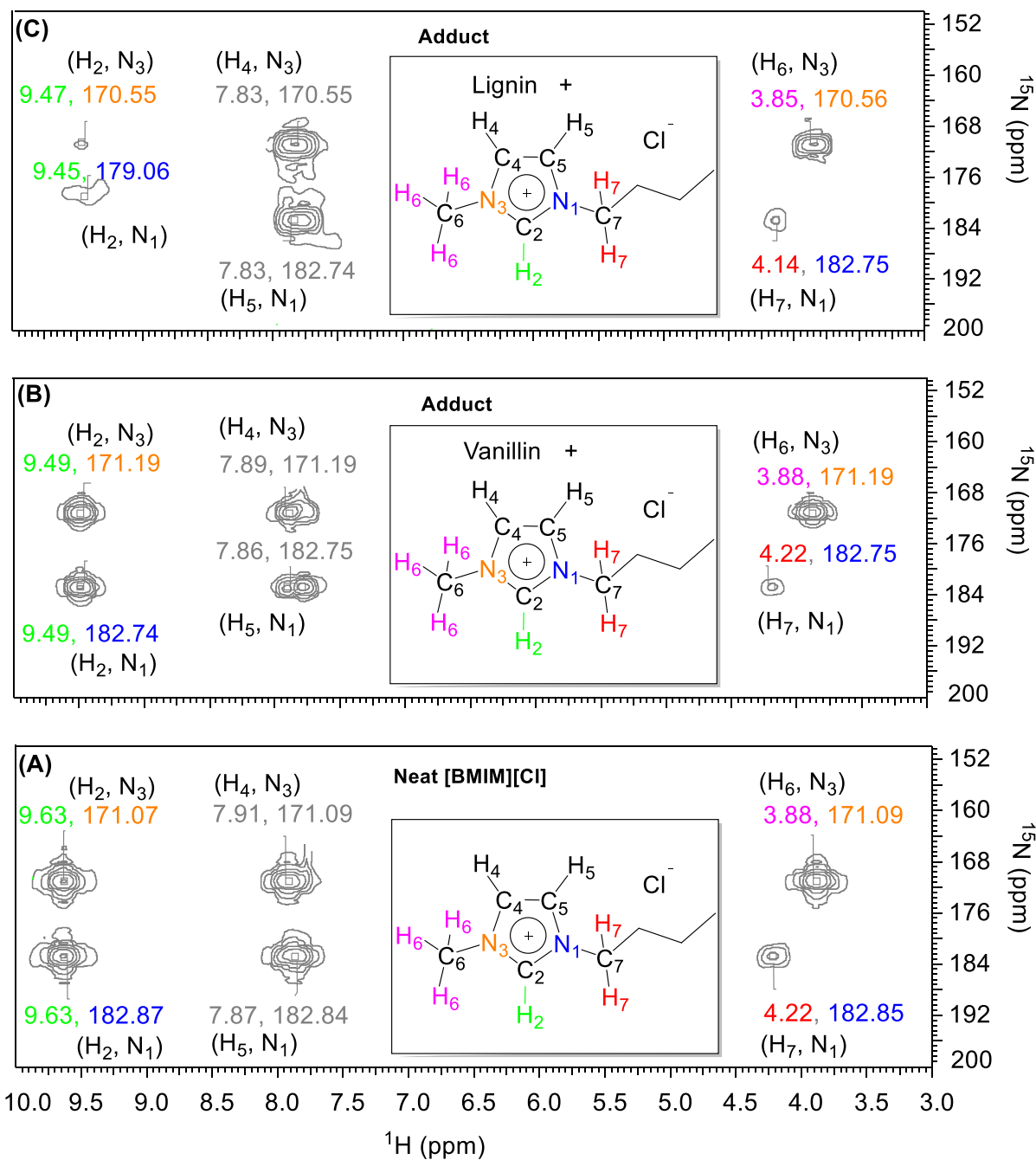
Figure 5.7. 2D (HMBC) NMR spectra and structures of (A) neat [BMIM][Cl], (B) vanillin-[BMIM][Cl] adduct and (C) lignin-[BMIM][Cl] adduct. All the spectra were recorded in DMSO-d$_6$ solvent.

Table 5.4. Assignment of chemical shifts in 2D heteronuclear multiple bond correlation (^{15}N/^{1}H, HMBC) NMR spectra of [BMIM][Cl], vanillin-[BMIM][Cl] adduct and lignin-[BMIM][Cl] adduct samples.

Sr. No.	Assignments	δ_N/δ_H (ppm) signals		
		Neat [BMIM][Cl]	Vanillin-[BMIM][Cl] adduct	Lignin-[BMIM][Cl] adduct
1	N_1-H_2	182.87/9.63	182.74/9.49	179.06/9.45
2	N_3-H_2	171.07/9.63	171.19/9.49	170.55/9.47
3	N_1-H_5	182.84/7.87	182.75/7.86	182.74/7.83
4	N_3-H_4	171.09/7.91	171.19/7.89	170.55/7.83
5	N_1-H_7	182.85/4.22	182.75/4.22	182.75/4.14
6	N_3-H_6	171.09/3.88	171.19/3.88	170.56/3.85

5.3.2.1.6. Elucidation of effect of cation and functional groups on chemical shifts

Since, it was expected that the positive charge on imidazolium ring would be in resonance, it should have shown similar change in chemical shifts for both the nitrogen atoms while studying interactions of IL with vanillin and lignin (Section 5.3.2.1.5). However, contrary to this, larger extent of shielding for N_1 compared with N_3 was observed (Table 5.4). This difference in behaviour encouraged us to probe this phenomenon in detail. As seen from Figure 5.8, in the NMR spectrum of 1-methylimidazole, peak for methyl (C_6) proton (H_6) was observed at 3.64 ppm. However, as per the expectation, peak for methylene (C_7) proton (H_7) was observed at slightly deshielded region (3.94 ppm) due to attachment of butyl chain to nitrogen which gives rise to difference in electronegativity on C_7 carbon attached to N_1 in 1-butylimidazole than C_6 carbon attached to N_3 in 1-methylimidazole (i.e. 1st carbon from nitrogen on alkyl side chain). The H_6 and H_7 protons are covalently bonded to 1-methyl or 1-butyl groups, which are further attached with nitrogen atoms at the imidazole ring but the major differences in the chemical shift is detected due to the difference in electronegativity of carbon (Electronegativity (Pauling scale)= 2.55) and hydrogen (Electronegativity (Pauling scale)= 2.20) atoms.[25-27] With the help of this data, it was possible to assign the signals for N_3 and N_1 in 2D (^{15}N/^{1}H, HMBC) NMR spectra as discussed earlier (Section 5.3.2.1.5, Figure 5.7, Table 5.4). Subsequently, 1D (^{1}H) NMR spectrum was recorded for [BMIM][Cl] and in this spectrum drastic differences from spectra for 1-methylimidazole and 1-butylimidazole were observed. As summarized in Table 5.5, both the peaks for H_6 (3.64→ 3.86 ppm) and H_7 (3.94→ 4.18 ppm) were deshielded in case of [BMIM][Cl] sample. This is because of electron deficient (cationic) nature of imidazole ring in [BMIM][Cl], which acts as electron withdrawing group that essentially reduces the electron density on carbon(s) of alkyl chain.
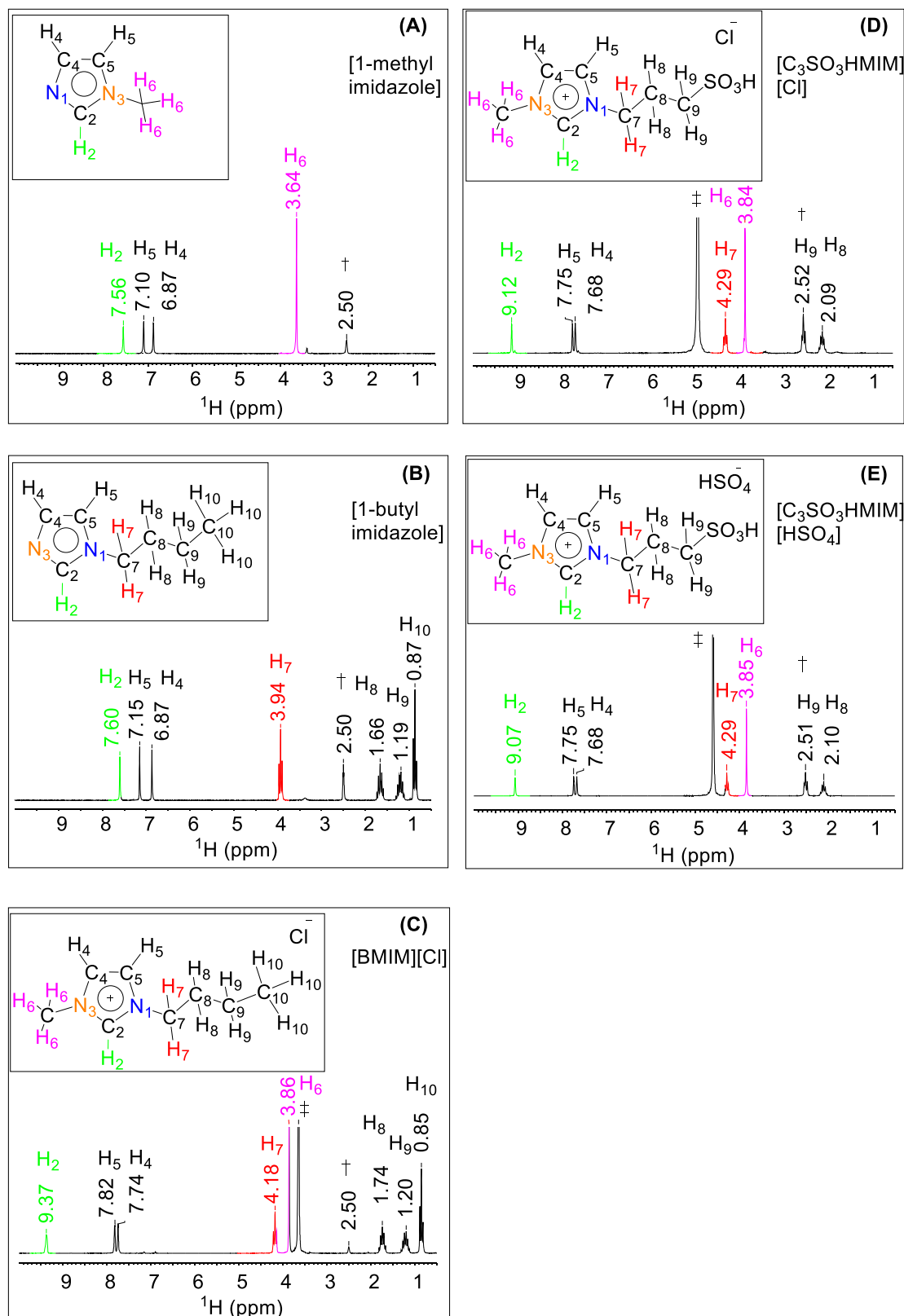
Figure 5.8. ^{1}H NMR of (A) 1-methylimidazole, (B) 1-butylimidazole, (C) [BMIM][Cl], (D) [C$_3$SO$_3$HMIM][Cl] and (E) [C$_3$SO$_3$HMIM][HSO$_4$] ILs. All the spectra were recorded in DMSO-d$_6$ solvent. †Peaks indicate for DMSO-d$_6$ solvent. ‡Peaks for water present in DMSO-d$_6$ solvent.

A further downshift of H_8 protons was also noticeable however, the extent was marginal. However, no change in chemical shift for H_9 and H_{10} protons was seen because with increase in carbon chain, decrease in effect of electron withdrawing or donating groups is known. It was interesting to see the extensive deshielding of H_2 proton (C_2-H_2 in imidazolium cation) in [BMIM][Cl] to 9.37 ppm from 7.60 ppm in case of 1-butylimidazole. Similarly, deshielding effect was also observable for H_4 and H_5 protons in [BMIM][Cl] compared to 1-butylimidazole. These observations in downshift of imidazole ring protons represents that the imidazole ring is electron deficient. Since, -$N_1C_2H_2N_3$- proton is slightly more acidic (electron deficient) than other protons on imidazole ring, it observed the highest deshielding.

While, due to fast exchange of protons under acidic conditions, it was impossible to carry out interaction studies between substrate and IL, the neutral [BMIM][Cl] was used as representative IL in NMR studies. However, to gain insights on chemical shifts in real environment, comparison studies between neutral [BMIM][Cl] and –SO_3H functionalized [C_3SO_3HMIM][Cl] BAIL were carried out (for not checking the interaction but to study effect of the –SO_3H group). Due to the presence of the electron withdrawing –SO_3H group on the alkyl chain in [C_3SO_3HMIM][Cl], it was expected that it would induce inductive effect. Additionally, NMR spectrum was also recorded for the actual catalyst, [C_3SO_3HMIM][HSO_4] used in lignin depolymerization study. As summarized in Table 5.5 (Figure 5.8), further deshielding of H_7 proton [4.18$\rightarrow$ 4.29 ppm, ($\Delta\delta$=0.11 ppm)] was observed in case of [C_3SO_3HMIM][Cl] and [C_3SO_3HMIM][HSO_4] BAILs because of presence of two electron withdrawing groups (imidazolium ring and –SO_3H) on either side of the alkyl chain. Nevertheless, compared to the H_7 proton, larger extent of deshielding effect was seen with H_9 [1.20$\rightarrow$2.52 ($\Delta\delta$=1.32 ppm)] and H_8 [1.74$\rightarrow$2.09 ($\Delta\delta$=0.35 ppm)] protons obviously because of their proximity to the electron withdrawing –SO_3H group. It is known from the literature that the chemical shift of the molecules usually depends on the nature of electron withdrawing groups[25, 26, 28] and from the results it is apparent that compared to the imidazolium ring (cation), the –SO_3H group has larger influence on the chemical shifts. This is because the presence of the -SO_3H group on the propyl chain exerts change of chemical shift even on the H_7 proton (4.18 $\rightarrow$ 4.29 ppm for [C_3SO_3HMIM][Cl] verses [BMIM][Cl]) but a similar effect was not observed in the case of the H_9 proton (1.20 ppm) with [BMIM][Cl] in comparison to 1-butylimidazole (1.19 ppm). This comparison between H_7 and H_9 proton was made because both of these proton are located on the 3rd carbon from the –SO_3H and imidazolium ring, respectively. It was interesting to see that the H_2 proton has shown shielding in [C_3SO_3HMIM][Cl] (9.12 ppm) than in [BMIM][Cl] (9.37 ppm), which implies that its acidic character has reduced. This might be because of extended interaction of Cl^- (anion) with H_2 and –SO_3H group in the case of [C_3SO_3HMIM][Cl]. However, there is an extended explanation based on the DFT study where HSO_4^- (anion) has shown interaction with both H_2 and –SO_3H groups

(Figures 5.10-5.12, Table 5.6). Similarly, the shielding of H_4 and H_5 protons was also observed, albeit to a lesser extent compared to H_2. This again suggests that C_2-H_2 is the most likely site for hydrogen bond formation with electron rich atom(s).

Table 5.5. Proton chemical shifts assignment in 1D (^{1}H) NMR of 1-methylimidazole, 1-butylimidazole, [BMIM][Cl], [C$_3$SO$_3$HMIM][Cl] and [C$_3$SO$_3$HMIM][HSO$_4$] samples.

Sr. No.	Assignments	δ_H (ppm) NMR				
		1-methyl imidazole	1-butyl imidazole	[BMIM][Cl]	[C$_3$SO$_3$HMIM] [Cl]	[C$_3$SO$_3$HMIM] [HSO$_4$]
1	H$_6$	3.64	-	3.86	3.84	3.85
2	H$_2$	7.56	7.60	9.37	9.12	9.07
3	H$_5$	7.10	7.15	7.82	7.75	7.75
4	H$_4$	6.87	6.87	7.74	7.68	7.68
5	H$_7$	-	3.94	4.18	4.29	4.29
6	H$_8$	-	1.66	1.74	2.09	2.10
7	H$_9$	-	1.19	1.20	2.52	2.51
8	H$_{10}$	-	0.87	0.85	-	-

When the NMR spectrum was recorded for [C$_3$SO$_3$HMIM][HSO$_4$], which is an actual catalyst used in lignin depolymerization study, it showed almost no difference in chemical shifts related to [C$_3$SO$_3$HMIM][Cl]. However, a slight shielding (9.07 ppm) of the -N$_1$C$_2$H$_2$N$_3$- proton was seen in [C$_3$SO$_3$HMIM][HSO$_4$] compared with [C$_3$SO$_3$HMIM][Cl] (9.12 ppm), maybe due to an extended interaction of anion, HSO$_4^-$ compared to the anion Cl$^-$ (Section 5.4, Figure 5.12). Considering this, in the DFT studies, it was possible to studied with acidic [C$_3$SO$_3$HMIM][HSO$_4$] and neutral [BMIM][Cl] ionic liquids.

5.3.2.2. RAMAN analysis

The RAMAN analysis of the neat vanillin, neat [BMIM][Cl] and vanillin-[BMIM][Cl] adduct are used to correlate and validate the explanation derived from 1D (^{1}H) and 2D (HSQC and HMBC) NMR interaction studies as discussed in the current Chapter. In RAMAN (Figure 5.9), characteristic peaks for the stretching mode of the -C=O bond are visible at 1661, 1667 and 1692 cm^{-1} for the neat vanillin sample, but those peaks are shifted to higher wavenumber or red shift (1667, 1699, 1758, 1770 cm^{-1}) in the vanillin-[BMIM][Cl] adduct form. It may be due to increasing the strength of bond character of –C=O (-CHO) present in the vanillin molecule because of electron pull from –OH group (which interacts with IL) located on para position. Simultaneously, in the vanillin-[BMIM][Cl] adduct, a negative shift or blue shift in wavenumber (3090 to 3068 cm^{-1}) for C-H (-N$_1$C$_2$H$_2$N$_3$-) of imidazolium ring (cation of IL) was noticed to neat [BMIM][Cl] sample. The observed positive shift was because of transfer of electron density from vanillin to imidazolium *via* aromatic ring and 'O' of -OH, which enhances the double bond

character of C=O as it is located to para position to –OH. Similarly, with increase in electron density on imidazolium, $^+\delta$ character is weakened and accordingly negative shift is spotted. These results yet again endorse the fact that –OH groups interact with imidazolium of IL.

The difference in chemical shifts in vanillin-[BMIM][Cl] adduct sample [1D (^{1}H) NMR, δ= 9.43$\rightarrow$9.36 ppm, and 2D NMR, δ_C/δ_H= 136.55/9.75$\rightarrow$136.74/9.37 ppm, (–N$_1$C$_2$H$_2$N$_3$-) upfield] and Ar-H in vanillin, 1D NMR, δ=10.27$\rightarrow$10.60 (H$_1$), 6.98$\rightarrow$7.10 ppm and 6.94$\rightarrow$7.06 ppm (H$_5$), and 2D NMR, δ_C/δ_H= 115.4/6.97$\rightarrow$115.63/7.11 ppm for 'H$_5$', downfield] correspond to neat [BMIM][Cl] and neat vanillin samples were detected (Figures 5.2-5.3). These results reinforce the observations made from RAMAN studies, characteristic peaks for -C=O stretching were visible at 1661, 1667 and 1692 cm^{-1} for neat vanillin, but those peaks were shifted to positive wavenumber (1667, 1699, 1758, 1770 cm^{-1}) in vanillin-[BMIM][Cl] adduct. The significant changes (e.g. chemical shifts and RAMAN shifts) arisen owing to their interaction.
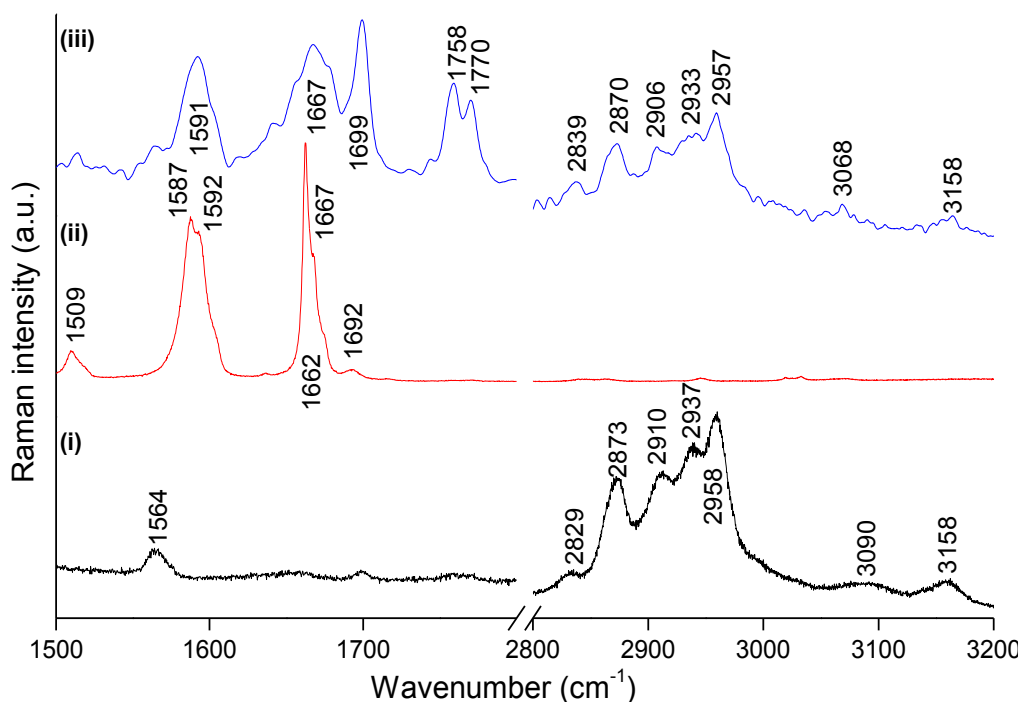
Figure 5.9. RAMAN spectra of (i) neat [BMIM][Cl], (ii) neat vanillin and (iii) vanillin-[BMIM][Cl] adduct at room temperature.

5.4. Theoretical validation

The optimized structures of vanillin and cumene are shown in Figures 5.10A-5.10B. For all the calculations discussed here, TZVP[18]/PBE[19] has been employed with Turbomole 7.0.[16] The experimental studies of proton NMR in deuterated DMSO solvent show that when vanillin interacts with [BMIM][Cl], the -O-H hydrogen of vanillin (atom O1, H1 in Figure 5.2) is deshielded, while the C-H hydrogen that is at the centre of the imidazole (atom C2, H2 in Figure 5.2) is shielded. In the adduct form, these are the two hydrogens that are the most shifted in the

proton NMR studies. In order to understand this experimental result, as observed from the mode of interaction between the vanillin -O-H and the -C-H of [BMIM][Cl]. Several conformers have been considered and the most stable structure obtained is reported here. The calculations indicate that there is an increase in the -O-H bond length (O1-H1, Figure 5.10A) of vanillin by 0.170 Å in the adduct (see Table 5.6) in comparison to the free vanillin structure (O1-H1, Figure 5.10A). This suggests that polarization of the bond occurs when the adduct is formed. This validates the experimental proton NMR result (Figure 5.2) with regard to the interaction. The bond length of the central -C-H bond (C2-H2, Figure 5.10A) in the imidazole moiety is seen to decrease by 0.014 Å (Table 5.6) in comparison to its free form (C2-H2, Figure 5.10C). The mode of interaction is essentially through O-H---Cl, where the Cl⁻ counter-anion forms an O-H---Cl strong hydrogen bond (Table 5.6, bond length (BL, 1.847 Å) and bond angle (BA, 170.8°) (Figure 5.10A)). The optimized geometry of the interaction of the substrate cumene with the [BMIM][Cl] catalyst shows that the most stable structure has negligible -C-H bond elongation in the catalyst (C2-H2, Figure 5.11B) in comparison to its free form (C2-H2, Figure 5.10C). The substrate cumene has no noticeable change in the *ortho* C-H bond distance (Table 5.6) and the C1-H1 distance (Figure 5.10B-5.11B). This suggests that the observations from the proton NMR experimental data match well with the calculated change in the bond lengths. Furthermore, a perusal of the mode of interaction shows that the Cl⁻ counter ion has a long range inefficient noncovalent interaction with the central -C-H (C2-H2, Figure 5.11A) of the imidazolium ring. It was experimentally found that the [C₃SO₃HMIM][HSO₄] catalyst produced a higher yield in the final product in comparison to the [BMIM][Cl] catalyst.

In order to provide the explanation for this and to get a possible idea of the interaction, the catalyst [C₃SO₃HMIM][HSO₄] was optimized in its free form (Figure 5.10D) as well as with the substrate vanillin in the adduct form (Figure 5.12). Different modes of interaction were considered and the most energetically favourable geometry is reported here (Figure 5.12A). This computational study with [C₃SO₃HMIM][HSO₄] is very valuable since it provides direct correlation with the activity of the catalyst. This is particularly more crucial since NMR studies could not be carried out with [C₃SO₃HMIM][HSO₄] due to its acidic nature (which hampers the recordings of H).

It was observed that with the catalyst [C₃SO₃HMIM][HSO₄], there is an extended interaction with the counter-anion HSO₄⁻, as well as with the attached -SO₃H moiety of the catalyst (atom O5, H11, O6 in Figure 5.12A) and the -OH moiety of vanillin (atom O1, H1 in Figure 5.12A). It was observed that the -O-H bond of vanillin increases in bond length by 0.208 Å (Table 5.6). This may be attributed to the greater polarization in the -O-H bond of vanillin in the adduct, due to the weak hydrogen bonding (BL-1.507 Å and BA-116.9°) with the HSO₄⁻.

This can be a possible reason for the higher percentage of yield in the final product. The adduct of cumene and $[C_3SO_3HMIM][HSO_4]$ was also optimized at the same level of theory and the geometry that has the most energetically favourable interaction was obtained. The interaction between cumene and $[C_3SO_3HMIM][HSO_4]$ shows that the central -C-H bond of the imidazole ring (atom C2-H2, Figure 5.12B) has a negligible noncovalent interaction with the oxygen atom of the counter ion HSO_4^- (atom number O5 in Figure 5.12B). The bond length of the -C-H bond (atom C2, H2 in Figure 5.12B) of the imidazole moiety shows only a negligible change in the bond distance, of 0.008 Å (Table 5.6) in comparison to its free form (Figure 5.10C). This suggests that there is little bond polarization in the adduct. The computationally optimized structure of free cumene shows that the bond length for the *ortho* hydrogen of the C-H bond (atom C1, H1 in Figure 5.12B) has not decreased (Table 5.6). This suggests that the substrate cumene does not polarize the C-H bond in the adduct.

Figures 5.11A-5.12A indicate that vanillin with [BMIM][Cl] and $[C_3SO_3HMIM][HSO_4]$ ILs shows weak and strong hydrogen bonding respectively, as also clear from Table 5.6. There is a significant change in bonding on going from neat [BMIM][Cl] to the vanillin-[BMIM][Cl] adduct. Depending on the bonding parameters, the weak hydrogen bond (WHB) and strong hydrogen bond (SHB) terms have been introduced.[29, 30] The adduct form of vanillin-[BMIM][Cl] has a bond length (H2---Cl1) of 2.739 Å and a bond angle (C2-H2---Cl1) of 123.8° (see Table 5.6) which suggests that a WHB compared to the neat form (Table 5.6 and Figure 5.10C). However, the H2---Cl1 bond length (2.307 Å) and C2-H2---Cl1 bond angle (154.0°), are noticed in the cumene-[BMIM][Cl] adduct and this is very similar to neat [BMIM][Cl]. So, this affirms that vanillin has greater affinity with the [BMIM][Cl] IL and that the Cl⁻ anion has a WHB with the –O-H of the vanillin group. It is also observed that the Cl⁻ anion forms WHB with the –C-H moieties attached with the imidazole ring. For more details descriptions, please see Table 5.6.

Additionally, the vanillin-$[C_3SO_3HMIM][HSO_4]$ adduct has a bond distance of H2---O1 (2.407 Å) and a bond angle of –C2-H2---O1 (156.7°) respectively. In the Figure 5.12A, it is observed that the bond length between the O6-H11 atoms is 1.592 Å and the bond angle (O6-H11---O5) is 178.3°, while in the neat sample, the bond length (O6-H11) is 1.438 Å and the bond angle (O6-H11---O5) is 172.5°, which suggests SHB (Figure 5.10). The interaction of the imidazole (C2-H2) shows that the WHB with the O2 of methoxy group has a bond distance of 2.185 Å (H2---O2) and a bond angle (C2-H2---O2) of 165.3°, compared to the bond distance (H2---O1) of 2.407 Å and bond angle (C2-H2---O1) of 156.1° in the vanillin molecule case (see Figure 5.12A). So, this affirms that the 'O' atom of the methoxy group has strong affinity for WHB compared to the hydroxyl group. Significantly, the extended WHB interaction represents the nature of the $[C_3SO_3HMIM][HSO_4]$ catalyst, which has better activity compared to the [BMIM][Cl] catalyst. It was also perceived that the cumene-$[C_3SO_3HMIM][HSO_4]$ adduct form has almost negligible

change in comparison to the neat structures. This may be due to the absence of hydroxyl and methoxy groups in cumene. This provides clear evidence of the effect of molecules having hydroxyl, methoxy and other groups and also shows that catalysts having a Brønsted proton will have good interaction with the hydroxyl and methoxy functionalities and provide better catalytic results, as shown in Figure 5.1.
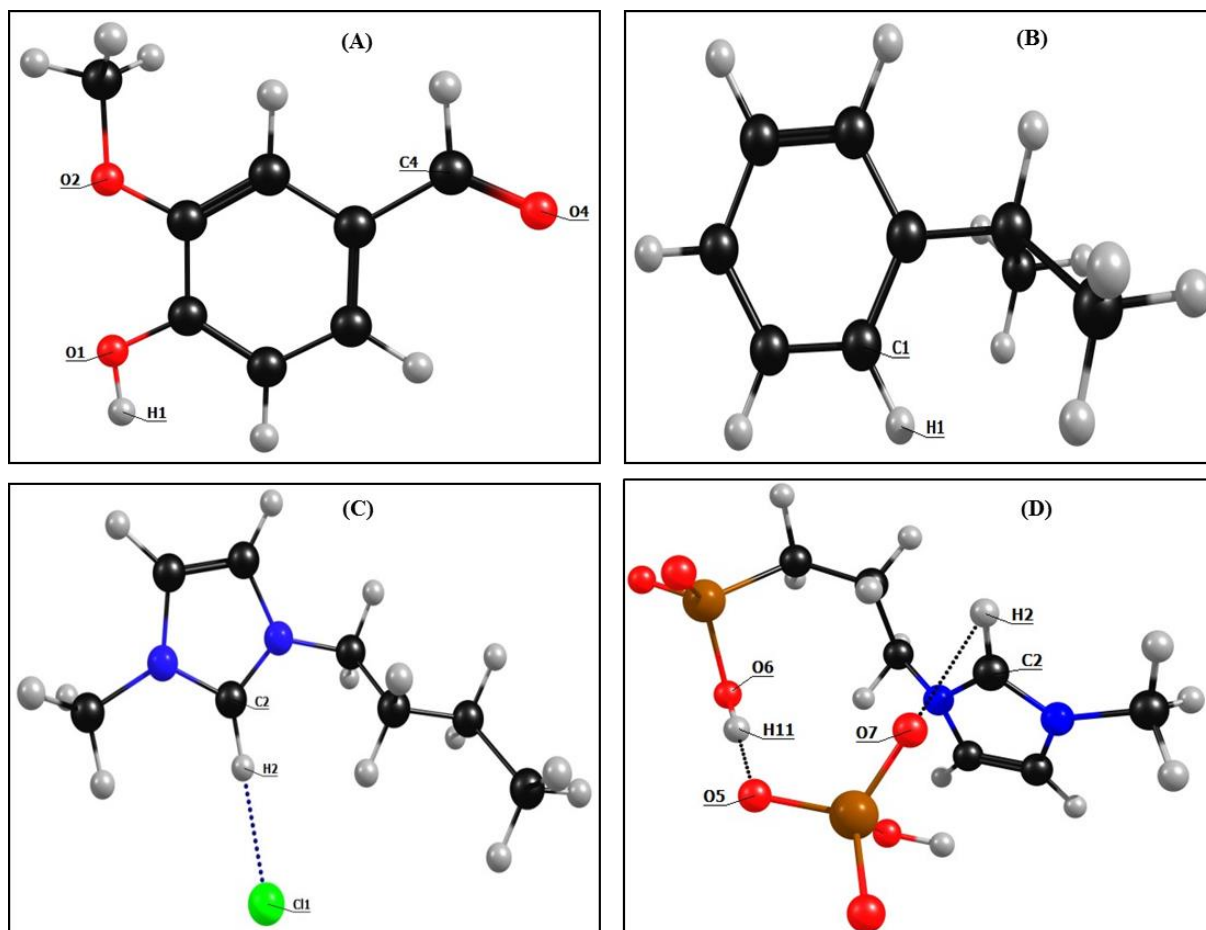
Figure 5.10. The optimized geometry of (A) vanillin, (B) cumene, (C) [BMIM][Cl] and (D) [C_3SO_3HMIM][HSO_4] molecules. The Figure uses color coding as follows: C (black), O (red), N (blue), H (grey), S (reddish brown), Cl (green). The interaction is shown by the fragmented bond (blue).
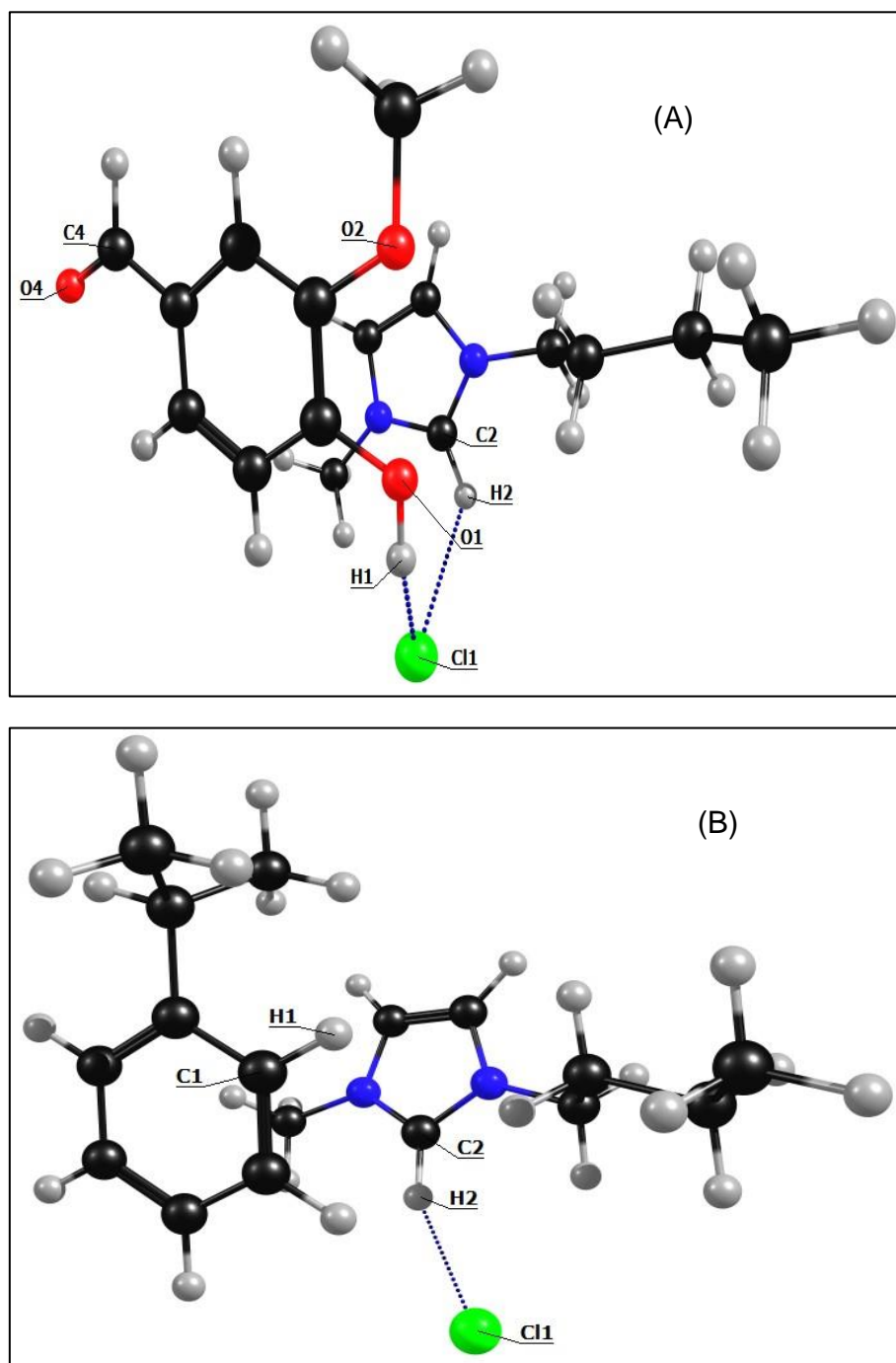
Figure 5.11. The optimized geometry of (A) vanillin–[BMIM][Cl] adduct and (B) cumene-[BMIM]Cl] adduct. The colour coding is as follows: C (black), O (red), N (blue), H (grey) and Cl (green). The interaction is shown by the fragmented bond (blue).
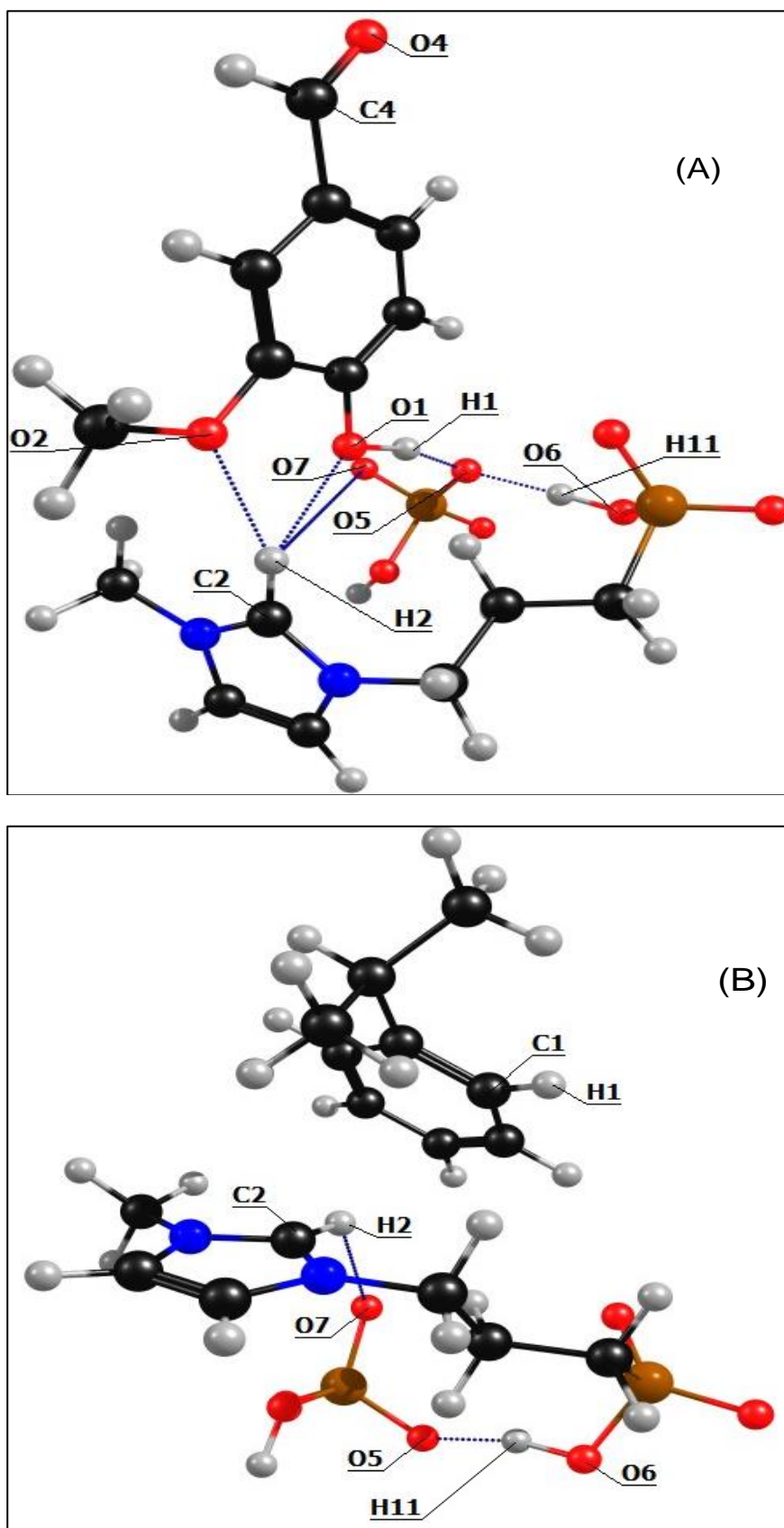
Figure 5.12. The optimized geometry of (A) vanillin-[C_3SO_3HMIM][HSO_4] adduct and (B) cumene-[C_3SO_3HMIM][HSO_4] adduct. The colour coding is as follows: C (black), O (red), N (blue), H (grey), S (reddish brown). The interaction is shown by the fragmented bond (blue).

Table 5.6. The bond lengths and bond angles for the different adducts and free species are indicated.

Substrate/ catalyst/ adduct	Bond length (Å)	Change in bond length in adduct (Å)	Bond length (Å)	Change in bond length in adduct (Å)	Bond angle (°)
Substrate					
Vanillin	O1-H1= 0.977	-	-	-	-
Cumene	C1-H1= 1.094	-	-	-	-
Catalyst					
[BMIM][Cl]	-	-	C2-H2=1.110 H2-Cl1=2.234	-	$\angle$C2-H2-Cl1=177.0
[C$_3$SO$_3$HMIM] [HSO$_4$]	-	-	C2-H2= 1.119 H2-O7= 2.116 H11-O6= 1.438	-	$\angle$C2-H2-O7=68.5 $\angle$O6-H11-O5= 172.5
Adduct					
Vanillin- [BMIM][Cl]	O1-H1= 1.147 H1-Cl1=1.847	O1-H1= 0.170	C2-H2= 1.096 H2-Cl1=2.739	C2-H2=-0.014 H2-Cl1= 0.505	$\angle$O1-H1-Cl1=170.8 $\angle$C2-H2-Cl1=123.8
Cumene- [BMIM][Cl]	C1-H1= 1.094 H1-Cl1=5.001	C1-H1= 0.000	C2-H2= 1.110 H2-Cl1=2.307	C2-H2= 0.000	$\angle$C2-H2-Cl1=154.0 $\angle$C1-H1-Cl1=76.7
Vanillin- [C$_3$SO$_3$HMIM] [HSO$_4$]	O1-H1= 1.185	O1-H1= 0.208	C2-H2= 1.108 H2-O7= 5.382 H2-O1= 2.407 H2-O2= 2.185 H1-O5= 1.507 H1-O7= 3.028 H11-O6=1.592	C2-H2=-0.011 H2-O7= 3.266 H11-O6= 0.154	$\angle$C2-H2-O7=79.8 $\angle$C2-H2-O1=156.7 $\angle$C2-H2-O2=165.3 $\angle$O1-H1-O5=116.9 $\angle$O6-H11-O5= 178.3 $\angle$O1-H1-O7=123.4
Cumene- [C$_3$SO$_3$HMIM] [HSO$_4$]	C1-H1= 1.094	C1-H1= 0.000	C2-H2= 1.111 H2-O7= 2.428 H11-O6=1.540	C2-H2=-0.008 H2-O7= 0.312 H11-O6=0.102	$\angle$C2-H2-O7=120.7 $\angle$O6-H11-O5= 164.6

From the 1D (^{1}H) NMR studies, it is easy to describe an interaction between lignin and the ionic liquid *via* the 'O' atom of –OH and -N$_1$C$_2$H$_2$N$_3$-. It is possible for C$_2$-H$_2$ (-N$_1$C$_2$H$_2$N$_3$-) to form hydrogen bonding because carbon (Pauling Scale= 2.55) is more electronegative than hydrogen (Pauling Scale= 2.20) and additionally carbon is attached to two more electronegative N atoms (Pauling Scale= 3.04). This led us to suggest that transfer of electron density from substrate

molecule to IL is possible, which eventually gives rise to high activity for BAILs. Although the essence of the interaction remains the same, by carrying out further studies with 2D ($^{15}N/^{1}H$, HMBC) NMR and DFT, it was observed that the anion plays an important role in these interactions. As seen, in the neat [BMIM][Cl] sample, Cl^- interacts with the most acidic proton (C_2-H_2) on the imidazole ring in a stable linear fashion. However, in case of the vanillin-[BMIM][Cl] adduct, Cl^- interacts with IL [$H_2(C_2$-$H_2)$] and also with the H atom of the –OH group in vanillin (Figure 5.11).[31] As seen from Figures 5.2-5.8, the most effective shielding and deshielding phenomenon were seen to occur with H_2 (C_2-H_2 in imidazolium ring) and H_1 (-OH group on vanillin) protons, respectively. This is because Cl^- has electronegativity (Pauling scale=3.16) between the C (Pauling scale=2.55) and O (Pauling scale=3.44) atoms. When Cl^- is replaced with HSO_4^- in [C_3SO_3HMIM][HSO_4], it also forms hydrogen bonding with the H_2 atom (C_2-H_2 in imidazolium ring) (Figure 5.12). However, unlike in [BMIM][Cl], extended interaction of C_2-H_2 with three oxygen atoms (HSO_4^-, -OH and –OCH_3) was also observed. This is contrary to the observation made with the Cl^- anion where Cl^- interacts with C_2-H_2 (imidazolium) and the H_1 atom of –OH in vanillin and no interaction between O atoms of –OH (vanillin) and C_2-H_2 was seen. This difference in hydrogen bonding is due to the fact that in case of [C_3SO_3HMIM][HSO_4], the most electronegative atom is oxygen, which is available for hydrogen bonding in the absence of Cl^- [BMIM][Cl]. Further, HSO_4^- also shows intramolecular interaction with the –SO_3H group attached to the propyl chain. The observance of increase in bond length between H2---O7 from 2.116 Å to 5.382 Å in neat [C_3SO_3HMIM][HSO_4] and its adduct with vanillin (Table 5.6) indicates that C2-H2 prefers to form hydrogen bonding with O2 (-OCH_3) and O1 (-OH) atoms on vanillin. The observation of stronger interaction with the O2 atom (-OCH_3) also may suggest that ether linkages present in lignin would interact extensively with IL and thus it would help cleave the ≡C-O-C≡ linkages. Though the extent of interaction generally depends on the size of the anion, due to the large difference in size of Cl^- and HSO_4^- and the nature of the anion, it was not possible to check this effect in the current work. In case of the real scenario where [C_3SO_3HMIM][HSO_4] is used for depolymerization, it interacts with oxygen of –OH (O1) and –OCH_3 (O2), and it is indicated that this interaction is very important to virtually tag around IL with lignin. Considering the above points, it is suggested that the IL and lignin extensively interact with each other where the anion plays a major role and this eventually leads to the availability of higher concentration of H^+ on BAIL (-SO_3H) close to ether (≡C-O-C≡) or ester (C-(O)O-C) linkages on lignin. This, in turn, has enhanced the depolymerization activity.

5.5. Mechanistic pathway

Lastly, based on the results an alternative mechanistic pathway (Figure 5.13) is advocated for $\equiv$C-O-C$\equiv$ bond cleavage wherein it is proposed that BAILs (Imidazolium cation) interact with lignin molecules *via* 'O' of –OH groups and make a virtual binding with the substrate, which is confirmed by experimental and theoretical studies (For more details please see the above Sections 5.3-5.4). This helps in easy supply of H^+ available with BAIL for protonation of 'O' of ether linkages which exist in lignin with almost 70% of all linkages. Once this is achieved, cleavage of $\equiv$C-O-C$\equiv$ bond and attack of water on the cation will take place to yield hydrolysis products with higher concentration of –OH groups which is again discussed through FT-IR study (For more details descriptions please see Chapter 3, Section 3B.6.5, Figure 3B.25). As change in concentration of H^+ in the solution showed difference in the products yields it is expected that this mechanism is credible (For more details please see Chapter 3, Section 3B.3.1, Figure 3B.2). Moreover, BAILs may not be able to catalyse cracking reactions at 120 ^{o}C and therefore solitary possibility is the hydrolysis reaction under the reaction conditions. Additionally, it is projected that since with alteration in BAIL, no distinction in product formation is seen, the foremost role of BAIL is to contribute the H^+ to the reaction solution and carry out the hydrolysis reaction. While, this role is major, the attachment of BAIL with substrate molecule enhances its probability for depolymerization because even if same concentration of H^+ was present when H_2SO_4 was used as catalyst still, most of the products formed were not low molecular weight aromatic monomers as is seen from GC-MS analysis (For more details please see the Chapter 3, Section 3B.3.1.5, Figure 3B.4).
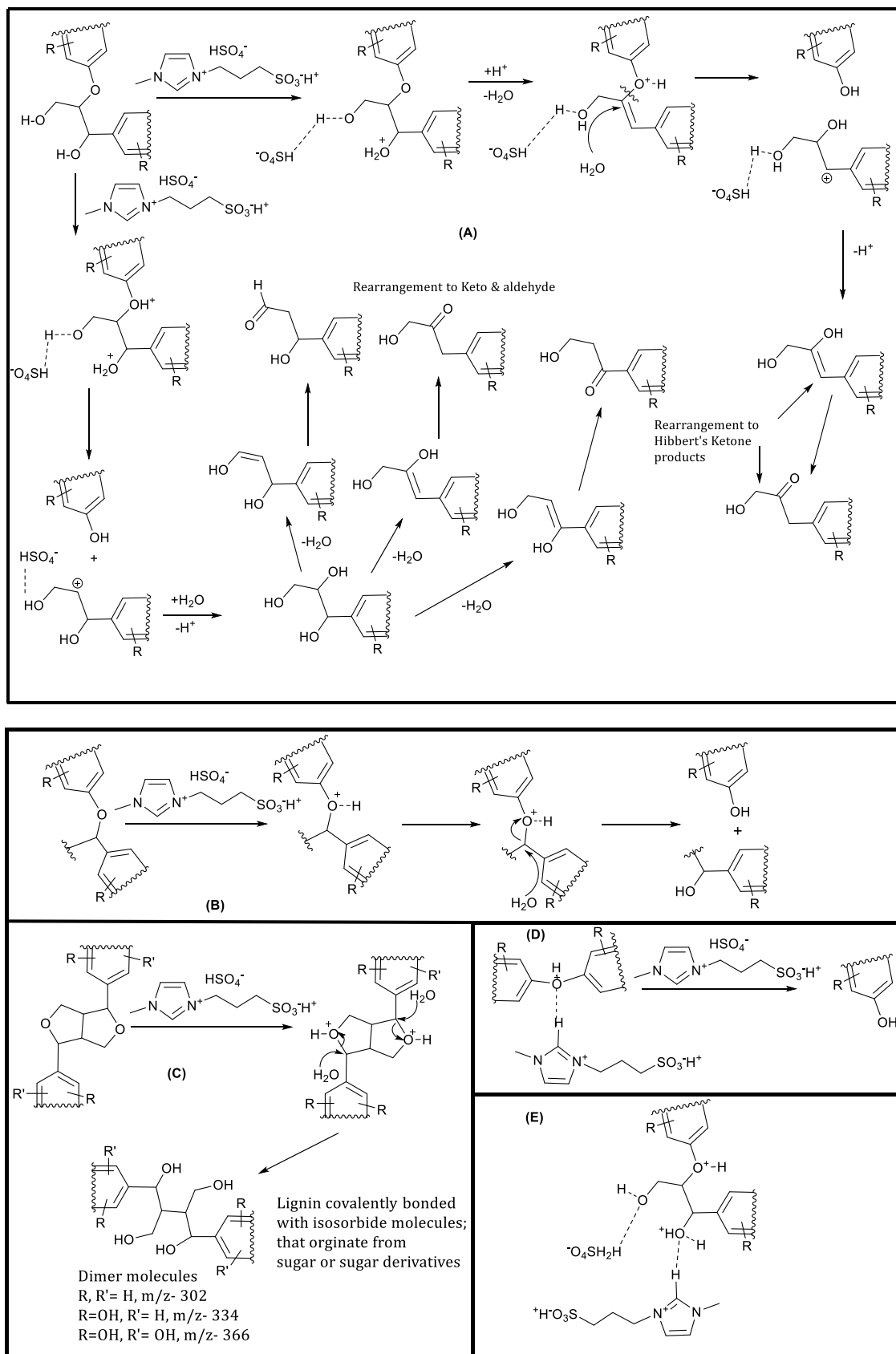
Figure 5.13. The proposed mechanism. (A) β-O-4, (B) α-O-4, (C) 4-O-5, (D) α-O-γ linkage present in the lignin molecules to form monomers and dimer units and (E) interaction of lignin with [C₃SO₃HMIM][HSO₄] BAIL.

5.6. Conclusions

In summary, lignin is linked *via* ≡C-O-C≡ and ≡C-C≡ bonds and decorated with various functional groups. Though, due to its intrinsic nature it is difficult to break these bonds and obtain low molecular weight aromatic products in good yields but with the help of Brønsted acidic ionic liquid (BAIL) such as [C_3SO_3HMIM][HSO_4], it was possible to yield 78% low molecular weight aromatic products at 120 °C in presence of water-methanol. In absence of acidity, with [BMIM][Cl] catalyst, products yield 18% was obtained under similar conditions. However, interestingly with mineral acid (H_2SO_4) with similar H^+ concentration as that with [C_3SO_3HMIM][HSO_4] comparatively very low yields of low molecular weight aromatic products was obtained. In order to comprehend the differences in activity between H_2SO_4 and BAIL, attempt was made to correlate the catalytic activity with the structure of IL employing both experiments and computations. This conclusion is substantiated by meticulous studies discussed with the help of experimental, RAMAN and 1D (^{1}H) and 2D (^{13}C/^{1}H HSQC, ^{15}N/^{1}H HMBC, ^{1}H/^{1}H NOESY) NMR and theoretical (DFT) studies, it has been established that the ILs form weak and strong hydrogen (inter and intra) bonding with the –OH and –OCH$_3$ groups on the substrate. These characterizations also helped to comprehend the mode of interaction as (preferably) perpendicular. It has been observed that, although the change in bond distance is negligible for the cumene-[BMIM][Cl] as well as cumene-[C_3SO_3HMIM][HSO_4] adduct. In case vanillin-[C_3SO_3HMIM][HSO_4] adduct, the changes in bond length and bond angle are greater than vanillin-[BMIM][Cl] adduct. This suggests that [C_3SO_3HMIM][HSO_4] plays a crucial role by having interactions with substrate, which, in turn, is responsible in producing higher yields. After compilation of all the data, hydrolysis mechanism is proposed for depolymerization of lignin into low molecular weight aromatic products *via* protonation of ≡C-O-C≡ linkages.

5.7. References

1.   S. K. Singh and P. L. Dhepe, *Bioresour. Technol.*, 2016, **221**, 310-317.

2.   J. Zakzeski, P. C. A. Bruijnincx, A. L. Jongerius and B. M. Weckhuysen, *Chem. Rev.*, 2010, **110**, 3552-3599.

3.   N. V. Plechkova and K. R. Seddon, *Chem. Soc. Rev.*, 2008, **37**, 123-150.

4.   S. K. Singh and P. L. Dhepe, *Green Chem.*, 2016, **18**, 4098-4108.

5.   S. Tsuzuki, M. Mikami and S. Yamada, *J. Am. Chem. Soc.*, 2007, **129**, 8656-8662.

6.   J.-Y. Ortholand, A. M. Z. Slawin, N. Spencer, J. F. Stoddart and D. J. Williams, *Angew. Chem. Int. Ed.*, 1989, **28**, 1394-1395.

7.   R. C. Remsing, R. P. Swatloski, R. D. Rogers and G. Moyna, *Chem. Commun.*, 2006, DOI: 10.1039/B600586C, 1271-1273.

8.   J. C. Ma and D. A. Dougherty, *Chem. Rev.*, 1997, **97**, 1303-1324.

9.   W. E. S. Hart, J. B. Harper and L. Aldous, *Green Chem.*, 2015, **17**, 214-218.

10.   C. S. Lovell, A. Walker, R. A. Damion, A. Radhi, S. F. Tanner, T. Budtova and M. E. Ries, *Biomacromolecules*, 2010, **11**, 2927-2935.

11.   B. G. Janesko, *Phys. Chem. Chem. Phys.*, 2014, **16**, 5423-5433.

12.   M. A. Petti, T. J. Shepodd, R. E. Barrans and D. A. Dougherty, *J. Am. Chem. Soc.*, 1988, **110**, 6825-6840.

13.   J.-Y. Ortholand, A. M. Z. Slawin, N. Spencer, J. F. Stoddart and D. J. Williams, *Angew. Chem. Int. Ed. Engl.*, 1989, **28**, 1394-1395.

14.   S. Tsuzuki, H. Tokuda and M. Mikami, *Phys. Chem. Chem. Phys.*, 2007, **9**, 4780-4784.

15.   R. P. Matthews, I. J. Villar-Garcia, C. C. Weber, J. Griffith, F. Cameron, J. P. Hallett, P. A. Hunt and T. Welton, *Phys. Chem. Chem. Phys.*, 2016, **18**, 8608-8624.

16.   R. Ahlrichs, M. Bär, M. Häser, H. Horn and C. Kölmel, *Chem. Phys. Lett.*, 1989, **162**, 165-169.

17.   TURBOMOLE GmbH, "TURBOMOLE V6.3 2011, a development of University of Karlsruhe and Forschungszentrum Karlsruhe GmbH, 1989–2007," 2011, http://www.turbomole.com/.

18.   A. Schäfer, C. Huber and R. Ahlrichs, *J. Chem. Phys.*, 1994, **100**, 5829-5835.

19.   J. P. Perdew, K. Burke and M. Ernzerhof, *Phys. Rev. Lett.*, 1996, **77**, 3865-3868.

20.   S. Grimme, J. Antony, S. Ehrlich and H. Krieg, *J. Chem. Phys.*, 2010, **132**, 154104-154123.

21.   K. Eichkorn, O. Treutler, H. Öhm, M. Häser and R. Ahlrichs, *Chem. Phys. Lett.*, 1995, **240**, 283-290.

22.   M. Sierka, A. Hogekamp and R. Ahlrichs, *J. Chem. Phys.*, 2003, **118**, 9136-9148.

23.   A. Klamt and G. Schuurmann, *J. Chem. Soc., Perkin Trans. 2*, 1993, DOI: 10.1039/P29930000799, 799-805.

24.   P. Batamack and J. Fraissard, *Catal Lett*, 1997, **49**, 129-136.

25.   G. V. D. Tiers, *Magn. Reson. Chem.*, 1999, **37**, 609-612.

26.   G. da Costa Resende and E. S. Alvarenga, *Magn. Reson. Chem.*, 2016, **54**, 968-974.

27.   L. Pauling, *The Nature of the Chemical Bond*, Cornell University Press, USA, 3 edn., 1060.

28.   A. Muhammad, A. Jalali and Y. M. Mahzia, *IOSR Journal of Applied Physics*, 2014, **6**, 45-56.

29.   G. R. Desiraju, *Chem. Commun.*, 2005, DOI: 10.1039/B504372G, 2995-3001.

30.   S. K. Panigrahi and G. R. Desiraju, *Proteins: Struct., Funct., Bioinf.*, 2007, **67**, 128-141.

31.   C. B. Aakeroy, T. A. Evans, K. R. Seddon and I. Palinko, *New J. Chem.*, 1999, **23**, 145-152.

Chapter 6:

Summary and conclusions

Summary and conclusions

The importance of the production of sustainable, eco-friendly and renewable resources of chemicals, fuels and energy from lignocellulosic biomass has been identified in the last few decades. Lignin is one of the major constituent of lignocellulose, and has wide range (e.g. chemicals, fuels, polymers, materials) of applications, due to its high energy efficiency (ca. 40% w.r.t. dry lignocellulosic biomass), than cellulose and hemicellulose. Ionic liquids are considered as green solvent and catalyst because of their important properties, such as low vapour pressure, excellent solubility, high thermal stability, tuneable acidity or basicity by changing the combination of cations or anions, etc. Lignin can be converted into fuels and chemicals, etc. using some transformation processes. The main aim of the current work is depolymerization of commercial and isolated lignins into low molecular weight aromatic products. In the previous Chapters, the obtained results on the lignin isolation, characterization and their depolymerization were discussed in details. Additionally, the mechanistic correlation of substrate with products and substrate with catalysts was also deliberated in details. However, the key results and conclusions obtained from each Chapter are consolidated in the current Chapter.

Chapter 1

In this Chapter, an overview on the fossil feedstocks, resources and its limitation such as nonrenewable, heterogeneous distribution, depletion, major cause of greenhouse gases, etc. is described and what are the alternative sources of fossil feedstocks is also drawn. There are several renewable, sustainable and locally available alternate sources available such as solar, geothermal, tidal, lignocellulosic materials etc. for the valorization. Among all the renewable resources, lignocellulosic biomass is the sole source of energy, fuels and chemicals, (rest for the energy). This non-edible lignocellulosic biomass is made up of mainly three units; cellulose, hemicellulose and lignin. The details on bio-synthesis, general structure, linkages, various functional groups present in the lignin copolymer are discussed in this Chapter. There are numerous ways for the extraction of lignin from the various resources (e.g. hardwood, softwood and grasses) by applying different process such as, Kraft, lignosulphate, enzymatic, organosolv, ionic liquids assisted etc. and the details on those have been mentioned. Based on the literature, several upgradation processes (e.g. thermal, chemical, enzymatic etc.) are used to valorise lignin into aromatic products. But most of the upgradation processes use very severe conditions (e.g. high temperature, high pressure, precious metal, time consuming, etc.) to break lignin into low molecular weight aromatic products. These processes convert lignin into maximum amount of degradation products such as char, tar, gases, etc. Considering the problems associated with known processes, it is important to develop a distinct and novel method to depolymerise lignin at milder reaction conditions using homogeneous catalyst. Moreover, it will be great advantage

to use acidic ionic liquids as a catalyst, they are already known for lignin depolymerisation as a solvent and also for conversion of polysaccharide in to value added products. It is essential to find an efficient method for the depolymerisation of lignin into aromatic products. Considering above discussion, the prime objectives of research works are shown as below;

➤ To develop a method for lignin (isolated and commercial) depolymerization into low molecular weight aromatic products at mild reaction conditions.

➤ Recycling and characterization of catalysts.

➤ Isolation of aromatic monomers from depolymerized products using column chromatography and their characterization.

➤ Correlation study of substrate with catalyst and substrate with products using experimental and theoretical studies.

Chapter 2

Section 2A

Considering the lignin depolymerization catalytic activity using acidic ionic liquids (ILs), imidazolium, benzimidazolium, ammonium and phosphonium cations based ILs catalysts were synthesized by the quaternization and direct combination methods and were evaluated for the lignin depolymerization reactions.

➤ Various ionic liquids with combination of cations (ammonium, phosphonium, imidazolium and benzimidazolium) and anions (hydrogen sulfate, dihydrogen phosphate, chloride, *p*-toluene sulphate) were synthesized by the quaternization and direct combination methods.

➤ ILs with Brønsted and Lewis acidity were synthesized for cleavage of $\equiv$C-O-C$\equiv$ and $\equiv$C-C$\equiv$ bonds. To check the interaction between pi-bonds among cations of ionic liquids and substrate.

➤ To find out the effect of geometry of catalysts such as tetrahedral (ammonium and phosphonium) and planar (imidazolium and benzimidazolium) for the interaction with substrate in lignin depolymerization reaction.

➤ The solubility of synthesized ILs was checked in several solvents having difference in polarity.

➤ The synthesized ILs were characterized by various physico-chemical characterization techniques such as elemental analysis (CHNS), TGA, FT-IR and NMR (^{1}H and ^{13}C). The UV-Vis analysis helped to know the Hammett acidity function (H_0) and thermodynamic parameters.

➤ Purity of ILs was proved by (^{13}C and ^{1}H) NMR, IR and elemental analysis. Moreover, thermal stability of ILs (250 ^{o}C) was measured by TGA.

Section 2B

By the immobilization of ILs, it would be helpful to use low quantity of ILs and would also be easy to recycle catalyst. Considering this points, an efficient, stable and maximum immobilized Brønsted acidic ionic liquid (I-BAIL) over the silica framework was synthesized by quaternization and crystallization methods.

➢ The immobilization on/in silica framework of imidazolium based cation and [HSO_4] anion IL was done by the quaternization and crystallization methods.

➢ I-BAIL catalyst was characterized by various physico-chemical analytical techniques.

➢ Solid state (^{29}Si and ^{13}C) NMR revealed that Q^3 and Q^4 Si sites are available in I-BAIL catalyst, similarly ^{13}C NMR confirmed that synthesized I-BAIL has all the imidazolium and side chains propane peaks.

➢ TGA analysis proved that $42 wt.\%$ immobilization of IL on/in silica framework, which is in line with the values obtained from elemental analysis.

➢ XRD pattern of the synthesized I-BAIL catalyst shows the amorphous nature of catalyst. An additional peak at $2\theta = 7.22^o$ was assigned to T^3 species of silica propyl (Si-$CH_2CH_2CH_2$-N) chain attached to the imidazole ring.

➢ SEM and TEM of I-BAIL showed the smoothness of surface and embedded void images respectively.

Chapter 3

Section 3A

Section 3A gives the details on the various types of lignin (e.g. dealkaline, alkaline, alkali and industrial lignin) substrates used in this work for acidic ionic liquids catalysed depolymerization of lignin. Physico-chemical properties of all these lignins were characterized using bulk and molecular level advance analytical techniques. The major findings of the current section are consolidated below.

➢ The solubility of lignin samples was recorded in the various neat or binary mixtures of solvents, which have different in both Hansen solubility parameters (HSP-14.3-48.0) and polarity index (PI- 1.0-9.0). From the lignin solubility results, water:methanol (1:5, *v/v*) ratios would be the best solvent, in this particular solvent ratio various lignin samples were soluble. This ratio was chosen to carry out the lignin depolymerization reactions.

➢ Hansen solubility parameters and polarity index of various solvents for lignin solubility and extraction of depolymerized products were also correlated.

➢ The molecular weight of dealkaline lignin was determined by the GPC and MALDI-TOF MS analysis. It was analyzed that dealkaline lignin has 60 kDa molecular weight.

➢ Based on elemental analysis, it was easy to find out the general monomer molecular formula ($C_{10}H_{12-13}O_3S_{0.01-0.09}$) of lignin samples. However, the finding of Sulphur in the lignin samples

revealed that isolation of lignin samples has been done with the use of Sulphur containing reagents like Na_2S or H_2SO_4.

➤ SEM-EDX and ICP-OES analysis for lignin samples confirmed the presence of sodium in the dealkaline, alkali and industrial lignin samples. It may be possible that Kraft process was used to extract these lignins.

➤ Non-uniform morphology of lignin samples with particle size ranging from <1 μm to 30 μm in the SEM images was seen.

➤ The FT-IR spectra of the lignin samples confirmed the presence of various types of functional groups like hydroxy, alkyl, alkoxy, carbonyl, alkenes etc.

➤ Amorphous nature and purity of the various lignin samples were recorded by XRD pattern. Peaks pattern present in dealkaline and industrial lignins correspond to Na_2SO_4 molecule.

➤ Presence of electronic transitions and chromophoric groups in the lignin samples were confirmed with the help of UV-Vis spectra.

➤ With the help of NMR [1D (^1H and ^{13}C) and 2D (HSQC)], presence of various types of carbon and hydrogen environment within the lignin molecules was confirmed. The various types of linkages and phenolic moieties (*S*, *G* and *H*) were confirmed by the 2D NMR analysis.

Section 3B

In the current section results on lignin depolymerization reaction into aromatic products using various ILs have been discussed. Furthermore, the lignin correlation studies with the obtained products have also been discussed in details.

➤ Various types of homogeneous acidic ionic liquids were used to evaluate lignin depolymerization into low molecular weight aromatic products. The optimum reaction conditions for lignin depolymerization are; lignin (2 *wt*.% solution $H_2O:CH_3OH$, 1:5 *v/v*= 30 mL), catalyst (0.5 g), 120 ᵒC, 1 h, 1000 rpm.

➤ Imidazolium, benzimidazolium, ammonium and phosphonium based cations with several anions were checked among all anions, [HSO_4] based anion with imidazolium, benzimidazolium, ammonium and phosphonium cations gave 78%, 42%, 19% and 10% THF soluble products yield respectively.

➤ Few THF soluble products were insoluble in EtOAc and DEE, it may be because of the dissimilarity in the Hansen solubility parameter (HSP) and polarity index of solvents.

➤ The qualitative and quantitative analyses of the low molecular weight aromatic products were done by GC, GC-MS, HPLC, and LC-MS analysis.

➤ Results obtained with catalytic amount of ILs were compared with solid and homogeneous acids.

➢ Lignin depolymerization results were evaluated on weight (1:1 *wt./wt.*, substrate to catalyst) and mol basis (2.78:2.78 mol/mol, substrate to catalyst), and higher yield (78%) of THF soluble products was obtained with weight basis reaction.

➢ Commercially procured aromatic monomers (identified by GC/GC-MS/LC-MS) were taken, mixed along with [C$_3$SO$_3$HMIM][HSO$_4$] catalyst in water:methanol (1:5 *v/v*= 30 mL) and scrutinized for their stability. The change in the concentrations of these aromatic monomers was monitored by GC and GC-MS analysis. When the study was performed at 120 ^{o}C for 1 h, slight change (±3%) in the peak areas was seen. Large decline (10-30%) in the peak areas for few chemicals due to char formation was noticed when the study was performed at 170 ^{o}C. These results elucidate the decline in yields for THF soluble products when reactions were done at higher temperatures.

➢ Recycle study with [C$_3$SO$_3$HMIM][HSO$_4$] catalyst was performed up to 6th run, and results showed that catalyst was possible to reuse after acid treatment. However, catalyst was stable (based on various physico-chemical characterization) under the reaction conditions.

➢ Column chromatography method was applied to isolate few aromatic monomers (e.g. vanillin, methyl vanillate and acetovanillone) in the pure form from the THF soluble low molecular weight aromatic products.

➢ To perceive the changes transpiring in lignin and products on bulk and molecular level, correlation studies were done using several analytical techniques (GPC, DSC, UV-Vis, FT-IR, 1D and 2D (HSQC) NMR, CHNS, TGA).

➢ UV-Vis correlation studies between lignin and THF soluble products showed that both contained similar chromophoric groups.

➢ In DSC analysis of lignin, peaks were observed at 230 and 245 ^{o}C, owing to melting (endothermic) and crystallization/char (exothermic) temperature, respectively. Nonetheless, these peaks are absent in products and observance of multiple new peaks at lower temperature (<180 ^{o}C) emphasized that lignin was depolymerized into low molecular weight aromatic products, which have diverse transition temperatures.

➢ The obtained GPC chromatograms of lignin and products samples showed that lignin undergoes depolymerization. The appearance of new peak(s) along with solvent was detected in GPC of products chromatogram, which reinforced that lignin underwent depolymerization.

➢ FT-IR studies of lignin and products were carried out. The emergence of new peaks for phenolic C-O stretch (1180 cm^{-1}) and enhancement in intensity for few peaks along with decrease in peak intensity for ether linkages (1040 and 1125 cm^{-1}) in products exhibits lignin depolymerization reaction.

➤ To ascertain the linkages and functional groups present in lignin and products, advance analytical tool, 2D (HSQC) NMR was employed, the disappearance of peaks for linkages regions in products sample confirmed that lignin underwent depolymerization. Similarly observance of new peaks for *H* type moieties in the products revealed for the lignin depolymerization reaction.

Section 3C

Discussions on the lignin depolymerization reactions using I-BAIL as a solid acid catalyst to yield low molecular weight aromatic products were carried out in the current section.

➤ Lignin depolymerization reaction into low molecular weight aromatic products (yield 90%) was done using I-BAIL as catalyst. The optimum reaction condition was; lignin (2 *wt*.% solution H_2O:CH_3OH, 1:5 *v/v*= 30 mL), I-BAIL (0.5 g), 200 ᵒC, 1 h.

➤ Depolymerization of lignin was optimized by applying the temperature in the range between 120 - 250 ᵒC. However, 200 ᵒC was observed to give higher yield (90%) of aromatic products in 1 h. Similarly, time study (0.25 h – 2 h) was performed.

➤ I-BAIL as solid acid catalyst was recycled and depolymerization results showed decrease in activity of catalyst.

➤ The change in the catalytic activity can be expected because dealkaline lignin contained ca. 29 mg/g of sodium, which can kill the Brønsted acidic sites present in the I-BAIL catalyst, which was affirmed by the ICP-OES analysis.

➤ Catalytic activity of homogeneous ($[C_3SO_3HMIM][HSO_4]$) and heterogeneous (I-BAIL) catalysts was correlated using GC-MS analysis of lignin depoleymrization products. It was observed that maximum amounts of aromatic monomers were obtained when $[C_3SO_3HMIM][HSO_4]$ catalyst was employed.

➤ Due to presence of Brønsted acidic proton and homogeneous reaction conditions, BAIL is giving maximum aromatic product yields (78%) than IL (18%, without Bronsted acidic proton) and I-BAIL (5%, heterogeneous catalyst) under similar reaction conditions i.e. lignin (0.5 g), catalyst (0.5 g), water:methanol, (1:5 *v/v*; 30 mL), 120 ᵒC, 1 h, 1000 rpm.

Chapter 4

Section 4A

Lignins were isolated from various crop waste samples using Klason method. They were characterized (bulk/molecular level) using various analytical tools such as, XRD, UV-Vis, ATR, NMR, etc. to understand the difference in their physico-chemical properties. The varying concentrations of *H*, *G*, *S* and T moieties were identified and their depolymerization activity was checked using acidic ionic liquids.

➤ The Technical Association of the Pulp and Paper Industry (TAPPI) method was applied to determine the chemical compositions of various crop waste [such as rice husk (RH I) from

Karnataka; bagasse (BG I) from Maharashtra; RH II, BG II and wheat straw (WS) from Uttar Pradesh and RH III from Odisha)] samples, which were collected from the different states of India. By TAPPI method determination of the chemical constituents such as lignin, α-, β- and γ- cellulose, pentosan, etc. in the various crop waste samples was possible.

➢ Klason method was used with 1.0 g of sample in 15 mL of 72% *wt./wt.* (12±0.02 M) of sulfuric acid (20±5 °C) solution and after 2 h diluted 3% *wt./wt.* sulfuric acid was added, which gave higher yield (21±3%) of Klason lignins (acid soluble and insoluble).

➢ Elemental analysis confirmed higher H/C and O/C ratios in isolated lignin than crop waste samples. Higher heat values of isolated Klason lignin were calculated using Dulong formula, which came to be ca. 2 times more than crop waste samples.

➢ Double bond equivalence (DBE) of the Klason lignin was calculated based on the C, H, N, S analysis and the resultant values were in the range between 4.4-5, which revealed that one benzene ring and one additional double bond in conjugation is present.

➢ Physico-chemical analysis with the help of UV-Vis, ATR and NMR spectra of Klason lignin samples confirmed the predominance of *G* units [UV-Vis (275±3 nm), ATR at 1220 and 1036 cm^{-1} and ^{13}C CP-MAS NMR (δ= 147.5±4 ppm) spectra].

➢ No impurity peaks for cellulose (15.26, 17.08° and 22.2°) and hemicellulose were seen in XRD patterns of Klason lignin samples.

➢ Depolymerization of Klason lignin derived from WS showed maximum organic solvent soluble products yield (99% with [C_3SO_3HMIM][HSO_4] and 92% with I-BAIL catalyst) than the other Klason lignin samples.

➢ As it was anticipated from the literature that substrate having different linkages (≡C-O-C≡ and ≡C-C≡) and moieties (*S*, *G* and *H*), after lignin depolymerization gave varying products yield. Similar trends are seen, when depolymerization of various Klason lignins were carried out using [C_3SO_3HMIM][HSO_4] and I-BAIL catalysts, which yielded 54-99% of organic solvent soluble products.

Section 4B

In this section, discussions on the isolation of organosolv lignins (ORGLs, 12±3% yield and 93±5% mass balance) from various crop waste and wood chip samples are done. The organosolv process was carried out using 1.024 mmol H_2SO_4 solution [60 mL distilled water-ethanol mixture (1:1 *v/v*)] at 180 °C in 1 h. To identify the possible alterations in lignin structures, several physico-chemical advanced characterization tools were employed.

➢ It was noted that though similar isolation method (organosolv process) was used to extract lignins from different crop waste and wood chip samples, their yields and physico-chemical properties seen to be varied.

➢ ATR spectra of ORGL derived from RHs, BG, WS and WC samples confirmed the presence of various types of functional groups (e.g. hydroxy, alkyl, alkoxy, carbonyl, alkenes etc.) with variable intensities.

➢ 2D (HSQC) NMR spectra of ORGL derived from crop waste and wood chip samples showed that the isolated lignin is in pure form without any polysaccharides contamination.

➢ Structural units in lignin were characterized by UV-Vis, ATR and 2D (HSQC) NMR analytical techniques, and observed that ORGL samples were composed of *S*, *G* and *H* units, among them *G* units were present in major quantity. This data is similar to observed with Klason lignin (section 4A).

➢ According to MALDI-TOF MS analysis, the average molecular weight of ORGL samples was ca. 1200 Da, which means that lignin comprises of ca. 6 to 7 consistent phenylpropenoid of *H, G, S* and T units (considering average molecular weight of lignin monomer as 180 g/mol).

➢ GPC analysis showed the *Mw;* 1082, 1093, 1366, 948, 1140, 1290 and 1436 Da, with a PDI of 1.7, 1.8, 1.7, 1.6, 1.6, 2.5 and 1.3 for RH I, II, III, IV, BG, WS and WC ORGL samples, respectively. MALDI-TOF MS results were in line with the observations made in GPC results (1301, 1387, 1402 1000, 1187, 1310 and 1510 verses 1082, 1093, 1366, 948, 1140, 1290 and 1436 Da) for RH I, II, III, IV, BG, WS and WC ORGL samples, respectively.

➢ Considering the physico-chemical properties of isolated ORGL samples, depolymerization of ORGL samples were carried out and the varying organic solvent soluble products yield (11-56%) with [C_3SO_3HMIM][HSO_4] and I-BAIL catalysts were obtained.

Chapter 5

Compared to H_2SO_4, Brønsted acidic ionic liquid (BAIL), [C_3SO_3HMIM][HSO_4] catalysed depolymerization of lignin yields higher amount of low molecular weight aromatic products as confirmed by GC and GC-MS analysis. This observation is contradictory to the fact that in reality H_2SO_4 catalyzed reaction showed higher weight basis yield (95%) compared to [C_3SO_3HMIM][HSO_4] (78%). To comprehend this disparity in catalytic activity between H_2SO_4 and BAIL experimental [1D (^{1}H) NMR, 2D (^{13}C/^{1}H HSQC, ^{15}N/^{1}H HMBC and ^{1}H/^{1}H NOESY) NMR and RAMAN] and theoretical (DFT) studies were carried out.

➢ With the help of experimental [RAMAN, 1D (^{1}H) and 2D (^{13}C/^{1}H HSQC; ^{15}N/^{1}H HMBC; ^{1}H/^{1}H NOESY) NMR] study, it has been established that the acidic proton (-NCHN- of imidazolium ring) in ILs form interaction through the –OH group of the substrate.

➢ To unravel interaction phenomenon between the catalyst and substrate, 1D (^{1}H) NMR studies were performed with monomers like cumene (without –OH group) and vanillin (with –OH, -OCH₃, -CHO groups), dimers like guaiacol glyceryl ether (-OH and ≡C-O-C≡ groups) and benzyl phenyl ether (≡C-O-C≡ group) and polymer, lignin (–OH, -OCH₃, -CHO, ≡C-O-C≡ etc. groups).

- In vanillin-[BMIM][Cl] adduct, shielding of chemical shifts of proton in IL (δ ppm= 9.43→9.36 (NCHN, 'h') and deshielding of chemical shifts of protons in vanillin (δ ppm= 10.27→10.60 (-OH, 'O'), 6.98→7.10 and 6.94→7.06 (doublet, Ar-H, 'k')] compared to neat spectra (of IL and vanillin) were observed.

- Through this finding it is explained that transfer of electron density (through 'O' of –OH) of vanillin to electron deficient imidazolium ring (cation of IL) is possible.

- To eliminate the possibility of involvement of Π electrons, ^{1}H NMR spectra were recorded with cumene (without –OH, -OCH$_3$ groups) and as anticipated no shift in proton NMR peaks was observed.

- Interaction studies with dimers indicate that IL interacts with substrate (guaiacol glyceryl ether (-OH and $\equiv$C-O-C$\equiv$)) having –OH groups as no interaction was visible with benzyl phenyl ether having only $\equiv$C-O-C$\equiv$ linkage.

- Lignin interacts with cation ($-N_1C_2H_2N_3$-, imidazolium ring) of IL *via* 'O' of –OH group, it can be affirmatively inferred from 2D (^{13}C/^{1}H, HSQC) NMR studies.

- From 2D (^{15}N/^{1}H, HMBC) NMR studies, the results obtained with 1D (^{1}H) and 2D (HSQC) NMR were corroborated and it is suggested that between lignin and cation of IL, a strong interaction is present.

- 2D (^{1}H/^{1}H, NOESY) NMR spectrum of vanillin-[BMIM][Cl] adduct helped to comprehend the mode of interaction as (preferably) perpendicular. This is because, no inter H---H interactions were observed between vanillin-[BMIM][Cl] adduct.

- In RAMAN, characteristic peaks for the stretching mode of the -C=O bond are visible at 1661, 1667 and 1692 cm^{-1} for the neat vanillin sample, but those peaks were shifted to higher wavenumber or red shift (1667, 1699, 1758, 1770 cm^{-1}) in the vanillin-[BMIM][Cl] adduct. It is due to increasing the strength of -C=O bond (-CHO) present in vanillin molecule because of electron pull from –OH group (which interacts with IL) located on para position.

- The theoretical (DFT) studies were performed using neutral [BMIM][Cl] and acidic [C$_3$SO$_3$HMIM][HSO$_4$] ILs with cumene and vanillin molecules. This study was interesting because, in NMR interaction studies with acidic ionic liquids were not possible due to fast exchange of protons under acidic conditions.

- Theoretical study with [C$_3$SO$_3$HMIM][HSO$_4$] catalyst was carried out with substrates (cumene and vanillin), which is very valuable since it provides direct correlation with the activity of the catalyst.

- It was observed that in vanillin-[C$_3$SO$_3$HMIM][HSO$_4$] adduct, extended interactions between HSO$_4$$^-$ and -SO$_3$H moieties (BAIL) with -OH (vanillin) groups were possible.

- The theoretical (DFT) studies also confirmed that the ILs form weak and strong hydrogen (inter and intra) bonding with the –OH and –OCH$_3$ groups on the substrate.

List of Publications and Patents

❖ Ionic liquids catalyzed lignin liquefaction: Mechanistic studies using TPO-MS, FT-IR, RAMAN and 1D, 2D-HSQC/NOESY NMR.

Sandip K. Singh, Paresh L. Dhepe* *Green Chem.*, 2016, 18, 4098-4108.

❖ Isolation of lignin by Organosolv process from different varieties of rice husk: Understanding their physical and chemical properties.

Sandip K. Singh, Paresh L. Dhepe* *Bioresour. Technol.*, 2016, 221, 310-317.

❖ Understanding interactions between lignin and ionic liquids with experimental and theoretical studies.

Sandip K. Singh, Subhrashis Banerjee, Kumar Vanka, Paresh L. Dhepe*, Catalysis Today, 2017, doi.org/10.1016/j.cattod.2017.09.050

❖ Effect of structural properties of organosolv lignins isolated from different rice husks on their liquefaction using acidic ionic liquids;

Sandip K. Singh, Paresh. L. Dhepe*, **Accepted-** Clean Technology Environmental and Policy - **2017**

❖ A comparative study on the physico-chemical properties of organosolv lignin obtained from rice husk, wheat straw, bagasse & wood chip.

Sandip K. Singh, Paresh L. Dhepe* Manuscript communicated -2017

❖ Role of cation, anoin, solubility & capping agent on lignin liquefaction: Mechanism endorse by ^{15}N NMR & H_0 of ionic liquids.

Sandip K. Singh, Paresh L. Dhepe* Manuscript communicated-2017

❖ Synthesis of an efficient, recyclable immobilized Brønsted acidic ionic liquids catalyst: Used for lignin liquefaction reaction.

Sandip K. Singh, Paresh L. Dhepe* Manuscript communicated-2017

❖ Acidic ionic liquids catalyzed depolymerization of lignin.

US Pat. Granted No. 9550710, Application No. IN *1387/DEL/2013; WO PCT/IN2014/000320; US Pat No. 14/890020; JP Pat. No. 2016-512484; CA Pat. No. 2911870; EP Pat. No. 14734241.4 2014*.

Sandip K. Singh, Babasaheb M. Matsagar, Ashutosh A. Kelkar, Paresh L. Dhepe.

❖ Synthesis of Supported Brønsted Acidic Ionic Liquids (SBAIL) Catalyst: Catalyst for Hydrolysis and Dehydration Reaction. Application No. IN 4057/DEL/2015.

Sandip K. Singh, Paresh L. Dhepe.

Work presented

❖ Attended 21st National Symposium on Catalysis "Catalysis for Sustainable Development" In Indian Institute of Chemical Technology, Hyderabad, India from 11 to 13th February 2013.

❖ Poster presented at International Conference on Global Opportunities for Latest Developments in Chemistry and Technology-2014 "GOLD-CT-14" In School of Chemical Science, North Maharashtra University Jalgaon, Maharashtra, India from 06 to 08th February 2014.

❖ Attended the National Academy of Sciences, India Workshop on "Scientific/Research paper writing" In Savitribai Phule Pune University, Pune, India from 16 to 17th December 2014.

❖ Poster Presented at 22nd National Symposium on Catalysis "Catalysis for Sustainable Development" In Central Salt and Marine Chemicals Research Institute, Bhavnagar, Gujarat, India from 07 to 09th January 2015.

❖ Attended IP licensing with a focus on patent, In CSIR-National Chemical Laboratory venture center, Pune, India 17th January 2015.

❖ Poster Presented at 17th CRSI National Symposium in Chemistry, In CSIR-National Chemical Laboratory, Pune, India from 06 to 08th February 2015.

❖ Poster Presented at National Science day celebration, In CSIR-National Chemical Laboratory, Pune, India from 25 to 26th February 2015.

❖ Poster Presented at International Conference on Sustainable Chemistry & Engineering, In Hotel Lalit, Mumbai, India from 08 to 09th October 2015.

❖ Attended one day National conference on "Conference on current trends in Catalysis for energy (CTCE)" at CSIR-National chemical Laboratory, Pune India, 28th October 2016.

❖ **An oral** presentation at 6th Asia-Oceania Conference on Sustainable and Green Chemistry at City University of Hong Kong, Hong Kong, from 27 to 30th November 2016.

❖ Poster Presented at National Science day celebration, In CSIR-National Chemical Laboratory, Pune, India from 23 to 24th February 2017.

❖ Poster Presented at National Science day celebration, In CSIR-National Chemical Laboratory, Pune, India from 23 to 24th February 2017.

List of Awards Received

❖ Poster Presented at National Conference on "Ionic liquids for Clean Energy and Environmental (ILCEE-2015)" at CSIR-National Chemical Laboratory, Pune, India from 16th to 17th December 2015 *[Best poster Award].*

❖ NCL RF- Agnimitra Memorial Award for Poster Presentation during National Science Day Celebration at CSIR- National Chemical Laboratory, Pune, India From 25th-26th February 2016 *[Best Poster Award].*

❖ **An oral** presentation at Asia-Pacific Congress on Catalysis-7th (APCAT–7) at Mumbai, India, from January 17th to 21st January 2017 *[Best Oral Award].*

Notes